Confinement of Normal and High-Strength Concrete Columns

by

SALIM RAZVI

A thesis submitted to
the Faculty of Graduate Studies and Research
in partial fulfilment of the requirements
for the degree of
DOCTORATE OF PHILOSOPHY
in Civil Engineering *

Department of Civil Engineering
University of Ottawa
Ottawa, Canada
June 1995

* The Ph. D. of Civil Engineering Program
is a joint Program with Carleton University
administered by the Ottawa-Carleton
Institute for Civil Engineering

ISBN 0-612-04970-1

UNIVERSITÉ D'OTTAWA
UNIVERSITY OF OTTAWA

Abstract

Reinforced concrete structures subjected to strong earthquakes are expected to develop inelastic deformations in their critical regions. First storey columns of a multi-storey frame structure are especially susceptible to a large number of inelastic deformation cycles. These columns are expected to maintain their capacity without a significant loss of strength while maintaining overall strength and stability of the structure. Deformability of concrete columns can only be improved through confinement of the core concrete. Therefore, current building codes (ACI 318-89, 1992: CSA A23.3, 1984) call for confinement steel for earthquake resistant columns. However, these design provisions are based on an arbitrary design criterion which does not consider some of the essential parameters of confinement including arrangement of reinforcement, axial load and lateral drift. Lack of a rational design procedure may be attributed to lack of a confinement model that is general enough to cover all the relevant parameters of confinement and simple enough to be used in design.

The use of high-strength concrete in the construction industry has gained acceptance during the last decade. High-strength concrete with strengths in excess of 100 MPa has been used successfully in columns of high rise buildings in large metropolitan centres where it has become available through ready mix companies. Economy and superior performance of high strength construction have been major reasons for widespread acceptance of the material. However, research on performance of structural members made with high-strength concrete has been lagging behind. Very little data are available in the literature on design and performance of high strength concrete structures. As a result, current building codes (ACI 318-89, 1992: CSA A23.3, 1984) do not address

important issues related to strength and deformability of high-strength concrete columns.

It has been established that strength and deformability of concrete are inversely proportional. This implies that deformability of structural members made with high-strength concrete may show undesirable characteristics in terms of performance of these members at or near their nominal capacities. This is especially true for compression members where failure may be governed by brittle compression crushing. Deformability of compression members gains a new dimension when seismic performance is under consideration. However, the provisions of current building codes have been developed on the basis of tests conducted on normal-strength concrete, where the 28-day strength does not usually exceed 40 MPa. Furthermore, effects of axial compression, reinforcement arrangement, and required drift level are not included in the current code procedure for normal strength concrete. Currently there is no design procedure for confinement of high strength concrete columns.

A comprehensive research project was conducted to investigate the behaviour and design of earthquake resistant normal-strength and high-strength concrete columns. The project included three essential components; testing of full size columns, development of an analytical model, and development of a design procedure.

The experimental program consisted of material research and structural testing. The first phase was designed to study mechanical properties of high-strength concrete, which involved testing of a large number of concrete cylinders. The second phase was designed to investigate performance of confined normal and high-strength concrete columns under concentric compression. The experimental program included tests of 46 full size square and circular columns, with concrete strength ranging between 60 MPa and 124 MPa. The parameters considered included; cross-sectional shape (circular and square), volumetric ratio and spacing of transverse reinforcement, distribution of longitudinal reinforcement and resulting tie arrangement, yield strength of transverse reinforcement, concrete compressive strength, influence of longitudinal reinforcement in circular columns, and type of circular reinforcement (continuous spiral and circular hoops).

The analytical component of the research program involved development of a mathematical model to represent stress-strain relationship of confined concrete. This was done in two steps. The first step included formulation of the relationship for normal strength concrete, for which extensive test data was available. The second step involved modification of the model for high-strength concrete. An extensive literature survey was first conducted, followed by evaluation of previous test data. This information was used, along with the results of the experimental phase of this investigation to develop a generalized confinement model for normal-strength and high-strength concrete columns.

The analytical and experimental research was used in developing a design procedure for confinement of earthquake resistant concrete columns. The procedure includes all the relevant parameters of confinement that have been observed to be important in column tests, and relates the design variables to deformation capacities. A displacement based design methodology was developed, where the lateral drift demand is a design parameter. This approach leads to different confinement steel requirements for columns with different deformability demands, an approach currently lacking in practice. Furthermore, the reinforcement arrangement is recognized as a design parameter, allowing lower volumetric ratio of confinement reinforcement for efficient arrangements. This may result in significant savings in steel, eliminating the common problem of steel congestion in earthquake resistant columns.

Acknowledgement

The author wishes to express his sincere appreciation to his thesis supervisor, Dr. M. Saatcioglu, for his guidance, advice, and financial support throughout the course of this research project.

Thanks are extended to Mr. Mongi Grira and the technical staff of the Civil Engineering Department for their assistance during the experimental part of this project.

Column Tests were conducted at the Fire Research Laboratory of National Research Council Canada (NRCC). Technical support received from NRCC staff, Mr. John Latour and Mr. John MacLaurin, is acknowledged.

Special thanks are due to Mr. Lee Pharo, operations manager of CBM ready mix concrete company of Ottawa, for his cooperation and valuable advice.

The research reported in this thesis was funded by the Portland Cement Association representing the North American cement industry, the Natural Sciences and Engineering Research Council of Canada (Research Partnership Program), and the Ontario Government University Research Incentive Funds. Their contributions are gratefully acknowledged.

The author would like to thank Canada Cement Lafarge, Steelco, and Conchem Co., for donating silica fume cement, high-strength steel, and superplasticizer, respectively.

Finally, I would like to thank my parents for their encouragement and prayer and my wife and children for their patience and continuous support.

Table of Contents

List of Tables

List of Figures

Notations

A_c Area of core concrete of column section.

A_{ch} Cross-sectional area of a column measured out-to-out of confining steel.

A_g Gross area of column section.

A_s Area of longitudinal steel.

A_{sh} Total cross-sectional area of transverse reinforcement within spacing 's'.

A_{sp} Area of spiral bar.

ΣA_s Summation of transverse reinforcement area.

ΣA_{st} Summation of transverse reinforcement area.

b_c Core dimension measured center-to-center of perimeter hoop.

b_{cx} ,b_{cy} Core dimension measured center-to-center of perimeter hoop.

b_d Bar diameter of transverse reinforcement.

c Depth of neutral axis.

d Effective depth of tension reinforcement.

d_s Diameter of spiral reinforcement.

E Modulus of elasticity.

E_c Modulus of elasticity of plain concrete.

E_{sec} Secant modulus of elasticity defined in Eq. 7.28.

f_c Stress in concrete.

f'_c Ultimate compressive strength of plain concrete obtained from standard cylinder test.

f'_{cc} Confined concrete compressive strength in member.

f'_{co} Unconfined concrete compressive strength in member.

f_l Lateral pressure defined in Eq. 7.10.

f_{lc} Equivalent lateral pressure that produces the same effect as uniformly applied pressure.

f_{lcx}, f_{lcy} Equivalent lateral pressure perpendicular to b_{cx} and b_{cy} respectively.

f'_{sp} Splitting tensile strength of plain concrete.

f_{test} Maximum stress carried by core concrete as observed in test.

f_{t1} Lateral pressure.

f_{t2} Axial strength of material under triaxial stress condition.

f_{u2} Axial strength of material under uniaxial stress condition.

f_{yt} Yield strength of transverse reinforcement.

H Column height at which deflection Δ_{as} is computed.

h_c Cross-sectional dimension of column core measured center-to-center of confining steel.

K Coefficient defined in Eq. 7.15.

k'_1, k_1 Coefficients defined in Eq. 7.5 and 7.7 respectively.

k_2 Coefficient defined in Eq. 7.19.

k_3, k_4 Coefficients defined in Eq. 7.22 and 7.23 respectively.

L Bar length defined in Eq. 8.10.

$P_{cc\,test}$ Maximum load carried by core concrete as observed in test.

P_o Nominal concentric column capacity defined in Eq. 5.1.

P_{oc} Nominal concentric capacity of column concrete defined in Eq. 5.2.

P_{occ} Nominal concentric capacity of column core concrete defined in Eq. 5.3.

P_{test} Maximum load carried by column as observed in test.

r Coefficient defined in Eq. 7.27.

s Spacing of transverse reinforcement in longitudinal direction.

s_l Spacing of longitudinal reinforcement, laterally supported by the corner of a hoop or the hook of a cross tie.

u Bond stress.

α	Angle between the leg of transverse reinforcement and the column side crossed by the same leg.
δ_{as}	Bar slip and/or extension.
Δ_{as}	Column end deflection due to bar slip and/or extension.
ϵ_c	Concrete strain.
ϵ_{tl}	Limiting transverse strain at failure under triaxial state of stress.
ϵ_{ul}	Limiting transverse strain at failure under uniaxial state of stress.
ϵ_1	Strain corresponding to peak stress of confined concrete.
ϵ_{01}	Strain corresponding to peak stress of unconfined concrete.
ϵ_{85}	Strain corresponding to 85% of peak stress of confined concrete on the descending branch.
ϵ_{085}	Strain corresponding to 85% of peak stress of unconfined concrete on the descending branch.
ρ_c	Area ratio of transverse reinforcement, defined in Eq. 7.17.
ρ_s	Volumetric ratio of transverse reinforcement, defined as volume of transverse steel divided by volume of concrete.
μ	Poisson's ratio.
θ_{as}	Rotation at column end due to bar slip and/or extension.

Chapter 1

Introduction

1.1 General

Reinforced concrete structures may develop inelastic deformations during strong earthquakes. These deformations usually occur at the ends of structural components, creating critical regions that are susceptible to rapid degradation of strength. Ductility and energy absorption capacity of these regions are essential for seismic resistance of structures.

In a well designed structure, the seismic induced energy is dissipated by formation of plastic hinges that can sustain a large number of inelastic deformation cycles, without a significant loss of strength. This can be achieved relatively easily in flexure dominant beams, where the reinforcing steel is designed to yield prior to concrete crushing. However, behaviour of compression members like columns may be dominated by concrete, which may lead to brittle failure. Therefore, it is desirable to dissipate earthquake induced energy by hinging of beams rather than columns. Furthermore, the consequence of a column failure is generally more severe than a local beam failure, since columns are usually responsible from overall strength and stability of structures.

However, it is difficult to avoid column hinging during a severe earthquake, especially at the first storey level. Figures 1.1 through 1.5 provide examples of column damage observed during past earthquakes. It is necessary to design reinforced concrete columns to withstand cycles of inelastic deformation. This can be achieved by confining the column concrete.

Column confinement can be attained by using closely spaced lateral reinforcement in the form of circular spirals or rectilinear ties. The presence of lateral reinforcement reduces internal cracking associated with lateral expansion of concrete under axial compression, and results in strength and ductility enhancements. Figures 1.6 through 1.8 illustrate examples of ductile performance observed in previous earthquakes.

The main variables affecting concrete confinement have been established by previous research. These include the volumetric ratio, strength, and spacing of confinement reinforcement, percentage and distribution of longitudinal reinforcement and resulting tie arrangement, concrete type and strength, section geometry and size, type and rate of loading, and the level of axial compression. A comprehensive survey of the available literature on concrete confinement has been conducted as part of the current investigation, and is presented in Chapter 2.

One of the recent developments in concrete technology, that has significance on column confinement, is the use of high-strength concrete. Strength of concrete used in practice has progressively increased over the years. While 40 to 50 MPa was considered to be high strength in 1970's, 60 to 80 MPa concretes have been used in columns of multistorey buildings in 1980's. More recently, a number of high-rise buildings were built, utilizing concrete strengths reaching up to 120 MPa. Consequently, a well planned research program on column confinement should follow the current trend in construction industry, and include research on confinement of high-strength concrete columns.

The strength level defining high-strength concrete is a source of controversy among researchers. Bertero (1979) considered strengths higher than 6000 psi (41 MPa) for normal-weight concrete, and 4000 psi (27 MPa) for light-weight concrete to be high strength. This was found to be justifiable since most of the ready-mix concrete supplied, and concrete used in experimental research, which provided basis for the majority of building code provisions, fell in the range of 3000 psi (20 MPa) to 6000 psi (41 MPa). The ACI Committee 363 on high-strength concrete, in its state-of-the-art report (ACI 363 1984), recognized the relative nature of the term high-strength, and defined its immediate concern as concretes with specified strengths higher than 6000 psi (41 MPa), since there was not enough information available in this range. The definition given by the FIP/CEB (1990) state-of-the-art report for high-strength concrete included a strength range between the presently stated limit in national codes, which is about 60 MPa, and the practical limit for making concrete with ordinary aggregates, which is about 130 MPa. Concrete with a cylinder strength higher than 40 MPa is referred to as high-strength concrete, in the current research program.

High-strength concrete has advantages in terms of performance and economy of construction. It results in high load carrying capacity per unit weight, which permits construction of very tall buildings and very long span bridges. Smaller member sizes may be used, resulting in reduced consumption of material. Furthermore, high-strength concrete allows for uniform column sections along the height, with higher strength concretes used in lower stories. This results in savings in formwork. It can also be used as an alternative to increasing reinforcement in compression members. This may result in savings in the material cost. Also, high-strength concrete permits early form removal, resulting from sufficiently high early age strength, increasing speed of construction. Lower deflections due to increased modulus of elasticity, lower creep, and greater resistance to physical and chemical deterioration form additional advantages associated with improved performance.

Although high-strength concrete has many advantages to offer, it has a major drawback for seismic applications. Since strength and ductility of concrete are inversely proportional, higher strength concretes are significantly more brittle than concretes within the normal-strength range. Therefore, concrete confinement becomes even more critical for high-strength concrete columns.

1.2 Research Needs

Performance of structures during past earthquakes have demonstrated that the confinement requirements for normal strength concrete, outlined in current building codes, provide satisfactory designs in most applications. However, the same requirements have been shown to produce unsafe column designs in certain cases, while also producing over conservative designs in other cases, resulting in congestion of reinforcement and associated constructibility problems (Saatcioglu 1989, Saatcioglu 1991). The state-of-knowledge on concrete confinement, on the other hand, has improved substantially since the pioneering research of Richart et al. (1928), which formed the basis of the current building code requirements. During the last two decades, a large volume of experimental data have been generated on confinement of normal-strength concrete, and a number of analytical models have been developed for stress-strain relationship of confined concrete. The new information, which could eliminate most of the shortcomings of the current design provisions, has not yet found its way in to the building codes. There is need for a rational design approach that reflects recent developments in the area of column confinement. More specifically, the effects of axial load, reinforcement arrangement, and inelastic deformation capacity need to be considered in design of columns for confinement. Such a design procedure requires proper analytical tools which have been lacking in the literature.

Analysis of confined columns requires a confinement model that incorporates all the relevant parameters. Early models, as well as some of the recent models, are not equipped to reflect the effect of reinforcement arrangement on concrete confinement. These models are deficient in distinguishing the differences resulting from various reinforcement arrangements. Among the two models that incorporate this effect, one is empirically derived and is only applicable to square columns (Sheikh and Uzumeri 1980), and the other (Mander, Priestley, and Park 1988 b) has limitations, as discussed later in Chapter 6. Currently, there is no model that is simple enough to be used for design purposes, and also incorporates all the main parameters of confinement. There is need for development of an analytical model that expresses stress-strain relationship of confined concrete, general enough to be applied to circular, square, and rectangular sections with different arrangements of confinement reinforcement.

Another area that lacks research data is confinement of high-strength concrete. Almost all the previous research on confinement, with few recent exceptions, were conducted on normal strength concrete, with strengths below 40 MPa. This is the range of concrete strength that is normally used in practice. It is also the strength range that is available through ready-mix companies. The recent trend towards using concretes in the range of 60 to 120 MPa leaves engineers and code writing authorities in the dark in terms of strength and deformability of high-strength concrete columns. The limited research that is available on high-strength concrete columns were mostly conducted on small specimens and standard cylinders, without longitudinal reinforcement. Therefore, there is need for experimental research on behaviour of confined high-strength concrete columns, preferably involving full size columns.

Lack of experimental data on high-strength concrete also resulted in lack of analytical tools for predicting strength and ductility of confined high-strength concrete columns. Current efforts in predicting the stress-strain relationship of high-strength concrete has been directed towards modifications of existing models developed for normal-strength concrete. Since the existing models were, by and large empirically developed, a large experimental data is required to introduce a rational modification. Since the test data in this area are scarce, the modifications introduced remain deficient. A confinement model, with capabilities for predicting the behaviour of both normal-strength and high-strength confined concrete can be developed if a sufficient experimental data are generated. This provides another justification for a well coordinated experimental research program.

The forgoing discussion clearly indicates that experimental and analytical research is needed for concrete confinement, in the newly growing field of high-strength concrete, as well as conventionally used normal-strength concrete columns.

1.3 Objective

The overall objective of this research project is to establish characteristics of confined concrete for normal-strength and high-strength concrete columns through experimental and analytical research . The columns investigated can be classified as short columns, not affected by secondary stresses. The specific objectives are outlined below:

- Generate experimental data on concrete mix design, mechanical properties, and test methods for high-strength concrete.

- Generate experimental data on high-strength concrete columns to establish relationships between confinement parameters, and strength and ductility characteristics of high-strength concrete in columns.

- Develop a generalized analytical model for confined concrete that can be used for normal-strength as well as high-strength concrete columns, with different geometric shapes and reinforcement arrangements, under different types of loading.

- Develop a displacement based design procedure for column confinement, based on the analytical model developed.

1.4 Scope

The following outlines the scope of the research program:

- Review of previous experimental and analytical research on confinement of normal and high-strength concrete columns.

- Parametric study to establish characteristics of mix design for high-strength concrete to be used in column tests. The study includes preparation and testing of standard cylinders with different amounts of superplasticizer, silica fume, and water/cement ratio, cured under different curing conditions, and tested at different ages.

- Tests of standard high-strength concrete cylinders to establish mechanical properties of concrete, including modulus of elasticity, modulus of rupture, and stress-strain relationships.

- Preparation and testing of high-strength concrete standard cylinders to investigate the effects of cylinder end conditions on standard cylinder tests. The end conditions considered include grinding, high-strength capping compound, and pad-caps filled with elastomeric pads.

- Design and construction of high-strength concrete spacer block to reduce the testing machine head room to appropriate level.

- Design, construction and instrumentation of 27 large scale square columns with different concrete strengths and confinement characteristics. The parameters of confinement include volumetric ratio, spacing, grade, and arrangement of transverse reinforcement.

- Design, construction and instrumentation of 23 large scale circular columns with different concrete strengths and confinement characteristics. The parameters of confinement include volumetric ratio, spacing, grade, and type of transverse reinforcement, and influence of longitudinal reinforcement.

- Testing of 46 large scale columns under monotonically increasing concentric compression.

- Processing of test data obtained from column tests, and evaluation of test parameters.

- Development of a confinement model for normal-strength concrete, based on existing test data, to be used for circular, square and rectangular columns, confined with different types and arrangements of transverse reinforcement, subjected to slow and fast rates of concentric and eccentric loadings.

- Modification of the model, on the basis of column tests conducted in the experimental phase, to include high-strength concrete.

- Verification of the model against existing test data reported in the literature on both normal and high-strength concrete columns.

- Development of a displacement based design procedure for column confinement.

- Presentation of results.

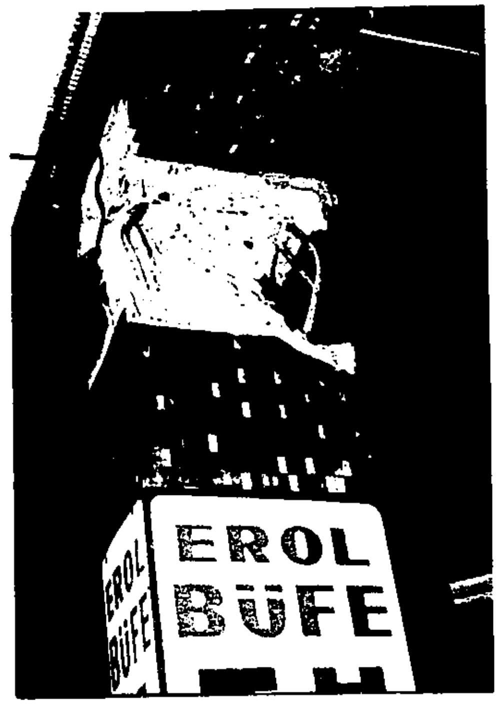

Figure 1.1: Column damage observed during the 1992 Erzincan Earthquake (Saatcioglu, and Bruneau 1993).

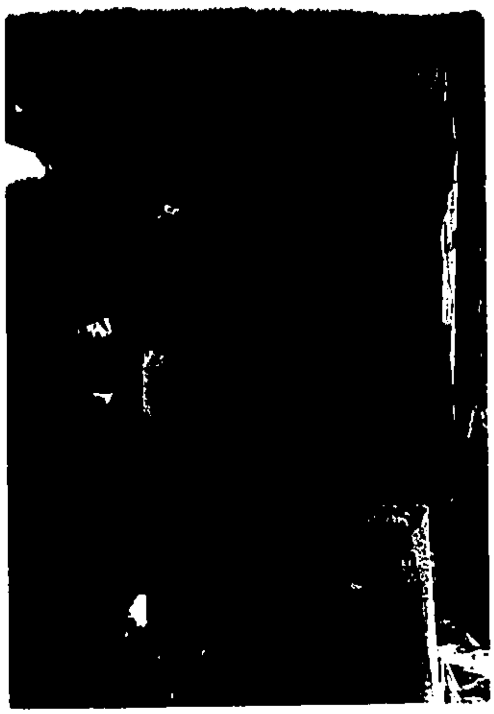

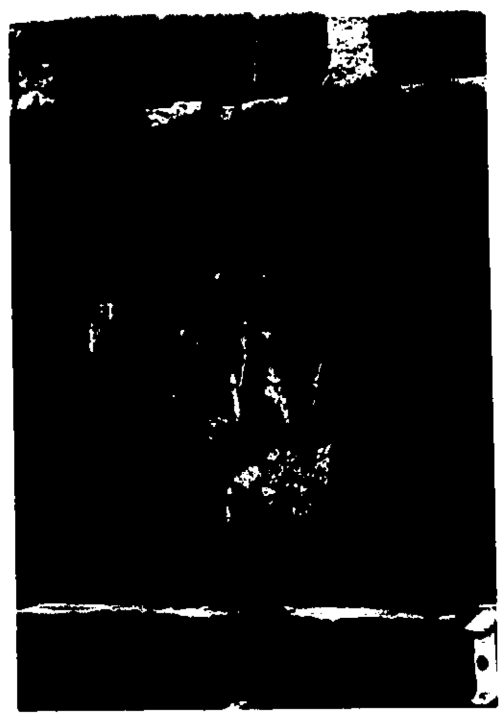

Figure 1.2: Damage to bridge columns during the 1994 Northridge Earthquake (Saatcioglu 1994).

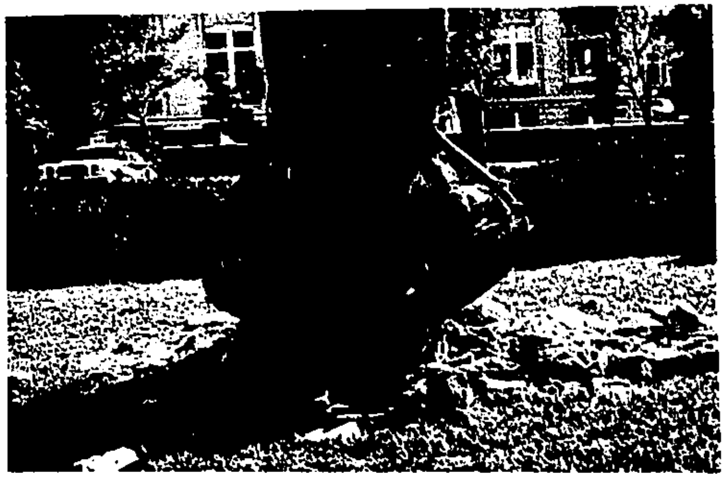

Figure 1.3: Column failure during the 1979 Imperial Valley Earthquake (Bertero 1985).

Figure 1.4: Column damage during the 1971 San Fernando Earthquake (Bertero 1985).

Figure 1.5: Bridge column damage in the 1971 San Fernando Earthquake (Bertero 1985).

Figure 1.6: Ductile behaviour of a spiral column during the 1971 San Fernando Earthquake (Bertero 1985).

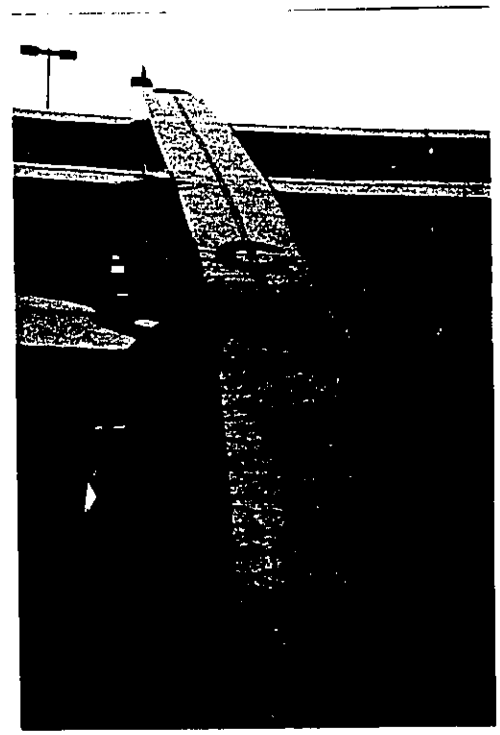

Figure 1.7: Ductile behaviour of a column during the 1994 Northridge Earthquake (Saatcioglu 1994).

Figure 1.8: Cover spalling of a well confined spiral column during the 1994 Northridge Earthquake (Saatcioglu 1994).

Chapter 2
Literature Review

2.1 General

Behaviour of confined concrete columns has been researched extensively during the last two decades. The majority of previous research was conducted on normal strength concrete columns, where the concrete strength was limited to 40 MPa. This research formed the basis for current design procedures for earthquake resistant columns, and provided a large volume of test data on behaviour of confined columns, also leading to development of analytical models for confined concrete. Research on column confinement can be grouped on the basis of type of applied loading. Such a grouping includes columns under monotonically increasing concentric and eccentric loadings, and columns under constant axial compression accompanied by lateral load reversals.

Recently, high-strength concrete has gained acceptance by the construction industry. Concretes with strengths of up to 120 MPa have been used in columns of multistorey buildings. Although limited, some research has been conducted in recent years on high-strength concrete columns. The research on high-strength concrete columns can also be classified on the basis of applied loading, in a manner similar to that described for normal-strength concrete columns. Review of previous research on normal-strength and high-strength concrete columns is presented separately in the following sections. A detailed review and inventory of previous analytical models for confined concrete are presented in Chapter 6, which forms part of a two-chapter section on development of a confinement model.

2.2 Previous Research on Normal-Strength Concrete Columns

Review of previous research on normal-strength concrete columns has been conducted by various researchers (Sheikh 1978, Yeh and Sheikh 1988, Sakai and Sheikh 1989), including the author in his M.A.Sc. thesis (Razvi 1988). Therefore, only a brief summary of previous research on normal-strength concrete columns will be provided in the following sections. Instead, the emphasis will be placed on literature review for high-strength concrete columns, presented in Section 2.3.

2.2.1 Columns Under Concentric Compression

Early research on concentrically tested concrete cylinders by Richart et al. (1928, 1929) provided some of the basic information on concrete confinement. The first set of tests included concrete cylinders confined by uniform fluid pressure (Richart et al.1928), followed by cylinders confined by circular spirals (Richart et al.1929). Subsequently, King (1946) studied the effect of confinement on ultimate strength of reinforced columns. Column confinement under concentric loading was a topic for many researchers. Chan (1955), Roy and Sozen (1964), and Kent and Park (1971) experimentally investigated the behaviour of confined concrete, and proposed analytical models to describe stress-strain relationships for confined concrete. The main variables considered were the size, strength, amount and spacing of lateral reinforcement. Other variables considered included cross-sectional size and shape, and rate of loading.

Most of the early research was conducted on small scale specimens and/or simple confinement arrangements (Szulczynski and Sozen 1961, Bertero and Felippa 1964, Stokl 1964, Shah and Rangan 1970). Researchers prior to 1975 did not consider the distribution of longitudinal reinforcement and the resulting tie arrangement as a confinement parameter (Bresler and Gilbert 1961, Pfister 1964, Hudson 1966, Somes 1970, Burdette and Hilsdorf 1971). This effect was discussed by Park and Paulay (1975), Vallenas, Bertero, and Popov (1977), and Sheikh and Uzumeri (1980). Sheikh and Uzumeri (1980) showed the effect of tie arrangement on square columns experimentally, for the first time. They also developed an analytical model based on the concept of effectively confined core area, where the area was defined on the basis of tie arrangement (Sheikh and Uzumeri 1982). The tie arrangement was not a parameter in earlier models, as well as some of the recent models (Park, Priestley, and Gill 1982, Fafitis and Shah 1985).

In 1988, Mander et al. reported test results of circular, square, and rectangular columns with different volumetric ratios and spacings of confinement reinforcement (Mander, Priestley, and Park 1988 a). The columns were tested under low and high strain rates. The researchers also developed an analytical model which utilized the effectively confined core area concept proposed earlier by Sheikh and Uzumeri (1982). The failure surface for concrete, under a multi-axial state of stress corresponding to the first hoop fracture, was theoretically calculated in the model (Mander, Priestley, and Park 1988 b).

Razvi and Saatcioglu (1989 a, 1989 b) tested columns with well distributed confinement steel in the form of welded-wire fabric. The results indicated that welded-wire fabric could be effective in confining the core concrete, resulting in significant improvements in strength and ductility of columns.

A critical review of previous research and code provisions for concrete confinement was reported by Sakai and Sheikh (1989). The main topics discussed included; properties of confined concrete, behaviour of confined sections and columns, and evaluation of confinement provisions in the building codes. An extensive list of references was also reported.

2.2.2 Columns Under Eccentric Compression

Effect of confinement on eccentrically loaded columns was first studied by Chan (1955). Sulaiman and Yu (1967) investigated the flexural behaviour of concrete confined by rectangular reinforcement. They indicated that the confinement pressure provided by transverse reinforcement would be different under strain gradient, than that developed under uniform compression. The researchers then proposed a stress-strain relationship for flexural analysis. The relationship included effects of spacing and tie size, and the ratio of confined concrete area to total area, as main parameters of confinement. Previous research indicates conflicting views on the effect of eccentricity on plain concrete. While Sturman et al. (1965) reported that the presence of strain gradient enhanced both the stress and strain at peak, Karsan and Jirsa (1970) indicated that there was no effect of strain gradient on the peak stress and corresponding strain, while the ductility of the descending branch improved.

Sargin et al. (1971) tested small scale columns under eccentric loading using specimens with rectangular ties, without longitudinal reinforcement. The experimental research resulted in an analytical model for confined concrete under eccentric loading. The effect of strain gradient was incorporated as improvements on strength and ductility of confined concrete, and was expressed in terms of the location of neutral axis.

Scott et al. (1982) tested large scale square columns under eccentric loading. They reported that the analyses based on stress strain relationships obtained from concentric column tests underestimated the deformability of columns recorded by tests. They further reported that a stress-strain relationship with a less steep falling branch would be more appropriate for members subjected to eccentric loading.

Sheikh and Yeh (1986), based on tests conducted by others, modified the Sheikh and Uzumeri model (1982) to reflect the ductility enhancement associated with strain gradient. Subsequently, they tested 16 columns under eccentric loading produced by different levels of constant axial load, accompanied by monotonically increasing lateral loading (Sheikh and Yeh 1990). The researchers reported that none of the confinement models available at the time was able to produce the experimental results accurately. While the Sheikh and Uzumeri (1982) model, as modified by Sheikh and Yeh (1986), produced good estimates of column behaviour under moderate levels of axial compression, it overestimated the column strength under high levels of compression. Therefore, the model was further modified to incorporate the strength reduction in concrete associated with increased axial compression (Sheikh and Yeh 1992). The descending branch of the original Sheikh and Uzumeri model was also modified based on the same data.

Saatcioglu et al. (1995) reported the results of large scale square columns tested under eccentric loading. Experimentally recorded moment-curvature relationships were reproduced analytically using the confined concrete model developed by Saatcioglu and Razvi (1992) on the basis of columns tested under concentric loading. The analytical relationships agreed well with those recorded experimentally for columns with different eccentricity of loading and confinement parameters. The researchers indicated that flexural behaviour of confined columns can be computed by using a confined concrete model developed for concentric loading, provided that the relevant parameters of confinement are incorporated in the model.

2.2.3 Columns Under Constant Axial Load and Incrementally Increasing Lateral Deformation Reversals

A number of experimental programs were conducted for columns under simulated seismic loading (Atalay and Penzien 1975, Zagajeski et al. 1978, Otani and Cheung 1981, Rabbat et al. 1982, Park et al. 1982, Saatcioglu and Ozcebe 1989). A comprehensive discussion of previous research under lateral load reversals was reported by Saatcioglu (1991). Test data were evaluated in terms of displacement ductility and drift ratios. It was concluded that column deformability reduced with increasing axial compression, shear stress, and rate of loading. On the other hand, deformability increased with reduced spacing and increased volumetric ratio and strength of confinement reinforcement.

The axial load level in the majority of previous tests under simulated seismic loading was limited to relatively low levels, although representing the majority of columns used in practice. However, because the level of axial compression is known to adversely affect column deformability, Sheikh and Khoury (1993) tested large scale columns under higher levels of constant axial load, combined with lateral load reversals. The main parameters considered were the amount and configuration of lateral steel, axial load level, and the stub effect. The researchers indicated that the stub effect was to enhance the strength of the adjacent section by 20%. It was also observed that the energy absorbtion capacity of columns, as well as the effectiveness of confinement reinforcement increased with reduction in axial load.

2.3 Previous Research on High-Strength Concrete Columns

Experimental and analytical studies on confinement of high strength concrete columns are scarce in the literature. This is partly because the use of high-strength concrete is a relatively recent development in concrete engineering. It may also be due to the difficulties associated with production, as well as testing of large scale specimens, which requires load levels that usually exceed capacities of testing machines in most research laboratories. The following is a summary of research carried out in the past, classified according to applied loading.

2.3.1 Columns Under Concentric Compression

2.3.1.1 Ahmed and Shah (1982)

Ninety six concrete cylinders were tested to study the effect of spiral confinement reinforcement on stress-strain relationship of normal and high-strength concrete. Fifteen of the cylinders had 75 x 300 mm dimensions. The remaining were 75 x 150 mm. Concrete strength, aggregate type, spiral pitch and yield strength of spiral reinforcement were considered as test variables. Concrete strengths of up to 69 MPa were considered with two types of aggregates. Steel strengths were 413 MPa, 1116 MPa, and 1433 MPa. No longitudinal reinforcement was placed in the specimens. The researchers reported that the efficiency of confinement by spiral reinforcement decreased with increased concrete strength. However, ductile behaviour of high strength concrete was achieved when spirals with sufficiently small pitch, and high yield strength were used. It was further reported that the effectiveness of spiral reinforcement, with 413 MPa yield strength, was low for low density aggregate concrete, as compared to normal density aggregate concrete.

An analytical procedure was proposed to predict the stress-strain relationship of confined concrete, on the basis of tri-axial stress-strain curves for plain concrete and stress-strain relationship of confining steel. An analytical investigation was conducted using the analytical procedure. It was concluded analytically that as the concrete strength increased the steel stress at peak concrete stress decreased. This was attributed to the small lateral strain of high strength concrete at the peak stress. However, the lateral strain of concrete increased rapidly after the peak, producing higher stresses in the spiral steel. It was further reported analytically that the stress in spiral steel, corresponding to peak concrete stress, was independent of the yield strength, for the same strength concrete. Hence, increasing the yield strength of spiral steel did not produce beneficial effects on strength enhancement. However, increasing the yield strength improved ductility of confined concrete.

2.3.1.2 Muguruma, Watanabe, Iwashimizu, and Mitsueda (1983)

Eighteen square columns with 147 x 147 x 400 mm dimensions were tested to study the effects of confinement on ductility of high strength concrete. Fourteen columns were laterally reinforced with circular spirals, having 50 mm spacing and 1390 MPa yield strength. The volumetric ratio of lateral reinforcement was 2.13%, except for two columns, which had 4.26% volumetric ratio. The remaining four columns were plain concrete specimens. The concrete strength ranged between 34 MPa and 89 MPa. No longitudinal reinforcement was provided in any column. Concrete strength and volumetric ratio of lateral reinforcement were studied as test parameters.

The results indicated that ductility of high strength concrete could be improved with the use of sufficient amount of confinement reinforcement, having high yield strength. Yielding of hoops was observed when the columns reached their peak stress. The stress-strain relationship originally proposed by the authors for normal-strength concrete (Watanabe et al. 1980) was modified based on the experimental data obtained in this study.

2.3.1.3 Martinez, Nilson and Slate (1983, 1984)

Tests were conducted on ninety four concrete cylinders with 102 x 203 mm, 102 x 406 mm, 127 x 610 mm, and 152 x 610 mm dimensions. The specimens were confined with spirals having yield strengths of 379 MPa to 414 MPa. Concrete strength varied between 21 MPa and 69 MPa, and the confinement pressure ranged from zero to approximately

21 MPa. No longitudinal reinforcement was provided in the specimens.

The researchers reported that both strength and ductility of concrete increased with increasing confinement pressure, regardless of unconfined concrete strength. However, the cylinders with higher unconfined strength showed reduced axial strain at peak stress, and faster rate of strength decay beyond the peak. The spiral steel did not yield in cylinders with high-strength concretes. Therefore, it was recommended that the yield strength of spiral steel be limited to 414 MPa. It was concluded that the ACI-318 building code (1977) requirements for spiral steel could lead to inadequate confinement of high-strength concrete columns. Small scale columns, designed on the basis of the ACI-318 building code (1977), were more ductile than larger scale columns. A stress-strain relationship was developed for confined concrete, based on the test data.

2.3.1.4 Faftis and Shah (1985 b)

An analytical investigation was carried-out to modify the original confinement model proposed by Fafitis and Shah (1985 a), to include high-strength concrete. The modification was based on column tests conducted under concentric loading by Martinez et al. (1983) and Muguruma et al (1983). The proposed relationship included concrete strength and lateral pressure as primary confinement parameters.

2.3.1.5 Basset and Uzumeri (1983, 1986)

Eighteen square columns were tested to study the behaviour of confined high-strength low-density concrete columns. The columns were 305 x 305 mm in cross-section, and 1956 mm in height. The concrete strength varied between 37 MPa and 40 MPa. The yield strength of ties ranged from 530 MPa to 600 MPa. The main variables considered in the experimental program included distribution of longitudinal reinforcement and the resulting tie configuration, amount of longitudinal steel, and the amount and spacing of transverse reinforcement. Although the columns contained low-density aggregate concrete, it was expected that some of the test results could be extended to normal-density high-strength concrete.

The results indicated that the brittle behaviour of low-density concrete could be improved significantly if large amount of lateral reinforcement was provided, and the longitudinal and lateral reinforcement were well distributed. Increasing the amount of longitudinal steel resulted in improved ductility. This was attributed to the importance of percentage of longitudinal steel in preventing premature buckling. Furthermore, increasing the amount of longitudinal steel increased the portion of load carried by steel, which prevented sudden drop of load at cover spalling. Minimum longitudinal and transverse reinforcement was recommended to maintain a reasonable level of ductility in columns. It was further reported that the behaviour of low-density aggregate concrete could not be predicted by Sheikh and Uzumeri (1982) and Modified Kent and Park (1982) models. These models resulted in unconservative results, overestimating column ductility.

2.3.1.6 Yong, Nour, and Nawy (1988)

Twenty four square columns were tested to study the behaviour of confined high-strength concrete columns. The column cross-section was either 152 x 152 mm or 133 x 133 mm, and the column height was 457 mm. The lateral reinforcement consisted of rectilinear ties having a yield strength of 496 MPa. Approximately the same grade of steel was used for longitudinal reinforcement. The concrete strength ranged from 84 MPa to 94 MPa. The variables considered included the volumetric ratio of lateral reinforcement, concrete cover, and distribution of longitudinal reinforcement. The amount of lateral reinforcement provided in each column was less than that required by the ACI-318 building code (1983).

The results indicated that the stress strain-strain relationship of high-strength concrete was improved by using lateral ties as confinement reinforcement. The improvement increased with the increase in the volumetric ratio of lateral steel. However, the lateral steel was less effective in confining high-strength concrete than confining normal-strength concrete. Tests indicated that the lateral steel did not yield at the first peak load. It was recommended that the spacing of lateral reinforcement should be less than the lateral column dimension. The distribution of longitudinal reinforcement improved ductility of concrete. Hence, it was recommended to use at least eight bars, distributed around the column perimeter. Concrete cover did not affect the stress-strain relationship of confined concrete. The available confinement models, i.e., those proposed by Sargin 1971, Vallenas et al. 1977, Park et al. 1982, Sheikh and Uzumeri 1982, and Fafitis and Shah 1985 failed to reproduce descending branches of experimentally obtained stress-strain relationships.

An empirical stress-strain relationship was proposed for high-strength concrete columns confined with rectilinear ties. The relationship consisted of two continuous polynomials. Strength enhancement due to confinement was assumed to be a function of concrete strength, spacing, diameter, volume, and yield strength of lateral steel, in addition to the number and diameter of longitudinal reinforcement.

2.3.1.7 Bjerkeli, Tomaszewicz, and Jensen (1990)

A major research program was undertaken on high strength concrete with normal-density and low-density aggregates. The normal-density aggregate concrete had cube strengths ranging between 65 MPa and 115 MPa, while the cube strength for low-density aggregate concrete varied between 60 MPa and 90 MPa. The scope included investigation of strength and deformation characteristics of plain and confined concrete, as well as sustained load effects on high-strength concrete. Short term behaviour of unconfined and confined concrete was investigated by testing 116 columns in four series. Series 1 consisted of small scale circular columns with 150 x 150 mm dimensions. Variables considered were concrete strength, and the amount and distribution of spiral reinforcement. Series 2 consisted of small scale square columns with 150 x 150 x 500 mm dimensions. Variables considered included the amount and distribution of confinement steel, the influence of longitudinal reinforcement, and strain rate. Series 3 consisted of small scale square columns with 150 x 150 x 1000 mm dimensions, tested under eccentric loading. Variables considered included concrete mix design, the eccentricity of loading, and the volumetric ratio of confinement reinforcement. Series 4 consisted of large scale rectangular columns with 300 x 500 x 2000 mm dimensions. Columns with 8-bar and 12-bar arrangements were tested to study the effects of longitudinal reinforcement distribution. Grade 613 MPa transverse reinforcement was used in the small scale square and circular columns. The steel grade varied between 506 MPa and 561 MPa for the transverse reinforcement used in large scale rectangular columns .

The results indicated that ductility of high-strength concrete could be improved through confinement. Use of large size longitudinal reinforcement did not produce any beneficial effect on ductility. However the number of longitudinal bars had significant influence on column ductility, showing improvements with increased number of bars. The strain rate was varied between 3.33×10^{-6} and 3.3×10^{-7} per second, and did not appear to have any significant effect on stress-strain relationship of confined concrete. Increase in concrete strength reduced the effectiveness of confinement reinforcement and resulted in reduced ultimate strain. Columns confined by circular spirals showed superior behaviour than corresponding rectangular columns confined by rectilinear reinforcement. The confinement efficiency for normal density concrete, in terms of strength enhancement, was about twice the efficiency observed for low-density concrete.

A stress-strain relationship was introduced for confined normal and low-density aggregate concretes. The expressions proposed by Martinez et al. (1984) were modified and used in defining the stress-strain relationship. The main parameters considered included concrete strength, confining pressure, and section geometry.

2.3.1.8 Rangan, Saunders, and Seng (1991)

Sixteen small scale columns were tested in this investigation. Ten columns had 160 x 160 x 800 mm dimensions, and were tested under concentric loading. The main variables considered were the amount and type of lateral steel (ties and welded wire fabric). The remaining six were slender columns with 100 x 100 x 2000 mm dimensions, and were tested under eccentric loading. The main variable considered in these tests was the eccentricity of loading. The concrete strength in all columns was 65 MPa.

The researchers concluded that there was no significant effect of confinement reinforcement on load-strain curves, despite the fact that yielding and fracture of confinement reinforcement was observed. This could be explained by the low amount of lateral steel used. It was also reported that recorded short column capacities agreed well with those computed using the current building code. The strength calculation and simplified stability analysis, proposed earlier by Rangan (1990), produced good agreements with the results of eccentrically tested columns.

2.3.1.9 Nagashima, Sugano, Kimura, and Ichikawa (1992)

Twenty six large scale columns, confined with high or ultra-high strength steel, were tested. The columns had 225 x 225 x 716 mm dimensions. Test variables included concrete strength, amount, strength, and configuration of confinement reinforcement, and yield strength of longitudinal steel.

The researchers reported that columns with concrete strength of 120 MPa showed a sudden strength drop at an axial strain of approximately 1% when $\rho_s f_{yt}$ was less than 18 MPa. The same columns developed strains in excess of 2% when this product was higher than 18 MPa. Columns with 6-bar, 8-bar, and 12-bar arrangements did not exhibit a major difference in strength and ductility. Strength enhancement due to confinement was observed to be independent of plain concrete strength, and was proportional to the square root of the effective lateral confinement capacity. Ductility of confined concrete was directly proportional to the capacity of lateral steel, and inversely proportional to concrete strength.

An analytical model was developed for confined high-strength concrete on the basis of the test data. The model incorporated the effectively confined concrete area concept for calculation of confined strength.

2.3.1.10 Itakura and Yagengi (1992)

A total of twenty-four square columns, with 218 x 218 x 500 mm dimensions, were tested (Itakura and Yagengi 1992, Yagenji et al. 1991, Ishiwata et al. 1990, Itakura et al. 1990). Test parameters included the amount, configuration, and hook length of lateral reinforcement, and the effect of longitudinal steel. Concrete strength was 74 MPa, and no concrete cover was provided in any of the columns.

It was reported that the confinement steel improved concrete strength tremendously. It was further reported that ties with hook lengths of six-bar-diameter were not as effective as those with ten-bar-diameter length. Columns with longitudinal bars were less ductile than those without longitudinal bars. It was observed that the confinement steel fractured as a result of buckling of longitudinal reinforcement.

2.3.1.11 Hatanaka and Tanigawa (1992)

Normal and high strength concrete cylinders, with 100 x 100 mm dimensions, were tested. The cylinders were confined by steel rings. Concrete strength ranged from 30 to 100 MPa. The objective of the test program was to establish a relationship between the amount of confinement steel and concrete ductility. Test variables included water-cement (w/c) ratio and confinement pressure. The results were used to modify the analytical model proposed earlier by the same researchers to include high-strength concrete.

2.3.1.12 Galeota, Giammatteo, and Marino (1992)

Small scale square columns with 60 MPa concrete were tested to investigate confinement of high-strength concrete. The columns had 150 x 150 x 450 mm dimensions and did not contain cover concrete. The main parameters considered were the amount and spacing of lateral reinforcement. No longitudinal reinforcement was placed in the columns. It was concluded that both the strength and ductility of concrete improved with confinement. However, the improvements were less than those associated with normal-strength concrete. An analytical modal was proposed based on the test data.

2.3.1.13 Polat (1992)

Twelve square concrete columns were tested to investigate the behavior of normal and high-strength concrete columns. The columns had 230 mm cross-sectional dimension and 1500 mm height. The variables considered included concrete strength (36 to 85 MPa), the strength of confinement steel (363 to 915 MPa), the amount of confinement steel (0 to 2.3%), and gage length (300 to 1500 mm). It was concluded that the strength and ductility of columns increased significantly when high volumetric ratios of lateral reinforcement were used. This improvement was found to be proportional to the square root of the yield strength of lateral steel. However, it was also concluded that high-strength concrete columns could fail at loads significantly lower than those computed on the basis of the ACI-318 building code (1989). When high-strength steel was used as confinement reinforcement, yielding of the steel was observed at peak column load. Column ductility was significantly affected by the gage length. The confinement models proposed earlier for normal-strength concrete (Sheikh and Uzumeri 1982, Modified Kent and Park 1982, Muguruma et al. 1983, Bjerkeli et al. 1990) were used to predict the stress-strain relationship of high-strength concrete. The results indicated that none of the models considered provided accurate predictions.

2.3.1.14 Nishiyama, Fukushima, Watanabe, and Muguruma (1993)

Tests were conducted on fourteen square columns, with 250 x 250 x 750 mm dimensions, and 110 MPa concrete. Test variables included yield strength (400 and 800 MPa), diameter (4 and 6 mm), the spacing (31, 41 and 60 mm) of confinement reinforcement, and concrete cover. Both monotonic and cyclic loadings were considered.

It was concluded that 4% volumetric ratio of grade 800 MPa reinforcement was required to achieve ductile behaviour. It was also reported that while the inner hoops yielded at peak concrete stress, the peripheral hoops did not yield. Columns with cover showed the same behaviour as those without the cover, after the spalling of the cover concrete.

2.3.1.15 Sudo, Masuda, Abe, and Yasuda (1993)

Tests were conducted on small scale cylindrical specimens, with 150 x 300 mm dimensions. The cylinders were confined with circular spirals. No concrete cover was provided. Concrete strength ranged between 39 and 120 MPa. Test variables included aggregate type, water/binder ratio, and the amount and spacing of spiral reinforcement.

It was reported that the improvements in peak concrete stress and corresponding strain were proportional to confinement pressure. It was also observed that increase in water/ binder ratio reduced the strength enhancement caused by confinement, while improving deformability.

2.3.1.16 Limsuwan (1993)

Four series of small scale square columns, with 150 x 150 x 1000 mm dimensions, were tested under concentric and eccentric compression. The main variables included the amount, type, and spacing of lateral reinforcement, and the amount of longitudinal steel.

Columns tested under concentric loading showed higher strength than computed on the basis of ACI-318 building code (1989). The use of 0.95 f'_c was recommended for computation of in-place strength of unconfined concrete, instead of 0.85 f'_c commonly used for normal-strength concrete. Columns tested under eccentric loading showed good agreement with axial load-moment interaction diagrams constructed using the ACI concrete stress block.

2.3.1.17 Al-Hussaini, Regan, Xue, and Ramadane (1993)

Eight columns were tested as part of a research program aimed at developing design guidelines for high-strength concrete columns. The columns had 250 mm square cross-section and 2000 mm height. Test parameters included tie spacing, and the amounts of lateral and longitudinal reinforcement. Concrete cube strength ranged between 112 and 144 MPa.

The results indicated that capacities of high-strength concrete columns could be computed fairly accurately using the equations given in the British Code (1985) for normal-strength concrete columns. However, the minimum lateral steel specified in the code was neither sufficient to produce ductile behaviour nor adequate to prevent buckling of longitudinal reinforcement.

2.3.1.18 Cusson and Paultre (1994)

Twenty seven square columns were tested to investigate the confinement of high-strength concrete columns. The columns had a cross-sectional dimension of 235 mm and a height of 1400 mm. Test parameters included concrete strength (53 to 100 MPa), lateral steel strength (392 to 770 MPa), the distribution of longitudinal reinforcement (4 to 12 bars), the volumetric ratio of lateral steel (1.4% to 4.9%), tie spacing (50 and 100 mm), the percentage of longitudinal reinforcement (2.2% and 3.6%), and concrete cover.

Early spalling of cover concrete was observed during testing. Hence, it was recommended to ignore the presence of cover concrete in capacity calculations. Well confined columns showed significant improvements in strength and ductility. It was reported that the amount of transverse reinforcement was the most important parameter that influenced stress-strain relationship of confined concrete. The efficiency of high-strength steel as confinement reinforcement increased with the degree of confinement.

2.3.1.19 Li (1994)

Tests of normal and high-strength concrete columns were performed in three series. The first series included 27 square columns with 240 mm cross-sectional dimension and 720 mm height, and 17 circular specimens with the same dimensions. These columns were tested under a low strain rate. Test parameters included concrete strength (35 to 82.5 MPa), the arrangement of longitudinal reinforcement (4-bar and 8-bar), and the volumetric ratio (0.8% to 5.0%), spacing (20 to 70 mm), and yield strength (445 and 1318 MPa) of lateral reinforcement. The second series included 11 square and 4 circular columns tested under a high strain rate. Column dimensions and test parameters were similar to those of the first series. The third series included 5 larger size square columns with 350 mm cross-sectional dimension and 3900 mm height. The columns were tested under a constant axial load and lateral load reversals. Test variables included the level of axial load, and the amount spacing, and yield strength of lateral reinforcement. Concrete strength was either 93 MPa or 98 MPa.

The results indicated that the most important confinement parameters were the amount and yield strength of confinement reinforcement. Increasing the amount and/or strength of confinement steel improved both the strength and ductility of confined concrete. It was observed that grade 430 MPa transverse reinforcement yielded at or shortly after the peak column load. However, grade 1300 MPa did not yield at the peak load. Columns confined with grade 1300 MPa steel behaved much better than those confined with grade 430 MPa. This indicated that the volumetric ratio of confinement steel could be reduced while increasing its yield strength. However, the usable yield strength of high strength steel was suggested to be limited to 900 MPa for columns with a shear-span-to-depth ratio of 4. It was also reported that the envelopes of stress-strain relationships for concrete tested under cyclic loading agreed well with those obtained under monotonic loading.

Columns tested under high strain rate showed higher strength, increased modulus of elasticity, and steeper slope of descending branch of the stress-strain relationship. However, higher strain rate did not produce higher strength for concrete confined with high-strength steel.

None of the confinement models for normal-strength concrete considered (Mander et al. 1988 b, Muguruma et al. 1991, Fafitis and Shah 1985 b, and Yong et al. 1988) was able to predict the behaviour of high strength concrete accurately. A stress-strain relationship was proposed for confined high-strength concrete on the basis of the test data. The form of the relationship was adopted from the three equations proposed earlier by Muguruma et al. (1991). Columns designed based on the New Zealand code (NZS 3101: 1982) showed brittle behaviour when tested under constant axial load and lateral load reversals.

2.3.2 Columns Under Eccentric Compression

Very little data is available in the literature on confinement of high strength concrete columns under monotonic eccentric loading. Early research conducted on the topic was either limited to small scale specimens (Schade 1992) or columns with concrete strength not exceeding 60 MPa (Kaar et al. 1978, Sandararaj 1991). Research prior to 1993 was discussed by Ozden (1992) and Ibrahim (1994). Some of the research programs discussed earlier under "Columns Under Concentric Compression" also included strain gradient as a test parameter (Rangan et al. 1991 and Ekasit 1993). These column tests are summarized in the preceding section along with columns tested under monotonic compression.

2.3.2.1 Ozden (1992)

Ten square columns, with a cross-sectional dimension of 230 mm and a column height of 1500 mm, were tested under strain gradient. The strain gradient was applied such that the strain on one side of the cross-section was always zero. Concrete strength varied between 55 MPa and 65 MPa. The main variables considered included the volumetric ratio (0% - 4.03%) and spacing (40, 80, 120 mm) of lateral ties.

The results indicated that strength and ductility of columns improved with confinement. However, when the spacing of ties was greater than one half of the cross-sectional dimension (h/2), there was no significant effect of confinement. In all the columns it was observed that the tie steel yielded at failure. It was suggested to reduce the multiplier that defines the intensity of rectangular stress block for flexural analysis from 0.85 to a lower value depending on the concrete strength.

2.3.2.2 Ibrahim and MacGregor (1994)

Fifteen rectangular and six triangular columns were tested under eccentric loading. The rectangular columns had 200 x 300 mm cross-sectional dimensions, and 3000 mm height. The triangular columns had 240 x 450 mm cross-sectional dimensions and 2950 mm height. The test parameters included concrete strength (59 to 131 MPa), the volumetric ratio (1.0% to 3.9%) and spacing (50, 100, 200 mm) of confinement reinforcement.

The results indicated that the column behaviour was dependent on the amount and spacing of lateral reinforcement. The deformation capacity of columns with very little confinement reinforcement was similar to that of plain concrete. The maximum tie spacing specified in the ACI code (1989) for non-seismic regions was not sufficient to produce ductile column behaviour. The ratio of unconfined in-place strength of column concrete to cylinder strength was found to be 0.92. However, the ACI rectangular stress block parameters were found to be unsafe for design of rectangular or triangular high-strength concrete columns. Four confinement models (Shah et al. 1983, Muguruma et al. 1989, Yong et al. 1988, and Bjerkeli 1990) were used to reproduce the experimental results. Non of these models produced sufficiently accurate results. Therefore, the researchers proposed modifications to Bjerkeli et al. (1990) model. The modified model agreed well with the test data.

2.3.2.3 Xie et al. (1994)

An analytical parametric investigation was conducted on high-strength concrete columns subjected to eccentric loading. A total of twenty one columns were analyzed using finite element method. The columns had three different cross-sectional dimension; 350 x 350 mm, 700 x 700 mm, and 200 x 300 mm. Concrete strength considered ranged from 37.5 to 75 MPa. The main parameters included were the configuration, size, and strength of confinement steel, concrete strength, depth of cover, and the amount of longitudinal reinforcement.

The results indicated that the confinement steel and depth of cover concrete had no effect on peak moment and the behavior prior to the peak. However, increasing the amount of confinement steel, decreasing the depth of concrete cover, and using a favourable tie configuration improved the post-peak behaviour.

2.3.2.4 Lioyd and Rangan (1995)

Experimental and analytical studies were conducted to investigate the behaviour of high strength concrete columns subjected to eccentric compression. The experimental program included testing of 36 columns. The columns had either 300 x 100 mm or 175 x 175mm cross-sectional dimensions and 1680 mm height. The main variables considered were; concrete strength (58, 92, and 97 MPa), eccentricity of load (0.1 to 0.4 times the column depth), and longitudinal reinforcement ratio (1.5% and 2.0%). All columns were confined laterally with 4 mm diameter high strength ties at 60 mm spacing. Confinement steel was in excess of the requirements of the Australian code (AS 3600 1994). It was reported that confinement steel was insufficient to produce ductile behaviour for columns with low load eccentricity (e=0.1 d). The failure of such columns was sudden, brittle, and explosive. One the other hand columns subjected to higher load eccentricities (e>0.3 d) behaved in a more ductile manner.

The analytical program included development of two computer programs to predict the failure load and load-deflection relationship of slender high strength concrete columns under axial load uniaxial bending.

2.3.3 Columns Under Constant Axial Load and Incrementally Increasing Lateral Deformation Reversals

Tests on high strength columns under reversed cyclic loading were scarce prior to 1990. However, a number of experimental and analytical studies were conducted during the past five years. The following is a summary of research on columns under reversed deformation cycles. The column length referred to in the following sections includes depths of top and bottom beams, or the depth of middle stub, wherever applicable.

2.3.3.1 Chung, Hayashi, and Kokusho (1980)

Twenty three rectangular columns were tested to investigate the behavior of reinforced concrete columns subjected to cyclic load reversals. The column dimensions were 150 x 200 x 1500 mm. The main parameters considered included concrete strength, axial load level, the amount of shear reinforcement, and loading history. The concrete strength ranged approximately from 20 to 80 MPa.

The results indicated that increasing the amount of shear reinforcement and reducing axial load level improved the ductility of high strength concrete columns. The effect of loading history on column deformability was investigated by testing two identical columns with two different loading histories. One of the columns was subjected to one cycle, while the other to ten cycles. The results showed a decrease in deformability with increasing number of inelastic deformation cycles.

2.3.3.2 Watanabe, Muguruma, Matsutani, and Sanda (1987)

Tests were conducted on three square columns, with 225 x 225 x 1340 mm dimensions.

The strength of concrete used was 58 MPa in all columns. Two of the columns were identical. They were designed to study the effect of direction of lateral loading. The columns were subjected to lateral load reversals applied either parallel to, or diagonal to the principal axis. The results indicated significant increase in deformability when the loading was applied diagonally. The third column was subjected to axial tension and lateral load reversals. This column showed reduced strength but improved deformability as compared to the companion column under axial compression.

2.3.3.3 Muguruma and Watanabe (1990)

Tests were conducted on eight square columns, with 200 x 200 x 1500 mm dimensions. Test variables included concrete strength (86 and 116 MPa), yield strength of confinement steel (328 and 792 MPa), and axial load level (25% and 63% of $A_g f'_c$). Twelve-grade 400 bars were used as longitudinal reinforcement. Plain reinforcement, with 6 mm diameter, was used as lateral confinement steel.

The tests indicated that the ductile behavior of high strength concrete columns could be achieved by using high-strength lateral reinforcement. It was also observed that the ductility enhancement was reduced with increasing concrete strength. Hence, the use of high-strength steel was recommended to confine high-strength concrete.

The test data was used to modify the confinement models proposed by Muguruma et al. (1983) and Modified Kent and Park (Park Preiestley and Gill 1982). The modified model was used to calculate moment-curvature relationships of high-strength concrete columns.

2.3.3.4 Sugano, Nagashima, Kimura, Tamura, and Ichikawa (1990)

Eight square columns were tested to study seismic behavior of high strength concrete columns. The columns had 250 mm square cross-sections and 2000 mm height. The variables considered included concrete strength, the capacity of lateral reinforcement

($\rho_s f_{yt}$), and the ratio of axial stress to specified concrete strength. Concrete strengths considered were 39, 59, and 78 MPa. The results indicated that the combined use of high-strength concrete and high-strength steel could be very effective in attaining improved deformability of columns.

2.3.3.5 Kabeyasawa, Li, and Huang (1990)

Three square columns were tested to investigate strength and ductility of high-strength concrete columns under high axial compression and lateral load reversals. The columns were 250 mm square in cross-section and 2210 mm in height. The lateral reinforcement was in the form rectilinear spirals and cross ties with a yield strength of 1334 MPa. Concrete strength was 91 MPa in all three columns. The main variables considered included axial load level (35% and 52% of $A_g f_c'$), and tie arrangement (8-bar and 12-bar arrangements).

The results indicated that both columns under low and high axial compression behaved in a ductile manner due to the efficiency of confinement reinforcement used. However, the one under high axial compression showed reduced ductility as compared to the other, under low axial compression. The column with a 12-bar arrangement developed a higher level of deformation at peak stress, when compared with a column with an 8-bar arrangement.

2.3.3.6 Sakai, Hibi, Otani, and Aoyama (1990)

Eight square columns were tested to study the effect of confinement on ductility of high-strength concrete columns. The columns had 250 x 250 mm cross-section and 2000 mm height, with 100 MPa concrete. The yield strength of ties ranged from 344 MPa to 1126 MPa. The main variables considered were the distribution of longitudinal reinforcement and resulting tie configuration, amount, diameter, and yield strength of transverse reinforcement, and axial load level.

The results indicated that the use of high-strength lateral steel was effective in improving deformability of high-strength concrete columns. Confinement efficiency improved with reduction of tie spacing in both the vertical and horizontal directions. The diameter of lateral steel had little effect on column deformability.

2.3.3.7 Shin, Kamara, and Ghosh (1990)

A research program was conducted to investigate the flexural ductility of high strength concrete members. Two series of tests were conducted. The first series consisted of twelve specimens with 150 x 300 mm cross-section and 3000 mm length, tested under monotonically increasing lateral loading. The concrete strength ranged from 28 MPa to 103 MPa. The second series consisted of twenty four specimens with 112.5 x 225 mm cross-section and 3000 mm length, tested under reversed cyclic loading. The concrete strength ranged from 35 MPa to 103 MPa. All the specimens were reinforced like columns, although they were tested under zero axial load. The main test variables were; concrete compressive strength, percentage of longitudinal reinforcement, and spacing of confinement steel.

It was observed that the ratio of tension reinforcement to balanced section reinforcement (ρ/ρ_s) was the most significant factor for flexural ductility. Increase in (ρ/ρ_s) resulted in reduced flexural ductility. The envelope of the load-deflection curves for specimens tested under cyclic loading showed the same features as those tested under monotonic loading. A reduction in load carrying capacity was observed with repetition of cycles at the same deflection level. The reduction in the load carrying capacity was more significant in specimens with higher concrete strength, wider tie spacing, and lower volumetric ratio of confinement steel. The equivalent rectangular stress block, suggested by the ACI-318 code, was found to produce good estimates of flexural strength, for members made with concrete strengths up to 103 MPa.

2.3.3.8 Muguruma, Nishiyama, Watanabe, and Tanaka (1991)

Four square columns were tested to study deformability of high-strength concrete columns confined with high-strength lateral steel. The columns were 200 mm square in cross-section and 1500 mm in height. The concrete strength was 130 MPa. The test variables included yield strength of transverse reinforcement (408 and 873 MPa) and level of axial load (34.3% and 47.3% of $A_g f_c'$). Eight laterally supported longitudinal bars were placed in each specimen.

The researchers concluded that high-strength concrete columns could be designed to behave in a ductile manner, even under high axial compression. It was also reported that when the axial load level was low, high-strength confinement steel did not result in ductility improvement, mainly because for these columns the volumetric ratio provided could be considered excessive. However, when the axial load was high, the yield strength of confinement steel played a major role in improving ductility. Furthermore, the rectangular stress block suggested by ACI 318-89 produced good estimates of experimental column capacity when the axial load level was moderate. However, the same approach underestimated the capacity of columns under high axial compression.

The researchers used the test data to modify a confinement model that was already modified once (Muguruma and Watanabe 1990). This model was originally developed by Muguruma et al. in 1983. The modification involved revision of strength reduction at large curvatures. It was assumed that concrete strength did not fall below 50% of the peak stress.

2.3.3.9 Mizoguchi, Arakawa, and Arai (1991)

Tests were conducted on twelve small scale square columns with 180 x 180 x 1250 mm dimensions. Four specimens were designed to fail in flexure and the remaining eight were designed to fail in shear. Strength of concrete used ranged between 30 and 60 MPa. The main test variables were; direction of lateral load, concrete strength, and axial load level.

The results indicated that the ultimate shear and flexural strengths of columns loaded under biaxial bending were similar to those loaded parallel to the principal axis. It was also reported that the columns failed in flexure showed smaller strength degradation than those that failed in shear.

2.3.3.10 Kabeyasawa, Shen, Kuramoto, and Rubiano (1991)

Two square columns were tested to study the behaviour of high-strength concrete columns under constant axial compression and biaxial moment reversals. The columns were 250 mm square in cross-section and 2000 mm in height. Both were reinforced with twelve laterally supported longitudinal bars. The lateral reinforcement consisted of square spirals and cross ties, having a yield strength of 969 MPa. Concrete strength was 64 MPa. The only variable considered was the axial load. The first column was subjected to constant axial load of 36.7 % of $A_g f_c'$. The second column was subjected to variable axial load, ranging from -10 % to 60 % of $A_g f_c'$.

The results indicated that the level of axial load had a significant effect on deformability of reinforced concrete columns. The column subjected to variable axial load showed reduced capacity when loaded in tension. However, it behaved in a more ductile manner and showed less damage compared to the companion column under constant axial compression.

2.3.3.11 Hibi, Mihara, Otani, and Aoyama (1991)

Five columns were tested to investigate deformability of high-strength concrete columns. The columns had a square cross-section with 300 mm sectional dimension, and 2125 mm height. Concrete strength was 100 MPa. The test variables considered included yield strength of confinement reinforcement (797 and 1251 MPa), lateral confinement pressure (6.0, 6.3, and 7.0 MPa), yield strength of longitudinal reinforcement (424, and 711 MPa), arrangement of longitudinal reinforcement (12 and 16-bar), and axial stress ratio (30 % and 45% of f_c'). The results indicated ductile behaviour of columns subjected to low axial compression and high lateral pressure. The strain readings indicated elastic behaviour of transverse reinforcement throughout testing.

2.3.3.12 Kuramoto and Minami (1992)

Six square columns were tested to study the shear strength of high-strength reinforced concrete columns. The columns had 300 x 300 x 2100 mm dimensions, and were prepared using 114 MPa concrete and 736 MPa longitudinal reinforcement. The main variables were; the amount (area ratio of 0.53% and 1.19%) and yield strength (407 to 766 MPa) of confinement reinforcement, and axial stress level (16.7 % and 33.3 % of f_c'). It was observed that the transverse reinforcement yielded in most of the columns at the peak load, regardless of the yield strength. It was also observed that the ultimate shear strength decreased with decreasing lateral confinement pressure and increasing axial compression.

2.3.3.13 Thomsen and Wallace (1992, 1994)

Experimental and analytical studies were conducted to investigate the possibility of using high-strength concrete columns in regions of moderate to high seismic risk. The experimental program included tests of twelve small-scale square columns with 152 mm cross-sectional dimension, and either 813 mm or 737 mm height. The concrete strength varied between 67 MPa and 103 MPa. All the columns had eight laterally supported longitudinal reinforcement. The primary variables were the spacing (25, 32, 38, 45 mm), configuration (hoops with cross ties or hoops with diamond shape ties), and yield strength (792, 1275 MPa) of transverse reinforcement, and the level of axial compression (0 %, 10 %, and 20 % of $A_g f_c'$).

The results of the experimental program indicated that the columns subjected to zero axial load developed lateral drifts in excess of 4% with no noticeable strength degradation. On the other hand, columns subjected to 10 % P_o to 20 % P_o showed stable behavior up to 2% lateral drift, with subsequent strength degradation. Since the confinement steel used was 50 % or less of that required by ACI 318-89, it was concluded that the current building code requirements were conservative for axial load levels of 0 to 20 % P_o. It was observed that at drift levels of less than 2% the configuration of transverse reinforcement did not play a significant role on concrete confinement. The use of higher strength steel (1275 MPa instead of 792 MPa) did not affect column ductility, in the drift range of practical interest, i.e. 2% or less. It was concluded that although the use of high-strength steel could permit using larger tie spacing, buckling of longitudinal reinforcement in such cases should be adequately prevented.

The analytical program included computations of monotonic lateral load-displacement relationships of columns using either the modified Kent and Park (1982) or Yong et al. (1988) confinement models. The model proposed by Yong et al. resulted in more accurate predictions of column behaviour than the modified Kent and Park model. The analytical program also included the computation of drift levels associated with longitudinal bar buckling. A parametric study was undertaken to evaluate the effect of high axial load on column performance. It was concluded that column ductility reduced significantly with increasing axial compression. More research was recommended in the axial compression range of 0.25 to 0.50 P_o.

2.3.3.14 Azizinamini et al. (1993) and Azizinamini et al. (1994)

Nine square columns were tested as part of a research program aimed at evaluating the ductility of columns designed according to the present ACI code (ACI 318-89). The columns had 305 mm cross-sectional dimension and 2440 mm height. The test parameters included the volumetric ratio (ρ_s= 2.36% to 3.82%), spacing (41, 67 mm), and yield strength (413 MPa, 827 MPa) of lateral reinforcement, concrete strength (26 to 104 MPa), and axial load level (20 %, 30 % and 40 % of P_o).

The test data indicated that an increase in concrete strength did not result in reduction of displacement ductility ratio. However, reducing spacing of lateral steel from 67 to 41 mm increased the maximum displacement by 40 %. Increasing the level of axial compression from 20 % to 40 % P_o caused a 30 % reduction in the maximum displacement. Increasing yield strength of transverse reinforcement from 413 to 827 MPa did not result in improvements in column deformability, when the columns were subjected to an axial load of 20 % P_o. It was concluded that high-strength concrete columns ($f_c' > 70$ MPa), designed in accordance with the present code (ACI 318-89) showed good ductilities when subjected to axial loads of 0.2 P_o or less. A linear reduction in the intensity of rectangular stress block was recommended from 0.85 to 0.60 for concrete strengths of greater than 70 MPa, in calculating the nominal moment capacity. The experimental data was also used to modify the confinement model proposed by Yong et al. (1988). Analytical moment-curvature relationships, based on the modified model, showed good agreement with those obtained experimentally.

2.3.3.15 Sheikh, Shah, and Khoury (1994)

Four reinforced concrete columns were tested to investigate the performance of high-strength concrete columns. The columns had 305 mm square cross-section, and approximately 2.3 m column height. Concrete strength ranged from 54 to 59 MPa. All columns were reinforced with eight laterally supported longitudinal bars. The volumetric ratio of lateral steel ranged from 1.68% to 4.3%, and the yield strengths were 464 MPa and 507 MPa. Axial load level ranged from 59 % to 62 % P_o.

The results were compared with those of normal-strength concrete columns. The comparisons indicated that the required amount of lateral steel was proportional to concrete strength, for certain column performance, if the axial load level was measured in terms of P_o rather than $A_g f_c'$. Improvement in column ductility appeared to be proportional to the amount of confinement steel.

2.3.3.16 Lipien and Saatcioglu (1995)

Ten square columns were tested as part of a research program aimed at evaluating the deformability of high strength concrete columns. The columns had 250 mm square cross-section, and 1.76 m column height. Test variables included concrete strength (64 and 104 MPa), yield strength (420, 575 and 1000 MPa), volumetric ratio(ρ_s= 1.90% to 5.58%) and spacing (45 to 100 mm) of confinement steel, reinforcement arrangement (8-bar and 12-bar), and axial load level (0.28% and 0.14% of $A_g f'_c$).

The tests indicated that the ductile behavior of high strength concrete columns could be achieved when sufficient amount of confinement steel was used. It was reported that increasing the amount of confinement steel and reducing tie spacing resulted in significant improvement in column ductility. The use of higher strength steel (1000 MPa instead of 575 MPa) did not have significant effect on column ductility, when the axial load was low.

2.3.3.17 Baingo and Saatcioglu (1995)

Nine columns were tested to investigate deformability of high-strength concrete columns. The columns had a circular cross-section with 250 mm diameter, and 1760 mm height. The test variables included; concrete strength (60 MPa, and 90 MPa), Type (circular spirals and circular hoops), amount (ρ_s=1.6% to 3.7%), spacing (50 mm and 100 mm), and yield strength (f_y = 400 MPa and 1000 MPa) of confinement steel, axial load level (0.21, 0.33, and 0.43 $A_g f'_c$), thickness of concrete cover (0, 10 mm).

The test results indicated that high strength concrete columns behaved in extremely brittle manner. However, the behaviour was improved by increasing the amount and/or reducing the spacing of confinement steel. The results also showed a superior performance of columns confined with high strength steel as compared to those confined with normal strength steel. This was especially true for columns subjected to high axial load levels. The type (continuity) of lateral steel did not have a significant effect on column performance.

2.3.3.18 Legeron and Paultre (1995)

Six square columns were tested as part of a research program aimed at evaluating the behaviour of high strength concrete columns. The columns had 305 mm square cross-section, and 2.65 m column height. Concrete strength ranged between 92.4 MPa and 104.3 MPa. Test variables included volumetric ratio (ρ_s= 1.96% and 4.26%) and spacing (60 and 130 mm) of confinement steel, and axial load level (0.14% to 0.39% of $A_g f'_c$).

The test results indicated that high strength concrete columns with sufficient amount and closely spaced confinement steel behaved in a ductile manner. It was observed that column ductility was reduced significantly when the axial load level was increased from 14% to 39% of $A_g f'_c$.

2.3.3.19 Bayrak and Sheikh (1995)

Five columns were tested under axial load and cyclic displacements to simulate earthquake forces. The columns had 305 x 305 x 1473 mm dimensions with 508 x 702 x 813 mm stubs. Unconfined concrete strengths were either 72 MPa or 102 MPa. Other test variables included; amount (ρ_s=3.15% to 4.29%), and spacing (70, 90, and 95 mm) of confinement steel, tie configuration, and axial load level (0.36, 0.48, and 0.50 Po).

Test results indicated that high strength concrete columns were less ductile than normal strength concrete columns subjected to the same level of axial load. The distribution of laterally supported longitudinal bars improved column ductility significantly. Columns with 4-bar arrangement designed according to the current codes (ACI 318-89, CSA A23.3, 1984) showed brittle behaviour under high axial load levels. The increase in axial load level was observed to reduce column ductility and increase stiffness degradation.

2.4 Conclusions Drawn From Previous Research

The following conclusions may be drawn from previous research on normal and high-strength concrete columns.

- Column deformability is a function of three groups of parameters; those related to applied loading, those related to confinement reinforcement and those related to concrete type. The parameters related to applied loading include axial load, eccentricity of axial load, shear stress, rate of loading, direction of lateral loading, and loading history. The parameters related to confinement reinforcement include the volumetric ratio, spacing, and yield strength of confinement reinforcement, percentage and distribution of longitudinal reinforcement and resulting tie arrangement, and section geometry. The parameters related to concrete type include concrete strength and mass density of aggregate.

- Axial compression reduces column deformability. However, it is possible to obtain high deformabilities in highly compressed columns, provided the columns are well confined.

- The effect of increasing shear stress on normal-strength concrete is to reduce ductility. However, well confined columns may develop high deformabilities even under high shear force reversals. The effect of shear stress on deformability of high-strength concrete columns has not been investigated.

- The effect of high strain rate on normal-strength concrete is to increase strength and reduce deformability. The same effect was observed by Li (1994) on high strength concrete columns confined with normal strength lateral steel. Tests by Bjerkeli et al. (1990) on high-strength concrete indicate no significant effect between low and very low strain rates.

- The effect of eccentricity of loading and the resulting strain gradient on deformability of confined concrete is a source of controversy. Although some researchers reported that strain gradient improved ductility of normal-strength concrete, others were able to reproduce moment-curvature relationships for columns using confined concrete stress-strain relationships obtained under concentric loading. There is little research reported in the literature on the effects of strain gradient on stress-strain relationship of confined high-strength concrete. However, some researchers were able to reproduce moment-curvature relationships for high-strength concrete columns using stress-strain relationships developed for concentric loading, implying that the strain gradient effect may not be significant on column deformability.

- The effect of number of inelastic deformation cycles is to decrease column deformability with increasing number of cycles.

- Strength and ductility of confined concrete increase with increasing volumetric ratio of confinement steel. This is true for both normal and high-strength concrete. However, significantly higher volumetric ratio is required for high-strength concrete columns to achieve deformabilities usually expected of normal-strength concrete columns.

- Previous research indicates conflicting views on the use of high-strength steel for column confinement. Some researchers believe that the extra strength present in high-strength steel can not be utilized prior to the failure of concrete. Therefore, these researchers suggested limits on yield strength. Others feel that the use of high-strength steel is necessary to produce ductile behavior of high strength concrete columns, even if very high-strength steel does not yield at the peak load.

Examination of available test data indicates that the use of high strength steel may not improve deformability of columns subjected to low axial load ($P \leq 0.2\ A_g f'_c$). However, there is a strong evidence that the behaviour of column subjected to high axial load improves significantly with the use of high strength lateral steel.

- Reductions in tie spacing, and spacing of laterally supported longitudinal reinforcement improve both the strength and deformability of confined normal and high-strength concrete columns. The effect of spacing is more significant in columns with relatively high volumetric ratio of confinement steel. The spacing of laterally supported longitudinal reinforcement may play an important role on column confinement.

- Circular spirals are more effective than most rectilinear ties. However, when legs of rectilinear ties and cross ties are closely spaced in the cross-sectional plane, the confinement efficiency can be increased to the same level as that of spirally reinforced columns.

- High-strength concrete is more brittle than normal-strength concrete. Therefore, more confinement steel is needed for high strength concrete to achieve deformabilities usually expected from normal strength concrete.

- Confinement efficiency changes with mass density of aggregate used in concrete. Strength and ductility enhancements attained in light-weight aggregate (LWA) concretes are much less than those for normal-weight aggregate (NWA) concretes.

- Unconfined strength of concrete in the column core varies approximately between 85% and 100% of concrete strength determined by a standard cylinder test. The average value of this variation appears to be higher for high-strength concrete.

- Existing analytical models for stress-strain relationship of confined concrete have limitations. Previous research indicates that analytical models developed based on normal-strength concrete are not applicable to high-strength concrete. Available confinement models for high strength concrete are mostly modified versions of normal-strength models, which are only applicable, in most cases, to test data based on which they were derived. There exists a need for a generalized analytical model that includes all essential parameters of confinement in normal-strength and high-strength concrete.

- Confinement steel requirements of ACI-318 (1989) building code for normal-strength concrete, are based on an arbitrary design concept. The code requirements tend to be conservative for columns subjected to low axial load, and unsafe for columns under high axial load. There exist a need for a more rational design approach which includes all relevant confinement parameters.

- No specific confinement steel requirements for high-strength concrete are available in the ACI-318 (1989) building code. However, the extension of the current normal-strength concrete requirements to high-strength concrete may lead to conservative design under low axial load, and unsafe design under high axial load.

Chapter 3

Mechanical Properties of High Strength Concrete

3.1 General

Mechanical properties of plain (unconfined) high-strength concrete have to be established first before the characteristics of confined concrete can be investigated. Currently used properties of concrete is mostly based on tests of normal-strength concrete. The applicability of these properties to concretes with strengths reaching up to 130 MPa becomes questionable since the stress-strain characteristics of concrete are known to change with strength. Therefore, selected properties of plain high-strength concrete were studied through a materials test program prior to the column tests presented in Chapter 4 for investigation of concrete confinement. The mechanical properties investigated include relationships between mix design and compressive strength, modulus of elasticity, splitting tension, and concrete stress-strain relationship. Parameters affecting standard cylinder testing were also investigated. The test program considered and the results obtained are presented in this chapter.

3.2 Compressive Strength

Compressive strength is perhaps the most important property of concrete for structural applications. Compressive strength is also used as a measure of other mechanical properties like; tensile strength, modulus of elasticity, durability, abrasion resistance, and creep. Careful selection of constituent materials and their proportions play an important role on concrete strength. Therefore, mix-design was investigated as a primary parameter. Other parameters considered to investigate concrete strength include; type of curing, age of concrete, cylinder size, type of cylinder moulds used, and cylinder end conditions. The effects of these parameters are discussed below.

3.2.1 Mix Design

A large number of standard cylinders were prepared from different trial mixes to study relationships between strength and mix design. Table 3.1 summarizes the mix designs considered, including those used in producing concrete for the column tests discussed in Chapter 4. Mix design variables include water/cement ratio, aggregate type, and roles of superplasticizer, silica fume, and slag. Table 3.2 summarizes strengths obtained at various ages from each mix design .

3.2.1.1 Water/Cementitious Material Ratio

Water/cementitious material ratio is one of the important parameters that affects concrete strength. Cementitious materials, in addition to cement, are often used in producing concretes of very high strength for reasons discussed in subsequent sections. Therefore, this ratio is used in place of water/cement ratio, which is commonly used for normal-strength concrete mixes. However, it is referred to as water/cement ratio, whenever applicable, because of its familiarity.

High-strength concrete can be produced by lowering the water/cement ratio and increasing cement content. However, low water/cement ratio leads to an unworkable mix. Therefore, it is necessary to use superplasticizers to improve workability. The water/cement ratio used in the current investigation range between 0.19 and 0.41. The low ratio of 0.2 was needed to produced concrete strengths in excess of 100 MPa. It was also observed that mixes with low water/cement ratios and high cement contents developed early shrinkage cracks.

3.2.1.2 Amount of Superplasticizer

Superplasticizer is essential to increase workability of low water/cement ratio mixes. However, the use of high amount of superplasticizer may lead to bleeding and reduced compressive strength of concrete. The amount of superplasticizer used in the mixes produced ranged between 2.9 L/m^3 to 20 L/m^3.

Mixes 9 and 10 were designed to study the effect of superplasticizer on concrete strength. The design for both mixes was identical except for the amount of superplasticizer. The results indicate that the amount of superplasticizer has little effect on the compressive strength of concrete. The two-month strength of mix 10 was reduced by 5% when the amount of superplasticizer was increased from 11.2 L/m^3 to 18.6 L/m^3. The effect of superplasticizer was also studied by Aitcin et al. (1984). These researchers indicated that the three-month strength dropped from 100 MPa to 90 MPa when the amount of superplasticizer was increased from 14 L/m^3 to 21 L/m^3, while no reduction was observed in the 7-days and 28-days strength.

It was observed that mixes with low water/cement ratio and high dosage of superplasticizer suffered loss of workability at a faster rate than those with high water/cement ratios and lower dosage of superplasticizer. Figure 3.1 shows the loss of workability in mixes with low and high water/cement ratios.

3.2.1.3 Silica Fume

Silica fume is usually required for strengths higher than 80 MPa (FIP/CEB state-of-the-art report 1990). Goldman and Bentur reported (1989) that the use of silica fume improved interface bond strength between the mortar and aggregate, and resulted in improved concrete strength .

Two types of cement were used in this investigation; Normal Portland Cement (Type 10), and Normal Portland Cement Blended with Silica Fume (Type 10SF). Type 10SF cement contained 7% silica fume. Comparison of test results for mix #1 (with Type 10SF cement) and mix #10 (with Type 10) indicates no significant effect of silica fume on compressive strengths of these two mixes. Comparisons of mix #2 (with Type 10SF) and mix #8 (with Type 10) shows that mix #2 developed slightly higher strength at 28 days although it had a higher water/cement ratio. However, the 2 and 3-month strength of mix #2 was lower than those for mix #8. The influence of silica fume on strength was apparent in mixes with low water/cement ratios. Mixes # 4 and 14 contained 75 L/m^3 of liquid silica fume. Each litre of liquid silica fume contained 0.5 kg of water and 0.7 kg of silica. The strength attained in 28 days was approximately 100 MPa, increasing to approximately 120 MPa after 6 months.

The presence of silica fume improved workability . This observation was also reported by Tachibana et al. (1990), who reported that "in high-strength concrete with low water/cement ratio, silica fume is considered to act as if it were water, dispersing between the cement particles, and producing high flowability". Mixes with high content of cementitious material and silica fume were observed to get more sticky, with a rapid loss of workability with time.

3.2.1.4 Blast Furnace Slag

Blast furnace slag is normally used to improve workability, resistance to alkali-aggregate reaction, and to control thermal cracking due to heat of hydration (Tachibana et al. 1990). Djellouli et al. (1990) indicated that slag can also be used in high-strength concrete mixes as a retarder to prolong workability of concrete. The researchers reported that the major disadvantage of high-strength concrete with low water/cement ratio was the rapid loss of workability due to the reactivity of cement. The loss of workability made it practically impossible to deliver concrete to construction sites only one hour from the concrete plant. Therefore, it was suggested that slag be added to these mixes as partial replacement of cement, since it was less reactive than cement, to control workability (Djellouli et al. 1990).

In the current investigation, slag was used in batches made with low water/cement ratios to avoid loss of workability and to reduce thermal cracking.

3.2.1.5 Size, Shape, and Type of Aggregate

Previous studies have shown that limiting the size of coarse aggregate to 10 to 12 mm improves the compressive strength of concrete. Cordon and Gillespie (1963) reported that smaller size aggregates produced higher concrete strength due to the increased bond stress between the aggregate particles and the cement paste. Mehta and Aitcin (1990) reported that for most types of aggregates the smaller particles of coarse aggregate were stronger than larger particles. The size reduction process eliminated internal defects, such as large pores, and micro cracks.

The particle shape is another factor that affects the compressive strength. ACI-363 (1984) reported that the crushed stones produce higher compressive strength than rounded gravel due to the greater mechanical bond associated with angular particles.

Crushed limestone with maximum size of 10 mm was used in all mixes considered in this research program. Aggregates from two different locations were used. Those from Doschenes Construction Limited , Hull, Quebec were used in earlier mixes. In one of the mixes tested the expected strength level was not achieved. Investigation of crushed cylinders indicated a possibility of concrete strength being controlled by the strength of aggregate. In subsequent mixes aggregates from United Aggregates Limited, Ottawa, Ontario were used to produce higher strength concretes. This location was known to have stronger aggregates, and it was possible attain strengths of up to 124 MPa when proper mix design was used.

3.2.2 Curing

The effect of curing was studied by considering two types of curing regime. All cylinders were covered with polyethylene sheets immediately after casting. The moulds were removed after 24 hours. Half of the cylinders were placed in the moist curing chamber. The other half were kept outside the chamber and covered with wet burlap. This group was sprayed water once a day until the day of testing. Test results indicated that the 28-day strength was not affected by the curing regime. However, the moist cured cylinders showed slightly higher strength at six months. These results are in line with those obtained by others (Read et al 1990).

3.2.3 Age

Strength development with time was monitored through period testing. Mixes with silica fume and w/c ratio of more than 0.3 showed a faster rate of strength development up to twenty eight days. However, this trend was reversed after twenty eight days. Similar observation was also made by Maage et al. (1990).

The effect of silica fume on long term strength development was studied by many researchers. Cadette et al. (1989) reported that the compressive strength of 2 years old silica fume concrete was lower than the 91 days strength. Similar observation was reported by Li (1994). The researcher indicated that cylinders tested after 400 days showed 9% reduction in strength as compared to 56 days strength. The long-term strength loss was explained by De Larrard (1993) by a self stress field that was generated in concrete. Drying of concrete resulted in skin tension which was balanced by a compression in the core. The core compression was comparable to the long term strength loss. Other researchers, however, found that there was no effect of silica fume on long term strength development of concrete. No strength loss was observed in concretes made either with or without silica fume, during a 10-year study period (Maage et al. 1990).

Silica fume was used to produce 124 MPa concrete in this research program. A large number of concrete cylinders were tested to monitor concrete strength. Test results indicate that the compressive strength increased with age during the first six months and remained constant thereafter up to the end of the study period, which was two years. This is shown in Table 4.3.

3.2.4 Cylinder Size

Previous researchers studied the effect of cylinder size on compressive strength and the possibility of using small size cylinders as standard size (Neville 1966, Malhotra 1976). Advantages of using small size cylinders include savings in materials (concrete, capping, and moulds), storage space, reduced capacity of testing machines, and ease in handling and transportation (Day and Haque 1992). Analysis of test data conducted on concrete cylinders with strengths of up to 50 MPa indicate that compressive strength of 100 mm diameter cylinders was statistically identical to that of 150 mm cylinders (Day and Haque 1992).

The study of size effect becomes more important for high-strength concrete. Testing high-strength concrete cylinders requires high machine capacity which may not be available in most concrete laboratories. Tests of high-strength concrete cylinders in the past showed conflicting results on the effect of cylinder size. Some researchers found that small scale cylinders (100 x 200 mm) gave higher strengths than those of standard cylinders (150 x 300 mm). The difference was reported to range between 2 and 9% by Tomosawa et al. (1993), and not more than 3% according to Novokshchenov (1993). Other researchers indicated that standard cylinders were 2% stronger than small scale cylinders (100 x 200 mm) (Radain et al. 1993).

In this study, small scale cylinders (100 x 200 mm) and standard cylinders (150 x 300 mm) were tested to study the size effect. Test results of small cylinders consistently showed lower compressive strength than those of standard cylinders. However, the difference was within 5%. Strengths reported elsewhere in this thesis were obtained by testing standard size cylinders.

3.2.5 Cylinder End Conditions

The effect of cylinder end condition on concrete strength was studied by a number of researchers (Novokshchenov 1993, Tomosawa et al. 1993, Boulay and de Larrard 1993, and Li 1994). The FIP/CEB State of the Art Report (1990) stated that "high-strength concrete in compression testing is more sensitive to geometrical imperfections on the ends of the specimens than concrete of a lower strength. The brittle behaviour of this material reduces the ability to redistribute any stress-concentrations that might arise due to partial contact between the plates and the specimen".

Four methods were used in this research program to prepare the ends of cylinders for testing. These methods are described below.

Grinding: Grinding of both ends was done using a special machine designed for this purpose. The machine was available at the Energy Mines and Resources (EMR) laboratory in Ottawa. This method produced highest compressive strengths as compared to other methods.

Using Pad-Caps: Pad-caps used consisted of solid aluminum restraining caps filled with tough elastomeric material to ensure uniform application of the load. The aluminum caps were useful in confining the ends and preventing premature failure of the cylinders. The test results were very close to those obtained by grinding the ends. The difference between the two methods did not exceed 5%. Figure 3.2 illustrates the failure mode of concrete cylinders tested using pad-caps.

<u>**Capping with High-Strength Sulphur Compound:**</u> Cylinders capped with high-strength sulphur compound produced results which were comparable to those obtained from the previous two methods, up to approximately 75 MPa. Beyond this strength level, however, the failure took place in the capping compound prior to cylinder failure.

<u>**Cutting the Ends by Steel or Diamond Saw:**</u> Steel and diamond saws available in the geology laboratory of the University of Ottawa, EMR, and a marble factory in Ottawa were used to cut the cylinder ends. This method did not produce good results. Compressive strengths obtained were consistently low. This was attributed to the difficulty of cutting the ends perfectly perpendicular to the longitudinal axis of cylinders.

Among the procedures considered above, grinding of cylinder ends produced the best results. However, this method may be time consuming and/or expensive. Boulay and de Larrard (1993 a, 1993 b) suggested capping high-strength concrete cylinders with a 'sand-box system'. This system contained dry compacted sand for uniform distribution of load. This method, not employed in the current investigation, produced test results with good agreement with those obtained by grinding the ends. The method has been used successfully in two major bridge projects in France (de Larrard 1993).

3.2.6 Type of Cylinder Moulds

Two types of moulds were used in this study; disposable plastic moulds and reusable steel moulds. Cylinders made using steel moulds showed higher compressive strength than those made using plastic moulds. The difference was in the range of 2 to 5%. This observation is consistent with that made earlier by Novokshchenov (1993).

3.3 Modulus of Elasticity

Modulus of elasticity of concrete is an important mechanical property that is used in deflection calculations and in estimating the modular ratio used for flexural analysis. Previous research showed a strong relationship between modulus of elasticity and concrete compressive strength. Most of the available expressions for modulus of elasticity are based on tests of concrete with strengths of 40 MPa or less. The following is a summary of some of these relationships recommended by current building codes and researchers:

ACI-318 (1989):

$$E_c = 4730\sqrt{f_c'} \tag{3.1}$$

CSA A23.3 (1984):

$$E_c = 5000\sqrt{f_c'} \tag{3.2}$$

Norwegian Standard NS 3473 (1989) for $f'_c < 85$ MPa:

$$E_c = 9500(f_c')^{0.3} \tag{3.3}$$

CEB / FIP Model Code 90 (1988), $f'_c \leq 80$ MPa :

$$E_c = 21500\ \sqrt[3]{f_{cm}/10}\ \alpha_\beta \tag{3.4}$$

where; f_{cm} is compressive strength in MPa of 150 x 300 mm cylinders, and α_β=0.9 for limestone aggregate.

Carrasquillo et al. (1981) for (21 MPa ≤ f'$_c$ ≤ and 83 MPa):

$$E_c = 3320\sqrt{f_c'} + 6900 \tag{3.5}$$

Radain et al. (1993) for (40 MPa ≤ f'$_c$ ≤ 90 MPa):

$$E_c = 2173\sqrt{f_c'} + 1456 \tag{3.6}$$

Tomosawa et al. (1993) for (20 ≤ f'$_c$ ≤ 160 MPa):

$$E_c = 33500\ k_1 k_2 (\gamma / 2.4)^2\ (\sigma_B / 60)^{1/3} \tag{3.7}$$

where; k_1 is a correction factor for aggregate. $k_1 = 0.968$ for concretes with crushed limestone and silica fume < 10%.

k_2 is a correction factor for mineral additions. $k_2 = 0.950$ for concretes with silica fume, slag, and fly ash.

σ_B is concrete compressive strength (MPa).

γ is concrete unit weight (kN/m^3).

The expressions given above are compared with values obtained from cylinder tests conducted in this investigation. The comparisons presented in Table 3.3 indicate that while both ACI-318 and CSA A23.3 expressions overestimate the modulus of elasticity of high-strength concrete, the expression proposed by Radain et al. (1993) underestimates it significantly. Equations suggested by NS 3473 (1989) code, CEB/FIP Model Code 90, and Tomosawa et al. (1993) provide reasonably good estimates of experimental data. Carrasquillo et al. (1981) equation provides the best correlation with test data. It was reported (Russell 1990) that the ACI-318 equation overestimated test results for concretes made with small size aggregates and underestimated those for large-size aggregate concretes. Therefore, it was recommended to report the modulus of elasticity as part of concrete mix design. In addition, it was reported that the applicability of the modulus of elasticity obtained from a 152 x 305 mm cylinder to large size structural members was questionable. Test results indicated that concrete in large size members might have a lower modulus of elasticity.

3.4 Tension Strength

The tensile capacity of concrete is usually ignored in calculating flexural capacity of members (ACI 318-1989, CSA A23.3-1984). However, it is one of the important properties of concrete, since bond and development of reinforcement, shear and torsion resistance of concrete, as well as deflection of members are usually related to tensile strength of concrete.

The tensile strength of concrete is usually expressed in terms of its compressive strength. The ratio of tensile to compressive strength becomes smaller for high-strength concrete (Tomosawa et al. 1990, Favre et al. 1990). The following methods are used to determine the tensile strength of concrete:

- **Direct method**, in which the specimen is subjected to uniaxial tensile stress.
- **Indirect methods**, which can be performed in two ways;
  - **Flexural tension test**. In this test a plain concrete beam is subjected to concentrated loads and fails in flexure. Modulus of rupture is calculated assuming elastic material properties.
  - **Split cylinder test**. In this test a cylinder is placed horizontally in the testing machine, and loaded in compression along two opposite sides. The cylinder splits in tension along the loading plane.

The tensile strength of concrete was evaluated in this research program using split cylinder tests. The tests were conducted according to ASTM C 496, using 150 x 300 mm standard cylinders. The test results, presented in Table 3.4 , represent the average of at least three tests for each concrete mix. Table 3.4 also includes the splitting tensile strength computed by previously proposed analytical expressions. The expressions used are presented below.

ACI-363 (1984) for (21 MPa ≤ f'$_c$ ≤ 83 MPa):

$$f'_{sp} = 0.59 \sqrt{f_c'} \tag{3.8}$$

FIP / CEB State of the Art Report (1990) for f'$_c$ < 75 MPa:

$$f'_{sp} = 0.54 \sqrt{f_c'} \tag{3.9}$$

Nilson (1985):

$$f_{sp} = 0.68 \sqrt{f_c'} \tag{3.10}$$

Wafa and Ashour (1992):

$$f_{sp} = 0.58 \sqrt{f_c'} \tag{3.11}$$

Bakhsh et al. (1990), Tachibana et al. (1990), and Radain et al. (1993):

$$f_{sp} = 0.62 \sqrt{f_c'} \tag{3.12}$$

Gerd (1992) for f'$_c$ < 80 MPa:

$$f_{sp} = 0.40 f_c^{0.58} \tag{3.13}$$

Imam et al. (1993) for (70 MPa ≤ f'$_c$ ≤ 115) MPa:

$$f_{sp} = 0.85 f_c^{0.44} \tag{3.14}$$

The comparisons of experimental and analytical values shown in Table 3.4 indicate very good correlations with the expressions proposed by Bakhsh et al. (1990), and Radain et al. (1993). The expression proposed by Nilson (1985) consistently overestimate the results.

The splitting tensile strength of concrete was reported to be influenced by curing conditions (Nilson 1985, Nilson 1987). De Larrard (1993) reported that in his research program the maximum tensile strength was developed at 7 days. The tensile strength decreased thereafter up to 3 years, as the compressive strength continued increasing. This behaviour was attributed to the formation of shrinkage cracks that weakened the concrete in tension. In the research project reported in this thesis, however, both tensile and compressive strengths were observed to increase up to 1 years.

3.5 Stress-Strain Relationship

The stress-strain relationships of high-strength concrete, obtained by testing standard cylinders, are shown in Figure 4.12. Each relationship was obtained by testing at least three concrete cylinders. The cylinders were tested using a Forney testing machine that had a capacity of 2200 kN. The machine had no deformation control feature which made it impossible to obtain the complete descending branches of stress-strain relationships. The main features of these relationships are summarized below, relative to those of normal-strength concrete.

- High slope of the ascending branch due to the increased modulus of elasticity.
- Higher strain corresponding to peak stress.
- Steeper descending branch beyond the peak, as observed by failure mode.

The same features were reported by other researchers (Li 1994, FIP/CEB state-of-the-art report 1990).

3.6 Summary and Conclusions

The following conclusions can be drawn from the study reported in this chapter:

- It is necessary to use low water/cement ratio, water reducing agent (superplasticizer), and silica fume to produce high-strength concrete. In addition, high quality control is essential.
- Compressive strength of high-strength concrete is influenced by mix design, age, and cylinder type.
- Addition of silica fume is essential to produce very high strength concrete (higher than 100 MPa). Silica fume also improves workability.
- Small size crushed stone, used as coarse aggregate, is more effective than large size round stone in producing high strength concrete, mainly due to increased bond stress.
- It is important to use good quality cylinder moulds to cast cylinders, and to grind the ends to obtain reliable compressive strength results.
- The expressions given in ACI-318 (1989) and CSA A 23.3 (1984) overestimate the modulus of elasticity for high-strength concrete. The expression suggested by Carrasquillo et al. (1981) agrees well with the experimental data.
- The splitting tensile strength of high-strength concrete is related to the square root of concrete compressive strength. Predictions of splitting tensile strength based on the equations proposed by Bakhsh et al. (1990), Tachibana et al. (1990), and Radain et al. (1993) agree well with test data on high-strength concrete.
- The stress-strain relationship of plain high-strength concrete shows higher strain at peak stress and steeper ascending and descending branches as compared to those of normal-strength concrete.

Table 3.1 Mix designs for trial mixes and column tests.

Mix #	1	2	3	4	5	6	7	8	9	10	11	12	13	14	15
Cement (kg)	485	420	420	373	485	420	420	420	485	485	420	500	500	362	336
Slag (kg)	N/A	N/A	N/A	164	N/A	N/A	N/A	N/A	N/A	N/A	N/A	N/A	N/A	156	144
Silica Fume (L)	N/A	N/A	N/A	75	N/A	N/A	N/A	N/A	N/A	N/A	N/A	N/A	N/A	75	N/A
Total Water (kg)	156	171	151	118	144	160	139	160	148	153	160	170	158	109	163
Sand (kg)	762	762	762	740	762	762	762	762	762	762	762	750	750	726	613
Coarse Aggregate (kg)	1143	1143	1143	1120	1143	1143	1143	1143	1143	1143	1143	1140	1150	1122	1130
Superplasticizer (L)	3.4	2.9	3.1	10.0	6.3	6.3	6.3	4.2	11.2	18.6	4.2	20.0	10.0	6.0	5.0
Retarding Admixture (L)	0.95	N/A	N/A	1.60	0.95	N/A	N/A	N/A	0.95	0.95	N/A	1.10	0.90	1.60	1.50
Water/Cementitious Ratio	0.322	0.407	0.360	0.200	0.297	0.381	0.331	0.381	0.305	0.315	0.381	0.340	0.316	0.191	0.340
Slump (mm)	70	90	80	65	25	120	40	50	55	125	50	195	100	50	85

Notes:

1. Coarse aggregate: 10 mm crushed limestone.
2. Superplasticizer : Conchem S.P.N. (Water reducing plasticizer). Each liter of superplasticizer contained 0.708 kg water and 0.490 kg solids.
3. Retarding Admixture: Conchem Protard (Water reducing set retarding admixture). Each liter contained 0.790 kg water and 0.410 kg solids.
4. Silica Fume: Grace Force 10000 (in liquid form). Each liter contained 0.5 kg of water and 0.697 kg of silica.
5. Mixes 1, 2, and 3 contained silica fume cement SF type 10. All other mixes contained Ordinary Portland Cement Type 10.
6. Total water includes added water, moisture content of sand and aggregate, and water contents of superplaster and retarding admix.
7. Mixes 4, 11, 13, 14, and 15 contained coarse aggregate which was obtained from a quarry in Ottawa, Ont. All other mixes contained aggregate from Hull, Quebec.

Table 3.2: Development of concrete compressive strength with time.

Age (Days)		1	7	28	56	91	182
Mix #	**Curing**						
1	M	N/A	58	74	75	75	82
1	D	N/A	59	73	77	78	79
2	M	N/A	45	59	63	62	63
2	D	N/A	45	58	61	59	60
3	D	N/A	49	64	64	65	66
4	D	49	79	107	112	115	121
5	D	N/A	67	69	73	81	86
6	D	N/A	42	51	56	N/A	N/A
7	D	N/A	64	76	80	82	91
8	D	N/A	44	52	59	70	77
9	D	N/A	61	72	80	N/A	N/A
10	D	N/A	61	71	76	N/A	N/A
11	D	N/A	42	51	60	72	80
12	D	N/A	39	53	66	69	72
13	D	N/A	54	65	69	78	85
14	D	52	63	80	102	110	123
15	D	30	41	50	56	58	59

Notes:

'D' indicates that cylinders were kept outside the curing chamber and sprayed water daily.

'M' indicates that cylinders were cured in the moist curing chamber.

Table 3.3: Moduli of elasticity for high-strength concrete.

Concrete Strength (MPa)	60	81	92	124
Experimental	30.8	37.9	40.2	43.7
ACI - 318 (1989)	36.6	42.6	45.0	35.5
CSA A23.3 (1984)	38.7	45.0	47.9	55.7
NS 3473 (1989)	32.4	35.5	36.9	40.3
CEB/FIP (1990)	35.2	38.9	40.5	44.8
Carrasquillo et al. (1981)	32.6	36.8	38.7	43.9
Radain et al. (1993)	18.3	21.0	22.3	25.7
Tomosawa et al. (1993)	30.8	35.8	37.4	39.2

Note: All units for moduli of elasticity are in GPa.

Table 3.4: Splitting tensile strength of high-strength concrete.

Concrete Strength (MPa)	60	81	92	124
Experimental	4.49	5.69	6.09	7.33
ACI - 318 (1989)	4.57	5.31	5.66	6.57
CEB/FIP (1990)	4.18	4.86	5.18	6.01
Nilson (1985)	5.26	6.12	6.52	7.57
Wafa and Ashour (1992)	4.49	5.22	5.56	6.46
Bakhsh et al. (1990)	4.80	5.58	5.90	6.90
Gerd (1992)	4.30	5.11	5.50	6.55
Immam et al. (1993)	5.15	5.88	6.21	7.09

Note: All units are in MPa.

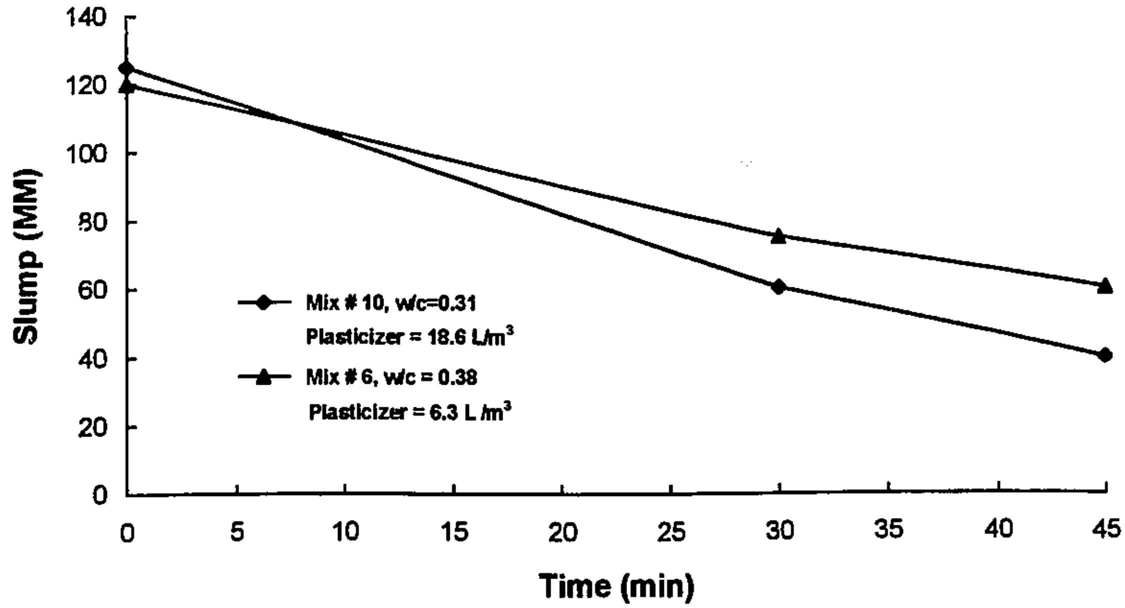

Figure 3.1: Loss of concrete workability with time.

Figure 3.2: Failure mode of concrete cylinders tested using pad-caps.

Chapter 4
Experimental Program

4.1 General

A comprehensive experimental program was conducted to investigate the behaviour of high-strength concrete columns confined with circular and rectilinear reinforcement. The test program included a total of forty six square and circular columns subjected to monotonicaly increasing concentric compression. Test specimens were designed to investigate the influence of main parameters of confinement. The parameters included cross-sectional shape, volumetric ratio and spacing of transverse reinforcement, distribution of longitudinal reinforcement and resulting tie arrangement, yield strength of transverse reinforcement, concrete strength, and type of circular reinforcement. The tests produced invaluable data for development of behavioral models and design guidelines for earthquake resistant high-strength concrete columns. The details of test specimens, material properties, test set-up, instrumentation, test procedure, observed behaviour, and test results are presented in this chapter. Analysis of test data and evaluation of test parameters are presented in Chapter 5.

4.2 Properties of Test Specimens

A total of 26 square and 20 circular columns were prepared for testing. The columns were labelled as either CS or CC, where the first letter "C" identified the type of loading, as being concentric, and the second letter identified the cross-sectional shape, as either "S" for square or "C" for circular.

4.2.1 Square Columns

The square columns had 250 mm square cross-section, and 1500 mm height. They were cast horizontally in four sets. Each set had a different batch of concrete with different strength. Concrete compressive strengths, established by standard cylinder tests, were f'_c = 60 MPa, 81 MPa, 92 MPa, and 124 MPa, for the period in which column tests were performed. Two of the columns were prepared as plain (unconfined) concrete specimens to establish the in-place strength of concrete in columns, as opposed to strength determined by standard cylinder tests. These were CS-10, and CS-21, with 124 MPa and 81 MPa concretes, respectively. The remainder twenty four columns were confined with three different reinforcement configurations. Configurations 2, 3, and 4 contained 4, 8, and 12 longitudinal bars, respectively, all laterally supported by transverse reinforcement. Column geometry and tie configurations are shown in Figures 4.1 and 4.2. All longitudinal bars were 16 mm in diameter (No.15), and had yield strength of 450 MPa. The percentage of longitudinal reinforcement was 1.28 %, 2.56 %, and 3.84 %, for 4-bar, 8-bar, and 12-bar configurations, respectively. The lateral confinement reinforcement had volumetric ratios (ρ_s) that varied between 1.0 % and 4.6 %. The spacings of transverse reinforcement were 40 mm, 55 mm, 85 mm, and 120 mm. Grades 400, 570, and 1000 MPa steel were used as transverse reinforcement. All the ties had 135-degree hooks at the ends, with at least 10-bar diameter extensions in to the core concrete. A clear concrete cover of 10 mm was provided in all reinforced specimens. The core size, measured from outside-to-outside of the perimeter tie was kept constant at 230 x 230 mm. The properties of square columns are summarized in Table 4.1. The reinforcement cages for square columns are illustrated in Figure 4.3.

The square columns were cast horizontally using a formwork made with 6.35 mm-thick plywood. The forms were stiffened by wooden brackets. Threaded rods were used to tie the opposite faces of formwork to prevent bulging during casting. Figure 4.4 illustrates preparation of square columns for casting. A large number of standard cylinders were cast from each batch to establish the stress-strain characteristics of concrete. The formwork was removed approximately 24 hours after casting. The specimens were covered with wet burlap and plastic sheets. Curing of specimens continued until the required strength level was attained. Figure 4.5 illustrates the columns during curing. All specimens were confined at the ends externally by steel brackets, and internally by closely spaced transverse reinforcement, to avoid premature failure at the loading ends, outside the test region. Figure 4.6 depicts the end brackets placed prior to testing.

4.2.2 Circular Columns

The circular columns had a 250 mm cross-sectional diameter and 1500 mm column height, as illustrated in Figure 4.1. They were cast using three different batches of concrete with three different strengths. Concrete compressive strengths, determined by standard cylinder tests were $f'_c = 60$ MPa, 92 MPa, and 124 MPa, for the period in which column tests were performed. All the columns were confined with circular spiral transverse reinforcement, with the exception of column CC-4 which was confined with circular hoops. Columns CC-5, CC-6, CC-17, and CC-18 were confined by circular spirals without any longitudinal reinforcement. The remainder 16 columns had 8-16 mm diameter (No.15) longitudinal bars, with yield strength of 450 MPa. The percentage of longitudinal reinforcement for these columns was 3.26%. The volumetric ratio (ρ_s) of confinement steel varied between 0.4% and 3.0%. The spacings of circular reinforcement were 60 mm, 70 mm, 100 mm, and 135 mm. Grades 400, 660, and 1000 MPa steel were used as transverse reinforcement. A clear concrete cover of 10 mm was provided in all columns. The diameter of the core, measured from outside-to-outside of the spirals or hoops, was kept constant at 230 mm. Figure 4.7 illustrates the reinforcement cages used for circular columns.

The circular columns were cast vertically using sona tubes. Figure 4.8 illustrates the sona tubes and preparation of columns for casting. The specimens were covered with plastic sheets after casting. The formwork was removed after approximately one day. The columns were covered with wet burlap and plastic sheets for curing. The curing of specimens continued until the required strength was attained. Figure 4.9 illustrates the columns during curing. All specimens were confined at the ends, externally by steel brackets, and internally by closely spaced transverse reinforcement, to avoid premature failure near the loading ends, outside the test region. Figure 4.10 shows the end brackets for circular columns. A summary of column properties is provided in Table 4.2.

4.3 Casting of Columns

A total of four batches of concrete were prepared for all columns. An arrangement was made with a local ready mix concrete company to supply the desired quantities of fine and coarse aggregates, and silica fume with a ready mix concrete truck. The moisture content of the sand and aggregate was reported by the ready-mix company to account for the extra water present. The moisture in the drum was also estimated prior to adding water. For Batch No.1, the desired quantities of water, cement, retarder, and superplasticizer were added in the structures laboratory, as shown in Figure 4.11(a). The concrete was mixed in the truck for at least five minutes before the first slump test was conducted. Subsequently, the specimens were cast along with a large number of standard cylinders. For Batches No.2, No.3, and No.4, the cementitious materials and 50% of the superplasticizer were added at the ready mix plant, in addition to the aggregates. All concrete batches had enough superplasticizer to maintain workability of concrete. A team of people were available to perform casting before the hardening of concrete.

Concrete was cast in layers and vibrated very well. Casting each set of columns took between 1.5 to 2.0 hours. Figure 4.11 (b) illustrates casting of square columns in the laboratory.

4.4 Material Properties

4.4.1 Concrete

Four different mix designs were used for four batches of concrete. Strength and workability were the main criteria in mix designs. Low water-cement ratio (w/c) and high cement content were used to achieve the strength level required. It was necessary to use superplasticizer to achieve workability. Normal Portland Cement and local aggregates were used in all batches. The course aggregate used was 10 mm crushed limestone. The silica fume used in some batches was in liquid form. The concrete compressive strengths attained were 60, 81, 92, and 124 MPa. Table 4.3 provides the material quantities used in each of the four batches. A Large number of standard cylinders were cast to determine the properties of unconfined concrete. Cylinder tests were performed at predetermined time intervals to monitor strength gain with time. The cylinders were either ground at the ends prior to testing, or capped with Pad-Caps to ensure the uniform application of load. Table 4.4 illustrates the development of strength in each batch of concrete with time.

The stress-strain relationship for each batch of concrete, as recorded by standard cylinder tests, are shown in Fig. 4.12. These relationships represent the average of at least three cylinders per batch. The cylinder tests were conducted using a Forney testing machine with 2200 kN capacity. The machine had no deformation control feature. Therefore, it was not possible to obtain the descending branches of the curves.

4.4.2 Steel

All the longitudinal reinforcement used were 16 mm diameter (#15) deformed bars. The yield strength was 450 MPa. Five different grades and sizes of reinforcing steel were used as lateral reinforcement. The lateral steel used for square columns consisted of 11.3 mm diameter (#10) deformed bars, two different grades of 6.5 mm-diameter plain bars, and 7.5 mm-diameter plain bars, with yield strengths of 400 MPa, 400 MPa, 570 MPa, and 1000 MPa, respectively. The circular columns contained either 11.3 mm diameter (#10) deformed bars, 6.3 mm diameter plain reinforcement or 7.5 mm diameter plain reinforcement, with 400 MPa, 660 MPa, and 1000 MPa yield strengths, respectively. The deformed bars showed clear yield strength and yield plateau. However, this was not the case for plain reinforcement. Therefore, the 0.2% offset method was used to establish yield strengths of plain reinforcement. Stress-strain relationships, established by coupon tests, are shown in Figs. 4.13 and 4.14. The coupon tests were obtained using a Tinious Olsen testing machine with a 1300 kN capacity. Each relationship shown in the figures represents the average of at least three coupon tests.

4.5 Instrumentation

The specimens were instrumented with linear variable differential transducers (LVDT) to measure axial deformations. A total of four LVDT's, with 100 mm stroke and 300 mm gauge length were mounted, one on each column face. The LVDT's were secured on threaded rods that had been cast in column concrete. This enabled continuous data recording, even after the spalling of cover concrete. Figure 4.15 shows the LVDT' on typical square and circular columns.

Electric strain gauges were placed on lateral and longitudinal reinforcement to measure steel strains. Most square columns had eight gauges placed on tie steel, four on the central tie, and two on each of the ties immediately above and below. Figure 4.16 shows the locations of strain gauges on lateral reinforcement in square columns. Square columns with 60 MPa concrete had eight strain gauges placed on longitudinal reinforcement, in addition to the eight placed on the tie steel. Each corner bar had two gauges placed, one above and the other below the cental tie. Most circular columns had six strain gauges placed on spiral steel. Two strain gauges were provided at mid-height, and two other pairs immediately above and below. Figure 4.17 shows the arrangement of strain gages in circular columns.

A pressure transducer was used to measure the applied load. The LVDT readings, steel strains, and applied load were recorded using a Sciemetric System 200 Data Acquisition System and a micro computer as illustrated in Figures 4.18 and 4.19.

4.6 Test Set-up and Test Procedure

The specimens were tested under monotically increasing concentric compression. A 10,000 kN capacity testing machine, located at the Fire Research Laboratory of the National Research Council of Canada (NRC) was used, because of the high concentric capacity of columns resulting from large cross-sectional size and high strength of concrete. The columns were prepared in the Structures Laboratory of the University of Ottawa before being shipped to NRC Laboratory, also located in Ottawa. The testing machine is illustrated in Figure 4.19. The machine head was set up for columns of approximately 4.0 m height. The specimens, on the other hand were 1.5 m high to avoid slenderness effects. Therefore, a high-strength concrete spacer block was used to reduce the machine head room to an appropriate level. Figure 4.20 shows the reinforcement cage and casting of the spacer block. Figure 4.21 illustrates the inside view of the testing machine, depicting the spacer block. An end plate, matching with the head of the testing machine, was secured to the end of each specimen by means of threaded rods that had been cast in column concrete, prior to testing. Upon fixing the steel brackets at the ends of a column, it was pulled into the machine by a self contained crane, and fixed at the top of the machine. Figure 4.22 shows various stages of installation of test specimens into the machine for testing. Four LVDTs were mounted on four sides of the column, at column mid-height. The LVDTs and strain gauges were connected to the data acquisition system.

The load was applied by compressing the column between the top of the machine and the spacer block. The initial load was applied slowly, and the deflections on four sides of the column were monitored. If the deflections were not approximately the same, this was an indication of the load not being concentric. The column was then unloaded and the ends were shimmed to minimize the accidental end eccentricity. This procedure continued until all four LVDT's indicated approximately the same reading, signifying that the initial load was concentric.

The load was applied continuously at a slow rate until the first sign of cover spalling was observed. The rate of loading was further reduced after the development of initial cracking in cover concrete. In some columns, the load was cycled a few times near the peak load to record sufficient data points prior to failure. The tests were stopped when the load dropped significantly.

4.7 Observed Behaviour and Recorded Data

The experimental observations made during column tests are presented and discussed in this section, along with the raw data recorded. The data presented include axial force-axial strain relationships as recorded by LVDT's, and steel strains as recorded by strain gauges. The recorded data is then processed to obtain the behaviour of confined core concrete and the effects of test parameters. The latter is presented and discussed in Chapter 5.

Figures 4.23 to 4.48 illustrate axial load-axial strain relationships recorded during tests of square columns. Observed behaviour of these columns are also shown in the same figures. Two plain concrete specimens, with a square cross-section, were tested to investigate the behaviour of unconfined concrete. These were columns CS-10 and CS-21.

Neither longitudinal nor transverse reinforcement was placed in these columns. Both specimens were observed to behave in a similar manner. The ascending branch of the recorded load-strain relationship was almost linear. Column CS-10, with 124 MPa concrete, showed steeper ascending branch (i.e. higher modulus of elasticity) than CS-21 with 81 MPa concrete. When the peak load was reached both columns failed in a sudden, brittle, and explosive manner. The strain corresponding to the peak load was 0.0025 and 0.0022, for CS-10 and CS-21, respectively. The recorded peak strength was equal to 89% and 92% of concrete strengths determined by standard cylinder tests (f_c') for CS-10 and CS-21, respectively.

The remainder of the square specimens were reinforced with different reinforcement arrangements. In general these specimens showed similar behaviour as the previous two, prior to the peak load. The specimens were continuously monitored during testing for development of surface cracks. It was observed that the surface cracks developed at an early stage of loading at approximately 0.0015 and 0.002 strains for 124 MPa and 60 MPa concrete columns, respectively. These cracks eventually resulted in spalling of cover concrete. Large pieces of cover concrete were observed to separate from the core and spall off, suggesting that the spalling was due to instability rather than crushing of the shell concrete. The spalling often resulted in some drop in load resistance.

The formation of cracks was not uniform on all sides. Usually the cracks were observed on one side of the column, before resulting in spalling. The column was then subjected to eccentric loading due to the uneven spalling of cover. The cracks soon propagated to other sides, causing complete spalling of the cover. The loading became approximately concentric after complete spalling of the cover, in the test region. At this load stage, the applied load was resisted by core concrete and longitudinal reinforcement. Therefore, the post peak behaviour varied depending on the confinement characteristics of the core concrete. It was also observed that the concrete strength was an important parameter that influenced column behaviour.

Square columns with 124 MPa suffered early spalling of concrete cover due to the instability of cover under high compressive stresses. Columns with less than 2% volumetric ratio of lateral steel (i.e. CS-5, CS-6, and CS-7) failed in a brittle and explosive manner. A sudden loss of strength was observed in these columns immediately after the peak load. The failure was associated with hoop fracture, buckling of longitudinal reinforcement, and crushing of core concrete. Column CS-1 failed in a similar manner, although it was confined by 3.33 % volumetric ratio of lateral steel. This may be attributed to poor confinement characteristics of the 4-bar arrangement used in this column. Columns with more than 3 % volumetric ratio of lateral steel, and better arrangement of reinforcement showed relatively more stable behaviour, with a gradual strength decay beyond the peak. Columns CS-8 and CS-9 fall under this category. Among the columns with 2.2% lateral steel, column CS-4 with 1000 MPa lateral steel was the most ductile column. This indicates that the grade of transverse steel played a significant role on column confinement.

Almost all the square columns with 81 MPa or 92 MPa concretes (with the exception of CS-17 and CS-18) behaved in a fairly ductile manner, showing a well developed yield plateau, until the fracture of one or more ties occurred. Once the first tie fractured, one or more longitudinal bars buckled causing the load to drop at a fast rate. Columns CS-17 and CS-18 had less than 1.5% lateral steel. They behaved in a brittle and explosive manner. A sudden drop was observed in the load resistance immediately after the peak load. The drop in load was attributed to the spalling of cover concrete. The load continued to drop at a fast rate due to buckling of longitudinal reinforcement and lack of sufficient transverse reinforcement.

Square columns with 60 MPa concrete can be viewed in two groups. Columns CS-24, CS-25, and CS-26, with more than 2% volumetric ratio of lateral steel, formed the first group and behaved in a fairly ductile manner. These columns showed high deformability, with little degradation of strength. On the other hand, columns CS-22, and CS-23, with less than 1.5% volumetric ratio of lateral steel, behaved in a less ductile manner. Strength of these columns dropped at a fast rate beyond the peak. Severe buckling of longitudinal reinforcement was observed at the end of the tests.

Figures 4.49 to 4.68 illustrate the axial load-axial strain relationships recorded during tests of circular columns. Observed behaviour of these columns are also shown in the same figures. The behaviour of circular columns showed essentially the same trend as those observed in square columns. It was clear that the concrete strength was a major contributor to column behaviour. Columns with 60 MPa and 92 MPa concrete showed superior performance when compared with those with 124 MPa. Significantly high volumetric ratio and/or yield strength of lateral steel was required in high strength concrete columns to achieve the same level of deformability exhibited by 60 MPa concrete columns.

Circular columns with 124 MPa and less than 1.5% volumetric ratio of lateral steel (i.e. CC-8, CC-9, and CC-11) failed in an extremely brittle and explosive manner. A sudden loss of strength was observed in these columns immediately after the peak load. The failure was associated with hoop fracture, buckling of longitudinal reinforcement, and crushing of core concrete. However, column CC-12 with 1.32% volumetric ratio of high strength lateral steel behaved in a ductile manner. The column showed high deformability, with very little drop in the load carrying capacity prior to the first hoop fracture. This indicates that high strength lateral steel was effective in confining the core concrete. Once the first hoop fractured, one or more longitudinal bars buckled causing a sudden drop in the load carrying capacity. Column CC-10 with high volumetric ratio of lateral steel (3.05%), exhibited ductile behaviour and showed relatively stable behaviour, and a well developed yield plateau.

Circular columns with 92 MPa and less than 2% volumetric ratio of normal strength lateral steel (i.e. CC-19, CC-20, CC-21, and CC-22) failed in an extremely brittle and explosive manner. However, the behaviour was improved when high strength lateral steel was used. Columns CC-14 and CC-16 with 1000 MPa lateral steel showed a more stable and ductile behaviour compared to those with normal strength lateral steel. Column CC-15 also behaved in a fairly ductile manner due to the high volumetric ratio of lateral steel provided (3.05%).

All of the circular columns made with 60 MPa concrete had low volumetric ratio of lateral steel (i.e. less than 1.5%). Therefore, none of the columns behaved in a ductile manner. Columns CC-5 and CC-6, with low volumetric ratio of transverse reinforcement, and without any longitudinal reinforcement, behaved similar to the plain concrete columns. These columns failed suddenly after the peak load. Therefore, it was not possible to record any data for the descending branches of the load-deformation relationships of these columns.

Square columns CS-22 to CS-26 had strain gages placed on longitudinal reinforcement. Each column had a total of eight strain gages located on corner bars. Figures 4.69 and 4.72 present typical axial load-average axial steel strain relationships. The figures also include axial load-average axial concrete strain relationships. The results indicate very good agreement between axial concrete and steel strains prior to the yielding of longitudinal steel. This indicates that there was no bond slip between steel and concrete.

Buckling of longitudinal steel was not observed in columns with closely spaced lateral steel until after the fracture of transverse reinforcement. In columns with widely spaced lateral steel, however, longitudinal bars buckled between the ties, prior to fracture. The axial load level at buckling varied depending on size and spacing of lateral reinforcement.

Strains in transverse reinforcement were measured using electric strain gages. Eight and six strain gages per column were provided for square and circular columns respectively. It was observed that transverse reinforcement, in square and circular columns, yielded at or shortly after the peak load was reached. This observation was made regardless the yield strength of transverse steel. Figures 4.73 and 4.88 present typical axial load - lateral steel strain relationships.

Table 4.1: Properties of square columns.

Column Number	Reinforcement Arrangement	f'_c (MPa)	b_c (mm)	b_d (mm)	s (mm)	ρ_s (%)	f_{yt} (MPa)
CS-1	2	124	218.7	11.3	55	3.33	400
CS-2	3	124	223.5	6.5	55	2.16	570
CS-3	4	124	223.5	6.5	55	2.16	570
CS-4	3	124	222.5	7.5	55	2.17	1000
CS-5	4	124	222.5	7.5	120	1.32	1000
CS-6	3	124	223.5	6.5	85	1.05	400
CS-7	4	124	223.5	6.5	120	0.99	400
CS-8	3	124	218.7	11.3	85	3.24	400
CS-9	4	124	218.7	11.3	120	3.06	400
CS-10	1	124	Plain	concrete			
CS-11	2	81	218.7	11.3	40	4.59	400
CS-12	2	81	218.7	11.3	55	3.33	400
CS-13	3	92	223.5	6.5	55	2.16	570
CS-14	4	92	223.5	6.5	55	2.16	570
CS-15	3	81	222.5	7.5	55	2.17	1000
CS-16	4	81	222.5	7.5	85	1.87	1000
CS-17	3	81	223.5	6.5	85	1.05	400
CS-18	4	81	223.5	6.5	85	1.40	400
CS-19	3	92	218.7	11.3	85	3.24	400
CS-20	4	92	218.7	11.3	85	4.32	400
CS-21	1	81	Plain	concrete			
CS-22	3	60	222.5	7.5	85	1.40	1000
CS-23	4	60	222.5	7.5	120	1.32	1000
CS-24	3	60	218.7	11.3	85	3.24	400
CS-25	4	60	218.7	11.3	120	3.06	400
CS-26	4	60	223.5	6.5	55	2.16	570

Notes: 1. Columns CS-2 and CS-13 had double layers of cross ties.
2. Reinforcement arrangements are shown in Figure 4.2.

Table 4.2: Properties of circular columns.

Column Number	Reinforcement Arrangement	f'_c (MPa)	b_c (mm)	b_d (mm)	s (mm)	ρ_s (%)	f_{yt} (MPa)
CC-1	5	60	223.7	6.3	135	0.41	660
CC-2	5	60	218.7	11.3	135	1.35	400
CC-3	5	60	223.7	6.3	70	0.80	660
CC-4	5	60	223.7	6.3	70	0.80	660
CC-5	6	60	223.7	6.3	70	0.80	660
CC-6	6	60	223.7	6.3	135	0.41	660
CC-8	5	124	223.7	6.3	70	0.80	660
CC-9	5	124	218.7	11.3	135	1.35	400
CC-10	5	124	218.7	11.3	60	3.05	400
CC-11	5	124	223.7	6.3	60	0.93	660
CC-12	5	124	222.5	7.5	60	1.32	1000
CC-14	5	92	222.5	7.5	60	1.32	1000
CC-15	5	92	218.7	11.3	60	3.05	400
CC-16	5	92	222.5	7.5	100	0.79	1000
CC-17	6	92	222.5	7.5	60	1.32	1000
CC-18	6	92	222.5	7.5	100	0.79	1000
CC-19	5	92	218.7	11.3	100	1.83	400
CC-20	5	92	223.7	6.3	100	0.56	660
CC-21	5	92	223.7	6.3	70	0.80	660
CC-22	5	92	218.7	11.3	135	1.35	400

Notes: 1. Column CC-4 had circular hoops tied with mechanical connectors.
2. Reinforcement arrangements are shown in Figure 4.2.

Table 4.3: Mix design for high strength concrete columns.

Mix #	1	2	3	4
Concrete Strength, f'_c (MPa)	81	92	124	60
Cement (kg)	500	500	362	336
Slag (kg)	N/A	N/A	156	144
Silica Fume (L)	N/A	N/A	75	N/A
Added Water (kg)	128	123	39	135
Water in Ready Mix Drum (kg)	4.5	4.5	4.5	4.5
Fine Aggregate (kg)	750	750	726	613
Coarse Aggregate (kg)	1140	1150	1122	1130
Superplasticizer (L)	20	10	6	5
Retarding Admixture (L)	1.1	0.9	1.6	1.5
Slump (mm)	195	100	50	85

Notes:
1. Coarse aggregate: 10 mm crushed limestone.
2. The fine aggregate contained approximately 3% by weight water.
3. Superplasticizer : Conchem S.P.N. (Water reducing plasticizer). It contained 0.708 kg of water and 0.490 kg of solids per liter.
4. Retarding Admixture: Conchem Protard (Water reducing set retarding admixture). It contained 0.790 kg of water and 0.410 kg of solids per liter.
5. Silica Fume: Grace Force 10000 (in liquid form). It contained 0.5 kg of water and 0.697 kg of silica per liter.
6. Cement: Ordinary Portland Cement Type 10.
7. The drum contained approximately 4.5 kg of water.

Table 4.4: Developement of concrete strength with time.

	Concrete compressive strength (MPa)			
Age (days) \ Mix #	1	2	3	4
1	N/A	N/A	52	30
2	39	54	63	41
7	53	65	80	50
28	66	69	102	56
91	69	78	110	58
182	72	85	123	59
365	80	91	124	60
730	81	92	124	60

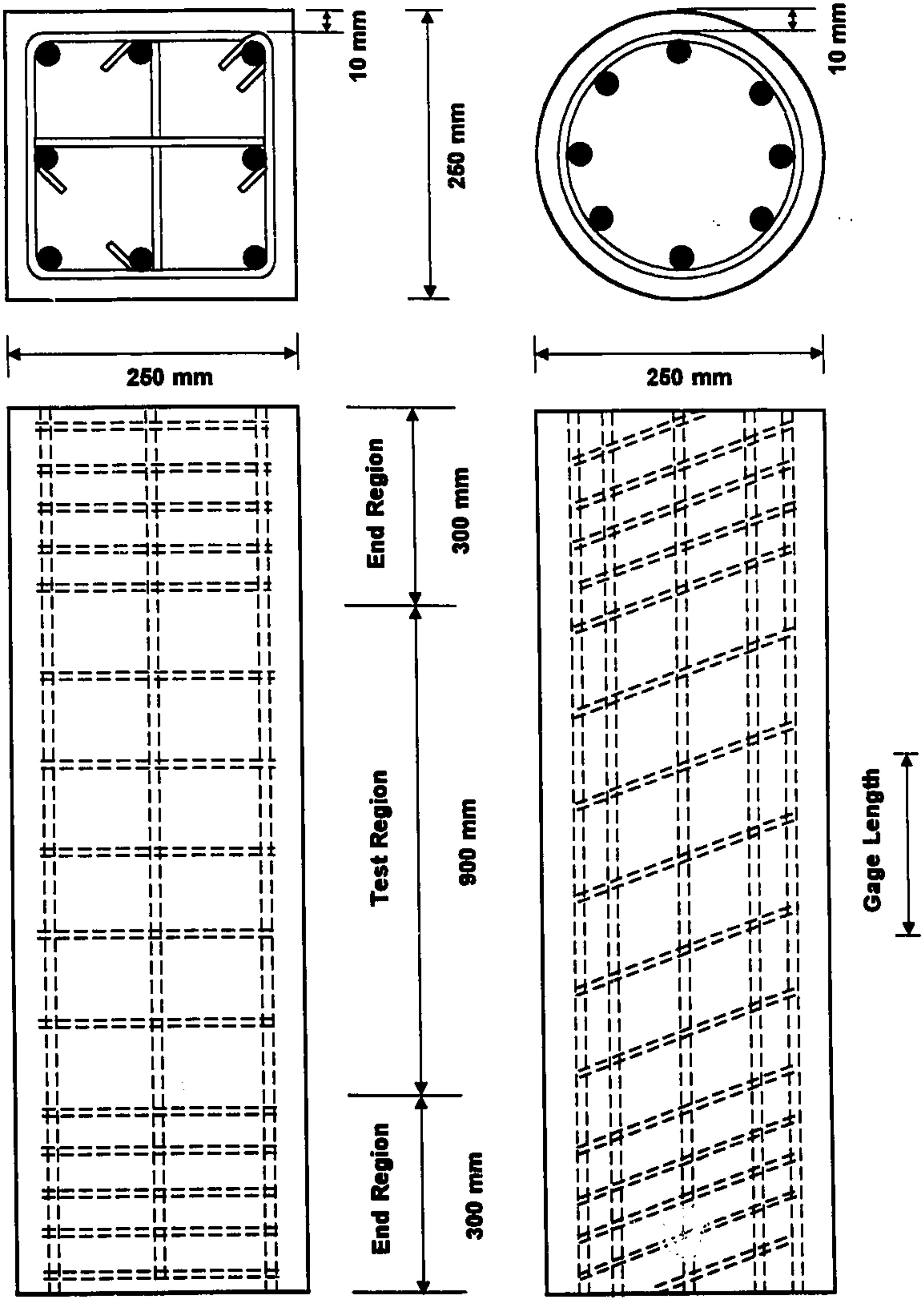

Figure 4.1: Geometry of columns tested

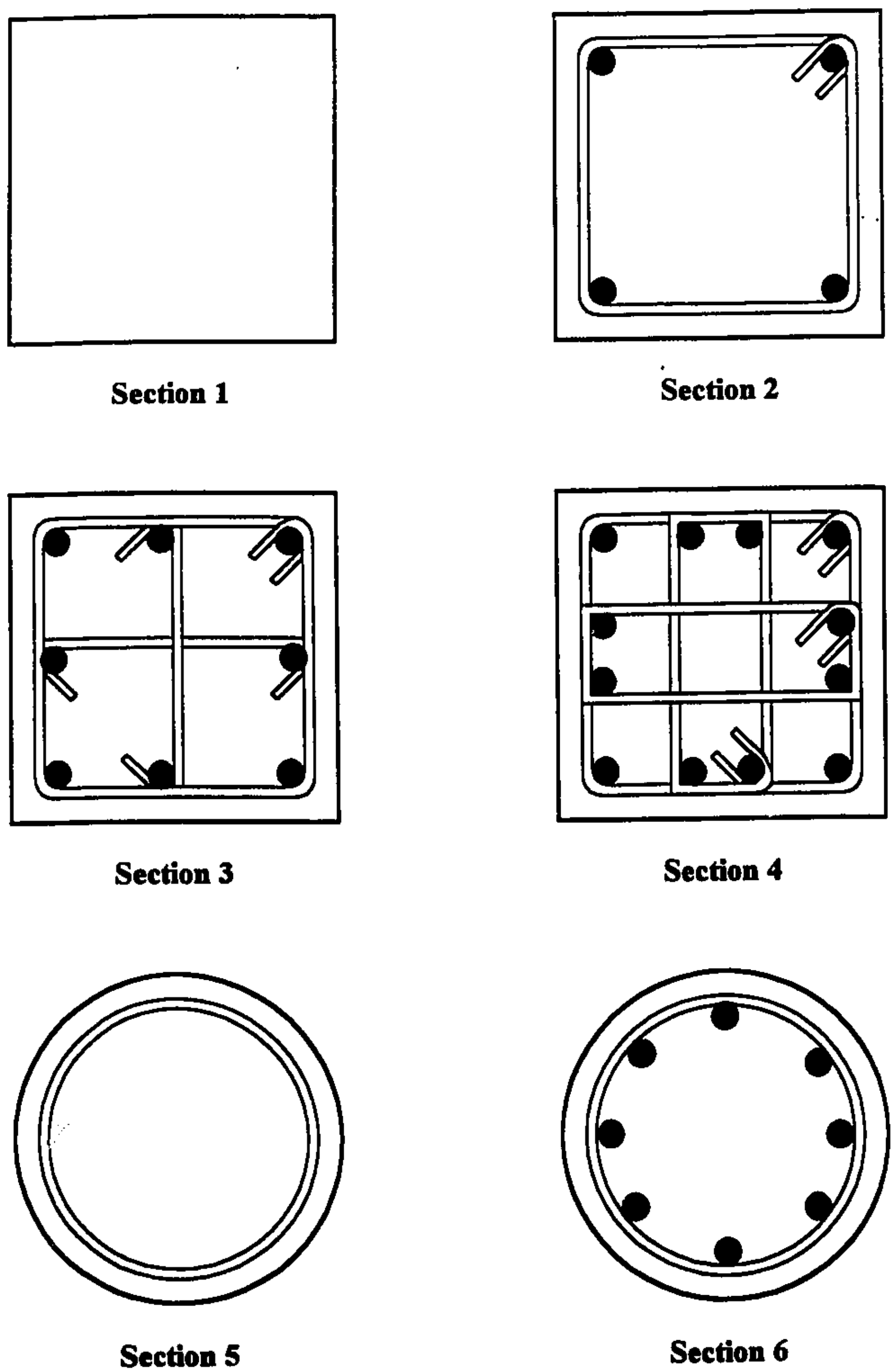

Figure 4.2: Cross-sectional arrangements considered in the experimental progeam.

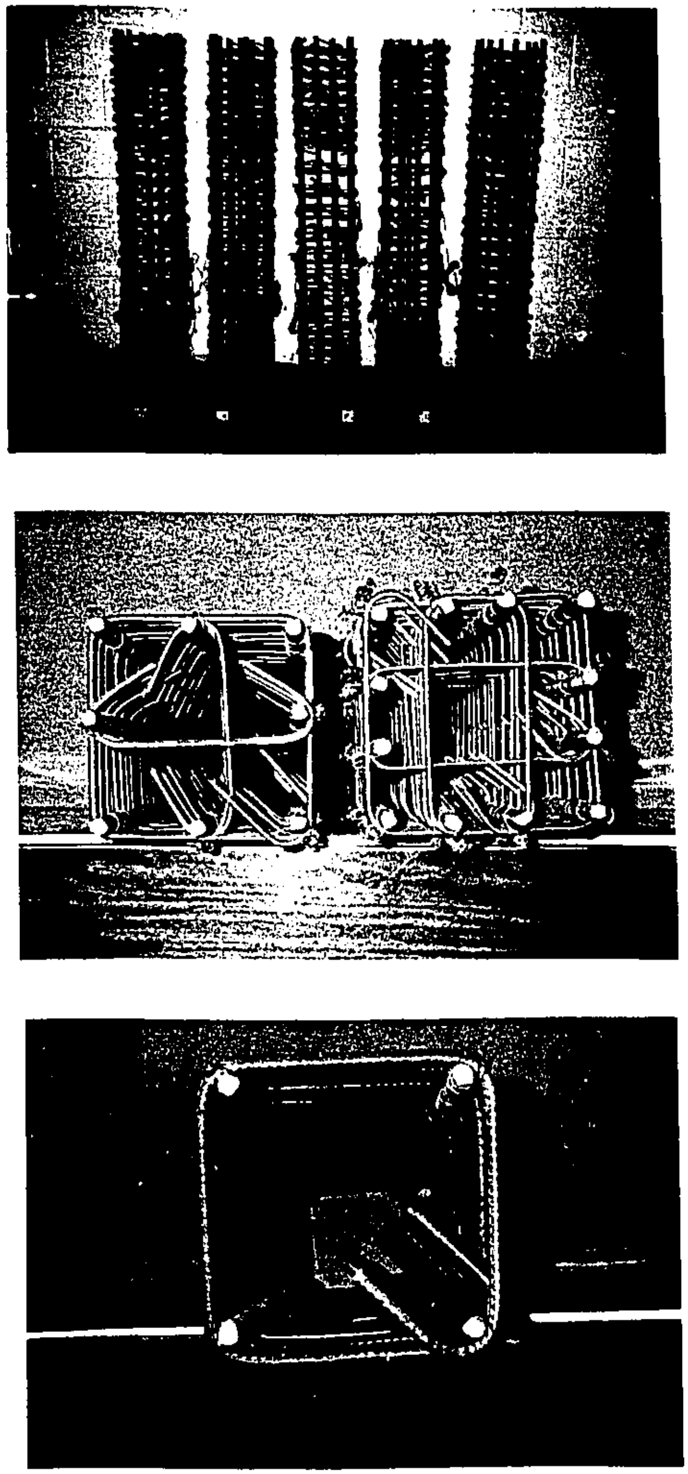

Figure 4.3: Reinforcement cages for square columns.

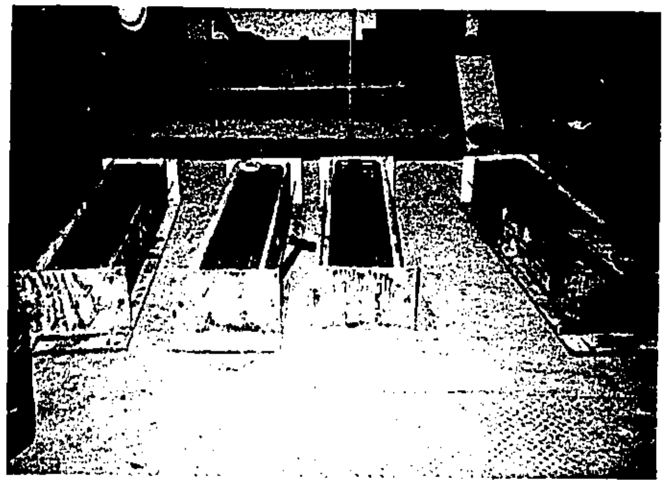

Figure 4.4: Preparation of square columns for casting.

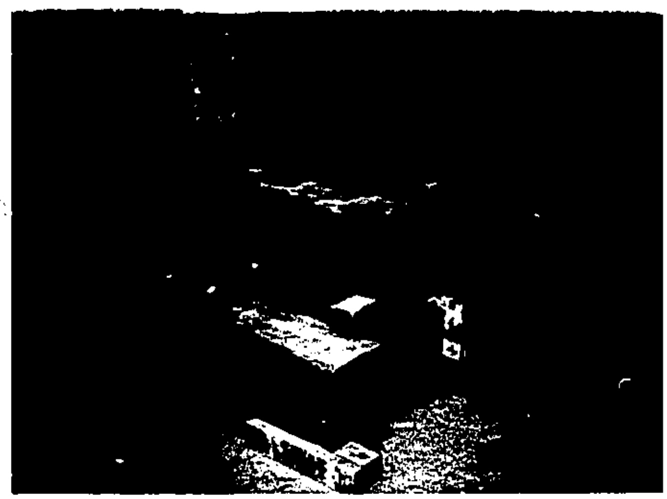

Figure 4.5: Curing of square columns in the laboratory.

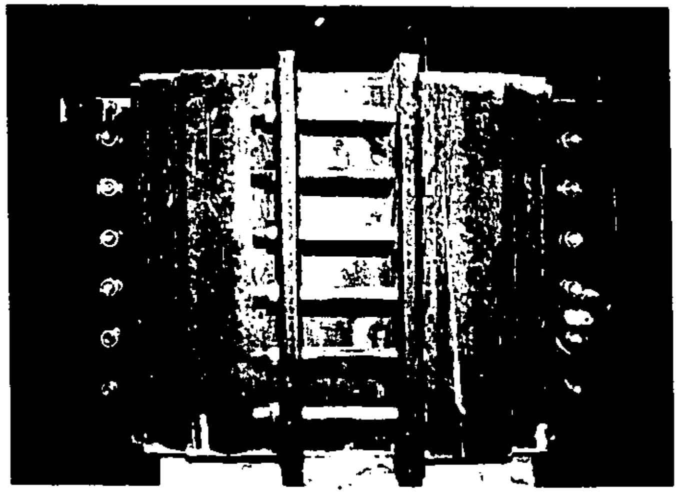

(a) Front view

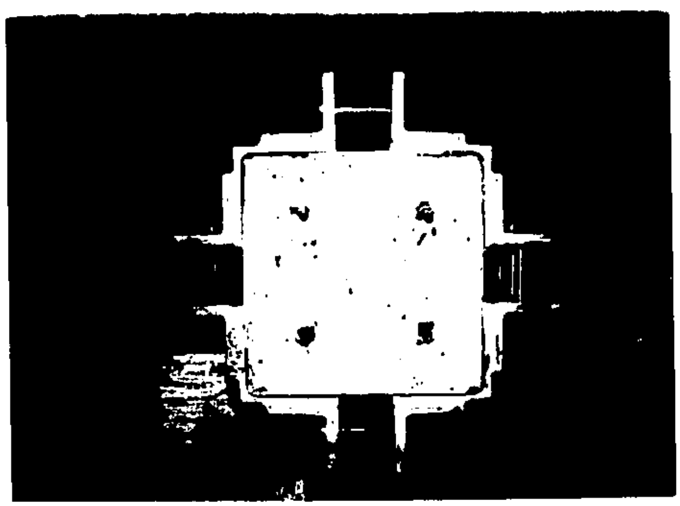

(b) Top view

Figure 4.6: End brackets for square columns.

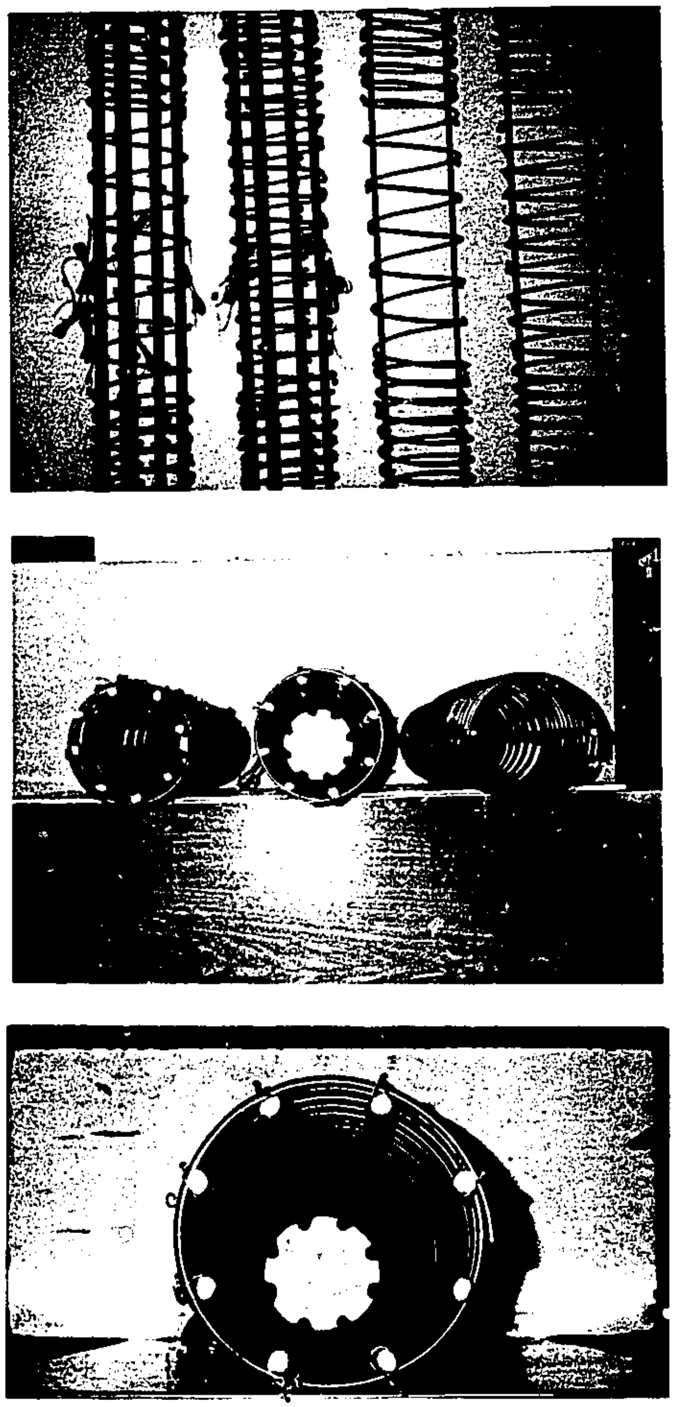

Figure 4.7: Reinforcement cages for circular columns.

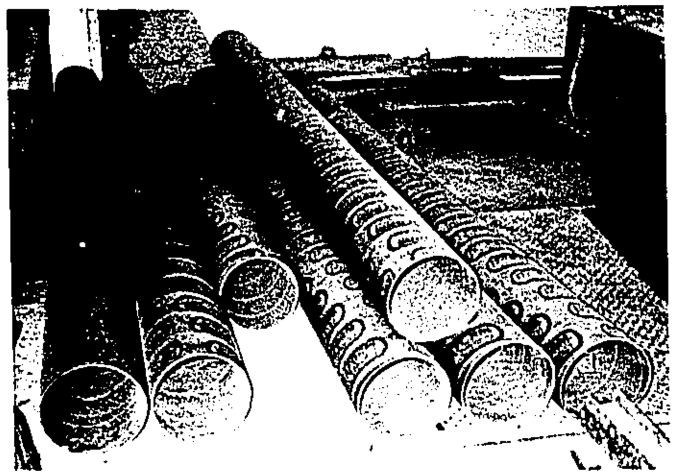

(a) Sona tubes

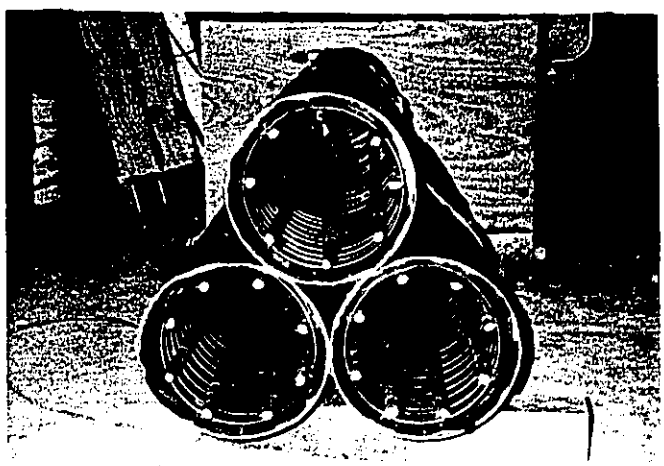

(b) Circular columns prior to casting.

Figure 4.8: Sona tubes and preparation of circular columns for casting.

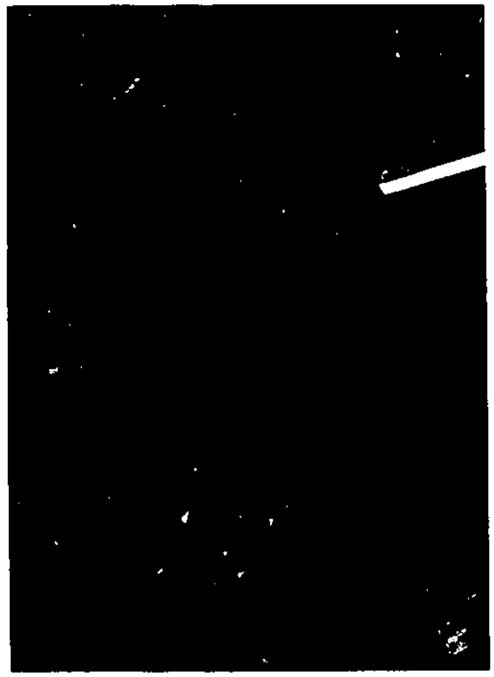

Figure 4.9: Curing of circular columns in the laboratory.

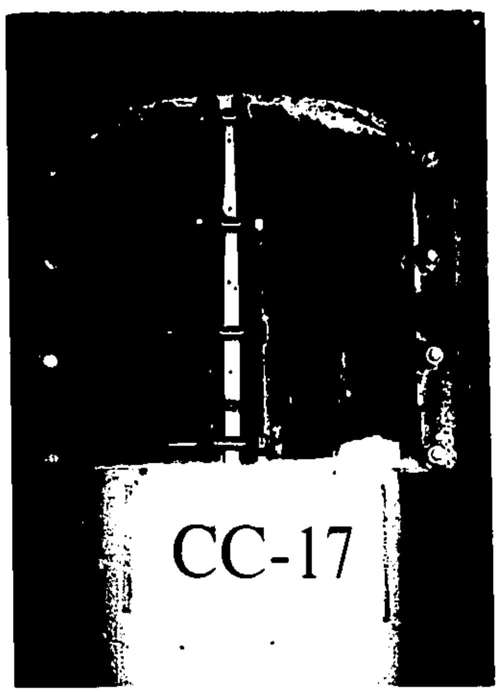

Figure 4.10: End bracket for circular columns.

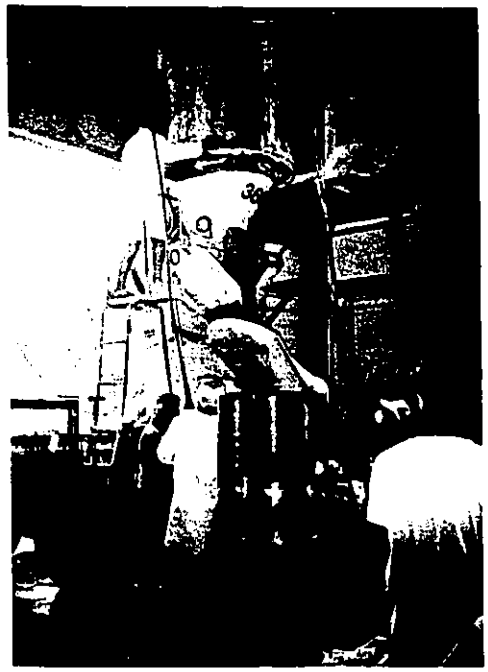

(a)

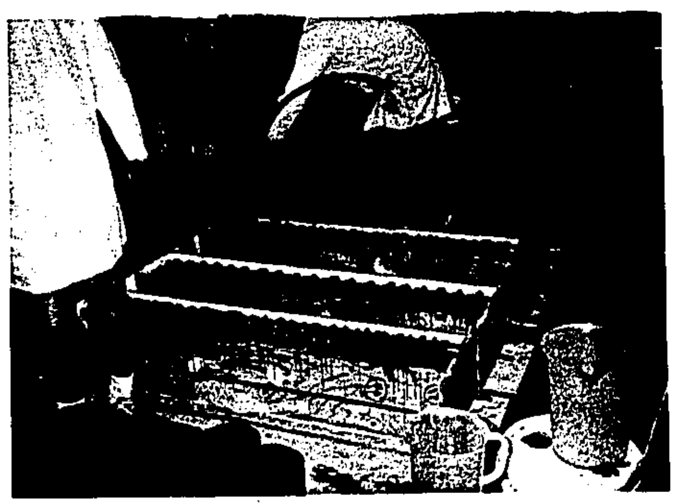

(b)

Figure 4.11: Casting high strength concrete in the laboratory.

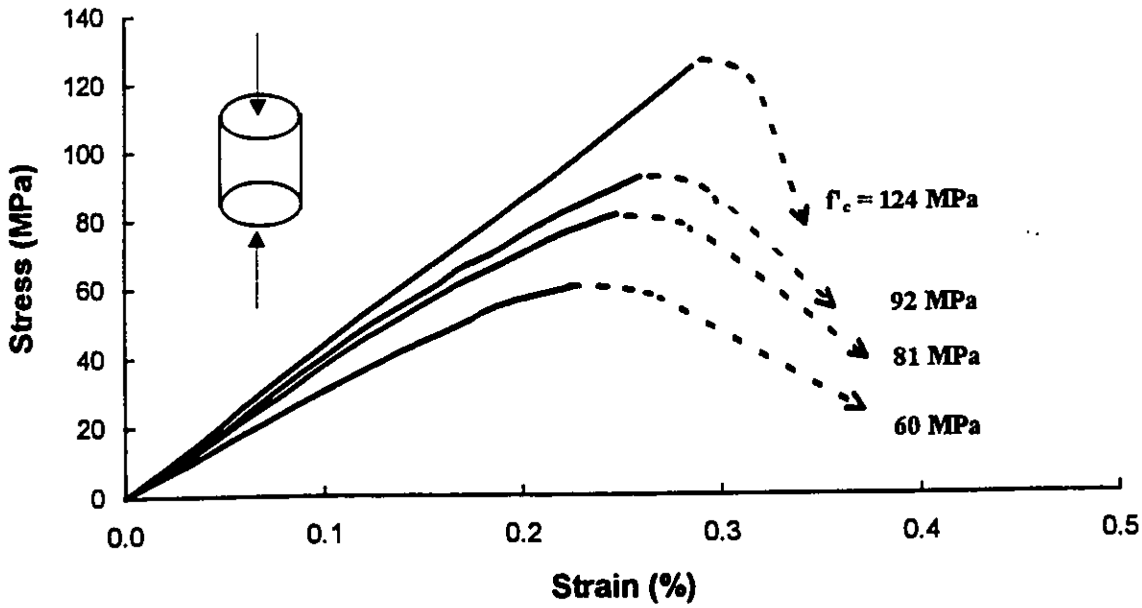

Figure 4.12: Stress-strain relationship for plain concrete.

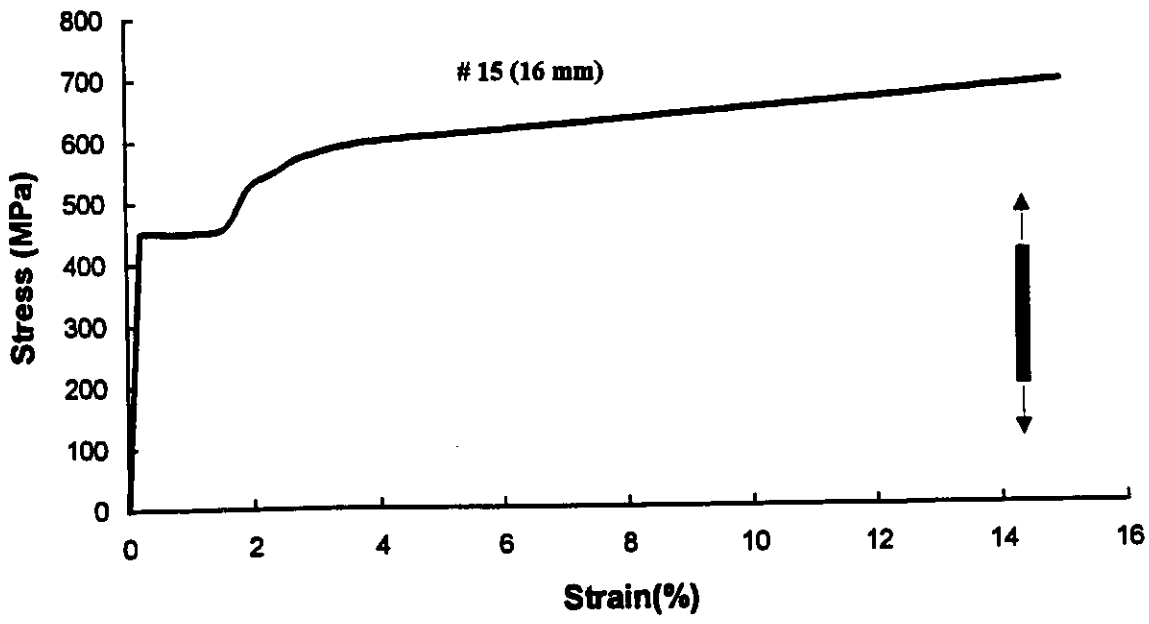

Figure 4.13: Stress-strain relationship for longitudinal reinforcement.

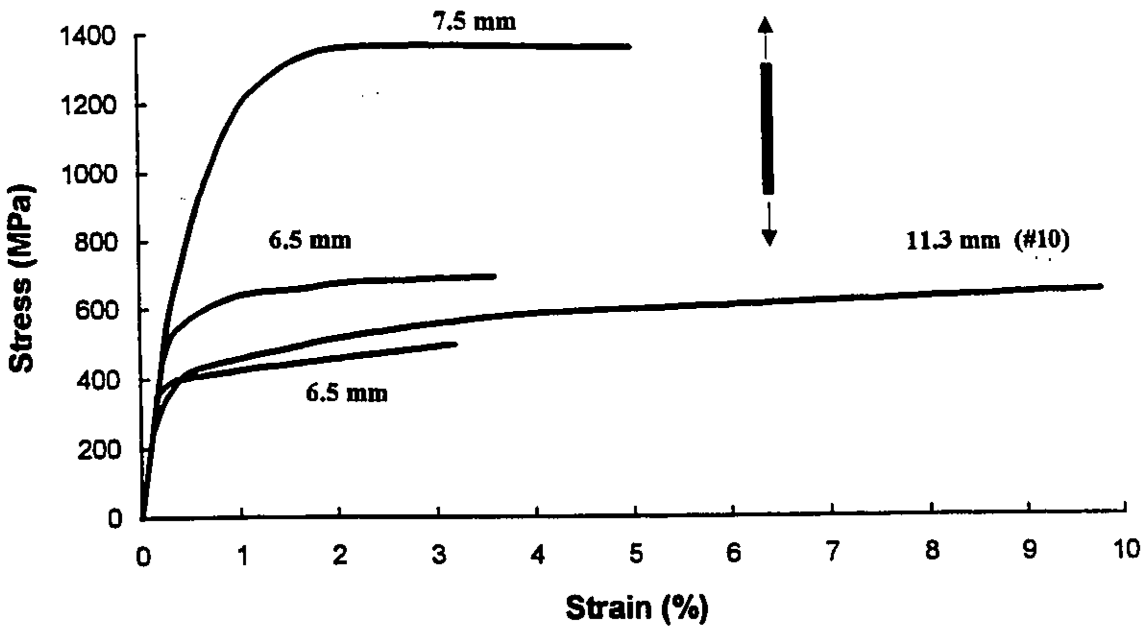

(a)

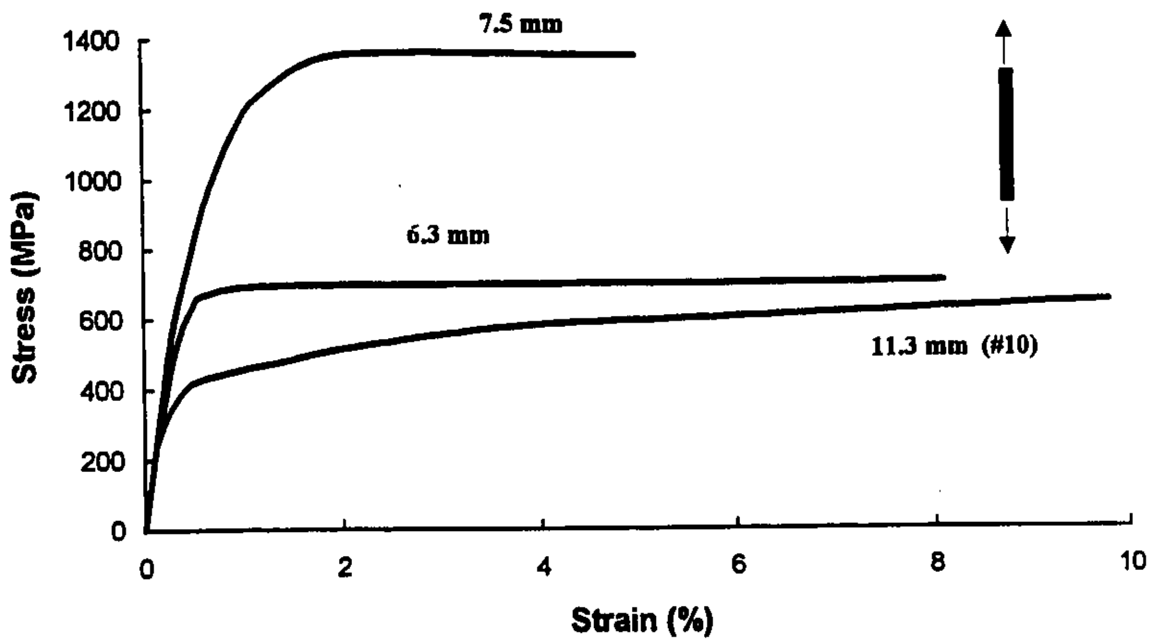

(b)

Figure 4.14: Stress-strain relationship for lateral reinforcement.

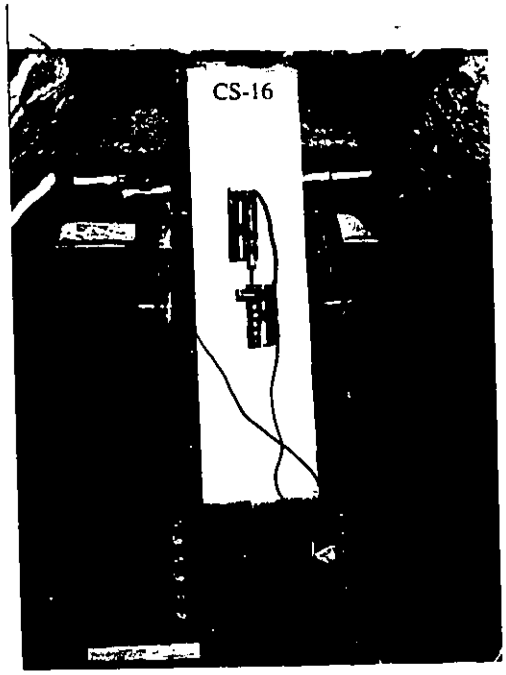

(a) Square column

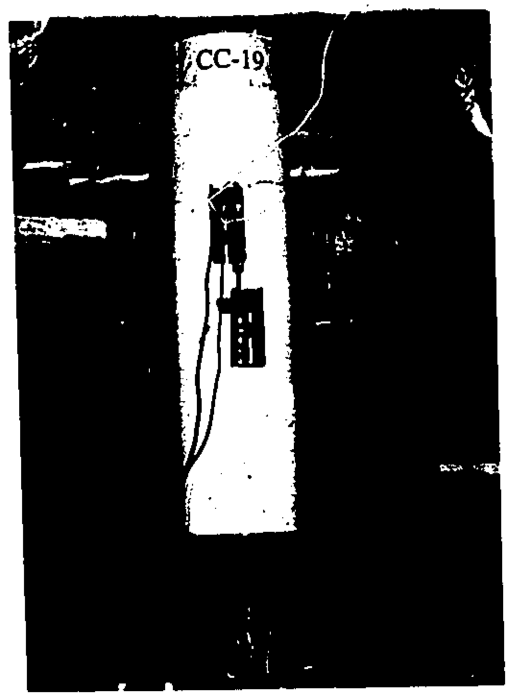

(b) Circular column

Figure 4.15: Instrumentation of testing region for axial strain measurement.

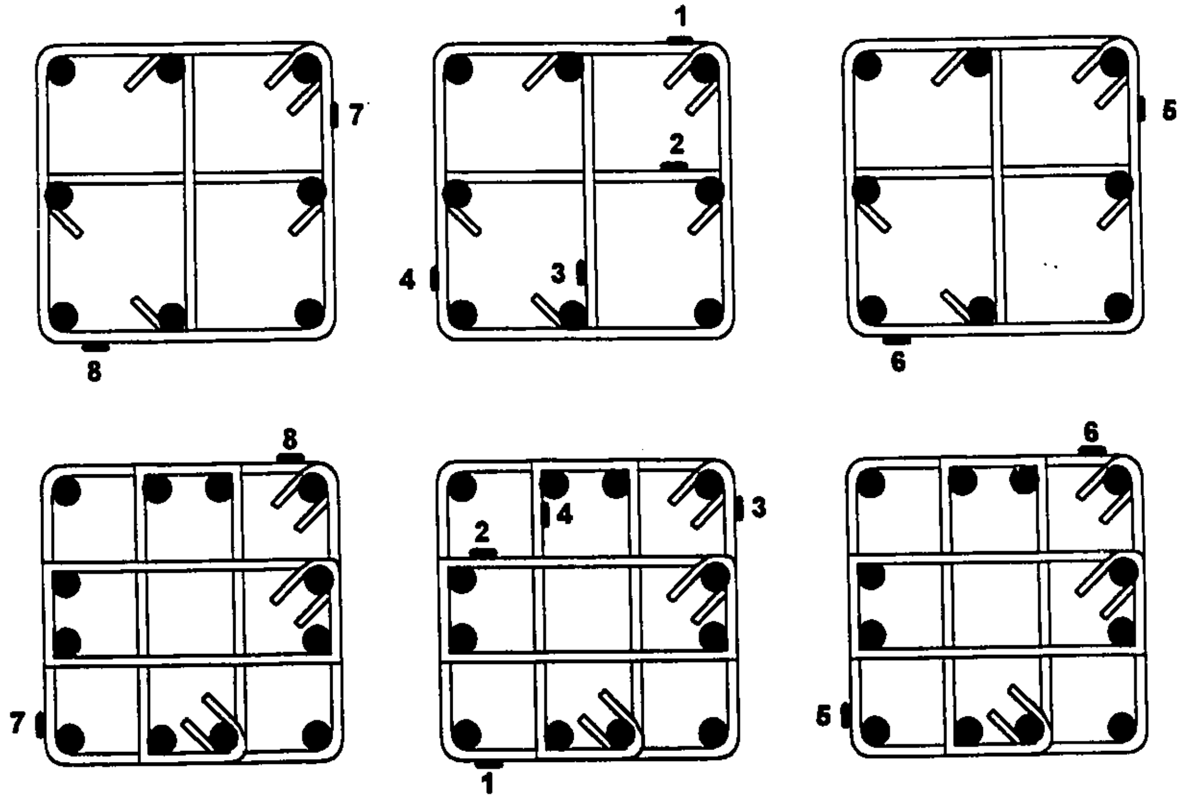

Figure 4.16: Location of strain gages on lateral steel in square columns.

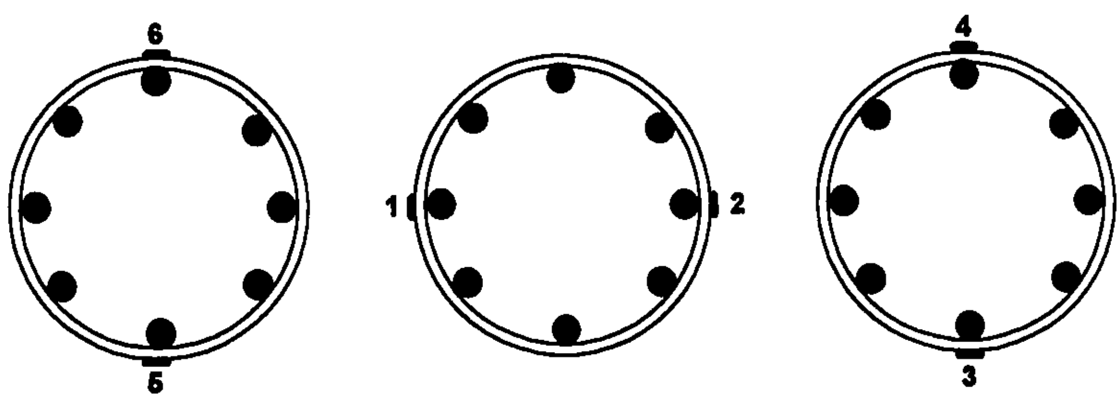

Figure 4.17: Location of strain gages on lateral steel in circular columns.

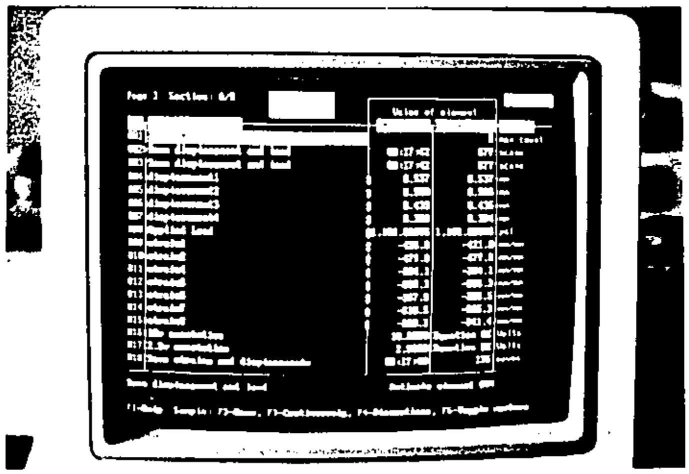

Figure 4.18: Recorded test data

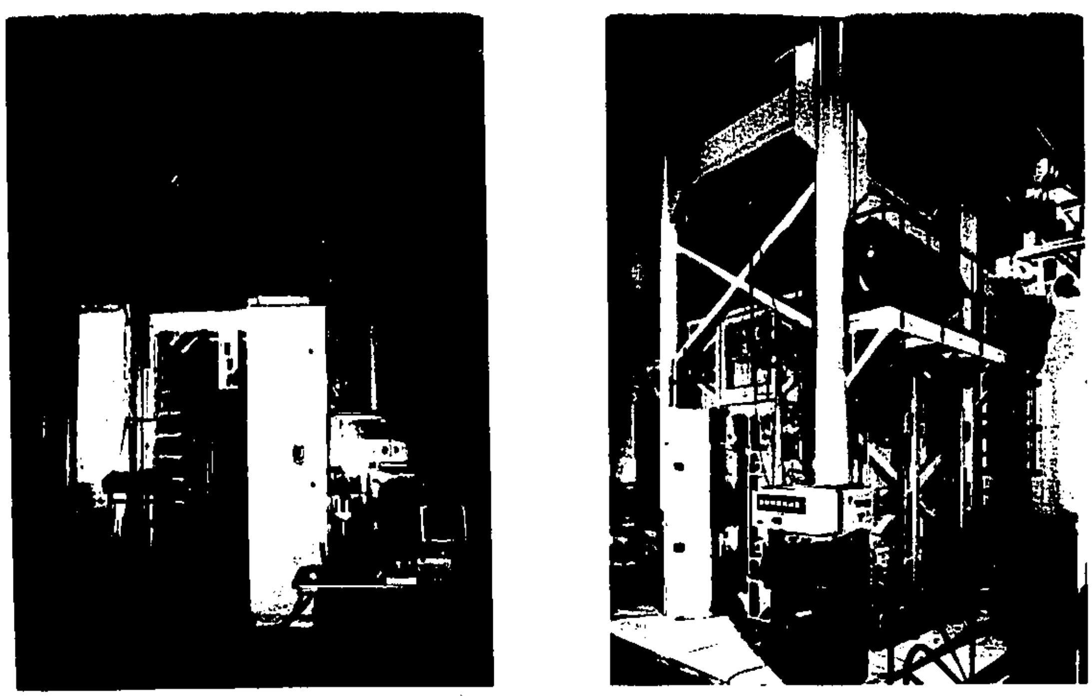

Figure 4.19: Testing machine

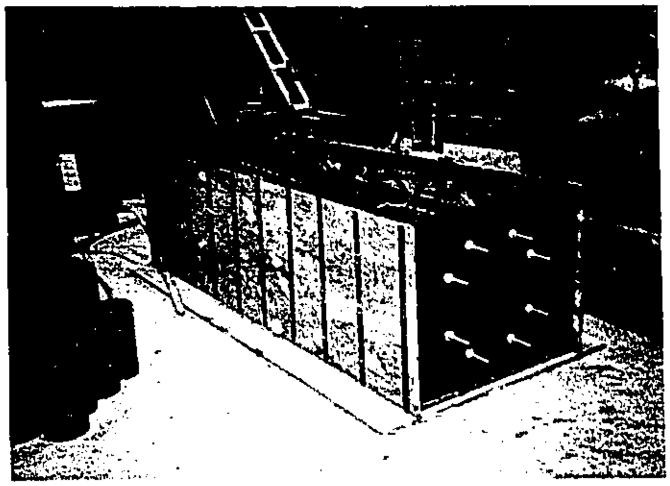

(a) Reinforcement cage

(b) Casting in the laboratory

Figure 4.20: Reinforcement cage and casting of spacer block.

Figure 4.21: Inside view of the testing machine.

Figure 4.22: Installation of a column specimen by means of self contained crane.

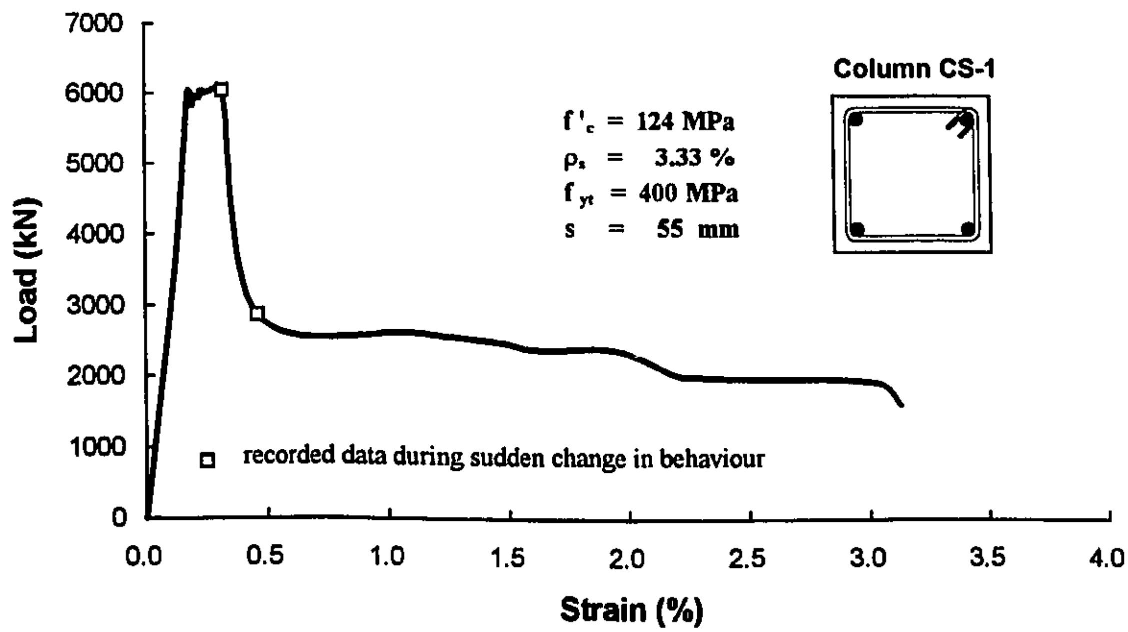

(a) Axial force-axial strain relationship.

(b) Column behaviour during different stages of loading.

Figure 4.23: Column CS-1

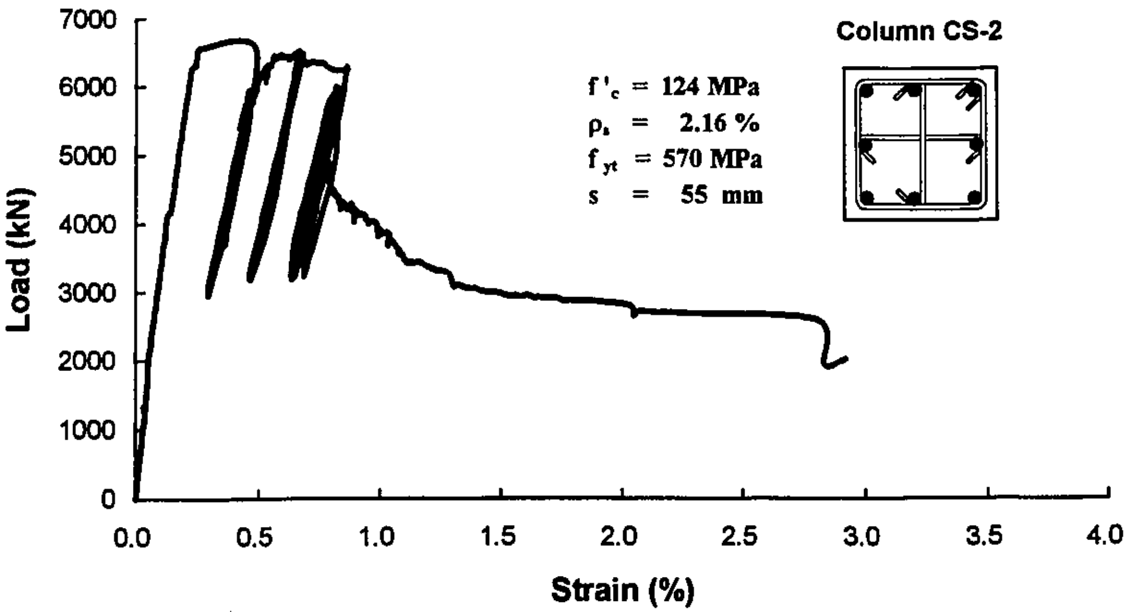

(a) Axial force-axial strain relationship.

(b) Column behaviour during different stages of loading.

Figure 4.24: Column CS-2

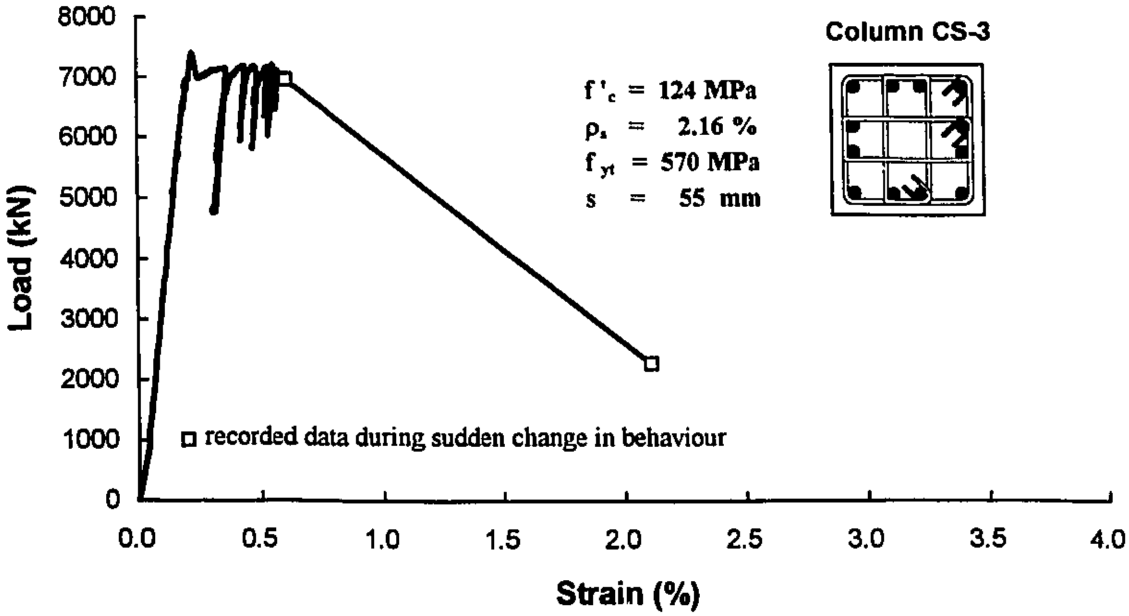

(a) Axial force-axial strain relationship.

(b) Column behaviour during different stages of loading.

Figure 4.25: Column CS-3

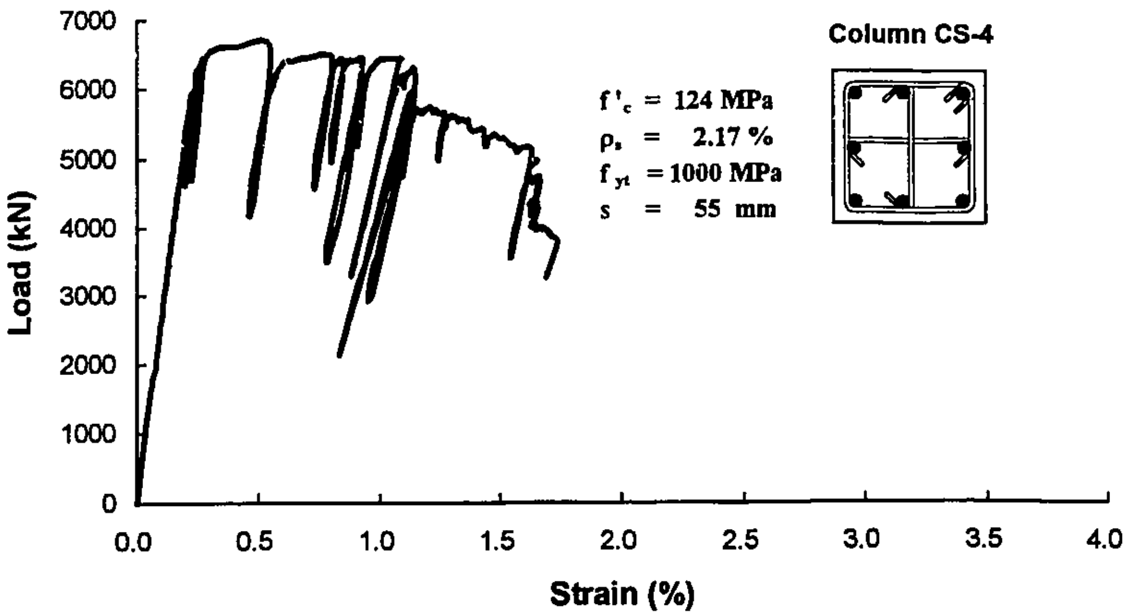

(a) Axial force-axial strain relationship.

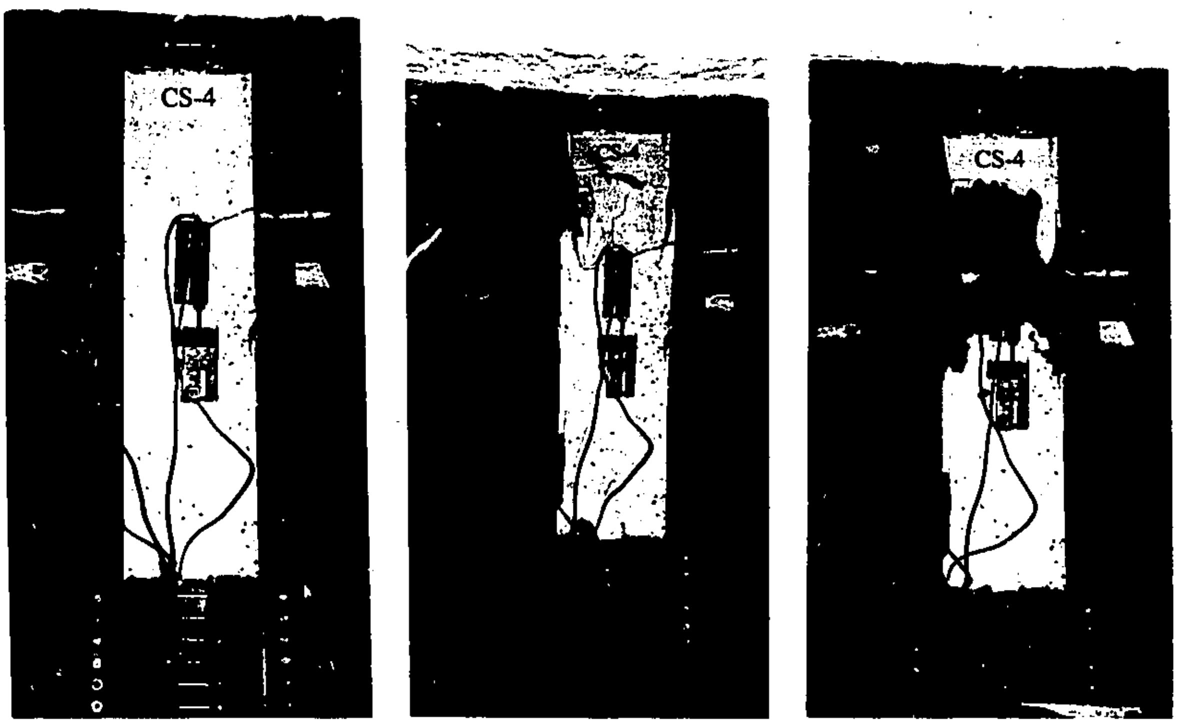

(b) Column behaviour during different stages of loading.

Figure 4.26: Column CS-4

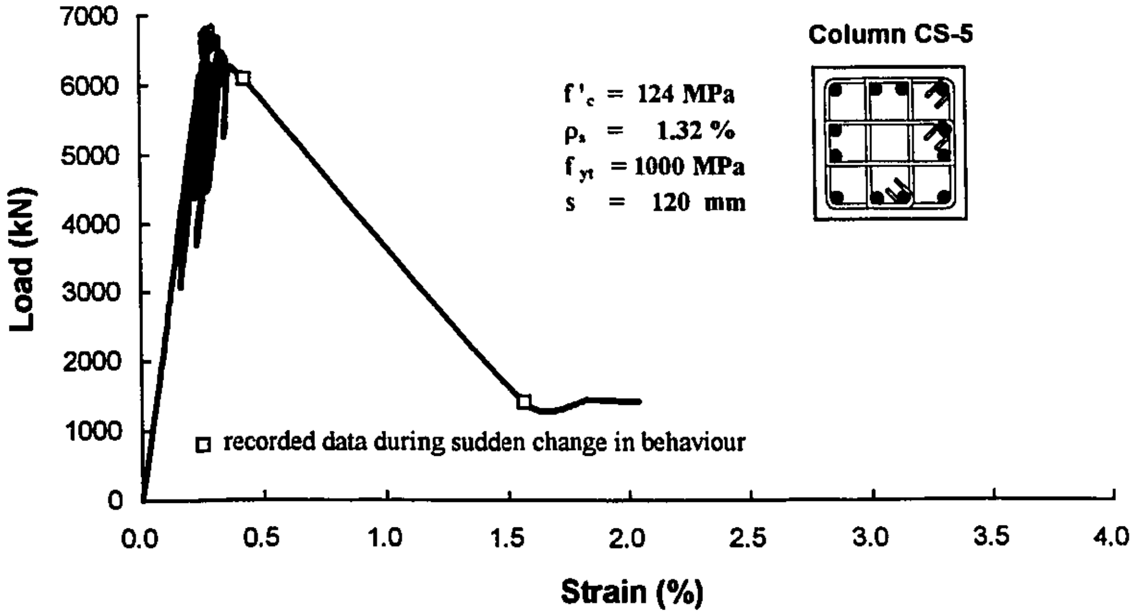

(a) Axial force-axial strain relationship.

(b) Column behaviour during different stages of loading.

Figure 4.27: Column CS-5

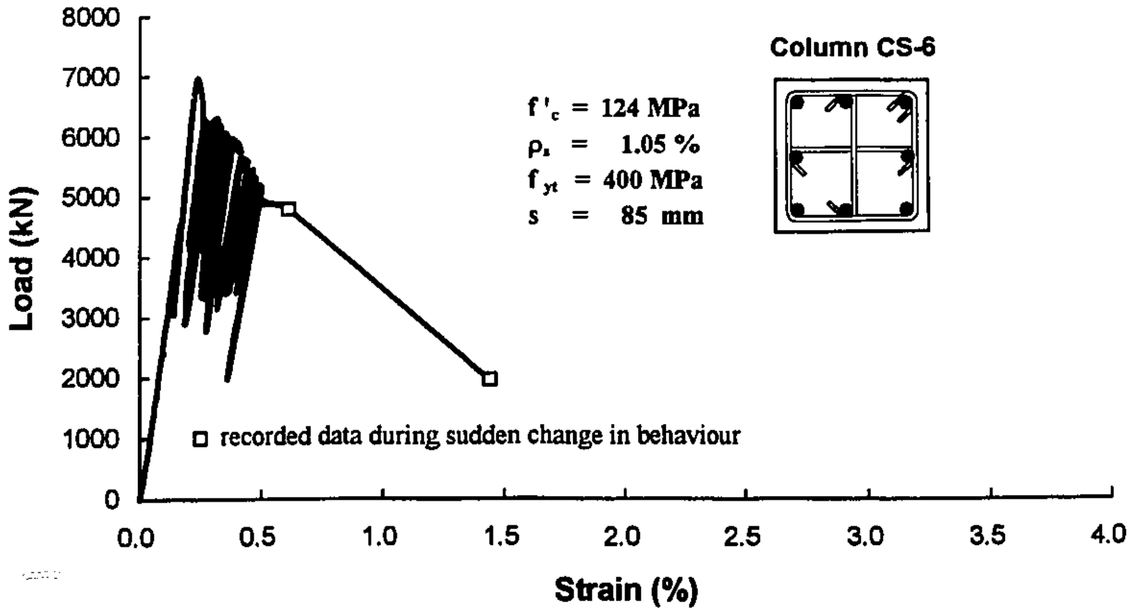

(a) Axial force-axial strain relationship.

(b) Column behaviour during different stages of loading.

Figure 4.28: Column CS-6

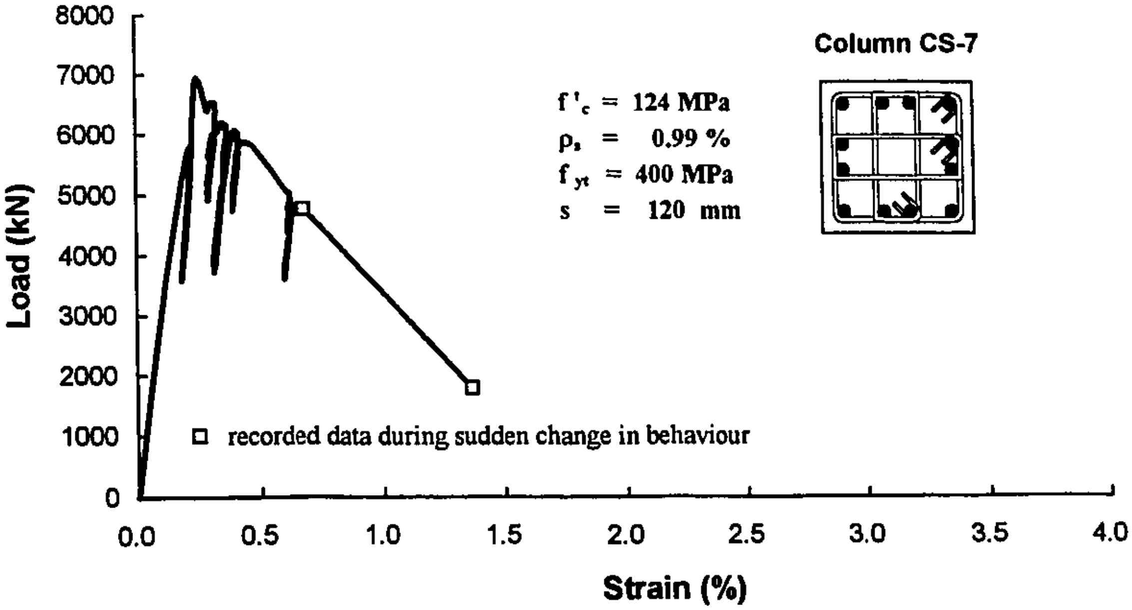

(a) Axial force-axial strain relationship.

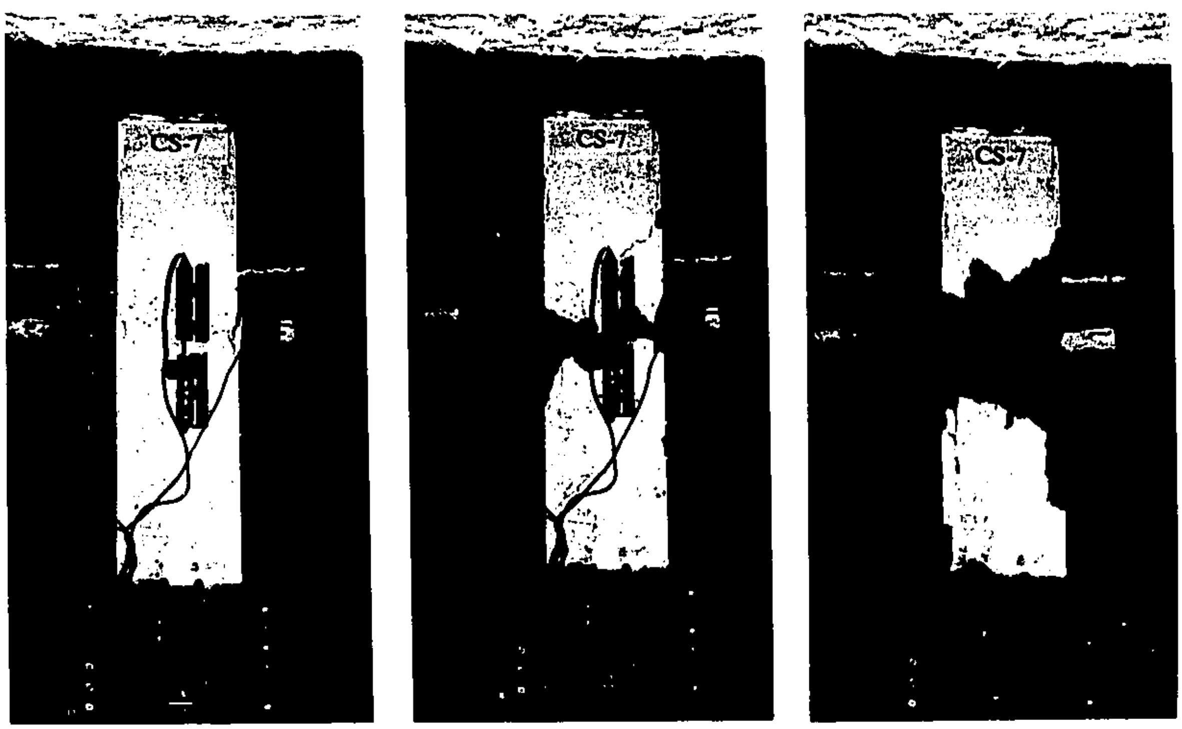

(b) Column behaviour during different stages of loading.

Figure 4.29: Column CS-7

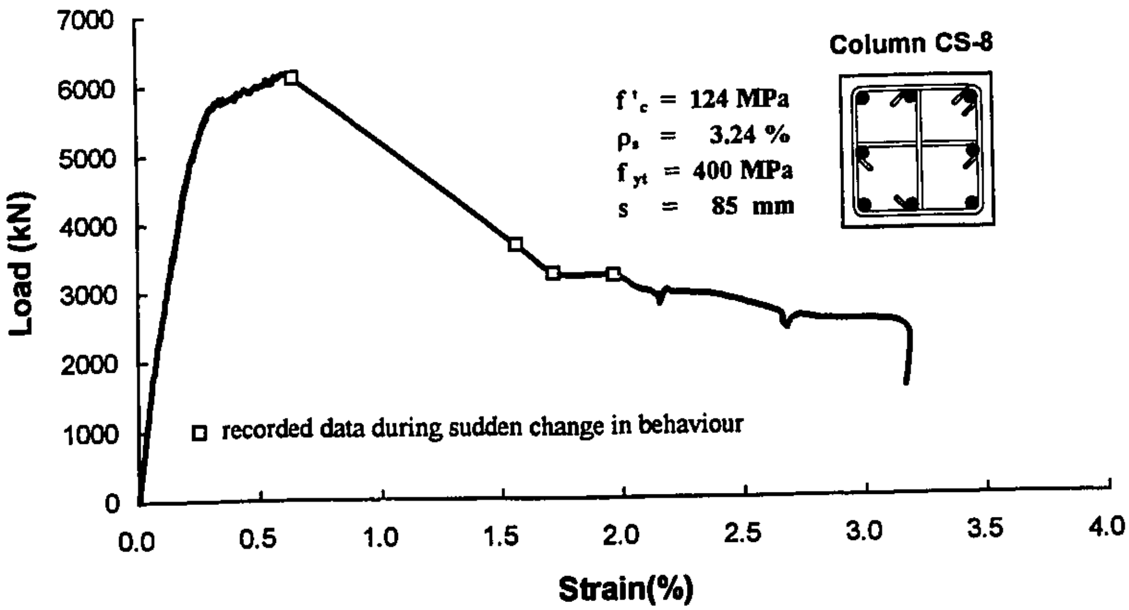

(a) Axial force-axial strain relationship.

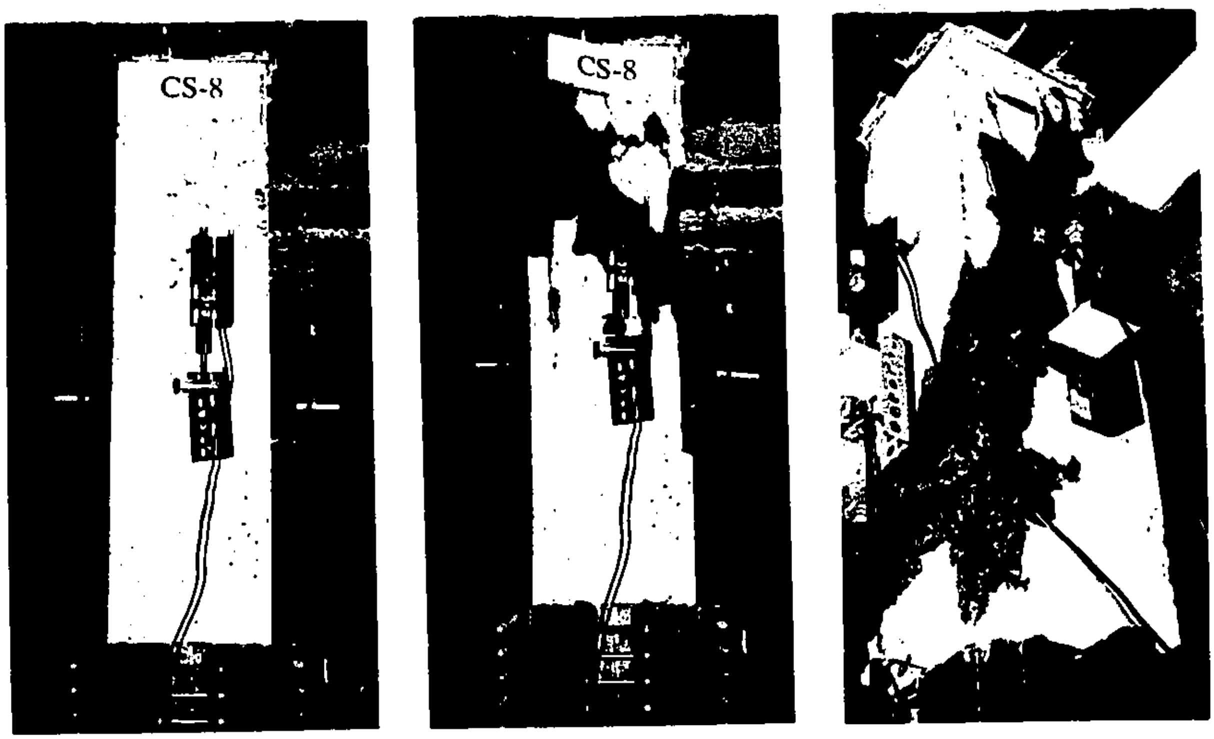

(b) Column behaviour during different stages of loading.

Figure 4.30: Column CS-8

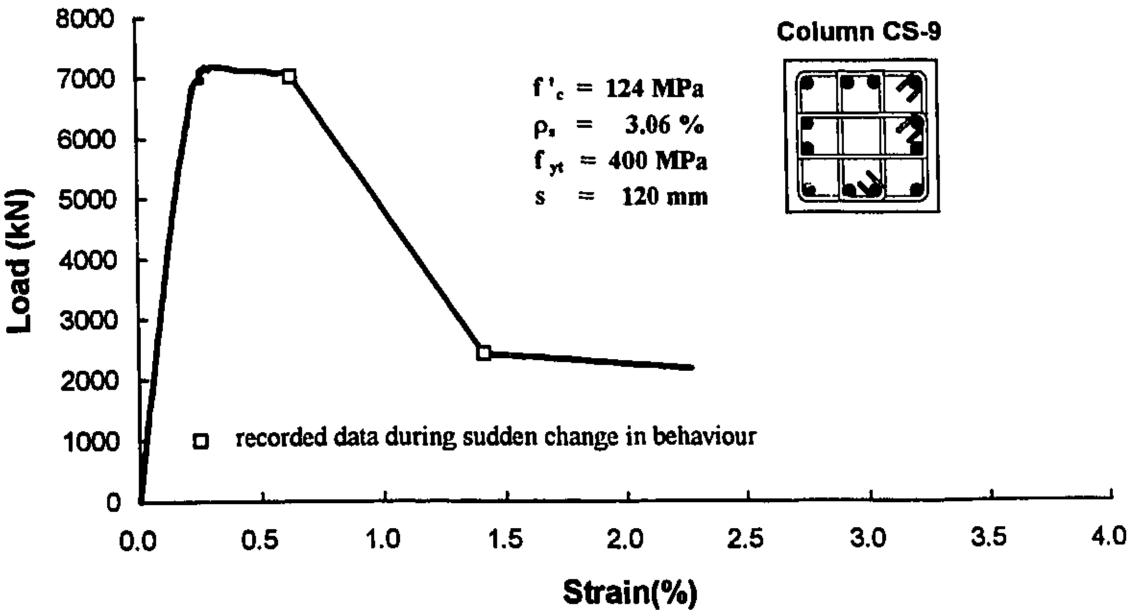

(a) Axial force-axial strain relationship.

(b) Column behaviour during different stages of loading.

Figure 4.31: Column CS-9

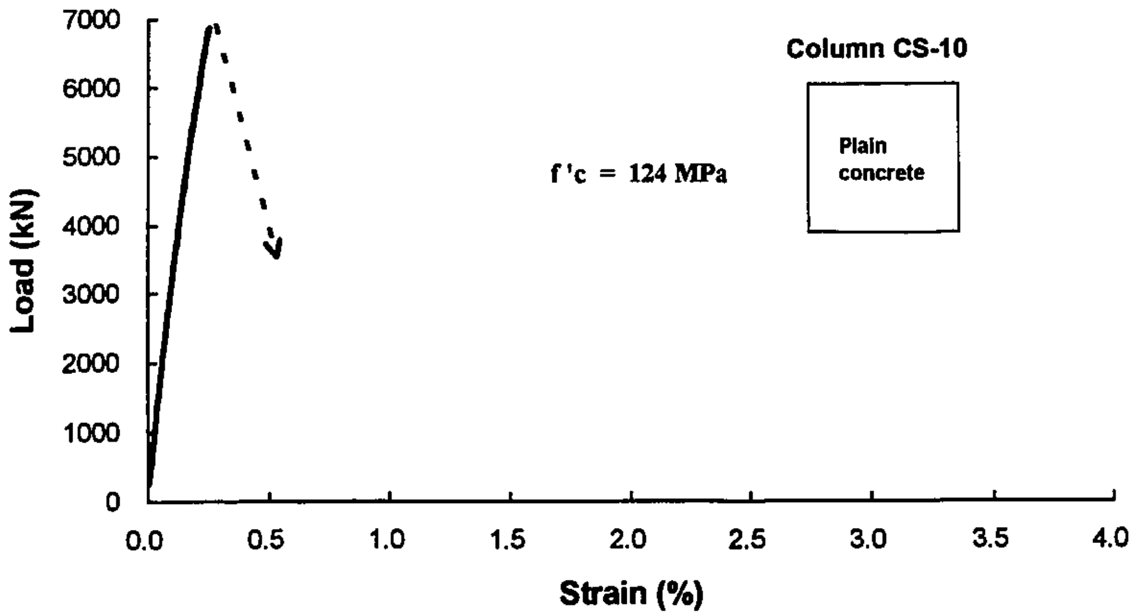

(a) Axial force-axial strain relationship.

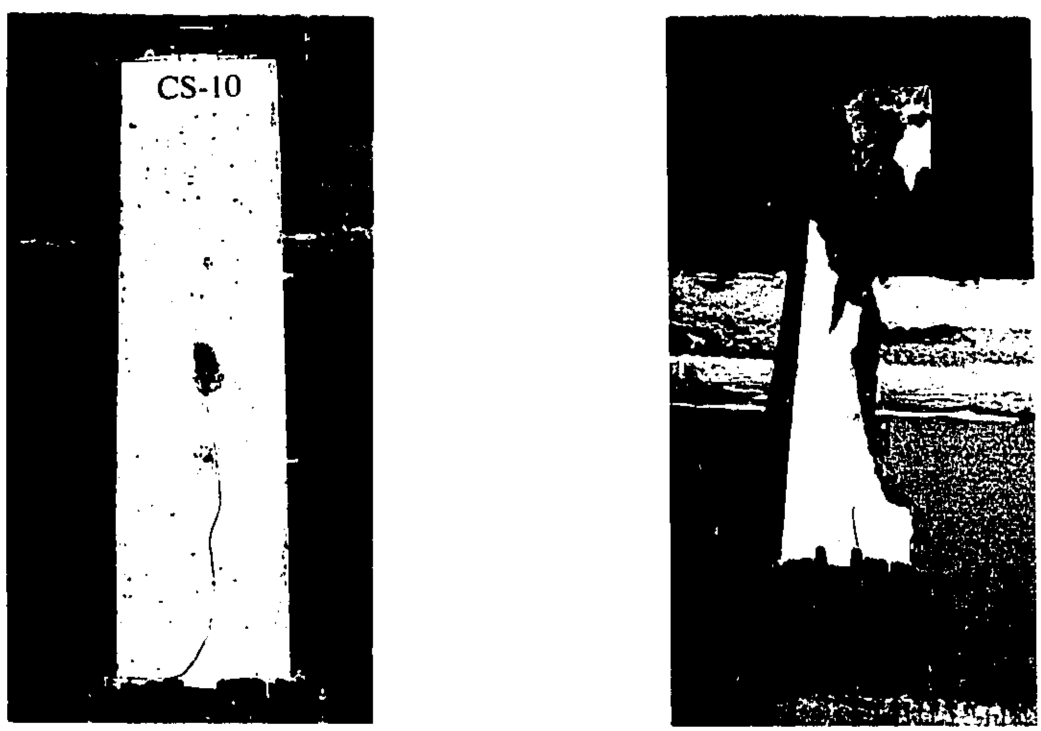

(b) Column behaviour during different stages of loading.

Figure 4.32: Column CS-10

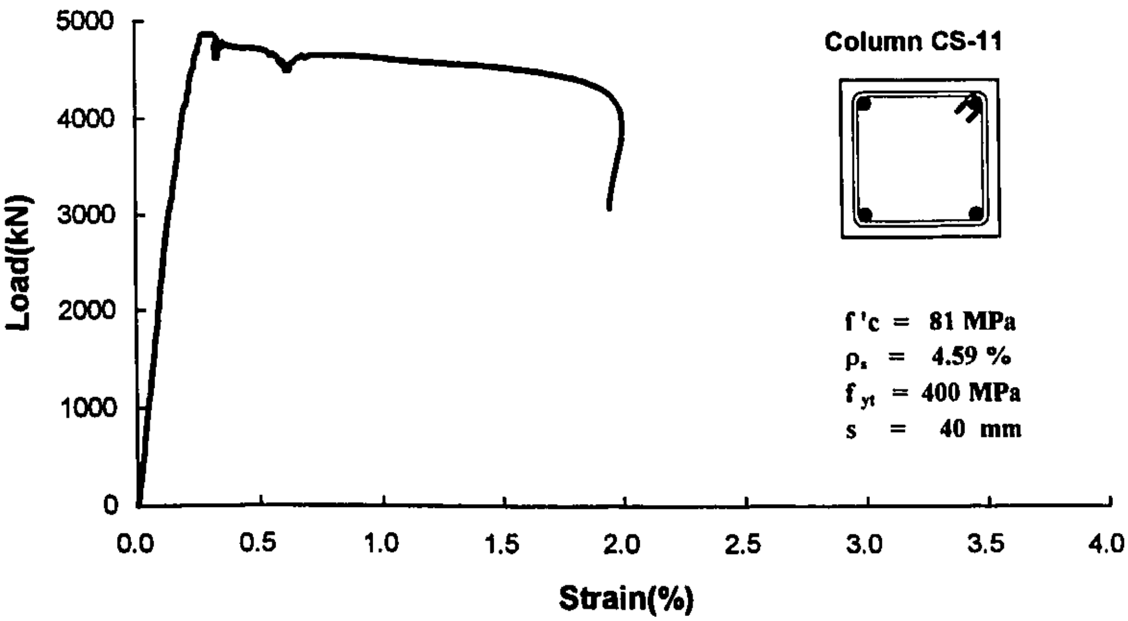

(a) Axial force-axial strain relationship.

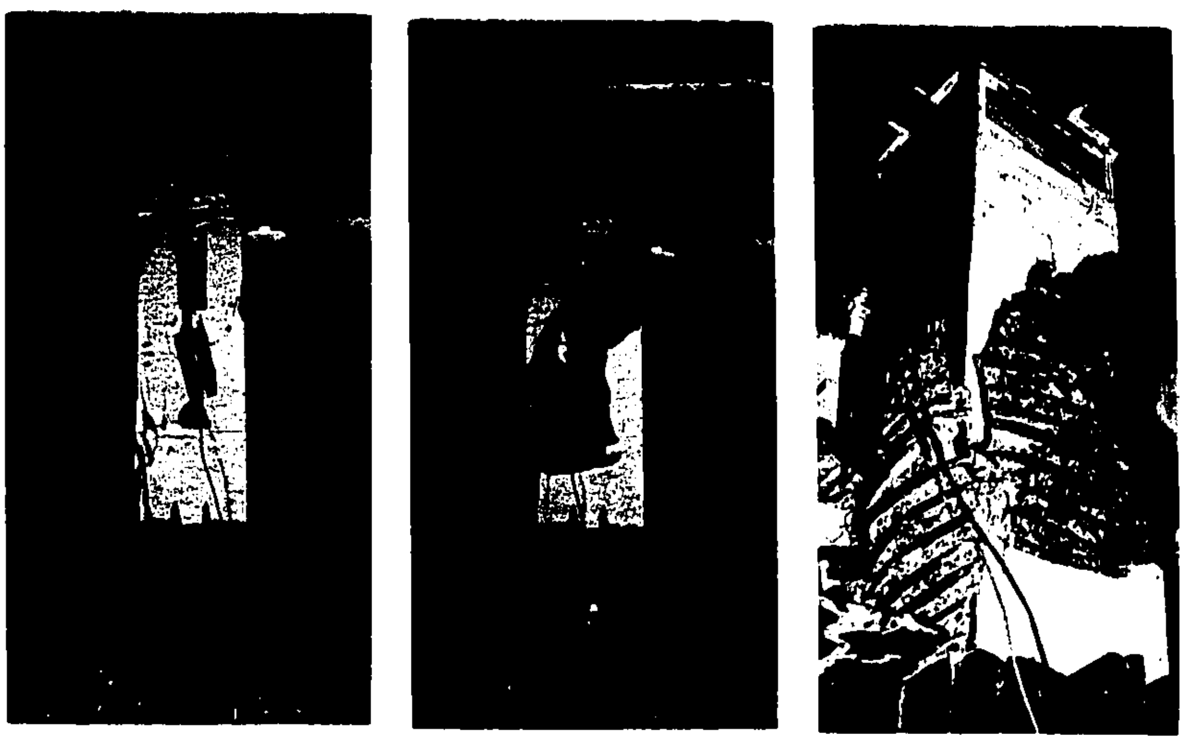

(b) Column behaviour during different stages of loading.

Figure 4.33: Column CS-11

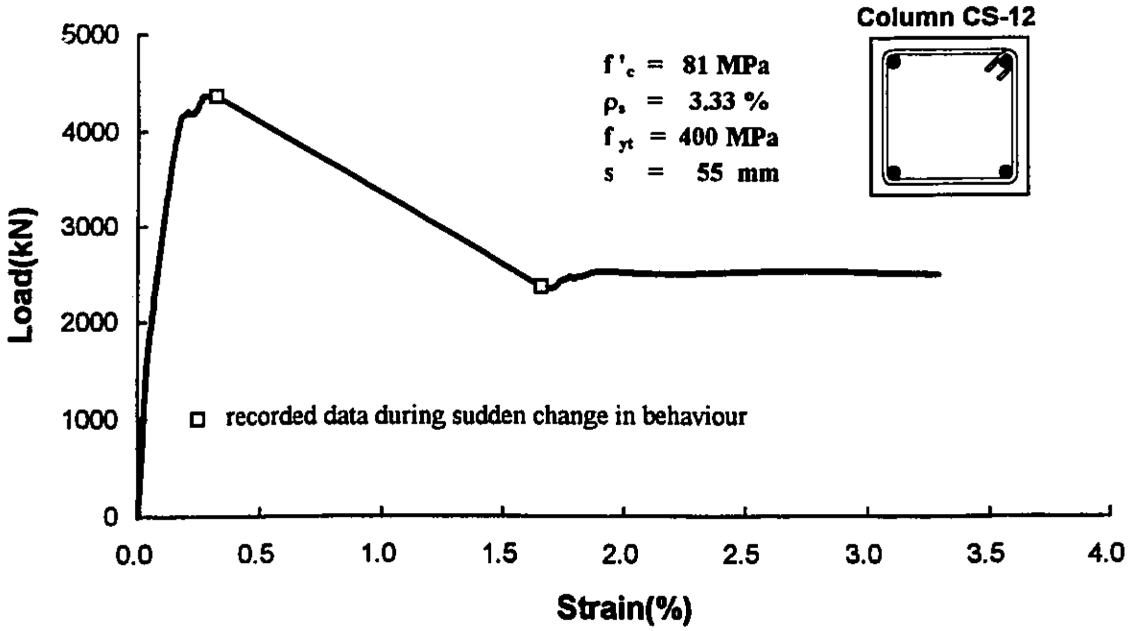

(a) Axial force-axial strain relationship.

(b) Column behaviour during different stages of loading.

Figure 4.34: Column CS-12

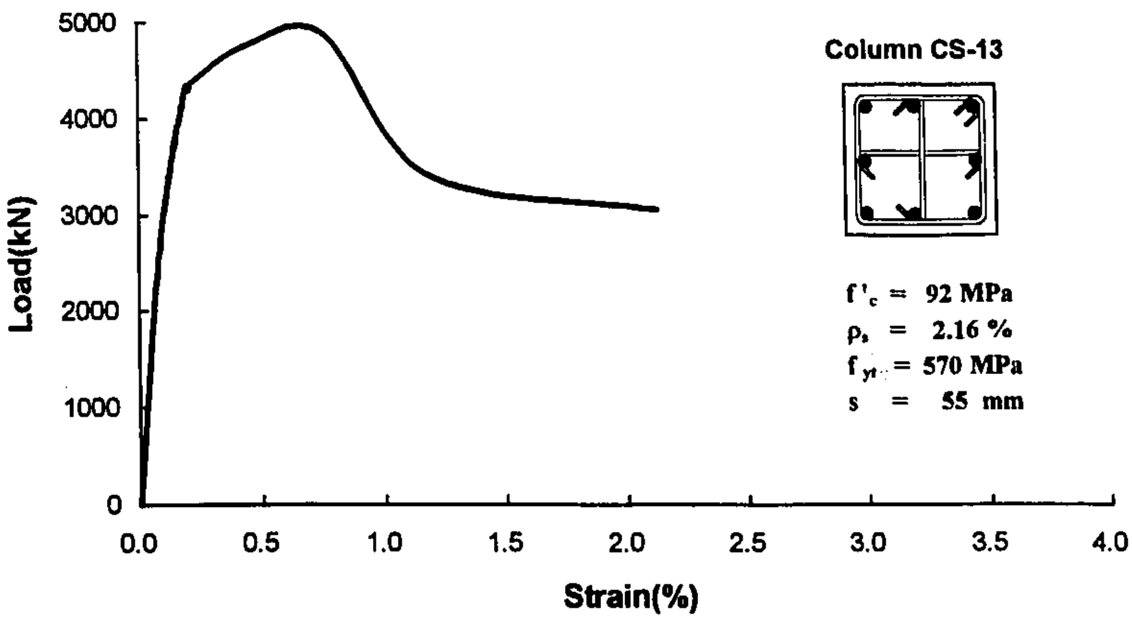

(a) Axial force-axial strain relationship.

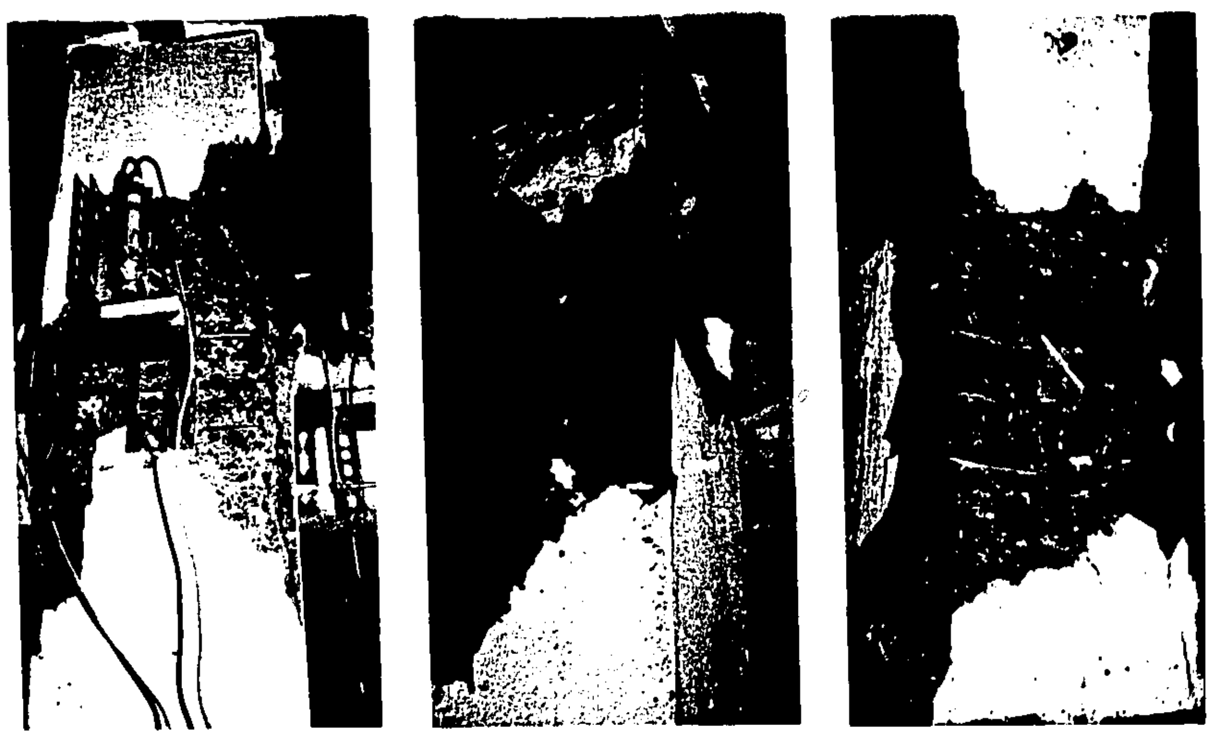

(b) Column behaviour during different stages of loading.

Figure 4.35: Column CS-13

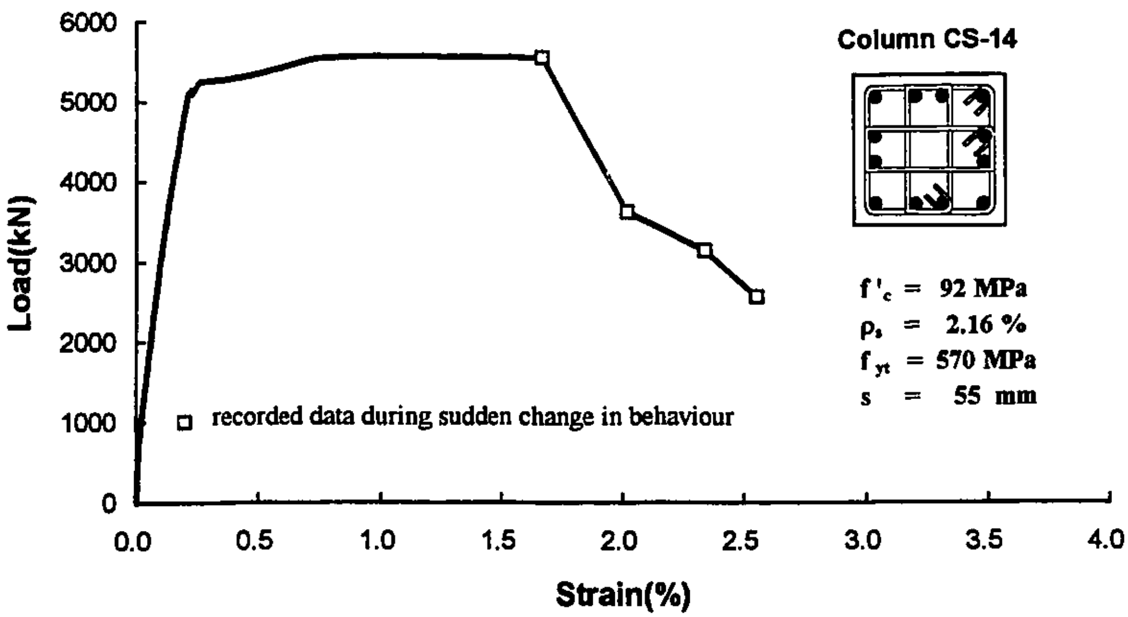

(a) Axial force-axial strain relationship.

(b) Column behaviour during different stages of loading.

Figure 4.36: Column CS-14

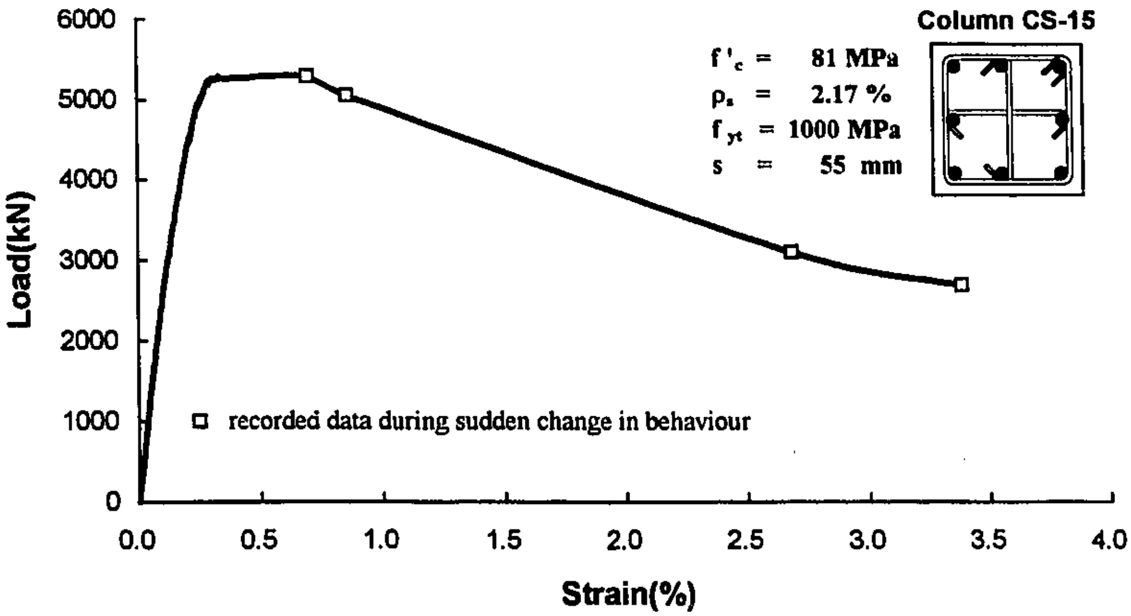

(a) Axial force-axial strain relationship.

(b) Column behaviour during different stages of loading.

Figure 4.37: Column CS-15

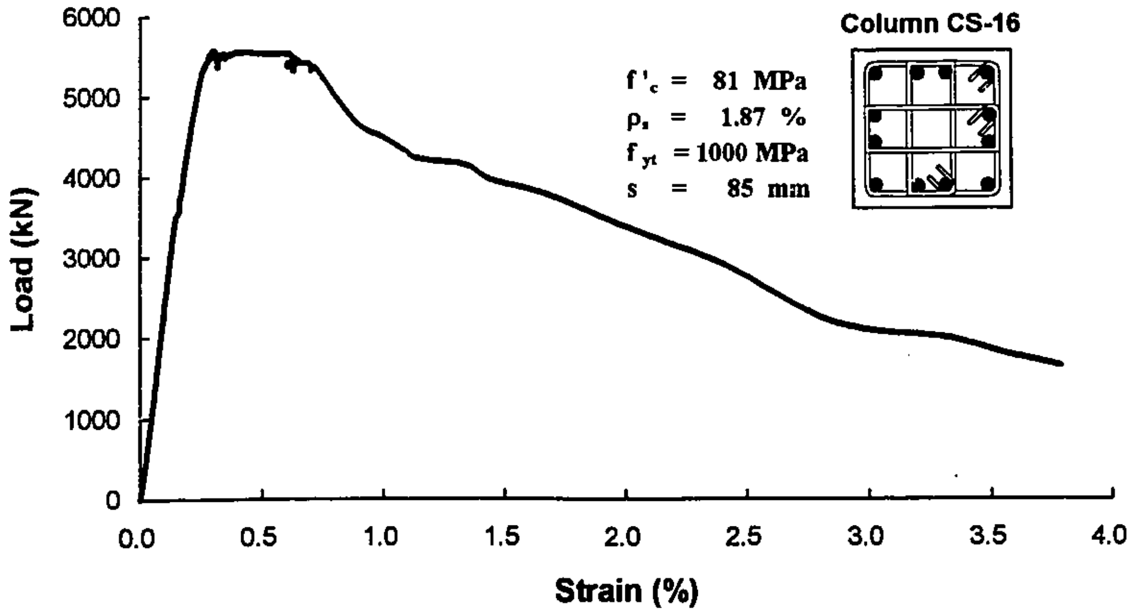

(a) Axial force-axial strain relationship.

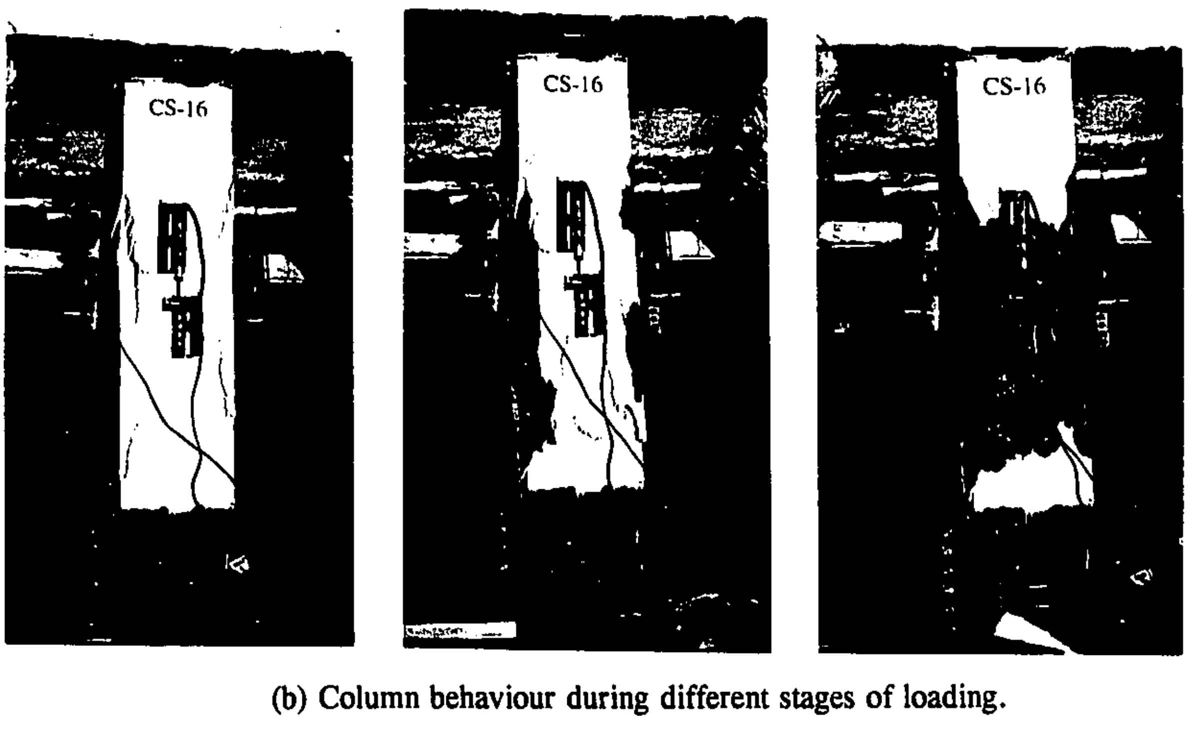

(b) Column behaviour during different stages of loading.

Figure 4.38: Column CS-16

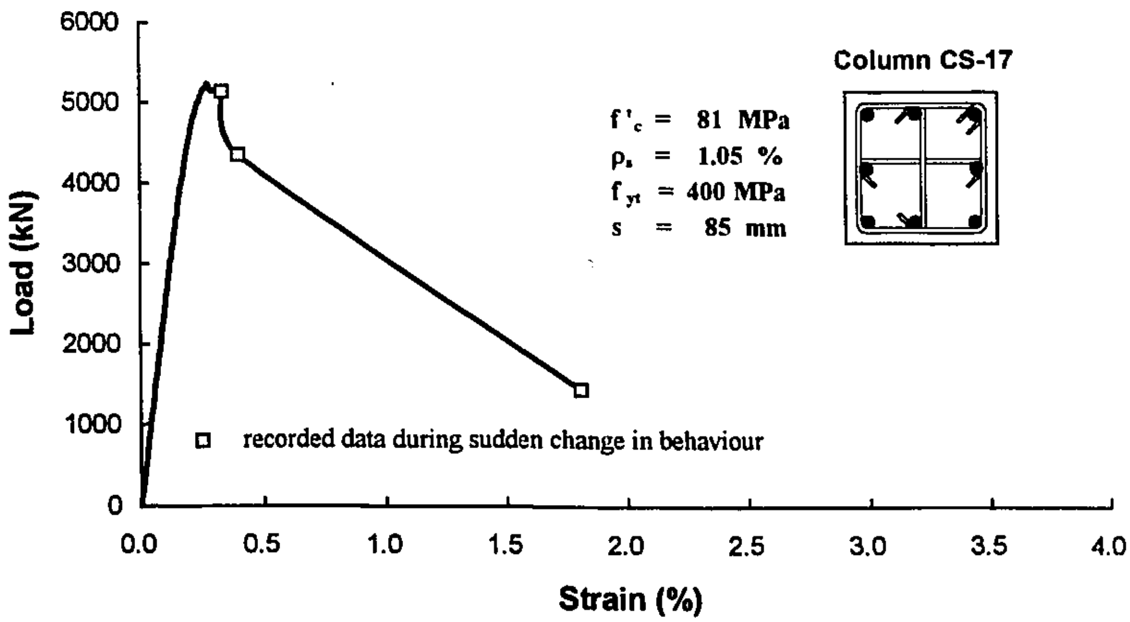

(a) Axial force-axial strain relationship.

(b) Column behaviour during different stages of loading.

Figure 4.39: Column CS-17

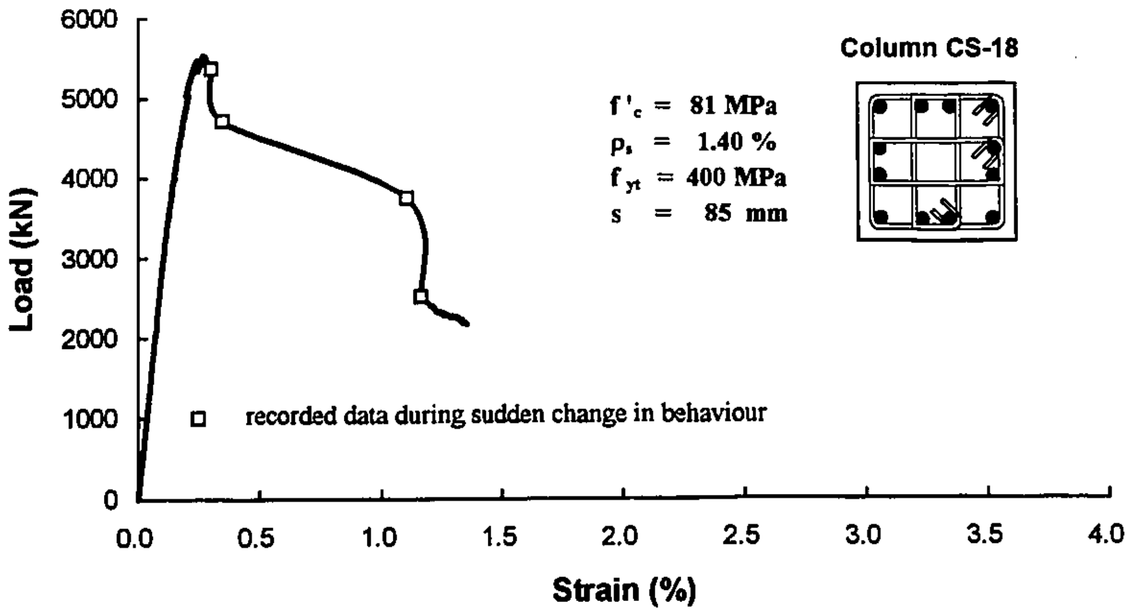

(a) Axial force-axial strain relationship.

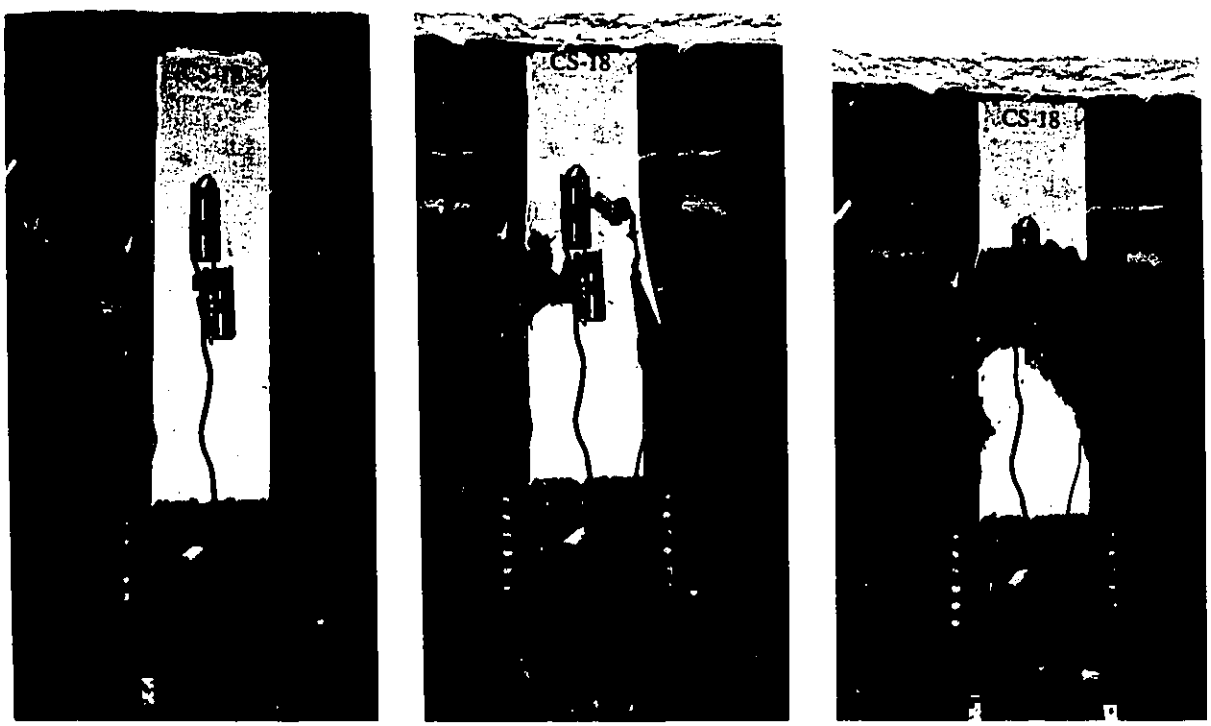

(b) Column behaviour during different stages of loading.

Figure 4.40: Column CS-18

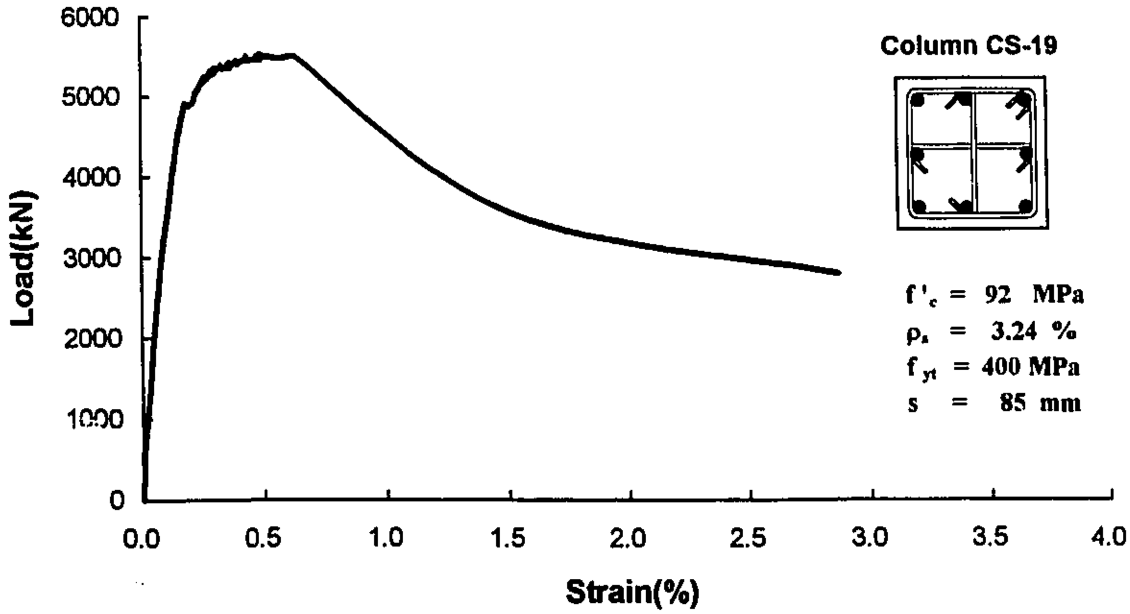

(a) Axial force-axial strain relationship.

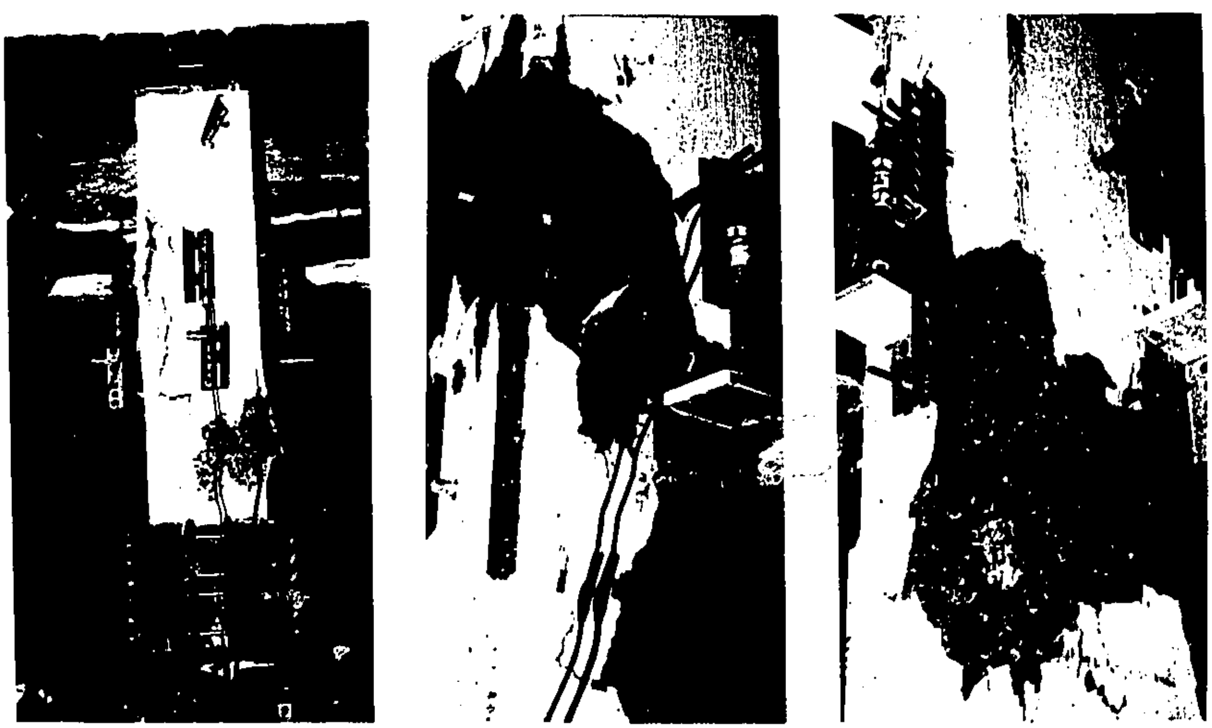

(b) Column behaviour during different stages of loading.

Figure 4.41: Column CS-19

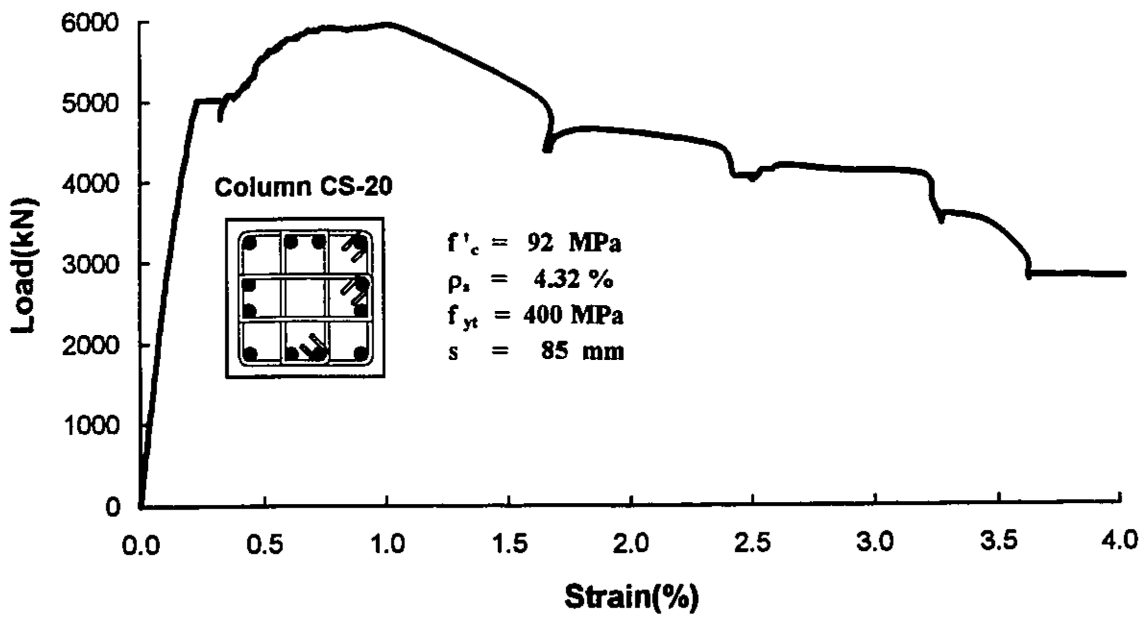

(a) Axial force-axial strain relationship.

(b) Column behaviour during different stages of loading.

Figure 4.42: Column CS-20

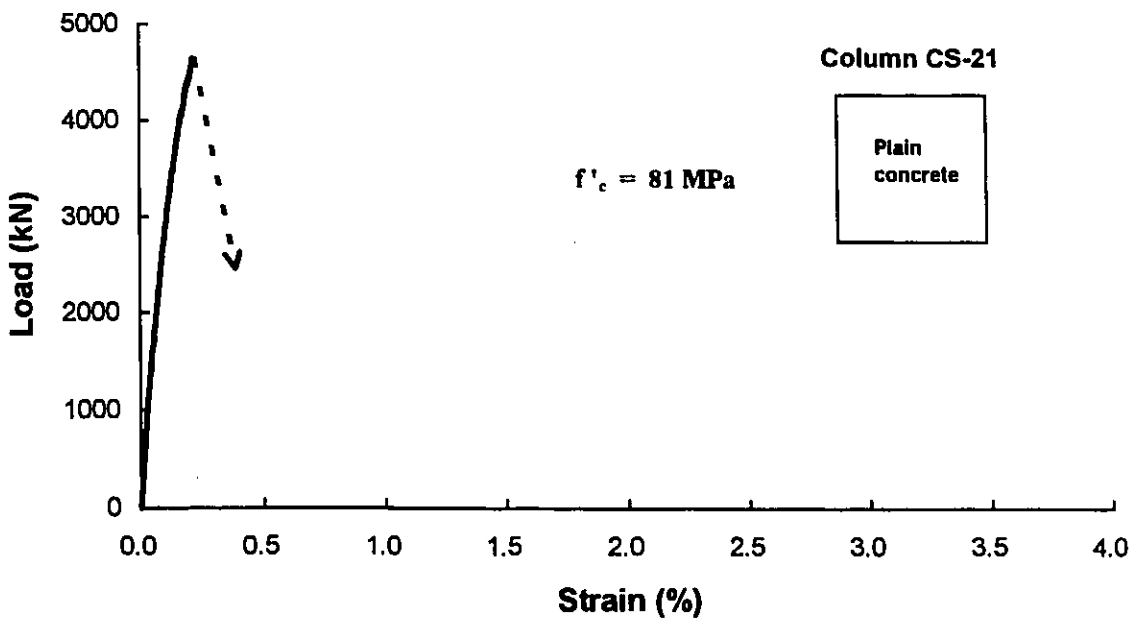

(a) Axial force-axial strain relationship.

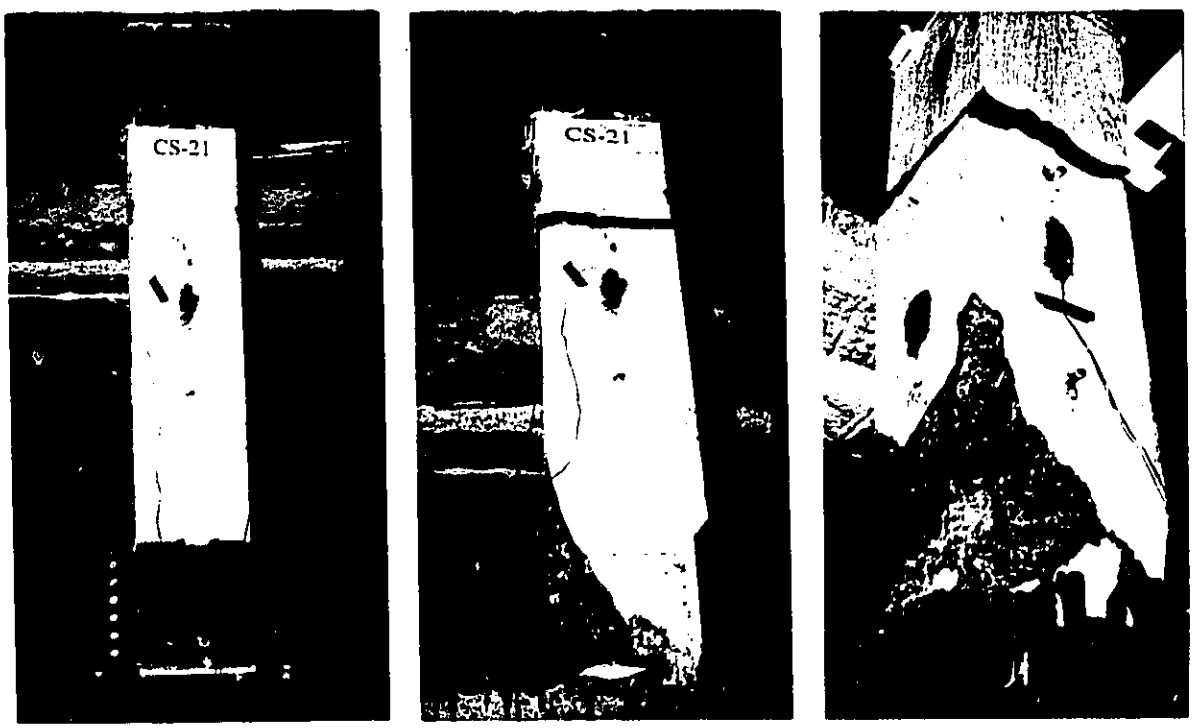

(b) Column behaviour during different stages of loading.

Figure 4.43: Column CS-21

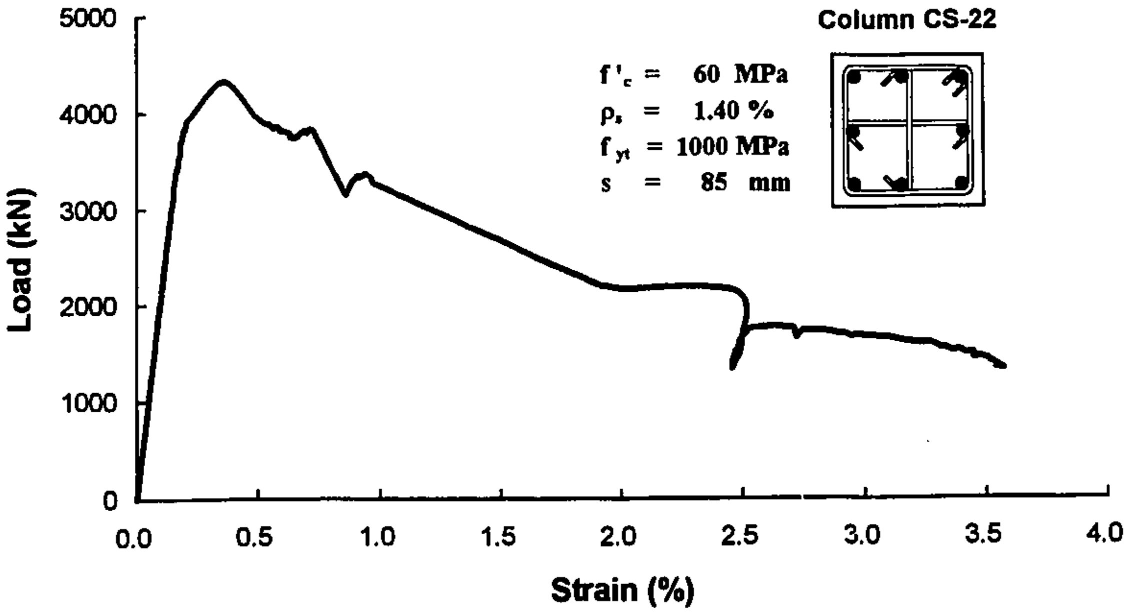

(a) Axial force-axial strain relationship.

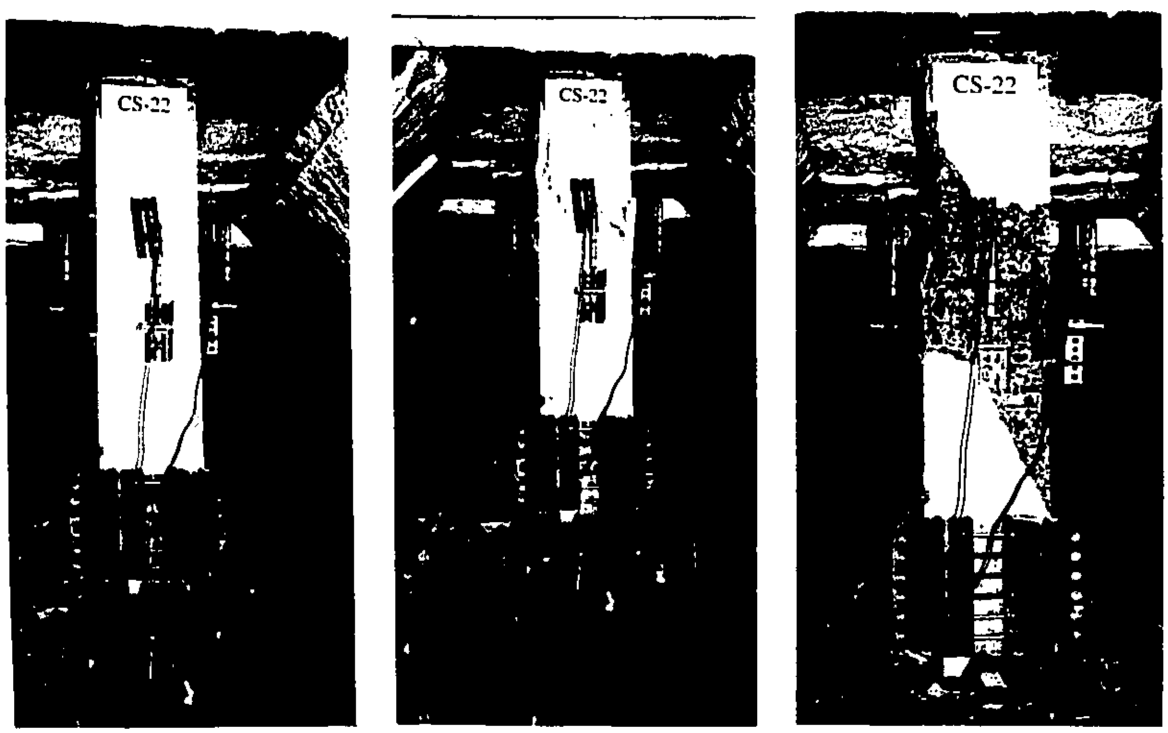

(b) Column behaviour during different stages of loading.

Figure 4.44: Column CS-22

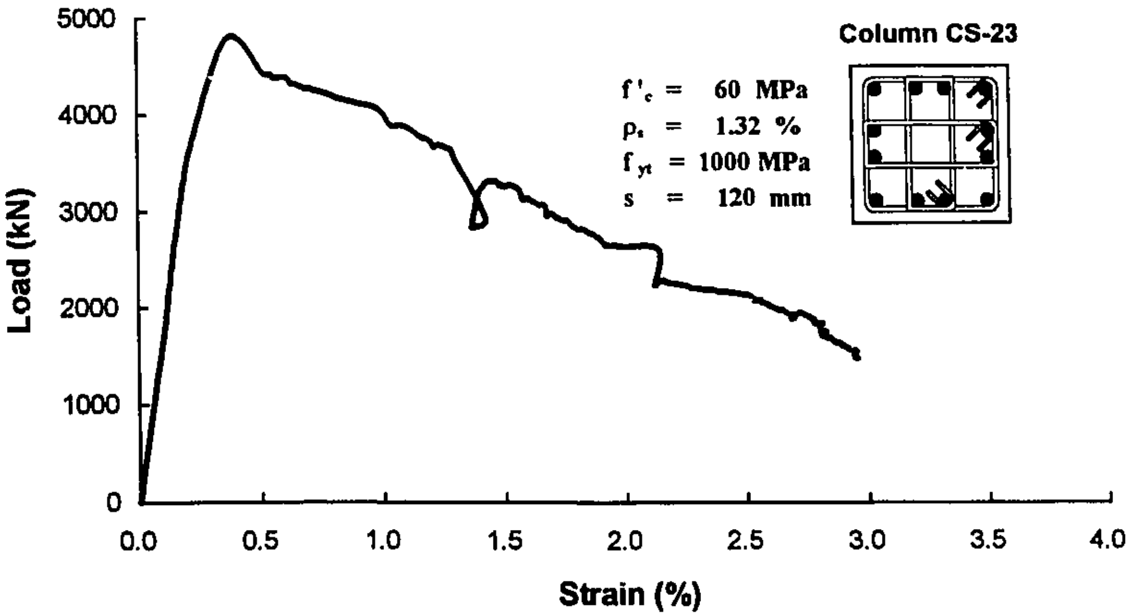

(a) Axial force-axial strain relationship.

(b) Column behaviour during different stages of loading.

Figure 4.45: Column CS-23

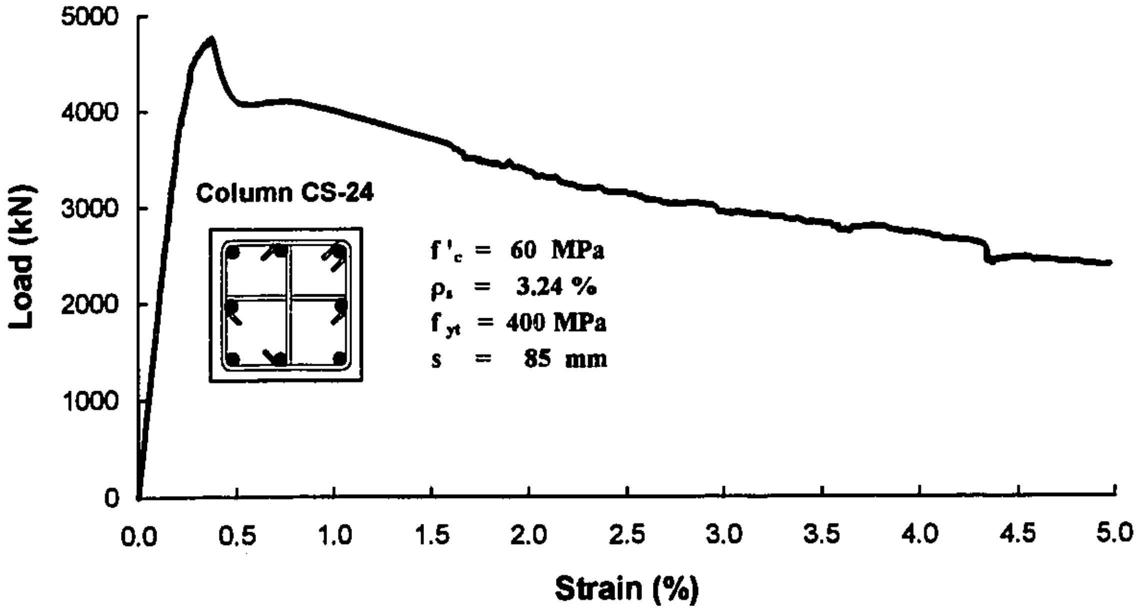

(a) Axial force-axial strain relationship.

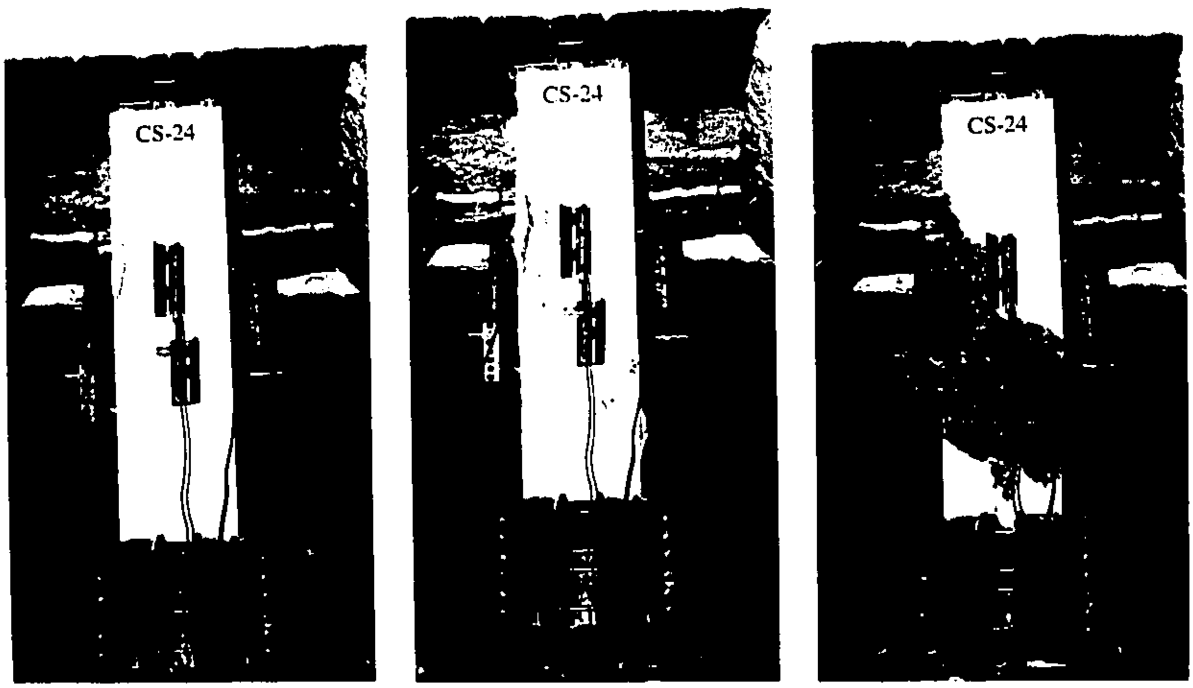

(b) Column behaviour during different stages of loading.

Figure 4.46: Column CS-24

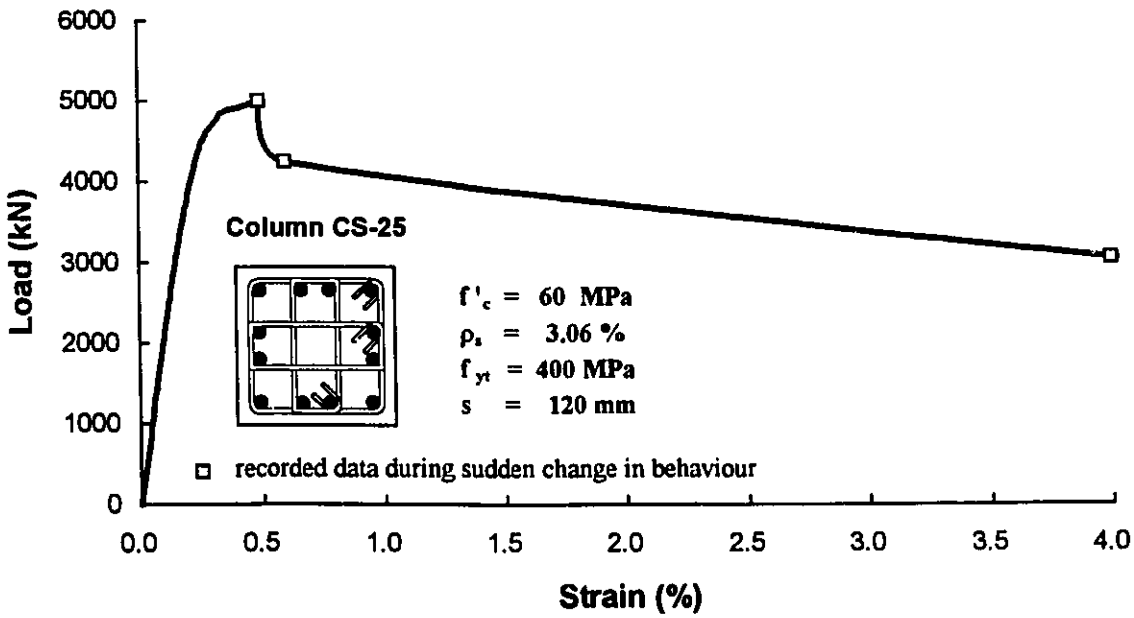

(a) Axial force-axial strain relationship.

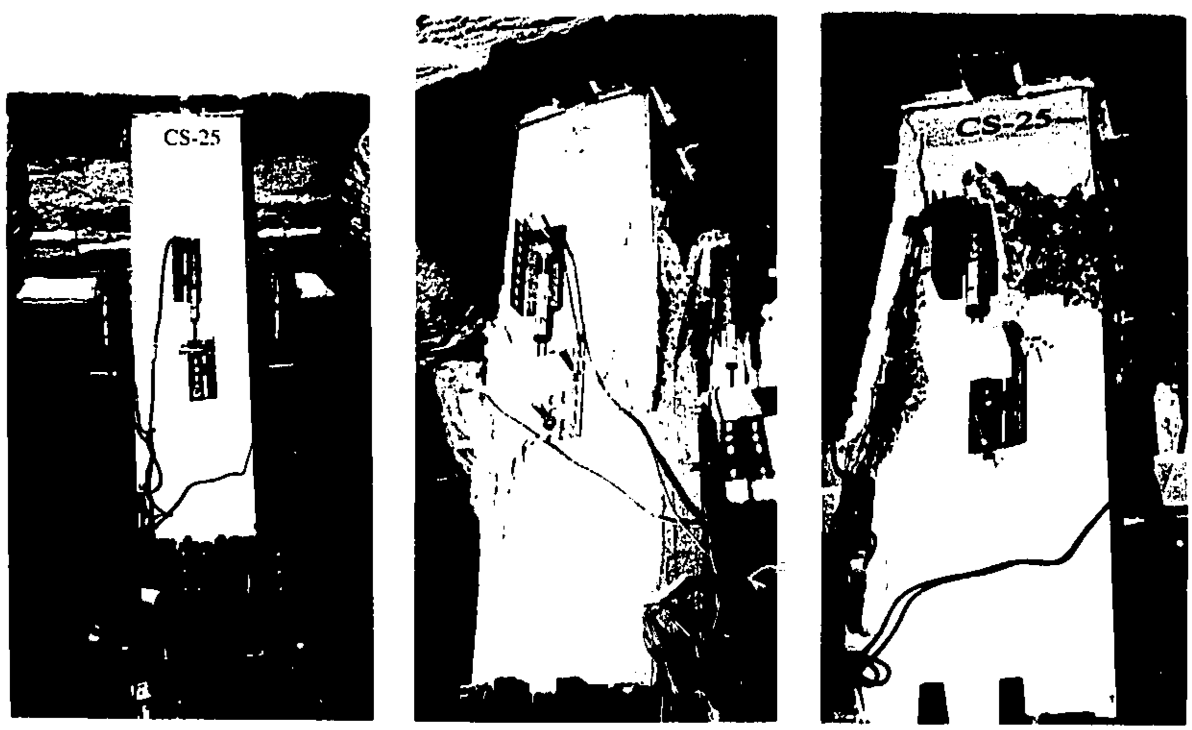

(b) Column behaviour during different stages of loading.

Figure 4.47: Column CS-25

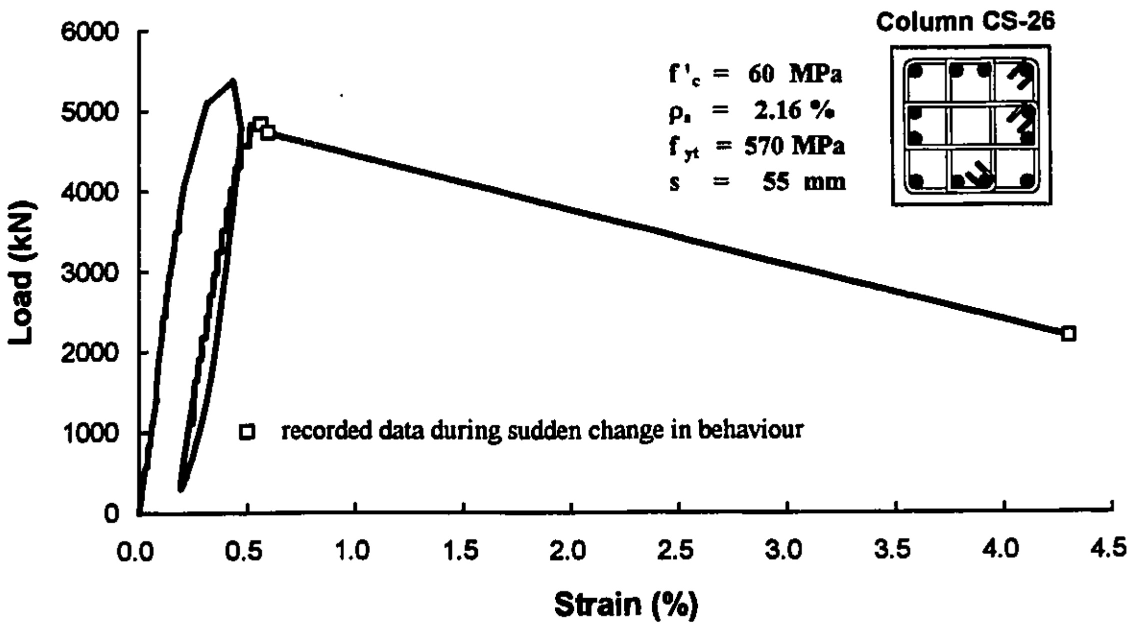

(a) Axial force-axial strain relationship.

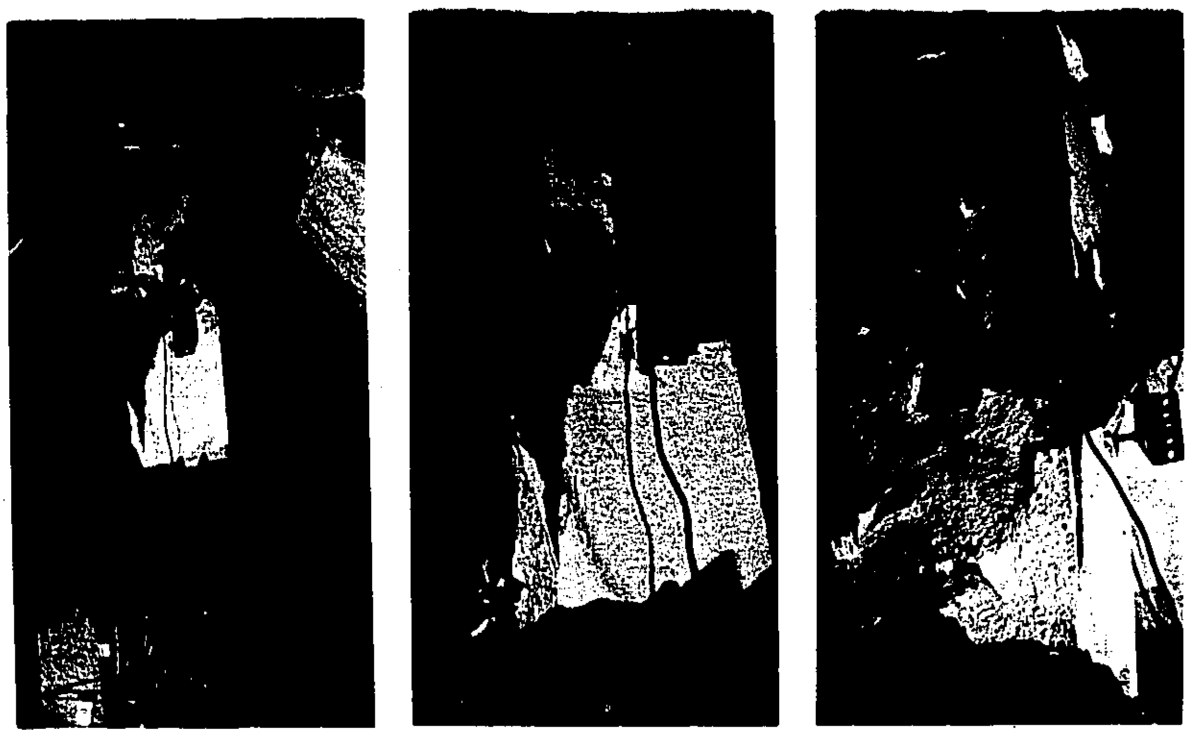

(b) Column behaviour during different stages of loading.

Figure 4.48: Column CS-26

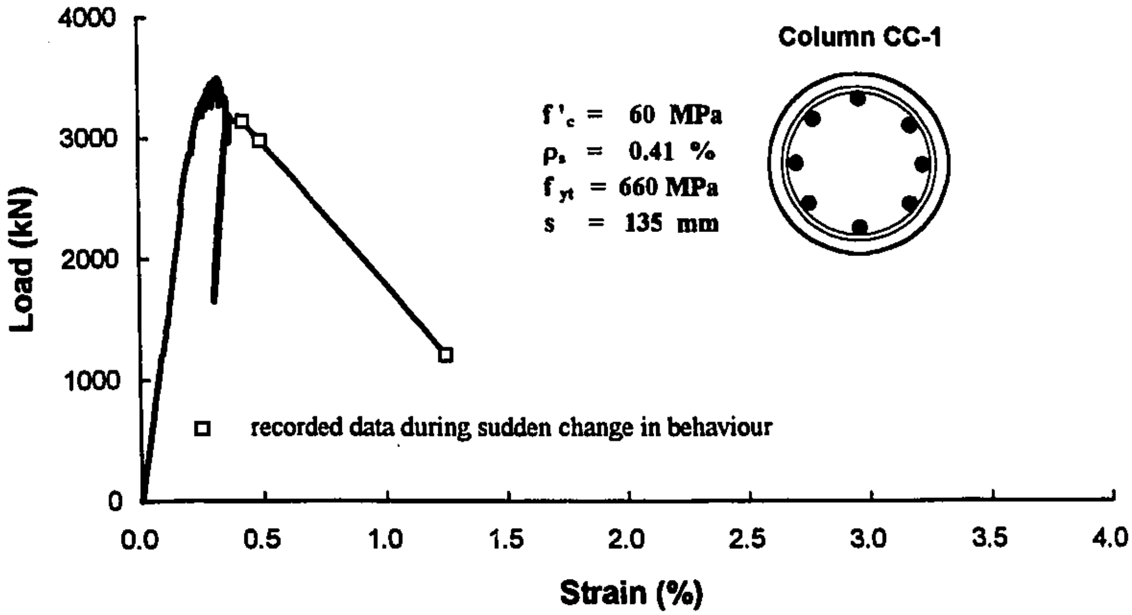

(a) Axial force-axial strain relationship.

(b) Column behaviour during different stages of loading.

Figure 4.49: Column CC-1

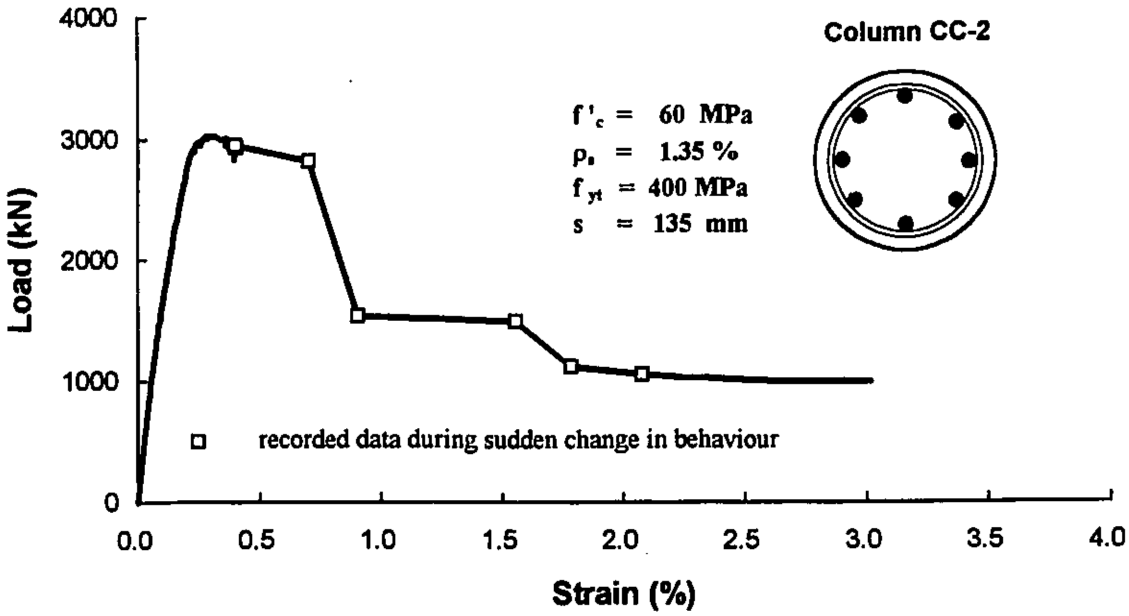

(a) Axial force-axial strain relationship.

(b) Column behaviour during different stages of loading.

Figure 4.50: Column CC-2

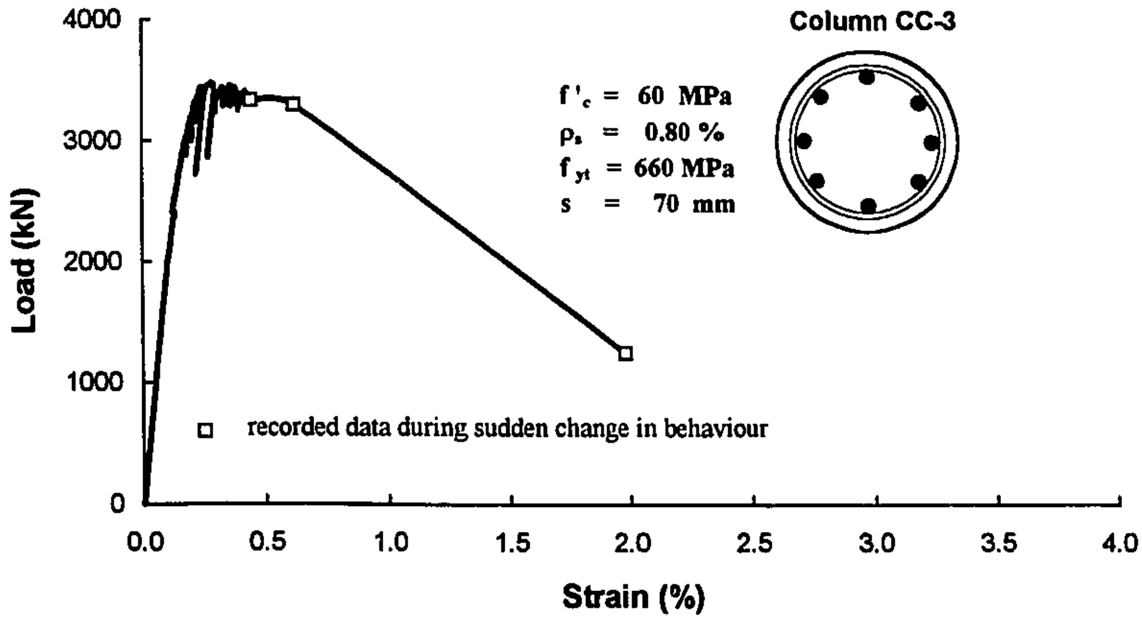

(a) Axial force-axial strain relationship.

(b) Column behaviour during different stages of loading.

Figure 4.51: Column CC-3

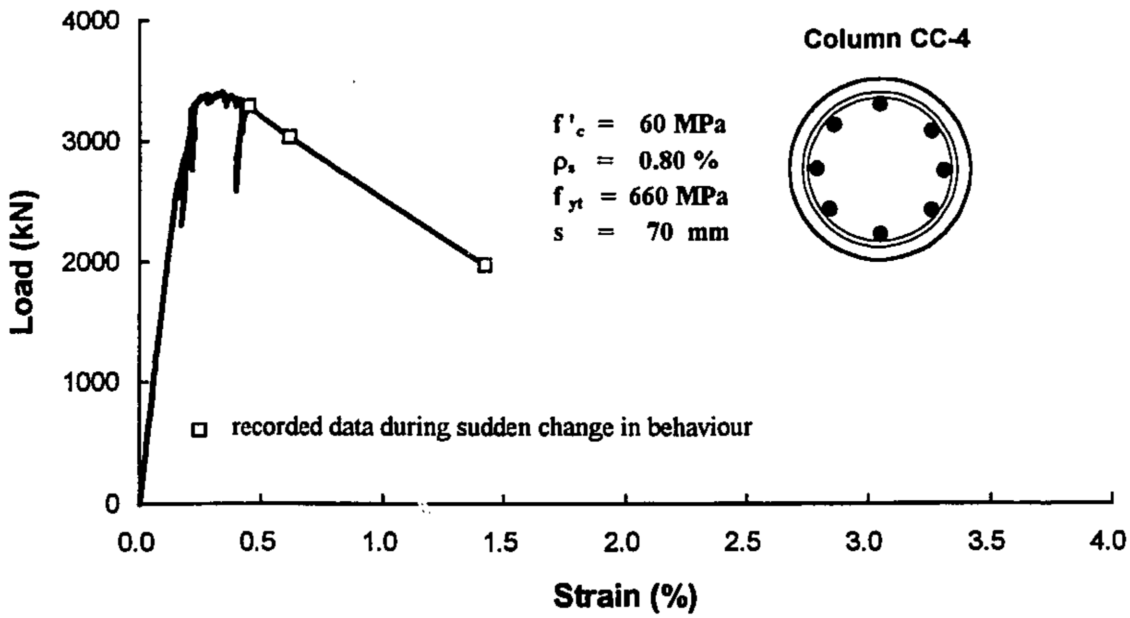

(a) Axial force-axial strain relationship.

(b) Column behaviour during different stages of loading.

Figure 4.52: Column CC-4

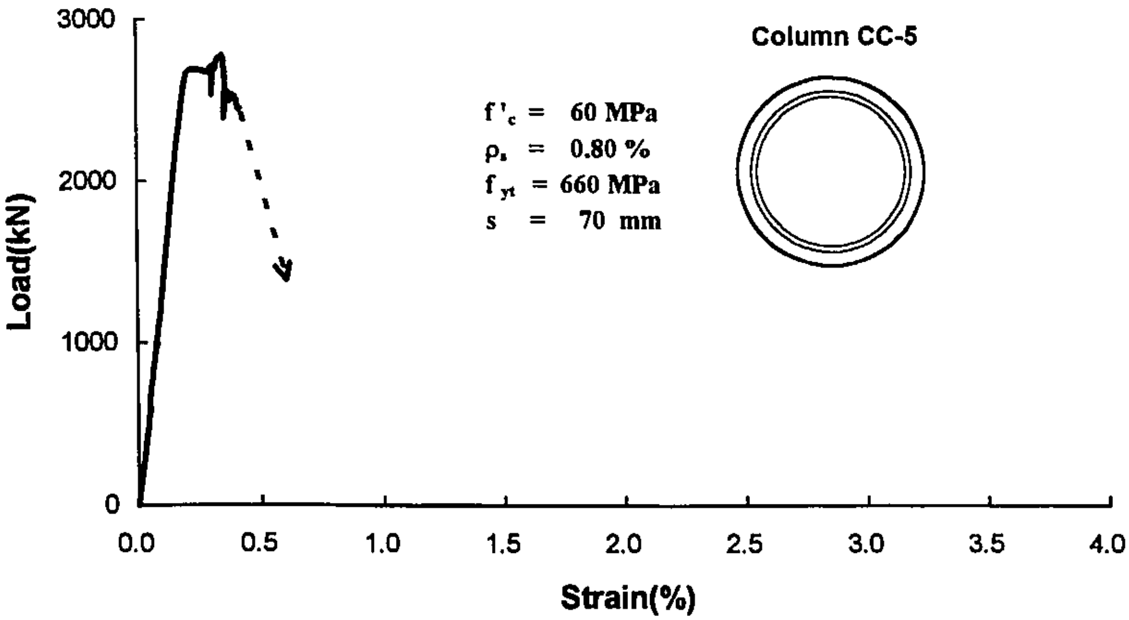

(a) Axial force-axial strain relationship.

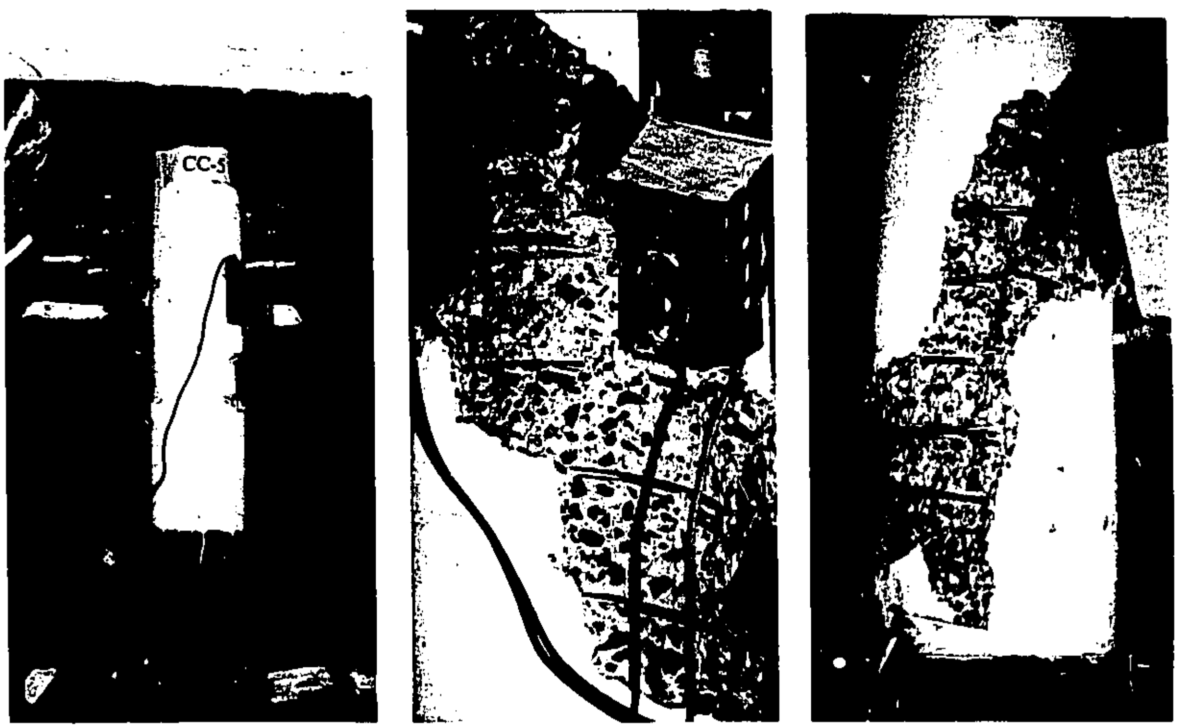

(b) Column behaviour during different stages of loading.

Figure 4.53: Column CC-5

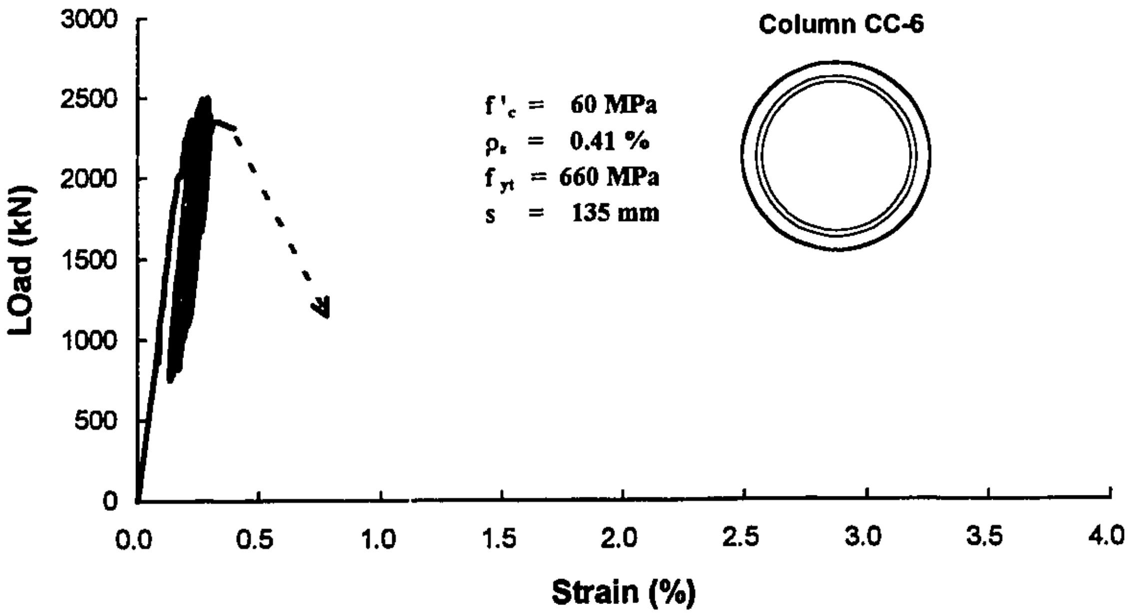

(a) Axial force-axial strain relationship.

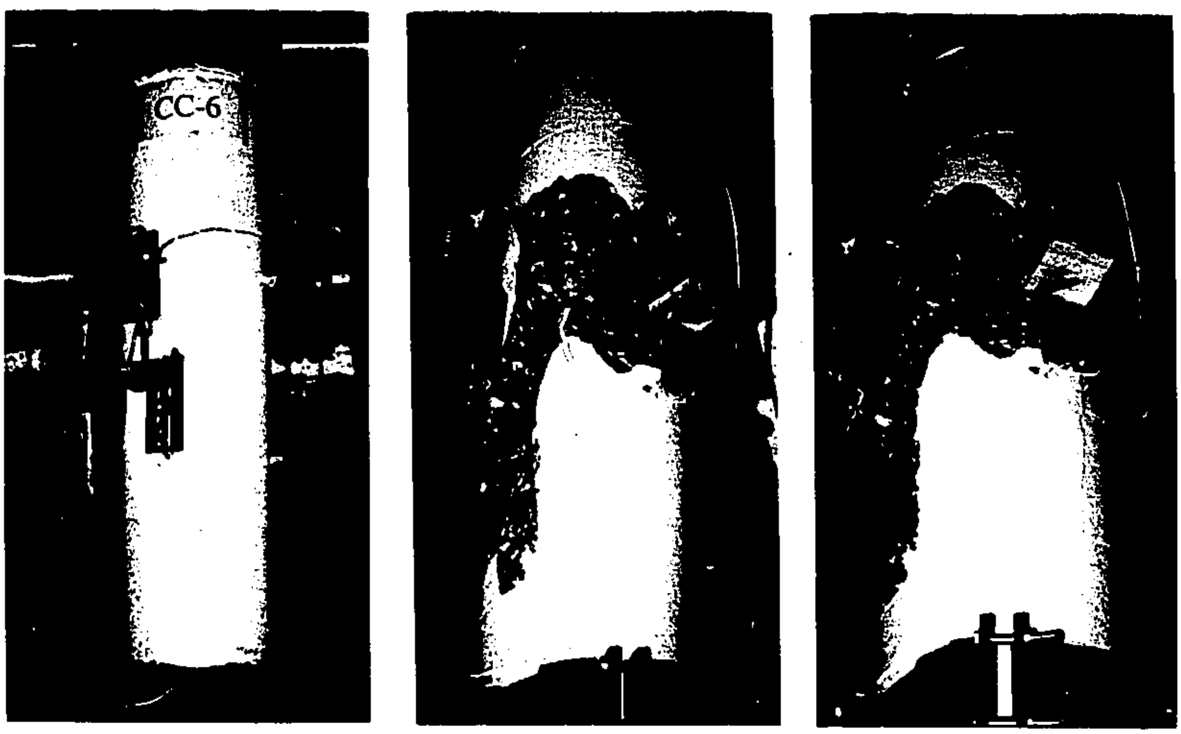

(b) Column behaviour during different stages of loading.

Figure 4.54: Column CC-6

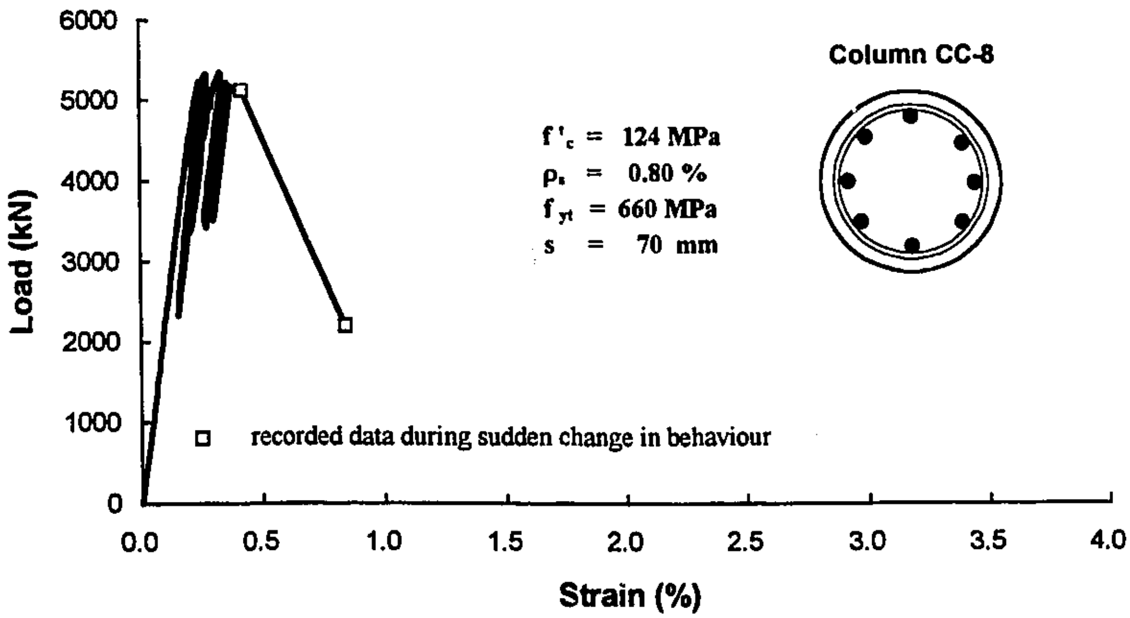

(a) Axial force-axial strain relationship.

(b) Column behaviour during different stages of loading.

Figure 4.55: Column CC-8

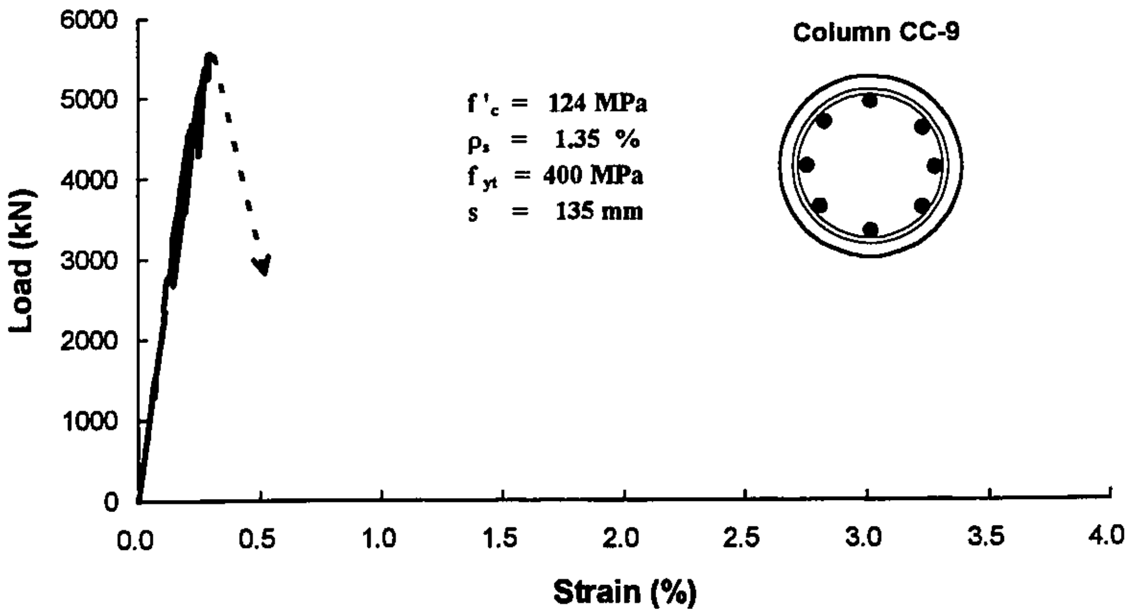

(a) Axial force-axial strain relationship.

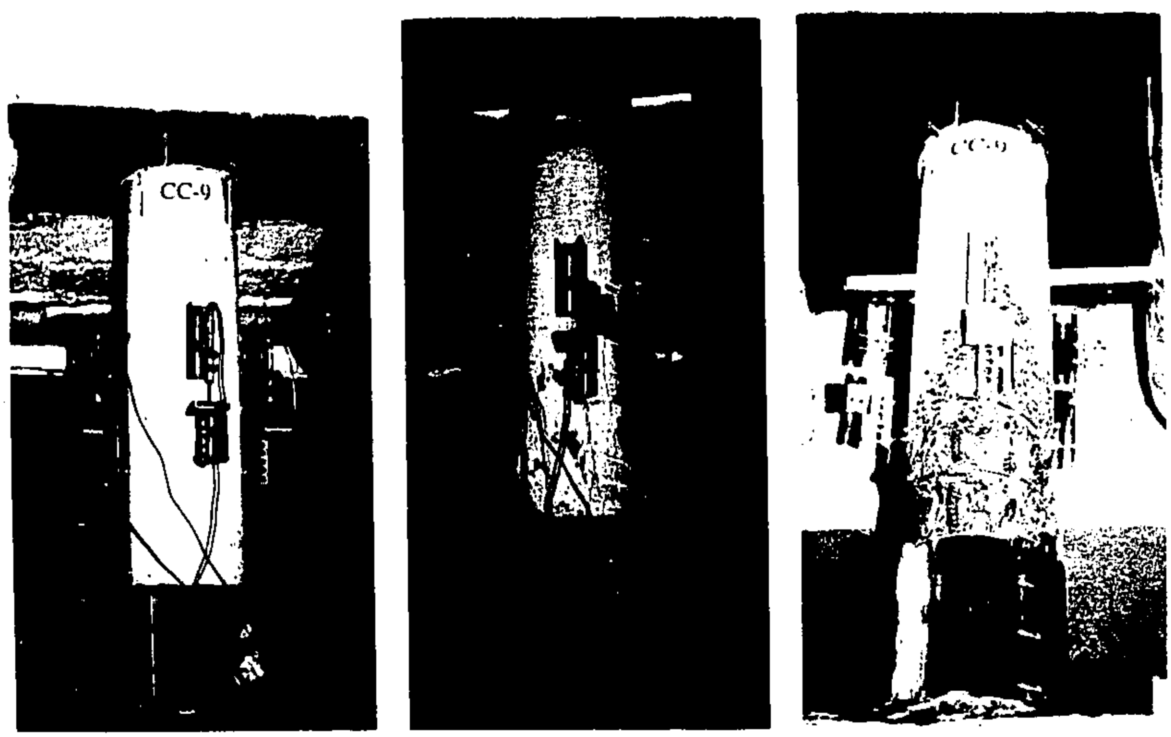

(b) Column behaviour during different stages of loading.

Figure 4.56: Column CC-9

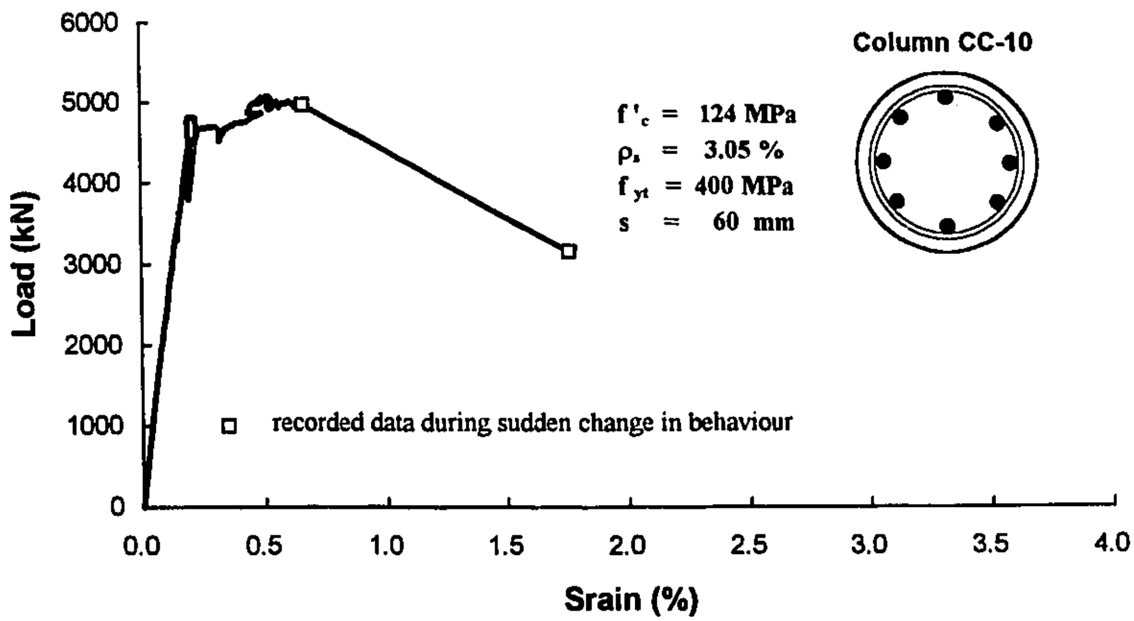

(a) Axial force-axial strain relationship.

(b) Column behaviour during different stages of loading.

Figure 4.57: Column CC-10

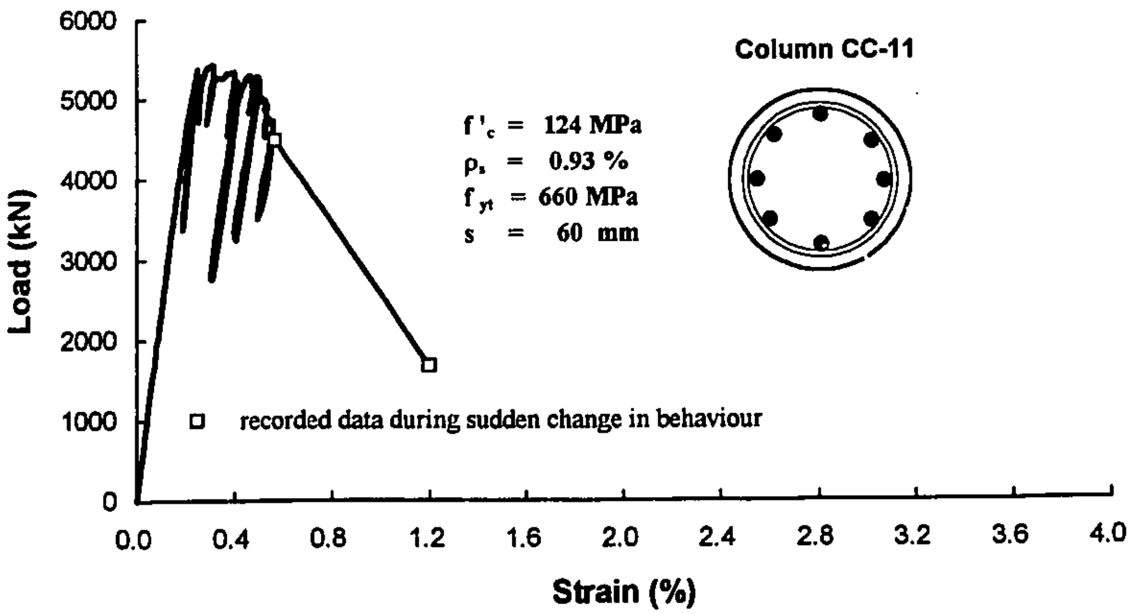

(a) Axial force-axial strain relationship.

(b) Column behaviour during different stages of loading.

Figure 4.58: Column CC-11

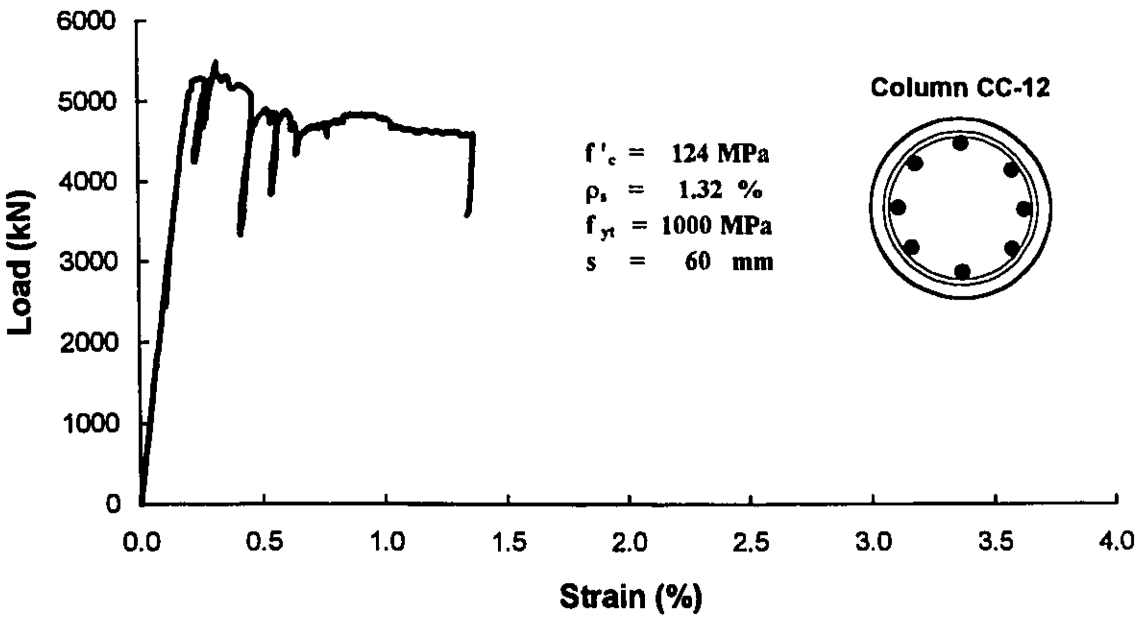

(a) Axial force-axial strain relationship.

(b) Column behaviour during different stages of loading.

Figure 4.59: Column CC-12

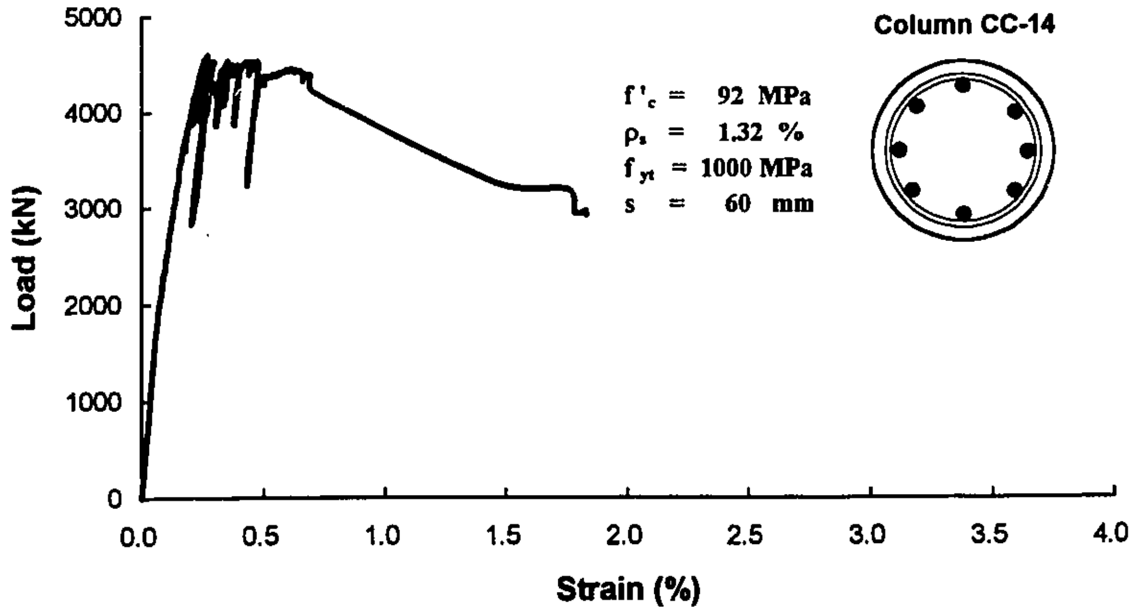

(a) Axial force-axial strain relationship.

(b) Column behaviour during different stages of loading.

Figure 4.60: Column CC-14

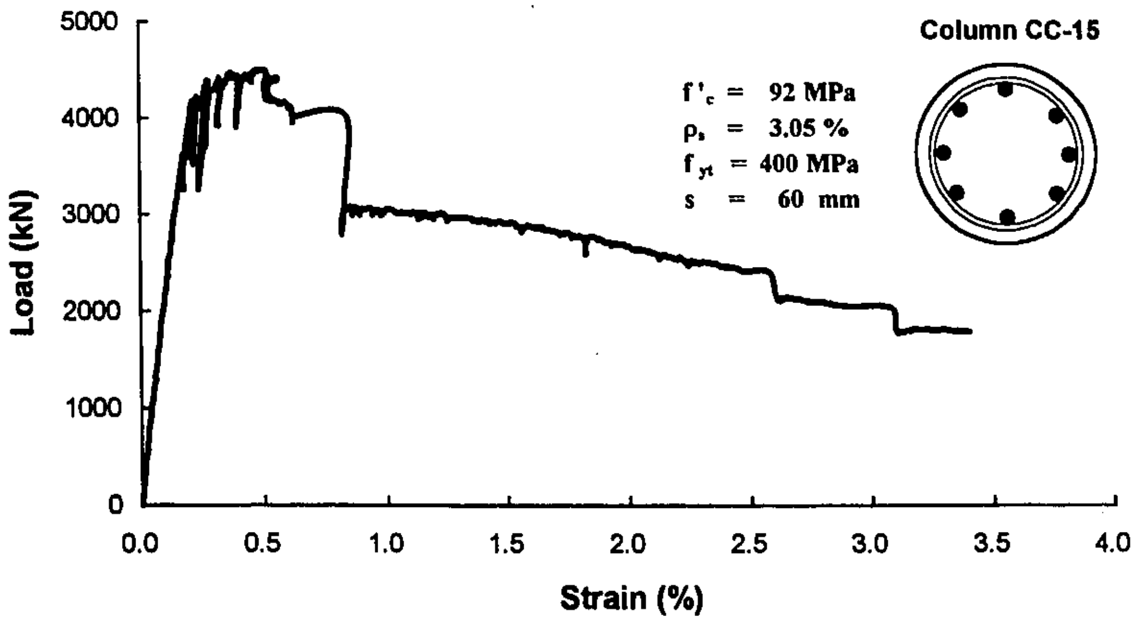

(a) Axial force-axial strain relationship.

(b) Column behaviour during different stages of loading.

Figure 4.61: Column CC-15

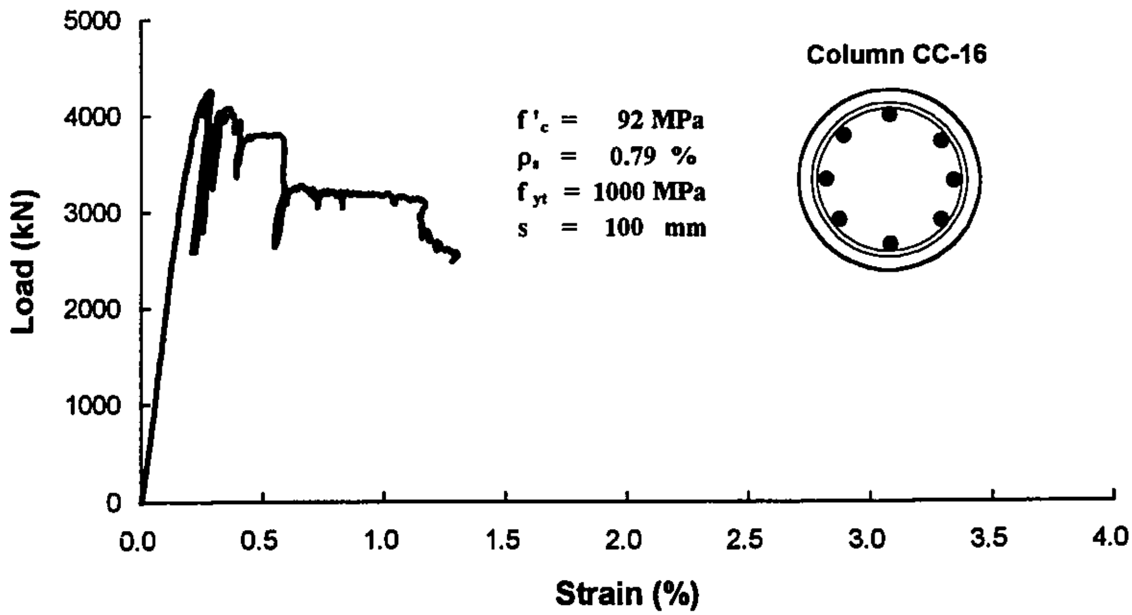

(a) Axial force-axial strain relationship.

(b) Column behaviour during different stages of loading.

Figure 4.62: Column CC-16

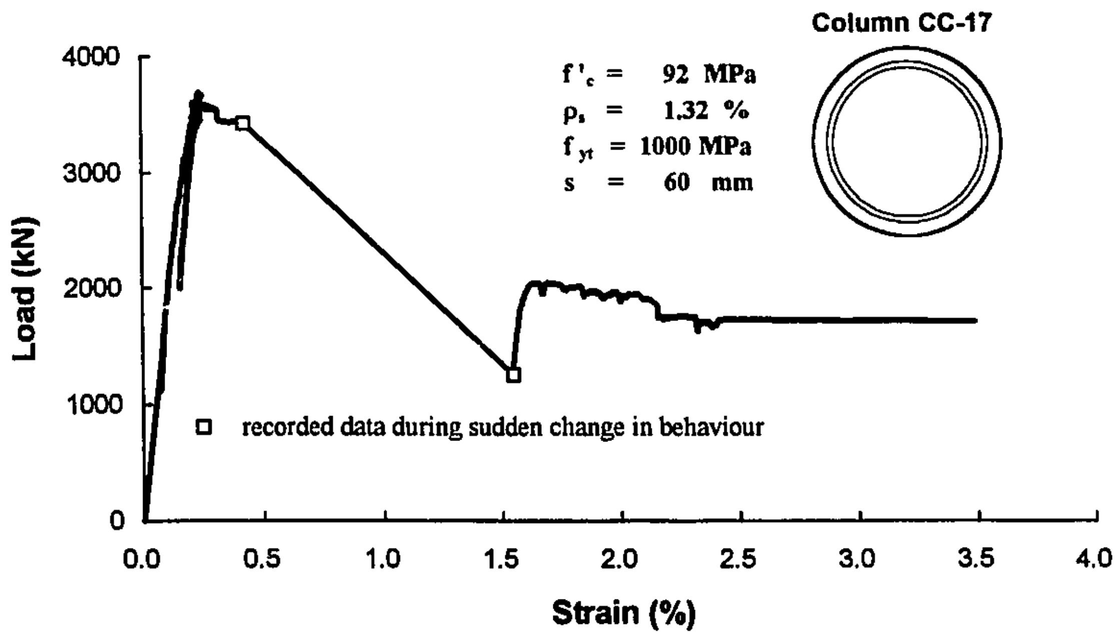

(a) Axial force-axial strain relationship.

(b) Column behaviour during different stages of loading.

Figure 4.63: Column CC-17

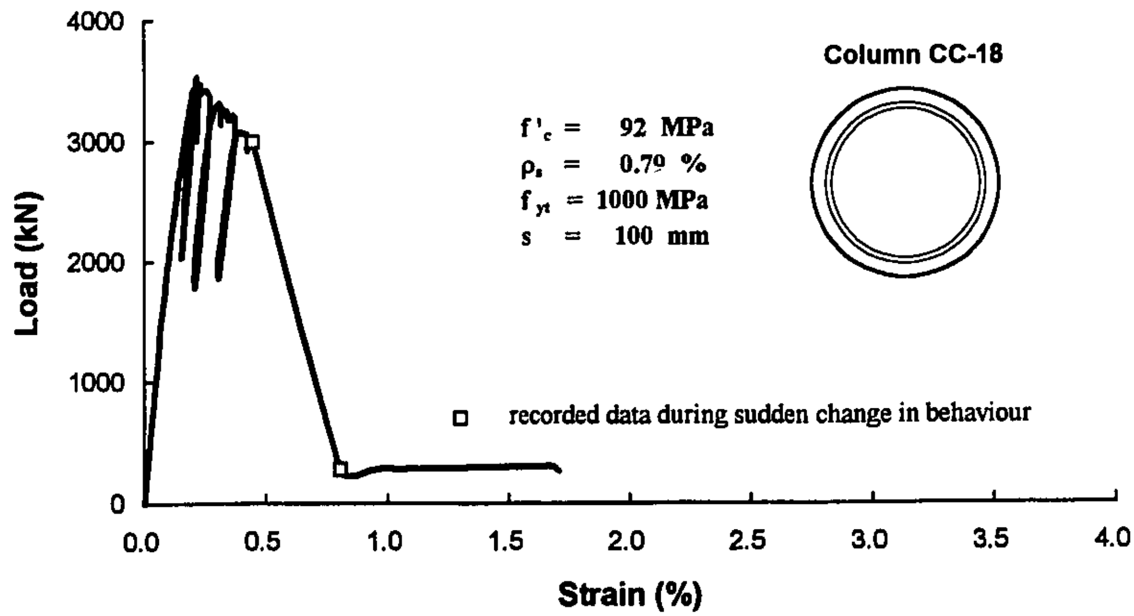

(a) Axial force-axial strain relationship.

(b) Column behaviour during different stages of loading.

Figure 4.64: Column CC-18

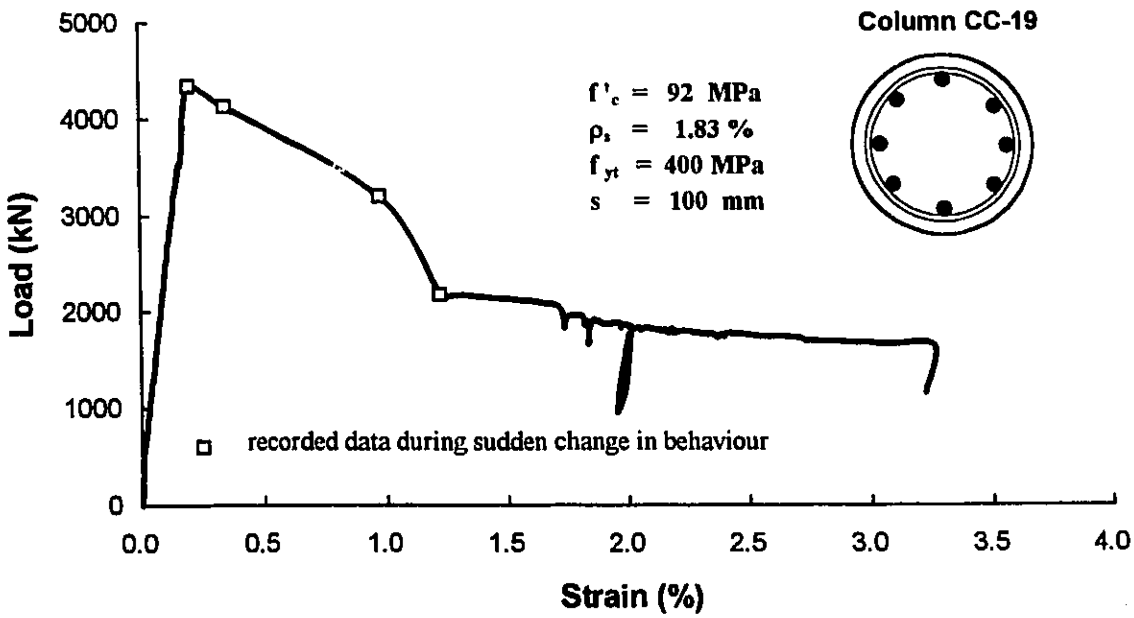

(a) Axial force-axial strain relationship.

(b) Column behaviour during different stages of loading.

Figure 4.65: Column CC-19

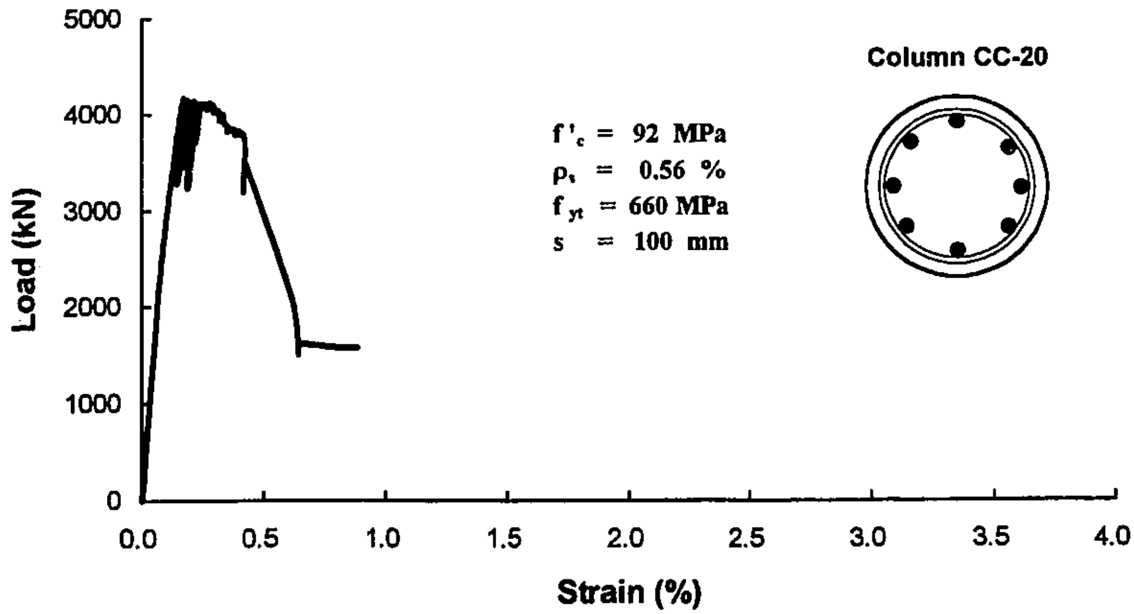

(a) Axial force-axial strain relationship.

(b) Column behaviour during different stages of loading.

Figure 4.66: Column CC-20

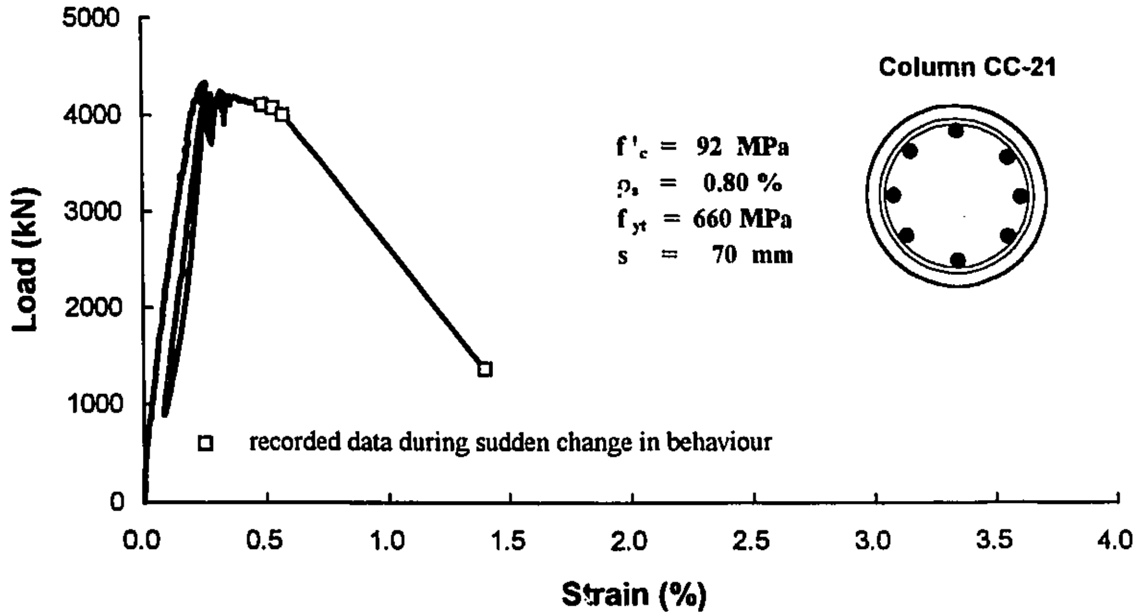

(a) Axial force-axial strain relationship.

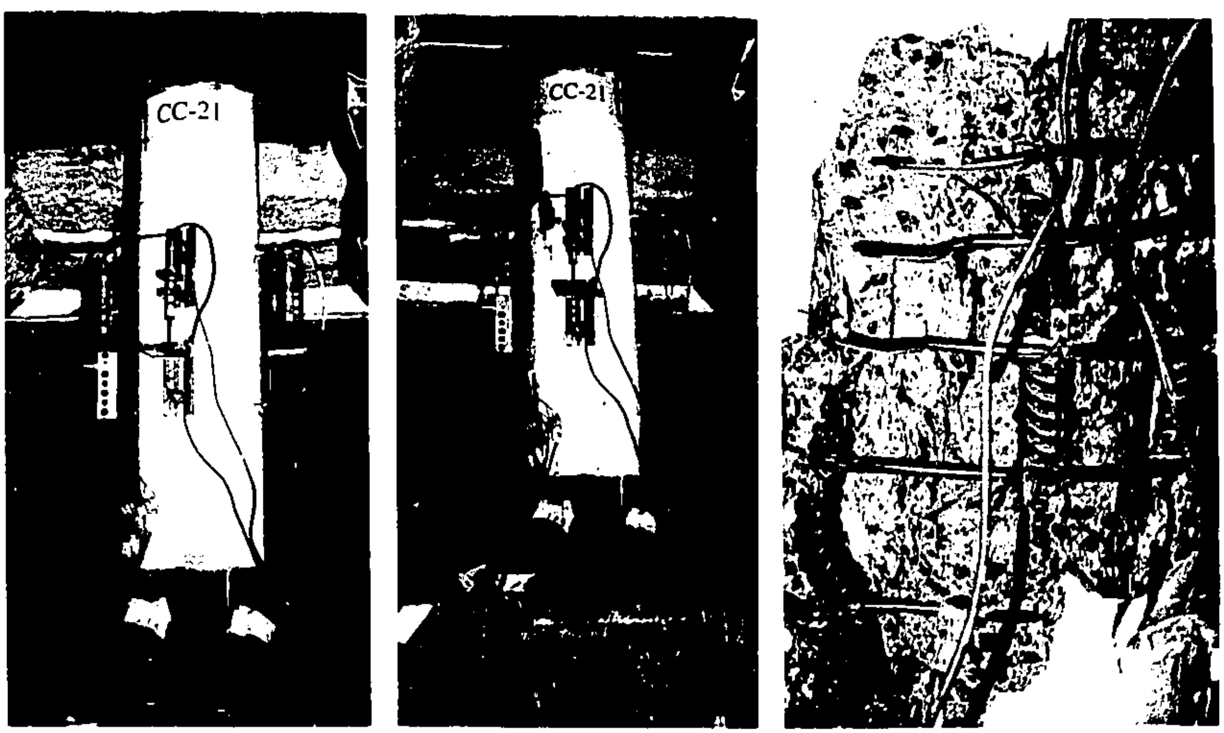

(b) Column behaviour during different stages of loading.

Figure 4.67: Column CC-21

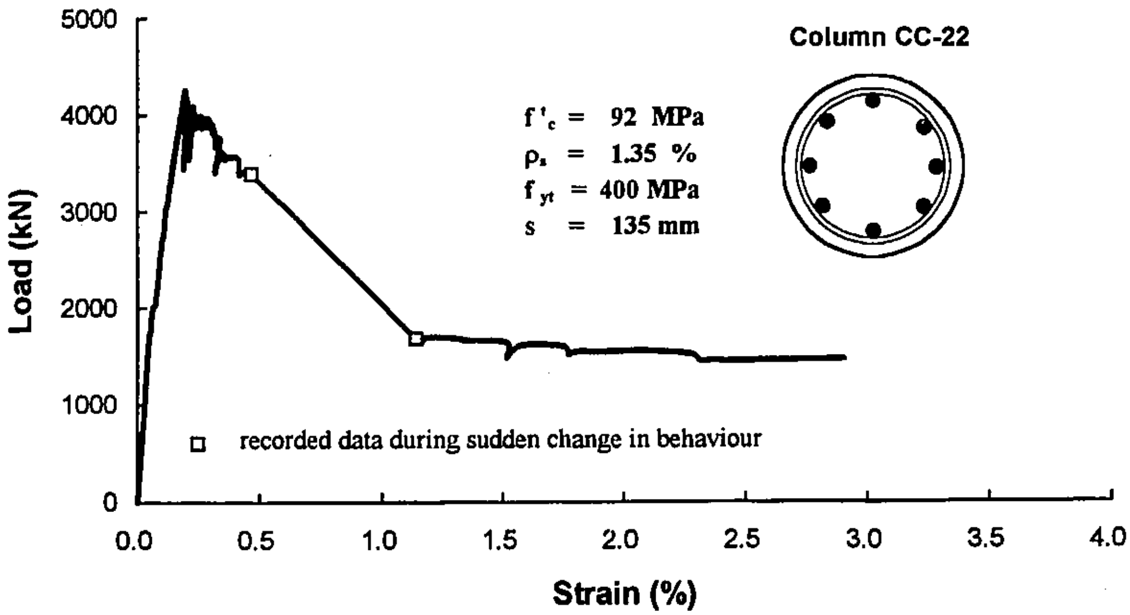

(a) Axial force-axial strain relationship.

(b) Column behaviour during different stages of loading.

Figure 4.68: Column CC-22

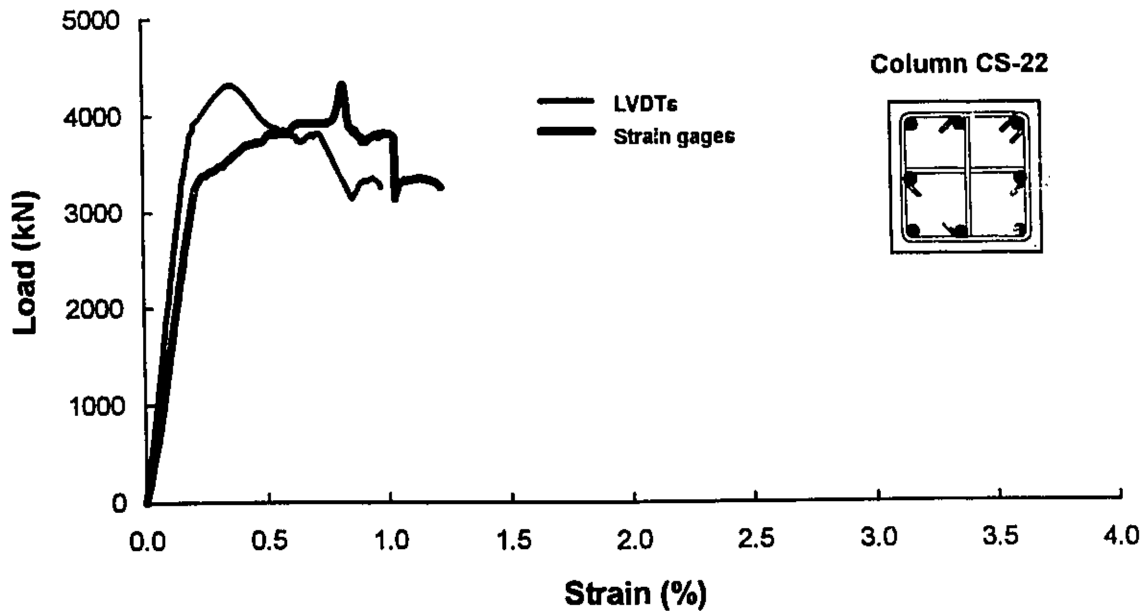

Figure 4.69: Column load versus longitudinal steel strain for column CS-22

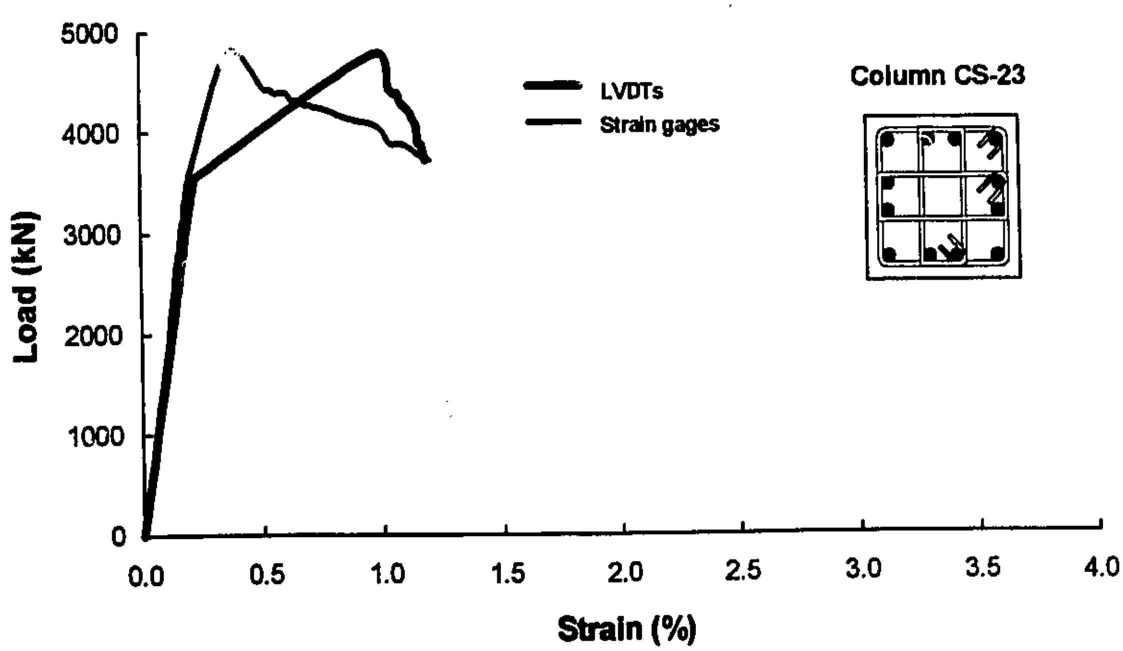

Figure 4.70: Column load versus longitudinal steel strain for column CS-23

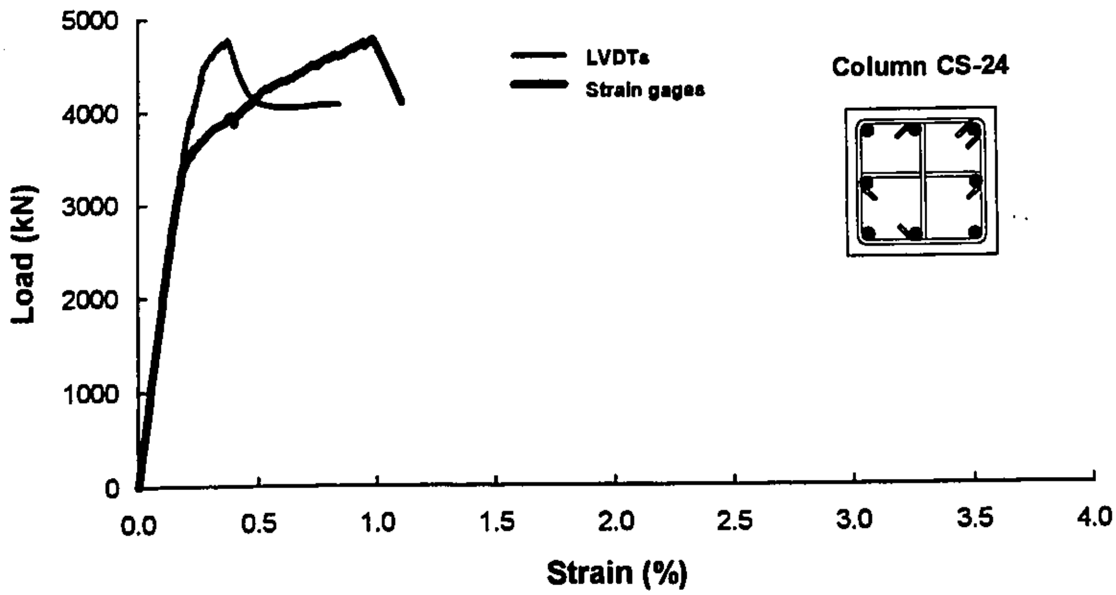

Figure 4.71: Column load versus longitudinal steel strain for column CS-24

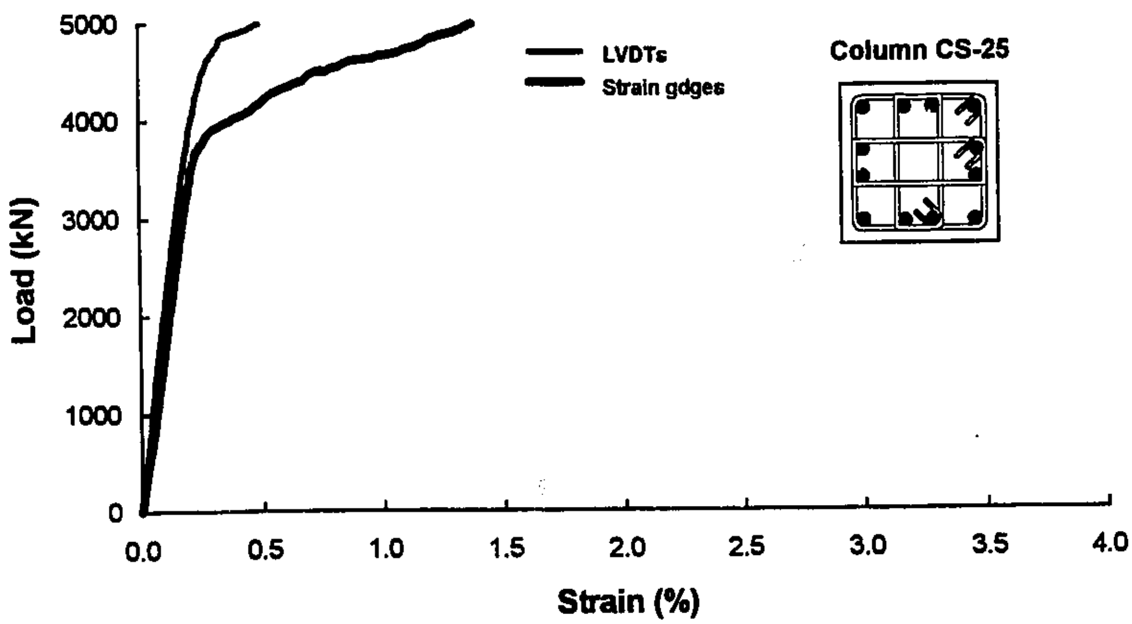

Figure 4.72: Column load versus longitudinal steel strain for column CS-25

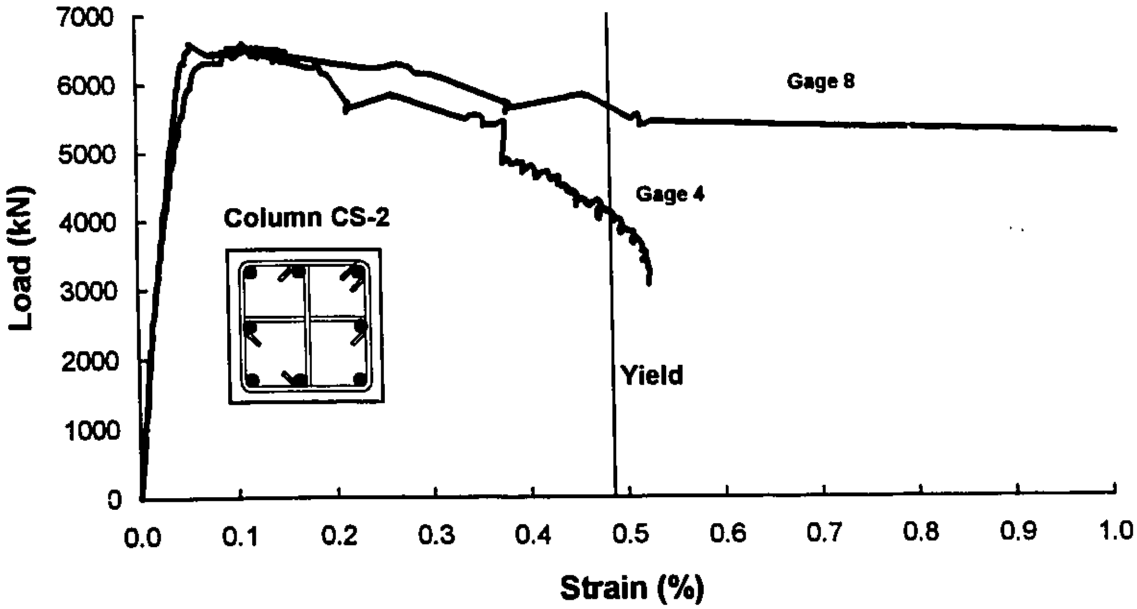

Figure 4.73: Column load versus transverse steel strain for column CS-2.

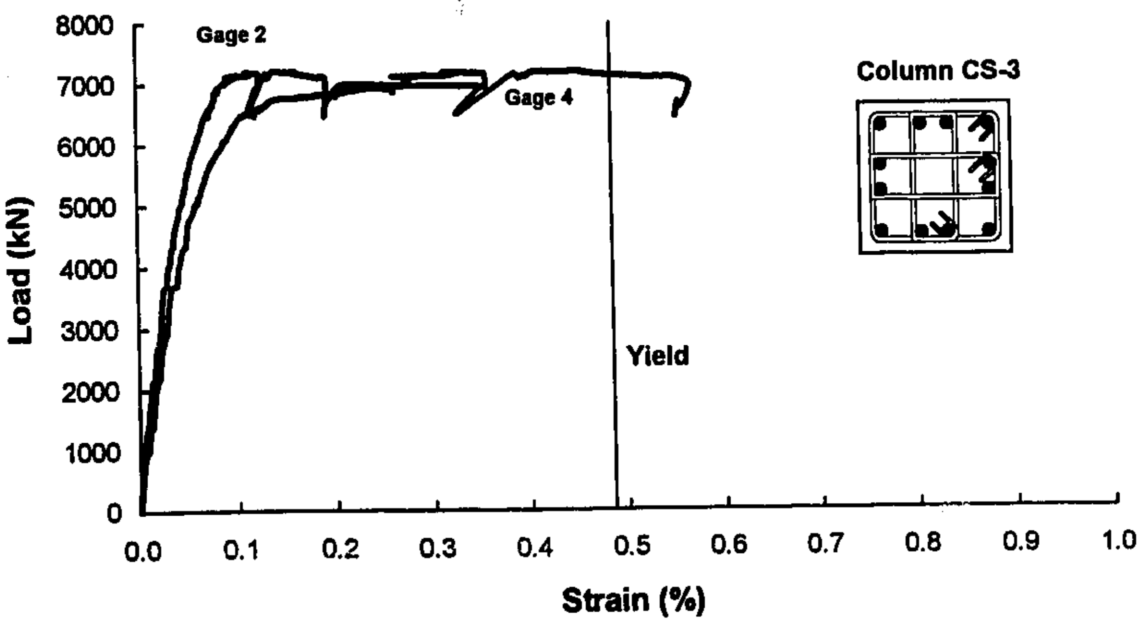

Figure 4.74: Column load versus transverse steel strain for column CS-3

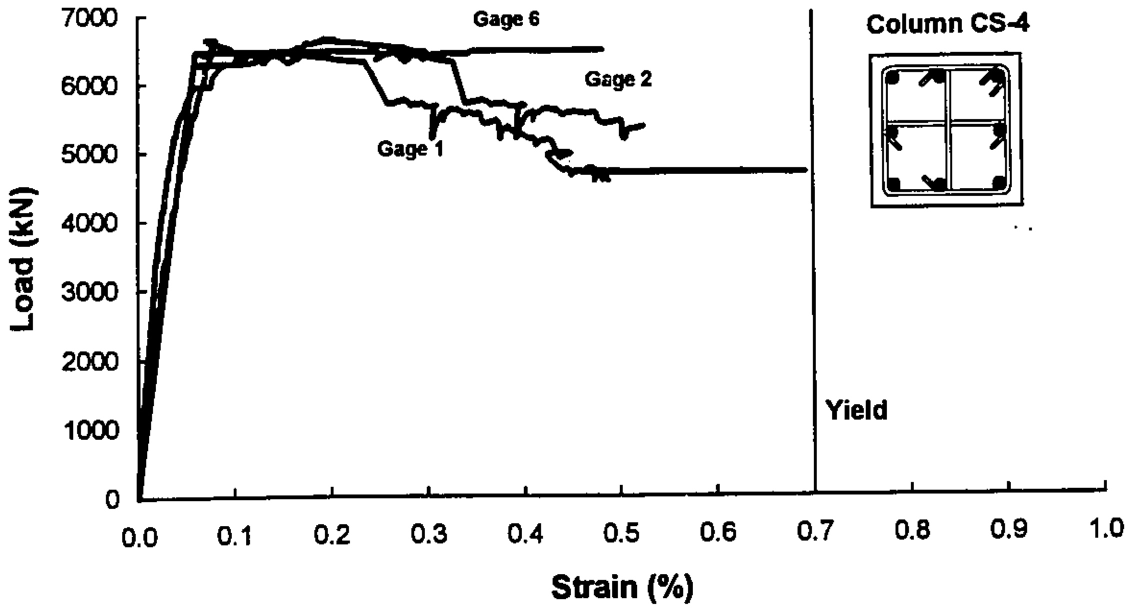

Figure 4.75: Column load versus transverse steel strain for column CS-4.

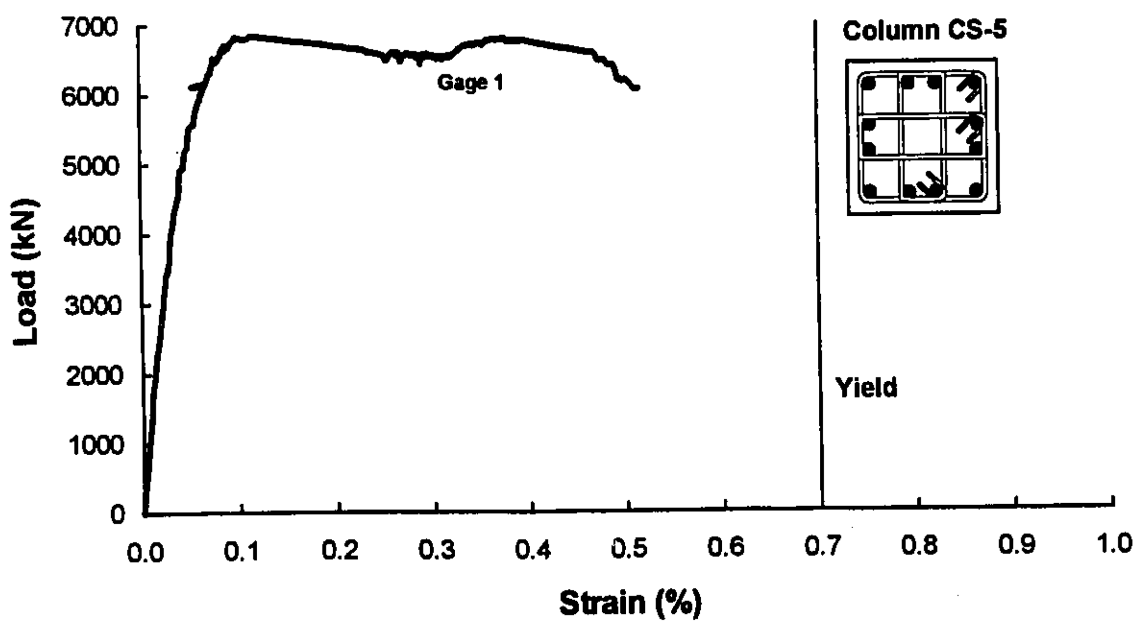

Figure 4.76: Column load versus transverse steel strain for column CS-5.

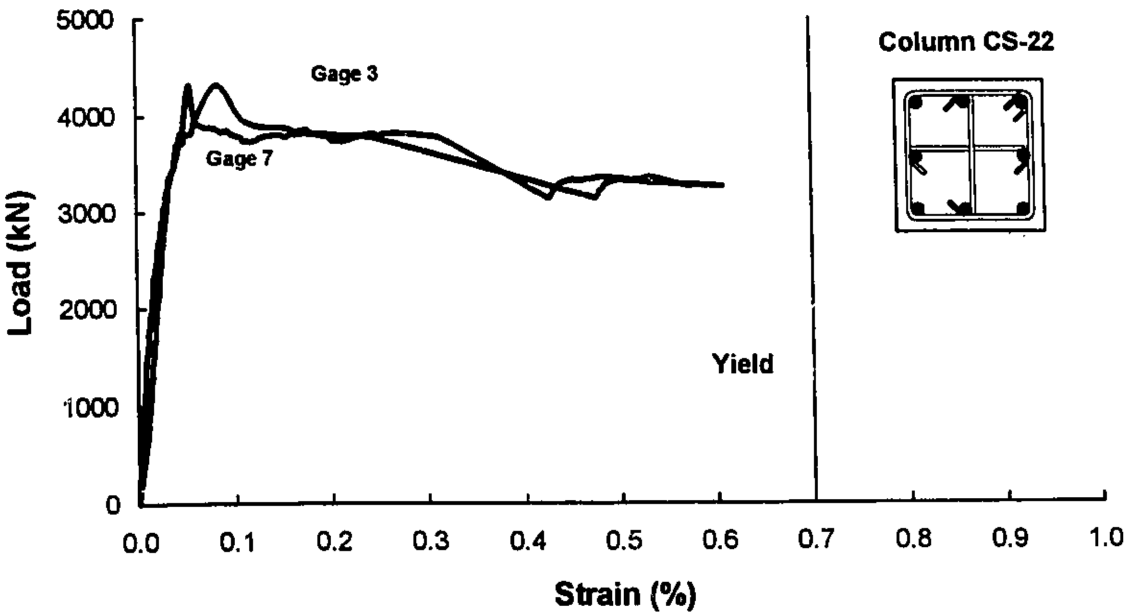

Figure 4.77: Column load versus transverse steel strain for Column CS-22.

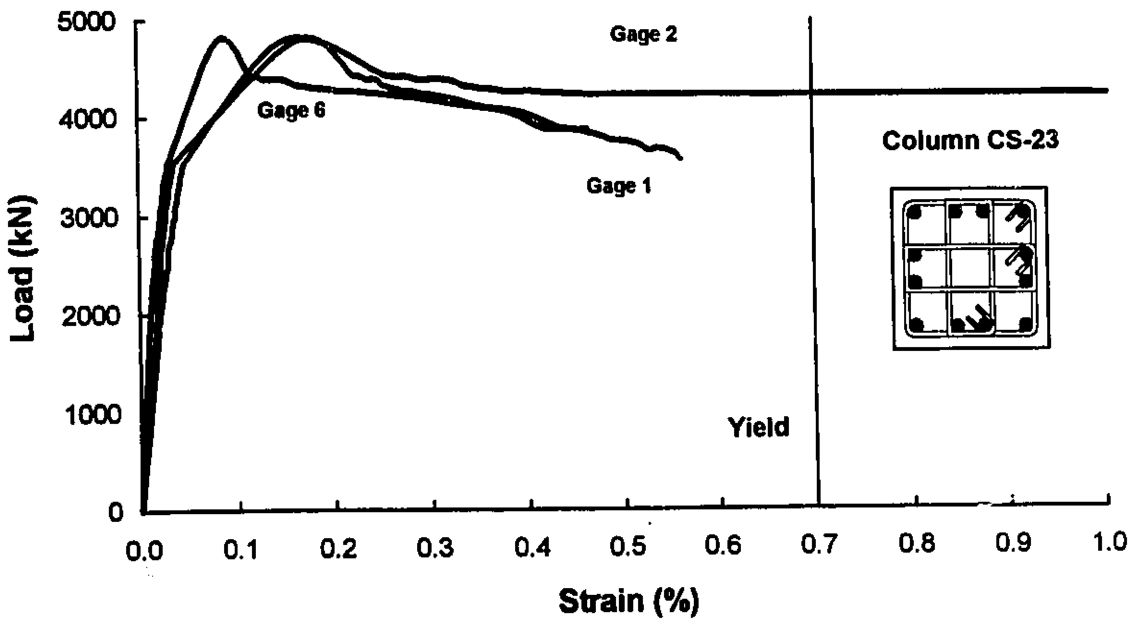

Figure 4.78: Column load versus transverse steel strain for Column CS-23.

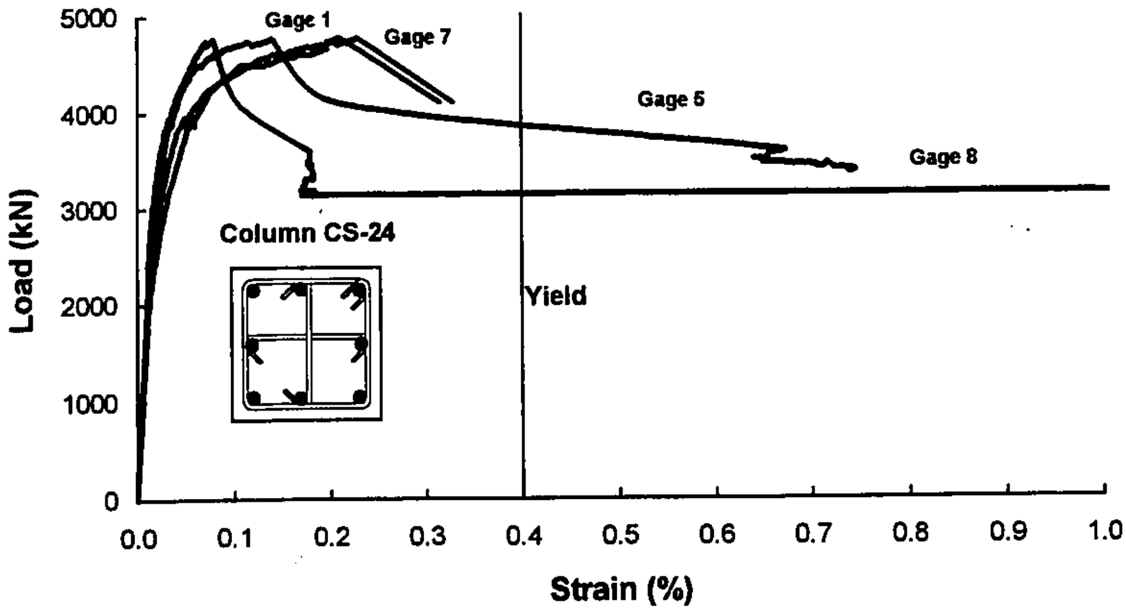

Figure 4.79: Column load versus transverse steel strain for column CS-24.

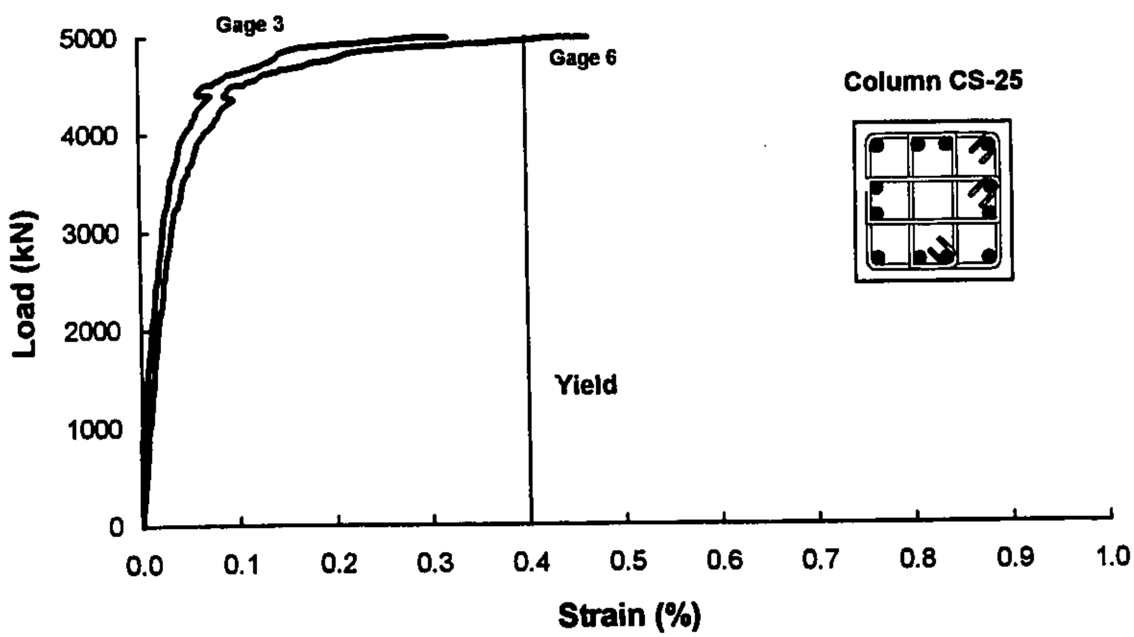

Figure 4.80: Column load versus transverse steel strain for column CS-25.

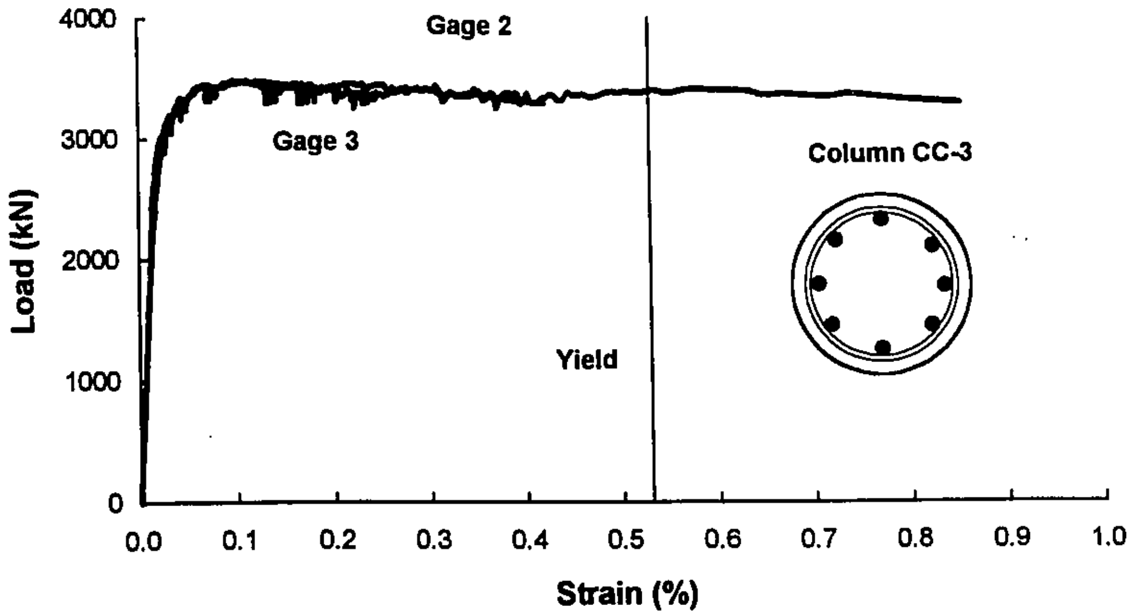

Figure 4.81: Column load versus transverse steel strain for column CC-3.

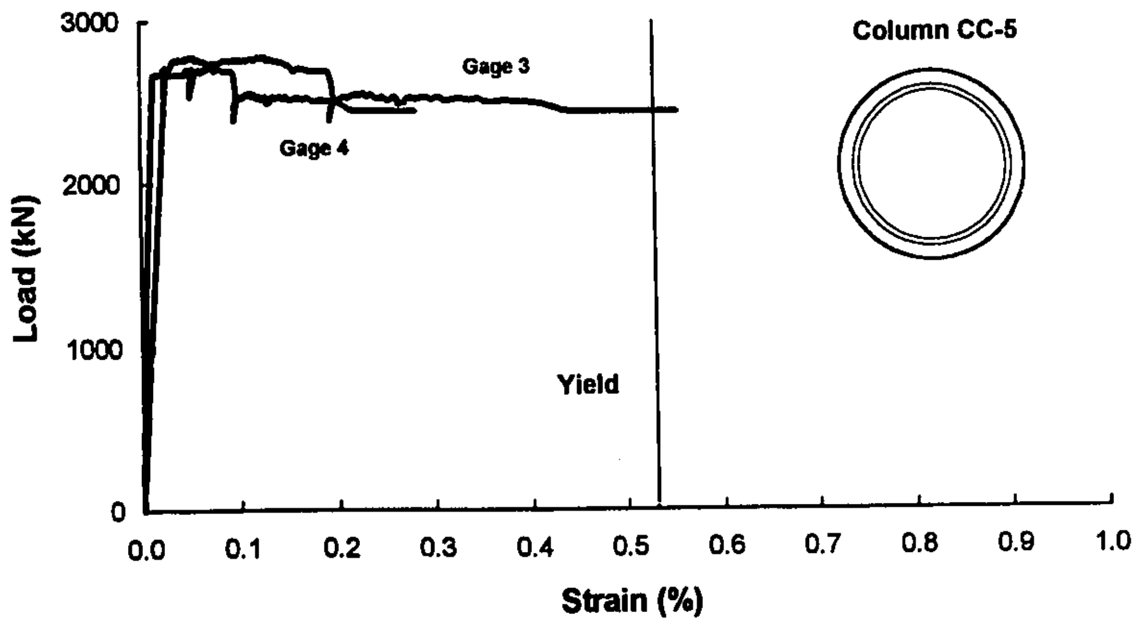

Figure 4.82: Column load versus transverse steel strain for column CC-5.

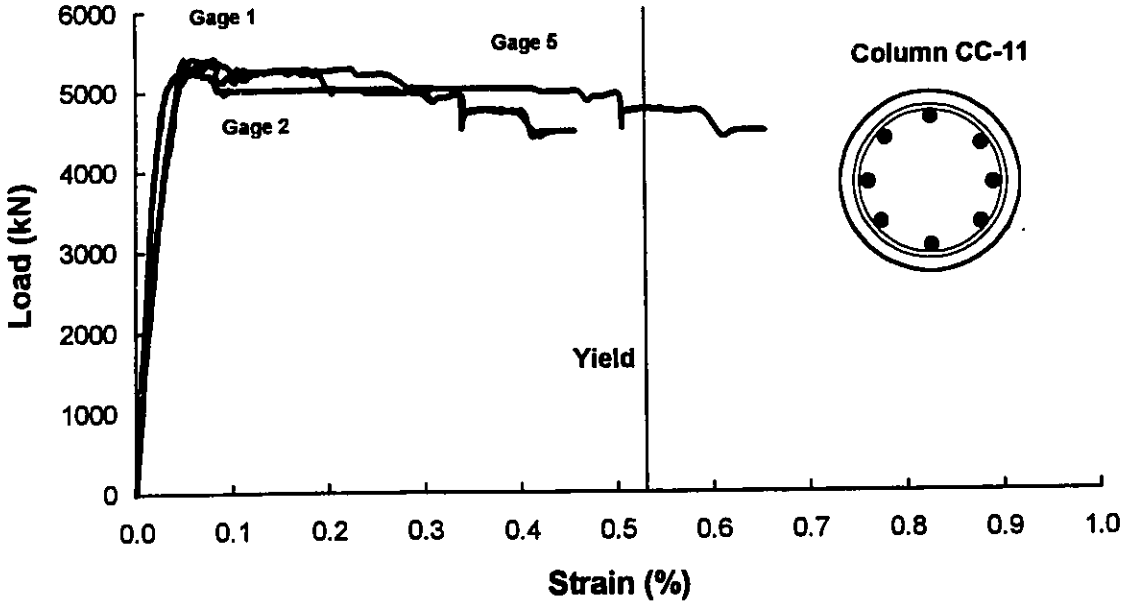

Figure 4.83: Column load versus transverse steel srain for column CC-11.

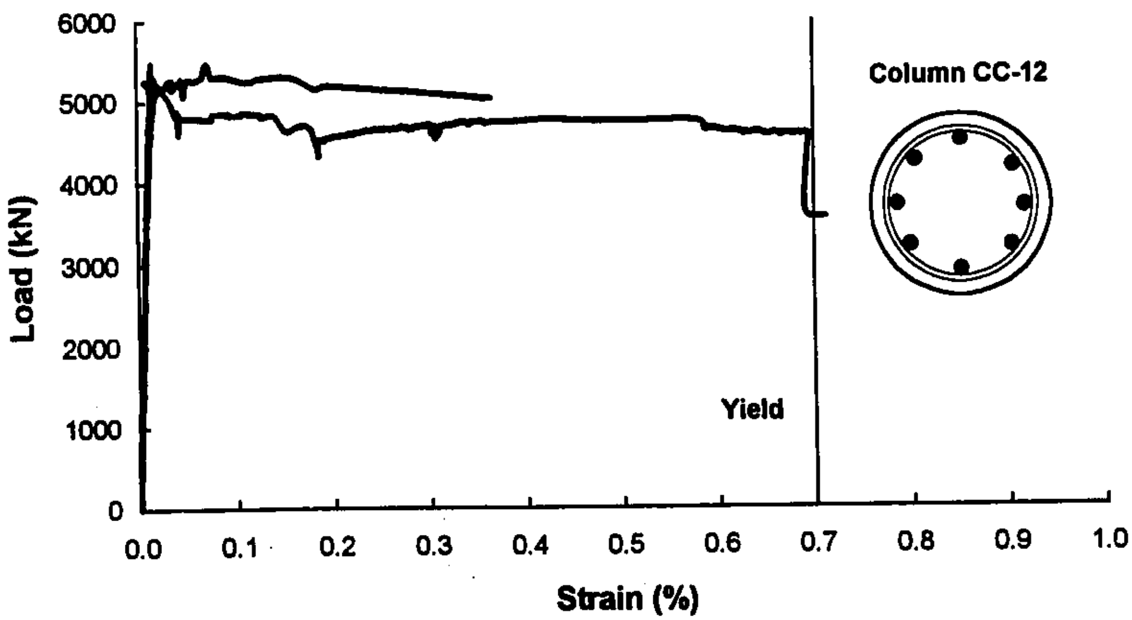

Figure 4.84: Column load versus transverse steel srain for column CC-12.

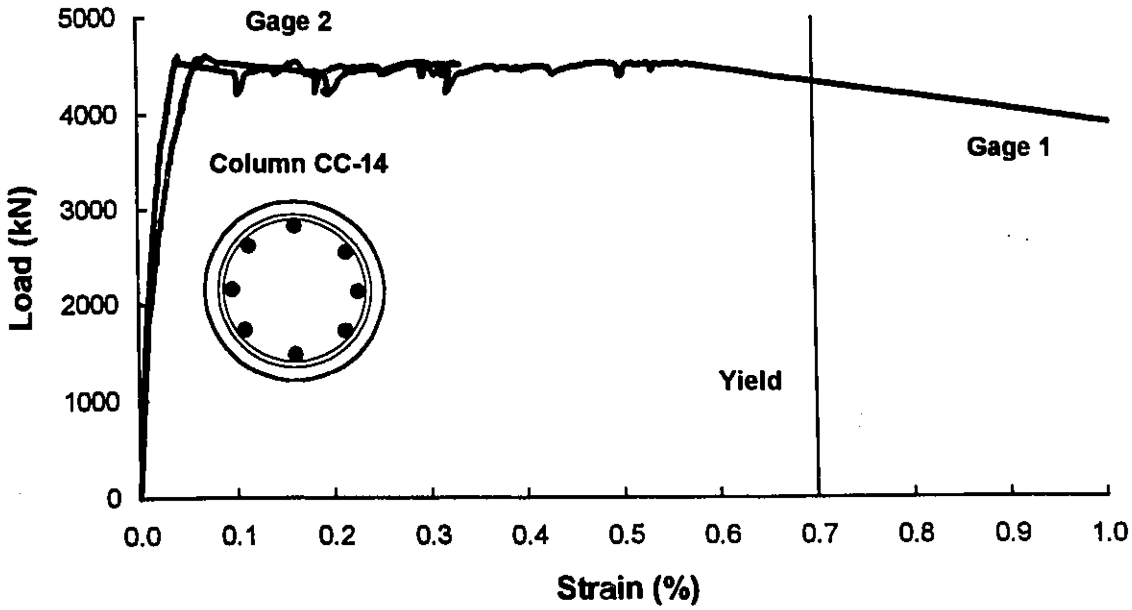

Figur 4.85: Column load versus transverse steel strain for column CC-14

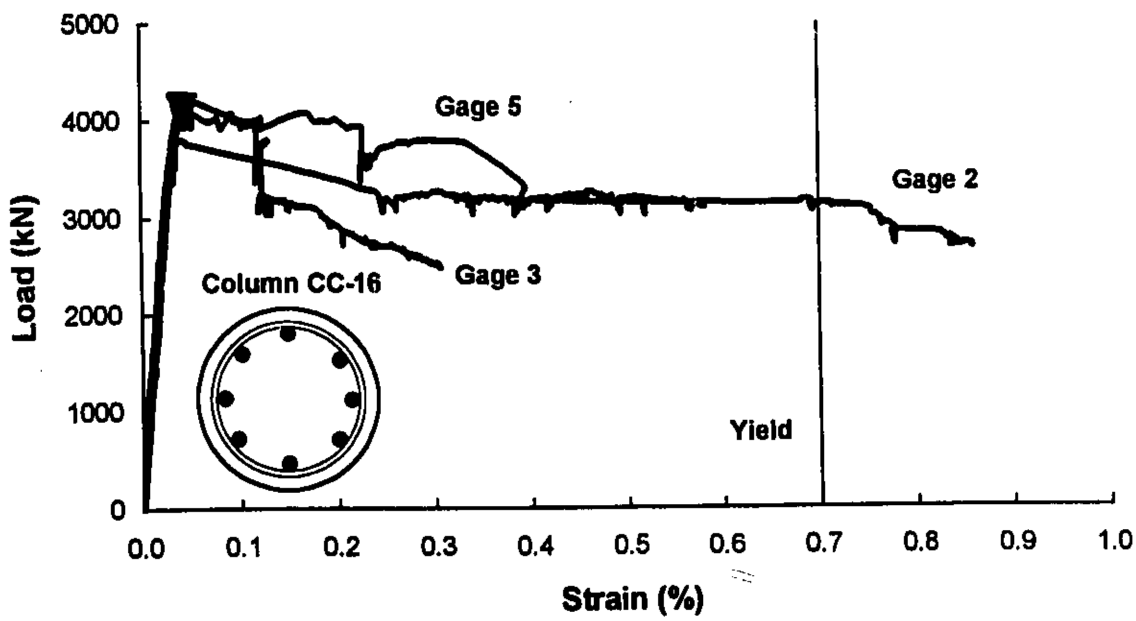

Figur 4.86: Column load versus transverse steel strain for column CC-16

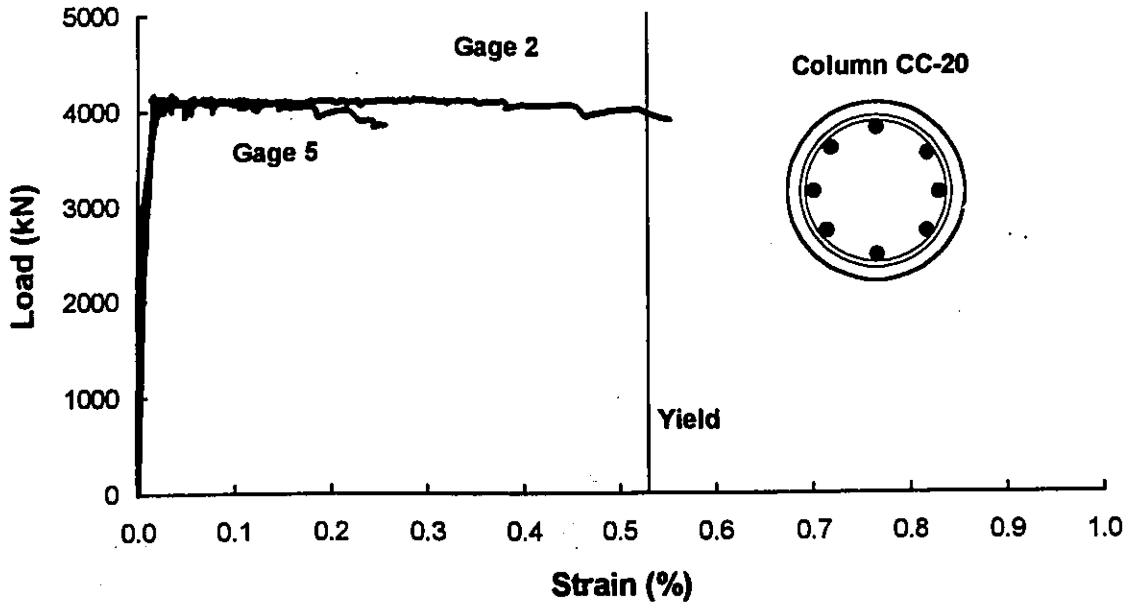

Figure 4.87: Column load versus transverse steel strain for column CC-20

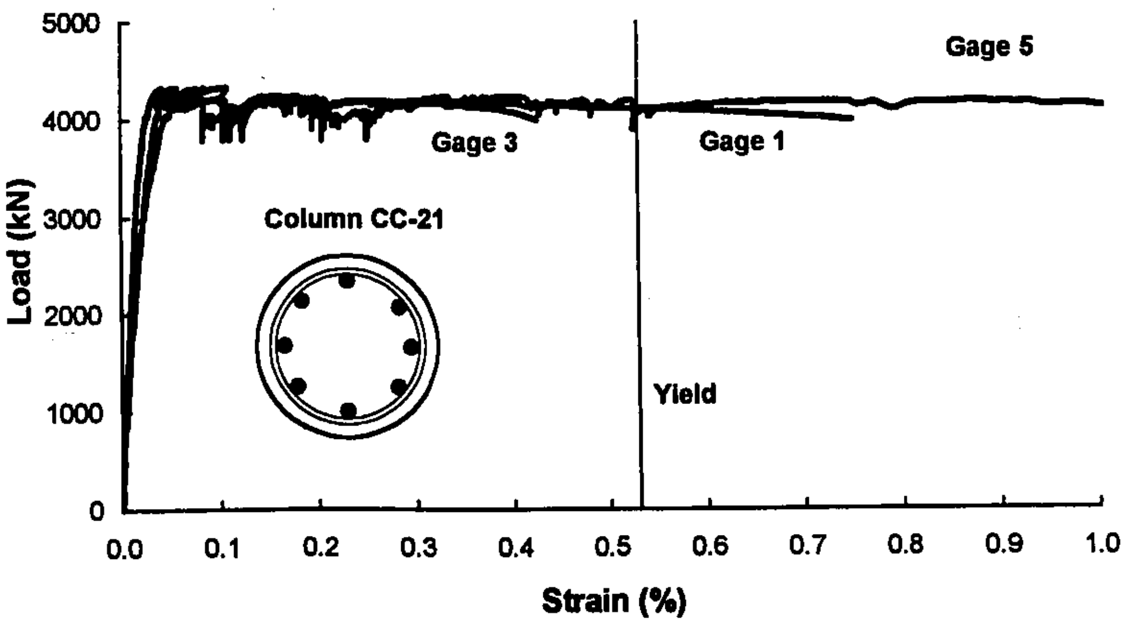

Figure 4.88: Column load versus transverse steel strain for column CC-21

Chapter 5

Analysis of Test Results

5.1 General

The test data presented in Chapter 4 was analyzed to establish strength and ductility of confined concrete in columns. This was done by computing stress-strain relationships of core concrete from recorded test data. The evaluation of test data, concentric capacities of columns, and the effects of confinement parameters are presented and discussed in this Chapter.

5.2 Evaluation of Test Data

The raw data recorded during column tests provided force-axial strain relationships for columns. This data was used to generate the stress-strain relationship of core concrete. The load carried by cover concrete and/or longitudinal reinforcement was subtracted from recorded column capacity, depending on whether the capacity was attained before or after the spalling of the cover concrete, to obtain load resisted by the core concrete. The following assumptions were made for this purpose:

- Strain in longitudinal steel was assumed to be equal to that of the surrounding concrete.

- A bilinear stress-strain relationship was assumed for longitudinal reinforcement, ignoring the strain hardening of steel. This was found justifiable in light of the experimental data that indicated bending and/or buckling of longitudinal bars either prior to, or shortly after the onset of strain hardening.
- It was assumed that the effect of confinement was negligibly small up to a certain level of axial strain that depended on concrete strength. These limiting strains were assumed to be 0.15%, 0.17%, 0.18%, and 0.20% for 124 MPa, 92 MPa, 81 MPa, and 60 MPa concretes, respectively. Therefore, the core and cover concretes were assumed to behave in a similar manner up to these limiting strains, with total cross-sectional area of concrete providing full resistance to applied loading. This assumption is consistent with the experimental observations discussed in Section 5.3.
- Concrete cover was assumed to spall off completely beyond a certain level of axial strain that depended on concrete strength. This strain level was assumed to be 0.25%, 0.30%, 0.35% and 0.50% for 124 MPa, 92 MPa, 81 MPa, and 60 MPa concretes, respectively. This assumption is consistent with the experimental observations discussed in Section 5.3.
- Gradual spalling of cover concrete was assumed between the two limiting values of axial strains specified above.

Stress-strain relationships of core concrete, computed from experimental data, are used in Sec. 5.5 to evaluate the effects of test parameters. They are also presented in Chapter 7 for comparison with analytical predictions.

5.3 Evaluation of Column Strength

Column strength under concentric loading was recorded during testing. Experimental observations indicated that cover spalling had occurred in most cases prior to the attainment of the load capacity. In these columns, the maximum load was resisted by the core concrete, including the contribution of longitudinal reinforcement. Columns with well confined core were able to resist loads higher than those computed based on gross cross-sectional area and unconfined concrete strength. However, those that did not have sufficient confinement were not able to develop unconfined column capacities based on total cross-sectional area and unconfined concrete strength. Tables 5.1 and 5.2 contain recorded strengths of square and circular columns, respectively. The tables also contain nominal concentric capacity (P_o), computed by Eq. 5.1, following the requirements of current building codes (ACI 318-89, CSA A23.3, 1984). Figure 5.1 illustrates the variation of strength gain in columns with concrete confinement.

$$P_o = 0.85 f'_c \ (A_g - A_s) + A_s f_y \tag{5.1}$$

The load resistance provided by concrete, and the core concrete alone, are included in Tables 5.1 and 5.2, as computed below.

$$P_{oc} = 0.85 f'_c \ (A_g - A_s) \tag{5.2}$$

$$P_{occ} = 0.85 f'_c \ (A_{co} - A_s) \tag{5.3}$$

Tests of plain concrete columns, discussed in Chapter 4, showed that the in-place strength of concrete (unconfined) in columns varied between 89% and 92% of strength determined by a standard cylinder test (f'_c). This implies that 0.85 f'_c may be used conservatively to represent the in-place strength of unconfined concrete in columns, as commonly done for concretes in the normal-strength range. The in-place strength of high-strength concrete, however, appears to be closer to the cylinder strength than that of normal strength concrete.

Strength enhancement due to confinement was established by comparing strengths of core and unconfined concretes. The core capacity was established by subtracting the contribution of cover concrete and/or longitudinal reinforcement from the recorded column capacity, as discussed in Sec. 5.2. The ratios of confined to unconfined concrete strengths are listed in Tables 5.1 and 5.2 for square and circular columns, respectively. These ratios range between 1.09 and 1.50 for confined square columns, and 1.06 and 1.35 for circular columns, indicating up to 50 % and 35 % increase in concrete strength due to confinement.

The test data was re-examined to assess concentric capacities of columns, and the influence of cover spalling. The strain data indicated that the premature spalling of cover concrete had occurred in columns with very high strength concretes, prior to the development of strains associated with concrete crushing. This observation, combined with visual observations of cover spalling during testing suggested that the cover concrete suffered stability failure under high compressive stresses. Fig. 5.2 illustrates cover spalling typically observed in columns. It was hypothesized that the presence of closely spaced longitudinal and transverse reinforcement, forming a mesh of reinforcement, produced a natural plane of separation between the cover and the core. The separation of this plane was triggered by high compressive stresses and the differences in behaviour between the core and cover concretes. Early spalling of the cover concrete resulted in lower capacities than those computed using Eq. 5.1, for those columns where the strength enhancement in the core was not sufficient to make-up for the loss of cover. Beginning of cover spalling was visually observed and marked during testing. Accordingly, the initial signs of cover spalling began at approximately 0.15% to 0.30% for 124 MPa, 0.12 % to 0.25% for 92 MPa, 0.18% to 0.29% for 82 MPa, and 0.20% and 0.41% for 60 MPa concretes. It should be noted that these strain ranges only indicate the initial signs of cover spalling and not accurate representations of spalling load.

The test data was further analyzed with those reported by other researchers, to explore the possibilities of generalizing some of the conclusions drawn. Figure 5.3 depicts the variation of column strength with concrete confinement. Those tested by Rangan et al. (1991), and some of the columns tested by Yong et al. (1988) contained widely spaced low volumetric ratio transverse reinforcement. These columns were able to develop unconfined column capacities, P_0, as given by Eq. 5.1. Columns tested by Itakura and Yagenji (1992), without any cover, consistently showed higher capacities than those computed based on gross cross-sectional area and unconfined concrete, since they did not suffer strength loss due to cover spalling. Those that were sufficiently confined to offset the effects of cover spalling consistently developed higher strengths than P_0. However, the group that contained insufficient volumetric ratio of closely spaced transverse reinforcement could not sustain capacities computed on the basis of total cross-sectional area and unconfined concrete strength. Therefore, it may be concluded that high-strength concrete columns may be classified into three groups in terms of their capacities under concentric loading. The first group consists of plain or lightly reinforced unconfined columns, where early separation of cover concrete is not likely to occur. These columns may be able to develop capacities based on the current practice for normal-strength concrete, as given by Eq. 5.1. Columns confined with closely spaced longitudinal and transverse reinforcement experience loss of strength due to the early separation of cover. Depending on the thickness of the cover, concrete strength, and the degree of confinement of the core, the unconfined strength P_o, based on gross cross-sectional area may or may not be attained. When core confinement is not sufficient, the loss of strength associated with cover spalling can not be compensated by the concrete confinement. These columns form the second group. It may be more appropriate to compute concentric capacities of these columns on the basis of the core area. The third group consists of columns with sufficient confinement of the core to develop unconfined column capacities with core alone. Equation 5.1 may still be applicable to these columns, provided that the attainment of the ultimate load capacity beyond the spalling of the cover is an acceptable limit state for design purposes. More research is needed to establish the governing conditions for each category of columns, and the associated concentric load capacities.

5.4 Evaluation of Column Deformability

Column deformability reflects the ability of columns to deform without a significant loss of strength. Deformability of columns tested in this research program were investigated by examining the experimentally obtained axial stress-axial strain relationships of core concrete. To quantify column deformability; the axial strain ductility ratio was used. The strain ductility ratio was determined as the ratio of axial strain of confined concrete at 15% strength loss beyond the peak stress (ϵ_{85}) divided by 0.002. These strain ratios are listed in Tables 5.3 and 5.4.

The axial strain ductility ratios provide some measure of column deformability. However, a better assessment of deformability can be achieved by examining the complete stress-strain relationships. This is done in the following section, as the effects of confinement parameters are examined.

5.5 Effects of Test Variables

The experimental program was designed to establish relationships between confinement parameters, and strength and ductility of high-strength concrete. The following includes the parameters considered in the test program:

1. Concrete compressive strength.
2. Amount of lateral confinement reinforcement.
3. Strength of lateral reinforcement.
4. Tie spacing.
5. Distribution of longitudinal reinforcement and the resulting tie arrangement.
6. Influence of longitudinal reinforcement in circular columns.
7. Type of circular reinforcement (continuous spiral and circular hoop).
8. Section geometry.

At least two companion columns were tested to investigate the effect of each parameter. These columns had otherwise identical properties.

5.5.1 Concrete Compressive Strength

Strength and ductility of unconfined concrete are known to be inversely proportional. High-strength concrete is more brittle than normal-strength concrete. Therefore, concrete strength was one of the primary variables that was studied extensively in the test program. Columns with the same amount and arrangement of reinforcement, but with distinctly different concrete strengths were tested to quantify the effects of this parameter. Both square and circular columns, with low and high levels of confinement, were considered. The results are compared in terms of stress-strain relationships of confined core concrete. However, to facilitate the comparison of concretes with different unconfined strengths, the stress axis was normalized relative to concrete cylinder strength (f'_c).

Figure 5.4 shows comparisons of companion square columns with a 12-bar arrangement, and either 60 MPa or 124 MPa concretes. The results indicate that 60 MPa concrete benefited more from the same confinement reinforcement used in each companion pair, and developed higher strength enhancement. Furthermore, the 60 MPa concrete clearly showed better ductility characteristics than the companion concrete with 124 MPa. The difference in behaviour appeared to be more pronounced in columns with higher volumetric ratio of confinement reinforcement. Similar comparisons, showing the effects of concrete strength on strength and deformability of core concrete are shown in Figs. 5.5 and 5.6 for columns confined with 8-bar and 4-bar arrangements, respectively.

The effects of concrete strength on strength and deformability of spirally reinforced circular columns are shown in Figs. 5.7. The sudden drops in strength observed in Fig. 5.7(b) are attributed to the buckling of longitudinal reinforcement associated with increased spiral pitch of 135 mm.

The comparisons described above indicate a consistent decrease in deformability with increasing concrete strength. However, strength gain due to confinement is approximately constant for concretes with different unconfined strengths. Columns with different concrete strengths but similar confinement characteristics indicate approximately the same absolute gain in strength due to confinement. Therefore, if the same percentage of strength enhancement is desired, higher strength concrete columns are required to be confined more than those with lower strength concretes.

5.5.2 Amount of Confinement Reinforcement

The amount of confinement steel is directly related to the passive confinement pressure that can be exerted by reinforcement. An increase in the amount of specific grade of confinement steel, usually expressed in terms of volumetric ratio, directly translates into a proportional increase in confinement pressure. In general, both the strength and ductility of confined concrete increase with increasing volumetric ratio.

The significance of the volumetric ratio of confinement reinforcement on square columns is illustrated in Figs. 5.8 and 5.9. The results indicate that both strength and ductility of confined high-strength concrete increase with an increase in volumetric ratio. Columns with low volumetric ratios exhibit brittle behaviour, showing high rate of strength decay immediately after the peak load. On the other hand, columns with increased lateral reinforcement are able to deform significantly with very little drop in capacity. The improvements observed are more pronounced in columns with closer spacing of transverse reinforcement. Similar observations can be made for circular columns, in Fig. 5.10.

5.5.3 Yield Strength of Transverse Reinforcement

Confinement pressure is generated from tensile forces that develop in transverse reinforcement. It is therefore likely to expect that the steel yield strength plays a role on concrete confinement. However, tensile stress in transverse reinforcement is generated as a result of lateral expansion of concrete, which in turn is dependent on the mechanical properties of concrete. If the lateral strain in concrete is not high enough to strain the transverse reinforcement to higher stresses, the extra strength of steel that may be present, will not be utilized.

The effect of yield strength was investigated by testing two pairs of square columns with the same volumetric ratio and spacing, but different yield strengths of lateral reinforcement. The comparisons, shown in Fig. 5.11, indicate that the columns confined with 1000 MPa lateral steel showed improved strength and ductility as compared to those with 570 MPa steel.

The effect of yield strength was further investigated by testing columns with different volumetric ratios (ρ_s) and yield strengths (f_{yt}) of confinement reinforcement, but the same $\rho_s f_{yt}$ product (representing lateral pressure). The comparisons shown in Fig. 5.12 indicate that, although higher grade confinement reinforcement increases lateral pressure and hence improves behaviour, the volumetric ratio plays a more dominant role on concrete deformability, especially when the tie spacing is large. Hence, the increase in the grade of transverse reinforcement could not totally make up for the proportional reduction in volumetric ratio, in square columns.

Fig. 5.13 shows the behaviour of three pairs of spirally reinforced circular columns where each column in a pair was reinforced with either grade 400 MPa or 1000 MPa transverse reinforcement. The results exhibit similar behaviour within each pair, indicating that the required lateral pressure could be provided either by increasing the volumetric ratio or the strength of transverse reinforcement. This implies that the increased confinement pressure required for high-strength concrete circular columns can be provided by increasing the strength of confinement steel. The apparent difference in behaviour between the square and circular columns could be explained by the difference in efficiency of confinement reinforcement, considered in the test program. When the transverse reinforcement is efficient, as in the case of circular spirals and closely spaced rectilinear ties, 1000 MPa transverse steel becomes fully effective in providing lateral confinement pressure. When the tie spacing approaches h/2, as in the case of columns in Fig. 5.12, using low volumetric ratio high-strength steel is not as effective as high volumetric ratio lower grade steel.

5.5.4 Distribution of Longitudinal Reinforcement and Resulting Tie Arrangement

Arrangement of transverse reinforcement is an important parameter that affects distribution of confinement pressure. If the lateral force applied by transverse reinforcement on concrete is well distributed around the perimeter of the core concrete, the distribution of lateral pressure becomes almost uniform, improving the efficiency of confinement reinforcement. The arrangement of transverse reinforcement has been shown to have significant effects on strength and ductility of normal-strength concrete columns.

Fig. 5.14 illustrates the behaviour of high-strength core concrete in two sets of three columns, confined with different arrangements of tie reinforcement. The reinforcement arrangements include 4, 8, and 12 longitudinal bars laterally supported either only by perimeter hoops, or perimeter hoops in combination with cross ties or interior hoops. The results indicate that as the spacing of laterally supported longitudinal reinforcement s_l decreases, strength and ductility of high-strength concrete increase. This implies that the tie spacing s in the longitudinal direction can be relaxed if the spacing s_l in the transverse direction is reduced to improve the efficiency of reinforcement. Figs. 5.15 and 5.16 indicate that there is a direct trade-off between s and s_l. For example, the spacing s of column CS-22, shown in Fig. 5.15(a), can be relaxed from 85 mm to 120 mm provided that the arrangement is improved from 8-bar to 12-bar, to attain similar behaviour.

5.5.5 Tie Spacing

Spacing of transverse reinforcement is one of the important parameters that affects the distribution of confinement pressure, as well as the stability of longitudinal reinforcement. Closer spacing of transverse reinforcement is known to increase the uniformity of lateral pressure and effectiveness of confinement reinforcement.

Behaviour of columns with different tie spacing is shown in Figs. 5.17 and 5.18. These columns also have different volumetric ratios of tie steel. The comparisons, shown in Figs. 5.17 and 5.18, indicate that the negative effects of increased tie spacing can be offset by increased volumetric ratio of transverse reinforcement, provided that premature buckling of longitudinal steel is prevented. However, the relationship between the effects of tie spacing and volumetric ratio is not linear. The effectiveness of transverse reinforcement diminishes quickly with increase in tie spacing. Columns with wide tie spacing may not develop any confinement, irrespective of the volumetric ratio used. High-strength concrete columns tested by Yong et al.(1988) did not develop any effect of confinement when the tie spacing was increased to be equal to the section size.

5.5.6 Effect of Longitudinal Reinforcement in Circular Columns

Although circular hoops provide uniform pressure at hoop level, the presence of longitudinal bars may provide additional restraining action against lateral expansion of concrete, and may improve the confinement efficiency. Previous research on circular columns was conducted mostly on small scale columns with no longitudinal reinforcement. Eight columns were tested to study the effect of longitudinal reinforcement on behaviour of circular columns. These include columns CC-5, CC-6, CC-17, and CC-18 without any longitudinal reinforcement, and columns CC-3, CC-1, CC-14, and CC-16 with eight longitudinal bars, uniformly distributed around the section perimeter. Figs. 5.19 and 5.20 indicate that the longitudinal reinforcement improves strength and ductility of circular columns. Therefore, previous research on circular columns, mostly conducted on small scale cylinders without any longitudinal reinforcement, has to be reassessed in view of these findings.

5.5.7 Type of Circular Reinforcement

One of the variables investigated in the experimental program was the significance of continuity in transverse reinforcement, as in the case of continuous spirals, as opposed to individual circular hoops. Columns CC-3 and CC-4 were tested for this purpose. These two columns had identical properties, with the exception of the type of transverse reinforcement. Column CC-3 had a continuous spiral, whereas CC-4 had circular hoops, the ends of which were connected with mechanical coupling devices to prevent opening under lateral pressure. Fig. 5.21 depicts the stress-strain relationships of core concretes for these two columns. The results indicate similar stress-strain relationships, implying circular spirals and hoops can be used interchangeably in confining concrete, provided that the hoop ends are connected not to allow opening under lateral pressure.

5.5.8 Section Geometry

It has been well established that circular spirals are more effective in confining concrete than rectilinear ties. The superiority of circular spirals come from their geometric shape which produces uniform and continuous pressure around the circumference of the core. Rectilinear ties produce non-uniform pressure which peaks at locations of transverse legs of tie steel. The effect of section geometry can be seen by comparing test results for square and circular columns with identical concrete strength and amount and spacing of confinement reinforcement. This is done in Fig. 5.22. The comparison clearly shows the superior performance of core concrete confined with circular spirals over a square core confined with perimeter hoops only. It is, however, possible to improve the behaviour of square columns up to the same level of performance as circular columns, or even higher level of performance, by improving the efficiency and/or the amount of confinement reinforcement. Figures 5.23 and 5.24 illustrate that similar behaviour was attained in square and circular columns when 8-bar or 12-bar arrangements were used for the square columns with increased volumetric ratio of transverse reinforcement.

5.6 Summary and Conclusions

The following conclusions can be drawn from the experimental parametric study reported in this chapter:

1. High-strength concrete columns under monotonically increasing concentric compression show extremely brittle behaviour unless confined with transverse reinforcement, providing sufficiently high lateral confinement pressure.

2. High lateral pressure required to confine high-strength concrete, relative to normal-strength concrete, can be provided either by increasing the volumetric ratio of confinement steel and/or using high-strength lateral steel. High strength steel, with 1000 MPa yield strength, can be fully utilized in confining high-strength concrete.

3. The beneficial effects of high strength concrete becomes more apparent when the transverse reinforcement is efficient, as in the case of circular spirals and closely spaced rectilinear ties.

4. Although higher grade confinement reinforcement increases lateral pressure and hence improves behaviour, the volumetric ratio plays a more dominant role on

concrete deformability. Hence, the increase in the grade of transverse reinforcement can not totally make up for a proportional reduction in volumetric ratio.

5. The test results indicate a consistent decrease in deformability with increasing concrete strength. However, strength gain due to confinement is approximately constant for concretes with different unconfined strengths. Columns with different concrete strengths but similar confinement characteristics indicate approximately the same absolute gain in strength due to confinement. Therefore, if the same percentage of strength enhancement is desired, higher strength concrete columns are required to be confined more than those with lower strength concretes.

6. Confined high-strength concrete columns with closely spaced reinforcement separating the core form the cover exhibit early spalling of cover concrete under concentric compression. Columns with efficient reinforcement arrangement and/or high volumetric ratio of confinement steel may be able to exceed their capacities based on the current building code approach. However, when confinement parameters are not favourable, columns may not develop the computed capacity based on the building code approach due to the early spalling of cover.

7. Reducing the spacing of lateral and/or longitudinal steel increases confinement efficiency, and improves strength and ductility of high-strength concrete columns.

8. Circular spirals are more effective in confining concrete than rectilinear ties. High-strength concrete columns confined with circular spirals showed improved strength and ductility when compared with columns confined with the same

volumetric ratio of rectilinear ties. However, it is possible to improve the behaviour of square columns up to the same level of performance as circular columns, or even higher level of performance, by improving the efficiency and/or the amount of confinement reinforcement

9. Circular hoops show similar effects of confinement as circular spirals.

10. Longitudinal reinforcement in circular columns has an effect on concrete confinement, when tied by closely spaced circular ties or spirals. Therefore, the characteristics of confined concrete in circular columns can not be assessed accurately by testing circular columns with transverse reinforcement only, as has commonly been done in previous research.

Table 5.1: Experimental and theoretical strengths for square columns.

Column Number	f'_c (MPa)	P_{test} (kN)	$P_{cc\,test}$ (kN)	f_{test} (MPa)	P_o (kN)	P_{oc} (kN)	P_{occ} (kN)	$\frac{P_{test}}{Po}$	$\frac{f_{test}}{f'co}$
CS-1	124	6040	5680	120.8	6863	5317	4957	0.88	1.15
CS-2	124	6597	5877	121.6	7139	5317	4597	0.92	1.15
CS-3	124	7402	6138	129.1	7415	5317	4237	1.00	1.22
CS-4	124	6631	5911	123.4	7139	5317	4597	0.93	1.17
CS-5	124	6849	5769	122.5	7415	5317	4237	0.92	1.16
CS-6	124	6927	5596	115.7	7139	5317	4597	0.97	1.10
CS-7	124	6910	5466	115.0	7415	5317	4237	0.93	1.09
CS-8	124	6165	5445	117.8	7139	5317	4597	0.86	1.12
CS-9	124	7177	6096	134.2	7415	5317	4237	0.97	1.27
CS-10	124	6863	6863	109.8	6588	5317	5317	1.04	1.04
CS-11	81	4856	4416	93.9	4608	5317	4957	1.05	1.36
CS-12	81	4366	3861	82.1	4608	5317	4957	0.95	1.19
CS-13	92	4874	4154	85.9	5482	5317	4597	0.89	1.10
CS-14	92	5561	4482	94.3	5780	5317	4237	0.96	1.21
CS-15	81	5296	4576	95.5	4913	5317	4597	1.08	1.39
CS-16	81	5578	4482	95.2	5218	5317	4237	1.07	1.38
CS-17	81	5242	3636	75.2	4913	5317	4597	1.07	1.09
CS-18	81	5536	3633	76.4	5218	5317	4237	1.06	1.11
CS-19	92	5536	4815	104.2	5482	5317	4597	1.01	1.33
CS-20	92	5911	4830	106.3	5780	5317	4237	1.02	1.36
CS-21	81	4645	4645	74.3	4303	5317	5317	1.08	1.08
CS-22	60	4322	3257	68.0	3826	5317	4597	1.13	1.33
CS-23	60	4790	3357	71.3	4145	5317	4237	1.16	1.40
CS-24	60	4763	3356	72.6	3826	5317	4597	1.24	1.42
CS-25	60	4996	3166	69.7	4145	5317	4237	1.21	1.37
CS-26	60	5365	3647	76.7	4145	5317	4237	1.29	1.50

Note: P_{test} is the maximum column load recorded during testing. $P_{cc\,test}$, f_{test} are the maximum load and stress resisted by core concrete. P_o, P_{oc}, and P_{occ} are defined in Equations 5.1, 5.2, and 5.3 respectively.

Table 5.2: Experimental and theoretical strengths for circular columns.

Column Number	f'_c (MPa)	P_{test} (kN)	$P_{cc\,test}$ (kN)	f_{test} (MPa)	P_o (kN)	P_{oc} (kN)	P_{occ} (kN)	$\frac{P_{test}}{Po}$	$\frac{f_{test}}{f'co}$
CC-1	60	3499	2259	59.9	3142	2643	1923	1.11	1.17
CC-2	60	3035	2241	62.3	3142	2554	1834	0.97	1.22
CC-3	60	3483	2580	68.4	3142	2643	1923	1.11	1.34
CC-4	60	3402	2543	67.4	3142	2643	1923	1.08	1.32
CC-5	60	2783	2415	61.8	2593	2094	1994	1.07	1.21
CC-6	60	2505	2214	56.6	2593	2094	1994	0.97	1.11
CC-8	124	5354	4634	122.9	5725	4694	3974	0.94	1.17
CC-9	124	5564	4845	134.7	5725	4511	3791	0.97	1.28
CC-10	124	5076	4356	135.3	5725	4511	3791	0.89	1.28
CC-11	124	5424	4704	124.8	5725	4694	3974	0.95	1.18
CC-12	124	5482	4762	127.7	5725	4650	3930	0.96	1.21
CC-14	92	4590	3820	102.5	4434	3635	2915	1.04	1.31
CC-15	92	4501	3781	105.2	4434	3532	2812	1.02	1.35
CC-16	92	4266	3546	95.1	4434	3635	2915	0.96	1.22
CC-17	92	3693	3452	89.2	3923	3125	3025	0.94	1.14
CC-18	92	3538	3216	83.1	3923	3125	3025	0.90	1.06
CC-19	92	4339	3402	94.6	4434	3532	2812	0.98	1.21
CC-20	92	4172	3331	88.4	4434	3668	2948	0.94	1.13
CC-21	92	4323	3522	93.4	4434	3668	2948	0.98	1.19
CC-22	92	4237	3210	89.3	4434	3532	2812	0.96	1.14

Note: P_{test} is the maximum column load recorded during testing. $P_{cc\,test}$, f_{test} are the maximum load and stress resisted by core concrete. P_o, P_{oc}, and P_{occ} are defined in Equations 5.1, 5.2, and 5.3 respectively.

Table 5.3: Axial strain ductility ratios for square columns.

Column Number	Reinforcement Arrangement	f'_c (MPa)	$\frac{s}{b_c}$	$\frac{\rho_s f_{yt}}{f'_c}$	ϵ_{85} (%)	$\frac{\epsilon_{85}}{0.002}$
CS-1	2	124	0.25	0.108	0.36	1.8
CS-2	3	124	0.25	0.099	0.78	3.9
CS-3	4	124	0.25	0.099	0.82	4.1
CS-4	3	124	0.25	0.175	1.19	5.9
CS-5	4	124	0.54	0.107	0.46	2.3
CS-6	3	124	0.38	0.034	0.46	2.3
CS-7	4	124	0.54	0.032	0.50	2.5
CS-8	3	124	0.39	0.104	0.93	4.7
CS-9	4	124	0.55	0.099	0.78	3.9
CS-10	1	124	N/A	0.000	N/A	N/A
CS-11	2	81	0.18	0.226	2.00	10.0
CS-12	2	81	0.25	0.165	0.74	3.7
CS-13	3	92	0.25	0.134	0.91	4.6
CS-14	4	92	0.25	0.134	1.80	9.0
CS-15	3	81	0.25	0.267	1.24	6.2
CS-16	4	81	0.38	0.231	0.83	4.1
CS-17	3	81	0.38	0.052	0.68	3.4
CS-18	4	81	0.38	0.069	0.78	3.9
CS-19	3	92	0.39	0.141	0.92	4.6
CS-20	4	92	0.39	0.188	1.54	7.7
CS-21	1	81	N/A	0.000	N/A	N/A
CS-22	3	60	0.38	0.234	0.78	3.9
CS-23	4	60	0.54	0.221	1.03	5.2
CS-24	3	60	0.39	0.216	1.65	8.3
CS-25	4	60	0.55	0.204	1.98	9.9
CS-26	4	60	0.25	0.205	1.46	7.30

Note: Reinforcement arrangements are shown in Figure 4.2.

Table 5.4: Axial strain ductility ratios for circular columns.

Column Number	Reinforcement Arrangement	f'_c (MPa)	$\frac{s}{b_c}$	$\frac{\rho_s f_{yt}}{f'_c}$	ϵ_{85} (%)	$\frac{\epsilon_{85}}{0.002}$
CC-1	5	60	0.60	0.045	0.66	3.3
CC-2	5	60	0.62	0.090	0.74	3.7
CC-3	5	60	0.31	0.088	0.90	4.5
CC-4	5	60	0.31	0.088	0.73	3.7
CC-5	6	60	0.31	0.088	N/A	N/A
CC-6	6	60	0.60	0.045	N/A	N/A
CC-8	5	124	0.31	0.042	0.50	2.5
CC-9	5	124	0.62	0.044	N/A	N/A
CC-10	5	124	0.27	0.098	1.00	5.0
CC-11	5	124	0.27	0.049	0.53	2.7
CC-12	5	124	0.27	0.107	1.00	5.0
CC-14	5	92	0.27	0.144	0.88	4.4
CC-15	5	92	0.27	0.133	0.85	4.3
CC-16	5	92	0.45	0.086	0.58	2.9
CC-17	6	92	0.27	0.144	0.63	3.2
CC-18	6	92	0.45	0.086	0.64	3.2
CC-19	5	92	0.46	0.080	0.72	3.6
CC-20	5	92	0.45	0.040	0.42	2.1
CC-21	5	92	0.31	0.057	0.67	3.4
CC-22	5	92	0.62	0.059	0.44	2.2

Note: Reinforcement arrangements are shown in Figure 4.2.

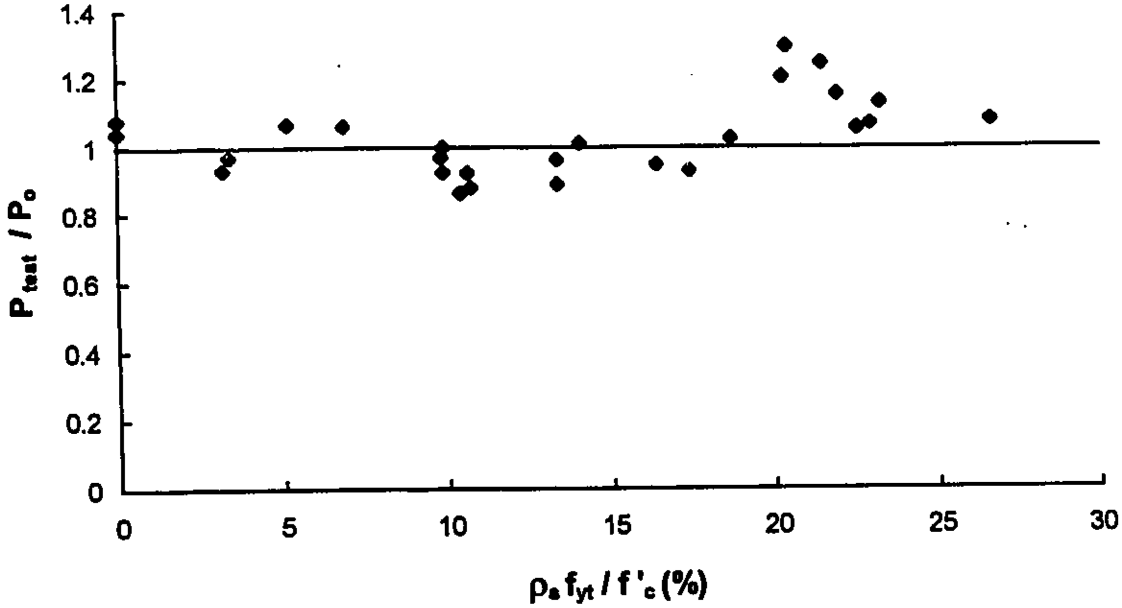

(a) Square Columns

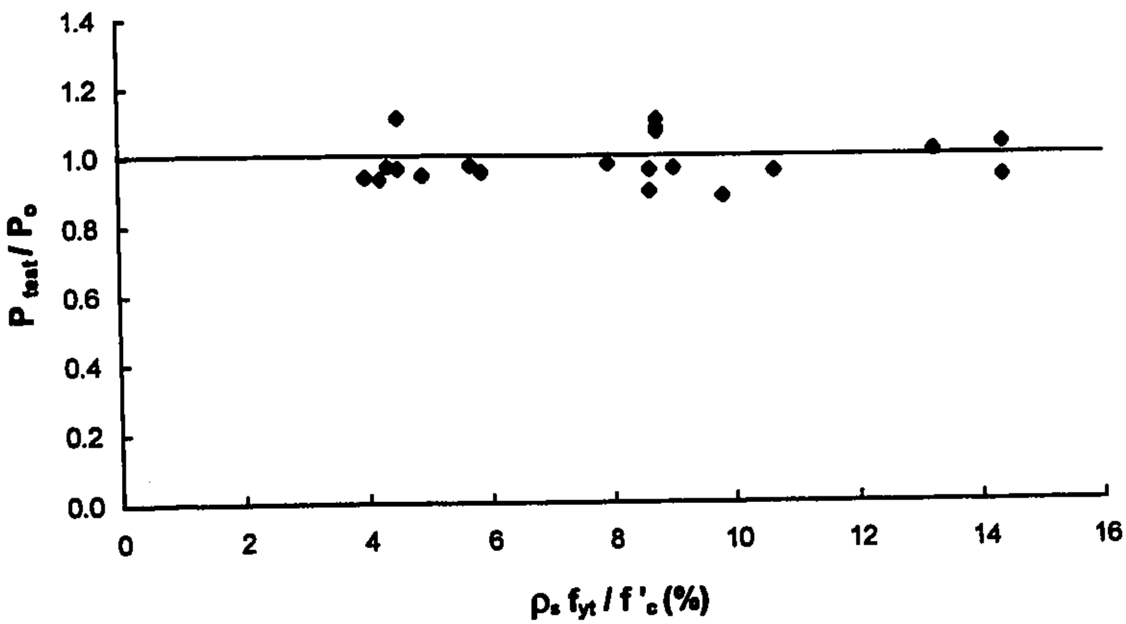

(b) Circular Columns

Figure 5.1: Variation of Column strength with $\rho_s\, f_{yt} / f'_c$

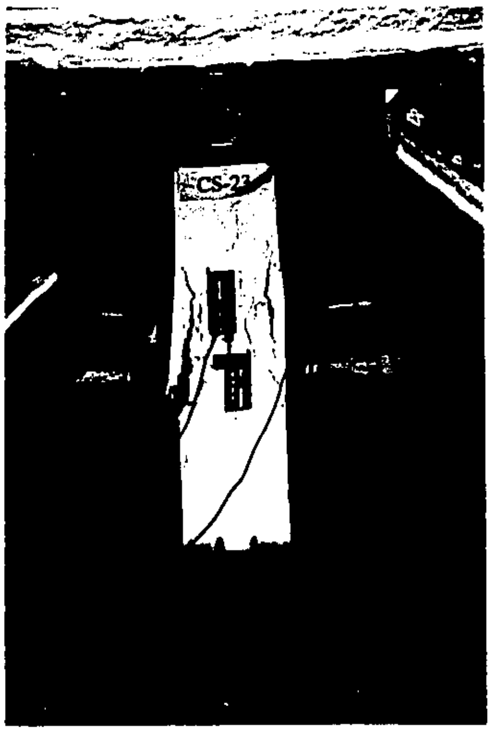

(a) Cover spalling in a square column.

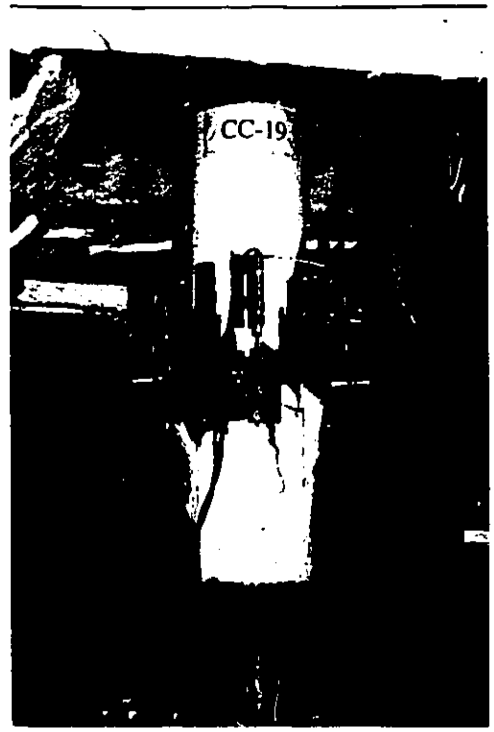

(b) Cover spalling in a circular column.

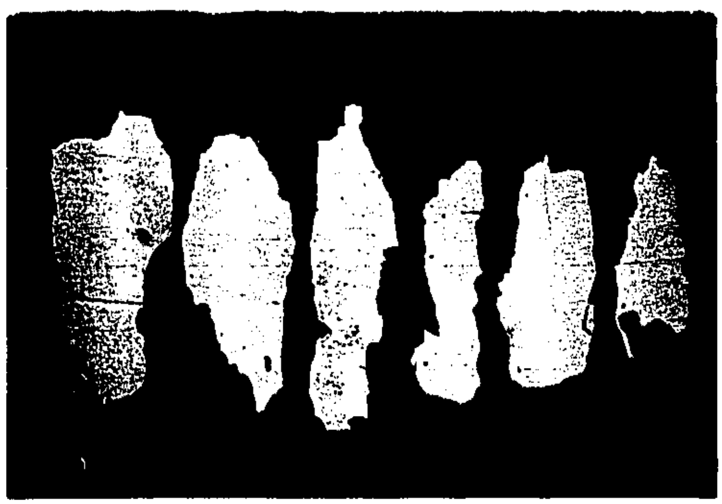

(c) Large pieces of spalled off cover concrete signifying instability failure.

Figure 5.2: Typical spalling of cover in high strength concrete columns.

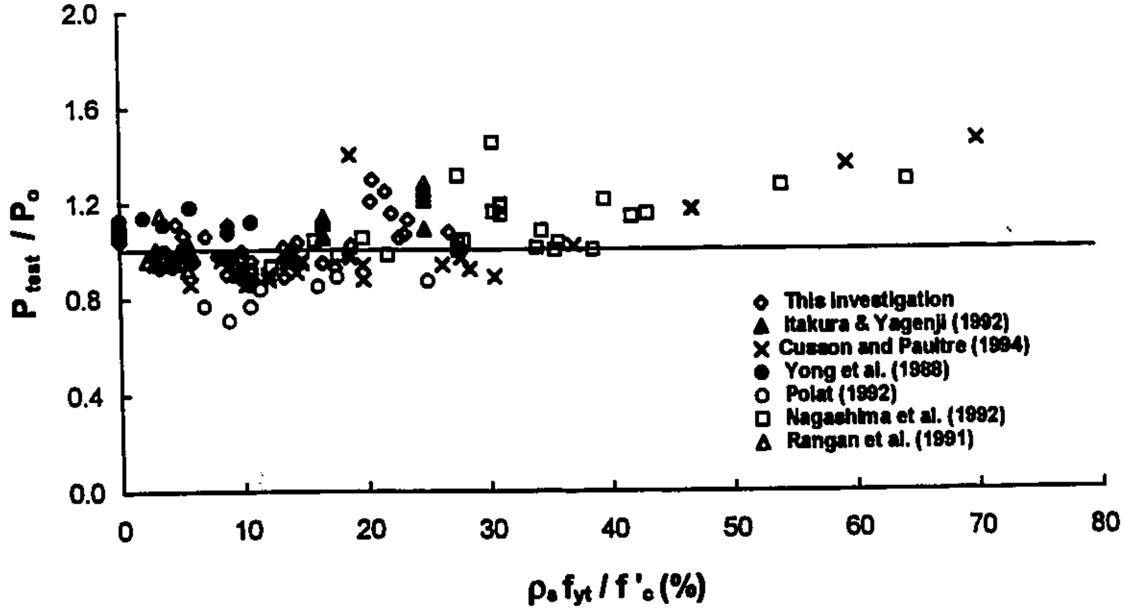

Figure 5.3 : Column strength data including those recorded by other researchers.

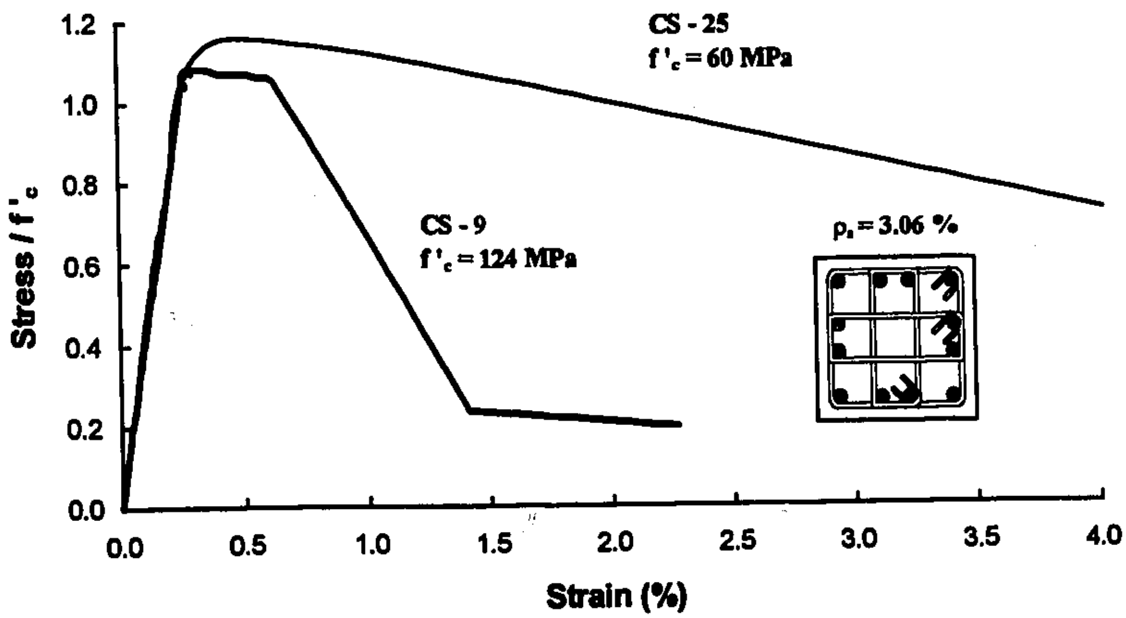

(a)

Figure 5.4: Effect of concrete strength for square columns with 12-bar arrangement.

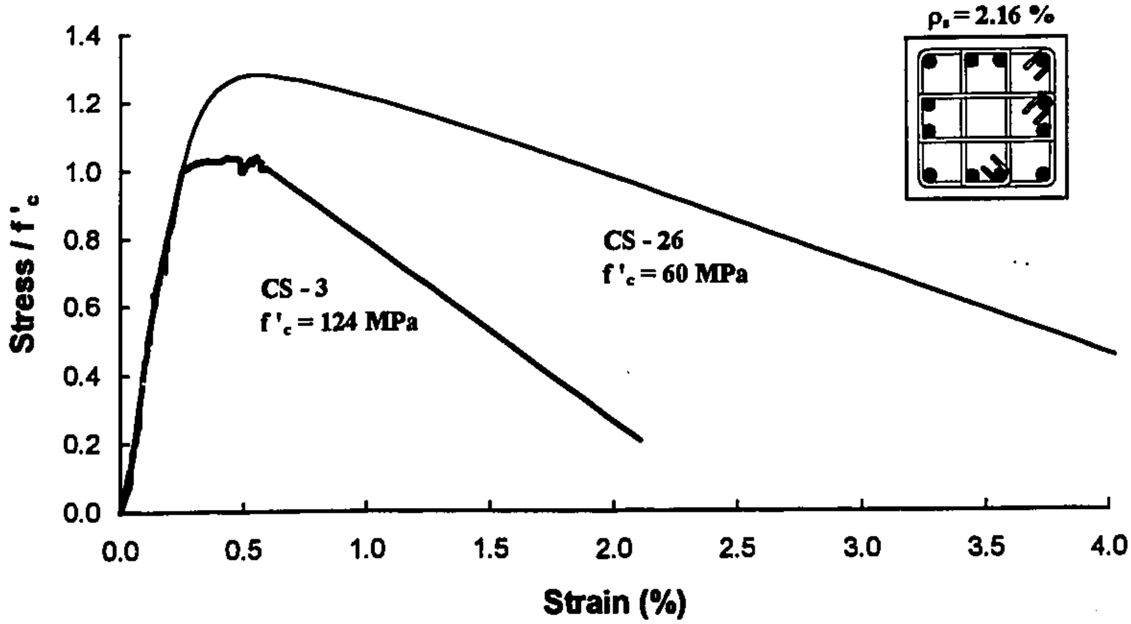

(b)

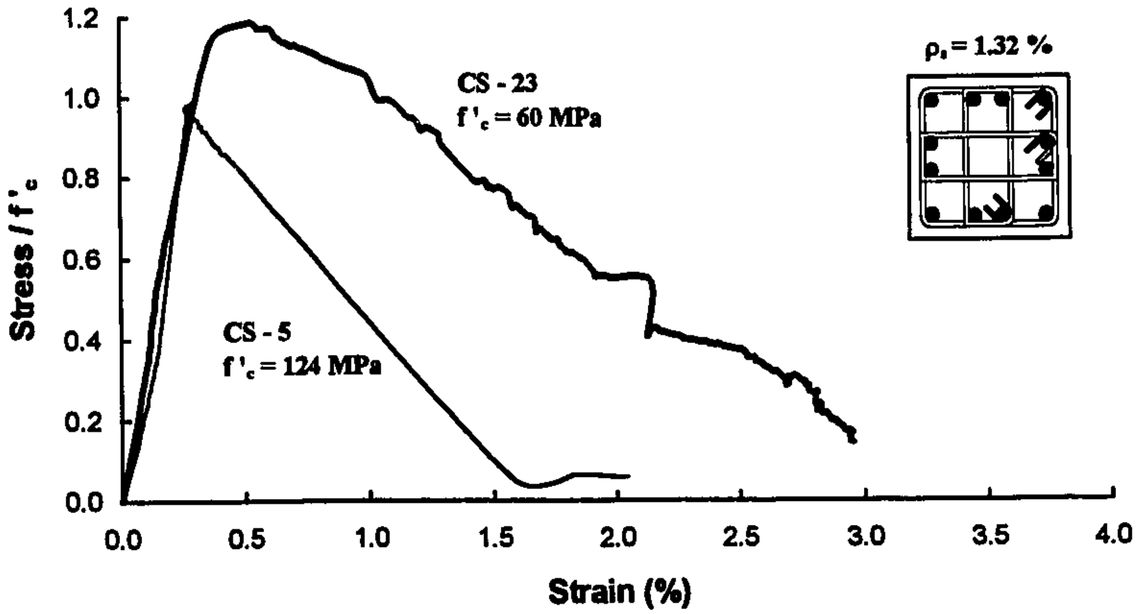

(c)

Figure 5.4: Continued

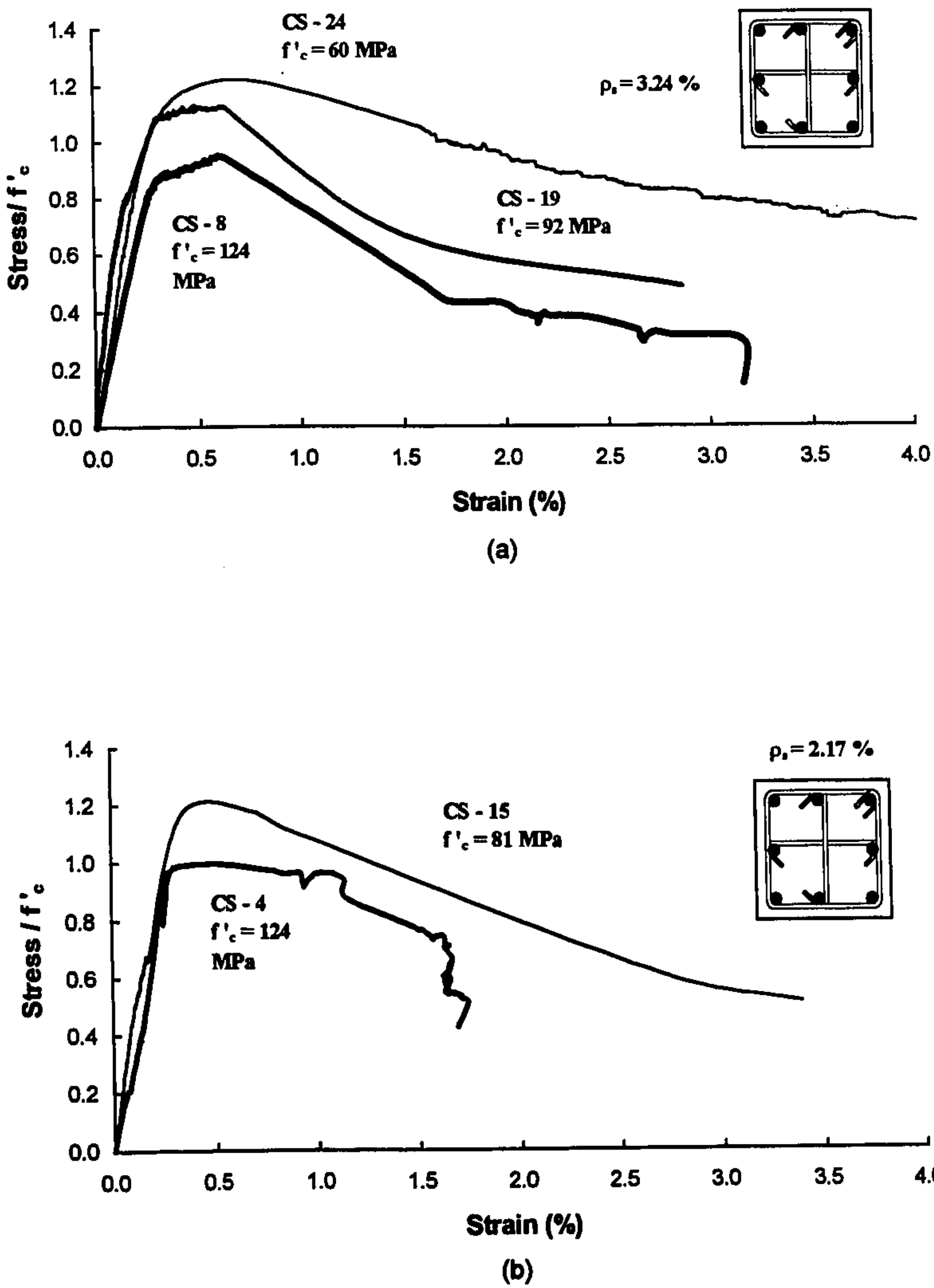

Figure 5.5: Effect of concrete strength for square columns with 8-bar arrangement.

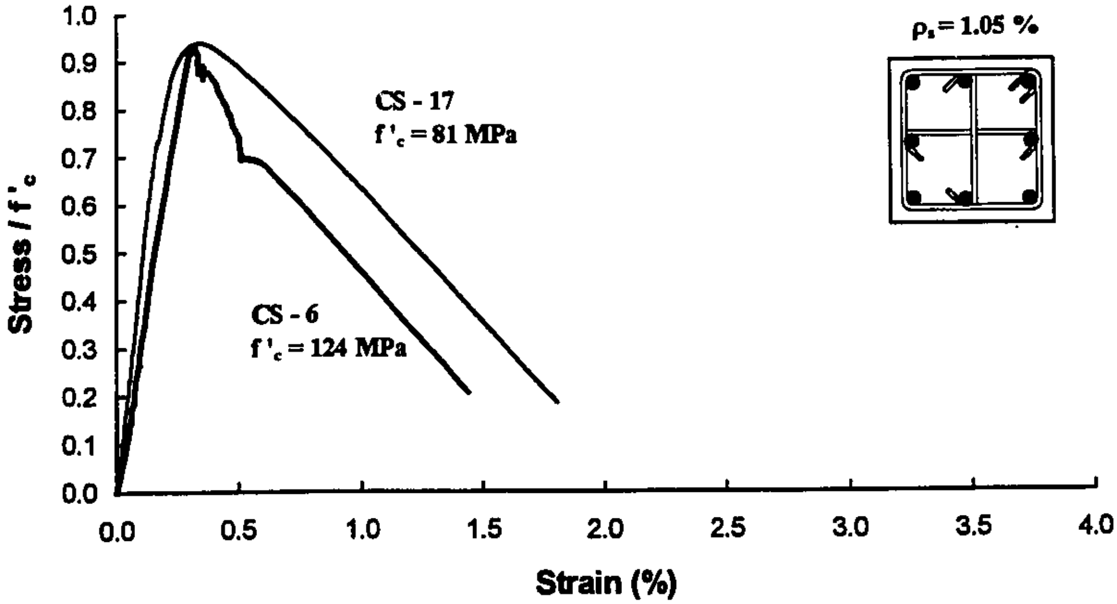

(c)

Figure 5.5: Continued

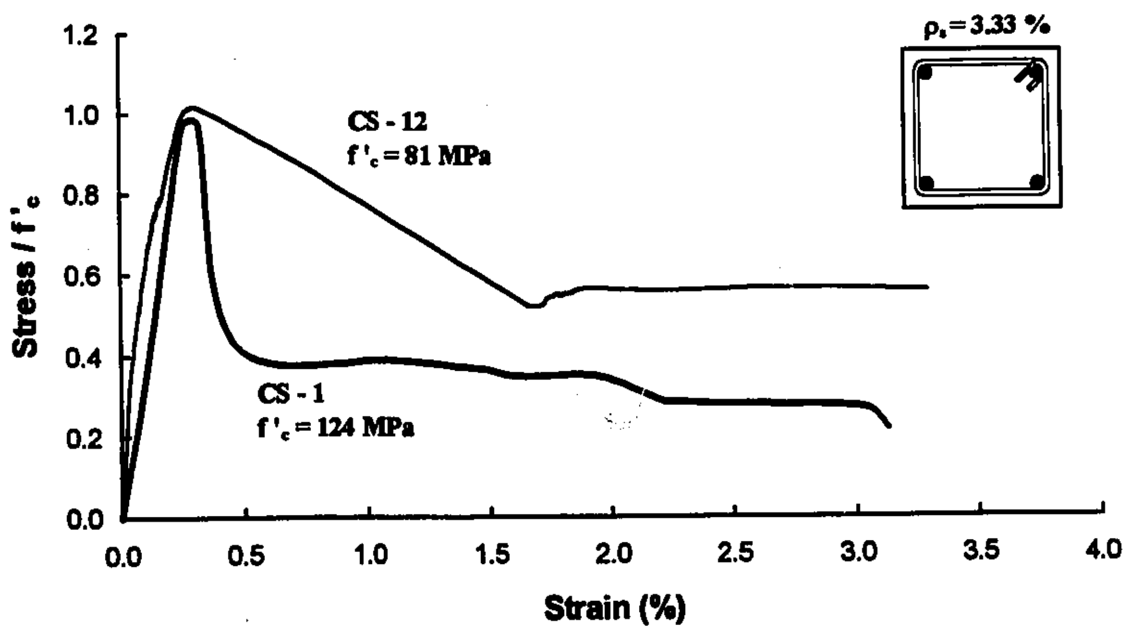

Figure 5.6: Effect of concrete strength for square columns with 4-bar arrangement.

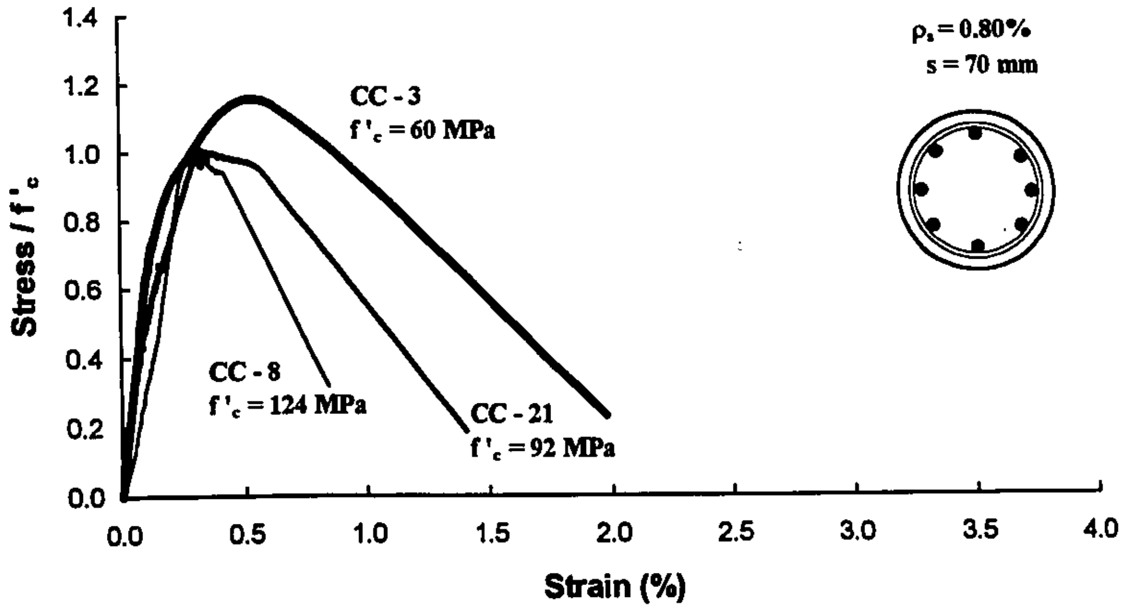

(a)

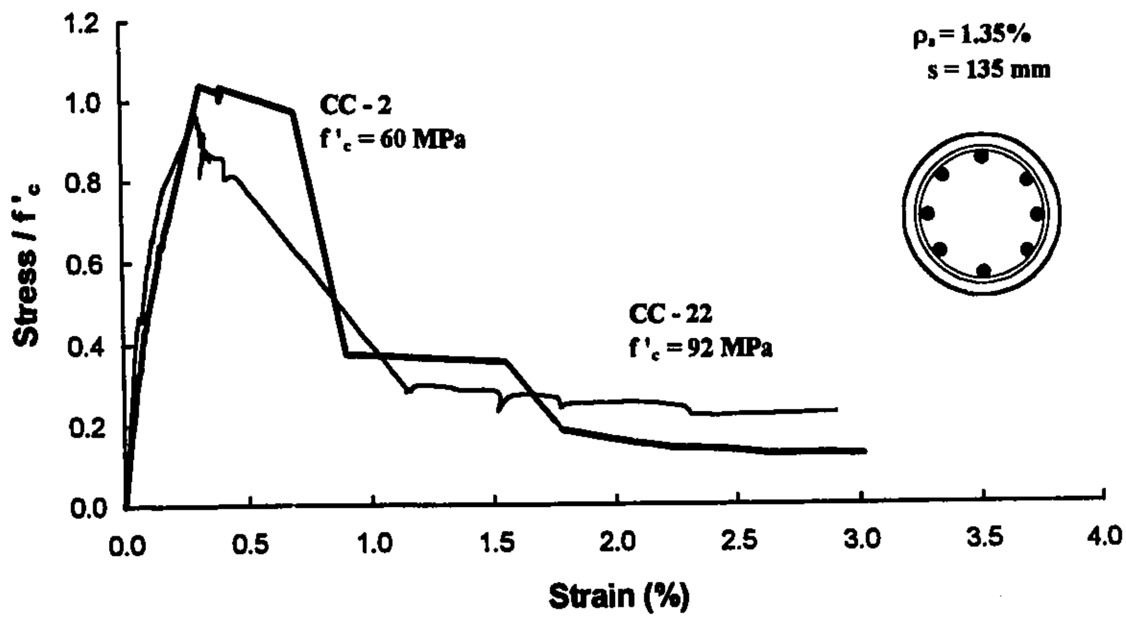

(b)

Figure 5.7: Effect of concrete strength for circular columns .

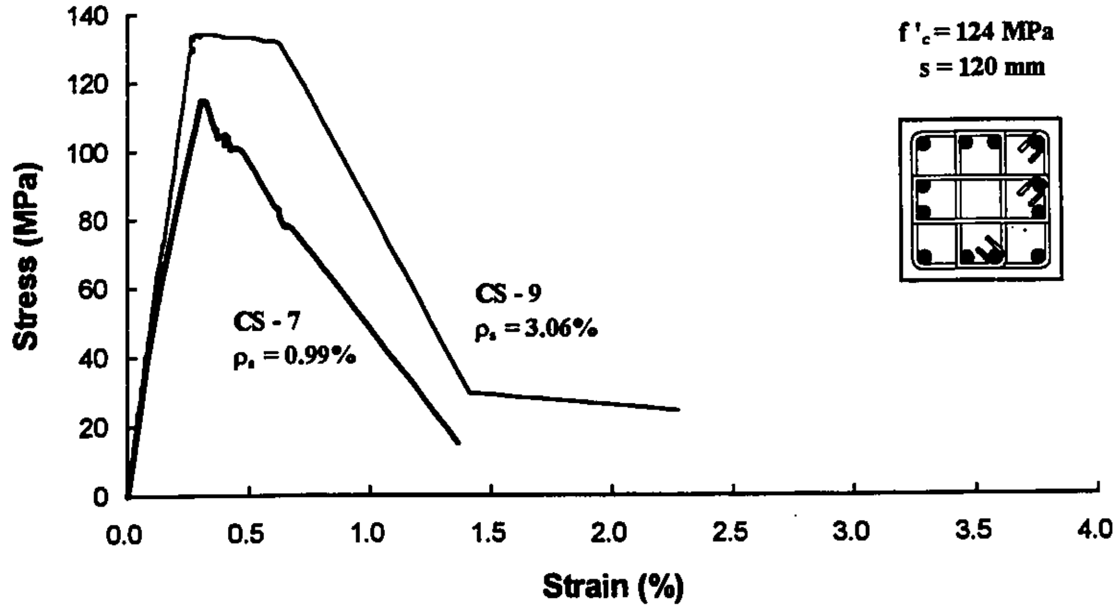

(a)

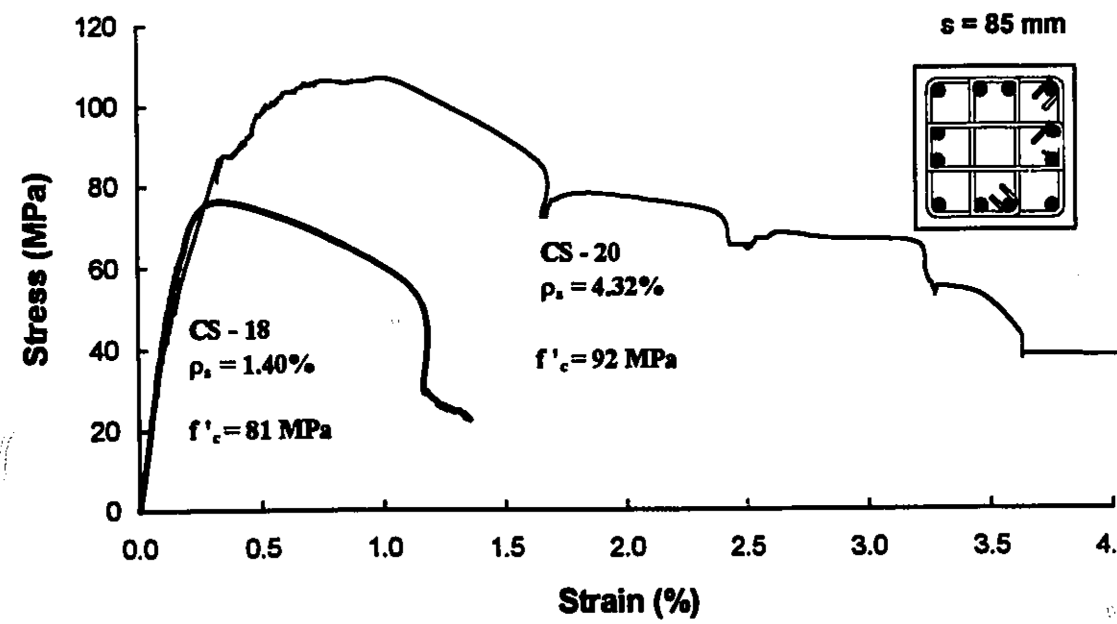

(b)

Figure 5.8: Effect of volumetric ratio of transverse reinforcement for square columns with 12-bar arrangement.

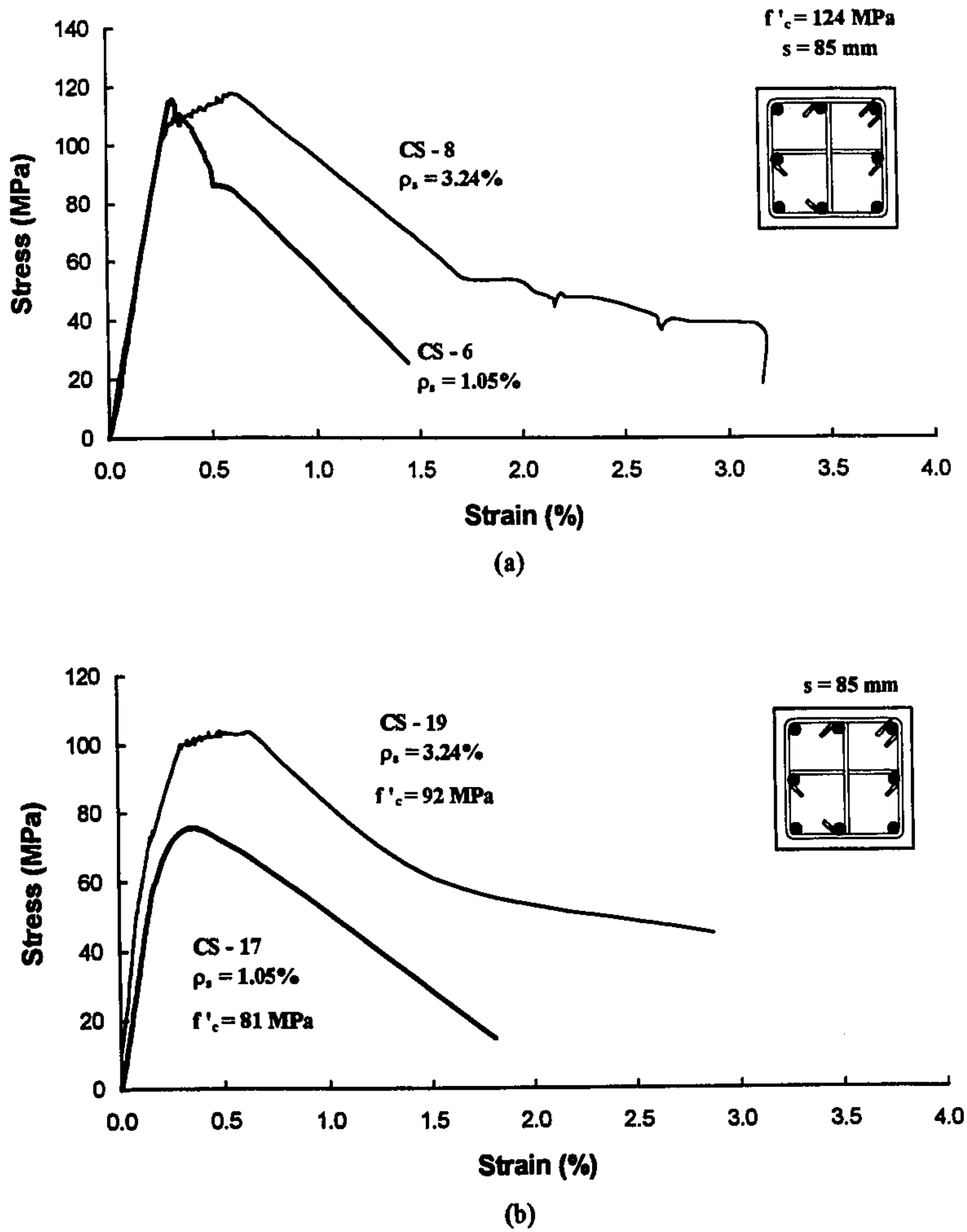

Figure 5.9: Effect of volumetric ratio of transverse reinforcement for square columns with 8-bar arrangement.

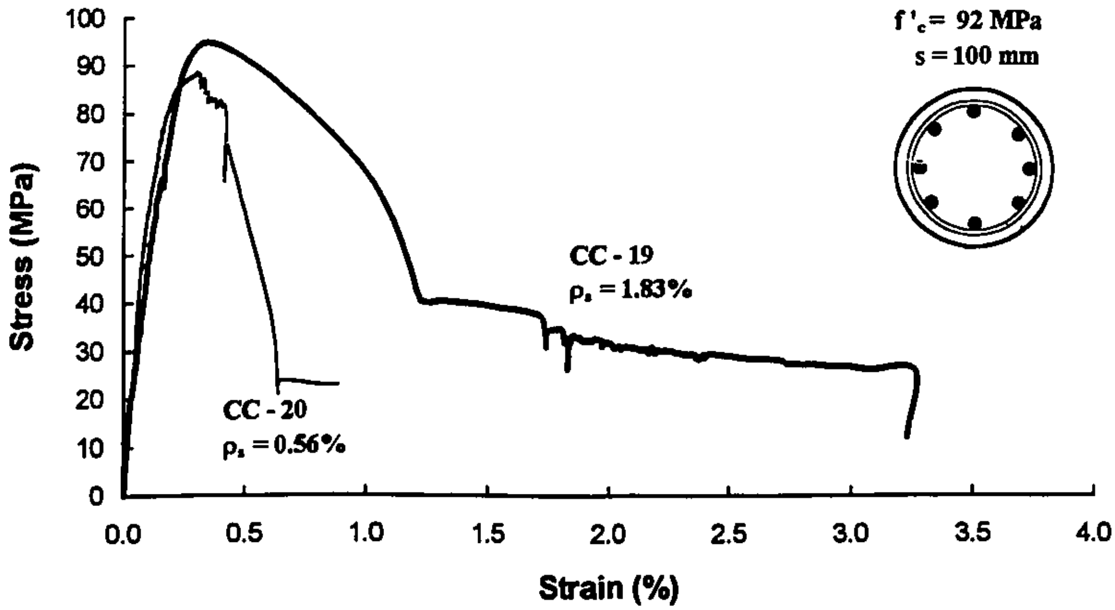

(a)

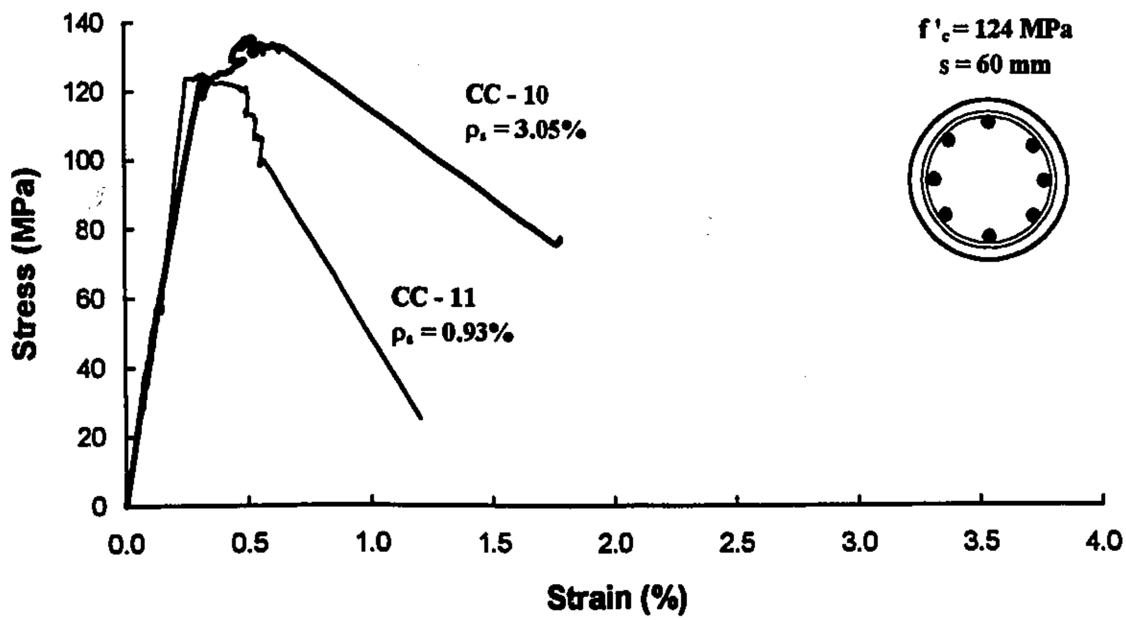

(b)

Figure 5.10: Effect of volumetric ratio of transverse reinforcement for circular columns.

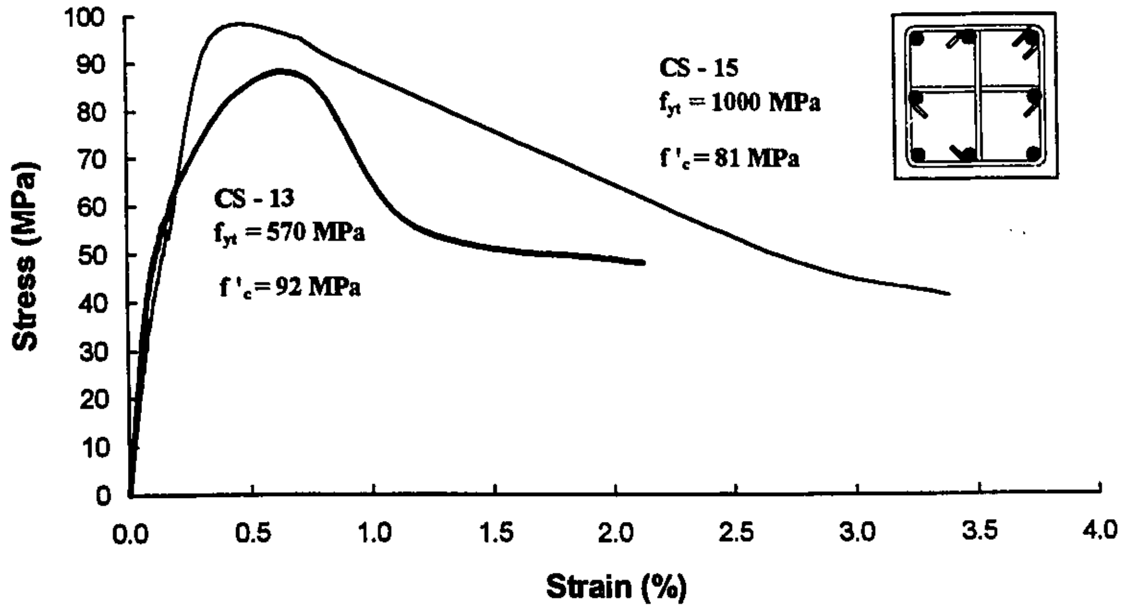

(a)

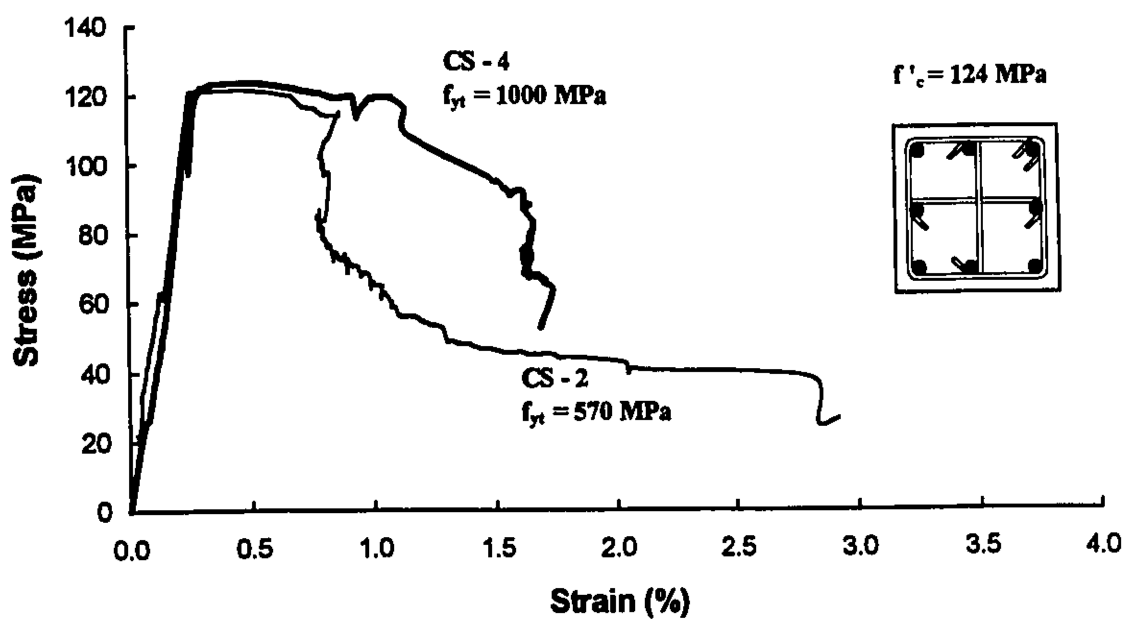

(b)

Figure 5.11: Effect of yield strength of transverse reinforcement for square columns.

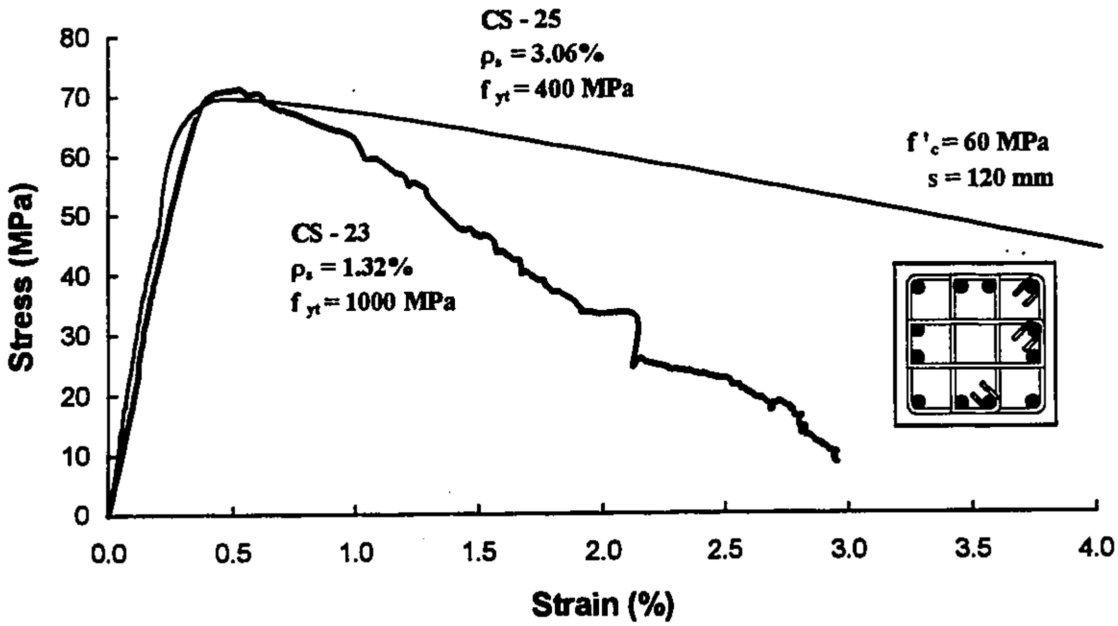

(a)

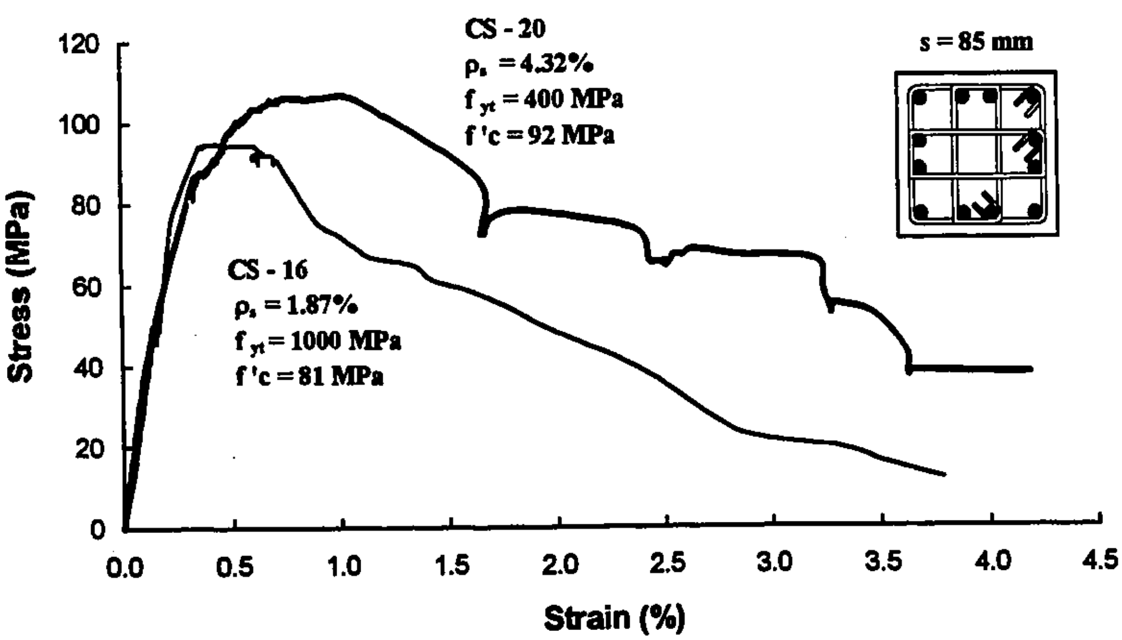

(b)

Figure 5.12 : Effect of $\rho_s f_{yt}$ for square columns.

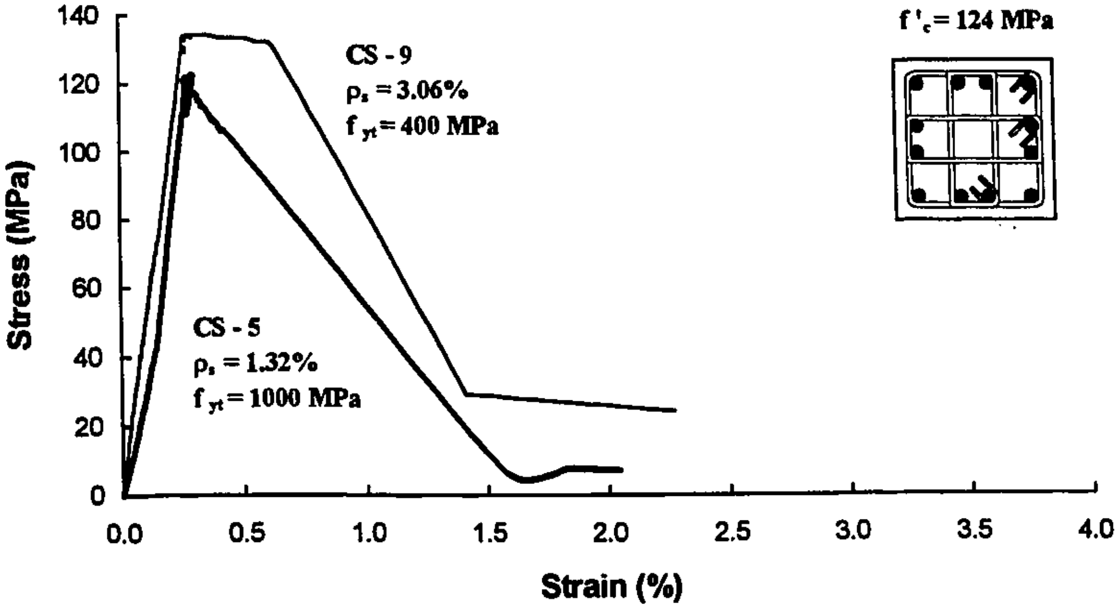

(c)

Figure 5.12: Continued

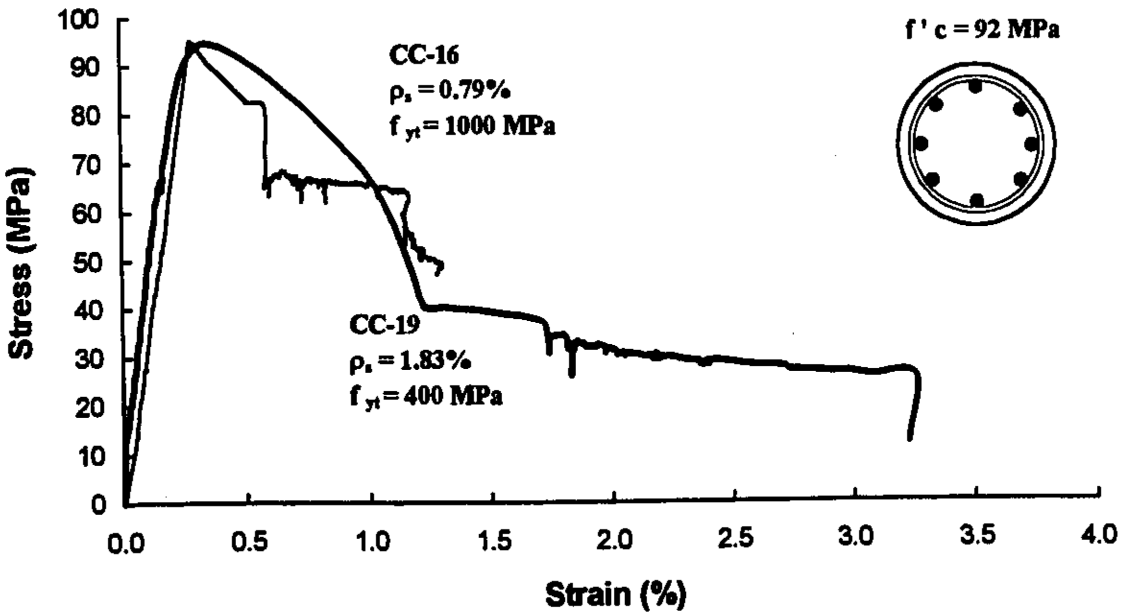

(a)

Figure 5.13 : Effect of $\rho_s f_{yt}$ for circular columns.

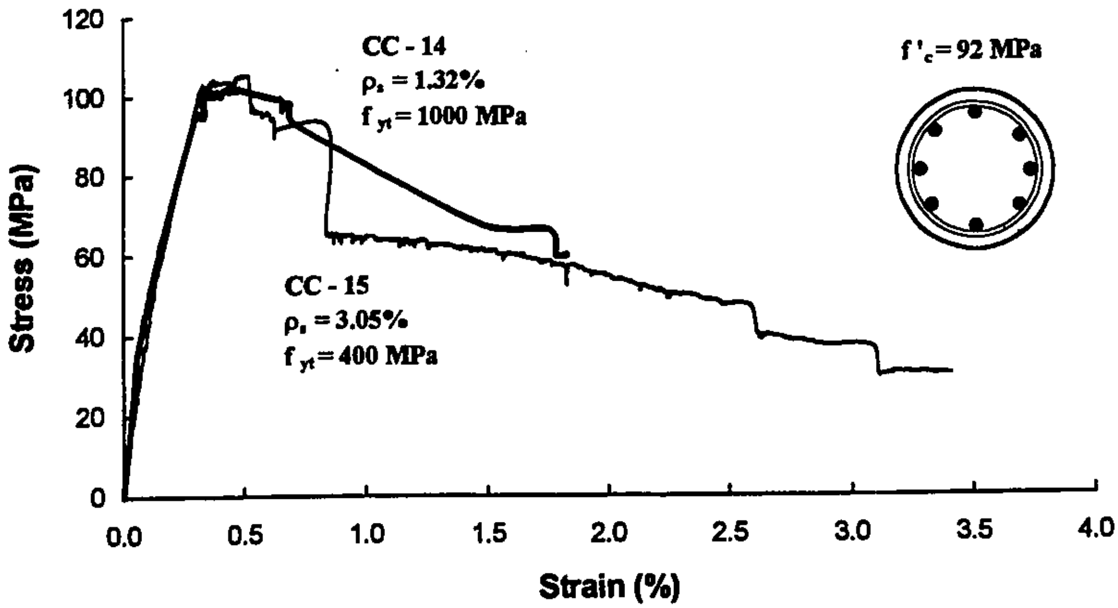

(b)

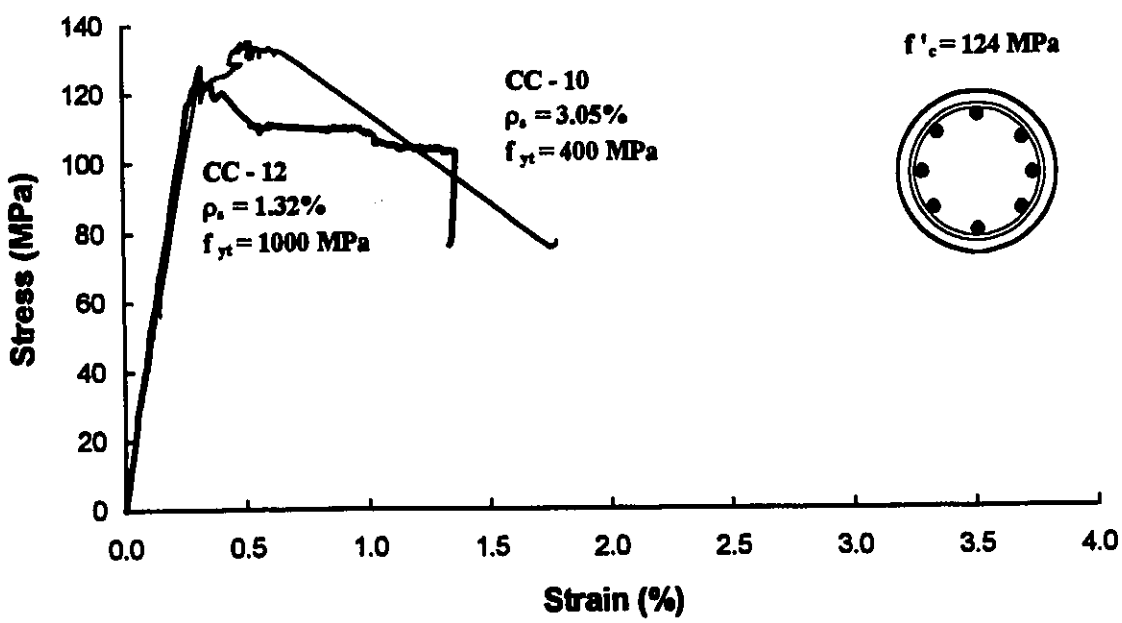

(c)

Figure 5.13: Continued

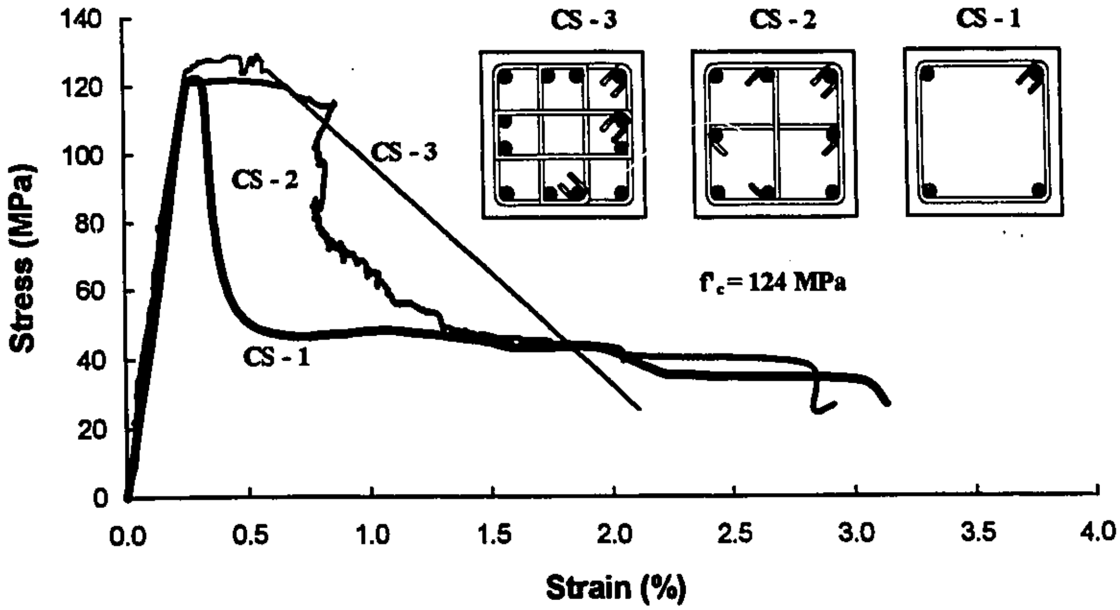

(a)

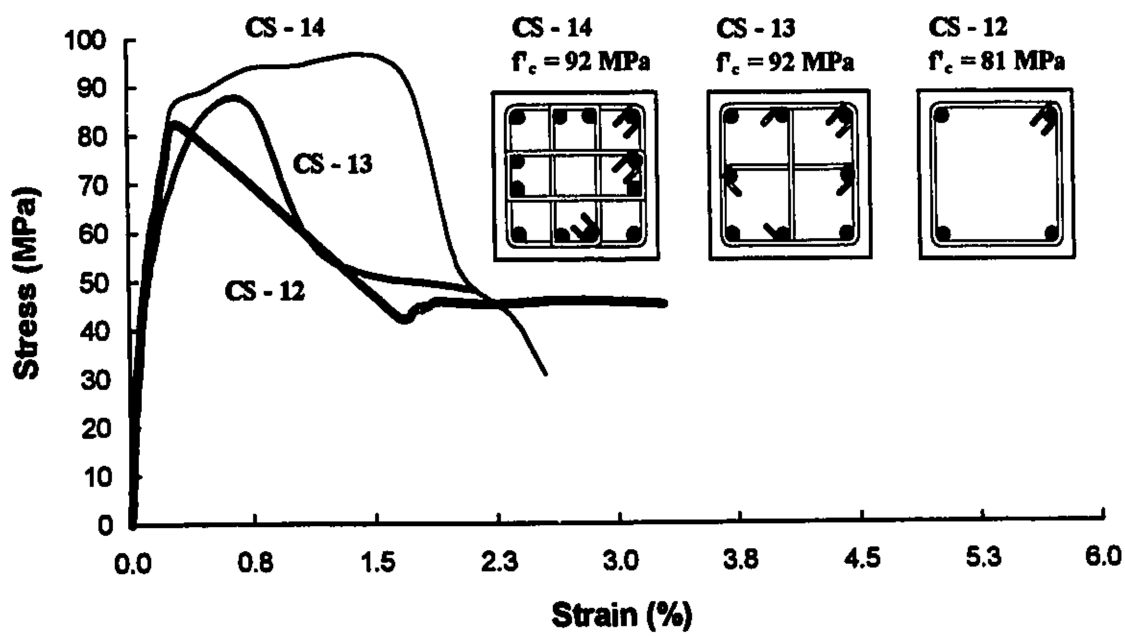

(b)

Figure 5.14: Effect of distribution of longitudinal reinforcement for square columns.

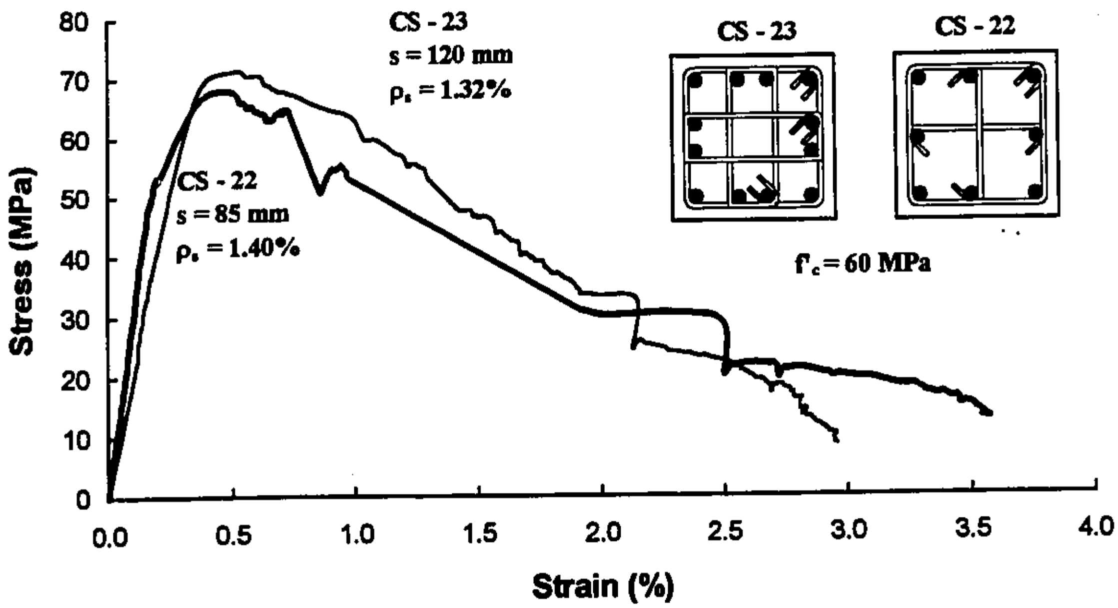

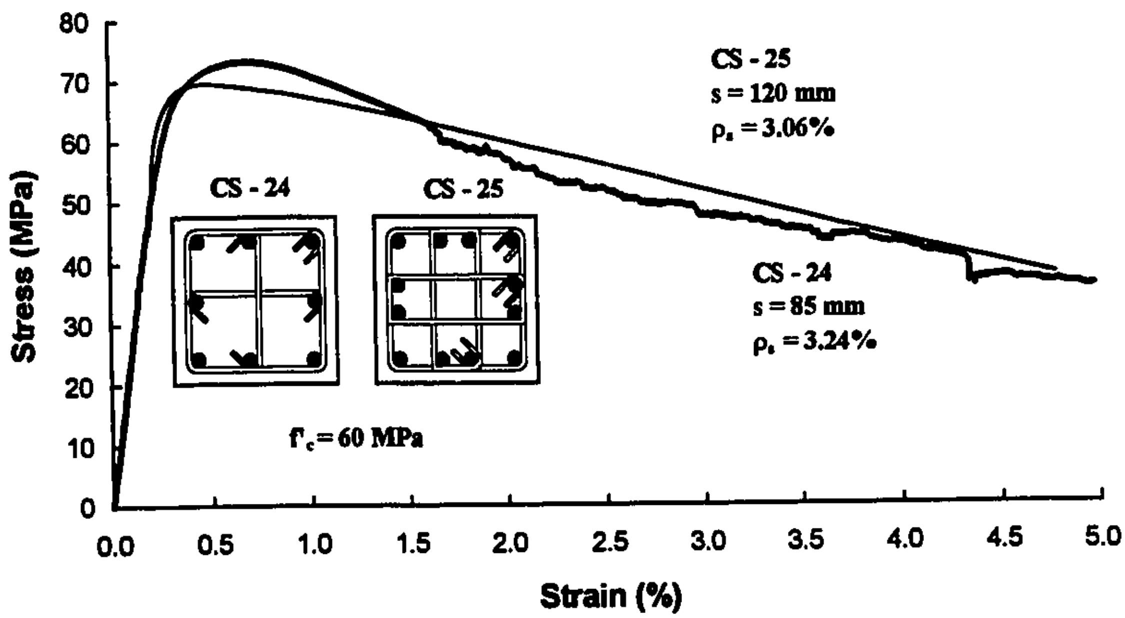

Figure 5.15: Effect of distribution of longitudinal and transverse reinforcement for square columns (f'$_c$ = 60 MPa).

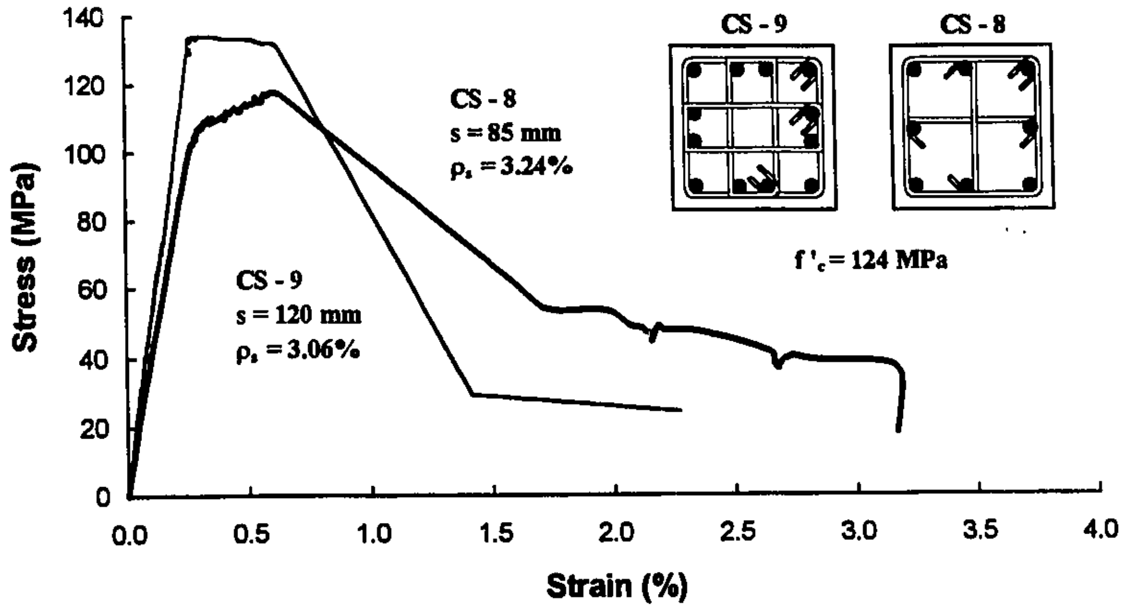

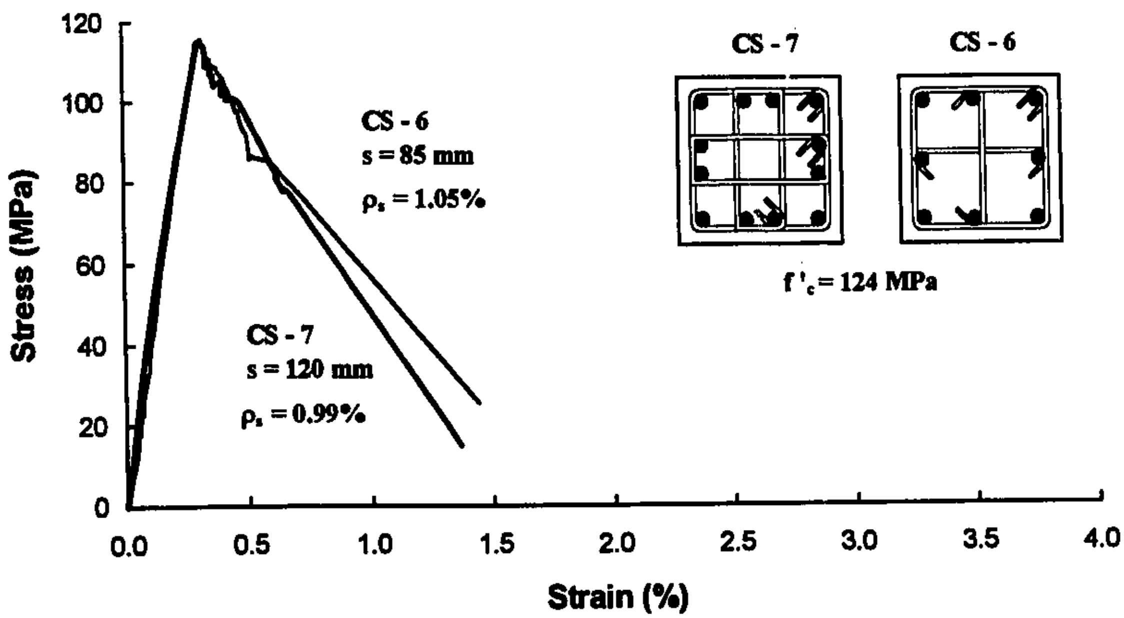

Figure 5.16: Effect of distribution of longitudinal and transverse reinforcement for square columns (f'_c = 124 MPa).

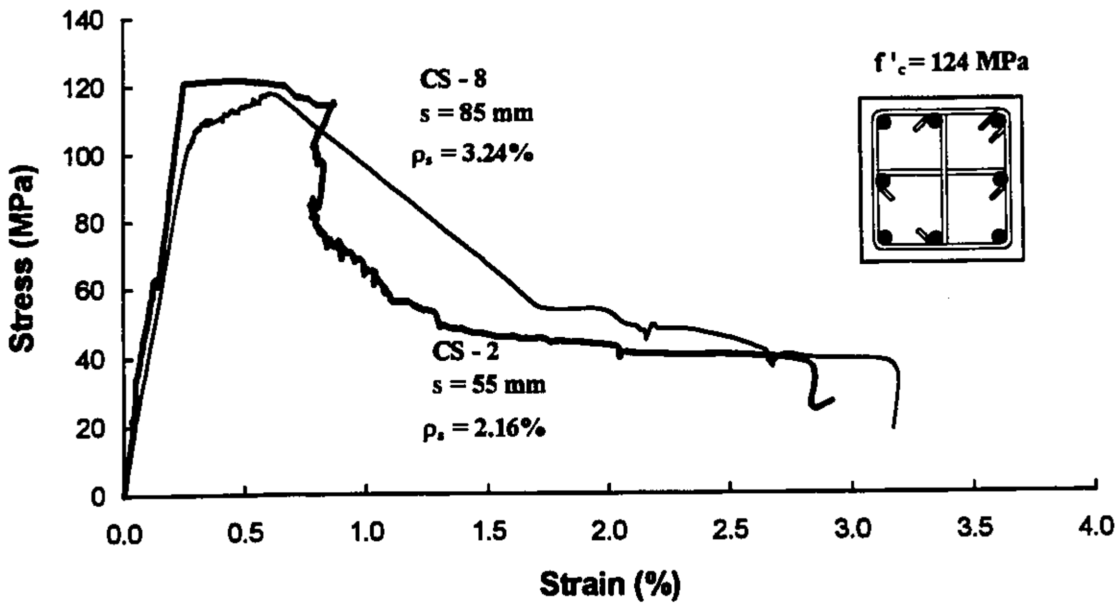

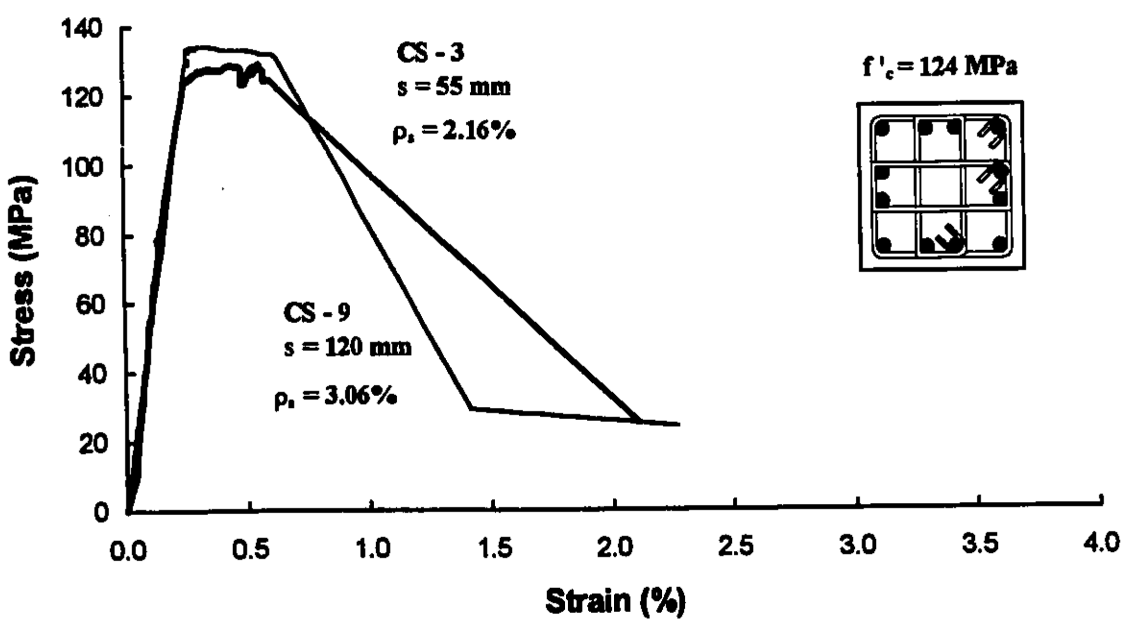

Figure 5.17: Effect of spacing of transverse reinforcement for square columns.

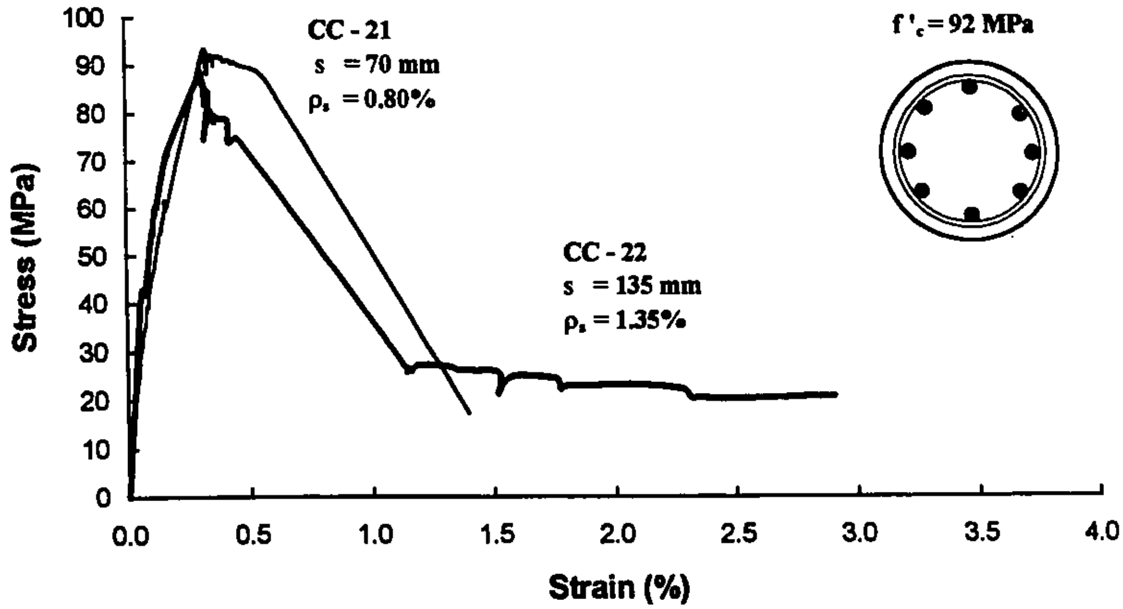

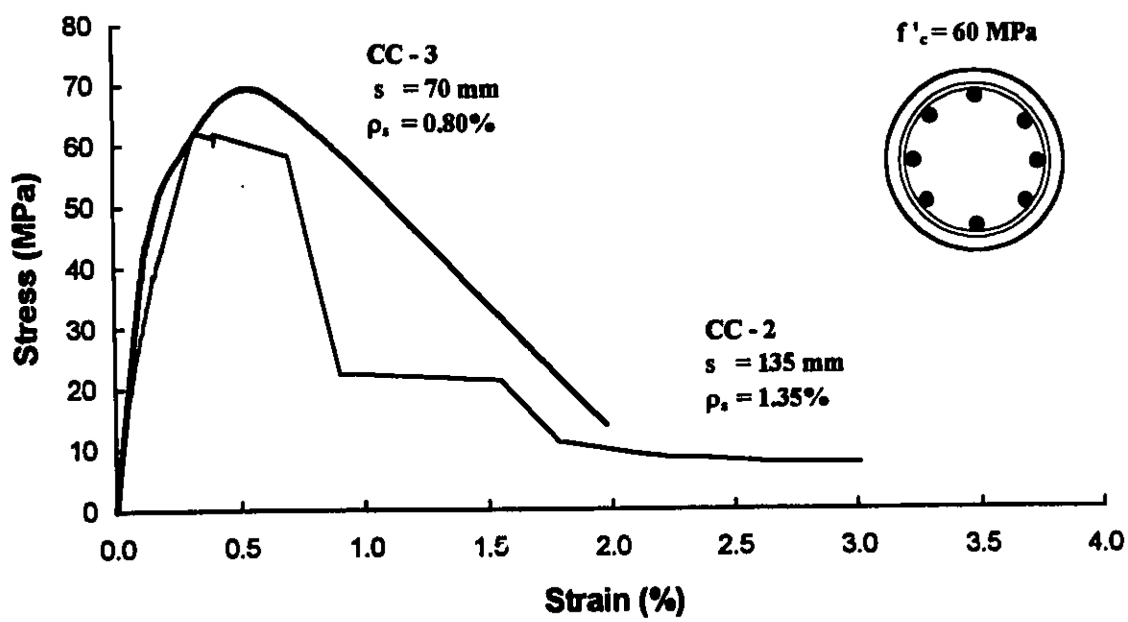

Figure 5.18: Effect of spacing of transverse reinforcement for circular columns.

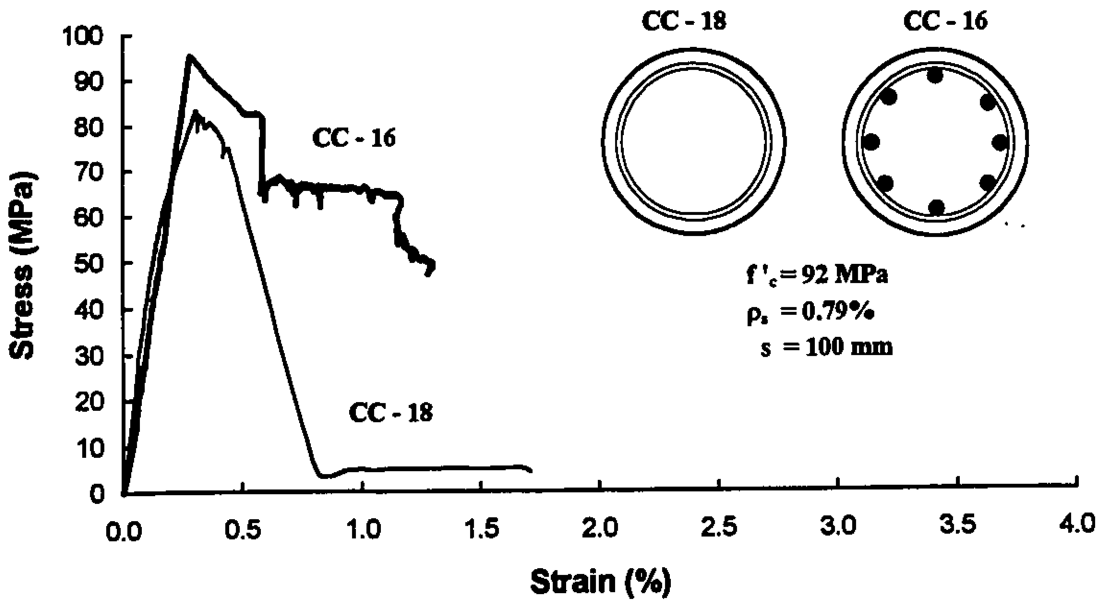

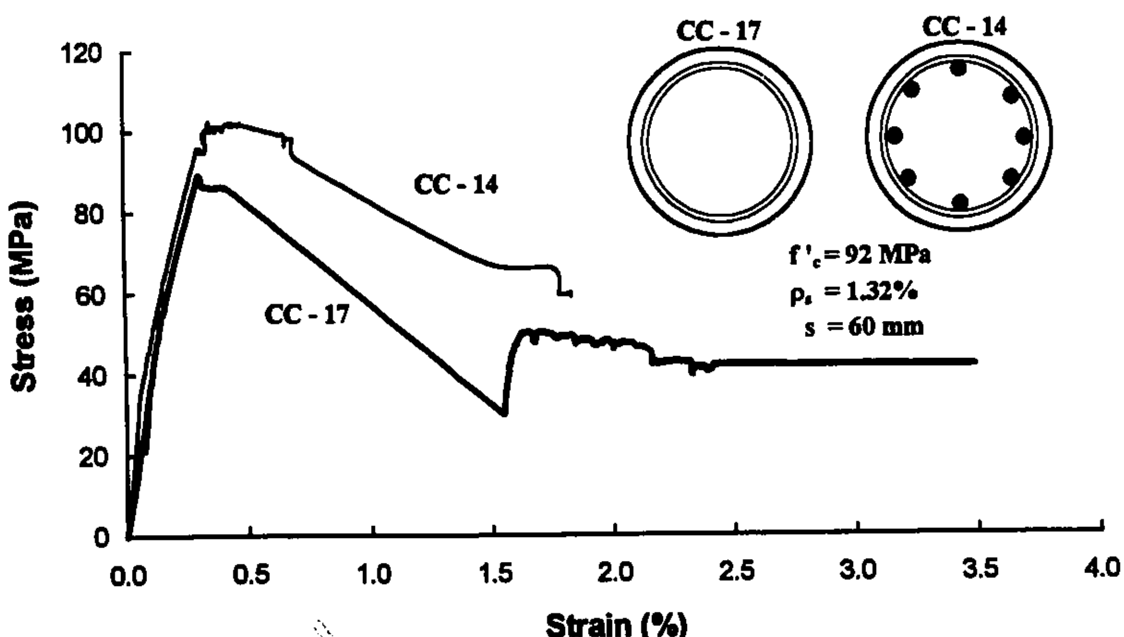

Figure 5. 19: Effect of longitudinal reinforcement in circular columns (f'$_c$ = 92 MPa).

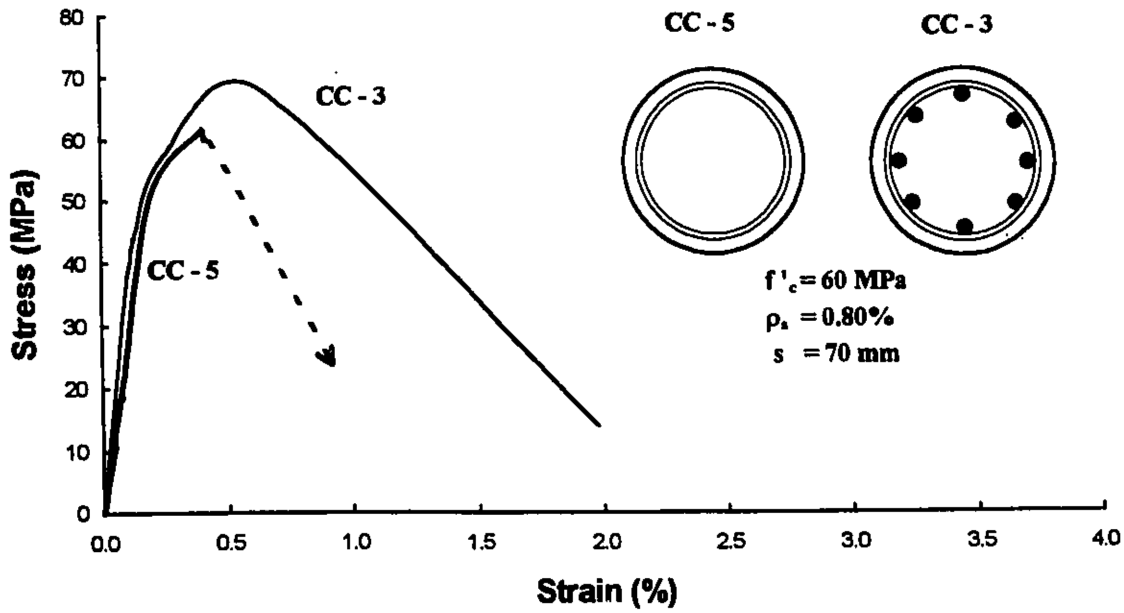

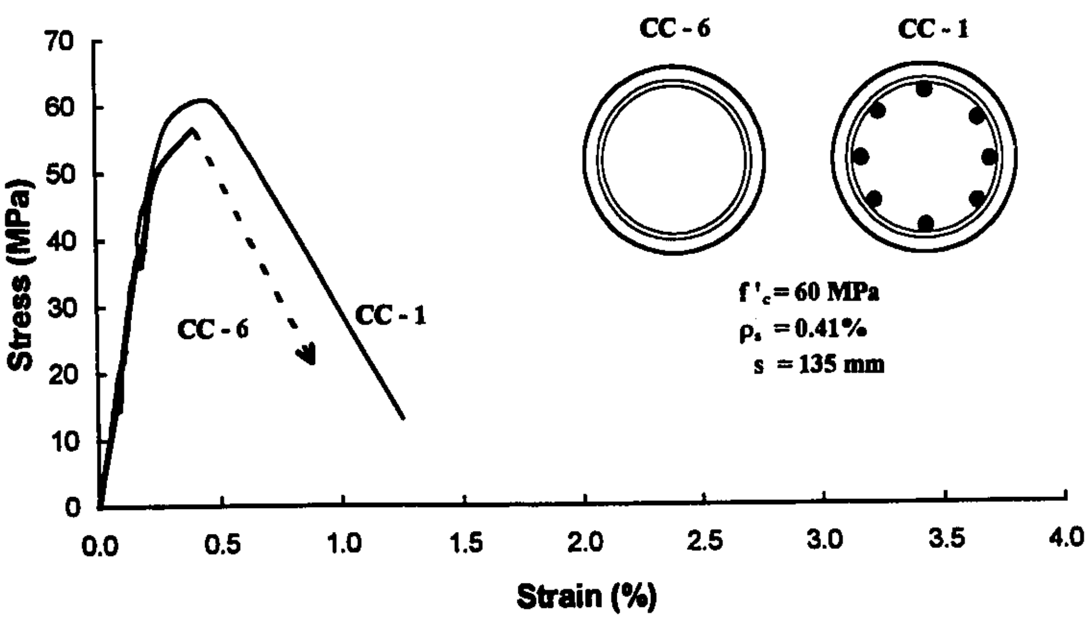

Figure 5. 20: Effect of longitudinal reinforcement in circular columns ($f'_c = 60$ MPa).

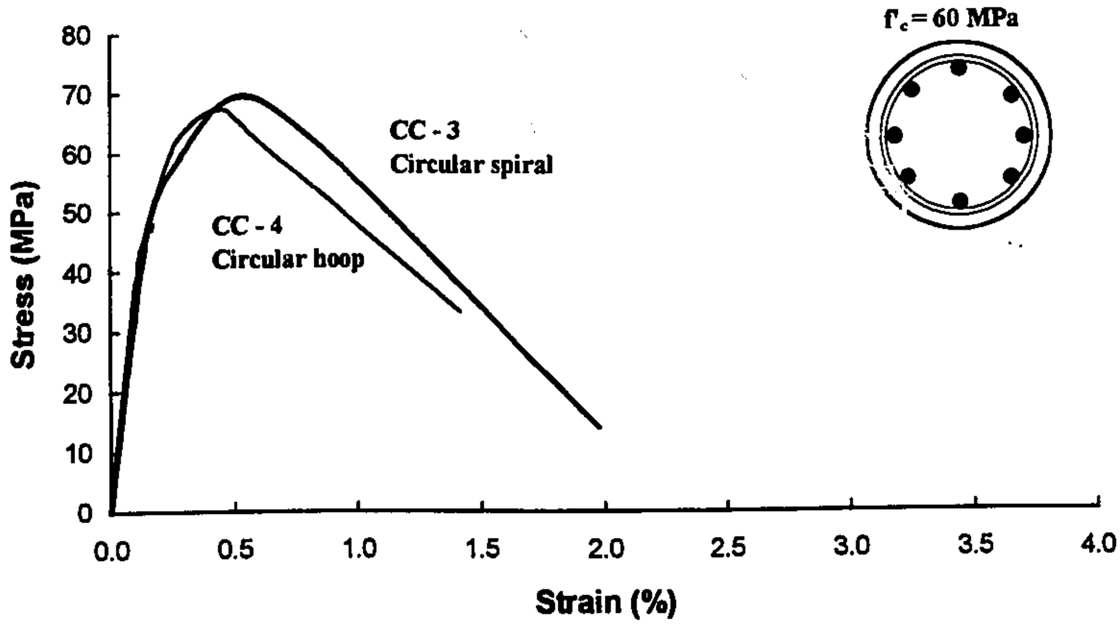

Figure 5. 21: Effect of type of circular reinforcement.

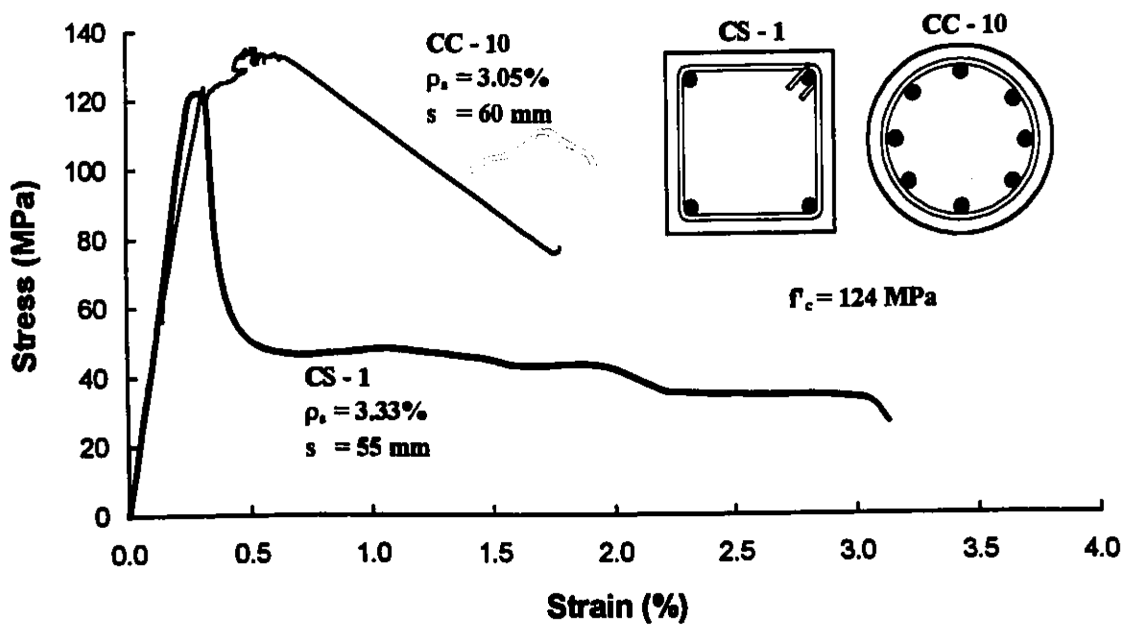

Figure 5. 22: Effect of section geometry (circular columns versus 4-bar arrangement square columns).

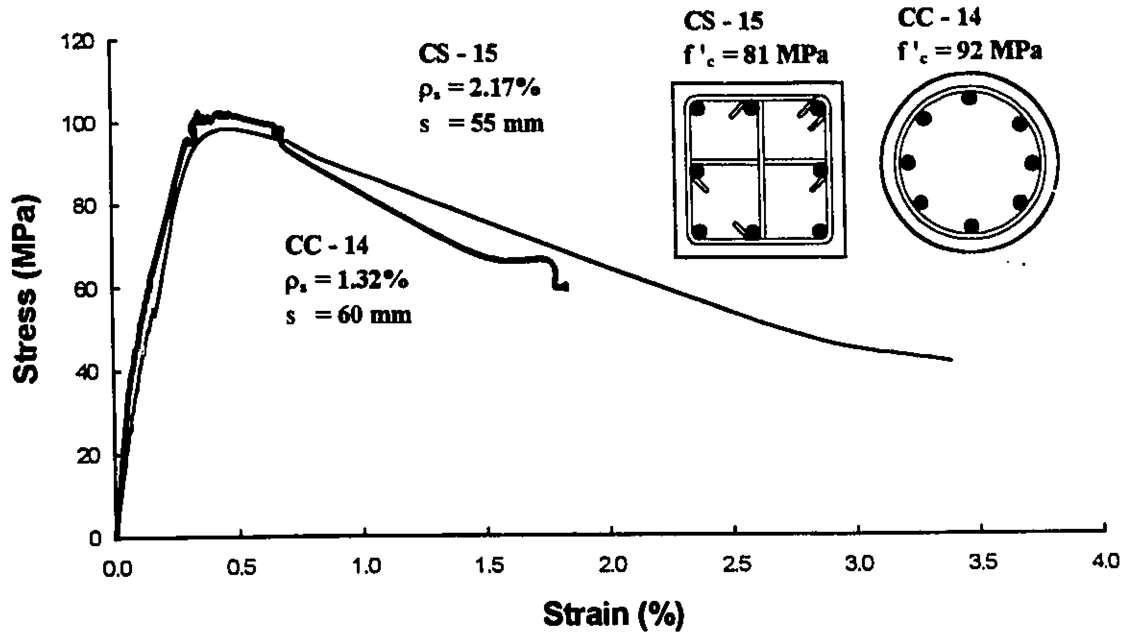

Figure 5. 23: Effect of section geometry (circular columns versus 8-bar arrangement square columns).

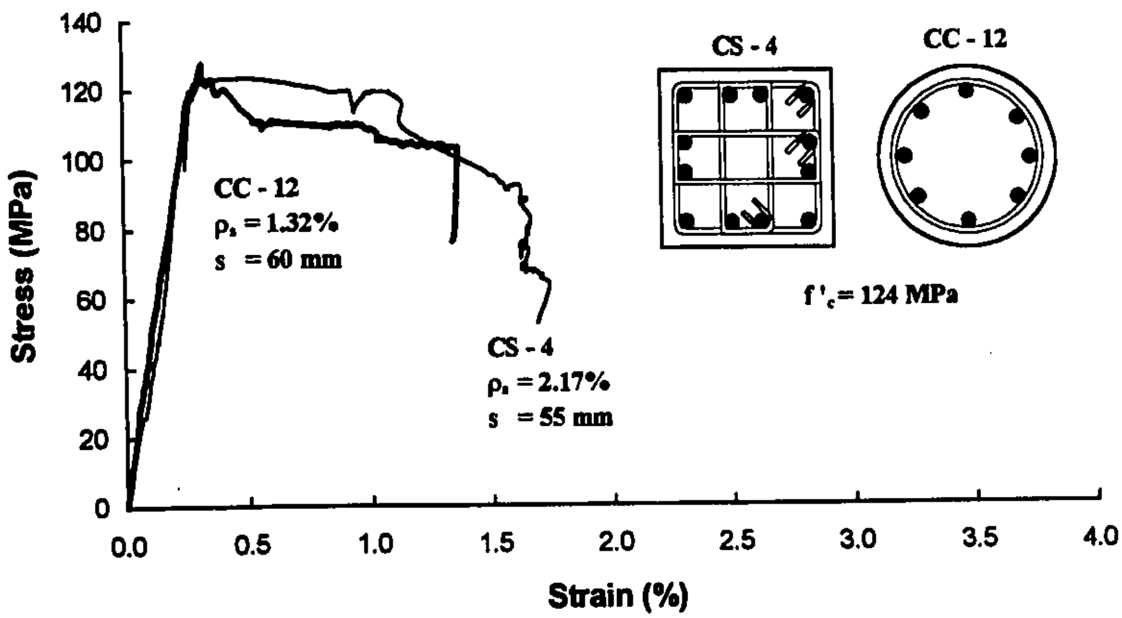

Figure 5. 24: Effect of section geometry (circular columns versus 12-bar arrangement square columns).

Chapter 6

Analytical Computations

Part 1- Review of Available Models

6.1 General

A critical review of previously proposed confinement models is presented in this Chapter. While the models for normal-strength and high-strength concretes are both included in the review, the emphasis is placed on those that were developed for high-strength concrete. A comprehensive review of available models for normal-strength concrete was presented earlier by the author (Razvi 1988). Development of a new confinement model, applicable to normal-strength and high-strength concretes, is discussed in Chapter 8 with extensive verifications, involving a large number of comparisons with experimental data.

6.2 Confinement Models for Normal Strength Concrete

Richart et al. (1928, 1928) were among the first researchers to study strength and ductility of confined normal-strength concrete. Their research on concrete cylinders, either confined by uniform fluid pressure or spiral reinforcement, provided some of the basic information on concrete confinement. Confinement by reinforcement was researched extensively in the past by Chan (1955), Roy and Sozen (1964), Sulaiman and Yu (1967), Sargin et al. (1971), Kent and Park (1971), and Vallenas et al. (1977). These researchers developed analytical models for the stress-strain relationship of confined concrete. The main variables considered in these models were the size, strength, amount and spacing of lateral reinforcement. Other variables considered included cross-sectional size and shape, rate of loading, and amount of longitudinal reinforcement.

Researchers prior to 1975 did not consider the distribution of longitudinal reinforcement and the resulting tie arrangement as a confinement parameter. This effect was discussed by Park and Paulay (1975), and Sheikh and Uzumeri (1980). The tie arrangement was not a parameter in the earlier models, as well as some of the more recent models (Park, Priestley, and Gill 1982, Fafitis and Shah 1985). The influence of this parameter on square columns was shown experimentally, for the first time, by Sheikh and Uzumeri (1980) The importance of tie arrangement was also shown by Scott, Park, and Priestley (1982) for columns under concentric and eccentric loadings, and by Ozcebe and Saatcioglu (1987) for columns under reversed cyclic loading. This effect was first modeled by Sheikh and Uzumeri (1982), using "effectively confined core area" concept, illustrated in Figure 6.1. A comparative study, conducted by Sheikh (1982), showed that models that did not include reinforcement arrangement as a parameter were not able to predict differences in response resulting from the tie arrangement. The Sheikh and Uzumeri model was subsequently modified by Sheikh and Yeh (1986) and Yeh and Sheikh (1988) to incorporate the effects of eccentric loading and high axial compression under eccentric loading. A comprehensive bibliography of available models prior to 1988 was compiled by the author (Razvi 1988).

A theoretical model was proposed by Mander, Priestley and Park (1988), with a wider scope than those previously proposed. The model was based on the effectively confined core area concept. The model was shown to produce good predictions of test data for circular, square, and rectangular sections subjected to high and low strain rates.

While the effectively confined core area concept, as proposed for symmetrically reinforced square columns (Sheikh and Uzumeri 1982) was a significant step forward in predicting the characteristics of confined concrete, the application of the concept to non-square sections raises questions, especially if the empirically derived coefficients for square sections are to be used. Figure 6.1 (b) illustrates a rectangular section where the parabolic arches defining the effectively confined core area overlap, resulting in negligibly small or negative effectively confined core area. Therefore, this section is expected to develop little or no confinement action. However, the same section can develop significant confinement when reinforced with closely spaced hoops, especially if it has high volumetric ratio of hoop steel. Therefore, the use of effectively confined core area concept for this column may result in erroneous results.

Additional difficulties arise when the same concept is applied to columns with asymmetric tie arrangement, and used to quantify lateral pressure, as done by Mander, Priestley and Park (1988). Figures 6.1 (c) and 6.1 (d) illustrate column sections with unequal lateral reinforcement arrangements in two orthogonal directions. In this case the lateral pressure in each direction is different. In rectangular sections, the pressure on the long side has a more pronounced effect than that acting on the short side. However, the effectively confined area is a sectional property which does not reflect the differences in confinement pressure in each direction.

The effectively confined core area concept has further limitations when applied to sections reinforced with different confinement reinforcement. Figure 6.1 (e) illustrates a square column reinforced with square hoops and a circular spiral. The concept as defined for square columns with rectilinear reinforcement, can not be applied to this type of columns.

6.3 Confinement Models for High Strength Concrete

Confinement models developed for normal-strength concrete may not be applicable to high-strength concrete. These models were shown to overestimate ductility when applied to high-strength concrete. Therefore, existing confinement models for normal strength-concrete are usually modified to be used for high-strength concrete. The following is a brief summary of confinement models proposed in the literature for high-strength concrete.

6.3.1 Ahmed and Shah (1982)

Ahmed and Shah were among the first group of researchers who propose a model for confined-high strength concrete. The model was developed on the basis of test data on up to 69 MPa concrete columns. It involves an iterative procedure, utilizing triaxial stress-strain relationship of plain concrete and stress-strain relationship of confinement steel. The model was verified against tests of concrete cylinders confined with circular spirals.

6.3.2 Martinez, Nilson, and Slate (1982)

Martinez et al. (1982) proposed a stress-strain relationship for confined concrete within the range of 21 to 83 MPa for normal-density concrete and 21 to 62 MPa for low-density concrete. The model is limited to steel grades of 414 MPa and lower. The relationship was derived on the basis of test data obtained from concrete cylinders confined with circular spirals, without any longitudinal reinforcement. Strength enhancement was expressed as a function of lateral pressure and spacing of confinement steel, as indicated below.

$$f'_{cc} = f'_{co} + \Delta f'_c \tag{6.1}$$

$$\Delta f'_c = 4.0\, f'_r \left(1 - \frac{s}{D'}\right) \tag{6.2}$$

$$f'_r = \frac{2\, A_{sp}\, f_{sp}}{s\, D'} \tag{6.3}$$

Ductility improvement is expressed in terms of concrete strength, lateral pressure, and spacing of confinement reinforcement.

$$\epsilon_1 = \epsilon_{01} + \Delta\epsilon_c \tag{6.4}$$

$$\Delta\epsilon_c = \frac{1.724\, f'_r \left(1 - \frac{s}{D'}\right)}{(f'_c)^2} \tag{6.5}$$

Where D' is the diameter of core concrete, A_{sp} is the area of circular hoop, and f_{sp} is the stress in circular hoop. It was assumed that the in place strength of concrete $f'_{co} = 0.85\, f'_c$, and the corresponding strain $\epsilon_{co} = 0.0025$. Substituting these values into the above equations leads to;

$$f'_{cc} = 0.85 f'_c + \frac{8.0 A_{sp}\, f_{sp}}{s\, D'} \left(1 - \frac{s}{D'}\right) \tag{6.6}$$

$$\epsilon_1 = 0.0025 + \frac{3.45 A_{sp}\, f_{sp}}{s\, D' (f'_c)^2} \left(1 - \frac{s}{D'}\right) \tag{6.7}$$

The mathematical expression for the ascending branch of the stress-strain relationship is given below.

For $\epsilon_c \le \epsilon_1$:

$$f_c = \frac{E_c\ \epsilon_c}{1+\left[\frac{E_c}{E_o}-2\right]\left[\frac{\epsilon_c}{\epsilon_1}\right]+\left[\frac{\epsilon_c}{\epsilon_1}\right]^2} \tag{6.8}$$

where;

$$E_c = (40000\sqrt{f'_c}+1.0x10^6)\left[\frac{w_c}{145}\right]^{1.5} \qquad psi \tag{6.9}$$

$$E_o = \frac{f'_{cc}}{\epsilon_1} \tag{6.10}$$

The descending branch was assumed to be a straight line, where the strain at 15% strength decay for confined concrete, ϵ_{85}, was defined as indicated below.

$$\epsilon_{85} = \epsilon_{085} + \frac{22.1x10^3 f'_r\left[1-\frac{s}{D'}\right]}{(f'_c)^3} \tag{6.11}$$

The strain at 15% stress decay for unconfined concrete, ϵ_{085}, was defined as;

$$\epsilon_{085} = 0.0025\left[\left(\frac{17.1}{f'_c}\right)^2+1\right] \tag{6.12}$$

6.3.3 Muguruma, Watanabe, Iwashimizu, and Mitsueda (1983)

Watanabe et al. (1980) had proposed a model for confined concrete with a strength of 26.2 MPa to 61.4 MPa. The model had been derived based on tests of concrete prisms and cylinders confined by lateral reinforcement having a yield strength between 161 and 1353 MPa. Muguruma et al. (1983) modified the model to increase the range of concrete strength. The modification was based on tests of small scale square columns confined with 1390 MPa lateral steel, without any longitudinal reinforcement. The concrete strength varied between 34 to 87.5 MPa. A confinement coefficient, C_c, was proposed as defined below, and used to express the peak stress and corresponding strain of confined concrete.

$$C_c = 0.313 \rho_s \frac{\sqrt{f_{yt}}}{f'_c} \left(1 - 0.5 \frac{s}{b}\right) \tag{6.13}$$

Where b is the largest dimension of confined core concrete.

The peak stress and strain are function of the confining coefficient, and given below.

$$f'_{cc} = (1 + 49 C_c) f'_c \tag{6.14}$$

$$\epsilon_1 = (1 + 341 C_c)\, \epsilon_{01} \tag{6.15}$$

The peak strain of unconfined concrete, ϵ_{01}, can be calculated as follows;

$$\epsilon_{01} = (0.814 k_m + 1.67) / 1000 \qquad k_m \leq 1.5 \tag{6.16}$$

$$\epsilon_{01} = 2.817 / 1000 \qquad k_m > 1.5 \tag{6.17}$$

Where k_m is a parameter that reflects the mix properties of fresh concrete, and can be calculated from the following equation.

$$k_m = (f'_c/54)\ (c/500)^2\ (w/200) \qquad (6.18)$$

The terms c and w refer to cement and water contents in (kg/m^3), respectively.

Ascending part of the proposed stress-strain relationship consists of two second degree parabolas. The first parabola is common to both unconfined and confined concretes, and starts at the origin and terminates at the peak point of unconfined concrete (f'_c , ϵ_{01}). The second parabola starts at (f'_c, ϵ_{01}) and terminates at the peak point of confined concrete (f'_{cc} , ϵ_1). The descending branch of the stress-strain relationship is a straight line. Starting at the peak of confined concrete (f'_{cc} , ϵ_1), and terminating at a point referred to as the available limit strain of confined concrete (f'_{cu} , ϵ_{cu}). The mathematical expressions for the three parts of the relationship are given below.

For $0 < \epsilon_c < \epsilon_{01}$:

$$f_c = E_i\ \epsilon_c + \frac{(f'_c - E_i \epsilon_{01})}{\epsilon_{01}^2}\ \epsilon_c^2 \qquad (6.19)$$

$$E_i = 4651\sqrt{f'_c} \qquad (6.20)$$

For $\epsilon_{01} < \epsilon_c < \epsilon_1$:

$$f_c = \frac{(f'_c - f'_{cc})}{(\epsilon_{01} - \epsilon_1)^2}\ (\epsilon_c - \epsilon_1)^2 + f'_{cc} \qquad (6.21)$$

For $\epsilon_1 < \epsilon_c$

$$f_c=\frac{(f_{cu}-f'_{cc})}{(\epsilon_{cu}-\epsilon_1)}(\epsilon_c-\epsilon_1)+f'_{cc} \tag{6.22}$$

Where f_{cu} and ϵ_{cu} are defined below.

$$f_{cu}=\frac{2(S_c-f'_{cc}\ \epsilon_1)}{\epsilon_1+\epsilon_{cu}}+f'_{cc} \tag{6.23}$$

$$\epsilon_{cu}=(1+509\,C_c)\ \epsilon_u \tag{6.24}$$

The strain ϵ_u is defined below.

$$\epsilon_u=1.31\epsilon_{01} \qquad k_m>1.5 \tag{6.25}$$

$$\epsilon_u=(-0.265k_m+1.71)\epsilon_{01} \qquad k_m\leq 1.5 \tag{6.26}$$

Where, S_c is the area under the stress-strain curve of confined concrete up to the peak.

For unconfined concrete, the model consists of two parts. The ascending branch is the same as for confined concrete. The descending branch is a straight line defined by the following equation;

$$f_c=f'_c+\frac{(f_u-f'_c)(\epsilon_c-\epsilon_{01})}{(\epsilon_u-\epsilon_{01})} \tag{6.27}$$

Where;

$$f_u = f'_c + \frac{2(S - f'_c \epsilon_{01})}{(\epsilon_u + \epsilon_{01})} \tag{6.28}$$

Where S is the area under the stress-strain curve up to f_c'.

6.3.4 Fafitis and Shah (1985)

Fafitis and Shah had developed a model for confined concrete, based on a large number of small cylindrical specimens with concrete strengths up to 62 MPa. (Fafitis and Shah 1985 a). The model was later modified to include the effects of higher strength concretes (Fafitis and Shah 1985 b). The modification was based on the tests conducted by Muguruma et al. (1983) and Martinez et al. (1982).

According to the model, the peak stress and the corresponding strain can be calculated as follows;

$$f'_{cc} = \lambda_2 \left[f'_c + \left(1.15 + \frac{21}{f'_c} \right) f_r \right] \tag{6.29}$$

$$\epsilon_1 = 1.49x10^{-5} f'_c + 0.0296\lambda_2 \frac{f_r}{f'_c} + 0.00195 \tag{6.30}$$

Where;

$$\lambda_2 = 1 + 15 \left(\frac{f_r}{f'_c} \right)^3 \tag{6.31}$$

$$f_r = \frac{2A_s\, f_{yt}}{s\ D} \tag{6.32}$$

A_s is the area of circular spiral or circular hoop. The model was developed for circular columns, and can be used for square columns with well distributed and laterally supported longitudinal reinforcement. The confining pressure, f_r, is calculated approximately by assuming an equivalent circular column with an effective diameter, D_e, equal to the side of the confined square core. For such square column, the confining pressure is given below;

$$f_r = \frac{2A_{sh}\, f_{yt}}{s\ D_e} \tag{6.33}$$

A_{sh} is the total cross-sectional area of rectilinear ties, including cross ties if any. The proposed stress-strain relationship consists of two continuous branches. The ascending branch is a parabolic curve that starts at the origin and terminates at the peak (f'_{cc}, ϵ_1). The descending branch is an exponential curve that starts at the peak and reaches zero stress at infinite strain. The expressions defining the stress-strain relationship are given below.

For $\epsilon_c \leq \epsilon_1$:

$$f_c = f'_{cc}\left[1 - \left(1 - \frac{\epsilon_c}{\epsilon_1}\right)^A\right] \tag{6.34}$$

For $\epsilon_c \geq \epsilon_1$:

$$f_c = f'_{cc}\ \exp\left[-k(\epsilon - \epsilon_1)^{1.15}\right] \tag{6.35}$$

Where;

$$A = \frac{E_c \epsilon_1}{f'_{cc}} \tag{6.36}$$

$$k = 24.7 f'_c \exp\left(-1.45 \frac{f_r}{\lambda_1}\right) \tag{6.37}$$

$$\lambda_1 = 1 + 25 \frac{f_r}{f'_c}\left[1 - \exp\left(-\frac{f'_c}{44.79}\right)^9\right] \tag{6.38}$$

$$E_c = 33\ w^{1.5}\ \sqrt{f'_c} \qquad psi \tag{6.39}$$

It is to be noted that the model is applicable to unconfined concrete with $f_r = 0$.

6.3.5 Yong, Nour, and Nawy (1988)

Yong et al. (1988) proposed a stress-strain relationship on the basis of experimental data obtained from tests of small scale square columns with concrete strengths of 84 to 94 MPa. Three sets of parameters are required to define the complete stress-strain relationship. These include; the peak stress and corresponding strain (f_{cc}', ϵ_1), the stress defined as inflection stress on the descending branch and corresponding strain (f_i, ϵ_i), and the stress and strain at an arbitrarily selected point on the descending branch (f_{2i}, ϵ_{2i}) where ϵ_{2i} is equal to ($2\epsilon_i$ - ϵ_1). The proposed peak stress is similar to that suggested originally by Sargin (1971), and modified later by Vallenas et al. (1977). The expression is given below;

$$f'_{cc} = K f'_c = \left[1 + 0.11 \left(1 - \frac{0.245s}{h} \right) \left(\rho_s + \frac{nd''}{8sd} \rho \right) \frac{f_{yt}}{\sqrt{f'_c}} \right] f'_c \qquad (6.40)$$

where, h is the length of one side of the rectangular tie, n is the number of longitudinal bars, d'' is the nominal diameter of lateral ties, d is the nominal diameter of longitudinal bars, and ρ is the volumetric ratio of longitudinal reinforcement.

The proposed strain corresponding to the peak stress is also similar to that proposed originally by Sargin (1971), as illustrated below.

$$\epsilon_1 = 0.00265 + \frac{0.008 \left(1 - \frac{0.734s}{h''} \right) (\rho_s f_{yt})^{2/3}}{\sqrt{f'_c}} \qquad (6.41)$$

The other variables can be calculate from the following equations;

$$f_i = f'_{cc} \left[0.25 \left(\frac{f'_c}{f'_{cc}} \right) + 0.4 \right] \qquad (6.42)$$

$$\epsilon_i = K \left[1.4 \left(\frac{\epsilon_1}{K} \right) + 0.0003 \right] \qquad (6.43)$$

$$f_{2i} = f'_{cc} \left[0.025 \left(\frac{f'_c}{6.9} \right) - 0.065 \right] \geq 0.30 f'_{cc} \qquad (6.44)$$

$$\epsilon_{2i} = 2\epsilon_i - \epsilon_1 \tag{6.45}$$

The proposed stress-strain curve consists of three parts. The first part (ascending branch) and second part (descending branch) are polynomials, similar in form to that originally proposed by Sargin (1971). They are used to produce a smooth continuous curve. The two equations meet with a slope continuity at the peak stress point. The third part of the curve is a horizontal segment, starting at the end of the second part where the stress reaches 30% of the peak, and shows constant stress beyond this point. The mathematical expressions for the stress-strain relationship are given below.

For $\epsilon_c \le \epsilon_1$;

$$Y = \frac{AX + BX^2}{1 + (A-2)X + (B+1)X^2} \tag{6.46}$$

For $\epsilon_c \ge \epsilon_1$;

$$Y = \frac{CX + DX^2}{1 + (C-2)X + (D+1)X^2} \tag{6.47}$$

Where;

$$X = \frac{\epsilon_c}{\epsilon_1} \tag{6.48}$$

$$Y = \frac{f_c}{f'_{cc}} \tag{6.49}$$

$$A = E_c \frac{\epsilon_1}{f'_{cc}} \tag{6.50}$$

$$B = \left[\frac{(A-1)^2}{0.55}\right] - 1 \tag{6.51}$$

$$C = \frac{(\epsilon_{2i} - \epsilon_i)}{\epsilon_1}\left[\frac{\epsilon_{2i}\, E_i}{(f_{cc}' - f_i)} - \frac{4\epsilon_i\, E_{2i}}{(f_{cc}' - f_{2i})}\right] \tag{6.52}$$

$$D = (\epsilon_i - \epsilon_{2i})\left[\frac{E_i}{(f'_{cc} - f_i)} - \frac{4E_{2i}}{(f'_{cc} - f_{2i})}\right] \tag{6.53}$$

$$E_i = \frac{f_i}{\epsilon_i} \tag{6.54}$$

$$E_{2i} = \frac{f_{2i}}{\epsilon_{2i}} \tag{6.55}$$

$$E_c = 27.55\, w^{1.5} \sqrt{f'_c} \qquad psi \tag{6.56}$$

6.3.6 Bjerkeli, Tomaszewecz, and Jensen (1990)

Bjerkeli et al. (1990) proposed a generalized model for high-strength concrete, applicable to circular, square, and rectangular sections. The behavior of confined concrete was assumed to be controlled by three parameters; concrete strength, confinement pressure, and section geometry. The model is applicable to normal density and low density concretes up to 90 MPa and 70 MPa, respectively. The equations presented here are only those applicable to normal density concrete. The proposed peak stress is given below.

$$f'_{cc} = f'_c + 4K_g f_r \qquad 45MPa < f'_c \leq 80MPa \tag{6.57}$$

$$f'_{cc} = f'_c + 3K_g f_r \qquad 80MPa < f_c < 90MPa \tag{6.58}$$

The confinement pressure is defined as;

$$f_r = \frac{A_{sh} f_{yt}}{h' s} \tag{6.59}$$

K_g is the larger of K_{g1} and K_{g2}.

$$K_{g1} = 1 - \frac{s}{d} \tag{6.60}$$

$$K_{g2} = 1 - \frac{nC^2}{5.5A_c} \tag{6.61}$$

Where; h': outer size of confined section.

A_{sh}: total effective area of hoop ties and supplementary confining reinforcement, in the direction under consideration, within spacing s.

d: the shorter outer diameter of hoop ties.

n: number of laterally supported longitudinal bars.

C: distance between laterally supported bars.

A_c: gross area of concrete section measured to centre line of peripheral hoop.

The strain corresponding to the peak can be calculated from the following equation.

$$\epsilon_1 = 0.0025 + 0.050 K_g \left(\frac{f_r}{f'_c} \right) \tag{6.62}$$

The proposed stress-strain relationship is a modified version of Martinez et al. (1982) model. It consists of three parts. The ascending branch is a polynomial, starting at the origin and ending at the peak stress. It is followed by a linear descending branch which ends at a stress level of f_{cy}. Beyond this point the stress is assumed to be constant. The expressions for the stress-strain relationship is given below.

For $\epsilon_c \leq \epsilon_1$:

$$f_c = \frac{E_c \, \epsilon_c}{1 + \left(\frac{E_c}{E_o} - 2 \right) \left(\frac{\epsilon_c}{\epsilon_1} \right) + \left(\frac{\epsilon_c}{\epsilon_1} \right)^2} \tag{6.63}$$

Where;

$$E_o = \frac{f'_{cc}}{\epsilon_1} \tag{6.64}$$

$$E_c = 9500\left(\frac{w_c}{2400}\right)^{1.5}\left(f'_c\right)^{0.3} \tag{6.65}$$

For $\epsilon_c > \epsilon_1$:

$$f_c = f'_{cc} - Z(\epsilon_c - \epsilon_1) \tag{6.66}$$

Where

$$Z = \frac{0.15\, f'_{cc}}{\epsilon_{85} - \epsilon_1} \tag{6.67}$$

$$\epsilon_{85} = \epsilon_{085} + \frac{0.05 K_g \left(f_r / f'_c \right)}{(1 - F)} \tag{6.68}$$

$$\epsilon_{085} = 0.0025\left[\left(\frac{17.07}{f'_c}\right)^2 + 1\right] \tag{6.69}$$

$$F = \frac{1}{1 + \left(\frac{1}{f_r K_g}\right)^{0.25}} \tag{6.70}$$

When the stress reaches f_{cy} on the descending branch, it remains constant. This stress is defined below.

$$f_{cy} = 4.87 \frac{d A_{sh} f_{yt}}{s A_c} \tag{6.71}$$

The main deficiencies of the model were discussed by Razvi and Saatcioglu (1991). Accordingly, the section geometry factor K_g is defined as the larger of K_{g1} and K_{g2}. The tie spacing s is included only in the expression for K_{g1}, while the number of laterally supported longitudinal bars is included only in the expression for K_{g2}. This implies that there is no effect of laterally supported longitudinal bars when K_{g1} governs, and no effect of tie spacing, when K_{g2} governs. This is inconsistent with experimental observations, as the tie spacing and the number of laterally supported longitudinal reinforcement both affect concrete confinement, and these parameters are interrelated.

The expression used for K_{g2} was developed for square columns. The applicability of this equation to circular and rectangular columns is questionable. Variables 'n' and 'C' are not defined for circular columns, as well as rectangular columns, where the spacing of longitudinal reinforcement is likely to be different in two orthogonal directions. In rectangular columns, the lateral confining pressure in one direction may not be equal to the pressure in the orthogonal direction. This implies that lateral pressure f_r used in the model is not constant for a given section. Therefore, the analytical model appears to have limitations that have not been mentioned by the authors.

Another questionable point in the analytical model is the sudden change in the confined concrete strength at the 80 MPa strength level. It is not likely that the concrete confinement mechanism changes suddenly at this strength level.

6.3.7 Muguruma, and Watanabe (1990)

Two of the previously proposed models were modified by Muguruma and Watanabe (1990) to reflect recent experimental results. The results were obtained from eight large scale HSC columns with well distributed longitudinal steel, tested under constant axial load and lateral load reversals.

One of the models had been developed by Muguruma et al. (1983) for high strength concrete, on the basis of column tests conducted on small scale square columns without longitudinal steel and cross ties. It was found that the model underestimated the curvature ductility in test columns. Therefore, the model was modified by reducing the slope of the descending branch to produce a better agreement with test data. The modification was introduced by increasing the available limit of compressive strain ϵ_{cu}. The original expression is given below.

$$\epsilon_{cu}=(1+509C_c)\ \epsilon_u \qquad (6.72)$$

The modified expression is;

$$\epsilon_{cu}=(1+509\alpha\, C_c)\ \epsilon_u \qquad (6.73)$$

Where, α is the modification coefficient. The value of α varies between 1.22 to 1.43 based on test results. However, a value of 1.2 was recommended for practical applications involving the computation of section curvature. The model does not account for effects of longitudinal steel distribution on confinement.

The second model that was modified by the same researchers was the modified Kent and

Park model (Park et al. 1982), originally developed for normal-strength concrete. It was found that the original model overestimated the curvature ductility of high-strength concrete columns. Therefore, the model was modified by increasing the slope of the descending branch as a function of concrete strength. The original slope of the descending branch is given by the following expression:

$$\tan\theta = K\,Z_m\,f'_c \qquad (6.74)$$

The modified slope of the descending branch can be calculated from the following expression:

$$\tan\theta = \beta K\,Z_m\,f'_c \qquad (6.75)$$

where, β is a modification factor, which is a function of concrete and steel strength, as indicated below:

$\beta = 1.0$ for $f_{yt} = 328$ MPa and $f_c' = 43$ MPa or less
$\beta = 3.5$ for $f_{yt} = 328$ MPa and $f_c' = 97$ MPa
$\beta = 1.0$ for $f_{yt} = 792$ MPa and $f_c' = 57$ MPa or less
$\beta = 3.5$ for $f_{yt} = 792$ MPa and $f_c' = 120$ MPa

K is the ratio of confined to unconfined concrete. Z_m is the base value of slope which is a function of concrete strength, as well as the amount, strength, and spacing of confinement reinforcement.

6.3.8 Muguruma, Nishiyama, Watanabe, and Tanaka (1991)

Muguruma et al. (1991) modified one of the models already modified for high-strength concrete (Muguruma and Watanabe 1990). The original model was developed by Muguruma et al. (1983). The modification was based on recent experiments conducted under constant axial load and lateral load cycles, and involved four large scale columns with concrete strength of 130 MPa. The re-modified model consists of three parts. The ascending branch is a polynomial, starting at the origin and ending at the peak stress. It is followed by a linear descending branch which ends at a stress level of 0.50 f_{cc}'. Beyond this point the stress is assumed to be constant. The mathematical expression of the ascending branch and the slope of the descending branch are identical to those of the modified modal (Muguruma and Watanabe 1990). However, in the re-modified model it was assumed that concrete strength does not fall below 50% of the peak stress.

6.3.9 Nagashima, Sugano, Kimura, and Ichikawa (1992)

Nagashima et al. (1992) proposed a model base on the results of square column tests. The effectively confined core area concept, suggested by Sheikh and Uzumeri (1982) was adopted in calculating confined concrete strength. The concept reflects the effects of longitudinal reinforcement and tie spacing. Confined concrete strength can be calculated from the following equations:

$$f'_{cc} = f'_{co} + 31.4\sqrt{\lambda^* \, P'_w \, f_{yt}} \qquad (6.76)$$

$$\lambda^* = \left(\left(1 - \frac{\Sigma C_i^2}{6B^2}\right)\left(1 - \frac{s}{2B}\right)\right)^2 \qquad (6.77)$$

Where,

P_w' = area ratio of lateral reinforcement (A_s / (B s)).

B = centre-to-centre distance between the legs of perimeter ties.

C_i = centre-to-centre distance between the longitudinal perimeter bars.

The strain at peak stress is expressed by the following equation:

$$\epsilon_1 = \epsilon_{01}\left[1 + 138\left(\frac{\lambda^* \, P'_w \, f_{yt}}{f'_{cc}}\right)\right]^2 \qquad (6.78)$$

The stress strain relationship consists of three parts. The expression proposed by Popovics (1973) and used by Mander et al. (1988) was adopted for the first part (ascending branch). The second part of the curve (descending branch) is a straight line, starting at the peak and terminating when the stress reaches 30 % of the peak stress. A horizontal line is assumed beyond this point to form the third part, with constant concrete stress.

The following are the mathematical expressions proposed for the stress-strain relationship.

For $\epsilon_c \leq \epsilon_1$:

$$f_c = \frac{f'_{cc}\, X\, r}{r - 1 + X^r} \qquad (6.79)$$

For $\epsilon_c > \epsilon_1$:

$$f_c = f'_{cc}\left[1 - 0.5\,\frac{\epsilon_c - \epsilon_1}{\epsilon_{50} - \epsilon_1}\right] \geq 0.3 f'_{cc} \qquad (6.80)$$

Where,

$$X = \frac{\epsilon_c}{\epsilon_1} \tag{6.81}$$

$$r = \frac{E_c}{E_c - E_{sec}} \tag{6.82}$$

$$E_{sec} = \frac{f'_{cc}}{\epsilon_1} \tag{6.83}$$

The strain at 50% stress decay is given below.

$$\epsilon_{50} = \epsilon_{01} + 0.193 \left(\frac{\lambda^{*} P'_{w} f_{yt}}{f'_{cc}} \right) \tag{6.84}$$

6.3.10 Muguruma, Nishiyama, and Watanabe (1993)

Muguruma et al. modified their original model for the fourth time in 1993. The modification was based on the same earlier tests that formed the basis for the previous two modifications (Muguruma and Watanabe 1990, and Muguruma et al. 1991). The present modifications are summarized below.

1. The peak strain of unconfined concrete ϵ_u, was expressed as a function of compressive strength f_c', to avoid the inconvenience of specifying water and cement contents for a particular concrete strength. The following equation was proposed to calculate ϵ_u;

$$\epsilon_{01} = 0.0013\left(1+\frac{f'_c}{98.6}\right) \qquad (6.85)$$

2. The modulus of elasticity was increased by about 10 %, as given in the following equation:

$$E_i = 22700\sqrt{\frac{f'_c}{19.6}} \qquad (6.86)$$

3. The descending branch of unconfined stress-strain curve was assumed to be a straight line that started at the peak (ϵ_u, f_c') and terminated at (0.004, 0). The equation for the descending branch is expressed below:

$$f_c = \frac{f'_c}{\epsilon_{01} - 0.004}\,(\epsilon_c - 0.004) \qquad (6.87)$$

4. The available strain and stress limits for plain concrete were expressed as given below;

$$\epsilon_u = \sqrt{\frac{2A_1\,(0.008-\epsilon_m)\;\epsilon_m-(0.004-\epsilon_m)}{f'_c}} \qquad (6.88)$$

$$f_u = \frac{f'_c\;(0.004-\epsilon_u\;)}{(0.004-\epsilon_{01})} \qquad (6.89)$$

Where;

$$A_1 = \frac{\epsilon_{01}\,(E_i\,\epsilon_{01} + 2f'_c)}{6} \tag{6.90}$$

5. The descending branch of confined concrete curve was assumed to continue to the zero stress level.

The mathematical expressions for stress-strain relationship of confined concrete are similar to those used in the previous version, as outlined below.

For $\epsilon_c \leq \epsilon_{01}$:

$$f_c = E_i\,\epsilon_c + \frac{(f'_c - E_i\,\epsilon_{01})}{\epsilon_{01}^2}\,\epsilon_c^2 \tag{6.91}$$

For $\epsilon_{01} < \epsilon_c < \epsilon_1$:

$$f_c = \frac{(f_c - f'_{cc})}{(\epsilon_{01} - \epsilon_1)^2}\,(\epsilon_c - \epsilon_1)^2 + f'_{cc} \tag{6.92}$$

For $\epsilon_1 < \epsilon_c$:

$$f_c = \frac{(f_{cu} - f'_{cc})}{(\epsilon_{cu} - \epsilon_1)}\,(\epsilon_c - \epsilon_1) + f'_{cc} \tag{6.93}$$

where ϵ_{cu} is the available strain limit of confined concrete, and f_{cu} is the stress corresponding to ϵ_{cu}. These two variables are calculated from the following equations.

$$f_{cu} = f'_{cc} - \frac{2(A_2 - f'_{cc}\,\epsilon_1)}{\epsilon_1 + \epsilon_{cu}} \tag{6.94}$$

$$\epsilon_{cu} = (1 + 611 C_c)\ \epsilon_u \tag{6.95}$$

where A_2 is the area under the stress-strain curve of confined concrete up to the peak. The peak stress and the corresponding strain are functions of confining coefficient C_c, and are given below.

$$f'_{cc} = (1 + 49 C_c) f'_c \tag{6.96}$$

$$\epsilon_1 = (1 + 341 C_c)\ \epsilon_{01} \tag{6.97}$$

where b is the maximum dimension of confined concrete core, and the confining coefficient, C_c, is defined below.

$$C_c = 0.313 \rho_s \frac{\sqrt{f_{yt}}}{f'_c} \left(1 - 0.5 \frac{s}{b}\right) \tag{6.98}$$

The model is applicable to columns with normal and high-strength concretes, in the range of 20 to 130 MPa, confined with normal and high-strength steel.

6.3.11 Cusson and Paultre (1993)

Cusson and Paultre (1993) proposed a model for confined concrete based on tests of large scale high-strength concrete columns. The model utilizes the 'effectively confined core area' concept which was originally proposed by Sheikh and Uzumeri (1982) and modified by Mander et al. (1988). The proposed expressions for peak stress and corresponding are given below.

$$f'_{cc} = f'_{co}\left[1.0 + 3.0\left(\frac{f_{le}}{f'_{co}}\right)^{0.9}\right] \tag{6.99}$$

$$\epsilon_1 = \epsilon_{01} + 0.2\left(\frac{f_{le}}{f'_{co}}\right)^{1.7} \tag{6.100}$$

Where:

$$f_{le} = K_e\, f_l = \frac{\left(1 - \frac{\sum w_i^2}{6c_x\, c_y}\right)\left(1 - \frac{s'}{2c_x}\right)\left(1 - \frac{s'}{2c_y}\right)}{(1 - \rho_c)}\, f_l \tag{6.101}$$

$$f_l = \frac{f'_h}{s}\left(\frac{A_{shx} + A_{shy}}{c_x + c_y}\right) \tag{6.102}$$

f'_h	= stress in lateral steel at peak stress of confined concrete.
A_{shx}, A_{shy}	= total area of lateral steel perpendicular to x and y axes, respectively.
c_x, c_y	= widths of concrete core parallel to the x-axis and y-axis, respectively.
s	= centre to centre tie spacing.
w_i	= clear spacing between adjacent longitudinal reinforcement.
s'	= clear spacing of ties.
ρ_c	= ratio of longitudinal steel.

The stress-strain relationship consists of two parts. The expression for the ascending branch was originally proposed by Popovics (1973) and later used by Mander et al. (1988) and Nagashima et al. (1992). The expression for the descending branch was adopted from Fafitis and Shah (1985). Following are the mathematical equations for the two branches.

For $\epsilon_c \leq \epsilon_1$:

$$f_c = \frac{f'_{cc} \, X \, r}{r-1+X^r} \tag{6.103}$$

For $\epsilon_c > \epsilon_1$:

$$f_c = f'_{cc} \, \exp\left[k_1 \left(\epsilon_c - \epsilon_1 \right)^{k2} \right] \tag{6.104}$$

$$X = \frac{\epsilon_c}{\epsilon_1} \tag{6.105}$$

$$r = \frac{E_c}{Ec - E_{sec}} \tag{6.106}$$

$$k_1 = \frac{\ln \, 0.5}{\left(\epsilon_{c50\,c} - \epsilon_1 \right)^{k_2}} \tag{6.107}$$

$$k_2 = 0.4 + 15 \left(\frac{f_{le}}{f_{co}} \right)^{1.3} \tag{6.108}$$

$$E_{sec} = \frac{f'_{cc}}{\epsilon_1} \tag{6.109}$$

The strain corresponding to 50% stress decay is given below.

$$\epsilon_{c50c} = \epsilon_{c50u} + 0.2 \left(\frac{f_{lc}}{f'_{co}} \right)^{1.2} \tag{6.110}$$

Where;

$\epsilon_{c\,50\,c}$ = strain at 50% drop beyond the peak stress of confined concrete.

$\epsilon_{c\,50\,u}$ = strain at 50% drop beyond the peak stress of unconfined concrete. In the absence of test data, a value of 0.004 can be assumed.

The proposed relationship can be used with $f_{lc} = 0$, and $k_2 = 1.5$ to describe the stress-strain relationship of unconfined concrete.

6.3.12 Cusson and Paultre (1994)

Cusson and Paultre (1994) modified their original model (Cusson and Paultre 1993) on the basis of column tests conducted by Nagashima et al. (1992). An iterative procedure was introduced, as part of modifications, to calculate the stress in lateral steel. The modified stress-strain relationship consists of the same ascending and descending branches of the original model. However, some of the empirically obtained coefficients were modified based on the new data base. Accordingly, the peak stress and corresponding strain, the strain at 50% stress decay, and coefficient k_2, originally described in equations 6. 99, 6.100, 6.110, and 6.108 respectively, are modified as follows;

$$f'_{cc} = f'_{co} \left[1.0 + 2.1 \left(\frac{f_{lc}}{f'_{co}} \right)^{0.7} \right] \tag{6.111}$$

$$\epsilon_1 = \epsilon_{01} + 0.21 \left(\frac{f_{le}}{f'_{co}} \right)^{17} \qquad (6.112)$$

$$\epsilon_{c50c} = \epsilon_{c50u} + 0.15 \left(\frac{f_{le}}{f_{co}} \right)^{1.1} \qquad (6.113)$$

$$k_2 = 0.58 + 16 \left(\frac{f_{le}}{f'_{co}} \right)^{1.3} \qquad (6.114)$$

All other equations remained the same as those used in the original model.

6.3.13 Li (1994)

Li (1994) proposed a generalized stress-strain relationship for confined and unconfined concrete. The model was developed on the basis of a large number of column tests with a wide range of concrete strength. It is applicable to circular and square columns confined with normal and high-strength steel. The model is described below.

Unconfined Concrete

A continuous curve was proposed to represent the stress-strain relationship of unconfined concrete. The proposed curve is a modified version of that proposed by Popovics (1973). The mathematical expression is;

$$f_c = \frac{f'_{cc}\, X\, r}{r - 1 + X^{rk}} \qquad (6.115)$$

Where;

$$X = \frac{\epsilon_c}{\epsilon_{01}} \tag{6.116}$$

$$r = \frac{E_c}{E_c - E_{sec}} \tag{6.117}$$

$$E_{sec} = \frac{f'_{co}}{\epsilon_{01}} \tag{6.118}$$

$$E_c = 3320\sqrt{f'_{co}} + 6900 \tag{6.119}$$

$$k = 0.67 + \frac{f'_{co}}{62} \geq 1.0 \tag{6.120}$$

$$\epsilon_{01} = \frac{0.7(f'_{co})^{0.3}}{1000} \tag{6.121}$$

Confined Concrete

Li (1994) found experimentally that a modified form of Popovic's equation would not accurately model the ascending and descending branches of confined high-strength concrete. Therefore, the equations proposed by Muguruma et al. (1993) were adopted after modification. The expressions for the proposed stress-strain relationship are given below;

For $\epsilon_c \leq \epsilon_{01}$:

$$f_c = E_c\, \epsilon_c + \frac{(f'_{co} - E_i\, \epsilon_{01})}{\epsilon_{01}^2}\, \epsilon_c^2 \qquad \textbf{(6.122)}$$

For $\epsilon_{01} < \epsilon_c < \epsilon_1$:

$$f_c = f'_{cc} - \frac{(f'_{cc} - f'_{co})}{(\epsilon_1 - \epsilon_{01})^2}\, (\epsilon_c - \epsilon_1)^2 \qquad \textbf{(6.123)}$$

For $\epsilon_1 < \epsilon_c$:

$$f_c = f'_{cc} - \beta\, \frac{f'_{cc}}{\epsilon_1}\, (\epsilon_c - \epsilon_1) \geq 0.4 f'_{cc} \qquad \textbf{(6.124)}$$

The following values are assigned to the β coefficient:

For concrete confined by circular high-strength steel ($f_{yt} > 1200$ MPa):

$\beta = 0.08$ when; $f'_{co} \leq 80$ MPa

$\beta = 0.20$ when; $f'_{co} > 80$ MPa

For concrete confined by circular normal-strength steel ($f_{yt} \leq 550$ MPa):

$\beta = 0.20$ when; $f'_{co} \leq 80$ MPa

For concrete confined by rectilinear high strength steel ($f_{yt} \geq 1200$ MPa):

$\beta = 0.07$ when; $f_{co} \leq 80$ MPa

$\beta = 0.10$ when; $f'_{co} > 80$ MPa

For concrete confined by rectilinear normal-strength steel ($f_{yt} \leq 550$ MPa) and $f'_{co} > 75$ MPa;

$$\beta = (0.048 f'_{co} - 2.14) - (0.098 f'_{co} - 4.57) \sqrt[3]{\frac{f'_l}{f'_{co}}} \tag{6.125}$$

The expressions for strength and ductility of confined concrete are also expressed on the basis of concrete strength and type of confinement reinforcement, as follows:

High-strength concrete confined by circular normal-strength steel:

The following expression was proposed for peak stress, on the basis of tests conducted by Khaloo and Ahmed (1989). The expression is similar to that used by Mander et al. (1988).

$$f'_{cc} = f'_{co} \left(-0.413 + 1.413 \sqrt{1 + 11.4 \frac{f'_l}{f'_{co}}} - 2 \frac{f'_l}{f'_{co}} \right) \tag{6.126}$$

The effective lateral pressure, f'_l, can be calculated based on the confinement effectiveness coefficient, K_e, as follows:

$$f'_l = 0.5 K_e \rho_s f_{yt} \tag{6.127}$$

$$K_e = \frac{\left(1 - \frac{0.5s'}{d_s}\right)^2}{1 - \rho_{cc}} \qquad (6.128)$$

Where, s′ is the clear spacing between circular hoops or spirals, d_s is the core diameter measured centre-to-centre of circular hoops or spiral, ρ_s is the volumetric ratio of confining reinforcement to core concrete, and ρ_{cc} is the ratio of longitudinal steel area to core area. Strain corresponding to the peak stress is expressed below.

$$\frac{\epsilon_1}{\epsilon_{co}} = 1.0 + 384\left(\frac{f'_l}{f'_{co}}\right)^2 \qquad (6.129)$$

The above expressions are only applicable in the range of 60 to 80 MPa.

<u>High-strength concrete confined by rectilinear normal strength steel:</u>

The peak stress is calculated using Eq. 6.126 provided above for circular columns. However, the effective pressure is calculated using the 'effectively confined core area' proposed by Sheikh and Uzumeri (1982) and later modified by Mander et al. (1988), and also used by Cusson and Paultre (1993, 1994). Accordingly, the effective pressure can be calculated as follows:

$$f'_l = 0.5K_e\ (\ \rho_x + \rho_y\ )\ f_{yt} \qquad (6.130)$$

$$K_e = \frac{\left(1-\frac{\sum w_i^2}{6c_x\ c_y}\right)\left(1-\frac{s'}{2c_x}\right)\left(1-\frac{s'}{2c_y}\right)}{(1-\rho_{cc})} \tag{6.131}$$

where; ρ_x , ρ_y are lateral confining reinforcement ratios parallel to x and y-axes, respectively, c_x, c_y are the widths of concrete core parallel to x and y-axes, respectively, w_i is the spacing between adjacent longitudinal reinforcement, and s′ is the clear spacing of ties. The strain corresponding to the peak stress is given below:

In the range of 60 MPa ≤ f_{co}' < 80 MPa;

$$\frac{\epsilon_1}{\epsilon_{co}} = 1.0+11.3\left(\frac{f'_l}{f'_{co}}\right)^{0.7} \tag{6.132}$$

In the range of 80 MPa ≤ f_{co}' < 100 MPa;

$$\frac{\epsilon_1}{\epsilon_{co}} = -8.1+9.1\ \exp\left(\frac{f'_l}{f'_{co}}\right) \tag{6.133}$$

Concrete confined by circular high-strength steel:

The expression proposed by Mander et al. (1988), to predict the peak stress of normal-strength concrete, was modified as follows:

$$f'_{cc} = f'_{co}\left(-1.254+2.254\sqrt{1+7.94\alpha_s\ \frac{f'_l}{f'_{co}}} - 2\,\alpha_s\ \frac{f'_l}{f'_{co}}\right) \tag{6.134}$$

For $f'_{co} \leq 52$ MPa;

$$\alpha_s = (21.2 - 0.35 f'_{co}) \frac{f'_l}{f'_{co}} \tag{6.135}$$

For $f'_{co} > 52$ MPa;

$$\alpha_s = 3.1 \frac{f'_l}{f'_{co}} \tag{6.136}$$

The strain corresponding to the peak stress is given below:

For $f'_{co} \leq 52$ MPa;

$$\frac{\epsilon_1}{\epsilon_{01}} = 1.0 + (119.8 - 1.554\, f'_{co}) \left(\frac{f'_l}{f'_{co}} \right) \tag{6.137}$$

For $f'_{co} > 52$ MPa;

$$\frac{\epsilon_1}{\epsilon_{01}} = 1.0 + (71.4 - 0.623\, f'_{co}) \left(\frac{f'_l}{f'_{co}} \right) \tag{6.138}$$

<u>Concrete confined by rectilinear high-strength steel:</u>

The peak stress is calculated using the same form of equation used for circular columns, as shown below:

$$f'_{cc} = f'_{co} \left(-1.254 + 2.254 \sqrt{1 + 7.94 \alpha_s \frac{f'_l}{f'_{co}}} - 2 \alpha_s \frac{f'_l}{f'_{co}} \right) \tag{6.139}$$

Where;

$$\alpha_s = 1.56\left(\frac{f'_l}{f'_{co}}\right) \tag{6.140}$$

The strain corresponding to the peak stress:

For $f'_{co} \leq 52$ MPa;

$$\frac{\epsilon_1}{\epsilon_{01}} = 1.0 + (78.1 - 0.83\, f'_{co})\left(\frac{f'_l}{f'_{co}}\right) \tag{6.141}$$

For $f'_{co} > 52$ MPa;

$$\frac{\epsilon_1}{\epsilon_{01}} = 1.0 + (55.3 - 0.39\, f'_{co})\left(\frac{f'_l}{f'_{co}}\right) \tag{6.142}$$

6.3.14 Azizinamini, Kuska, Brungardt, and Hatfield (1994)

Azizinamini et al. (1994) modified Yong et al. (1988) model based on their test results and those conducted by Yong et al. (1988). The model consists of a linear ascending branch, followed by a linear descending branch and a constant residual stress of 0.3 f''_{cc}. The peak stress and corresponding strain of confined concrete were adopted from Yong et al. (1988) as given below:

$$f'_{cc} = K\, f'_c = \left[1 + 0.11\left(1 - \frac{0.245s}{h}\right)\left(\rho_s + \frac{nd''}{8sd}\rho\right)\frac{f_{yt}}{\sqrt{f'_c}}\right] f'_c \tag{6.143}$$

$$\epsilon_{cc} = 0.00265 + \frac{0.008\left(1 - \frac{0.734\, s}{h''}\right)(\rho_s\, f_{yt})^{2/3}}{\sqrt{f'_c}} \tag{6.144}$$

Where;

- h : rectilinear tie dimension
- n : number of longitudinal reinforcement
- d": nominal diameter of lateral ties
- d : nominal diameter of longitudinal reinforcement
- ρ : volumetric ratio of longitudinal reinforcement.
- ρ_s : volumetric ratio of longitudinal reinforcement.

The ascending branch of the stress-strain relationship is defined below.

For $\epsilon_c \le \epsilon_1$:

$$f_c = \frac{f'_{cc}}{\epsilon_1}\,\epsilon \tag{6.145}$$

For $\epsilon_c > \epsilon_1$:

$$f_c = f'_{cc}\left[1 - \alpha\,(\epsilon - \epsilon_1)\right] \ge f'_{cc} \tag{6.146}$$

Where;

$$\alpha = \frac{0.25\,\dfrac{\left(0.145f'_c - 0.6\right)}{0.145f'_{cc}}}{3.13K\left[1.4\left(\dfrac{\epsilon_1}{K}\right)+0.0003\right]} \tag{6.147}$$

6.4 Summary and Conclusions

The following observations can be made based on the review of previously proposed analytical models presented above:

- Most of the models proposed for high-strength concrete are modified versions of models developed for normal-strength concrete. The modifications are usually made based on limited test data. Therefore, the modified models may be limited to cases considered in a particular experimental program, and may have to be remodified for other cases. Many examples of this were presented in the previous section.

- Most of the proposed models for high-strength concrete are applicable to either circular or square columns, and are not general enough to cover both cases. Ahmed and Shah (1983), Martinez et al. (1982), and Fafitis and Shah (1985) models were developed for circular columns. All others, with the exception of that proposed by Li (1994), were developed for square columns.

- The parameters of confinement considered in developing models for high-strength concrete are the same as those considered for normal-strength concrete.

- Many of the models proposed for square columns do not include the distribution of longitudinal reinforcement as a confinement parameter. Those that include this parameter are based on the "effectively confined core area concept", with the exception of that proposed by Yong et al. (1988).

- With the exception of those proposed by Muguruma et al. (1991, 1993) and Li (1994), none of the previous models is applicable to a wide range of concrete strength, covering between 30 MPa, which is a commonly used normal-strength concrete, and 130 MPa, which is generally regarded as the highest strength that can be attained with ordinary materials of concrete. The two that have a relatively wide range of applicability in terms of strength, have other limitations, seriously hindering their use as generalized models.

- It can be concluded that there exists a need for an analytical model that is relatively simple to use and general enough to cover the cross-sectional shapes and reinforcement arrangements used in practice. This model should reflect all the relevant parameters of confinement with a smooth transition from normal-strength to high-strength concrete.

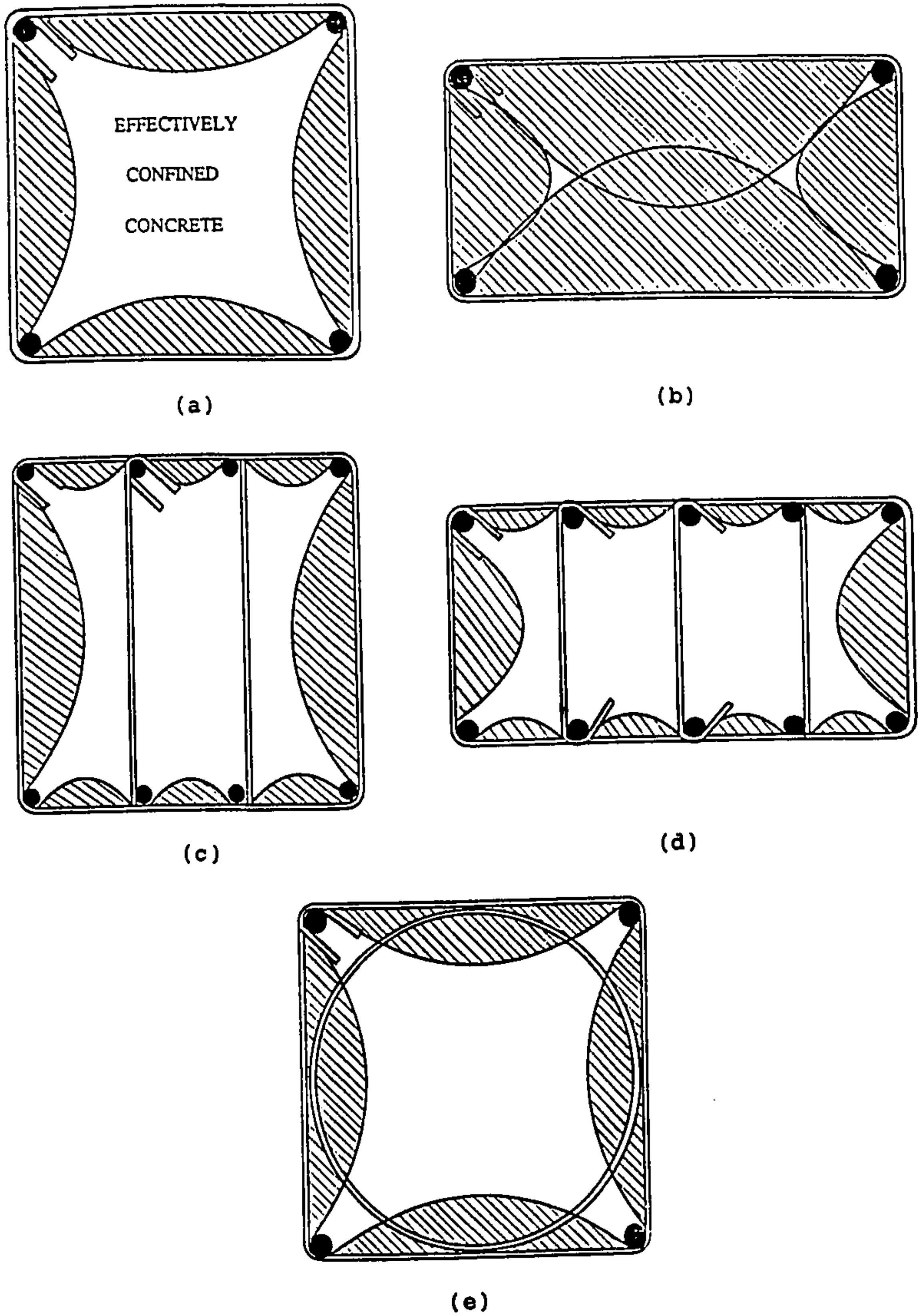

Figure 6.1: Generalization of effectively confined area concept.

Chapter 7

Analytical Computations

Part 2 - Development of a Confinement Model

7.1 General

A mathematical model was developed for stress-strain relationship of confined concrete. The model was developed in two stages. The first stage involved the formulation of the model for normal-strength concrete, for which extensive test data was available. The second stage involved the formulation of strength dependent parameters based on experimental research on high-strength concrete. The experimental research used for the latter stage included that reported in Chapter 4 and those previously conducted by others. Extensive verification of the analytical model has been done against available test data, covering a wide range of parameters.

The model is based on the computation of confinement pressure caused by circular or rectilinear transverse reinforcement, and the resulting improvement in strength and ductility of confined concrete. A large volume of test data, including those for poorly and well confined concretes, was evaluated to establish the parameters of the model. The model is general, and is applicable to circular, square, and rectangular columns, confined by different types of reinforcement arrangements. It can be used to predict concrete behaviour under concentric and eccentric loadings, applied with slow and fast strain rates. Development of the model, and the comparisons with experimental data, are presented in this chapter.

7. 2 Development of a Model for Normal-Strength Concrete

7.2.1 Confined Concrete Strength

Plain concrete subjected to longitudinal compression is in a uniaxial state of stress. Longitudinal strains generated by such loading give rise to transverse tensile strains, which may result in vertical cracking. As the material approaches its uniaxial compressive capacity, the transverse strains and vertical cracks reach their limiting values.

For a linearly elastic and isotropic material, the limiting value of lateral strain at failure can be expressed as shown below:

$$\epsilon_{u1} = -\mu f_{u2} / E \qquad (7.1)$$

The material failure can be prevented if the development of the limiting lateral strain is counteracted. This can be achieved either by active, or passive lateral pressure caused by the lateral restraint. The combination of lateral pressure and axial compression results in a triaxial state of stress.

Uniaxial and triaxial stress conditions are illustrated in Figure 7.1. Transverse strains caused by lateral pressure counteract the tendency of material to expand laterally, resulting in increased strength. For a linearly elastic and isotropic material, the limiting transverse strain can be determined from Hook's law as indicated below:

$$\epsilon_{t1} = \frac{f_{t1} - \mu \left(f_{t2} + f_{t1} \right)}{E} \tag{7.2}$$

Assuming failure under triaxial and uniaxial stress conditions take place at the same transverse strain level, Eq. 7.1 can be set equal to equation Eq. 7.2. Solving for f_{t2} provides the expression for axial strength of material under triaxial stress condition, in terms of lateral pressure.

$$\epsilon_{u1} \approx \epsilon_{t1} \tag{7.3}$$

$$f_{t2} = f_{u2} + k'_1 f_{t1} \tag{7.4}$$

where;

$$k'_1 = (1 - \mu)/\mu \tag{7.5}$$

Coefficient k_1' is a function of the Poisson's ratio μ. For Poisson's ratios of 0.1 and 0.3, the corresponding values of k_1' are 9.0 and 2.3 respectively, resulting in a higher value for a lower value of Poisson's ratio. The stress terms; f_{t1}, f_{t2}, and f_{u2} represent stresses under triaxial and uniaxial stress conditions, acting in directions 1 and 2. E is the elastic modulus.

The above equations are not directly applicable to concrete. The elastic modulus and the

Poisson's ratio of concrete change due to material nonlinearity and internal cracking. Furthermore, the stress-strain characteristics and Poisson's ratio may be different in all three orthogonal directions. However, the mechanism of load resistance described above can be used to explain the confinement of concrete in reinforced concrete elements.

The lateral pressure in reinforced concrete is provided by reinforcement where the transverse reinforcement plays a major role. In this case the lateral pressure may or may not be uniform. Furthermore, the coefficient that relates the lateral pressure to strength enhancement is different than that given by Eq. 7.5. Recognizing these differences between a linearly elastic isotropic material and concrete, Eq. 7.4 can be written to express triaxial strength of concrete in terms of uniaxial strength and lateral confinement pressure.

$$f'_{cc} = f'_{co} + k_1 f_l \tag{7.6}$$

where, f_{cc}' and f_{co}' are confined and unconfined strengths of concrete in member, respectively. While the coefficients k_1 and k_1' are not identical, it is reasonable to expect that k_1, like k_1', is a function of the Poisson's ratio, and as in the previous case, assumes lower values for higher values of this ratio. Since higher values of Poisson's ratio occur near failure, when the lateral pressure is maximum, lower values of coefficient k_1 corresponds to higher values of lateral pressure.

The variation of coefficient k_1 with lateral pressure f_l can best be obtained from experimental data. Figure 7.2 contains experimental data obtained from specimens subjected to different levels of hydrostatic pressure (Richart et al. 1928), and an analytical relationship obtained from regression analysis. The results show that coefficient k_1 does assume low values for high values of lateral pressure, approaching a constant value in the high pressure range. However, for normal-strength concrete, the lateral pressure provided by reinforcement, is generally in the low end of the pressure range shown in Fig. 7.2. The expression given below, obtained from regression analysis of test data, reflects the variation of coefficient k_1 with lateral pressure.

$$k_1 = 6.7\,(f_l)^{-0.17} \qquad (7.7)$$

where f_l is uniform confinement pressure in MPa. Tests conducted by Balmer (1949) and, Sato and Ibushi (1988) also indicate that coefficient k_1 attains low values for high values of lateral pressure.

Eq. 7.6 was also arrived at by Richart et al. (1928) from experimental data. Richart et al. performed a large number of cylinder tests under different levels of lateral fluid pressure (Richart, Brandtzaeg, Brown, 1928), as well as tests of spirally reinforced cylinders (Richart, Brandtzaeg, Brown, 1929). It was reported that Eq. 7.6 with a constant value of 4.1 for k_1 produced a good correlation with spirally reinforced test cylinders. Their recommendations have formed the basis for confinement steel requirements of the ACI 318 Building Code (1989) for many years.

The unconfined concrete strength f_{co}' in Eq. 7.6 is the plain concrete strength in a member under concentric loading. This may be different than that obtained from a standard cylinder test. Therefore it should best be determined from tests of plain concrete specimens of the same geometry, size, and concrete casting practice as those of the actual column member. In the absence of such test data, standard cylinder test results may be used with an appropriate modification. Modification factors ranging between 0.85 and 1.00 have been reported in the literature. For members subjected to high strain rates, the unconfined concrete strength f_{co}' should be determined under the same strain rate for which the confined concrete strength f_{cc}' is sought.

7.2.1.1 Circular Sections

The relationship between concrete strength and lateral confining pressure, given in Eq.

7.6, is valid for uniform lateral pressure. The pressure provided by closely spaced circular spirals and vertical column reinforcement can be considered to be uniform around the perimeter of the core. This lateral pressure can be computed from statics, as illustrated by Fig. 7.3. If the pressure is computed at the useful limit of the hoop steel, i.e. at yield, and taken equal to the uniform pressure f_l given in Eq. 7.6, and coefficient k_1 is obtained from Eq. 7.7, the confined concrete strength can be established for spirally reinforced circular columns.

Equations 7.6 and 7.7 were used to compute confined concrete strengths of 24 circular columns reinforced with circular spiral or circular hoop and longitudinal reinforcement. The columns were tested by two groups of researchers in two different research programs (Mender, Priestley and Park, 1988, and Sheikh and Toklucu, 1993). The columns were tested under both slow and fast rates of concentric loading. The results are shown in Table 7.1 and 7.2 and Fig. 7.4. Comparisons of experimental and analytical values indicate excellent agreement.

7.2.1.2 Square Columns

While the uniform confinement pressure for spirally reinforced columns can be found from hoop tension, it is difficult to determine the confining pressure exerted by a square or a rectangular hoop. Therefore, empirical expressions were used in the past to relate what was observed to be significant during the experiments, to the increase in concrete strength. However, a more general and rational approach, analogous to that used for spirally reinforced columns can be employed to compute the equivalent lateral pressure and the resulting confined concrete strength, starting from material and geometric properties.

The passive confinement pressure exerted by a square hoop is dependent on the restraining force developed in the hoop steel. The hoop steel can develop high restraining forces at the corners, where it is supported laterally by transverse legs, and low restraining action between the laterally supported corners. The restraining force at each corner depends on the force that can be developed in the transverse leg, which in turn is related to the area and stress of the hoop steel. The restraining action of the hoop between the corners is related to the flexural rigidity of the hoop steel, which depends on the size and unsupported length of the bar. This restraining action is proportional to the elastic rigidity of the hoop steel until yielding. Beyond yielding, the restraining action remains approximately constant until the strain hardening of steel produces additional restraining action. However, the flexural rigidity of the hoop between the laterally supported nodal points and the resulting restraining action is very small as compared to the restraining action of the corners and the other nodal points. Therefore, as the concrete expands laterally under axial compression, there will be higher reactive pressures building up at the nodal points, than at locations away from the nodes. Figure 7.5 illustrates the build-up of passive confinement pressure in a square column. If cross ties or inside hoops are used to support the middle bars, additional points of high lateral restraint are generated. It is clear that the shape of the pressure distribution is a function of the reinforcement arrangement. Shapes of pressure distributions for various tie arrangements are shown in Fig. 7.6.

Concrete confinement is a three dimensional phenomenon that can not be reduced to a sectional level. Therefore, it is essential to consider the variation of lateral pressure along member length. This is illustrated in Fig. 7.7. It should be noted that the pressure developed at a nodal point, where the longitudinal bar is supported by a lateral tie, is distributed reasonably uniformly along the length of the longitudinal bar. This is because the longitudinal bar in compression, with a short unsupported length between the ties, maintains the restraining action until it begins to lose its stability. The lateral pressure between the ties reduces with the distance from the longitudinal reinforcement. This reduction occurs at a faster rate than that of the pressure at the tie level.

For the case of closely spaced and laterally supported longitudinal reinforcement, the pressure distribution is close to uniform. In this case a transverse force of $A_s f_{yt}$ is developed in each transverse bar at the useful limit of reinforcement, where A_s and f_{yt} are the area and yield strength of transverse reinforcement, respectively. The summation of these forces divided by the area bound by the core dimension, measured center-to-center of perimeter hoop (b_c) and center-to center tie spacing (s) leads to an average uniform pressure for which Eq. 7.6 was derived. At the other extreme, columns with four corner bars tied by widely spaced perimeter hoops are subjected to pressure peaks at corner nodal points. The reduction of pressure in the longitudinal direction between the ties becomes more pronounced. In this case the assumption of uniform pressure, obtained by distributing these corner forces over the side of the core, results in overestimation of the actual effect of lateral pressure. Therefore, the average pressure can not reflect the true effect of the actual confinement pressure. In this case an equivalent uniform pressure, with the same effect as that of the actual non-uniform pressure, is needed if Eq. 7.6 is to be used. Figure 7.8 illustrates the actual, average, and equivalent lateral pressures in a square column section. The equivalent uniform pressure f_{le} can be established by reducing the average pressure with due considerations given to the appropriate parameters. Therefore, coefficient k_2 is introduced to reduce the average pressure. Equation 7.6 then becomes;

$$f'_{cc} = f'_{co} + k_1 f_{le} \qquad (7.8)$$

where;

$$f_{le} = k_2 f_l \qquad (7.9)$$

$$f_l = \left[\sum A_s f_{yt} \sin\alpha\right] / (s b_c) \qquad (7.10)$$

$$k_1 = 6.7\left(f_{le}\right)^{-0.17} \tag{7.11}$$

The equivalent lateral pressure in Eq. 7.11 is in MPa. Coefficient k_2 is equal to 1.0 for closely spaced spirally reinforced circular columns as well as square columns with closely spaced lateral and laterally supported longitudinal reinforcement. Angle α is the angle between transverse reinforcement and b_c, and is equal to 90 degrees if the transverse reinforcement is perpendicular to b_c.

A large volume of experimental data was examined to define k_2. It is clear from the above discussion that k_2 should have a smaller value for large spacings of laterally supported longitudinal reinforcement (s_l), and lateral ties (s), so that the reduction in the average stress is high. It was also found from experimental data that a high nodal force, resulting from a large area and/or strength of transverse steel, increases the stress concentration and sharpness of stress peaks at the nodes. This requires further reduction in the average stress so that the stress in regions away from the nodal points are not overestimated due to the sharpness of the stress peaks. The following is the expression derived from regression analysis of test data.

$$k_2 = 0.26\sqrt{\left(\frac{b_c}{s}\right)\left(\frac{b_c}{s_l}\right)\left(\frac{1}{f_l}\right)} \leq 1.0 \tag{7.12}$$

where, f_l is in MPa. It should be noted that Eq. 7.12 is applicable only if premature buckling of longitudinal reinforcement is prevented. Based on the results of column tests considered in developing the above expression, the maximum tie spacing for buckling specified in the ACI Building Code (ACI 318, 1989) appears to satisfy this requirement. Furthermore, the columns considered conformed to the building code limitation for maximum spacing of laterally supported longitudinal reinforcement. Therefore this may be taken as an upper limit for s_l.

Equations 7.8 through 7.12 were used to compute confined concrete strengths of 51 square columns tested by three groups of researchers in three different research programs (Razvi and Saatcioglu 1989, Scott et al. 1982, Sheikh and Uzumeri 1980). The columns included a wide range of confinement parameters, from poorly confined to well confined columns. Different reinforcement configurations were used, as indicated in Fig. 7.9. Both low and high rates of loadings were considered. The unconfined concrete strength f_{co}', was taken as reported, wherever available. When this value was not reported, the cylinder strength was factored as suggested by researchers who reported the test data. Comparisons between the analytical and experimental strength values are presented in Tables 7.3 through 7.5 and Fig. 7.10. The results indicate an excellent agreement between the analytical and experimental values.

7.2.1.3 Rectangular Sections

Rectangular columns may have different confinement reinforcement in two orthogonal directions. This may lead to different levels of confinement pressure along the long and short sides of the section. The pressure along each side can be determined following the same procedure outlined above for circular and square columns. Figure 7.11 illustrates lateral pressure distributions along the long and short sides of a rectangular column section. Confinement pressure along the long side plays a more dominant role on concrete strength than that along the short side. Examination of experimental data indicated that the effects of confinement pressures along long and short sides could be considered to be proportional to the cross-sectional dimensions. Therefore, Eq. 7.13, given below, can be used as overall equivalent lateral pressure to be used in Eq. 7.8.

$$f_{le} = \left(f_{lex} b_{cx} + f_{ley} b_{cy}\right) / \left(b_{cx} + b_{cy}\right) \tag{7.13}$$

where, f_{lcx} and f_{lcy} are effective lateral pressures acting perpendicular to core dimensions b_{cx} and b_{cy} respectively. Eq. 7.13 also provides equivalent lateral pressure for square columns where the pressure distributions in two orthogonal directions are not equal.

Results of rectangular column tests conducted by Mander, Park, and Priestley (1988) are compared with analytical calculations of concrete strength obtained by the use of Eqs. 7.8 through 7.13. The comparisons, shown in Table 7.6 and Figure 7.12, indicate an excellent agreement between experimental and analytical strength values. The reinforcement arrangements used in rectangular column tests are shown in Fig.7.9.

7.2.1.4 Concrete Confined by WWF

The analytical procedure discussed above can also be applied to columns reinforced with welded wire fabric. In this case the column is treated the same as a column reinforced with reinforcing bars, with due considerations given to the area and grid size of the welded wire fabric. The tie spacing is taken as the vertical grid dimension of the mesh. The spacing s_l, between the laterally supported longitudinal reinforcement is taken as the center-to-center distance between the outermost vertical wires unless there are lateral ties in between. The comparisons of experimental (Abdulkadir, 1991) and analytical results for columns reinforced with welded wire fabric are shown in Table 7.7. The comparisons are also shown in Fig. 7.10.

7.2.1.5 Combined Use of Different Confinement Reinforcement

The analytical procedure presented above also permits superposition of confinement effects resulting from the use of different types of confinement reinforcement. Razvi and Saatcioglu (1989) tested columns confined with welded wire fabric and square hoops. Figure 7.9 illustrates the reinforcement arrangements used in the experimental program. The core concrete in these columns was confined by a combination of hoop and welded wire fabric reinforcement. The analytical procedure for this case involves computation of equivalent lateral pressures separately for each type of confinement reinforcement.

The pressures acting over the same area are then superimposed to find the combined effect. This combined pressure is used in Eq. 7.8 to find the confined concrete strength. In the cross-sectional arrangement No. 9 shown in Fig. 7.9, the inner circular core is subjected to uniform pressure provided by the welded wire fabric, and the equivalent uniform pressure provided by the outside hoops. In the same column, the core area between the outer hoops and the inside mesh is confined only by the outside hoops. The comparisons of analytical and experimental strength values are shown in Table 7.7 and Fig. 7.10.

7.2.2 Ductility of Confined Concrete

Plain concrete under uniaxial compression shows brittle behaviour. Deformability of concrete improves with confinement. Confined concrete can sustain higher strains at the peak stress, and may show little strength degradation thereafter.

The strain at peak stress is affected by confinement, and can be expressed in terms of the ratio of confined to unconfined concrete strengths. The following expression, also used by previous researchers (Balmer 1949, Mander et al., 1988) is found to produce good agreement with experimentally obtained strain values.

$$\epsilon_1 = \epsilon_{01}(1+5K) \tag{7.14}$$

where;

$$K = k_1 f_{le} / f'_{co} \tag{7.15}$$

ϵ_{01} is the strain corresponding to peak stress of unconfined concrete, and should be determined under the same rate of loading as for confined concrete. In the absence of experimental data, a value of 0.002 may be appropriate for ϵ_{01} under slow rate of loading.

Deformability of concrete beyond the peak stress is significantly affected by the behaviour of longitudinal reinforcement. Longitudinal reinforcement in concrete is laterally restrained against buckling. However, spalling of cover concrete at approximately the peak stress level makes the longitudinal reinforcement susceptible to buckling. At this load stage, the lateral support provided by transverse reinforcement becomes important. If the amount of lateral reinforcement is sufficiently high in relation to the unsupported length of longitudinal reinforcement, the stability of longitudinal reinforcement between the ties is ensured. A stable reinforcement cage is essential to continue providing effective confinement against lateral expansion of concrete. Therefore, the amount of transverse reinforcement, expressed in terms of reinforcement ratio (ρ), plays a major role on the descending slope of the stress-strain relationship. Regression analysis of test data indicates that the following expression can be used to establish the strain at 85 % strength level beyond the peak (ϵ_{85}).

$$\epsilon_{85} = 260\rho_c\epsilon_1 + \epsilon_{085} \tag{7.16}$$

Where;

$$\rho_c = \sum A_s / \left[s\,(b_{cx} + b_{cy}) \right] \tag{7.17}$$

ϵ_{085} is the strain at 85 % strength level beyond the peak stress of unconfined concrete, and should be determined under the same rate of loading used for the confined concrete. In the absence of test data, a value of 0.0038 may be appropriate for ϵ_{085}, for slow rate of loading. The summation sign in Eq. 7.17 indicates the summation of transverse reinforcement area in two directions, crossing b_{cx} and b_{cy}, giving total area of transverse reinforcement in used in both directions. If an inclined reinforcement is crossing the core, the projection of the area should be included in the total area. If the section is spirally reinforced, or has identical reinforcement arrangement in each direction, Eq. 7.17 reduces to transverse reinforcement ratio in each direction. For columns with more than one type of confinement reinforcement, the reinforcement ratio consists of the summation of reinforcement ratios for each type, computed with due consideration given to the respective core dimensions. It is important to note that, while the deformability of confined concrete improves with increasing transverse reinforcement ratio, it is not realistic to expect this improvement to continue at the same rate, beyond a practical range of reinforcement ratio. Eq. 7.16 was obtained from test data that included columns with less than 2% lateral reinforcement ratio. This may be used as an upper limit for Eq. 7.16.

7.2.3 Stress - Strain Relationship of Confined Concrete

The stress-strain relationship shown in Fig. 7.13 is proposed for confined concrete. The relationship consists of a parabola for the ascending branch, and a linear portion for the descending branch. A constant residual strength is assumed at 20 % strength level. The following expression is suggested for the parabolic ascending portion.

$$f_c = f'_{cc}\left[2\left(\frac{\epsilon_c}{\epsilon_1}\right)-\left(\frac{\epsilon_c}{\epsilon_1}\right)^2\right]^{\frac{1}{1+2K}} \leq f'_{cc} \qquad (7.18)$$

where, coefficient K is defined in Eq. 7.15. The proposed relationship becomes identical to that proposed by Hognestad (1951) for unconfined concrete, when confinement effects are negligible and the lateral confinement pressure is zero. This expression was selected for its simple and familiar form, even though under certain combinations of confinement parameters it may result in a slight underestimation of confined concrete stiffness prior to the onset of the mechanism of confinement.

The analytical relationship is compared with a large volume of experimental data, covering a wide range of confinement parameters between poorly confined and well confined columns. Some of the typical comparisons are selected for presentation in Figs. 7.14 through 7.34 for circular, square and rectangular columns, tested under slow and fast rates of concentric compression. The comparisons indicate good correlation between the analytical and experimental results.

7.2.4 Confined Columns under Eccentric Loading

The applicability of confinement models derived on the basis of concentric column tests to eccentrically loaded columns is a source of controversy among researchers. Therefore, one of the objectives of this research program was to investigate the effects of strain gradient on concrete confinement.

Column tests performed under concentric loading indicate that transverse column reinforcement develops its yield strength at or near peak concentric column load. The same reinforcement may not be stressed to the same level under eccentric loading. While the tendency to expand in the lateral direction, and the associated transverse strains in concrete near the extreme core compression fiber may be comparable to those attained under concentric compression, concrete near the neutral axis is subjected to relatively low compressive strains in the longitudinal direction and comparably low tensile strains in the transverse direction. This translates into a lower passive pressure produced by confinement reinforcement. Hence, the lateral pressure predictions based on concentric loading are not representative of those generated under eccentric loading. Fig. 7.35 illustrates equivalent lateral pressure for concentrically and eccentrically loaded columns. A linear variation of equivalent pressure is more appropriate for the compression region of an eccentrically loaded column, undergoing a linear variation of longitudinal strains. However, the effects of confinement on stress-strain characteristics of concrete increase with increased compressive strain. This means that in the low compressive strain range, the range typically expected near the neutral axis is not likely to result in appreciable differences in overall section response. This is illustrated in Fig. 7.35. Concrete near the extreme compression fiber (Strip 1) has stress-strain characteristics that can be determined by the confined concrete model. The use of the same stress-strain relationship for compression regions towards the neutral axis (Strip 2 and 3) will produce overestimation of concrete confinement. However, in these regions the longitudinal strains are proportionately lower, and the corresponding portions of the stress-strain relationships are not significantly different than that established for Strip 1. Furthermore, the true confinement pressure near the perimeter hoop is higher than the uniform pressure used to establish the stress-strain relationship for Strip 1. Therefore, some overestimation of confinement effects for Strips 2 and 3 within the low longitudinal strain range are likely to be offset by the underestimation of confinement pressure for Strip 1. Hence, the use of the stress-strain relationship established for Strip 1 for the whole compression zone is not likely to result in any appreciable error in flexural analysis. This point has been verified extensively against test data. The analytical model described in previous sections was used to conduct plane section analyses of columns tested under eccentric loading. Column tests reported by Saatcioglu et al. (1995), Sheikh and Khoury (1993) and Ozcebe and Saatcioglu (1987), and Park et al. (1982) were used for this purpose. Analytically generated moment-curvature relationships are compared with those recorded experimentally, in Chapter 8. The results indicate that the model, although developed based on column tests conducted under concentric loading, is also applicable to columns under eccentric loading.

7.3 Modifications Introduced for High-Strength Concrete

Previous researchers concluded that models developed for normal-strength concrete overestimated ductility of high strength concrete (Yong et al. 1988, Polat 1992, Thomsen and Wallace 1992, Cusson and Paultre 1994). This observation was confirmed in the current investigation. Experimental results of high-strength concrete columns tested in this research program exhibited steeper descending branch of stress-strain relationships, and lower strains at peak stress, when compared with those computed by the model described above. Therefore, it was necessary to modify the expressions used for the model, without changing the main features, so that they would be applicable to high-strength concrete. The new expressions were derived based on experimental research involving both normal-strength and high-strength concrete columns, and hence are applicable to a wide range of concrete strength. The modified expressions are described in the following sections.

7.3.1 Confined Concrete Strength

Review of previous research indicated two conflicting views on strength enhancement in high strength concrete. While Nagashima et al. (1992) concluded that the additional strength gain due to confinement was independent of concrete strength, Galeota et al (1992) showed that the strength gain attained was lower in higher strength concretes. The experimental results of this study confirmed the findings of Nagashima et al. (1992), i.e. the absolute gain in strength was independent of concrete strength. Therefore, Equations 7.8 through 7.11, which are independent of concrete strength, can be used without modification to compute confined strength of high-strength concrete in columns. However, the yield strength of lateral steel f_{yt} used in Eq. 7.10 should be limited to 1000 MPa, to be consistent with experimental observations. Columns tested in this program showed yielding of 1000 MPa steel at or shortly after the peak. Polat (1992) also reported yielding of 950 MPa steel at the peak. However, Li (1994) indicated that high-strength steel with yield strength of 1300 MPa did not yield at the peak. Therefore, the useful limit of yield stress was assumed to be 1000 MPa.

A large volume of test data, including those of high-strength concrete, were examined to verify the applicability of Eq. 7.12 when the lateral pressure was relatively high, as required for high-strength concrete. It was concluded that while Eq. 7.12 produced accurate estimates of coefficient k_2 for the lateral pressure range usually used for normal-strength concretes, it may not produce acceptable results for high-strength concretes under high lateral pressure. Since the lateral pressure required to confine high-strength concrete is much higher than that required for normal-strength concrete, Eq. 7.12 underestimates coefficient k_2. Test results indicate that coefficient k_2 becomes independent of f_l beyond a certain limit of lateral pressure. Therefore, Eq. 7.12 is modified by substituting a constant value of $f_l = 3$ MPa, as shown below.

$$k_2 = 0.15\sqrt{\left(\frac{b_c}{s}\right)\left(\frac{b_c}{s_l}\right)} \leq 1.0 \tag{7.19}$$

It is to be noted that coefficient k_2 reflects the arrangement of confinement reinforcement, and is equal to unity for closely spaced spirally reinforced circular columns with well distributed longitudinal reinforcement.

Eqs. 7.8 through 7.11 and Eq. 7.19 were used to predict the strength of 40 confined high-strength concrete columns tested in this research program, in addition to 127 columns tested by six other groups of researchers. The columns were either circular or square in section, confined by different amount, spacing, grade and arrangement of transverse reinforcement. The concrete strength ranged approximately between 50 and 130 MPa. The reinforcement arrangements considered are shown in Fig. 7.9. The in-place strength of unconfined concrete f_{co}' was taken to be $0.85f_c'$ for the columns tested in this research program. Similar values are used for columns tested in other research programs, as reported or suggested by respective researchers.

The comparisons between analytical and experimental strength values are presented in Tables 7.8 to 7.16 and Figures 7.36 to 7.39. The results indicate good agreement of analytical strength values with those recorded in column tests.

7.3.2 Ductility of Confined Concrete

It is well known that the strength and ductility of concrete are inversely proportional. Ductility of confined concrete is indicated by the slope of the descending branch of the stress-strain relationship. The slope of the descending branch is a function of two strain values in the analytical model developed in this investigation. These values include strains corresponding to the peak stress (ϵ_1), and 85% of the peak within the descending branch of the stress-strain relationship (ϵ_{85}). The mathematical expressions for ϵ_1, and ϵ_{85}, as originally developed using normal-strength concrete test data, were not a function of concrete strength. The effects of concrete strength and lateral steel strength on ductility of confined concrete were subsequently introduced using coefficients k_3 and k_4 respectively as indicated below;

$$\epsilon_1 = \epsilon_{01} \ (1 + 5k_3 \ K) \qquad (7.20)$$

$$\epsilon_{85} = 260 \ k_3 \ \rho_c \ \epsilon_1 \ \left[1 + \ 0.5k_2 \ (k_4 \ -1)\right] + \epsilon_{085} \qquad (7.21)$$

$$k_3 = \frac{40}{f'_{co}} \leq 1.0 \qquad (7.22)$$

$$k_4 = \frac{f_{yt}}{500} \geq 1.0 \qquad (7.23)$$

where;

ϵ_{01} and ϵ_{085} are strains of unconfined concrete in column corresponding to the peak stress and 85% of the peak within the descending branch, respectively. These quantities are usually determined experimentally. In the absence of experimental data, however, the following expressions may be used;

$$\epsilon_{01} = \mathbf{0.0028 - 0.0008}\, k_3 \qquad \mathbf{(7.24)}$$

$$\epsilon_{085} = \epsilon_{01} + \mathbf{0.0018}\ k_3^2 \qquad \mathbf{(7.25)}$$

It is to be noted that Eq. 7.21 was obtained from test data that included columns with lateral reinforcement ratio, ρ_c, less than (0.04 - 0.02k_3). This may be used as an upper limit for the applicability of Eq. 7.21.

7.3.3 Stress - Strain Relationship of Confined Concrete

The ascending branch of the stress-strain relationship, proposed for normal-strength concrete, was a modified version of Hognestad's curve (1951). It was confirmed experimentally that the applicability of this curve was limited to normal-strength concrete. This relationship, given in Eq. 7.18, produced overestimation of the initial modulus of elasticity when applied to high-strength concrete. Therefore, another relationship which was reported to produce good agreement with experimental data for both normal-strength and high-strength concretes was adopted for the model. The relationship is applicable to confined and unconfined concretes within the normal and high-strength range. The curve was originally proposed by Popovics (1973), and later used by Mander et al. (1988) for normal-strength concrete, and by Nagashima et al. (1992), and Cusson and Paultre (1993, 1994) for high-strength concrete. The mathematical expression for the curve is given below.

$$f_c = \frac{f'_{cc}\left(\frac{\epsilon_c}{\epsilon_1}\right) r}{r-1+\left(\frac{\epsilon_c}{\epsilon_1}\right)^r} \tag{7.26}$$

$$r = \frac{E_c}{E_c-E_{sec}} \tag{2.27}$$

Where;

E_{sec} is the secant modulus of elasticity of confined concrete. It can be calculated from Equation 7.28.

$$E_{sec} = \frac{f'_{cc}}{\epsilon_1} \tag{7.28}$$

E_c is the modulus of elasticity of unconfined concrete. The following expression, originally proposed by Carrasllquillo et al. (1981) is found to produce good agreement with experimentally obtained values.

$$E_c = 3320\sqrt{f'_c}+6900 \tag{7.29}$$

7.3.4 Comparisons with Experimental Results

The analytical model, with the above stress-strain relationship and the modified expressions (Eqs. 7.19 to 7.27) defining strains, is compared with 40 high-strength concrete columns tested in this research program, in addition to 50 columns tested by three other groups of researchers (Nagashima et al. 1992, Nishiyama et al. 1993, and Li 1994). The comparisons include circular and square columns with a wide range of confinement parameters and concrete strengths. Figs. 7.40 through 7.83 , indicate good agreement between the experimental and analytical stress-strain relationships.

It is important to note that the model is applicable to both normal and high-strength concretes. This is because the model assumes that the absolute gain in strength due to confinement is independent of concrete strength. Therefore, Eqs. 7.8 through 7.11, Eq. 7.13, and Eq. 7.19 can be used to calculate the confined concrete strength for both normal and high-strength concretes. Furthermore, Eqs. 7.20, and 7.21, used to calculate concrete ductility, become identical to Eqs 7.14 and 7.16, when $k_3 = 1$ (for normal-strength concrete), and $k_4 = 1$ (for normal-strength steel). Therefore, the model can be used for columns with concrete strengths ranging between 30 and 120 MPa.

7.4 Conclusions

The analytical procedure and the stress-strain relationship developed in this research program can be used to predict strength and ductility characteristics of confined concrete. The procedure is relatively simple to use. It covers a wide range of concrete strength, ranging from 30 to 120 MPa, confined with normal or high-strength steel. It is applicable to concretes confined by spirals, rectilinear hoops, cross ties, welded wire fabric, and combinations of these reinforcement. Confined concrete behaviour under concentric and eccentric loadings, and slow and fast strain rates can be predicted by the proposed model. The stress-strain relationships established by the model compare well with those obtained experimentally.

Table 7.1: Strength enhancement for normal strength concrete in circular columns tested by Manderet al. (1988).

Col. Label	Reinf. Arrg.	b_c (mm)	d_b (mm)	f_{yt} (MPa)	s (mm)	$\hat{f}_l$ (MPa)	k_1	k_2	f_{co}' (MPa)	f_{cc}' (MPa) Exp	f_{cc}' (MPa) Anal	Anal / Exp
a	10	438	12	310	52	3.08	5.53	1.0	24.0	38.0	41.0	1.08
b	10	438	12	340	52	3.38	5.45	1.0	30.0	48.0	48.4	1.01
c	10	438	12	340	52	3.38	5.45	1.0	32.0	47.0	50.4	1.07
1	10	438	12	340	41	4.28	5.23	1.0	29.0	51.0	51.4	1.01
2	10	438	12	340	69	2.54	5.72	1.0	29.0	46.0	43.5	0.95
3	10	438	12	340	103	1.70	6.12	1.0	29.0	40.0	39.4	0.99
4	10	440	10	320	119	0.96	6.75	1.0	29.0	36.0	35.5	0.99
5	10	440	10	320	36	3.17	5.15	1.0	29.0	47.0	46.5	0.99
6	10	434	16	307	93	3.06	5.54	1.0	29.0	46.0	45.9	1.00
7	10	438	12	340	52	3.38	5.45	1.0	32.0	52.0	50.4	0.97
8	10	438	12	340	52	3.38	5.45	1.0	30.0	49.0	48.4	0.99
9	10	438	12	340	52	3.38	5.45	1.0	32.0	52.0	50.4	0.97
10	10	438	12	340	52	3.38	5.45	1.0	30.0	50.0	48.4	0.97
11	10	438	12	340	52	3.38	5.45	1.0	30.0	54.0	48.4	0.90
12	10	438	12	340	52	3.38	5.45	1.0	32.0	52.0	50.4	0.97

Notes:

1. Column 'a' was tested under a slow, and all others a high strain rate of 0.0133/sec.
2. Reinforcement arrangements are illustrated in Fig. 7.9.

Table 7.2: Strength enhancement for normal strength concrete in circular columns tested by Sheikh and Toklucu (1993).

Col. Label	Reinf. Arrg.	b_c (mm)	d_b (mm)	f_{yt} (MPa)	s (mm)	f_l (MPa)	k_1	k_2	f_{co}' (MPa)	f_{cc}' (MPa) Exp	f_{cc}' (MPa) Anal	Anal / Exp
1	10	301.5	10.0	452	56	5.4	3.4	1.0	30.5	51.9	57.5	1.11
2	10	301.5	10.0	452	76	3.9	3.2	1.0	30.5	48.5	51.4	1.06
3	10	301.5	10.0	452	112	2.7	3.0	1.0	30.5	41.5	45.7	1.10
4	10	301.5	10.0	452	152	2.0	2.9	1.0	30.5	43.0	42.3	0.98
5	10	303.5	8.0	607	56	3.6	3.4	1.0	30.5	44.6	49.9	1.12
6	10	303.5	8.0	607	76	2.6	3.2	1.0	30.5	47.9	45.5	0.95
7	10	303.5	8.0	607	112	1.8	3.0	1.0	30.5	46.7	41.4	0.89
8	10	305.8	5.7	593	56	1.8	3.4	1.0	30.5	46.1	41.3	0.89
9	10	301.5	10.0	452	76	3.9	3.2	1.0	30.5	49.1	51.4	1.05

Note:

1. Reinforcement arrangements are illustrated in Fig. 7.9.

Table 7.3: Strength enhancement for normal strength concrete in square columns tested by Razvi and Saatcioglu (1989).

Col. Label	Reinf. Arrg.	b_c (mm)	s_l (mm)	d_b (mm)	f_{yt} (MPa)	s (mm)	f_l (MPa)	k_1	k_2	f_{co}' (MPa)	f_{cc}' (MPa) Exp	f_{cc}' (MPa) Anal	$\frac{Anal}{Exp}$
3(a)	1	143	120	6.53	373	35	4.99	6.42	0.26	32.0	40.0	40.2	1.01
3(b)	1	143	120	6.53	373	35	4.99	6.42	0.26	32.0	38.4	40.2	1.05
4(a)	1	143	120	6.53	373	70	2.50	7.23	0.26	32.0	33.3	36.6	1.10
6(a)	1	138	120	6.53	373	35	5.17	6.44	0.24	39.0	51.9	47.1	0.91
6(b)	1	138	120	6.53	373	35	5.17	6.44	0.24	39.0	51.1	47.1	0.92
7(a)	1	138	120	6.53	373	70	2.59	7.25	0.24	39.0	43.3	43.6	1.01
7(b)	1	138	120	6.53	373	70	2.59	7.25	0.24	39.0	44.8	43.6	0.97
15(a)	1	143	120	6.53	373	70	2.50	7.23	0.26	29.0	35.1	33.6	0.96
15(b)	1	143	120	6.53	373	70	2.50	7.23	0.26	29.0	31.6	33.6	1.06
16(a)	1	143	120	6.53	373	35	4.99	6.42	0.26	29.0	38.0	37.2	0.98
16(b)	1	143	120	6.53	373	35	4.99	6.42	0.26	29.0	38.0	37.2	0.98

Note:
1. Reinforcement arrangements are illustrated in Fig. 7.9.

Table 7.4: Strength enhancement for normal strength concrete in square columns tested by Scott et al. (1982).

Col. Label	Reinf. Arrg.	b_c (mm)	s_l (mm)	d_b (mm)	f_{yt} (MPa)	s (mm)	f_l (MPa)	k_1	k_2	f_{co}' (MPa)	f_{cc}' (MPa) Exp	f_{cc}' (MPa) Anal	$\frac{Anal}{Exp}$
2	5	400	123	10	309	72	2.88	6.02	0.65	23.1	33.0	34.4	1.04
3	5	400	123	10	309	72	2.88	6.02	0.65	30.9	40.9	42.2	1.03
6	2	400	183	10	309	72	2.88	6.23	0.53	23.1	32.4	32.7	1.01
7	2	400	183	10	309	72	2.88	6.23	0.53	30.9	39.1	40.4	1.03
12	5	400	123	10	309	98	2.11	6.35	0.65	30.3	40.4	39.0	0.97
13	5	400	123	10	309	72	2.88	6.02	0.65	30.3	43.0	41.5	0.97
14	5	400	123	12	296	88	3.25	6.06	0.55	30.3	43.5	31.2	0.95
15	5	400	123	12	296	64	4.46	5.74	0.55	30.3	48.5	44.5	0.92
17	2	400	183	10	309	98	2.11	6.56	0.53	30.3	38.5	37.7	0.98
18	2	400	183	10	309	72	2.88	6.23	0.53	30.3	41.7	39.8	0.96
19	2	400	183	12	296	88	3.25	6.27	0.45	30.3	42.2	39.5	0.94
20	2	400	183	12	296	64	4.46	5.94	0.45	30.3	45.6	42.3	0.93
22	5	400	123	10	309	98	2.11	6.35	0.65	29.5	35.8	38.3	1.07
23	5	400	123	10	309	72	2.88	6.02	0.65	29.5	37.9	40.8	1.08
24	5	400	123	12	309	88	3.39	6.04	0.54	29.5	39.9	40.6	1.02
25	5	400	123	12	309	64	4.66	5.72	0.54	29.5	45.5	44	0.97

Notes:

1. Columns 2 and 6 were tested under slow strain rates, all other columns were tested under high strain rate of 0.0167/sec.
2. Reinforcement arrangements are illustrated in Fig. 7.9.

Table 7.5: Strength enhancement for normal strength concrete in square columns tested by Sheikh and Uzumeri (1980).

Col. Label	Reinf. Arrg.	b_c (mm)	s_l (mm)	d_b (mm)	f_{yt} (MPa)	s (mm)	f_l (MPa)	k_1	k_2	f_{co}' (MPa)	f_{cc}' (MPa) Exp	f_{cc}' (MPa) Anal	Anal / Exp
1	2	267	123	4.76	455	57.1	1.81	6.58	0.62	31.9	37.6	39.2	1.04
2	2	267	123	4.76	255	57.1	1.02	6.91	0.82	31.4	39.6	37.2	0.94
3	4	267	62	3.17	490	50.8	1.54	6.23	1.00	30.9	37.4	40.5	1.08
4	4	267	62	3.17	283	50.8	0.89	6.83	1.00	31.2	37.4	37.3	1.00
5	4	267	62	4.76	500	38.1	4.74	5.52	0.66	29.8	49.1	47.0	0.96
6	4	267	62	4.76	255	38.1	2.42	5.85	0.92	29.1	44.6	42.1	0.94
7	2	267	118	7.94	476	76.2	3.95	6.29	0.37	34.8	44.5	43.9	0.99
8	2	267	120	4.76	420	28.7	3.33	5.88	0.65	34.7	47.5	47.4	1.00
9	2	267	118	9.52	345	76.2	4.12	6.26	0.36	34.4	42.3	43.7	1.03
10	2	267	119	6.35	455	35.1	5.25	5.75	0.47	34.6	45.3	48.7	1.08
11	4	267	61	6.35	359	95.2	2.42	6.31	0.59	34.6	43.9	43.5	0.99
12	4	267	62	3.17	469	25.4	2.95	5.57	1.00	34.7	50.6	51.1	1.01
13	2	267	120	4.76	476	57.1	1.90	6.54	0.61	26.6	34.6	34.2	0.99
14	2	267	120	9.52	427	76.2	5.10	6.16	0.32	26.8	36.9	36.9	1.00
15	2	267	122	6.35	414	35.1	4.78	5.81	0.49	26.9	39.6	40.4	1.02
16	4	267	63	3.17	589	50.8	1.86	6.14	0.90	27.6	37.6	37.9	1.01
17	4	267	62	7.94	348	101.6	3.44	6.17	0.47	28.0	38.0	38.0	1.00
18	4	267	62	4.76	552	38.1	5.23	5.48	0.62	28.1	47.8	46.0	0.96
19	3	267	80	7.94	400	101.6	2.92	6.39	0.45	28.4	40.6	36.8	0.91
20	3	267	81	4.76	545	38.1	3.81	5.76	0.64	29.5	44.8	43.5	0.97
21	3	267	81	6.35	490	47.6	4.88	5.75	0.51	30.2	46.5	44.4	0.95
22	5	267	80	7.94	386	82.5	2.96	6.28	0.50	30.2	43.5	39.4	0.91
23	5	267	81	4.76	552	28.6	4.39	5.55	0.69	30.5	47.0	47.3	1.01
24	5	267	81	6.35	476	38.1	5.06	5.62	0.56	30.5	49.7	46.3	0.93

Note:
1. Reinforcement arrangements are illustrated in Fig. 7.9.

Table 7.6: Strength enhancement for normal strength concrete in rectangular columns tested by Mander et al.(1988).

Col. Label	Reinf. Arrg.	Section Side	b_c (mm)	s_l (mm)	d_b (mm)	f_{yt} (MPa)	s (mm)	f_l (MPa)	k_2	f_{le} (MPa)	k_1	f_{co}' (MPa)	f_{cc}' (MPa) Exp	f_{cc}' (MPa) Anal	Anal/Exp
1	11	Long	644	89	6	310	25	5.44	1.00	4.94	5.10	26.0	46.0	51.2	1.11
		Short	94	76				7.46	0.20						
2	11	Long	644	89	6	340	25	5.97	1.00	5.41	5.03	29.0	56.0	56.2	1.00
		Short	94	76				8.18	0.20						
3	12	Long	644	89	6	310	50	3.81	1.00	3.42	5.43	26.0	46.0	44.6	0.97
		Short	94	76				3.73	0.21						
4	13	Long	644	89	6	310	25	4.35	1.00	3.99	5.30	26.0	51.0	47.1	0.92
		Short	94	76				7.46	0.21						
5	11	Long	644	89	6	310	72	1.89	1.00	1.72	6.11	26.0	37.0	36.5	0.99
		Short	94	76				2.59	0.21						
6	11	Long	640	88	10	330	42	9.64	0.88	7.63	4.74	26.0	56.0	62.2	1.11
		Short	90	68				13.71	0.12						
9	11	Long	644	89	6	340	25	5.97	1.00	5.41	5.03	43.0	72.0	70.2	0.98
		Short	94	76				8.18	0.20						
10	11	Long	644	89	6	340	25	5.97	1.00	5.42	5.03	43.0	72.0	70.2	0.98
		Short	94	72				8.18	0.20						
11	11	Long	644	89	6	340	50	2.99	1.00	2.71	5.65	43.0	60.0	58.3	0.97
		Short	94	72				4.09	0.20						
12	11	Long	640	88	10	360	42	10.51	0.85	8.00	4.70	43.0	78.0	80.6	1.03
		Short	90	64				14.96	0.12						
13	14	Long	640	155	10	360	30	7.36	0.90	6.10	4.93	43.0	69.0	73.0	1.06
		Short	90	68				20.94	0.11						
14	14	Long	644	157	6	340	30	2.49	1.00	2.34	5.80	43.0	58.0	56.6	0.98
		Short	94	76				6.82	0.20						

Notes:

1. Columns 1, 3, 5, and 6 were tested under slow strain rates, all other columns were tested under high strain rate of 0.0133/sec
2. Reinforcement arrangements are illustrated in Fig. 7.9.

Table 7.7: Strength enhancement for normal strength concrete reinforced with welded wire fabric.

Col. Label	Reinf. Arrg.	Trans. Reinf.	b_c (mm)	s_l (mm)	d_b (mm)	f_{yt} (MPa)	s (mm)	f_l (MPa)	k_2	k_1	f_{co}' (MPa)	f_{cc}' (MPa) Exp	f_{cc}' (MPa) Anal	$\frac{Anal}{Exp}$
RC1	6	WWF	204	197	3.40	530	51	0.90	0.55	7.51	23.0	24.0	26.7	1.11
RC2	6	WWF	204	197	3.40	530	51	0.90	0.55	7.51	25.0	26.0	28.3	1.09
RC5	7	WWF	175	168	3.40	530	51	2.20	0.33	7.07	23.0	29.0	28.1	0.97
12 (a)	9	Ties	143	120	6.53	373	70	2.50	0.26	6.24	29.0	40.0	36.8	0.92
		WWF	135	N/A	1.90	375	25	0.90	1.00					
12 (b)	9	Ties	143	120	6.53	373	70	2.50	0.26	6.24	29.0	41.0	36.8	0.90
		WWF	135	N/A	1.90	375	25	0.90	1.00					
13 (a)	9	Ties	143	120	6.53	373	70	2.50	0.26	6.28	29.0	38.0	36.6	0.96
		WWF	135	N/A	1.45	300	13	0.80	1.00					
13 (b)	9	Ties	143	120	6.53	373	70	2.50	0.26	6.28	29.0	34.0	36.6	1.08
		WWF	135	N/A	1.45	300	13	0.80	1.00					
14 (a)	8	Ties	148	120	6.53	373	70	2.40	0.27	6.49	29.0	38.0	36.8	0.97
		WWF	140	139	1.45	300	13	0.60	1.00					
14 (b)	8	Ties	148	120	6.53	373	70	2.40	0.27	6.49	29.0	36.0	36.8	1.02
		WWF	140	130	1.45	300	13	0.60	1.00					

Notes:
1. Columns RC1 to RC5 were tested by Abdulkadir (1991), all other columns were tested by Razvi and Saatcioglu (1989).
2. Reinforcement arrangements are illustrated in Fig. 7.9.

Table 7.8: Strength enhancement for high strength concrete in circular columns tested in this investigation.

Col. Label	Reinf. Arrg.	b_c (mm)	d_b (mm)	f_{yt} (MPa)	s (mm)	f_l (MPa)	k_1	k_2	f_{co}' (MPa)	f_{cc}' (MPa) Exp	f_{cc}' (MPa) Anal	Anal/Exp
CC - 1	5	223.7	6.3	660	135	1.36	6.36	1.0	51.0	59.9	59.7	1.00
CC - 2	5	218.7	11.3	400	135	2.71	5.66	1.0	51.0	62.3	66.3	1.06
CC - 3	5	223.7	6.3	660	70	2.63	5.69	1.0	51.0	68.4	65.9	0.96
CC - 4	5	223.7	6.3	660	70	2.63	5.69	1.0	51.0	67.4	65.9	0.98
CC - 8	5	223.7	6.3	660	70	2.63	5.69	1.0	105.4	122.9	120.3	0.98
CC - 9	5	218.7	11.3	400	135	2.71	5.66	1.0	105.4	134.7	120.7	0.90
CC - 10	5	218.7	11.3	400	60	6.10	4.93	1.0	105.4	135.3	135.4	1.00
CC - 11	5	223.7	6.3	660	60	3.07	5.54	1.0	105.4	124.8	122.4	0.98
CC - 12	5	222.5	7.5	1000	60	6.62	4.86	1.0	105.4	127.7	137.6	1.08
CC - 14	5	222.5	7.5	1000	60	6.62	4.86	1.0	78.2	102.5	110.4	1.08
CC - 15	5	218.7	11.3	400	60	6.10	4.93	1.0	78.2	105.2	108.2	1.03
CC - 16	5	222.5	7.5	1000	100	3.97	5.30	1.0	78.2	95.1	99.2	1.04
CC - 19	5	218.7	11.3	400	100	3.66	5.37	1.0	78.2	94.6	97.9	1.03
CC - 20	5	223.7	6.3	660	100	1.84	6.04	1.0	78.2	88.4	89.3	1.01
CC - 21	5	223.7	6.3	660	70	2.63	5.69	1.0	78.2	93.4	93.1	1.00
CC - 22	5	218.7	11.3	400	135	2.71	5.66	1.0	78.2	89.3	93.5	1.05

Notes:
1. Column CC - 4 had circular hoops tied with mechanical connectors.
2. Reinforcement arrangements are illustrated in Fig. 4.2.

Table 7.9: Strength enhancement for high strength concrete in square columns tested in this investigation.

Col. Label	Reinf. Arrg.	b_c (mm)	s_l (mm)	d_b (mm)	f_{yt} (MPa)	s (mm)	f_l (MPa)	k_1	k_2	f_{co}' (MPa)	f_{cc}' (MPa) Exp	f_{cc}' (MPa) Anal	Anal/Exp
CS - 1	2	218.7	191.4	11.3	400	55	6.67	5.9	0.32	105.4	120.8	118.0	0.98
CS - 2	3	223.5	100.5	6.5	570	55	6.15	5.6	0.45	105.4	121.6	121.0	1.00
CS - 3	4	223.5	67.0	6.5	570	55	6.15	5.4	0.55	105.4	129.1	123.9	0.96
CS - 4	3	222.5	99.5	7.5	1000	55	10.83	5.1	0.45	105.4	123.4	130.4	1.06
CS - 5	4	222.5	66.3	7.5	1000	120	6.62	5.7	0.37	105.4	122.5	119.6	0.98
CS - 6	3	223.5	100.5	6.5	400	85	2.10	7.0	0.36	105.4	115.7	110.7	0.96
CS - 7	4	223.5	67.0	6.5	400	120	1.98	7.1	0.37	105.4	115.0	110.6	0.96
CS - 8	3	218.7	95.7	11.3	400	85	6.47	5.8	0.36	105.4	117.8	119.0	1.01
CS - 9	4	218.7	63.8	11.3	400	120	6.11	5.8	0.37	105.4	134.2	118.7	0.88
CS - 11	2	218.7	191.4	11.3	400	40	9.17	5.4	0.37	68.9	93.9	87.5	0.93
CS - 12	2	218.7	191.4	11.3	400	55	6.67	5.9	0.32	68.9	82.1	81.4	0.99
CS - 13	3	223.5	100.5	6.5	570	55	6.15	5.6	0.45	78.2	85.9	93.8	1.09
CS - 14	4	223.5	67.0	6.5	570	55	6.15	5.4	0.55	78.2	94.3	96.7	1.03
CS - 15	3	222.5	99.5	7.5	1000	55	10.83	5.1	0.45	68.9	95.5	93.8	0.98
CS - 16	4	222.5	66.3	7.5	1000	85	9.34	5.3	0.44	68.9	95.2	90.7	0.95
CS - 17	3	223.5	100.5	6.5	400	85	2.10	7.0	0.36	68.9	75.2	74.2	0.99
CS - 18	4	223.5	67.0	6.5	400	85	2.79	6.5	0.44	68.9	76.4	76.9	1.01
CS - 19	3	218.7	95.7	11.3	400	85	6.47	5.8	0.36	78.2	104.2	91.8	0.88
CS - 20	4	218.7	63.8	11.3	400	85	8.63	5.3	0.45	78.2	106.3	98.7	0.93
CS - 22	3	222.5	99.5	7.5	1000	85	7.01	5.7	0.36	51.0	68.0	65.5	0.96
CS - 23	4	222.5	66.3	7.5	1000	120	6.62	5.7	0.37	51.0	71.3	65.2	0.91
CS - 24	3	218.7	95.7	11.3	400	85	6.47	5.8	0.36	51.0	72.6	64.6	0.89
CS - 25	4	218.7	63.8	11.3	400	120	6.11	5.8	0.37	51.0	69.7	64.3	0.92
CS - 26	4	223.5	67.0	6.5	570	55	6.15	5.4	0.55	51.0	76.7	69.5	0.91

Notes:

1. Columns CS - 2 and CS - 13 had double layers of cross ties.
2. Reinforcement arrangements are illustrated in Fig. 4.2.

Table 7.10: Strength enhancement for high strength concrete in circular columns tested by Li (1994).

Col. Label	Reinf. Arrg.	b_c (mm)	d_b (mm)	f_{yt} (MPa)	s (mm)	f_l (MPa)	k_1	k_2	f_{co}' (MPa)	f_{cc}' (MPa) Exp	f_{cc}' (MPa) Anal	$\frac{\text{Anal}}{\text{Exp}}$
3A	10	204.0	6.0	445	20	6.17	4.92	1.0	63.0	93.0	93.3	1.00
6A	10	204.0	6.0	445	35	3.52	5.41	1.0	63.0	78.0	82.1	1.05
9A	10	204.0	6.0	445	50	2.47	5.75	1.0	63.0	74.7	77.2	1.03
12A	10	204.0	6.0	445	65	1.90	6.01	1.0	63.0	70.6	74.4	1.05
3B	10	204.0	6.0	445	20	6.17	4.92	1.0	72.3	108.8	102.6	0.94
6B	10	204.0	6.0	445	35	3.52	5.41	1.0	72.3	92.7	91.4	0.99
9B	10	204.0	6.0	445	50	2.47	5.75	1.0	72.3	85.0	86.5	1.02
12B	10	204.0	6.0	445	65	1.90	6.01	1.0	72.3	73.8	83.7	1.13
2HB	10	203.6	6.4	1318	20	15.80	4.19	1.0	52.0	126.0	118.2	0.94
4HB1	10	203.6	6.4	1318	35	9.03	4.61	1.0	52.0	87.5	93.6	1.07
6HB	10	203.6	6.4	1318	50	6.32	4.90	1.0	52.0	68.5	83.0	1.21
2HC1	10	203.6	6.4	1318	20	15.80	4.19	1.0	82.5	146.5	148.7	1.02
4HC	10	203.6	6.4	1318	35	9.03	4.61	1.0	82.5	106.8	124.1	1.16
6HC	10	203.6	6.4	1318	50	6.32	4.90	1.0	82.5	92.3	113.5	1.23

Note:
1. Reinforcement arrangements are illustrated in Fig. 7.9.

Table 7.11: Strength enhancement for high strength concrete in square columns tested by Li (1994).

Col. Label	Reinf. Arrg.	b_c (mm)	s_l (mm)	d_b (mm)	f_{yt} (MPa)	s (mm)	f_l (MPa)	k_1	k_2	f_{co}' (MPa)	f_{cc}' (MPa) Exp	f_{cc}' (MPa) Anal	Anal / Exp
1A	1	209	191.0	6	445	20	6.02	5.54	0.51	60.0	71.0	76.9	1.08
2A	2	209	95.5	6	445	20	10.28	4.77	0.72	60.0	90.0	95.2	1.06
4A	1	209	191.0	6	445	35	3.44	6.39	0.38	60.0	70.0	68.4	0.98
5A	2	209	95.5	6	445	35	5.87	5.50	0.54	60.0	71.0	77.5	1.09
7A	1	209	191.0	6	445	50	2.41	7.00	0.32	60.0	72.6	65.4	0.90
8A	2	209	95.5	6	445	50	4.11	6.03	0.45	60.0	72.6	71.2	0.98
10A	1	209	191.0	6	445	65	1.85	7.48	0.28	60.0	72.0	63.9	0.89
11A	2	209	95.5	6	445	65	3.16	6.44	0.40	60.0	72.4	68.1	0.94
1B	1	209	191.0	6	445	20	6.02	5.54	0.51	72.3	84.8	89.2	1.05
2B	2	209	95.5	6	445	20	10.28	4.77	0.72	72.3	107.4	107.5	1.00
4B	1	209	191.0	6	445	35	3.44	6.39	0.38	72.3	81.2	80.7	0.99
5B	2	209	95.5	6	445	35	5.87	5.50	0.54	72.3	81.5	89.8	1.10
7B	1	209	191.0	6	445	50	2.41	7.00	0.32	72.3	84.2	77.7	0.92
8B	2	209	95.5	6	445	50	4.11	6.03	0.45	72.3	80.5	83.5	1.04
10B	1	209	191.0	6	445	65	1.85	7.48	0.28	72.3	73.1	76.2	1.04
11B	2	209	95.5	6	445	65	3.16	6.44	0.40	72.3	81.7	80.4	0.98
1HA	2	208.6	95.1	6.4	1318	35	15.04	4.69	0.54	35.2	72.5	73.5	1.01
3HA	2	208.6	95.1	6.4	1318	53	9.93	5.21	0.44	35.2	51.8	58.0	1.12
5HA	2	208.6	95.1	6.4	1318	70	7.52	5.60	0.38	35.2	43.8	51.3	1.17
1HB	2	208.6	95.1	6.4	1318	20	26.33	4.07	0.72	52.0	118.5	128.8	1.09
3HB1	2	208.6	95.1	6.4	1318	35	15.04	4.69	0.54	52.0	81.4	90.3	1.11
3HB3	2	208.6	95.1	6.4	1318	35	15.04	4.69	0.54	52.0	84.4	90.3	1.07
5HB	2	208.6	95.1	6.4	1318	50	10.53	5.14	0.45	52.0	61.6	76.5	1.24
1HC1	2	208.6	95.1	6.4	1318	20	26.33	4.07	0.72	82.5	150.0	159.3	1.06
3HC1	2	208.6	95.1	6.4	1318	35	15.04	4.69	0.54	82.5	105.0	120.8	1.15
3HC3	2	208.6	95.1	6.4	1318	35	15.04	4.69	0.54	82.5	105.0	120.8	1.15
5HC	2	208.6	95.1	6.4	1318	50	10.53	5.14	0.45	82.5	87.7	107.0	1.22

Note:

1. Reinforcement arrangements are illustrated in Fig. 7.9.

Table 7.12: Strength enhancement for high strength concrete in square columns tested by Nishiyama et al. (1993).

Col. Label	Reinf. Arrg.	b_c (mm)	s_l (mm)	d_b (mm)	f_{yt} (MPa)	s (mm)	f_l (MPa)	k_1	k_2	f_{co}' (MPa)	f_{cc}' (MPa) Exp	f_{cc}' (MPa) Anal	Anal / Exp
1	3	214	64	6	813	31	14.67	4.49	0.72	92.4	145.0	139.8	0.96
2	3	214	64	6	813	31	14.67	4.49	0.72	92.4	137.0	139.8	1.02
3	3	214	64	6	813	31	14.67	4.49	0.72	92.4	145.0	139.8	0.96
4	3	214	64	6	813	45	10.11	4.93	0.60	92.4	122.0	122.2	1.00
5	3	214	64	6	813	60	7.58	5.31	0.52	92.4	120.0	113.2	0.94
6	3	214	64	6	813	60	7.58	5.31	0.52	92.4	110.0	113.2	1.03
7	3	214	64	6	813	60	7.58	5.31	0.52	92.4	120.0	113.2	0.94
8	3	216	64	4	840	31	6.68	5.12	0.73	92.4	120.0	117.3	0.98
9	3	214	64	6	462	31	8.34	4.94	0.72	96.2	134.0	125.9	0.94
10	3	214	64	6	462	31	8.34	4.94	0.72	96.2	133.0	125.9	0.95
11	3	214	64	6	462	45	5.75	5.43	0.60	96.2	117.0	114.9	0.98
12	3	214	64	6	462	60	4.31	5.84	0.52	96.2	115.0	109.2	0.95
13	3	214	64	6	462	60	4.31	5.84	0.52	96.2	115.0	109.2	0.95
14	3	216	64	4	481	31	3.83	5.63	0.73	96.2	115.0	111.9	0.97

Note:
1. Hoop ends were welded. No hooks were used.
2. Reinforcement arrangements are illustrated in Fig. 7.9.

Table 7.13: Strength enhancement for high strength concrete in square columns tested by Nagashima et al. (1992).

Col. Label	Reinf. Arrg.	b_c (mm)	s_l (mm)	d_b (mm)	f_{yt} (MPa)	s (mm)	f_l (MPa)	k_1	k_2	f_{co}' (MPa)	f_{cc}' (MPa) Exp	f_{cc}' (MPa) Anal	Anal/Exp
HH08LA	3	199.9	61.6	5.1	1387	55	7.13	5.37	0.52	98.8	122.8	118.5	0.97
HH10LA	3	199.9	61.6	5.1	1387	45	8.71	5.10	0.57	98.8	122.5	124.1	1.01
HH13LA	3	199.9	61.6	5.1	1387	35	11.20	4.79	0.65	98.8	131.5	133.4	1.01
HH15LA	3	198.6	60.7	6.4	1368	45	13.33	4.75	0.57	98.8	127.0	134.9	1.06
HH20LA	3	198.6	60.7	6.4	1368	35	17.14	4.45	0.65	100.4	148.2	149.7	1.01
HL06LA	3	200	61.7	5.0	807	45	7.03	5.29	0.57	100.4	118.2	121.6	1.03
HL08LA	3	200	61.7	5.0	807	35	9.04	4.96	0.65	100.4	133.2	129.4	0.97
LL05LA	3	200	61.7	5.0	807	55	5.58	5.60	0.51	51.3	68.9	67.4	0.98
LL08LA	3	200	61.7	5.0	807	35	9.04	4.96	0.65	51.3	79.4	80.3	1.01
LH08LA	3	199.9	61.6	5.1	1387	55	6.92	5.40	0.52	51.3	70.9	70.5	0.99
LH13LA	3	199.9	61.6	5.1	1387	35	11.20	4.79	0.65	51.3	85.7	85.9	1.00
HH13MA	3	199.9	61.6	5.1	1387	35	11.20	4.79	0.65	100.4	131.8	135.0	1.02
HH13HA	3	199.9	61.6	5.1	1387	35	11.20	4.79	0.65	100.4	129.2	135.0	1.05
LL08MA	3	200	61.7	5.0	807	35	9.04	4.96	0.65	51.3	79.6	80.3	1.01
LL08HA	3	200	61.7	5.0	807	35	9.04	4.96	0.65	51.3	78.0	80.3	1.03
LH15LA	3	198.6	60.7	6.4	1368	45	13.33	4.75	0.57	52.4	88.7	88.5	1.00
HH13LB	5	199.9	61.6	5.1	1387	27	12.39	4.60	0.74	100.4	131.7	142.3	1.08
HH13LD	2	199.9	92.4	5.1	1387	25	13.38	4.67	0.62	100.4	128.2	139.4	1.09
LL08LB	5	200	61.7	5.0	807	27	9.99	4.77	0.74	52.4	82.4	87.5	1.06
LL08LD	2	200	92.5	5.0	807	25	10.79	4.84	0.62	52.4	77.3	85.0	1.10
HH13MSA	3	199.9	61.6	5.1	1387	35	11.20	4.79	0.65	100.4	129.7	135.0	1.04
HH13HSA	3	199.9	61.6	5.1	1387	35	11.20	4.79	0.65	100.4	134.8	135.0	1.00
LL08MSA	3	200	61.7	5.0	807	35	9.04	4.96	0.65	52.4	79.0	81.4	1.03
LL08HSA	3	200	61.7	5.0	807	35	9.04	4.96	0.65	52.4	80.5	81.4	1.01

Note:
1. Reinforcement arrangements are illustrated in Fig. 7.9.

Table 7.14: Strength enhancement for high strength concrete in square columns tested by Cusson and Paultre (1994).

Col. Label	Reinf. Arrg.	b_o (mm)	s_l (mm)	d_b (mm)	f_{yt} (MPa)	s (mm)	f_l (MPa)	k_1	k_2	f_{co}' (MPa)	f_{cc}' (MPa) Exp	f_{cc}' (MPa) Anal	Anal/Exp
1A	1	195	166	9.5	410	50	5.96	6.00	0.32	81.1	99.7	92.6	0.93
1B	2	195	85.6	7.9	392	50	6.73	5.56	0.45	81.1	105.4	97.8	0.93
1C	5	195	58.6	7.9	392	50	6.73	5.38	0.54	81.1	101.4	100.7	0.99
1D	3	195	58.6	7.9	392	50	7.88	5.24	0.54	85.3	112.6	107.6	0.96
1D1	3	195	58.6	7.9	392	50	7.88	5.24	0.54	85.3	124.6	107.6	0.86
2A	1	195	167.6	7.9	392	50	3.94	6.44	0.32	81.9	91.8	90.1	0.98
2B	2	195	86.3	6.4	414	50	4.66	5.92	0.45	81.9	91.8	94.2	1.03
2C	5	195	59.1	6.4	414	50	4.66	5.73	0.54	81.9	99.1	96.3	0.97
2D	3	195	59.1	6.4	414	50	5.46	5.58	0.54	81.9	98.3	98.3	1.00
3A	1	195	166	9.5	410	100	2.98	7.16	0.23	83.4	81.7	88.2	1.08
3B	2	195	84.8	9.5	410	100	5.09	6.17	0.32	83.4	85.9	93.4	1.09
3C	5	195	58.1	9.5	410	100	5.09	5.98	0.38	83.4	90.1	95.1	1.06
3D	3	195	58.1	9.5	410	100	5.96	5.82	0.38	83.4	93.4	96.7	1.04
4A	1	195	160.3	9.5	410	50	5.96	5.98	0.33	79.1	96.5	90.8	0.94
4B	2	195	83.8	7.9	392	50	6.73	5.55	0.45	79.1	102.9	96.0	0.93
4C	5	195	55.9	7.9	392	50	6.73	5.36	0.55	79.1	106.0	99.1	0.93
4D	3	195	55.9	7.9	392	50	7.88	5.22	0.55	79.1	111.6	101.9	0.91
5A	1	195	160.3	9.5	705	50	10.25	5.46	0.33	84.9	99.4	103.2	1.04
5B	2	195	83.8	7.9	770	50	13.22	4.94	0.45	84.9	104.4	114.4	1.10
5C	5	195	55.9	7.9	770	50	13.22	4.78	0.55	84.9	110.4	119.8	1.09
5D	3	195	55.9	7.9	770	50	15.48	4.65	0.55	84.9	128.2	124.8	0.97
6B	2	195	83	9.5	715	50	17.75	4.70	0.45	98.5	122.2	136.4	1.12
6D	3	195	55.9	7.9	680	50	13.67	4.75	0.55	96.6	126.5	132.5	1.05
7B	2	195	83	9.5	715	50	17.75	4.70	0.45	64.5	107.1	102.4	0.96
7D	3	195	55.9	7.9	680	50	13.67	4.75	0.55	57.7	100.4	93.6	0.93
8B	2	195	83	9.5	715	50	17.75	4.70	0.45	44.7	89.4	82.6	0.92
8D	3	195	55.9	7.9	680	50	13.67	4.75	0.55	47.3	90.7	83.2	0.92

Notes:

1. Column 1D1 had no concrete cover.
2. Reinforcement arrangements are illustrated in Fig. 7.9.

Table 7.15: Strength enhancement for high strength concrete in square columns tested by Itakura and Yagenji (1992).

Col. Label	Reinf. Arrg.	b_c (mm)	s_l (mm)	d_b (mm)	f_{yt} (MPa)	s (mm)	f_l (MPa)	k_1	k_2	f_{co}' (MPa)	f_{cc}' (MPa) Exp	f_{cc}' (MPa) Anal	Anal/Exp
C8P6A-1	1	212	193.0	6	808	40	6.13	5.85	0.36	57.6	74	70.5	0.95
C8P6A-2	1	212	193.0	6	808	40	6.13	5.85	0.36	57.6	74	70.5	0.95
C8P9A-1	1	212	193.0	6	808	27	9.08	5.29	0.44	57.6	73	78.7	1.08
C8P9A-2	1	212	193.0	6	808	27	9.08	5.29	0.44	57.6	73	78.7	1.08
C8P6Am	1	212	193.0	6	808	40	6.13	5.85	0.36	57.6	75	70.5	0.94
C8P6B	*	212	96.5	6	808	60	6.13	5.71	0.42	57.6	73	72.2	0.99
C8P6B(6)	*	212	96.5	6	808	60	6.13	5.71	0.42	57.6	74	72.2	0.98
C8P6B(4)	*	212	96.5	6	808	60	6.13	5.71	0.42	57.6	73	72.2	0.99
C8P9B	*	212	96.5	6	808	40	9.19	5.15	0.51	57.6	87	81.8	0.94
C8P6C-1	2	212	96.5	6	808	70	5.98	5.81	0.39	57.6	76	71.0	0.93
C8P6C-2	2	212	96.5	6	808	70	5.98	5.81	0.39	57.6	75	71.0	0.95
C8P9C-1	2	212	96.5	6	808	47	8.90	5.25	0.47	57.6	87	79.6	0.92
C8P9C-2	2	212	96.5	6	808	47	8.90	5.25	0.47	57.6	85	79.6	0.94
C8P9D	3	212	64.3	6	808	66	7.43	5.38	0.49	57.6	84	77.1	0.92
C8P9D(6)	3	212	64.3	6	808	66	7.43	5.38	0.49	57.6	78	77.1	0.99

Notes:

1. All columns had no concrete cover.
2. Reinforcement arrangements are illustrated in Fig. 7.9. * indicates arrangement 3 in Fig. 4.2.
3. Columns C8P6A, C8P9A, and C8P6Am had 8, 12, and 10 longitudinal bars respectively.

Table 7.16: Strength enhancement for high strength concrete in square columns tested by Yong et al. (1988).

Col. Label	Reinf. Arrg.	b_c (mm)	s_l (mm)	d_b (mm)	f_{yt} (MPa)	s (mm)	f_l (MPa)	k_1	k_2	f_{co}' (MPa)	f_{cc}' (MPa) Exp	f_{cc}' (MPa) Anal	Anal/Exp
set A	2	130.2	58.7	3.2	496	25.4	4.12	5.91	0.51	81.0	99.0	93.3	0.94
Set B	2	130.2	58.7	3.2	496	50.8	2.06	7.06	0.36	84.3	101.6	89.5	0.88
Set C	2	130.2	58.7	3.2	496	76.2	1.37	7.83	0.29	80.5	90.9	83.6	0.92
Set D	2	130.2	58.7	3.2	496	152.4	0.686	9.34	0.21	81.5	83.1	82.8	1.00
Set N	2	130.2	58.7	3.2	496	50.8	2.06	7.06	0.36	78.6	90.9	83.8	0.92
Set L	2	130.2	117.5	3.2	496	76.2	1.37	8.30	0.21	86.7	89.0	89.0	1.00

Notes:
1. Set [illegible] had no concrete cover.
2. Reinforcement arrangements are illustrated in Fig. 7.9.

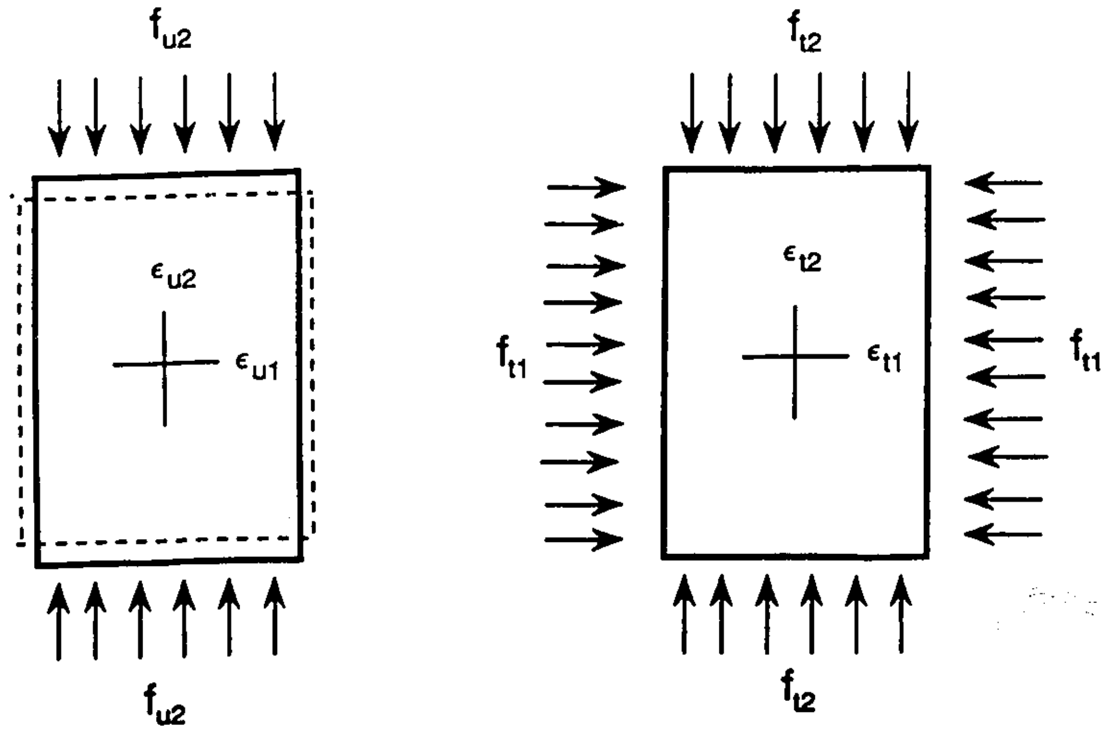

(a) Uniaxial

(b) Triaxial

Figure 7.1: States of stress.

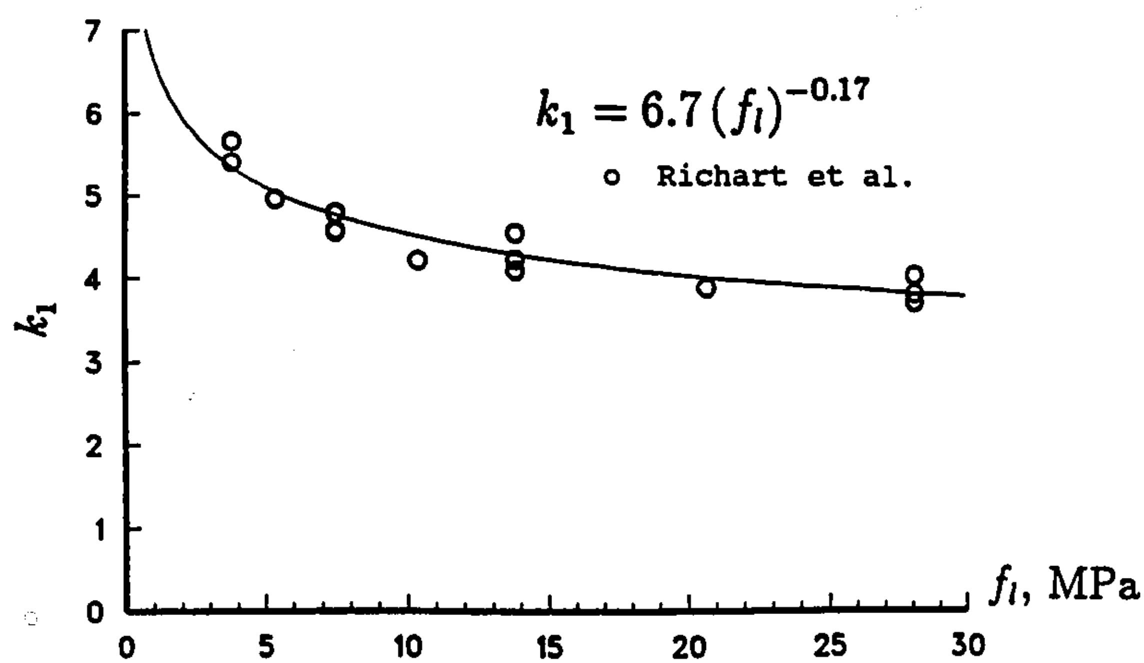

Figure 7.2: Variation of coefficient k_1 with lateral pressure.

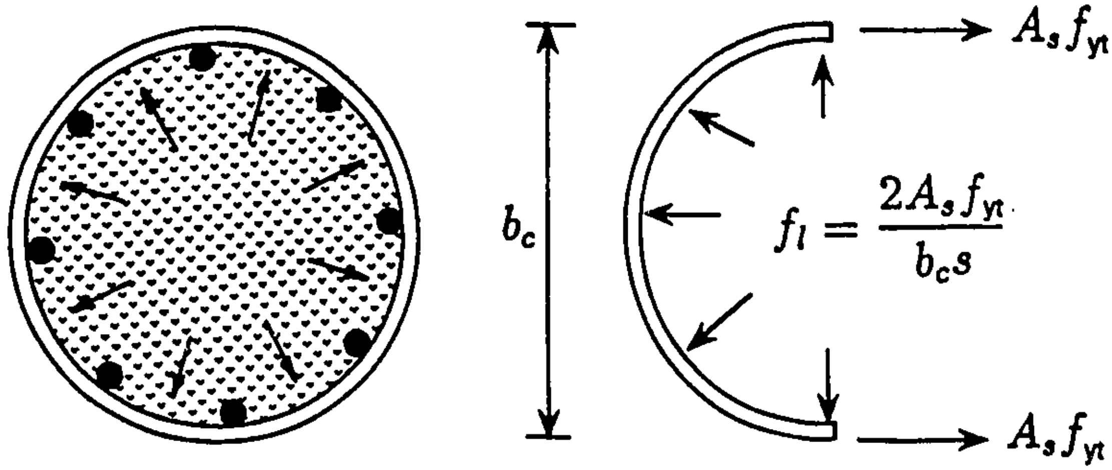

(a) Uniform built-up of pressure. (b) Computation of lateral pressure from hoop tension.

Figure 7.3: Lateral pressure in circular columns.

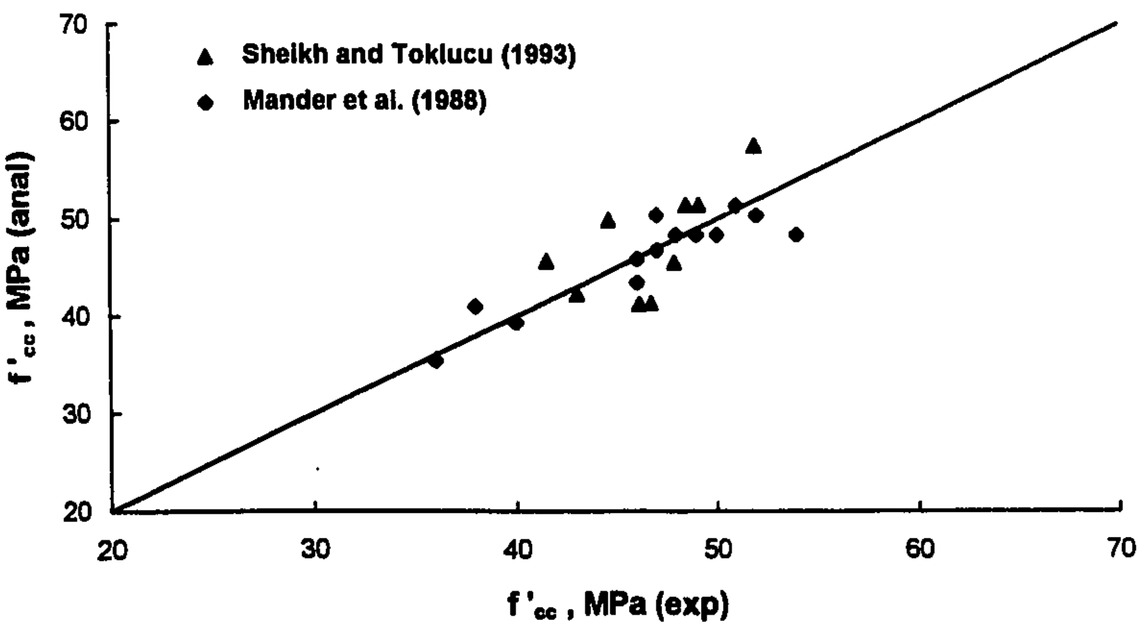

Figure 7.4: Comparison of analytical and experimental strength values for confined normal strength concrete in circular columns.

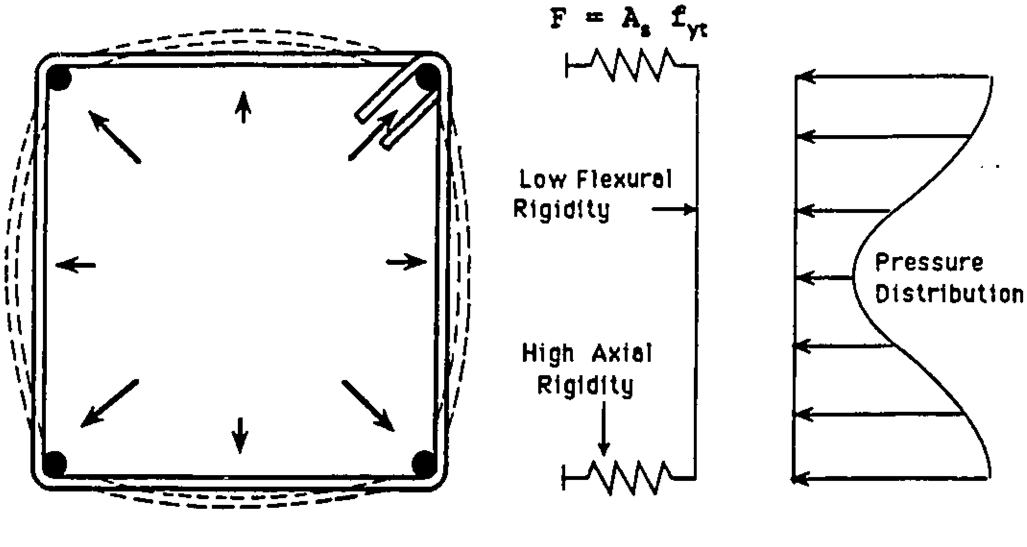

Figure 7.5: Lateral pressure built-up in square columns.

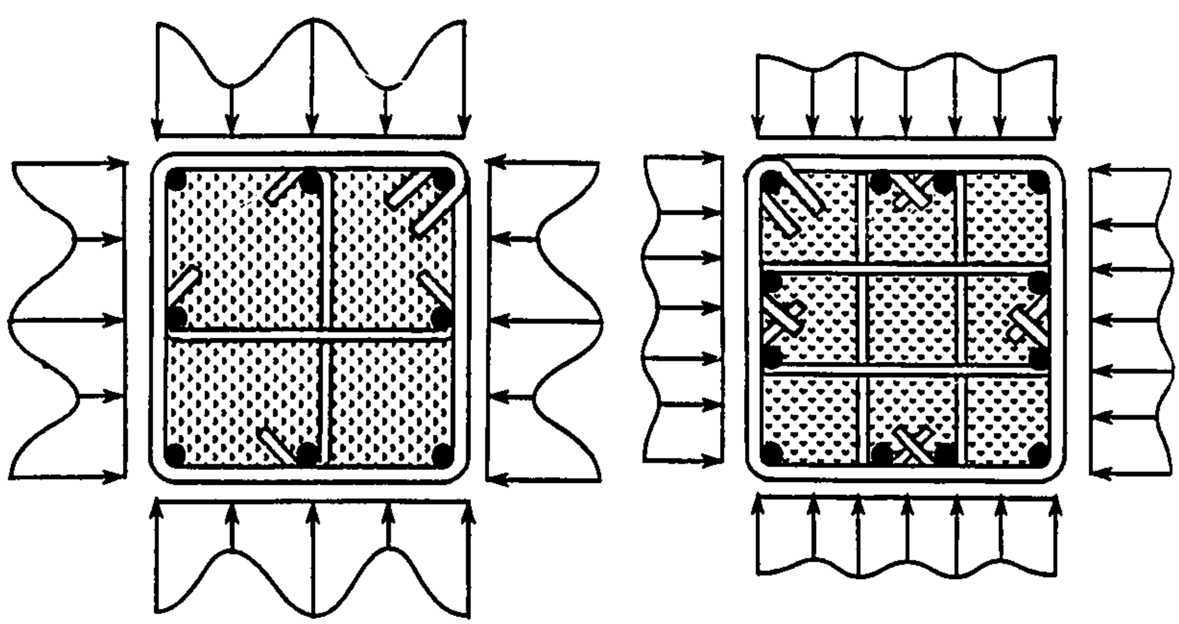

Figure 7.6: Pressure distribution resulting from different reinforcement arrangements.

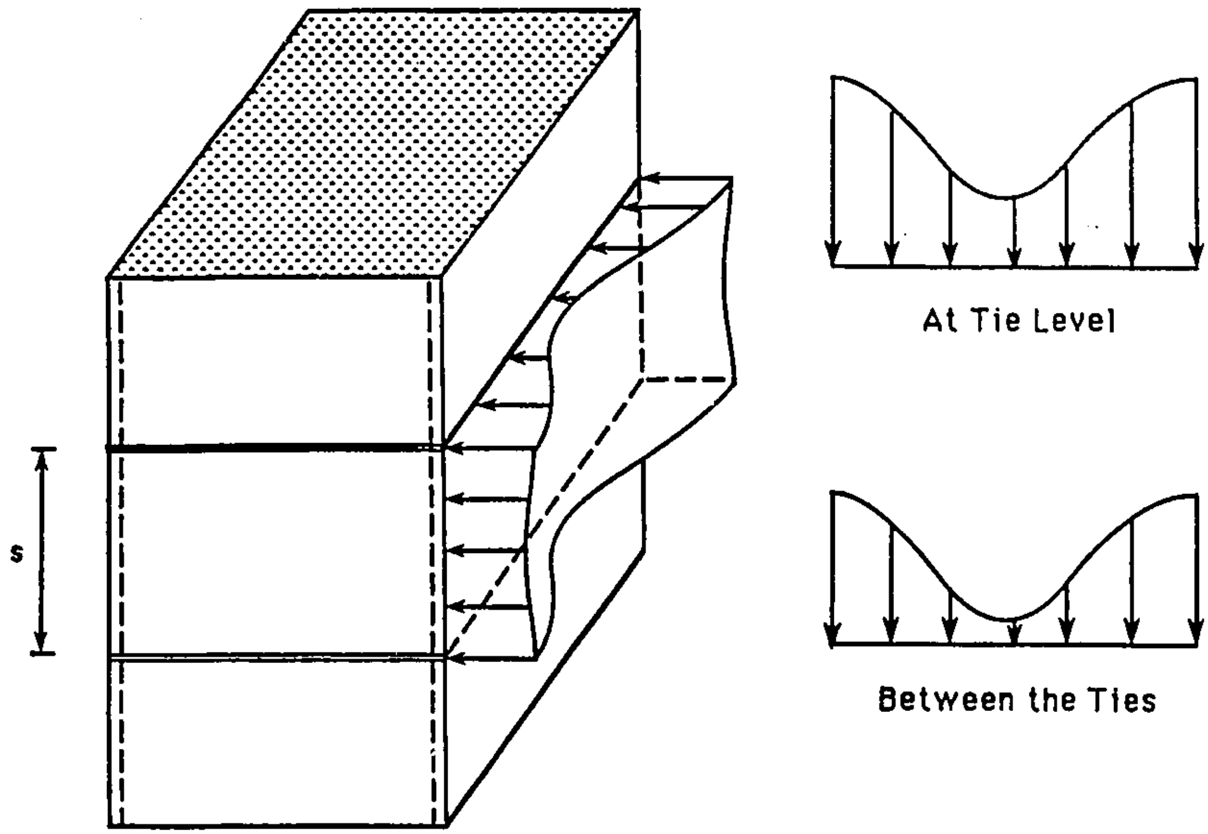

Figure 7.7: Distribution of lateral pressure along member length.

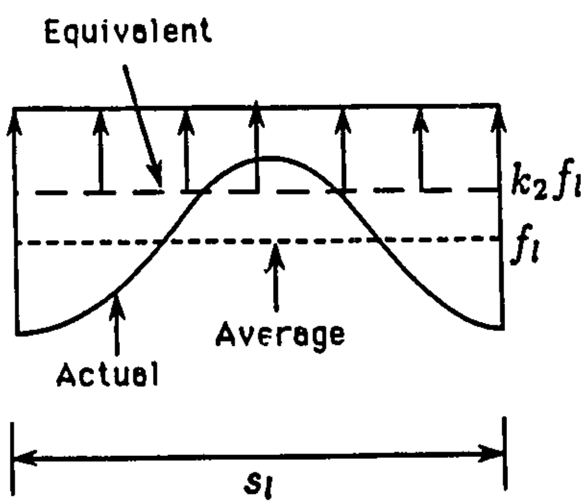

Figure 7.8: Actual, average, and equivalent lateral pressure.

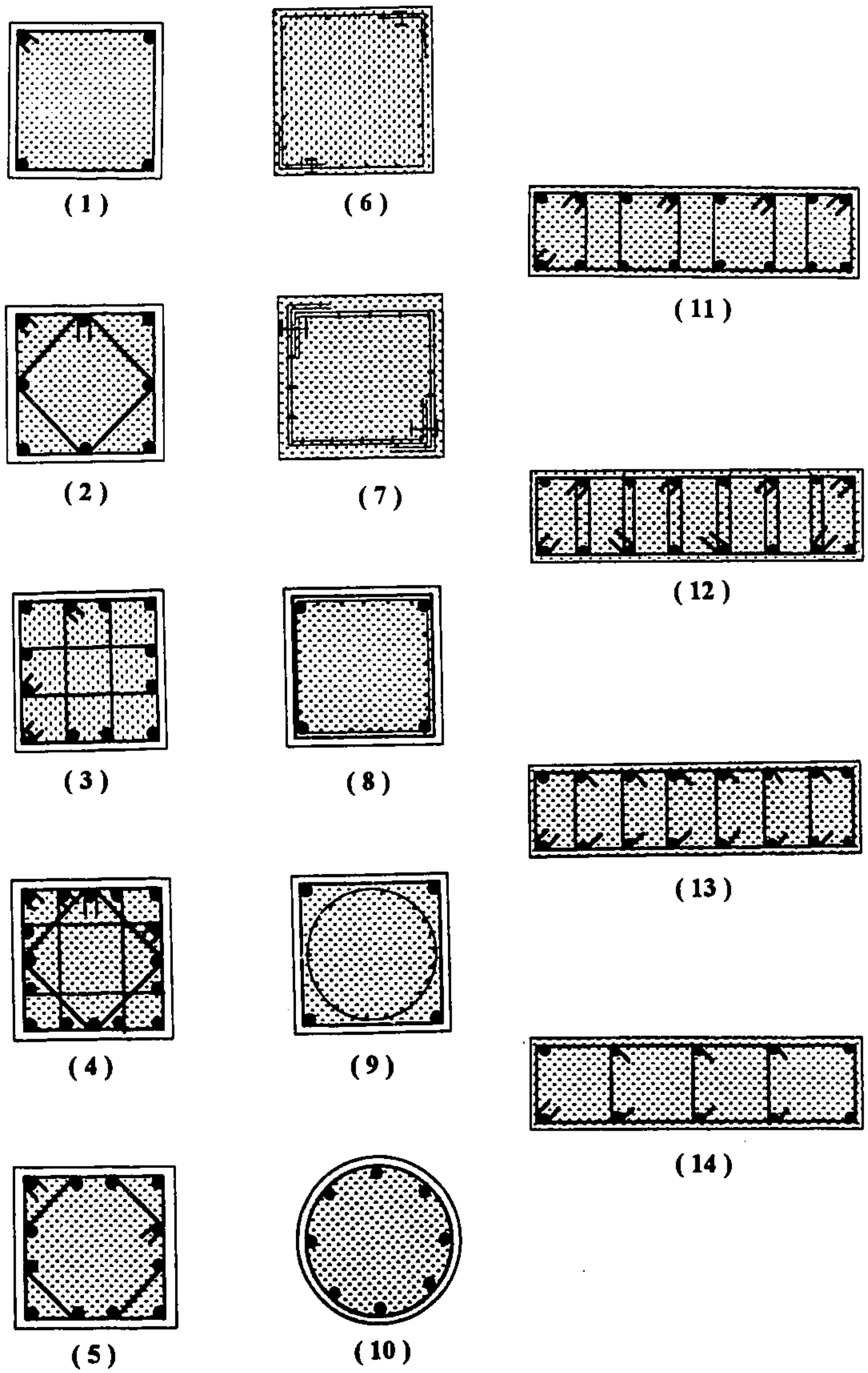

Figure 7.9: Reinforcement arrangements considered in column tests.

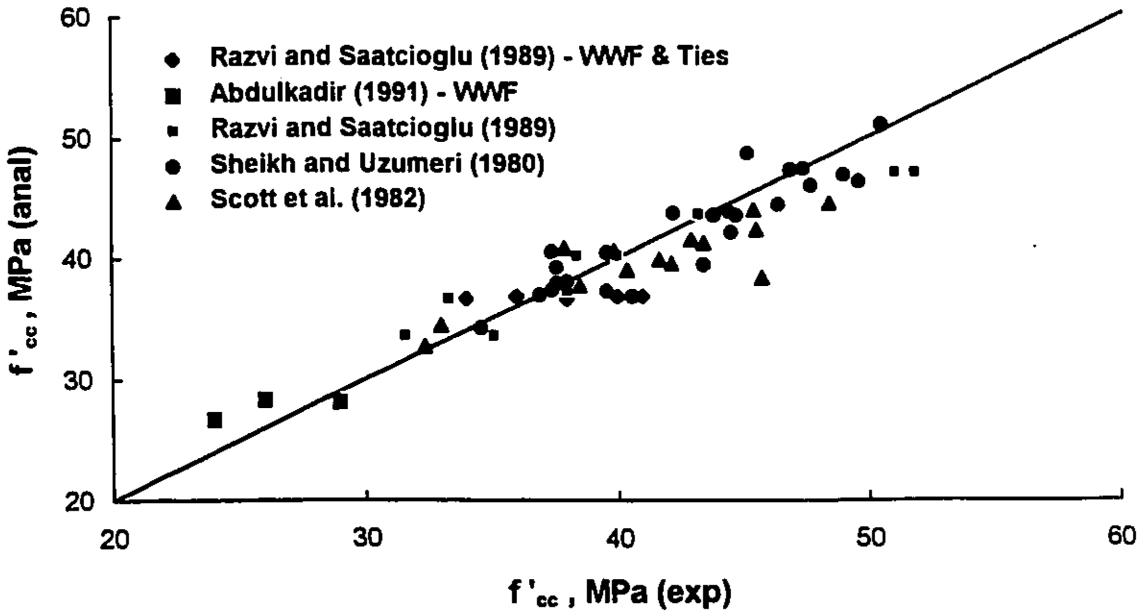

Figure 7.10: Comparison of analytical and experimental strength values for confined normal strength concrete in square columns.

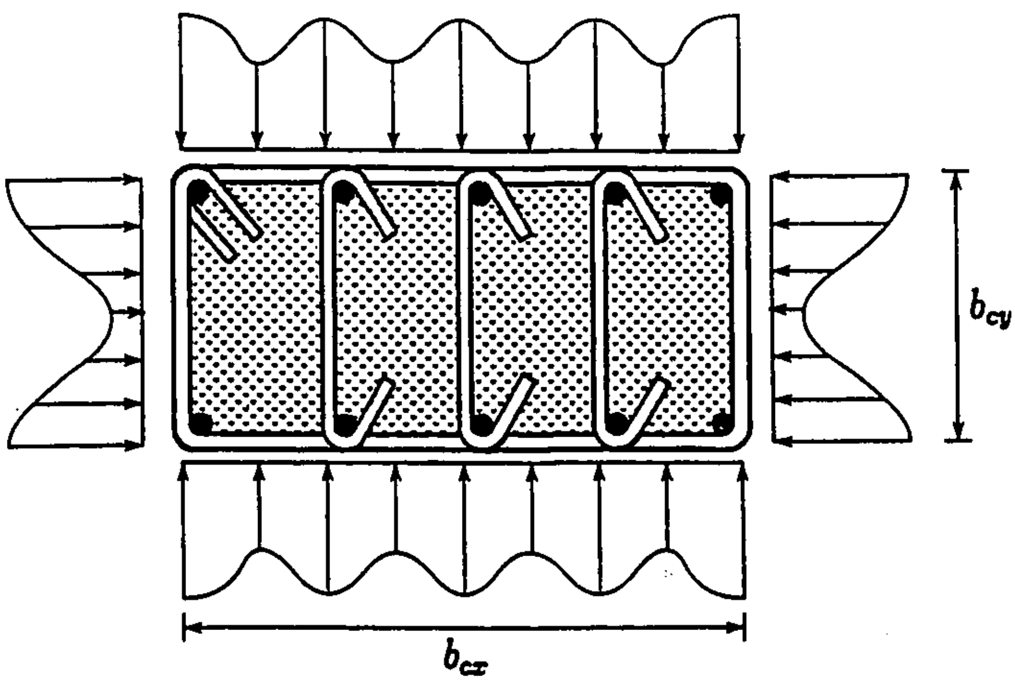

Figure 7.11: Lateral pressure distribution in rectangular columns.

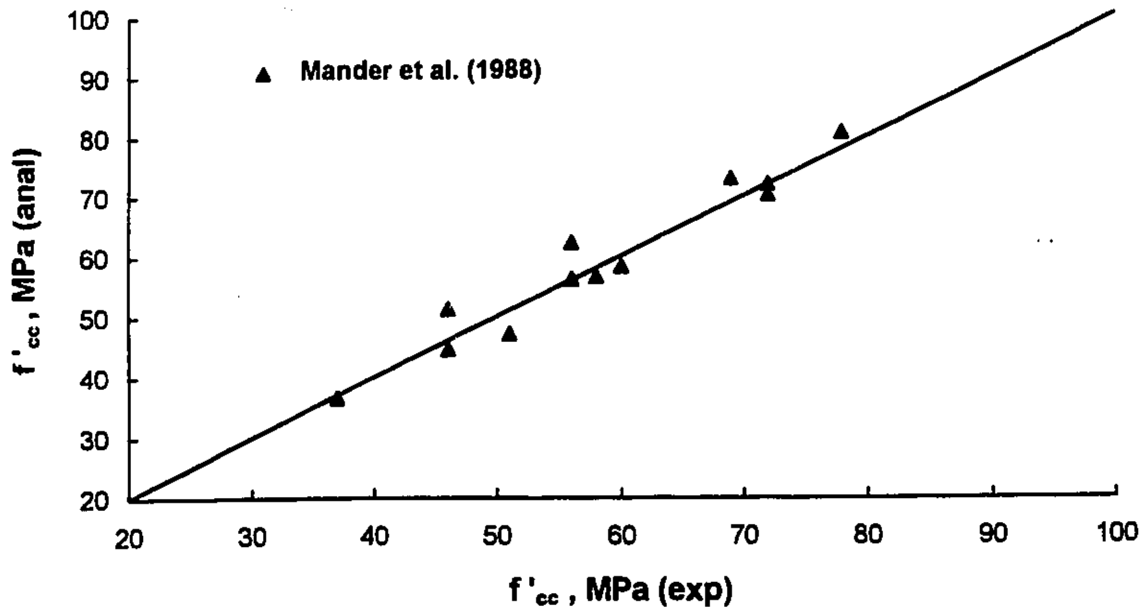

Figure 7.12: Comparison of analytical and experimental strength values for confined normal strength concrete in rectangular columns.

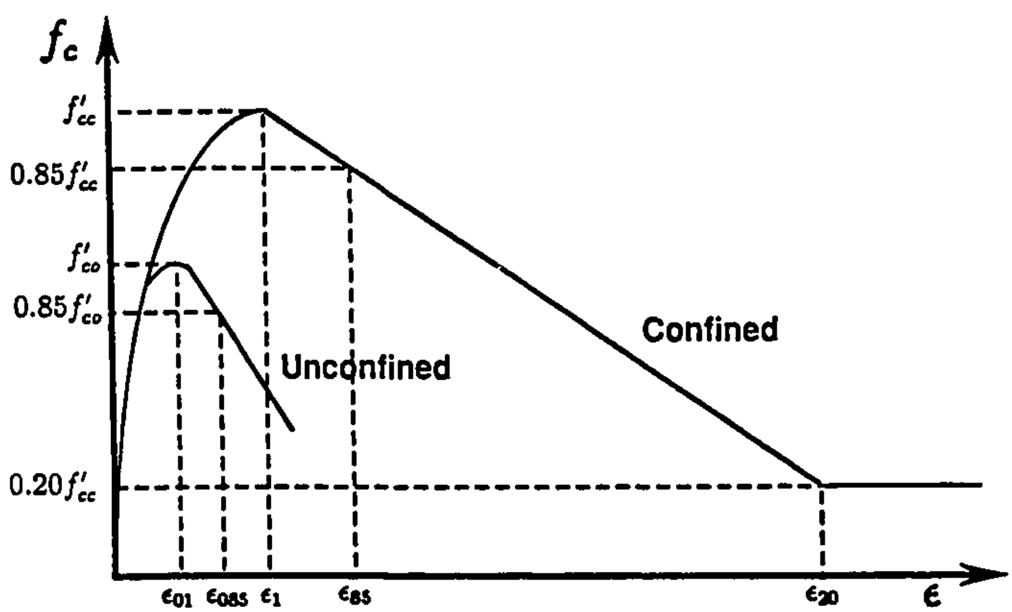

Figure 7.13: Proposed stress-strain relationship for confined concrete.

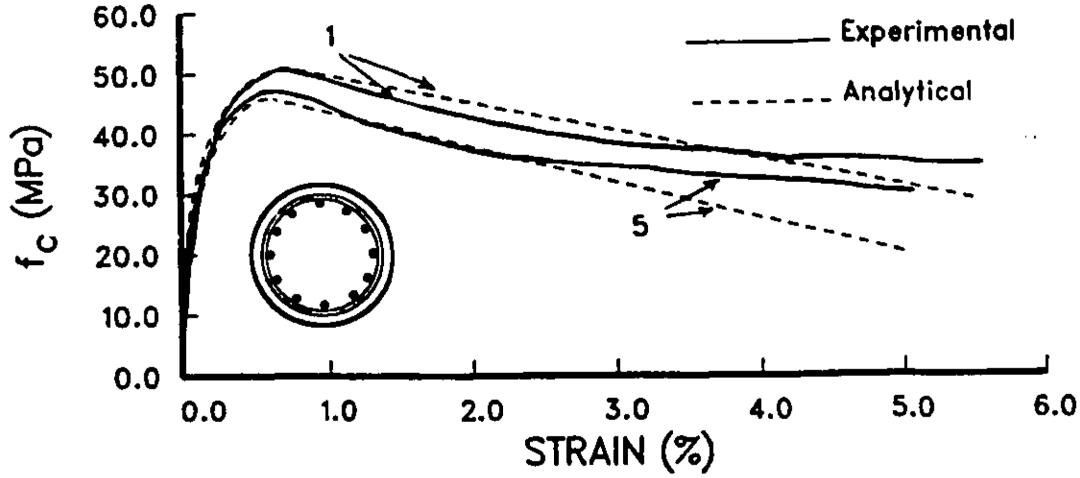

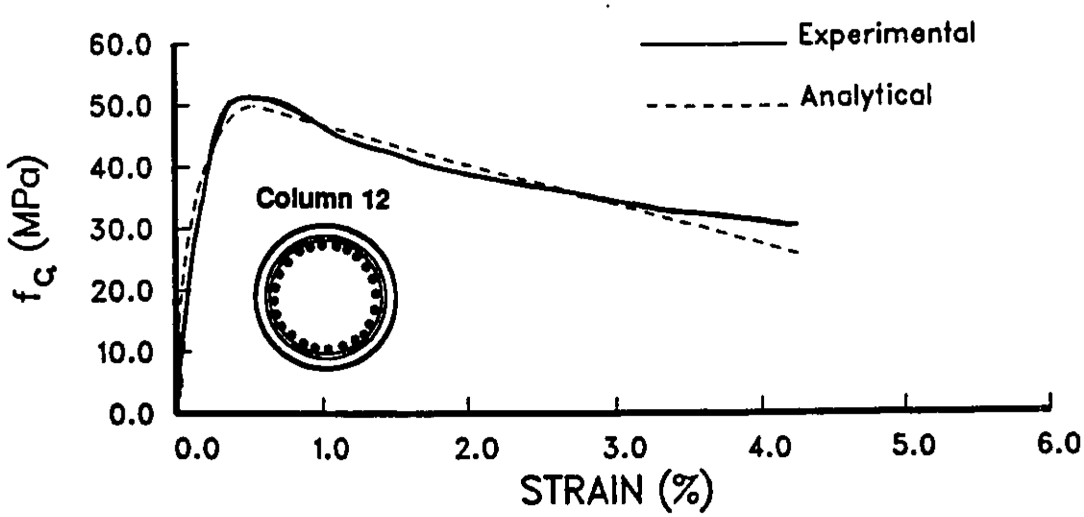

Figure 7.14: Circular columns (1, 5, and 12) tested by Mander et al. (1988) under a high strain rate of 0.0133/sec.

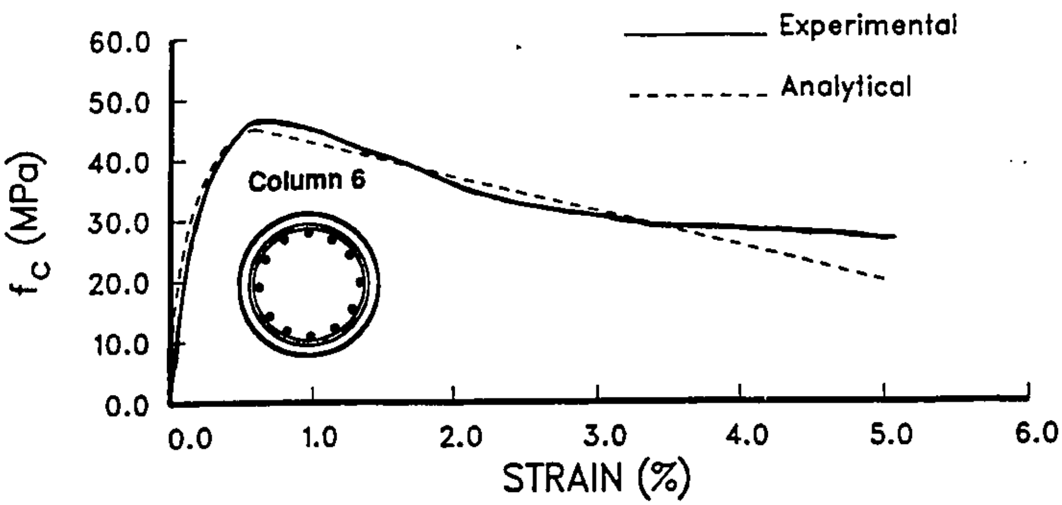

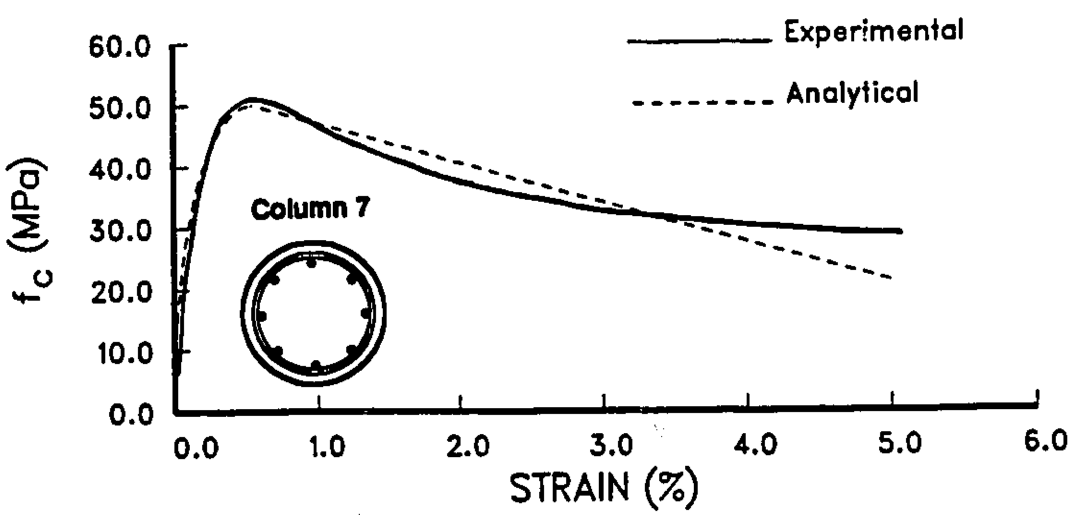

Figure 7.15: Circular columns (6 and 7) tested by Mander et al. (1988) under a high strain rate of 0.0133/sec.

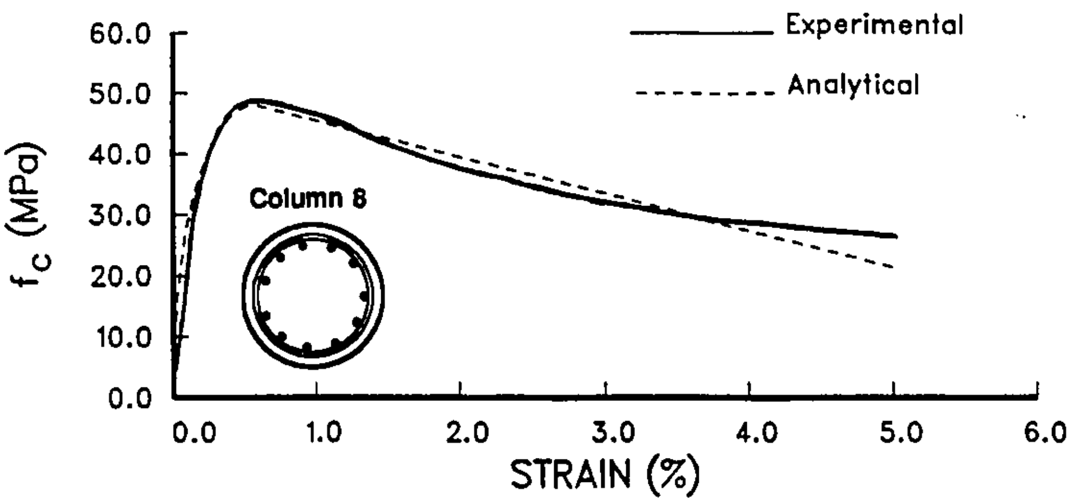

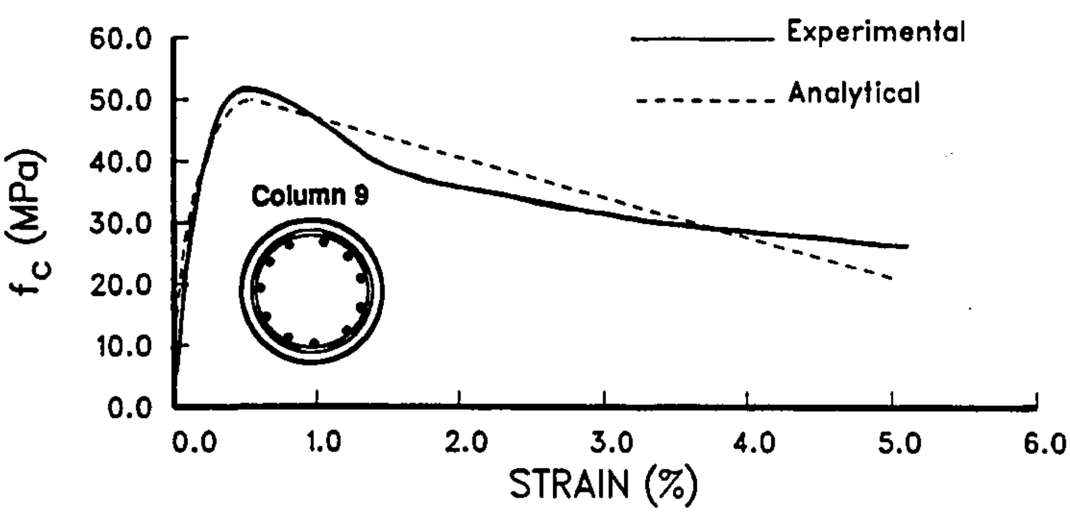

Figure 7.16: Circular columns (8 and 9) tested by Mander et al. (1988) under a high strain rate of 0.0133/sec.

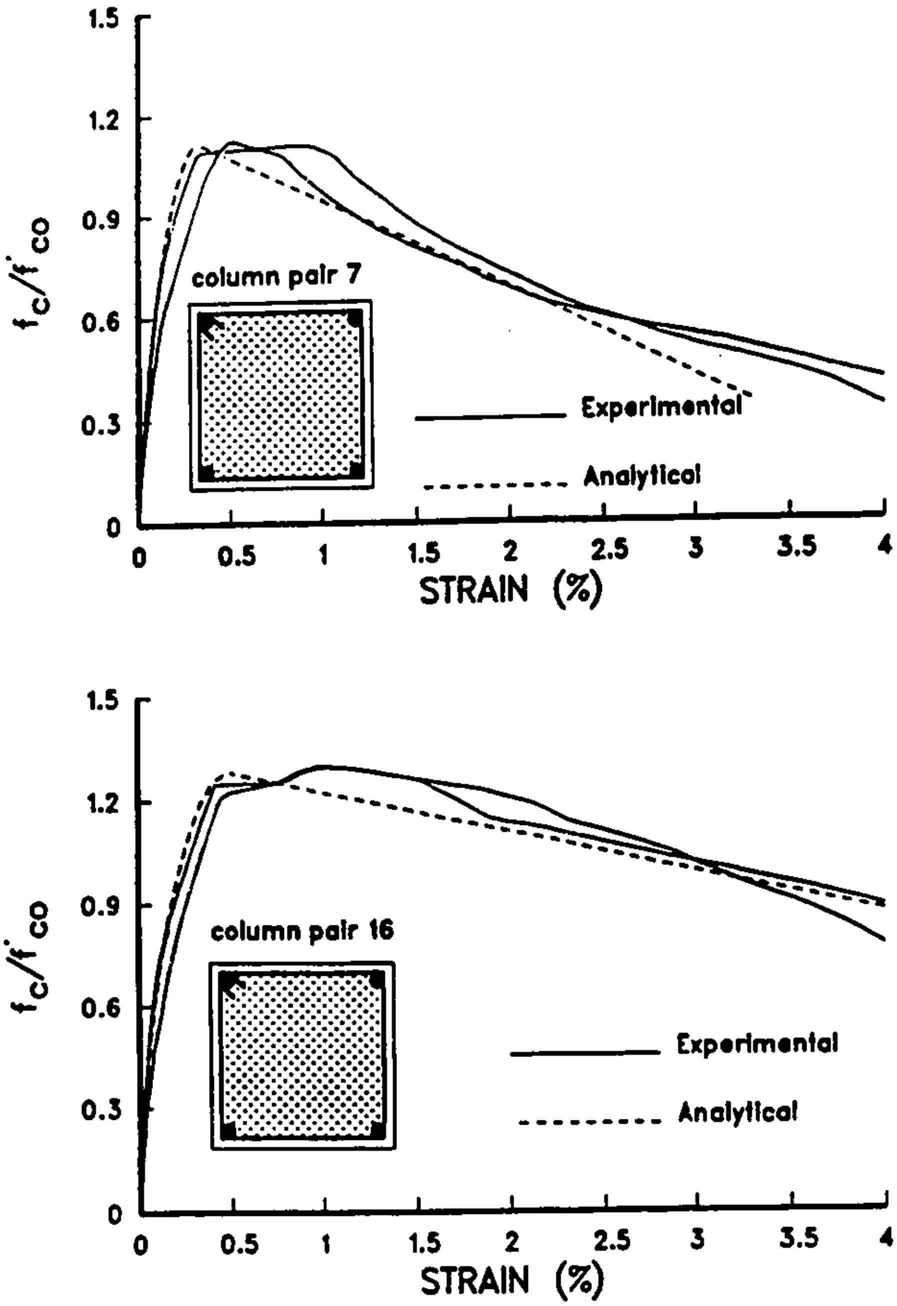

Figure 7.17: Square columns (7 and 16) tested by Razvi and Saatcioglu (1989).

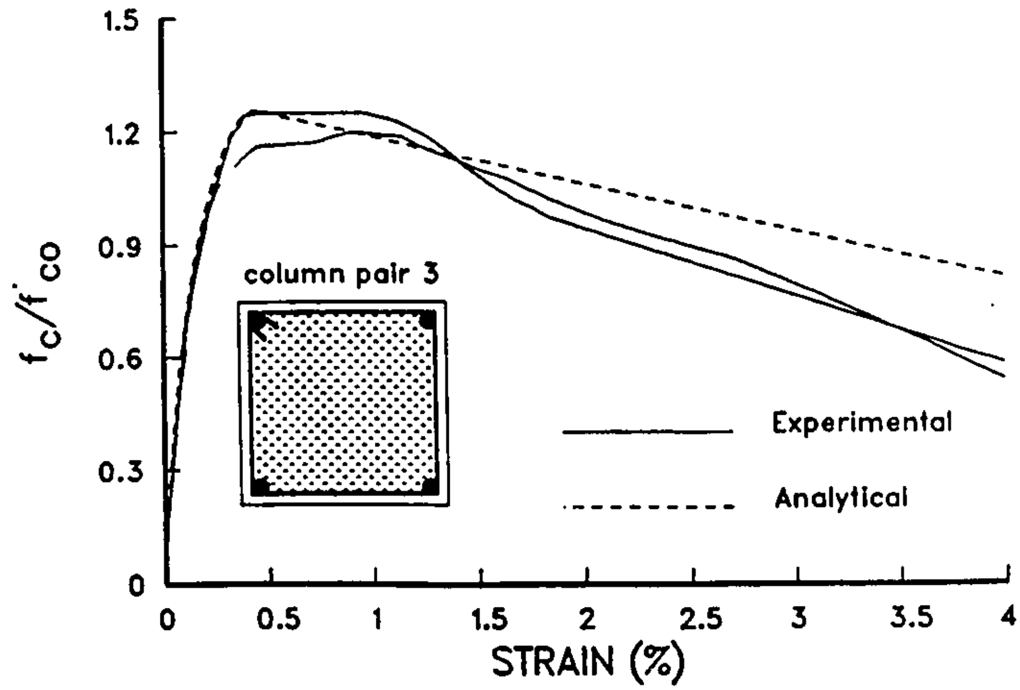

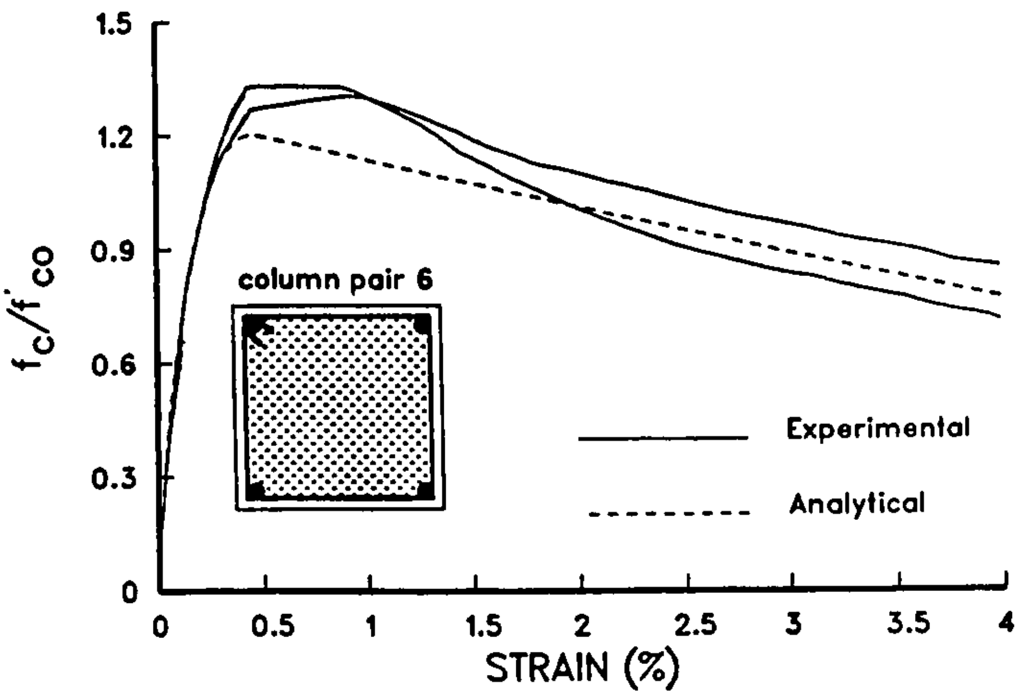

Figure 7.18: Square columns (3 and 6) tested by Razvi and Saatcioglu (1989).

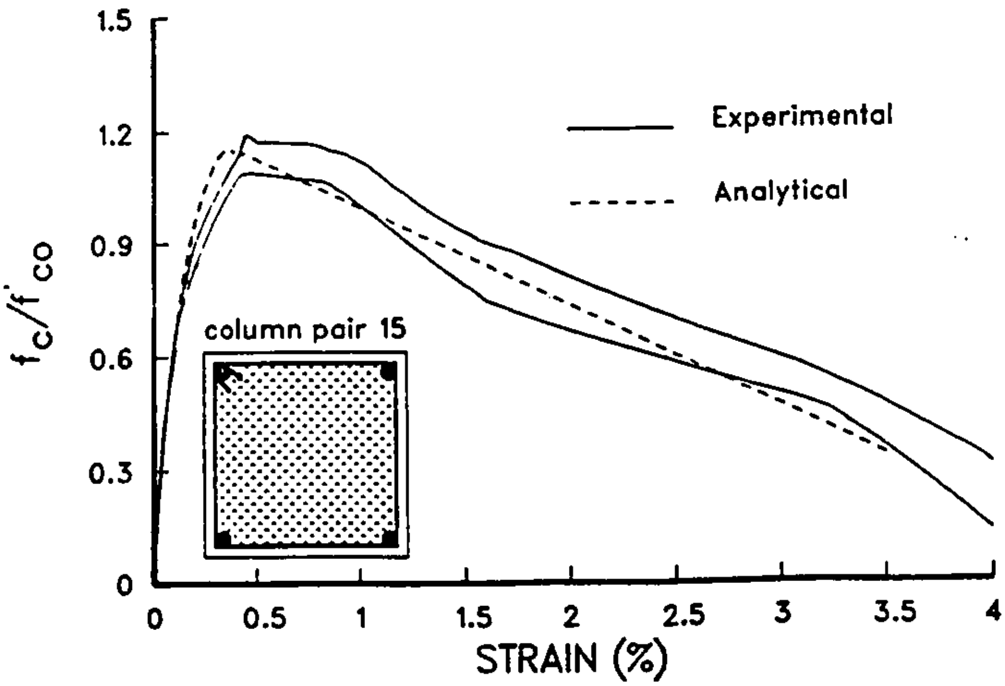

Figure 7.19: Square columns (pair 15) tested by Razvi and Saatcioglu (1989).

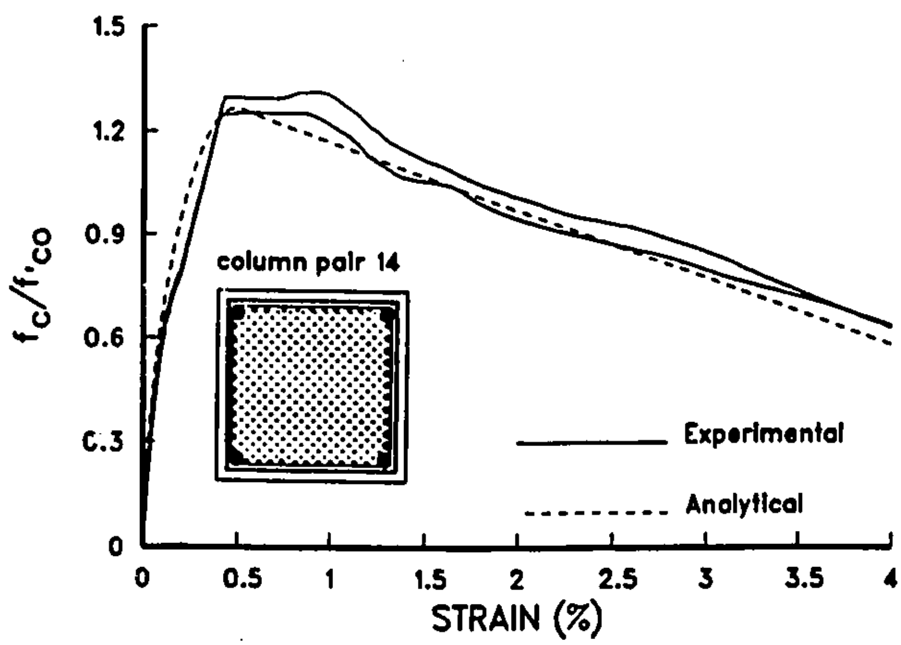

Figure 7.20: Square columns (pair 14) confined with WWF and hoops, tested by Razvi and Saatcioglu (1989).

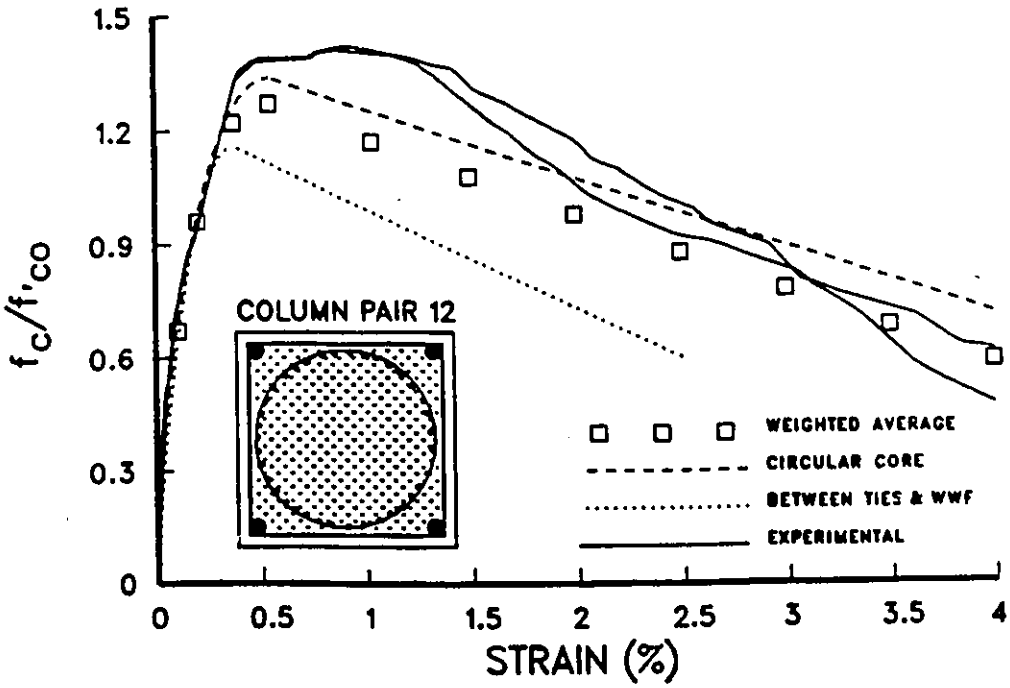

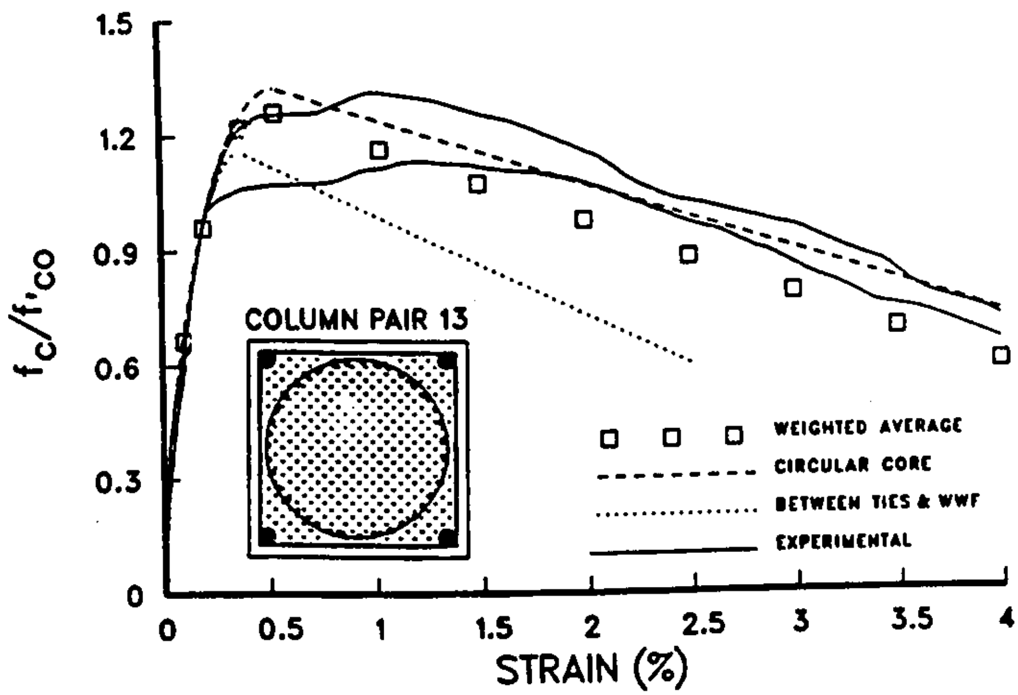

Figure 7.21: Square columns (pairs 12 and 13) confined with WWF, tested by Razvi and Saatcioglu (1989).

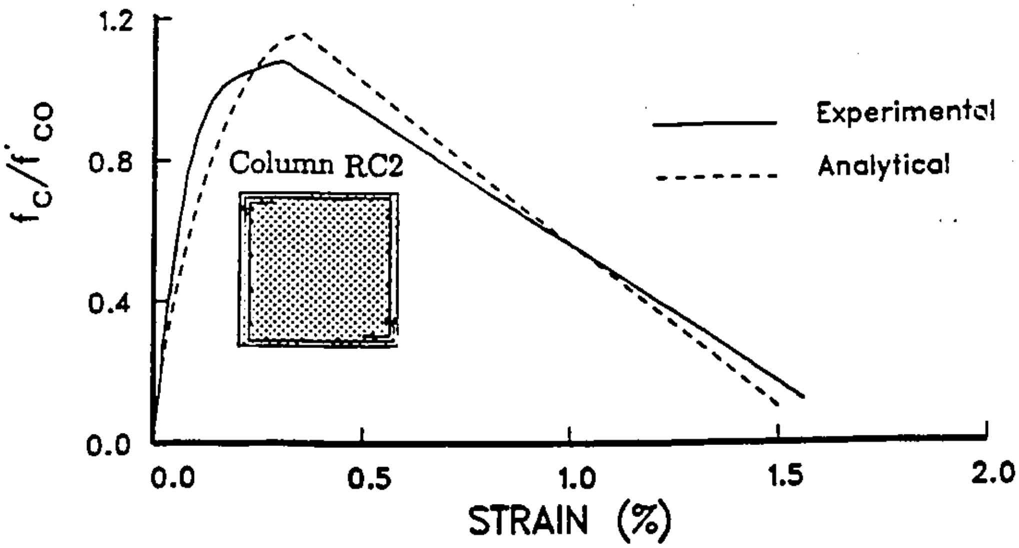

Figure 7.22: A square column (RC2) confined with WWF, tested by Abdulkadir (1991).

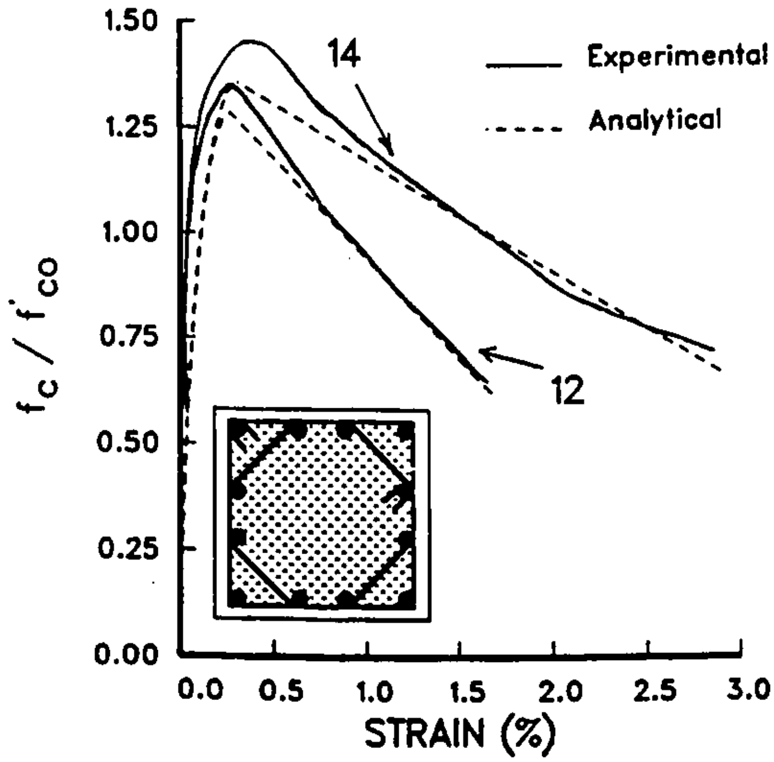

Figure 7.23: Square columns (12 and 14) tested by Scott et al. (1982) under a high strain rate of 0.0167/sec.

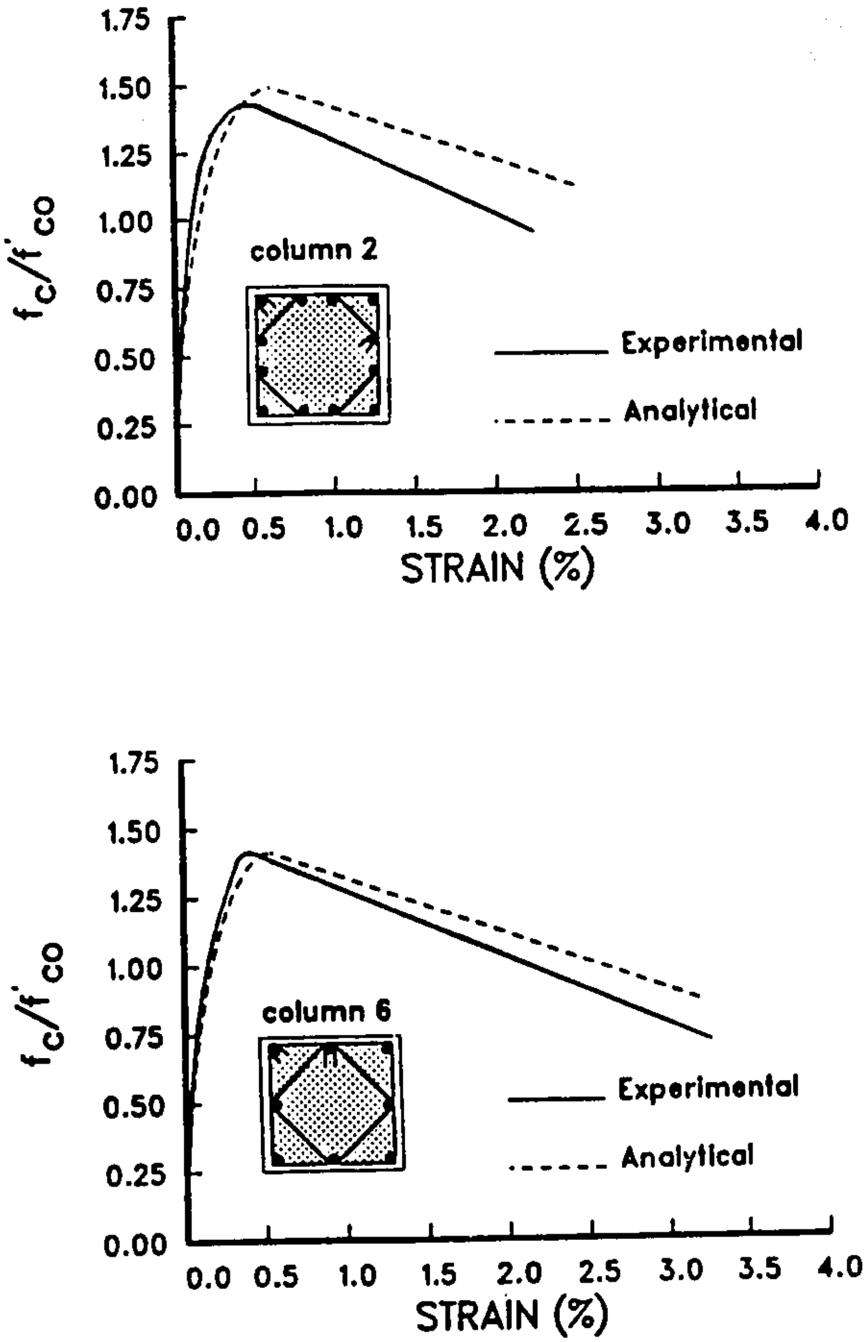

Figure 7.24: Square columns (2 and 6) tested by Scott et al. (1982).

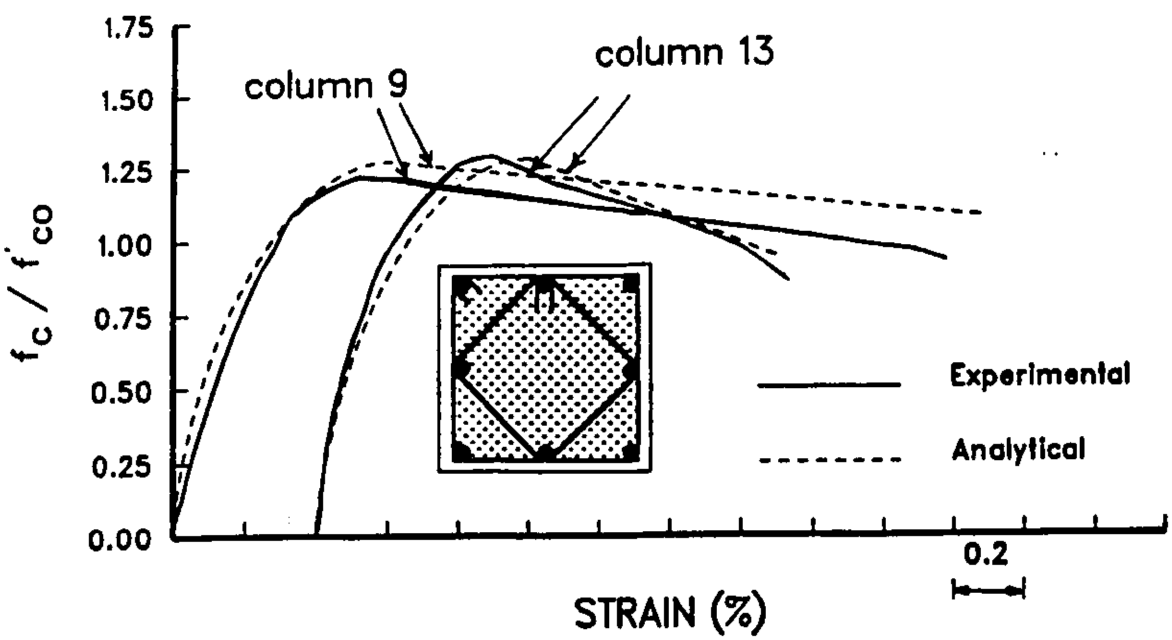

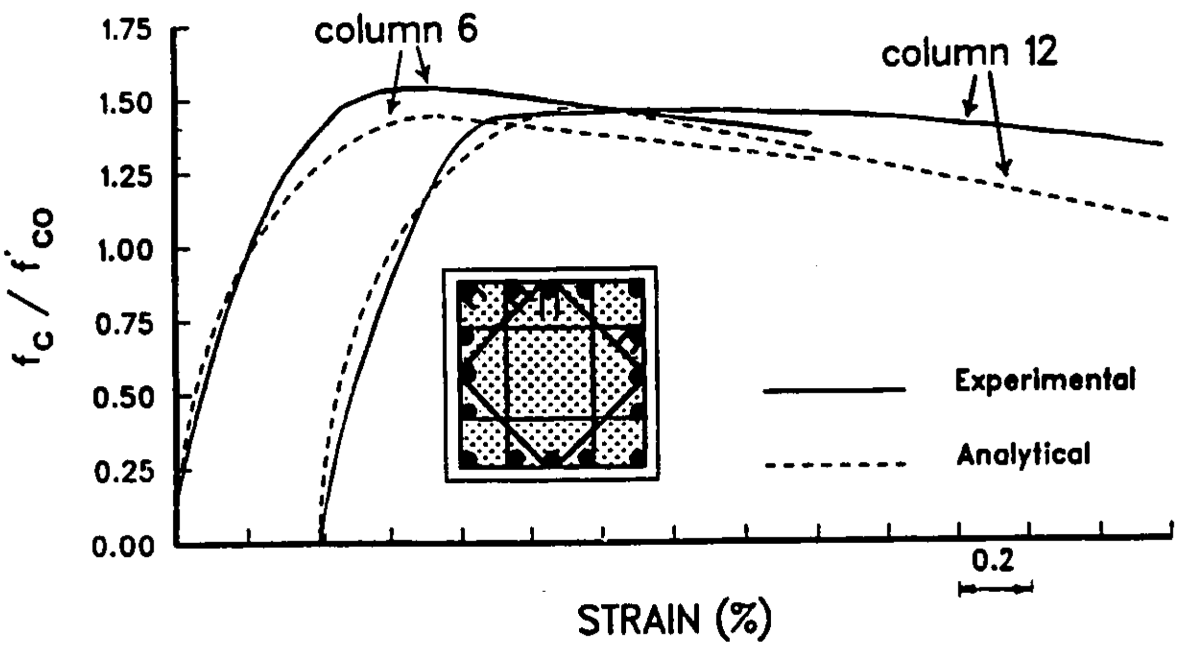

Figure 7.25: Square columns (6, 9, 12 and 13) tested by Sheikh and Uzumeri (1980).

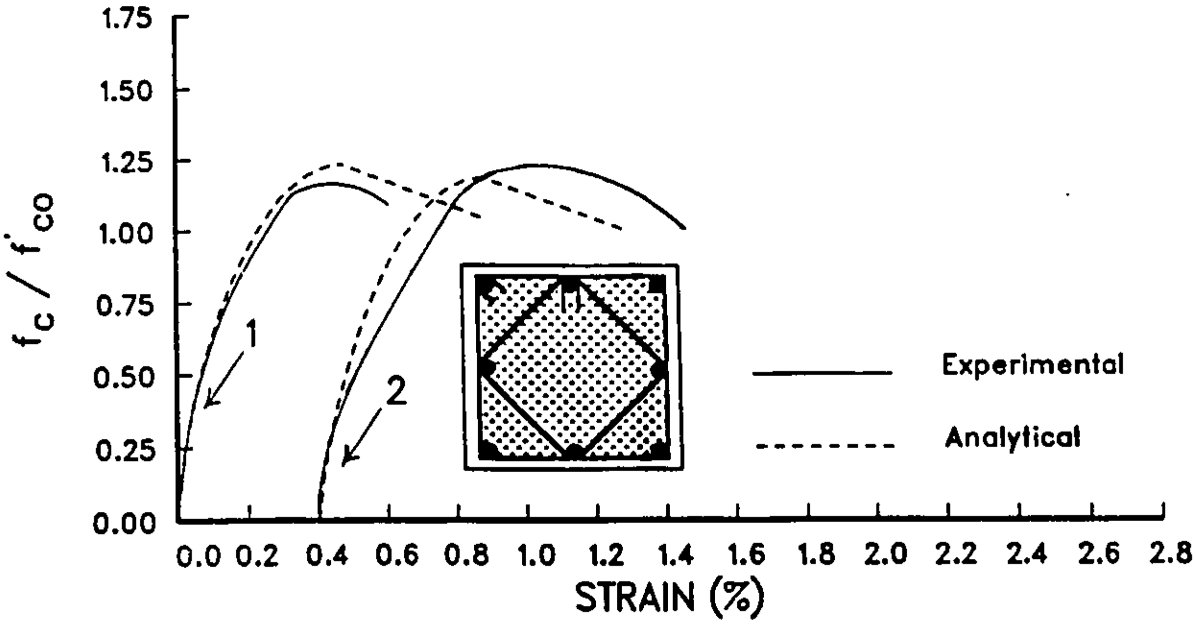

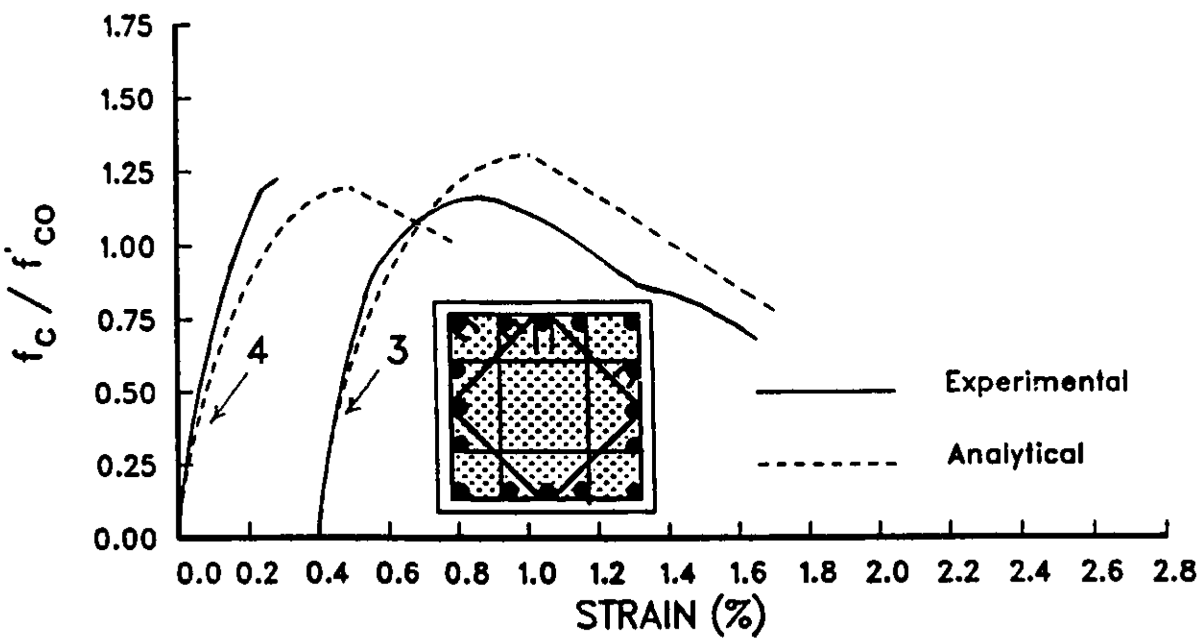

Figure 7.26: Square columns (1, 2, 3 and 4) tested by Sheikh and Uzumeri (1980).

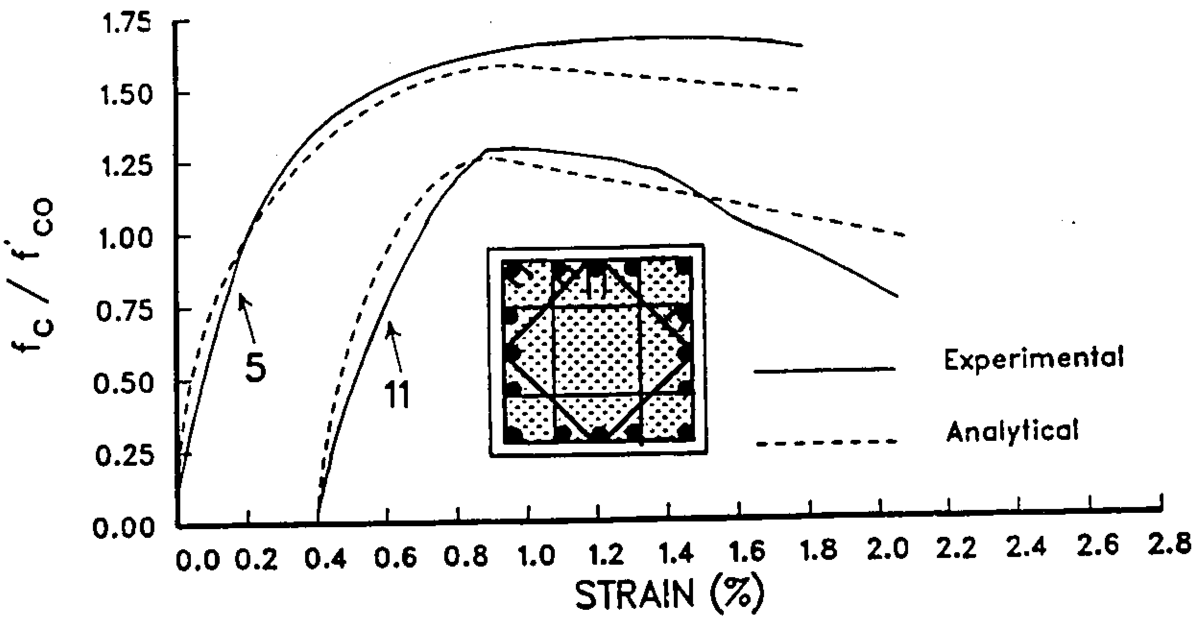

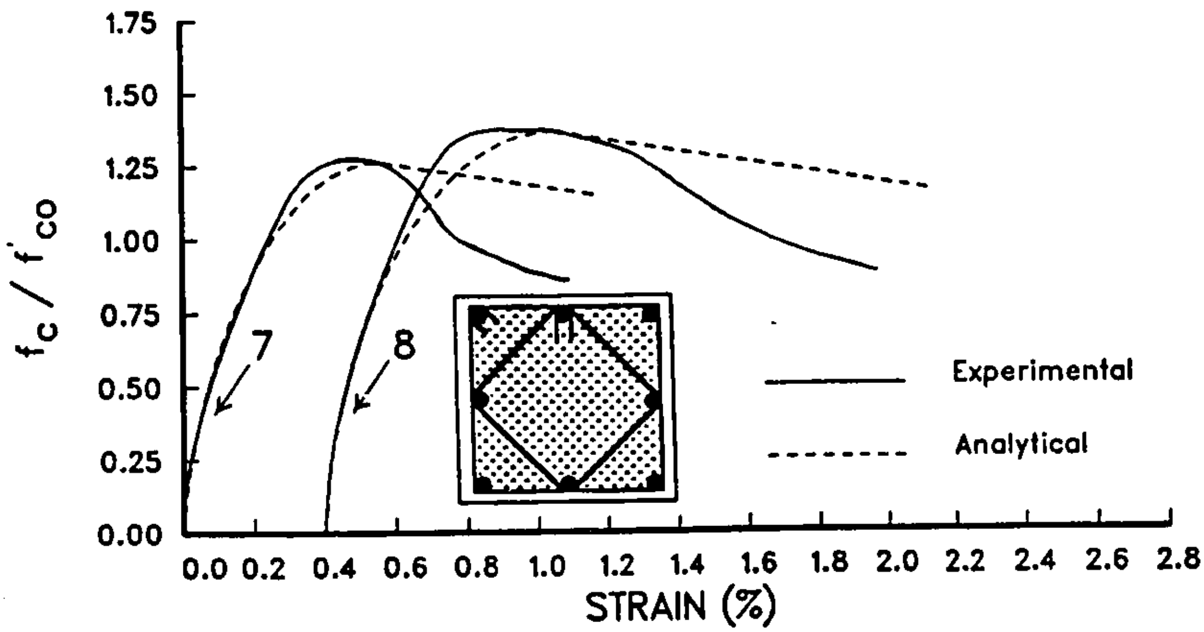

Figure 7.27: Square columns (5, 7, 8 and 11) tested by Sheikh and Uzumeri (1980).

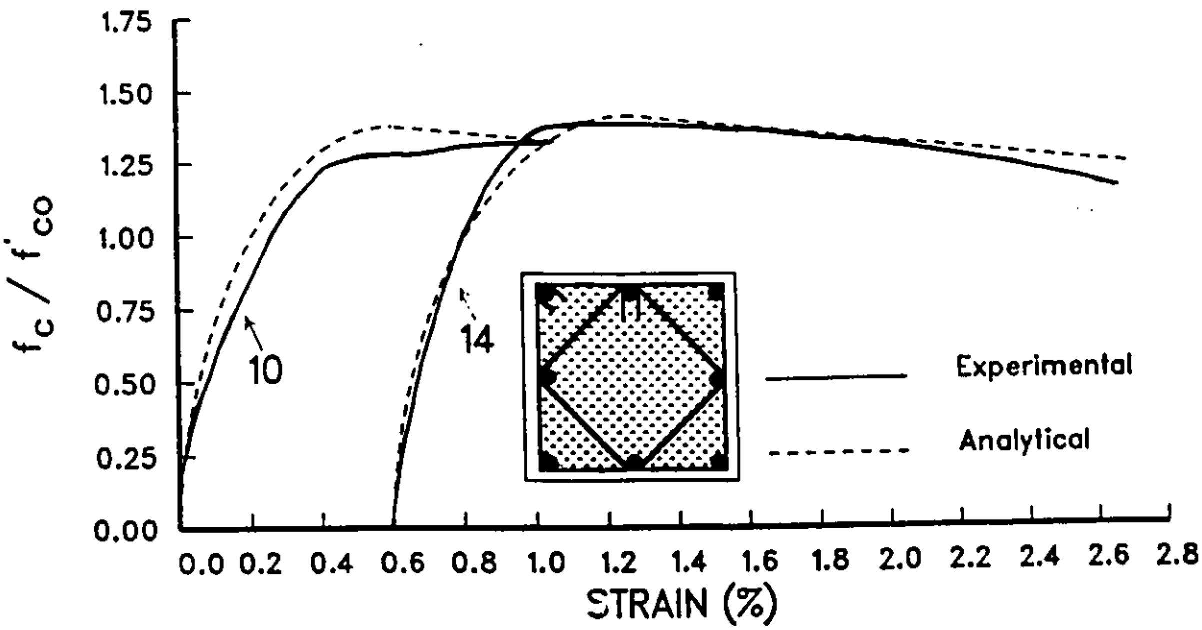

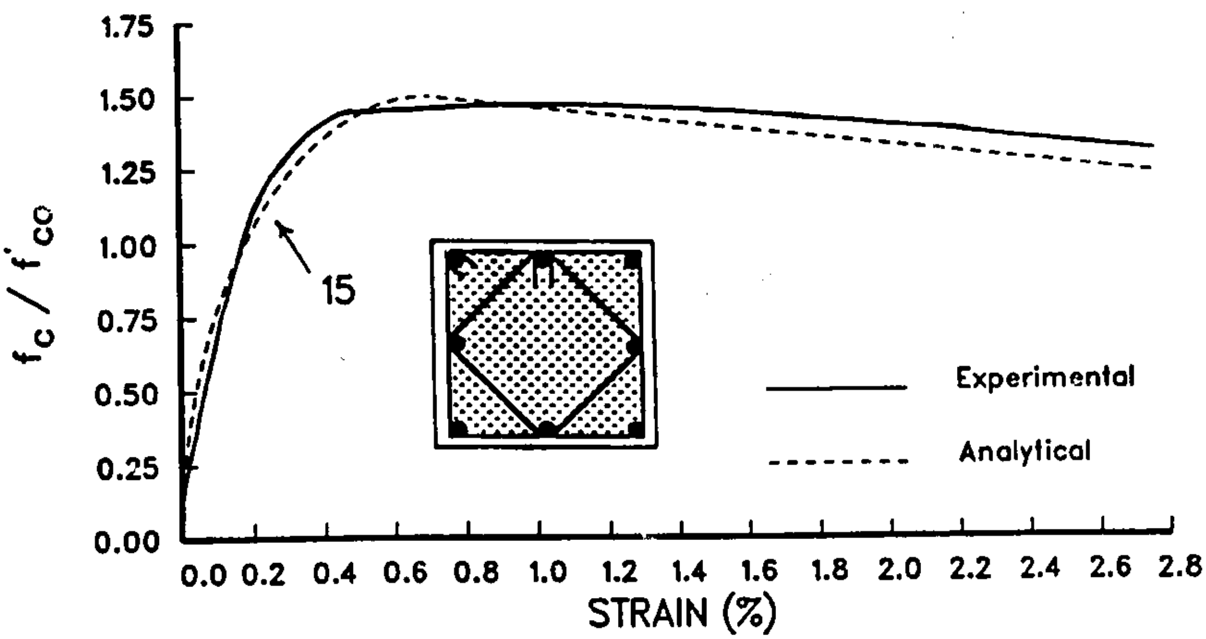

Figure 7.28: Square columns (10, 14 and 15) tested by Sheikh and Uzumeri (1980).

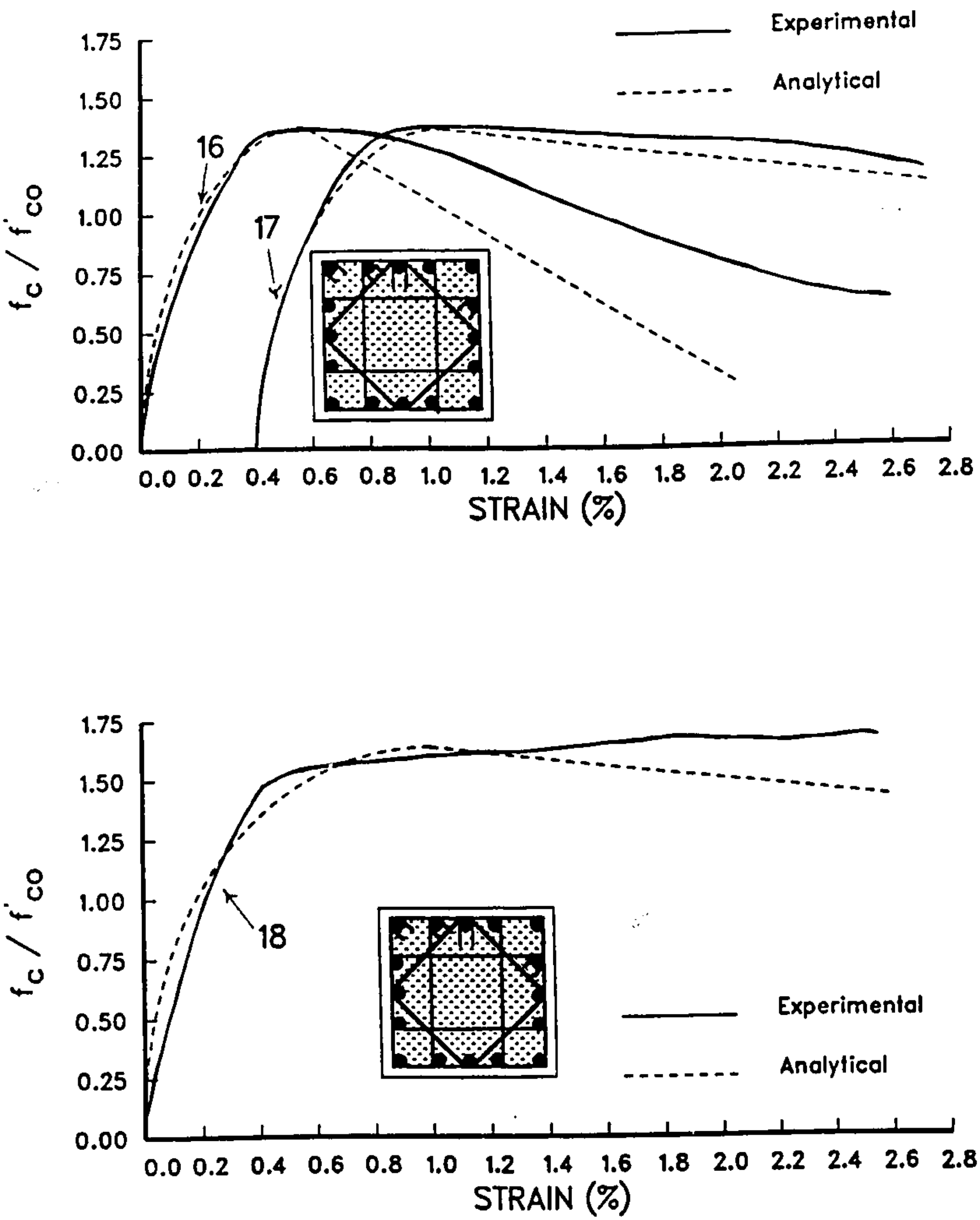

Figure 7.29: Square columns (16, 17 and 18) tested by Sheikh and Uzumeri (1980).

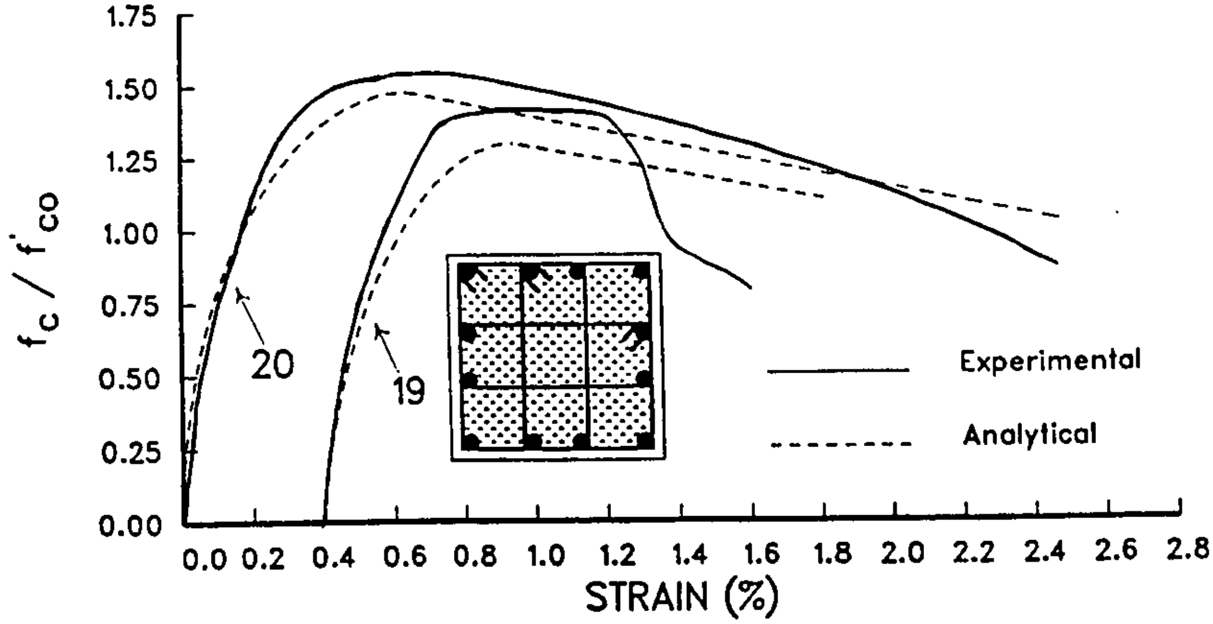

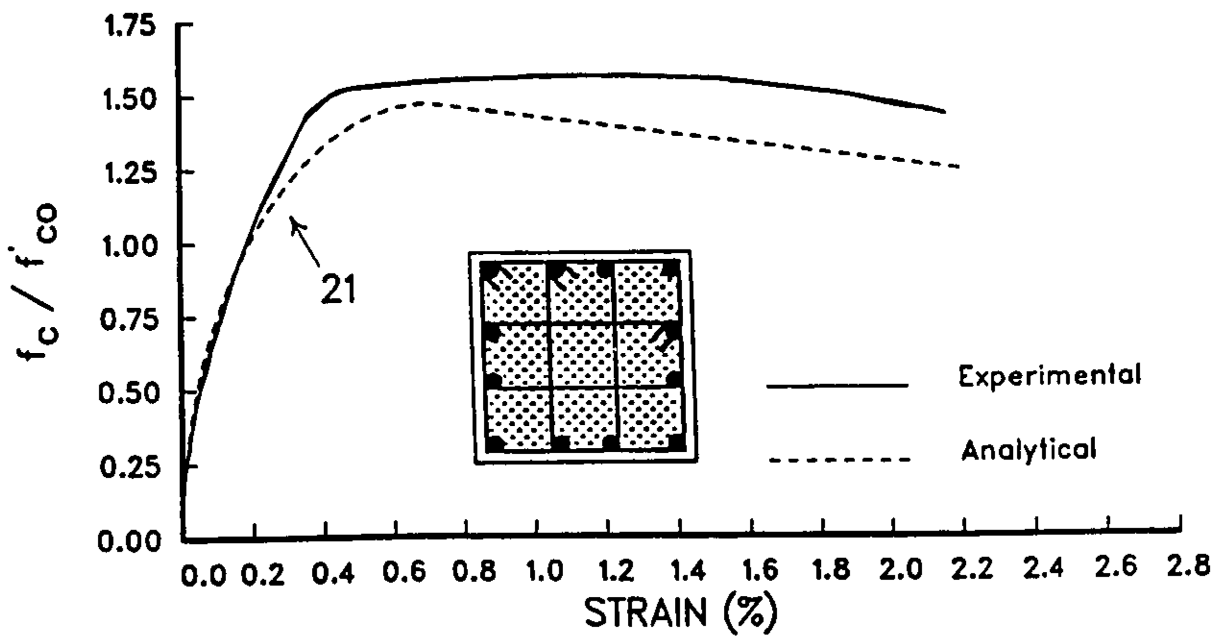

Figure 7.30: Square columns (19, 20 and 21) tested by Sheikh and Uzumeri (1980).

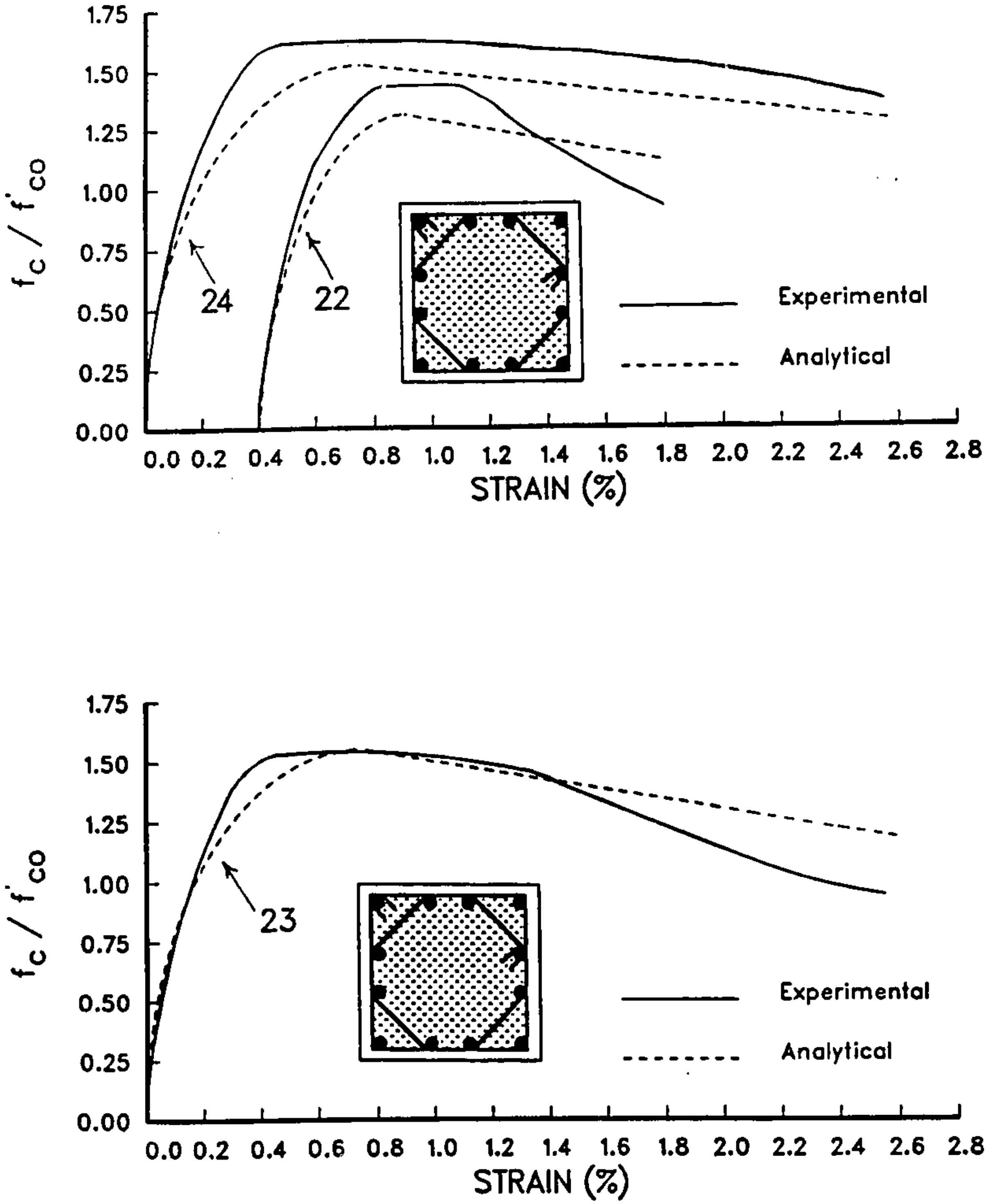

Figure 7.31: Square columns (23 and 24) tested by Sheikh and Uzumeri (1980).

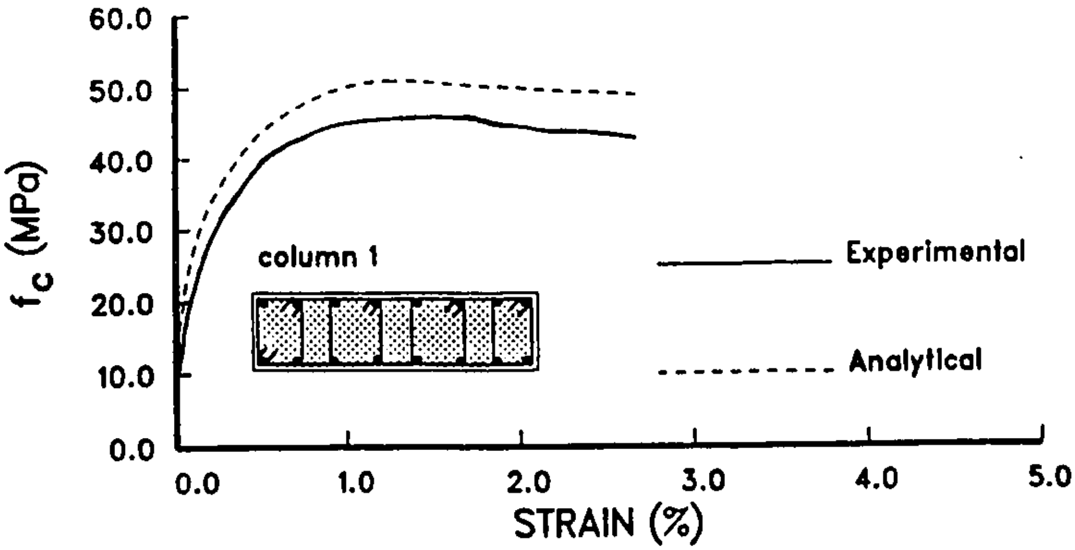

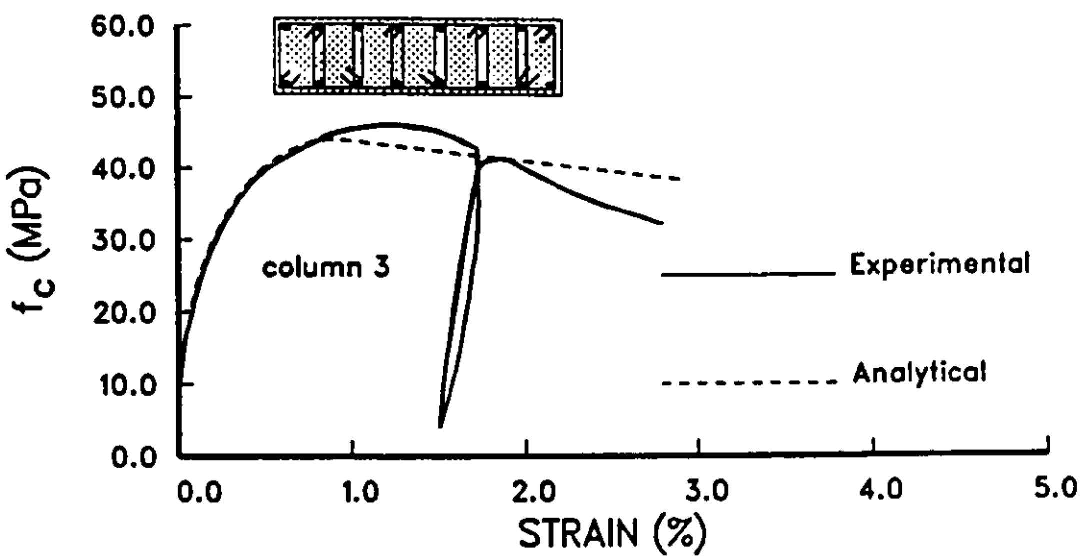

Figure 7.32: Rectangular columns (1 and 3) tested by Mander et al. (1988).

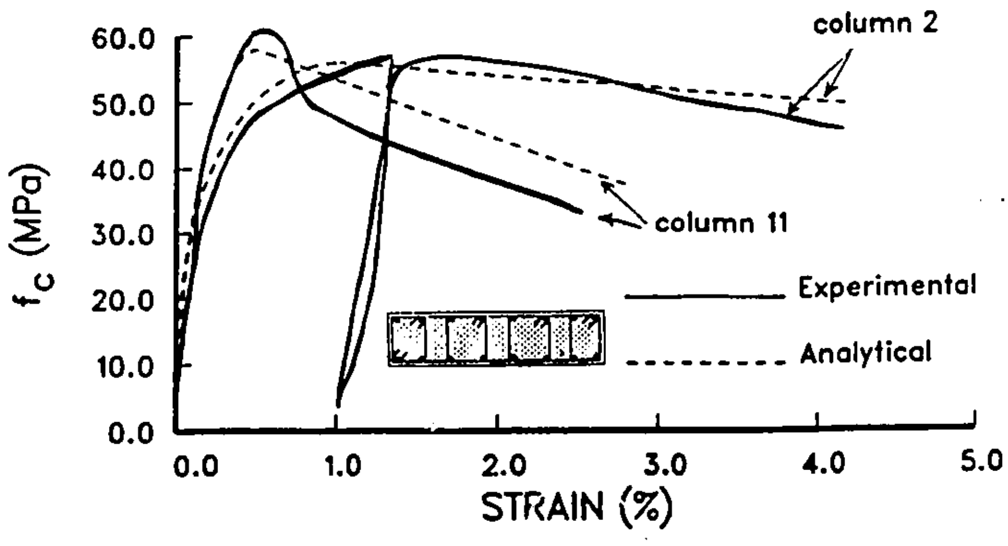

Figure 7.33: Rectangular columns (2 and 11) tested by Mander et al. (1988) under a high strain rate of 0.0167/sec.

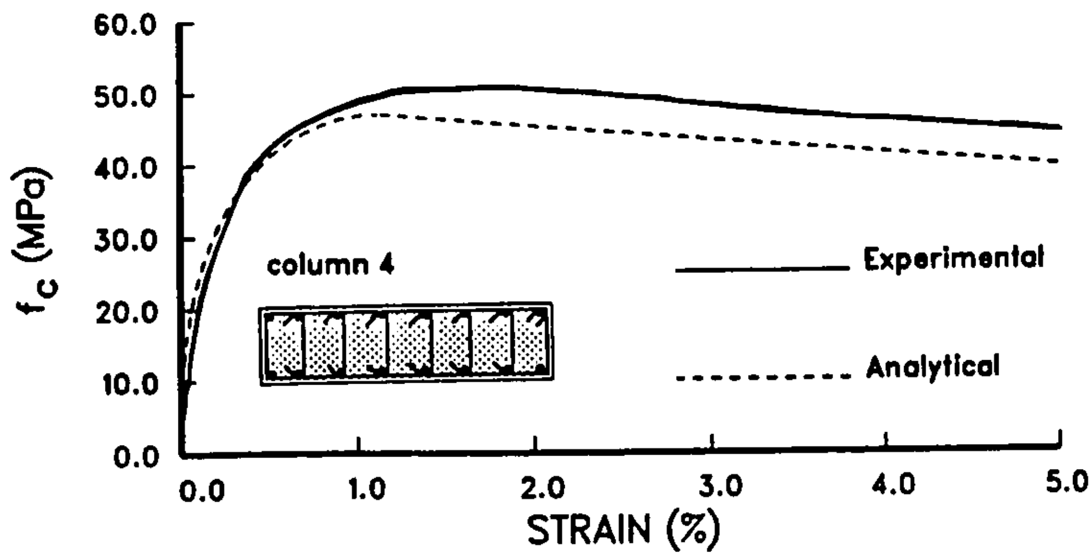

Figure 7.34: A rectangular columns (4) tested by Mander et al. (1988).

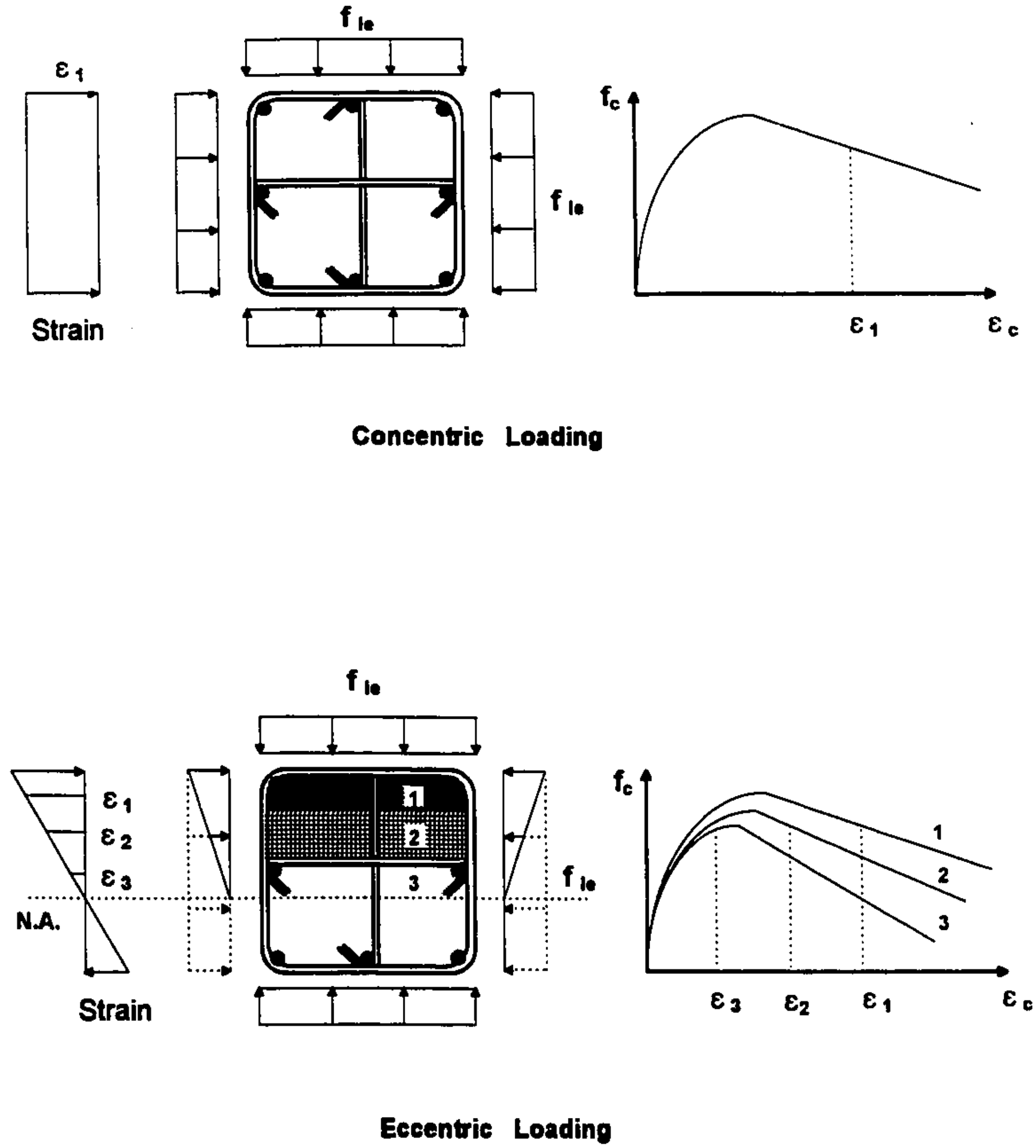

Figure 7.35: Equivalent lateral pressure and corresponding stress-strain relationships for concentric and eccentric loads.

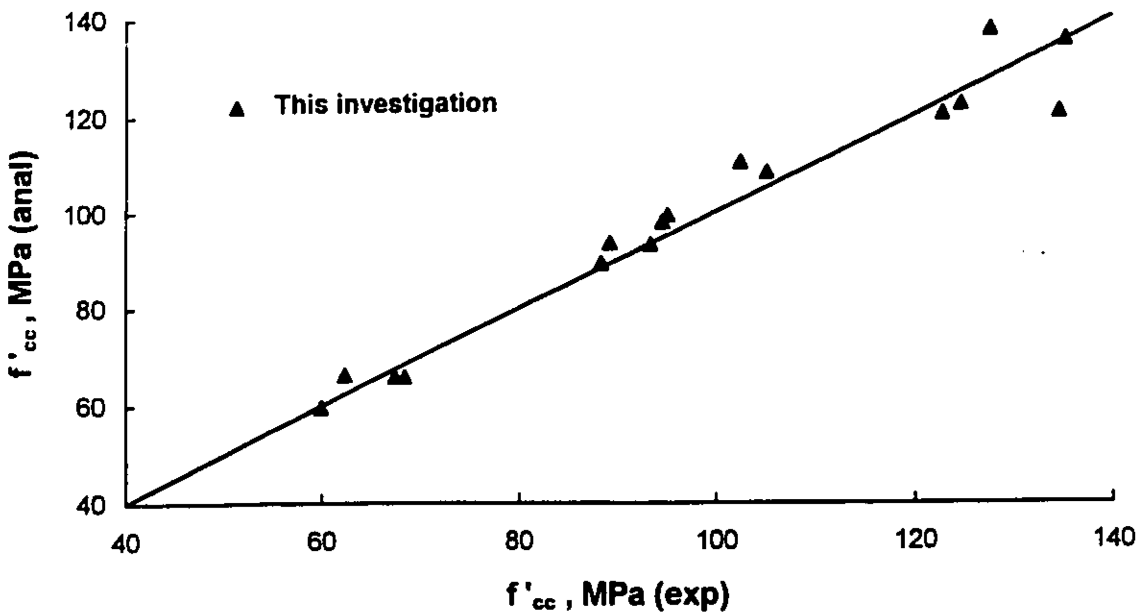

Figure 7.36: Comparison of analytical and experimental strength values for confined high strength concrete in circular columns tested in this investigation.

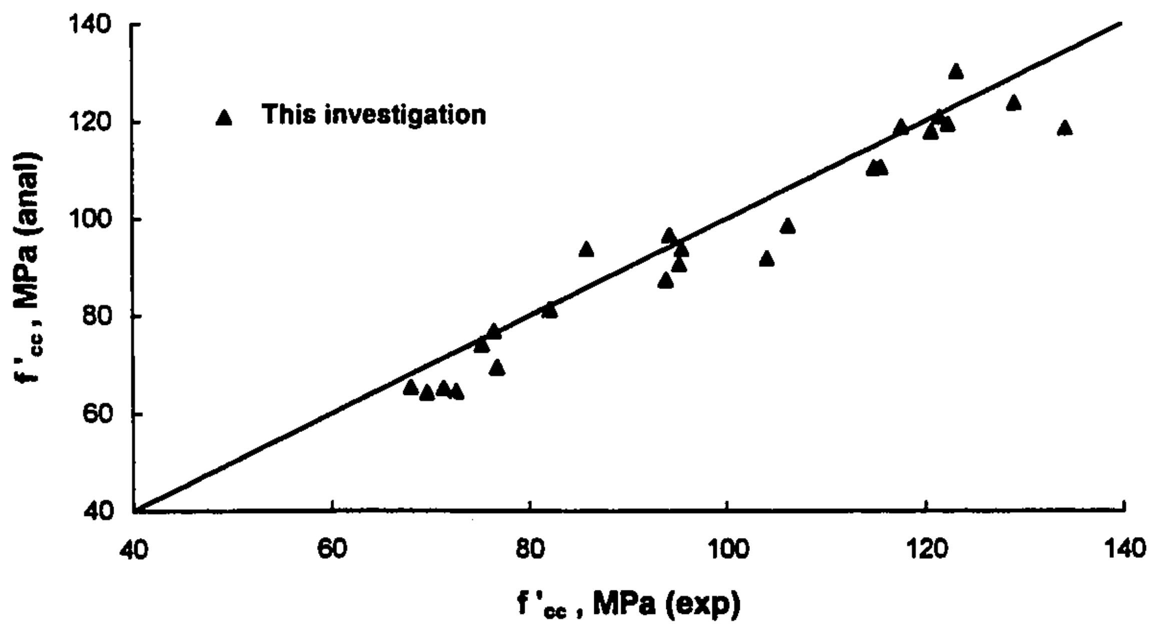

Figure 7.37: Comparison of analytical and experimental strength values for confined high strength concrete in square columns tested in this investigation.

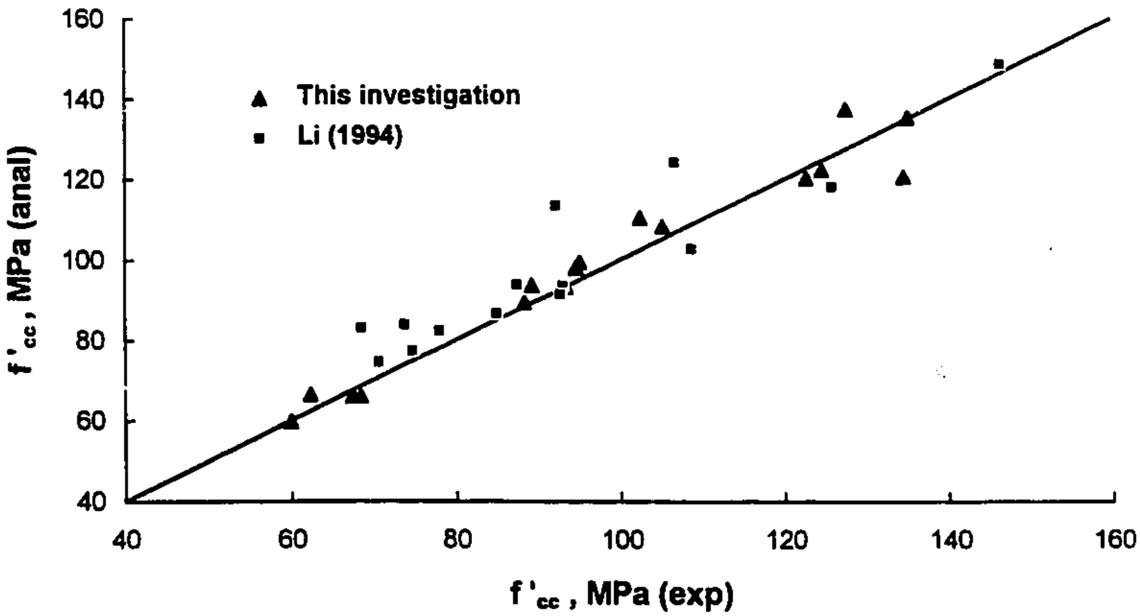

Figure 7.38: Comparison of analytical and experimental strength values for confined high strength concrete in circular columns including those tested by others.

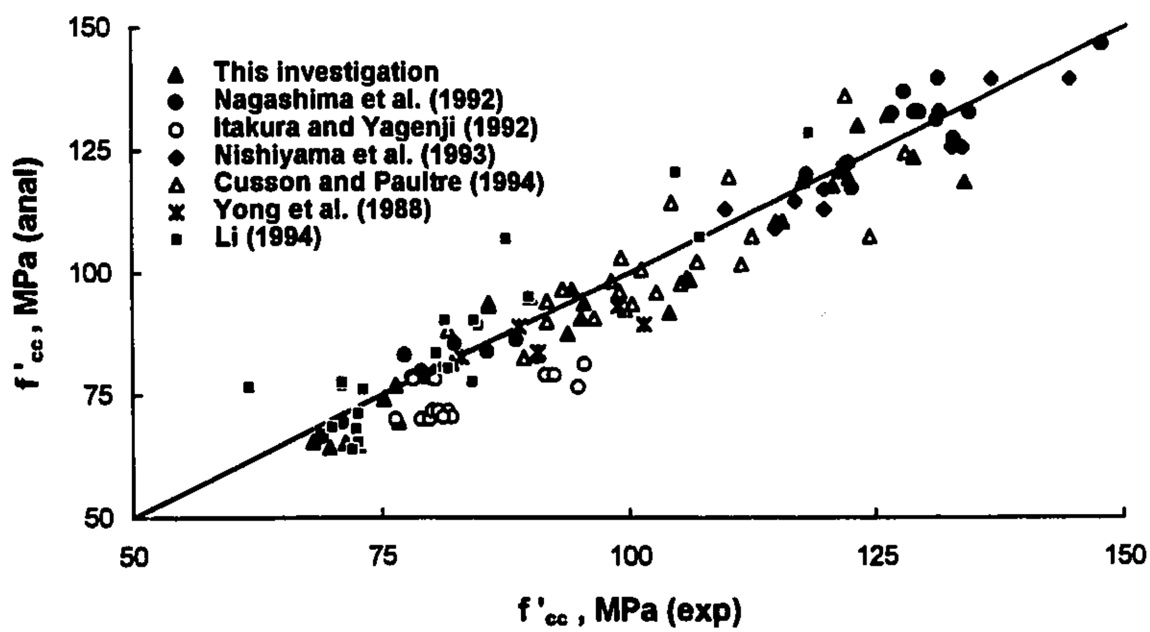

Figure 7.39: Comparison of analytical and experimental strength values for confined high strength concrete in square columns including those tested by others.

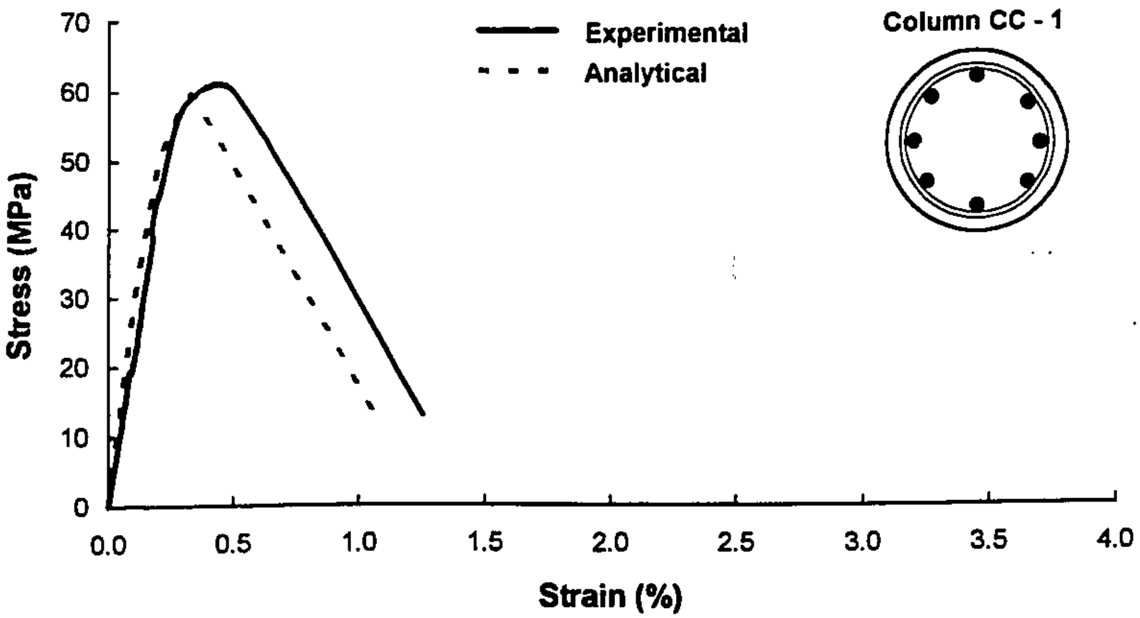

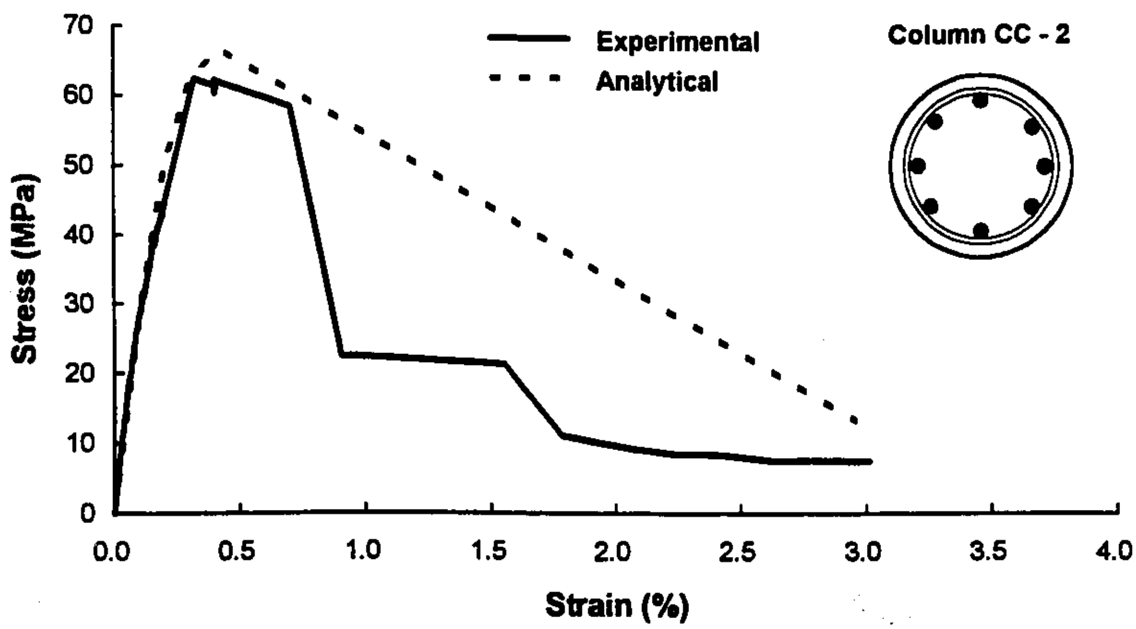

Figure 7.40: Circular columns (CC-1 and CC-2) tested in this investigation.

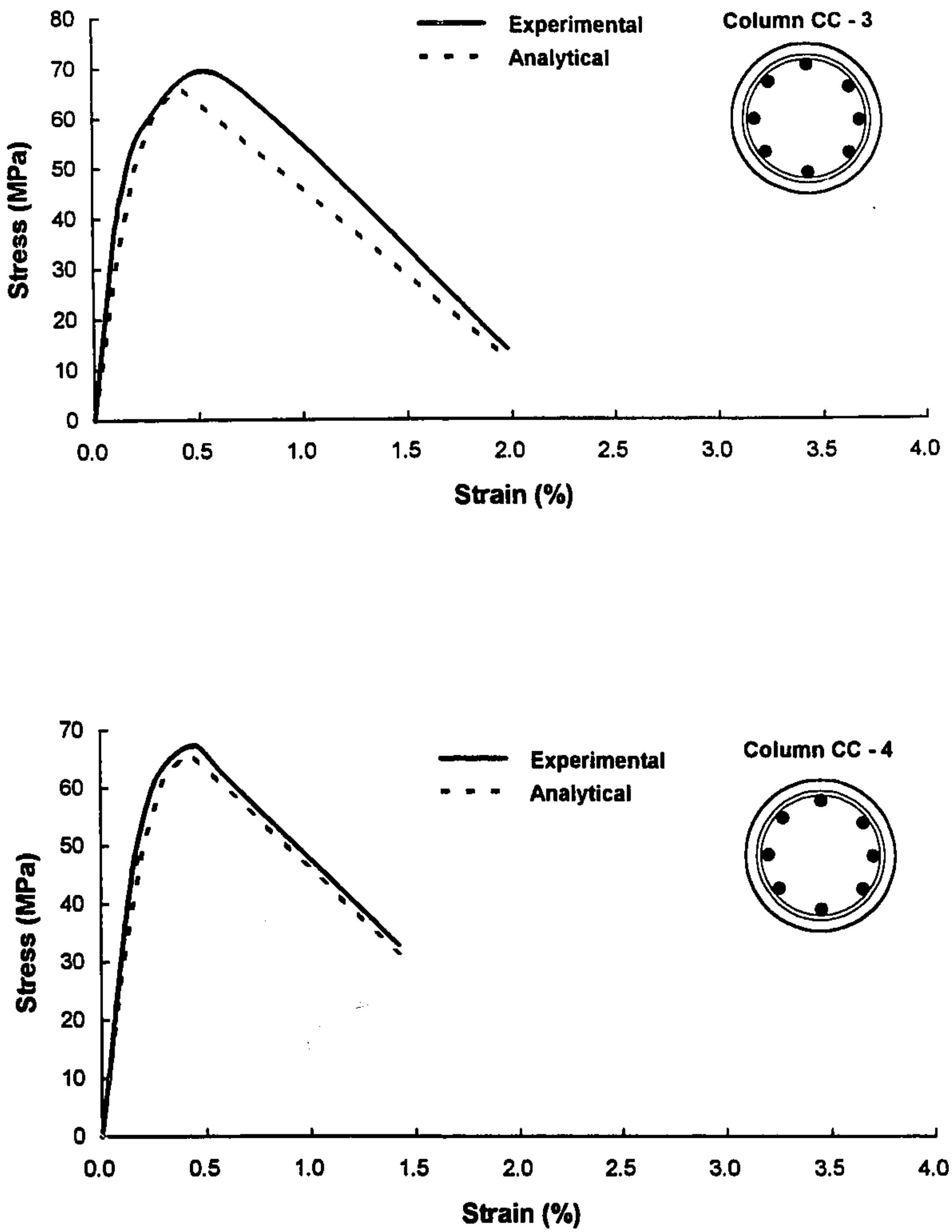

Figure 7.41: Circular columns (CC-3 and CC-4) tested in this investigation.

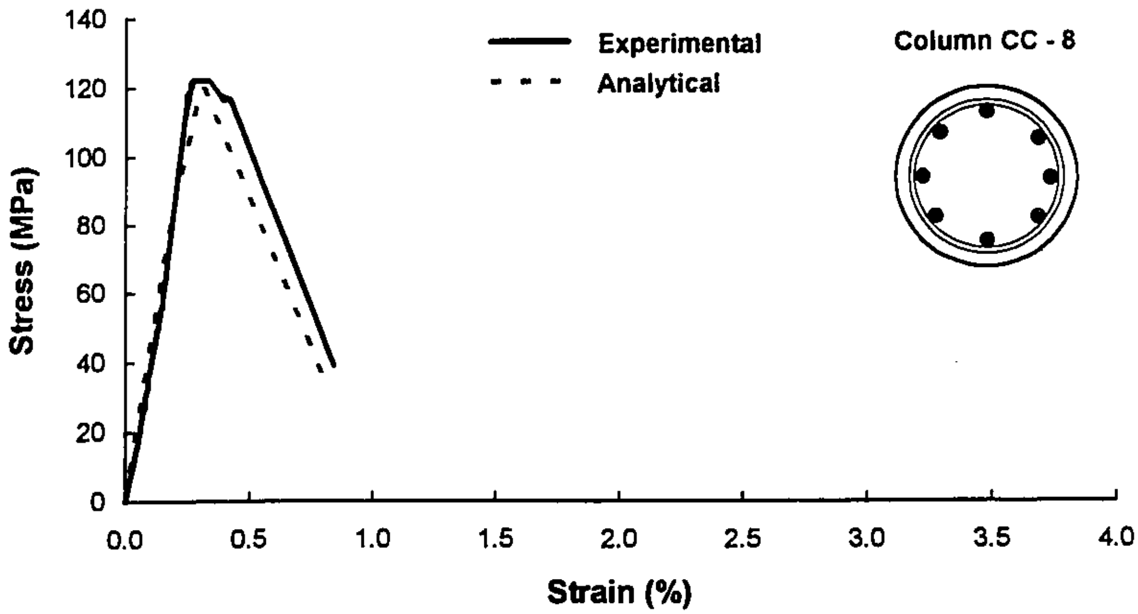

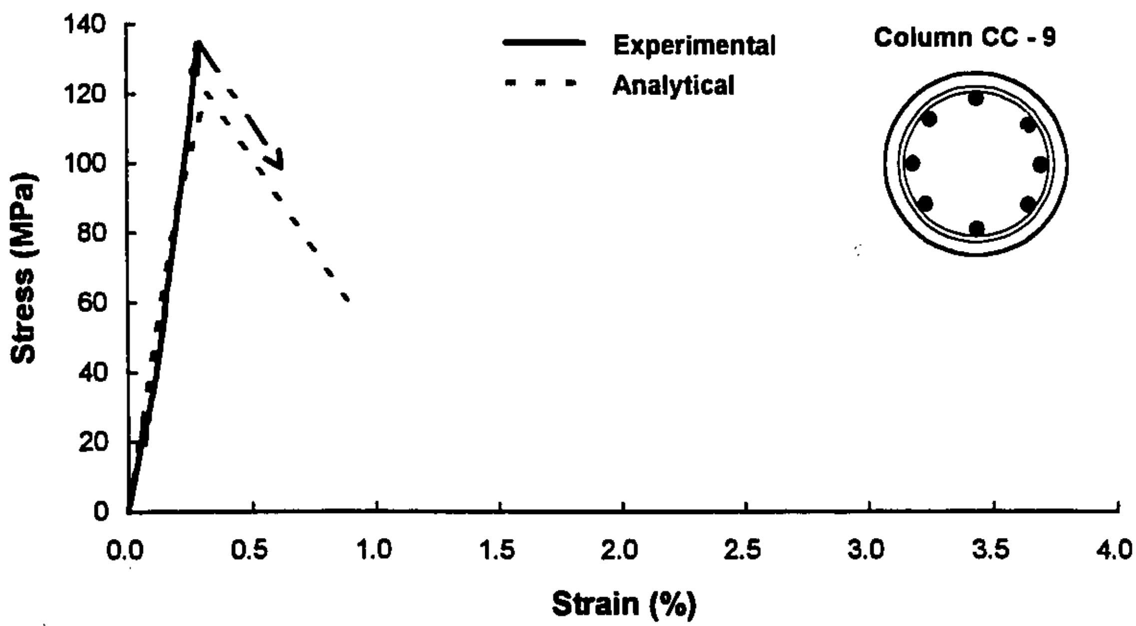

Figure 7.42: Circular columns (CC-8 and CC-9) tested in this investigation.

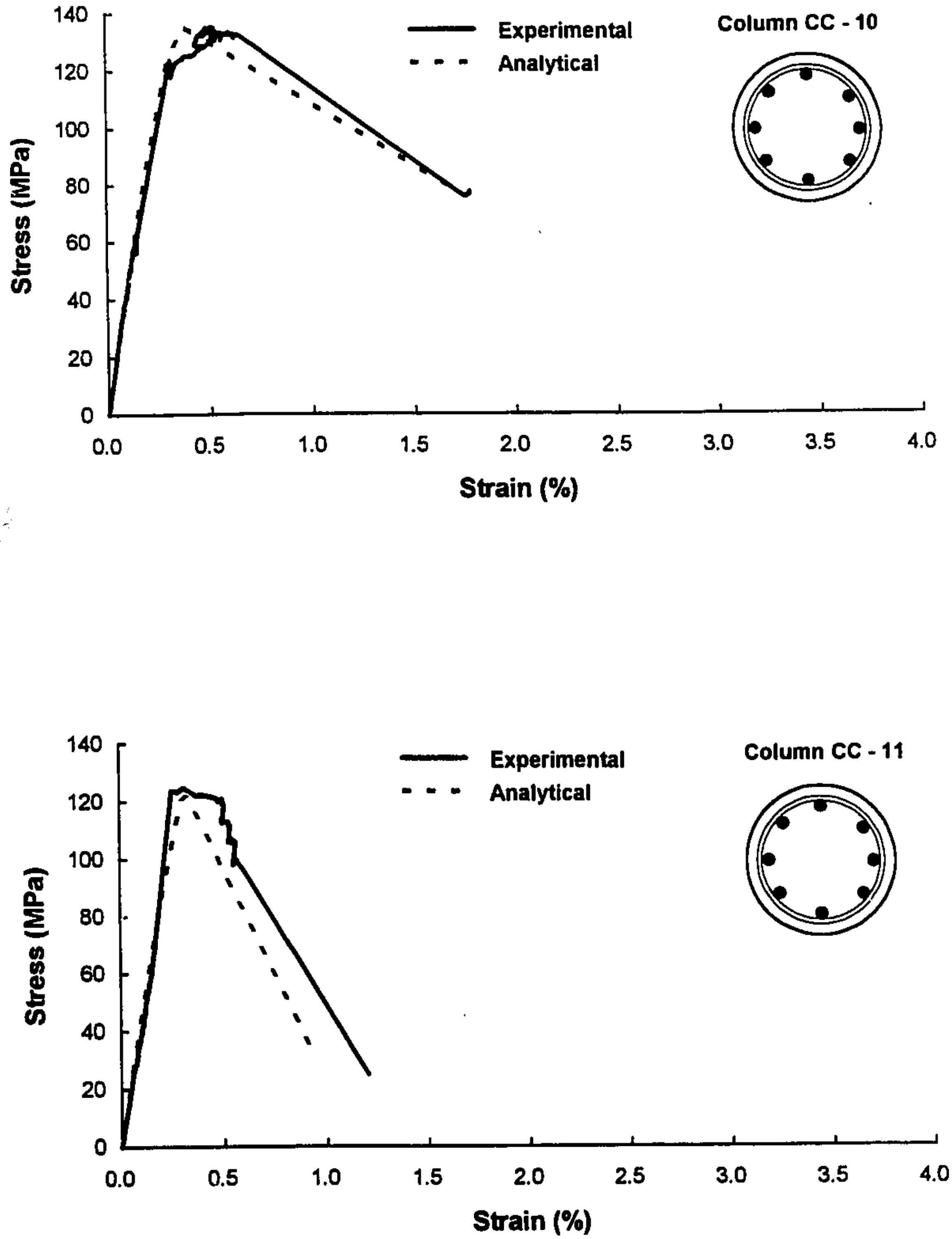

Figure 7.43: Circular columns (CC-10 and CC-11) tested in this investigation.

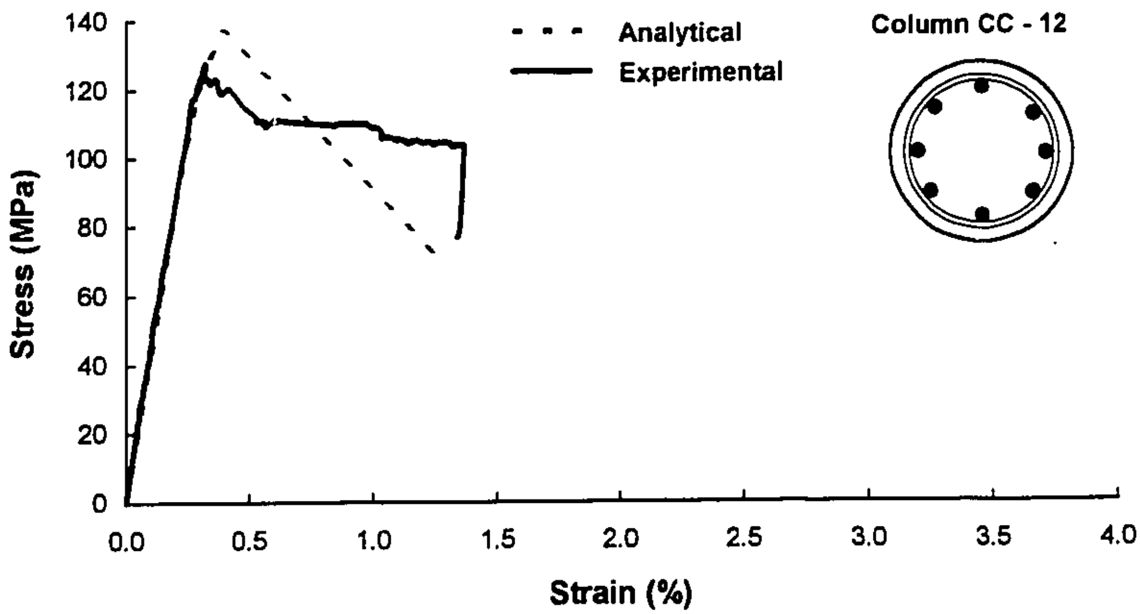

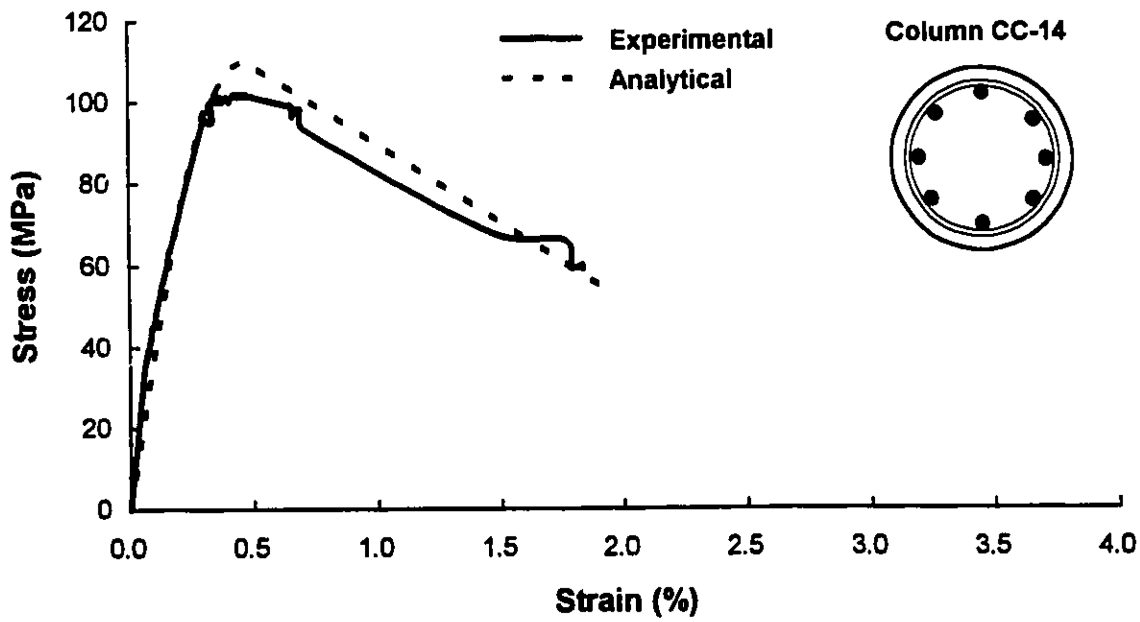

Figure 7.44: Circular columns (CC-12 and CC-14) tested in this investigation.

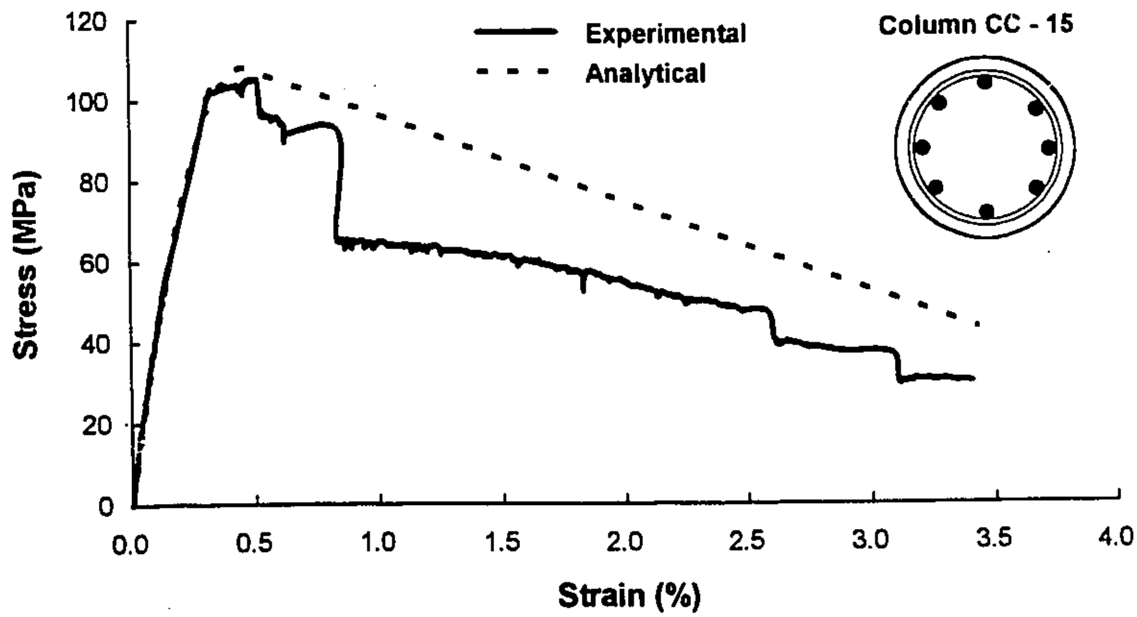

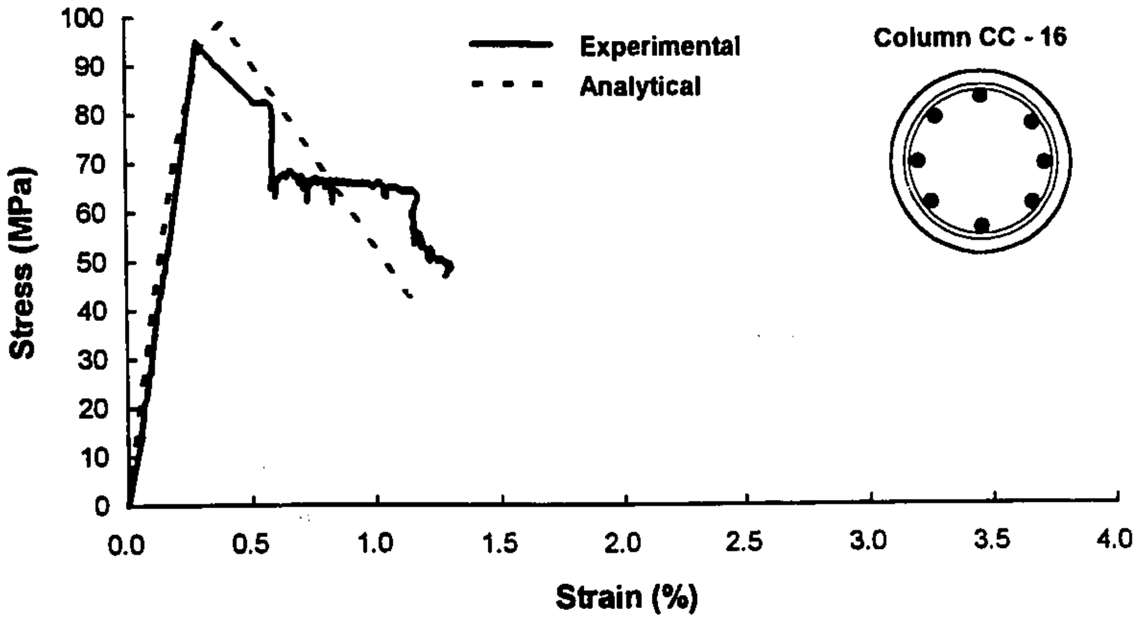

Figure 7.45: Circular columns (CC-15 and CC-16) tested in this investigation.

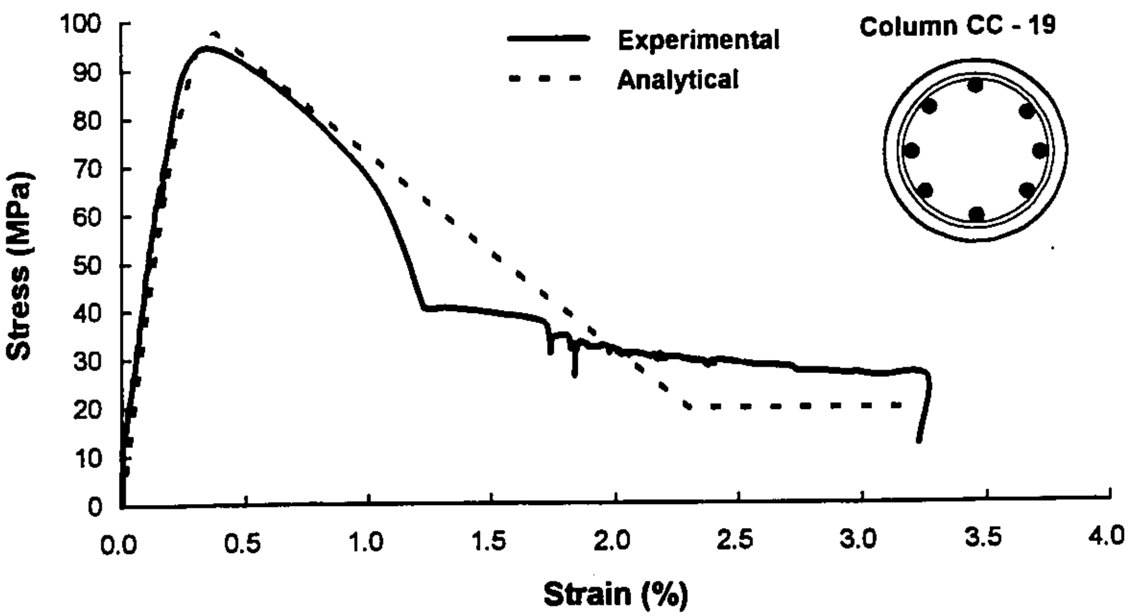

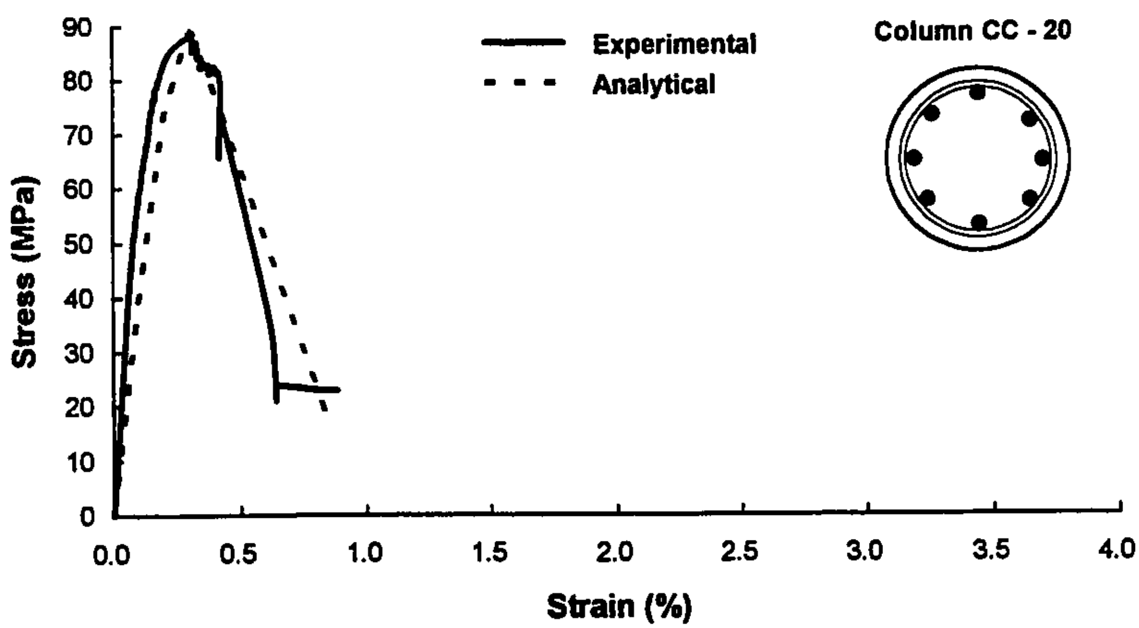

Figure 7.46: Circular columns (CC-19 and CC-20) tested in this investigation.

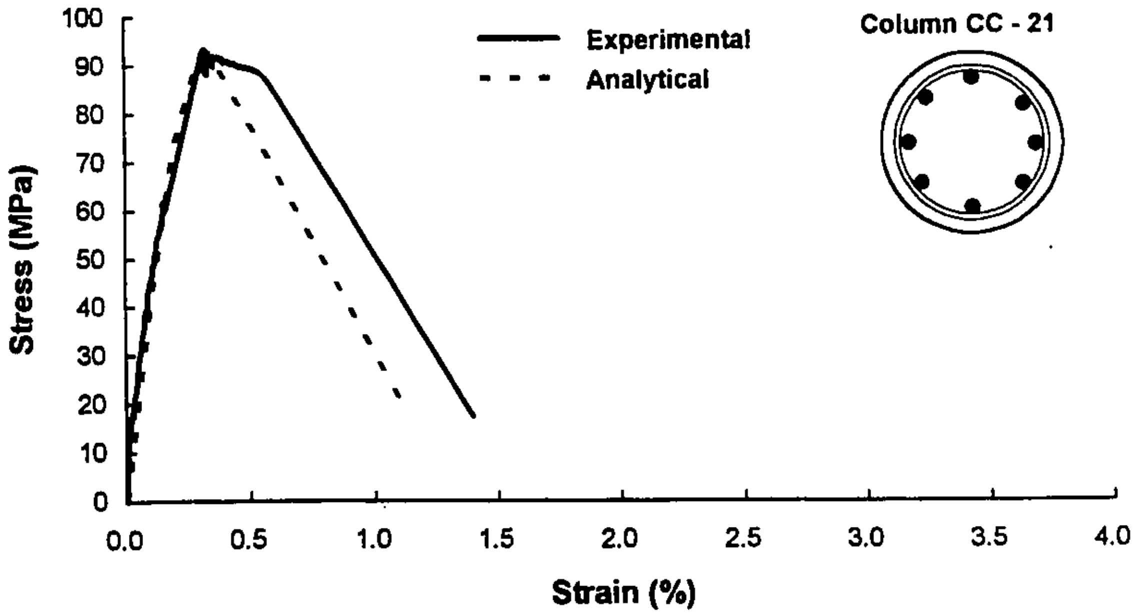

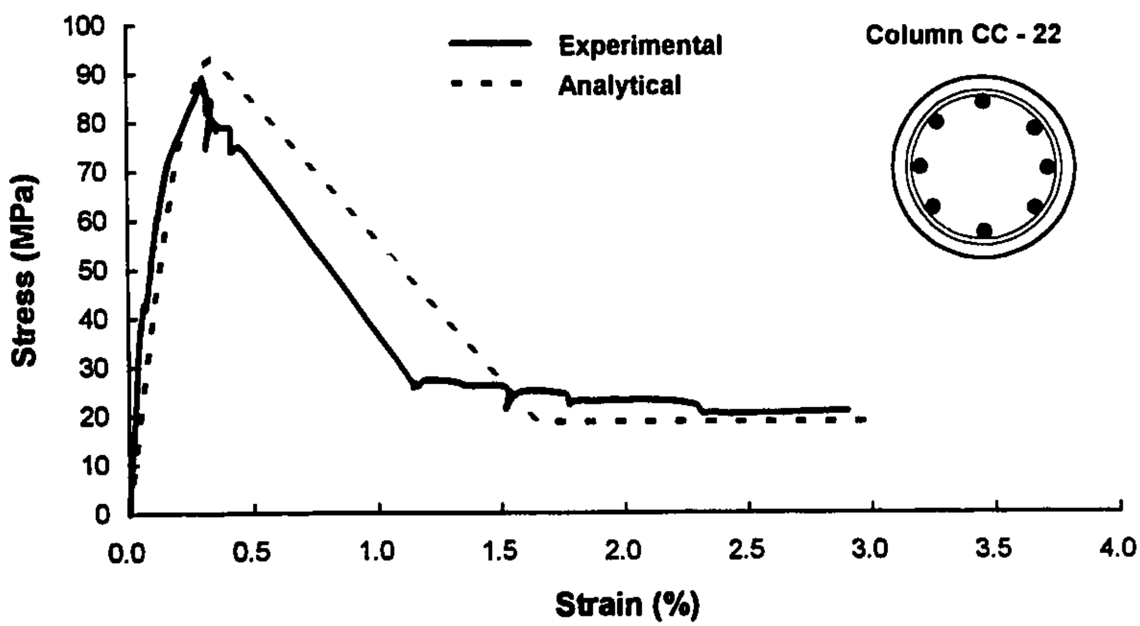

Figure 7.47: Circular columns (CC-21 and CC-22) tested in this investigation.

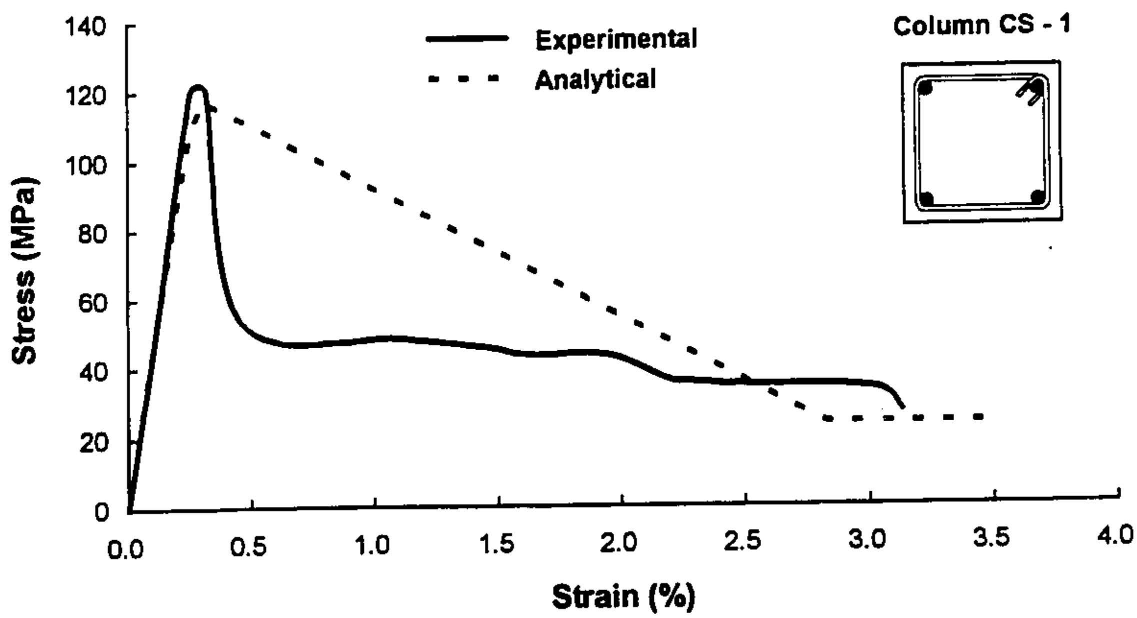

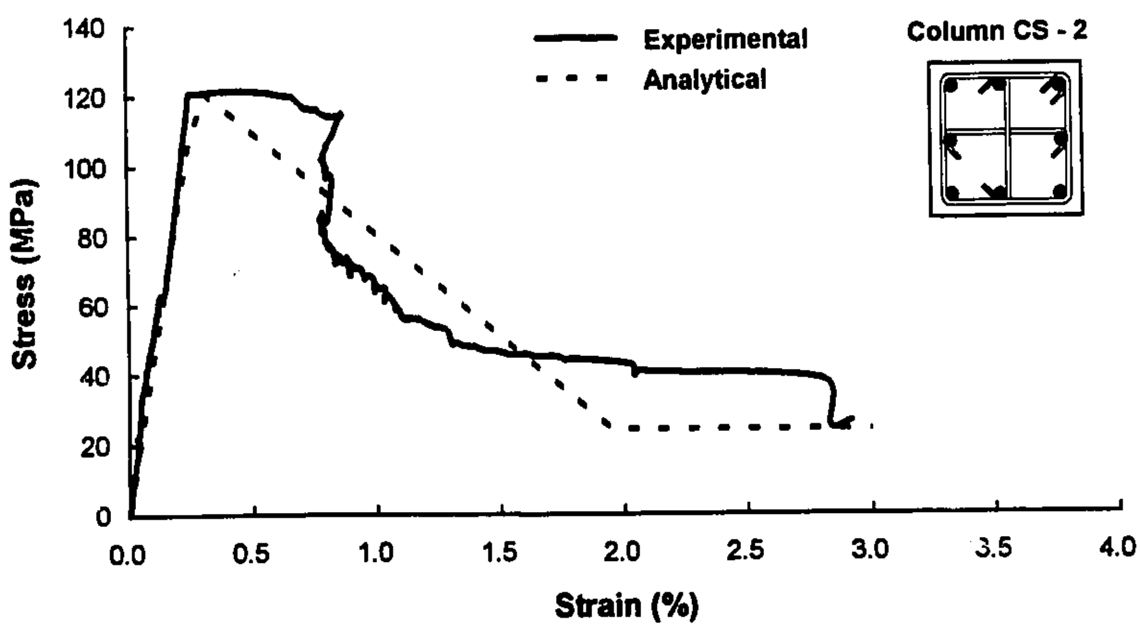

Figure 7.48: Square columns (CS-1 and CS-2) tested in this investigation.

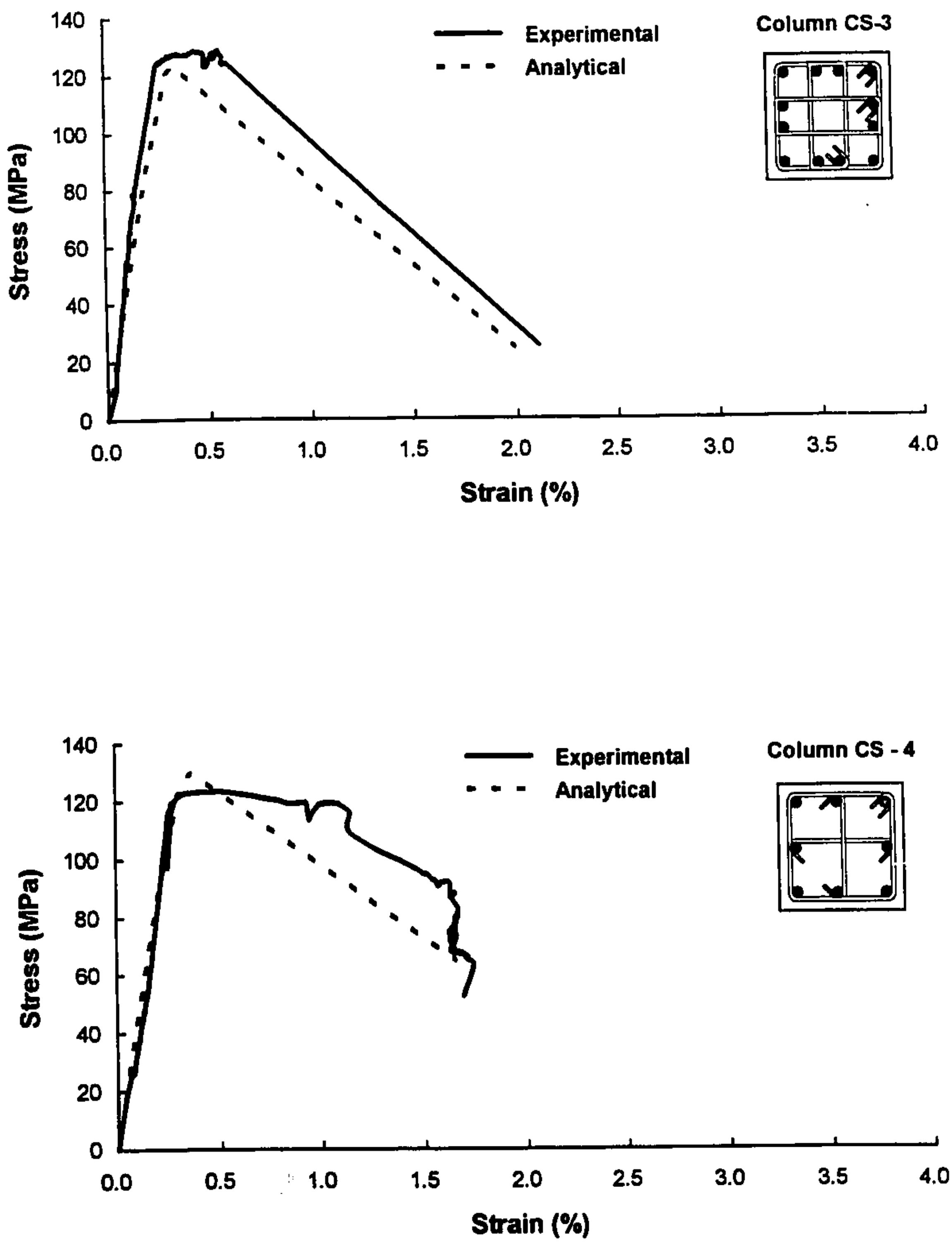

Figure 7.49: Square columns (CS-3 and CS-4) tested in this investigation.

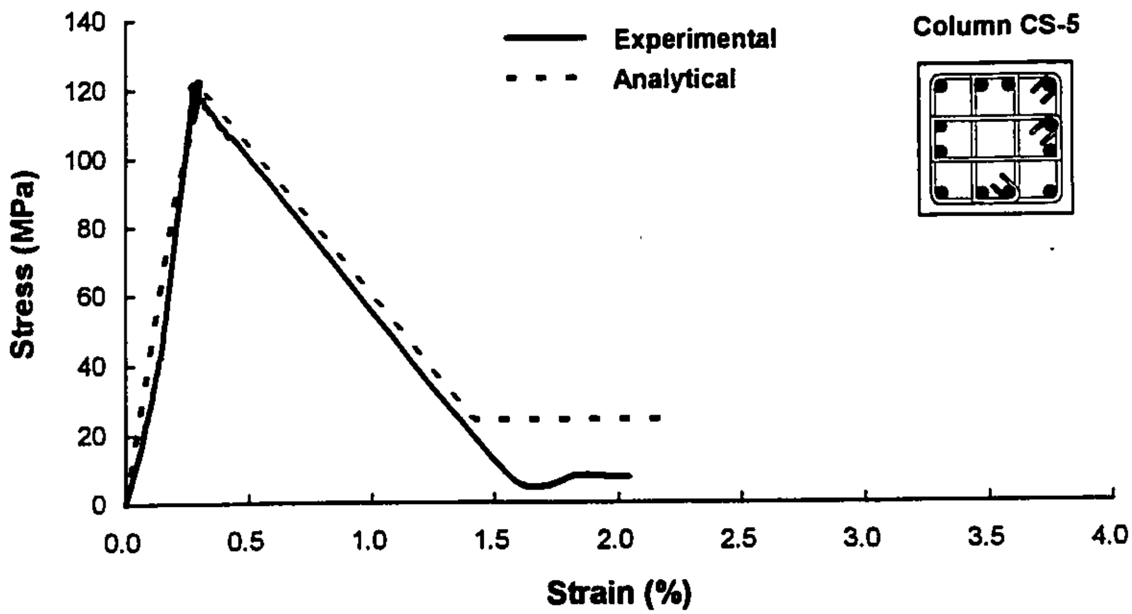

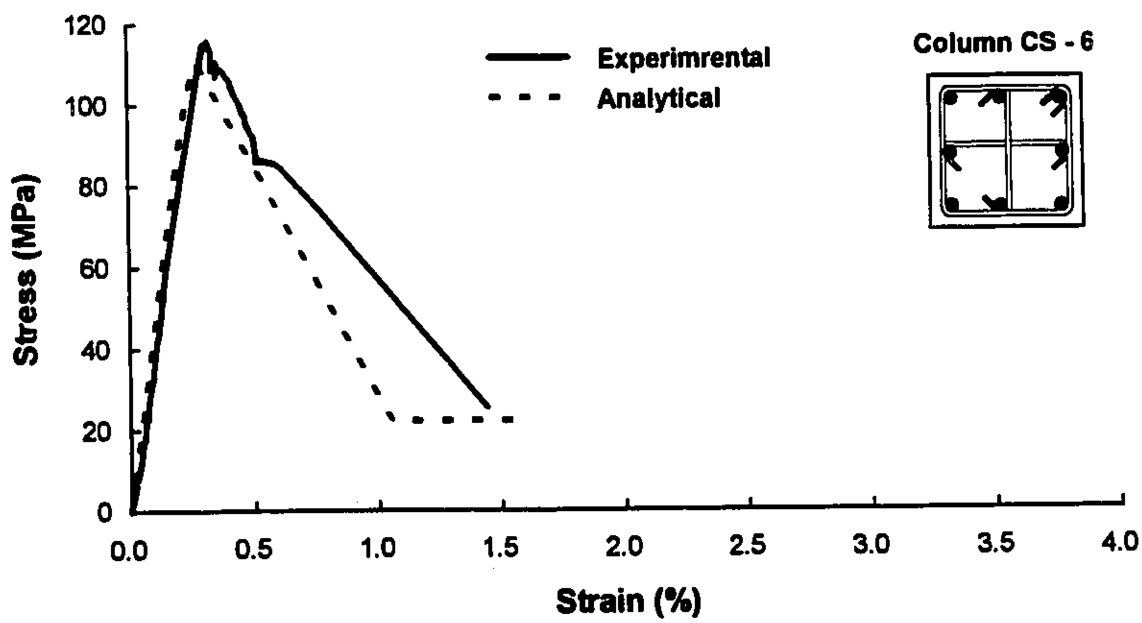

Figure 7.50: Square columns (CS-5 and CS-6) tested in this investigation.

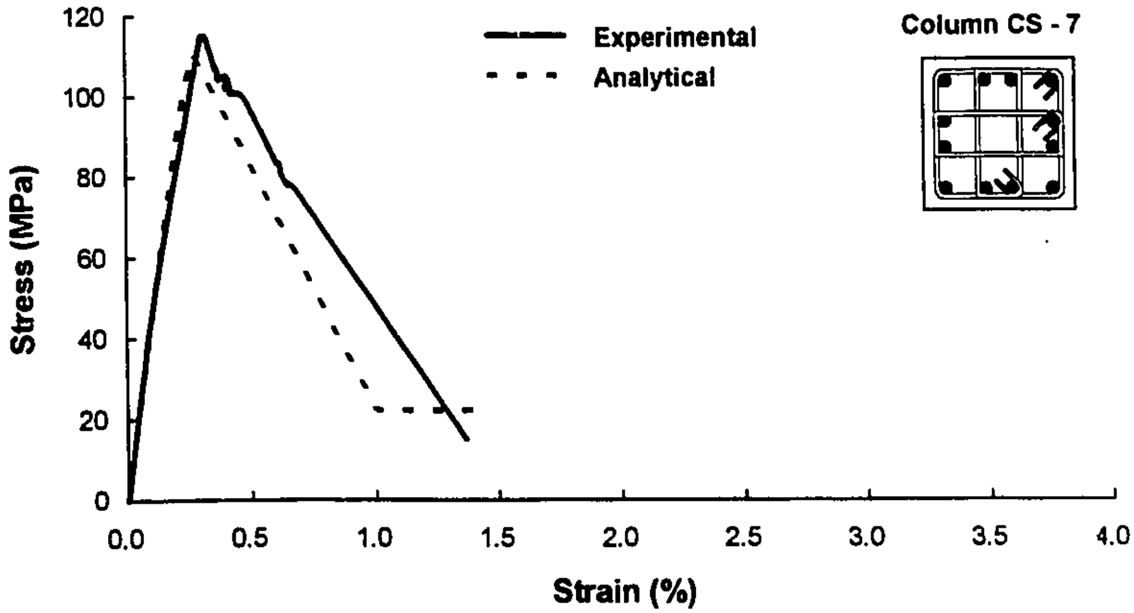

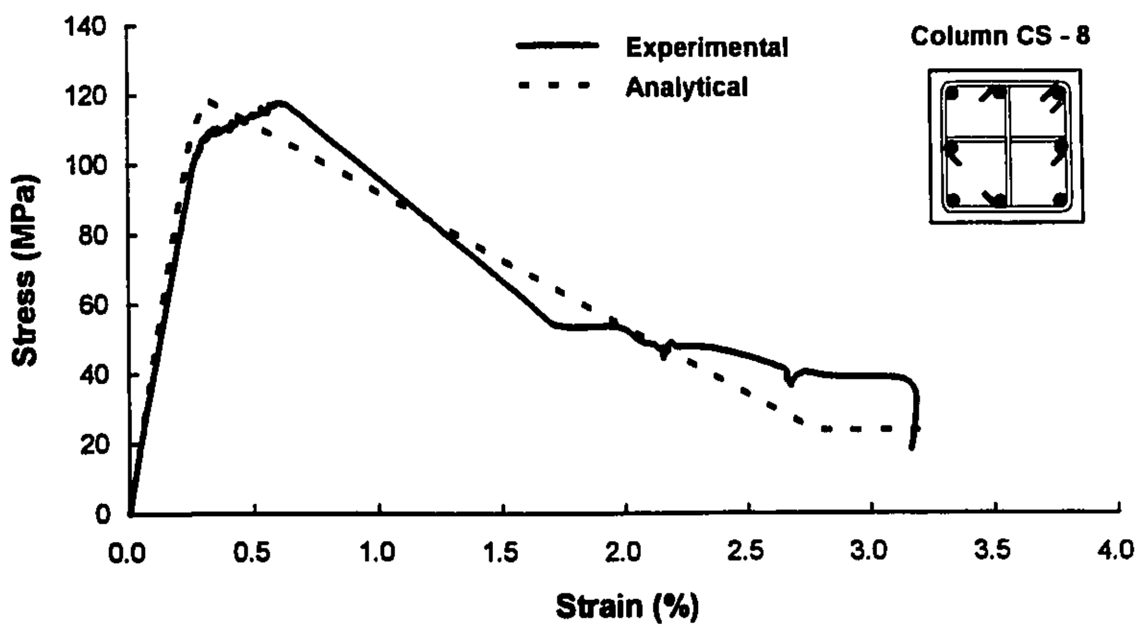

Figure 7.51: Square columns (CS-7 and CS-8) tested in this investigation.

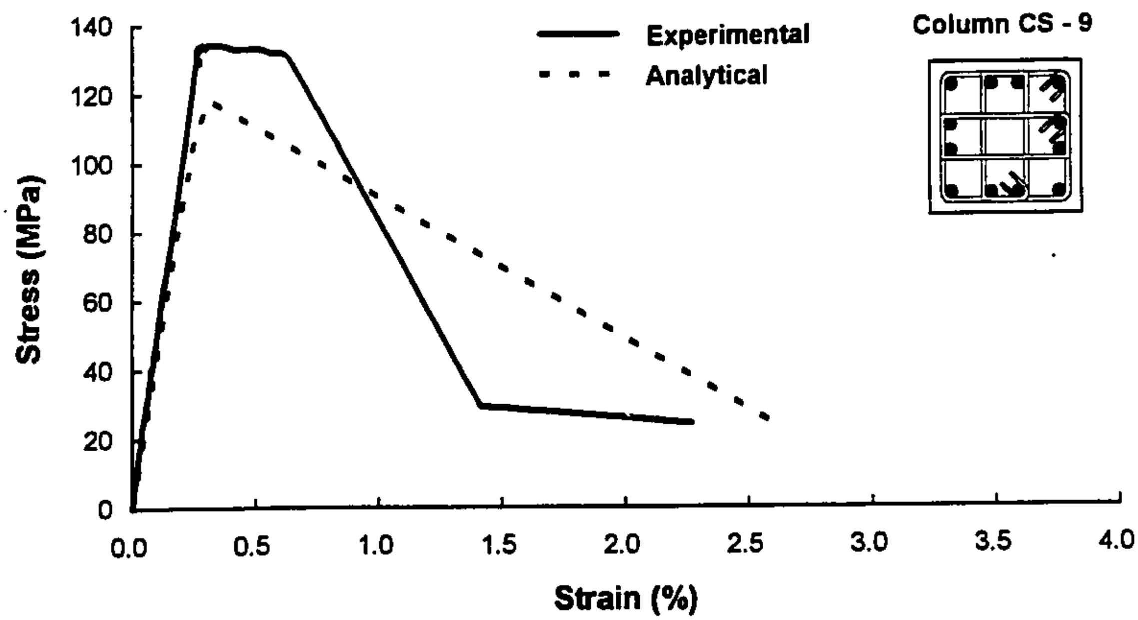

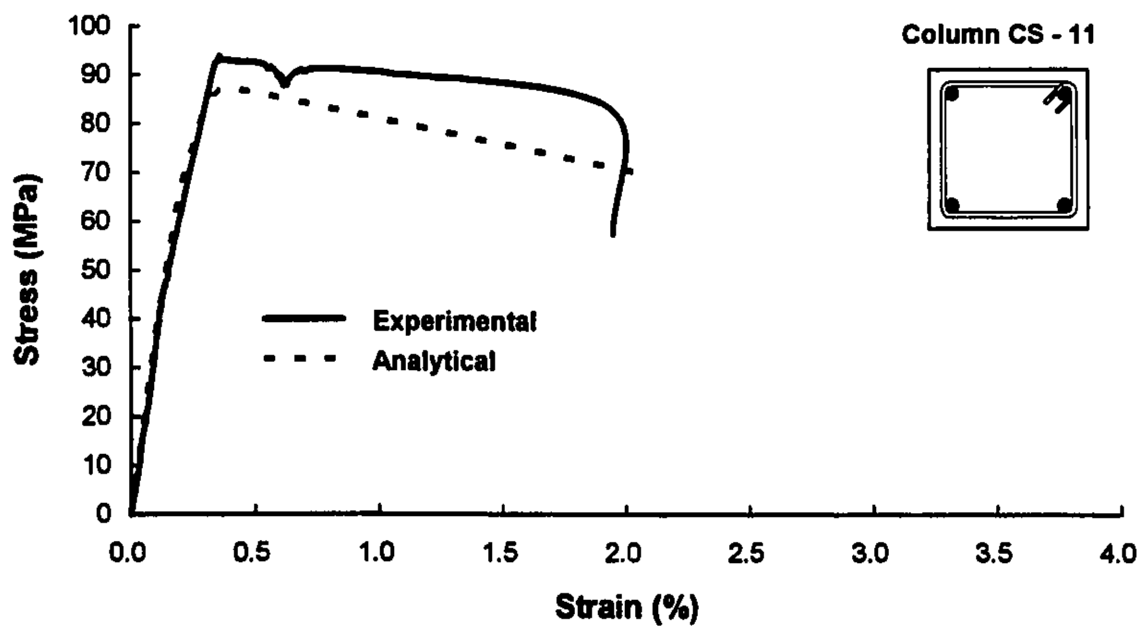

Figure 7.52: Square columns (CS-9 and CS-11) tested in this investigation.

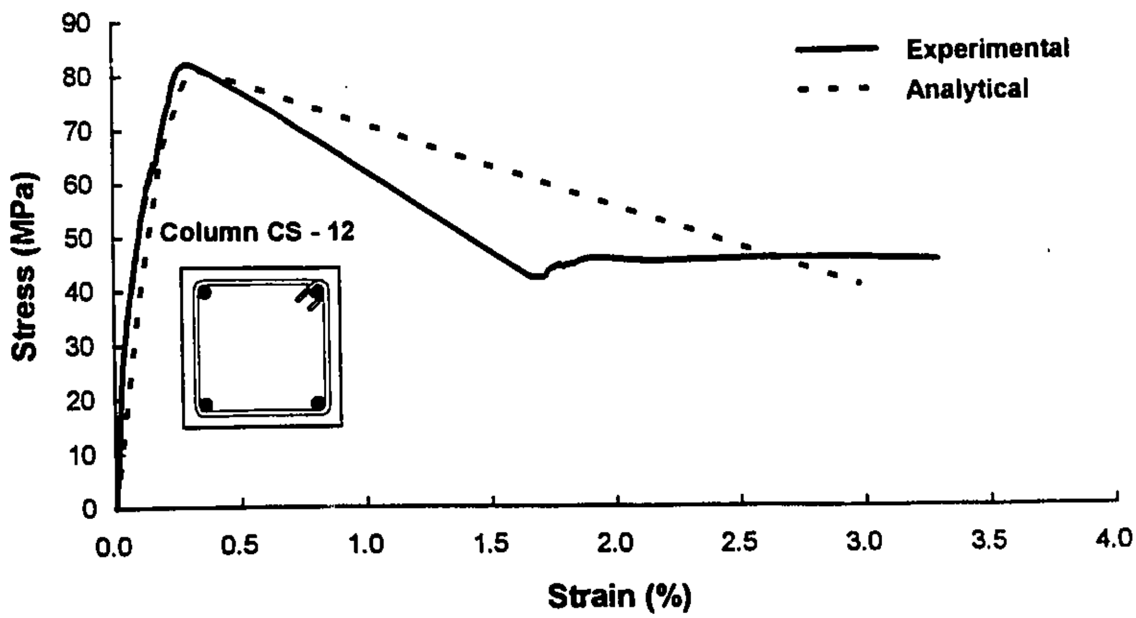

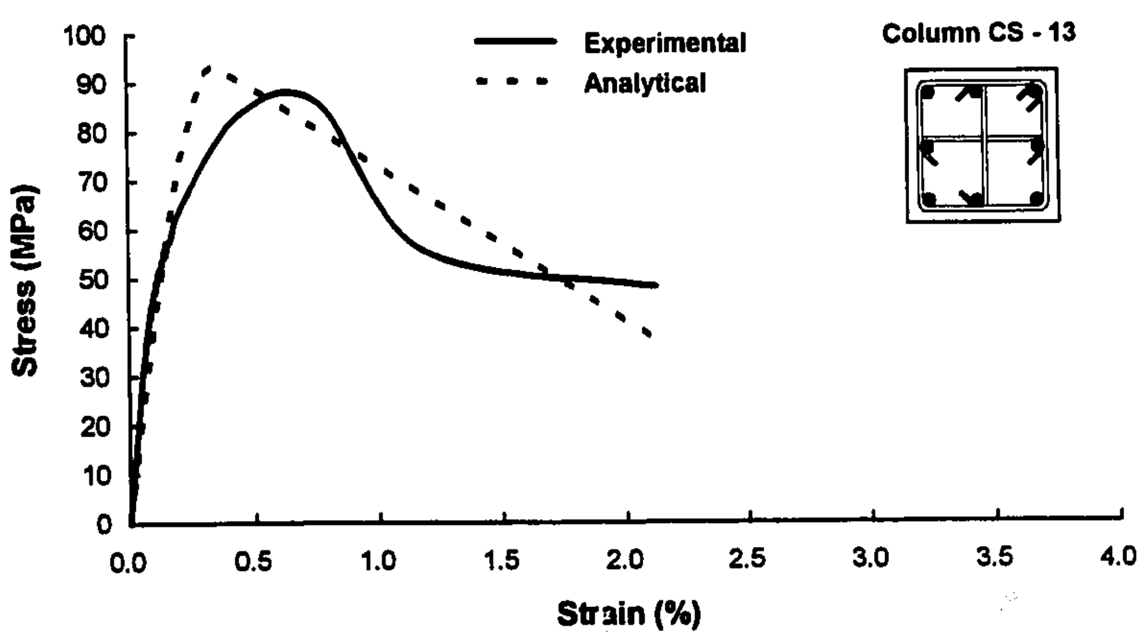

Figure 7.53: Square columns (CS-12 and CS-13) tested in this investigation.

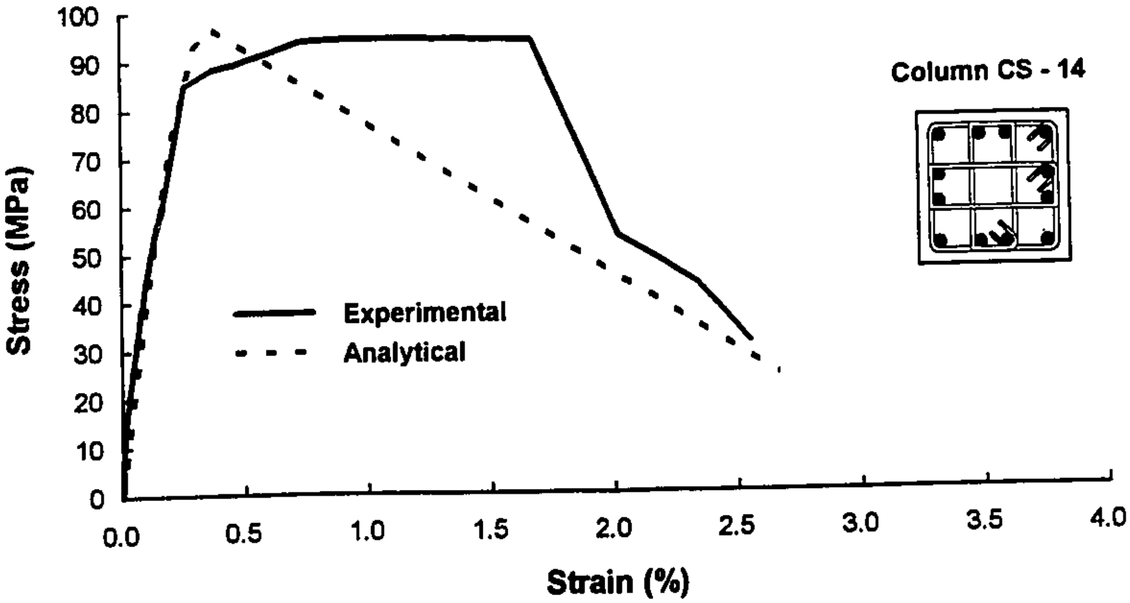

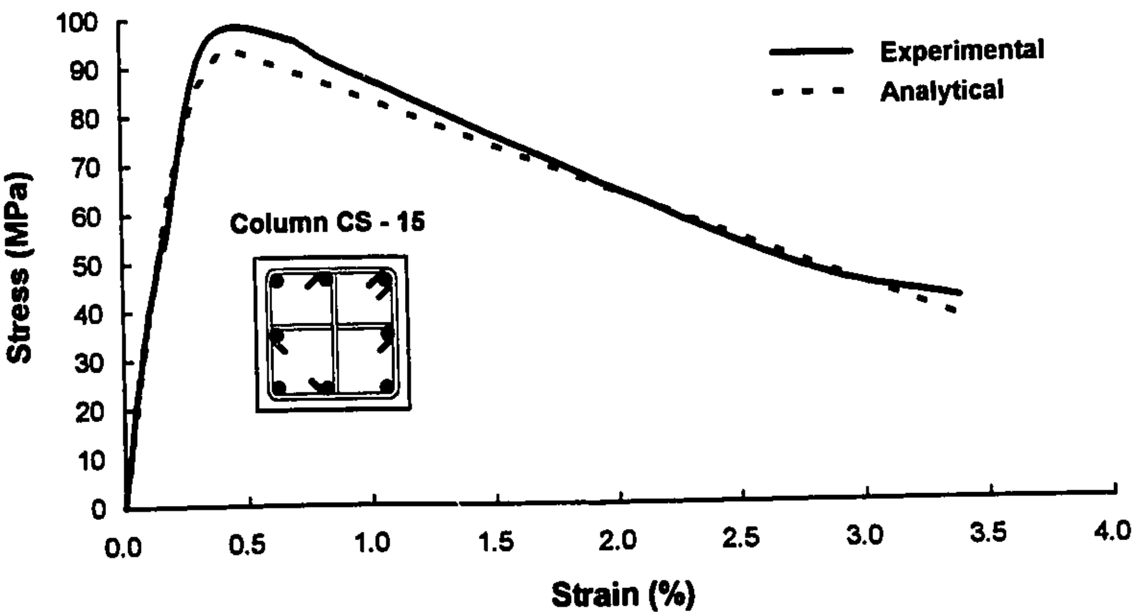

Figure 7.54: Square columns (CS-14 and CS-15) tested in this investigation.

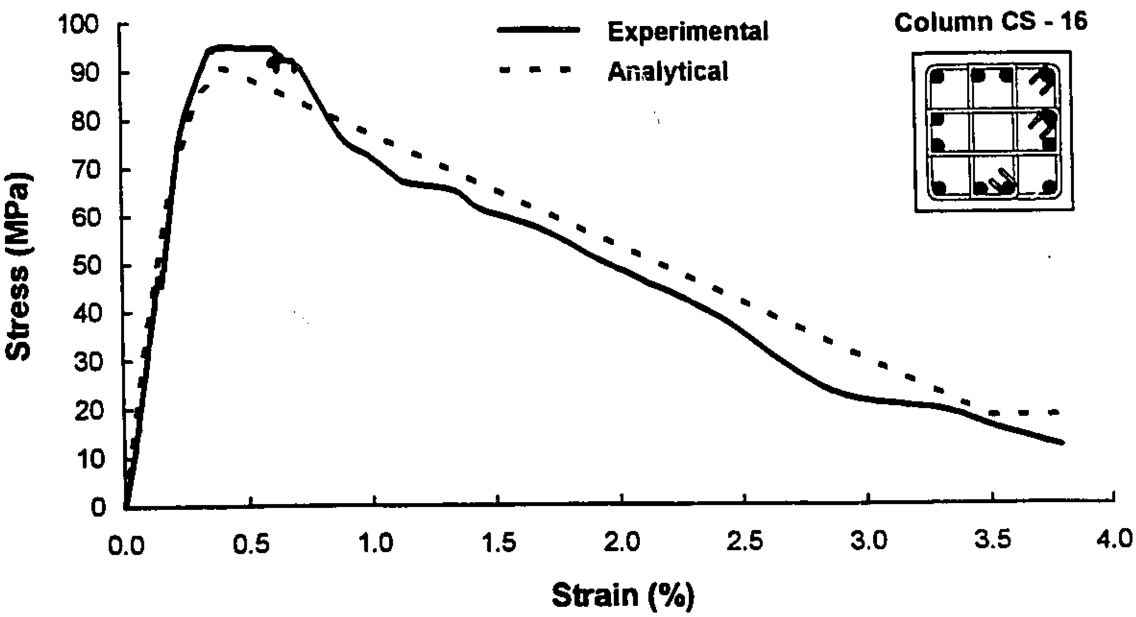

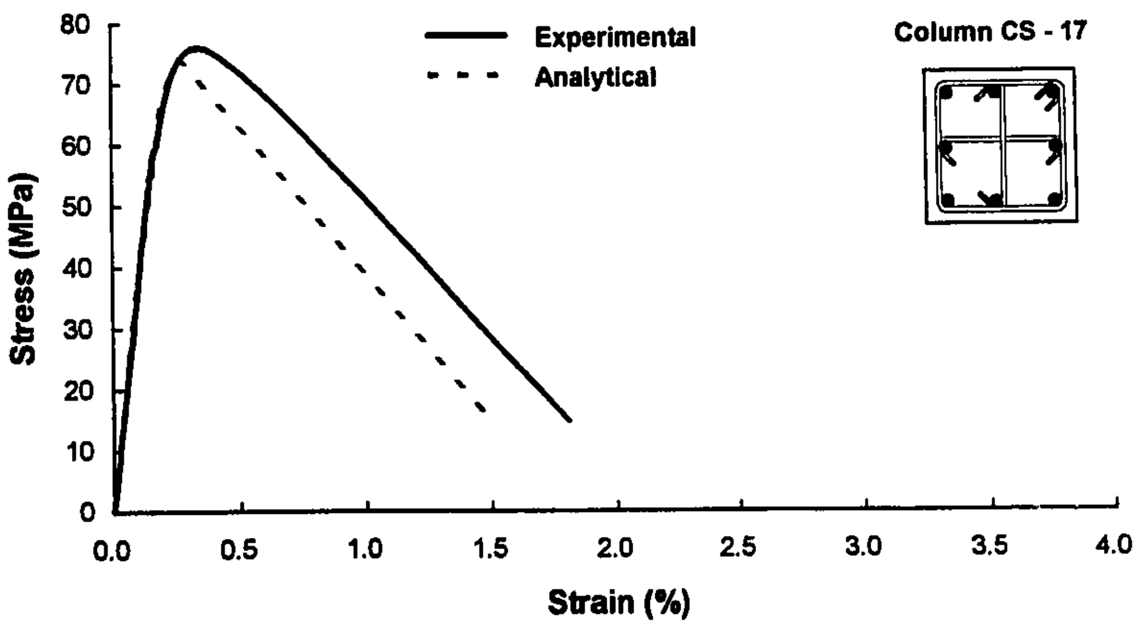

Figure 7.55: Square columns (CS-16 and CS-17) tested in this investigation.

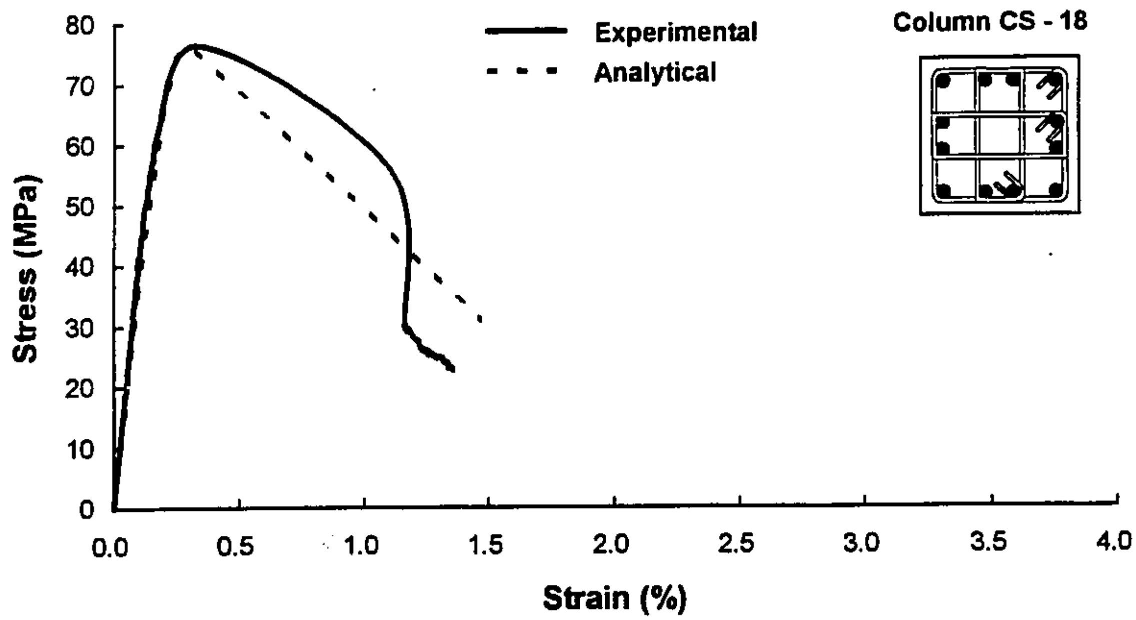

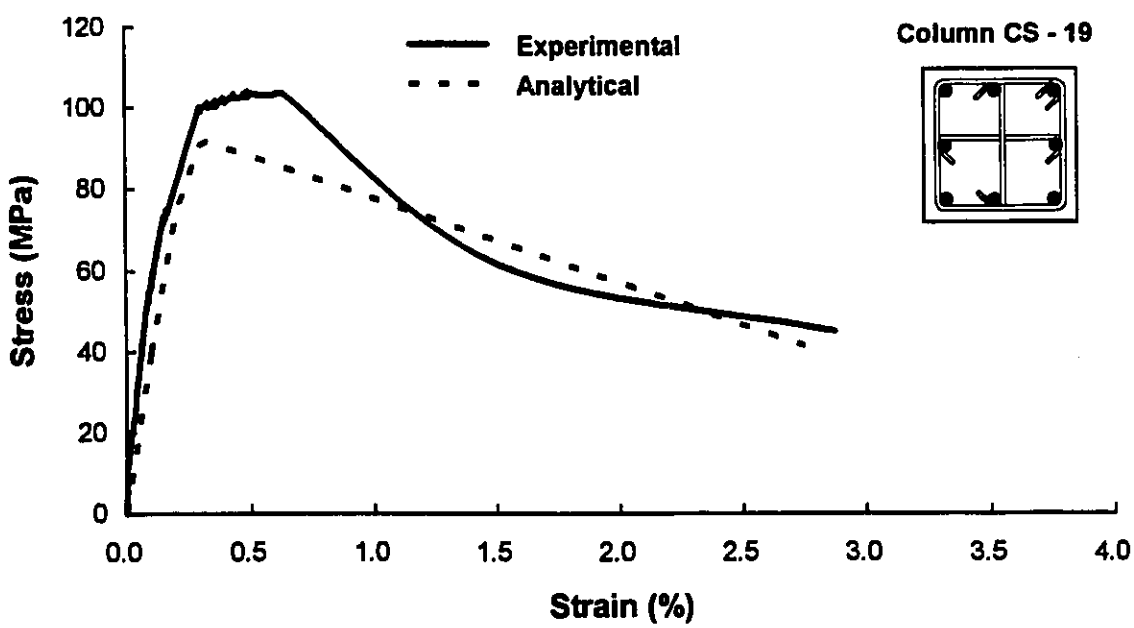

Figure 7.56: Square columns (CS-18 and CS-19) tested in this investigation.

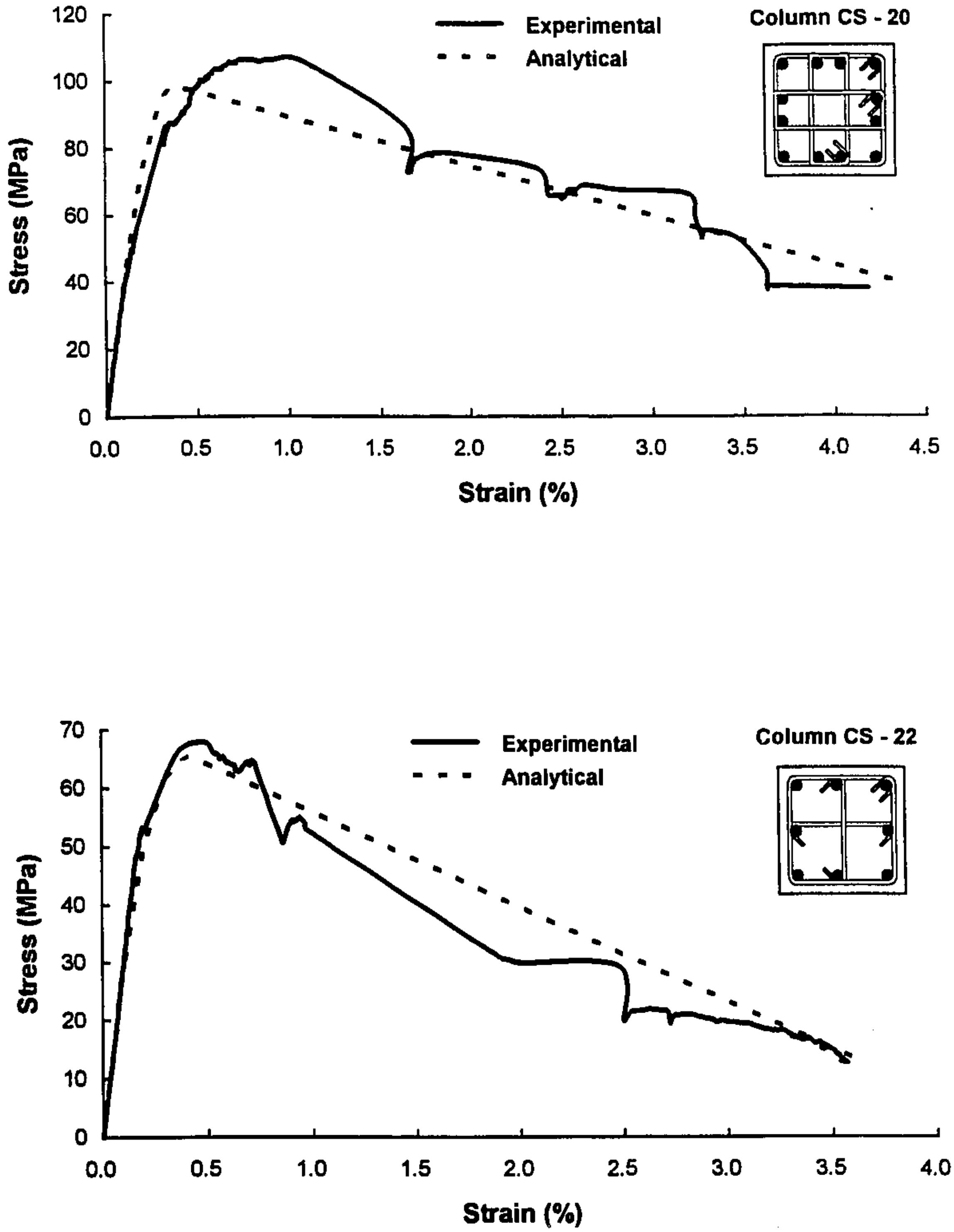

Figure 7.57: Square columns (CS-20 and CS-22) tested in this investigation.

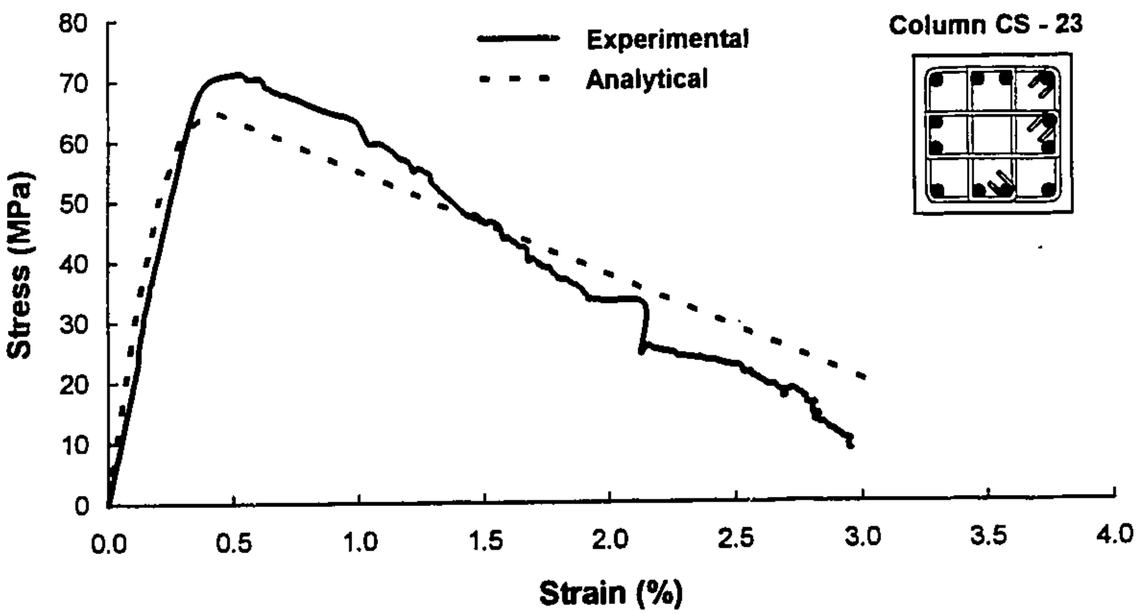

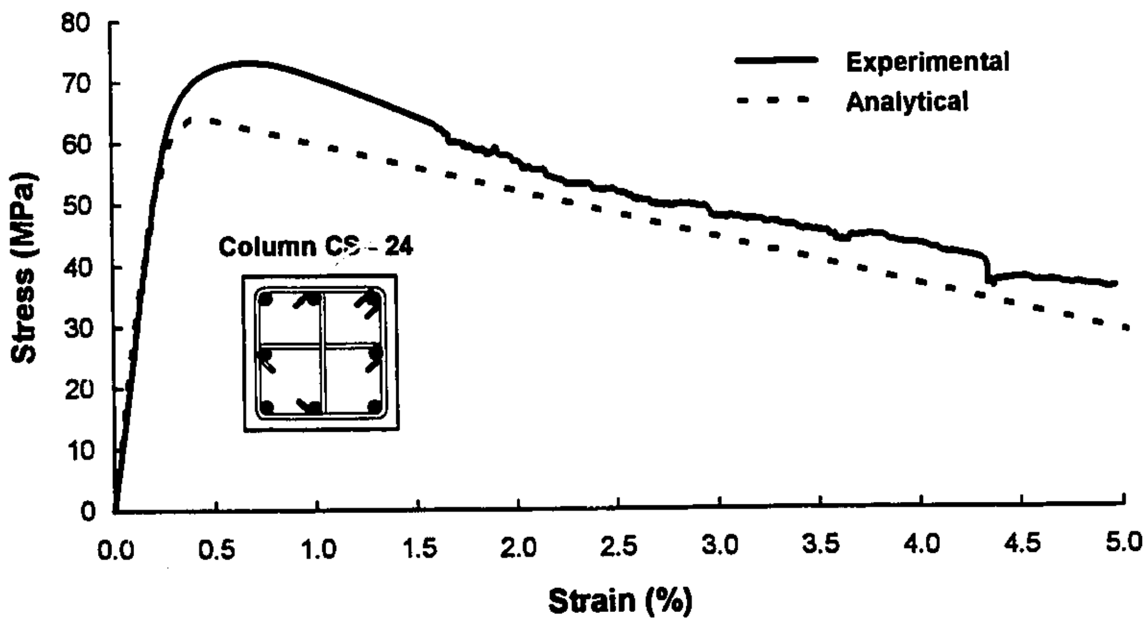

Figure 7.58: Square columns (CS-23 and CS-24) tested in this investigation.

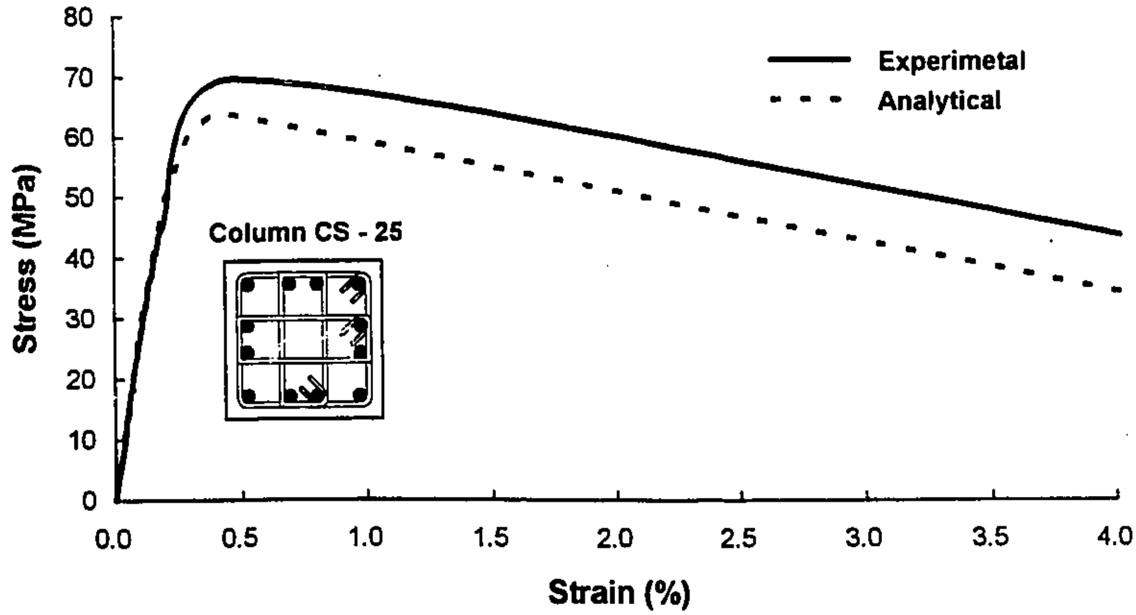

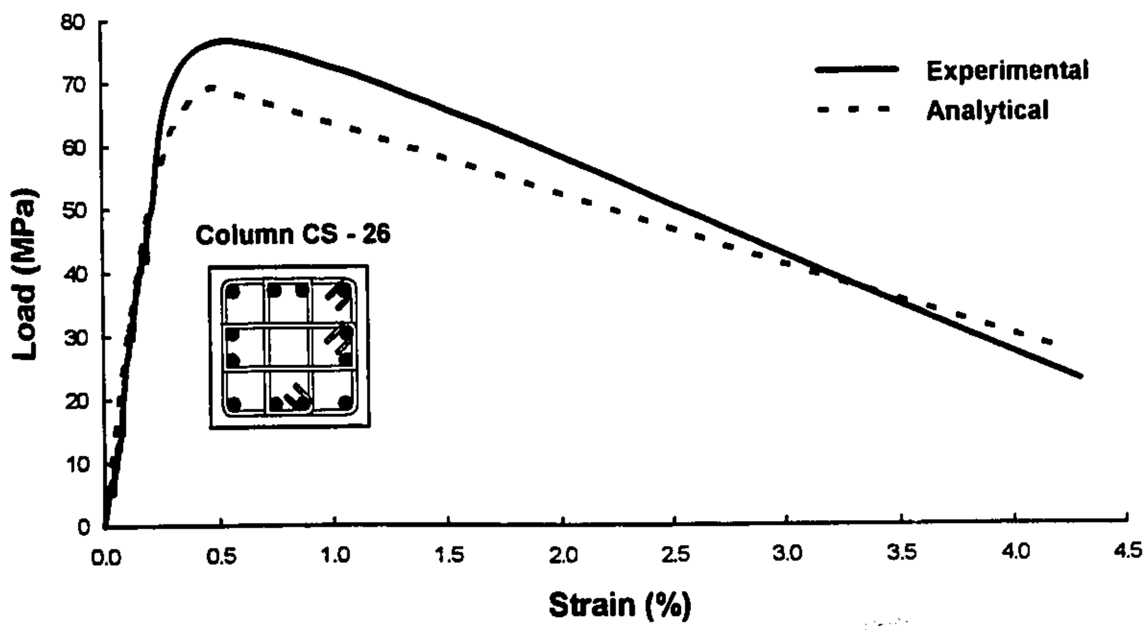

Figure 7.59: Square columns (CS-25 and CS-26) tested in this investigation.

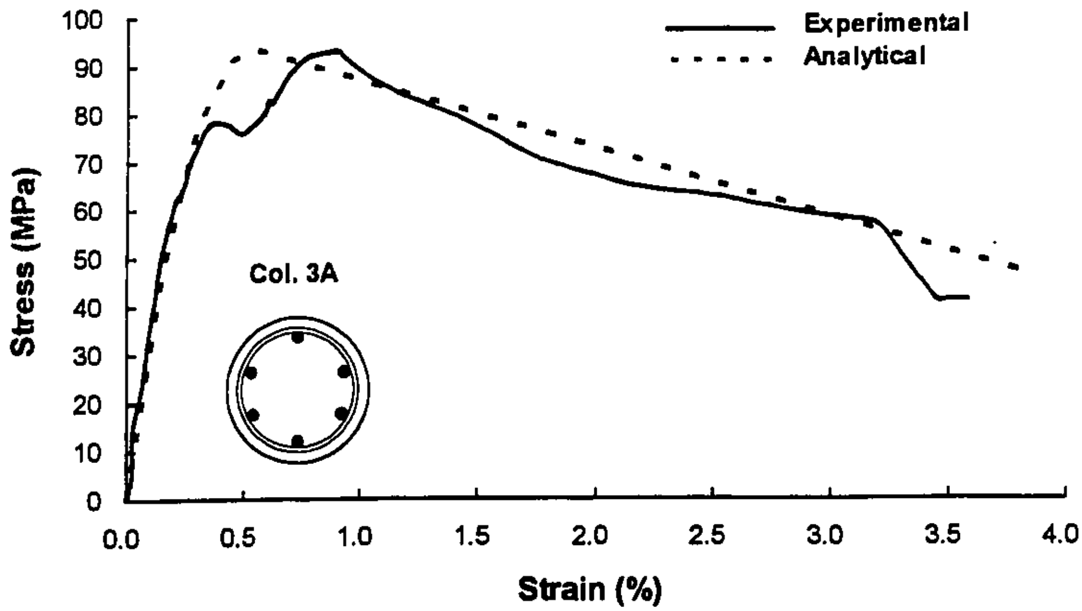

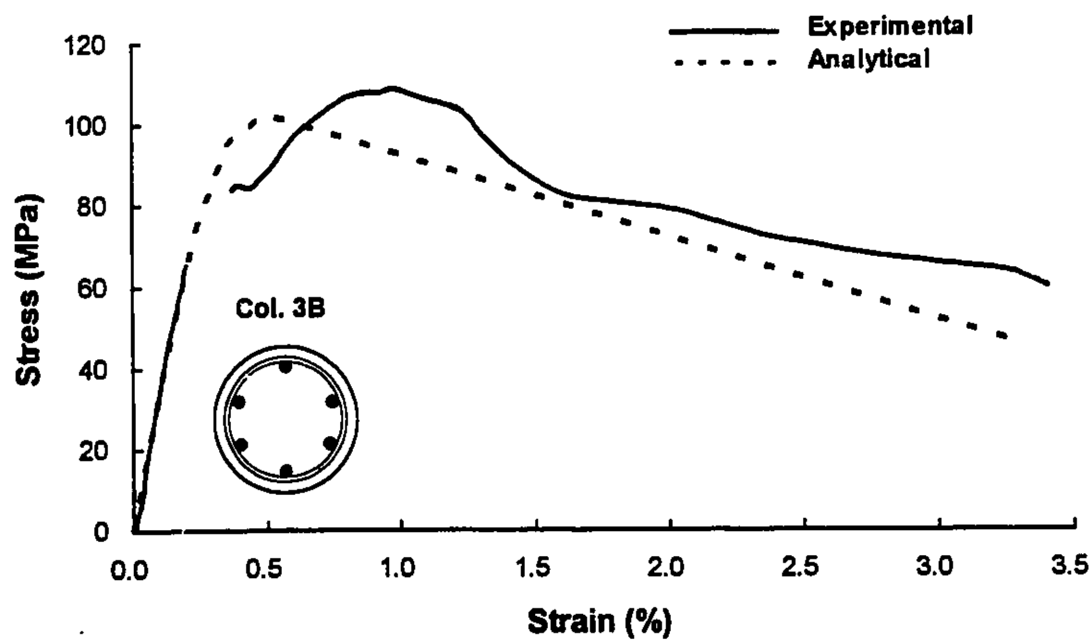

Figure 7.60: Circular columns (3A and 3B) tested by Li (1994).

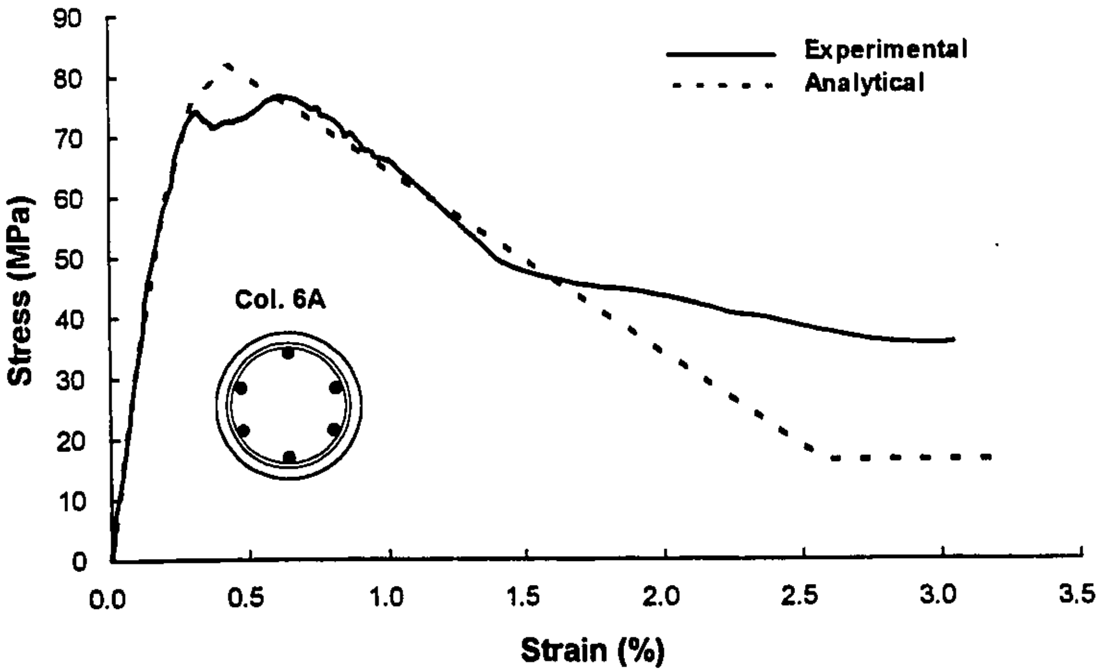

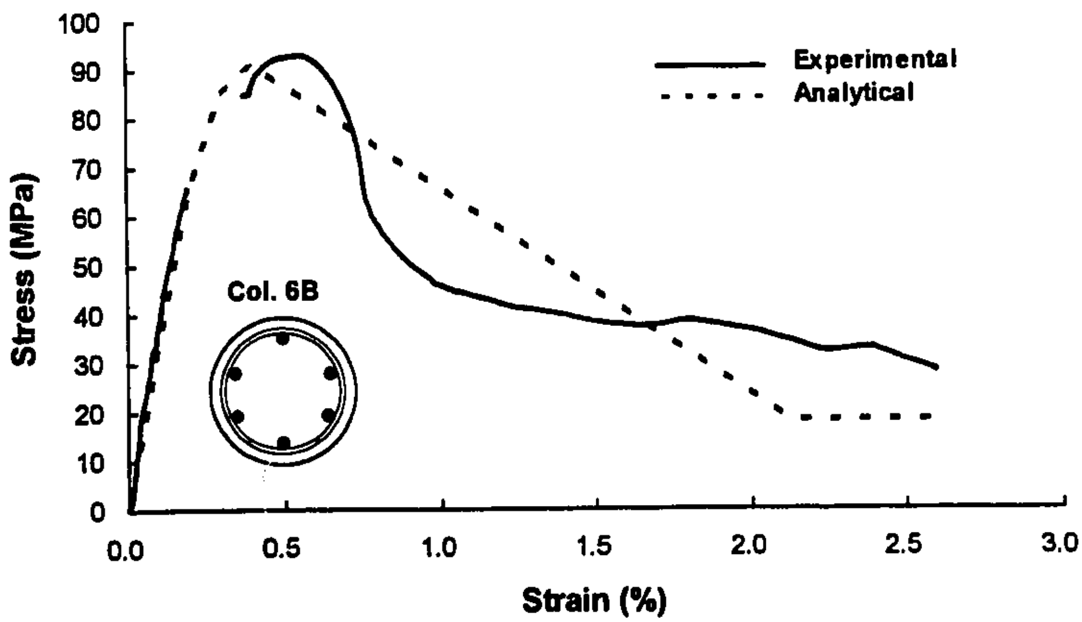

Figure 7.61: Circular columns (6A and 6B) tested by Li (1994).

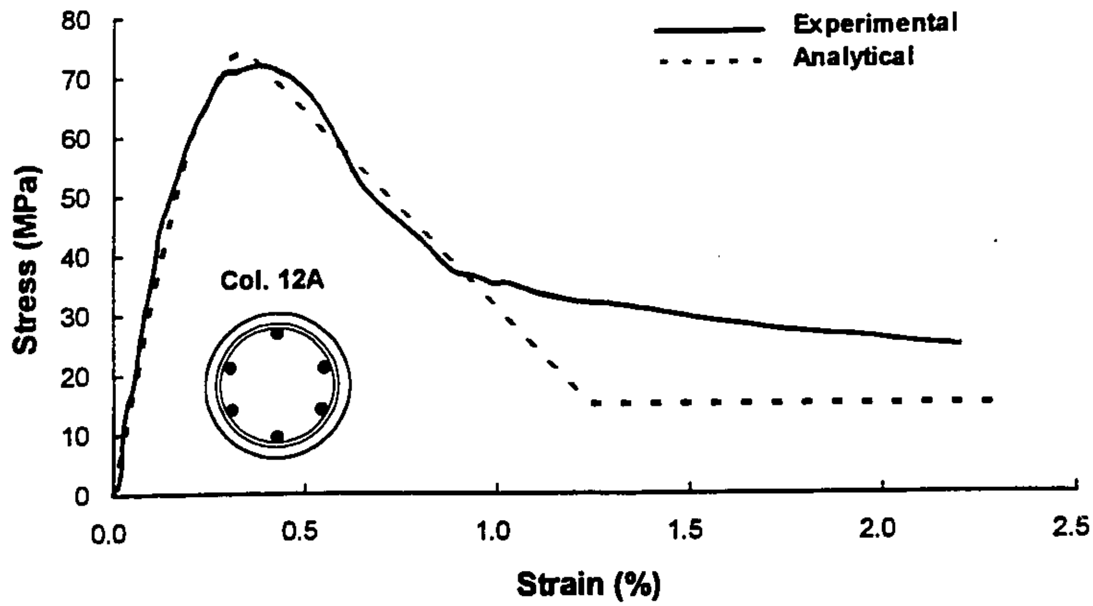

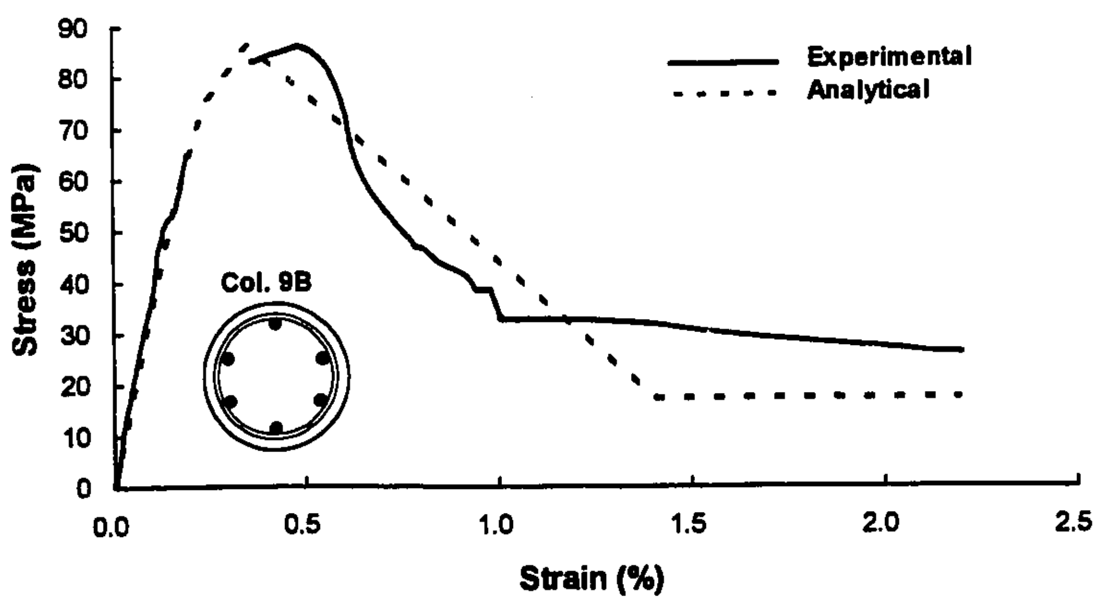

Figure 7.62: Circular columns (12A and 9B) tested by Li (1994).

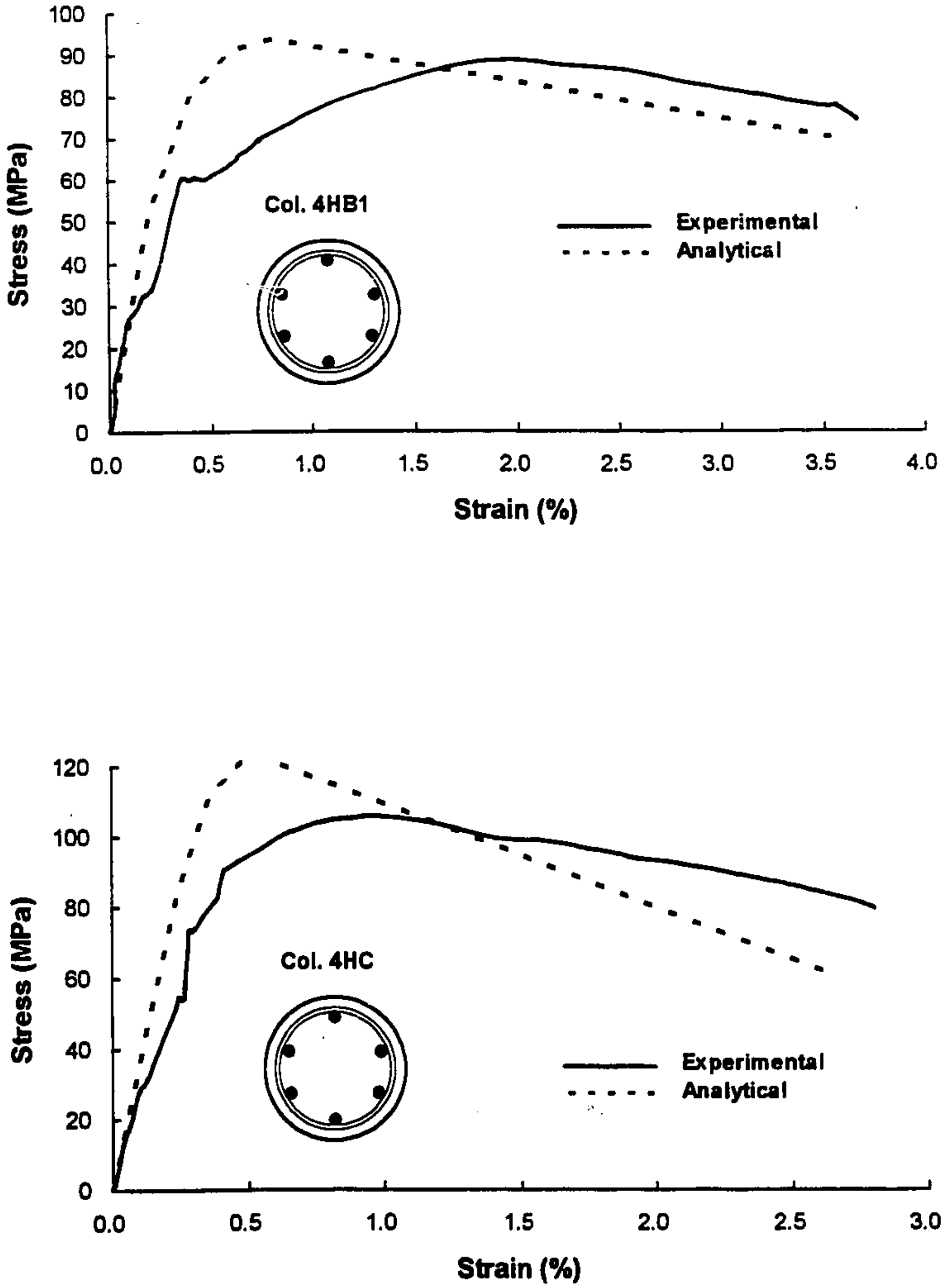

Figure 7.63: Circular columns (4HB1 and 4HC) tested by Li (1994).

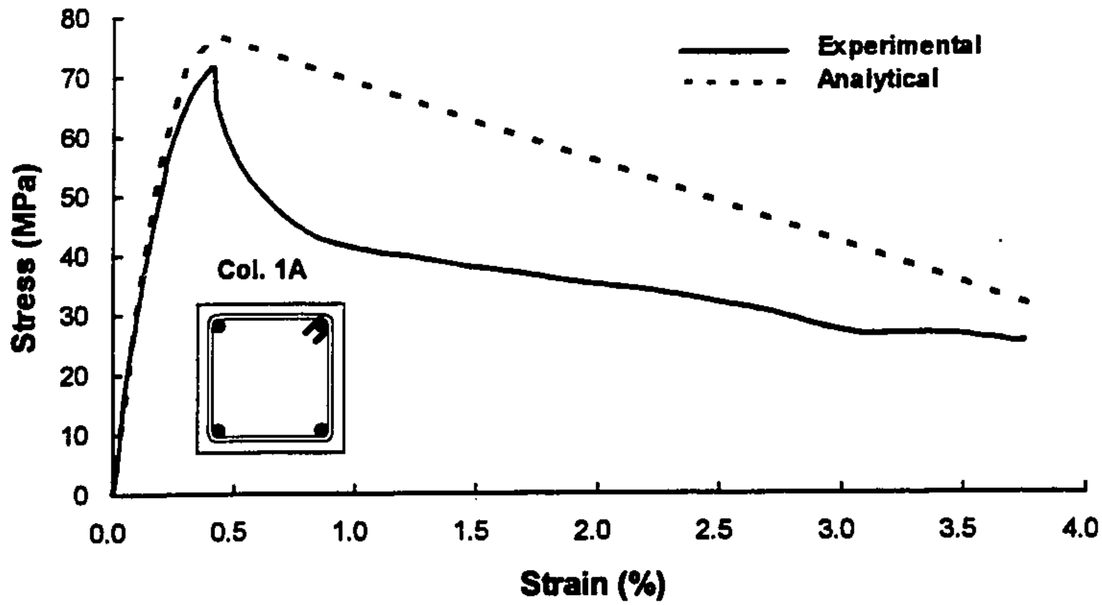

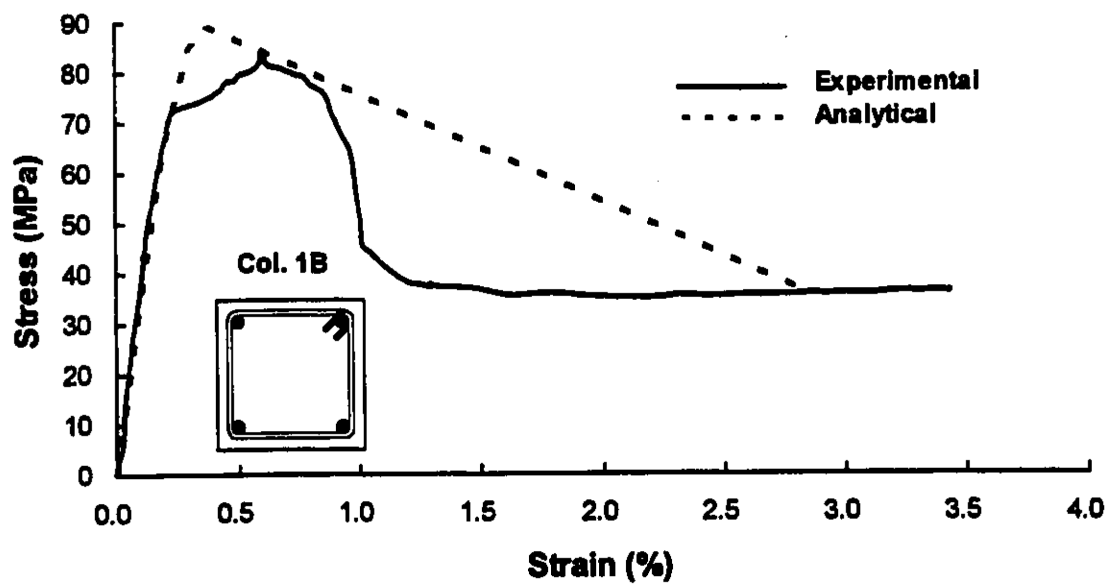

Figure 7.64: Square columns (1A and 1B) tested by Li (1994).

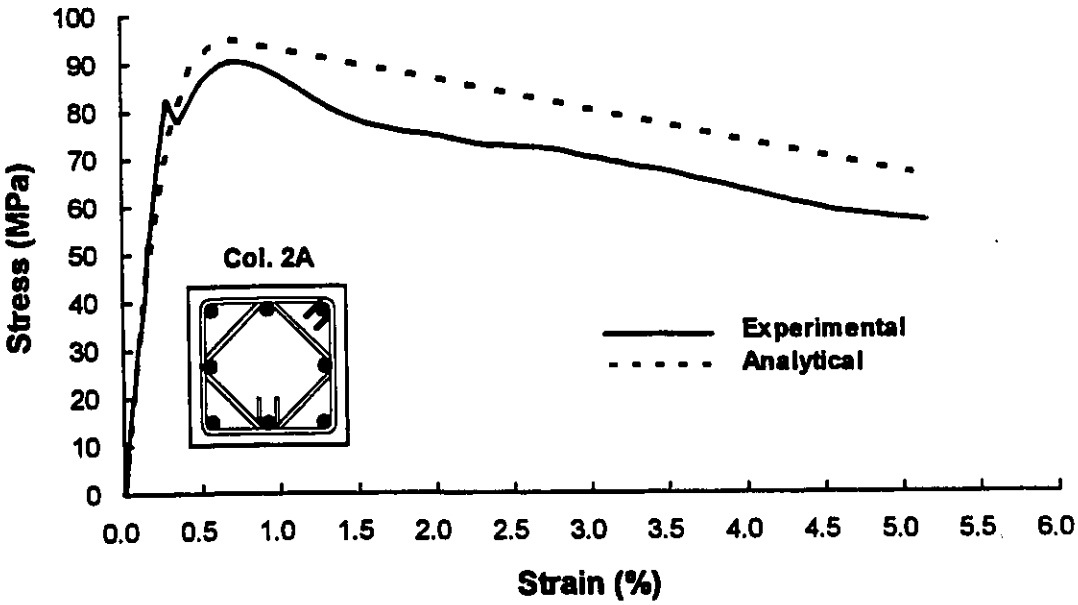

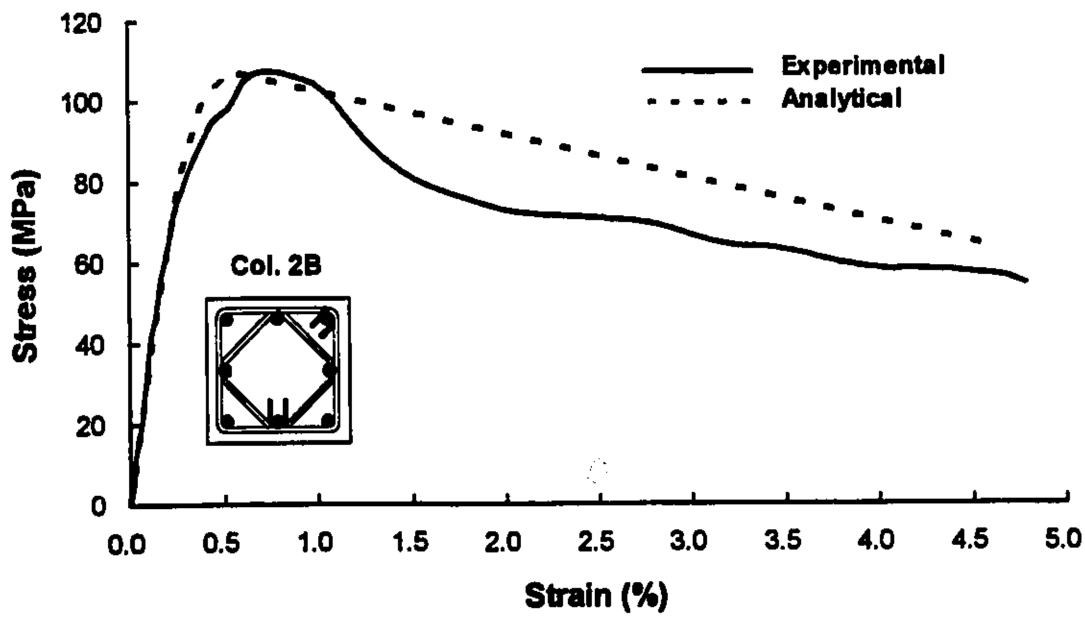

Figure 7.65: Square columns (2A and 2B) tested by Li (1994).

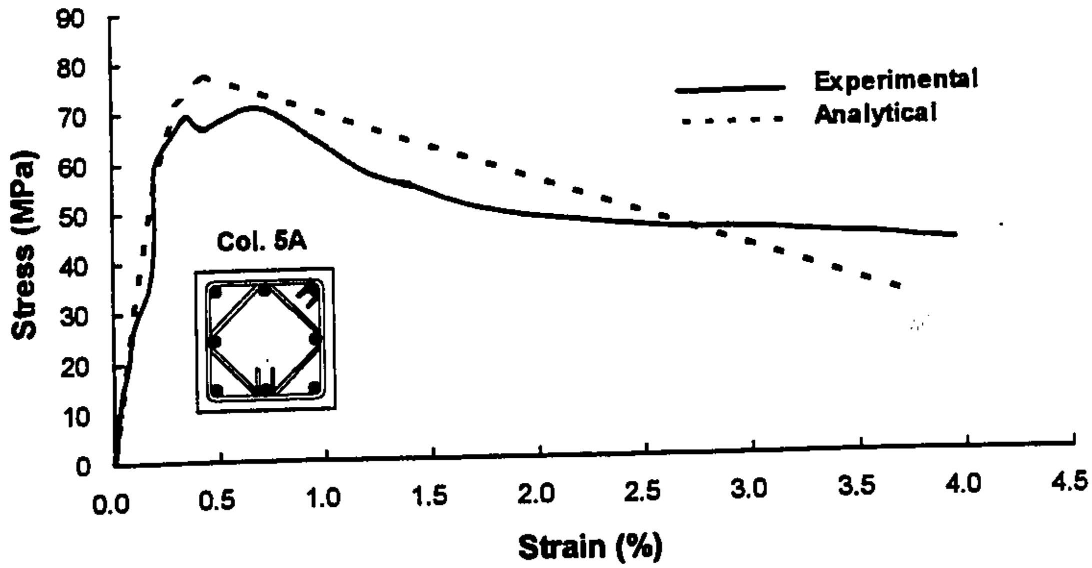

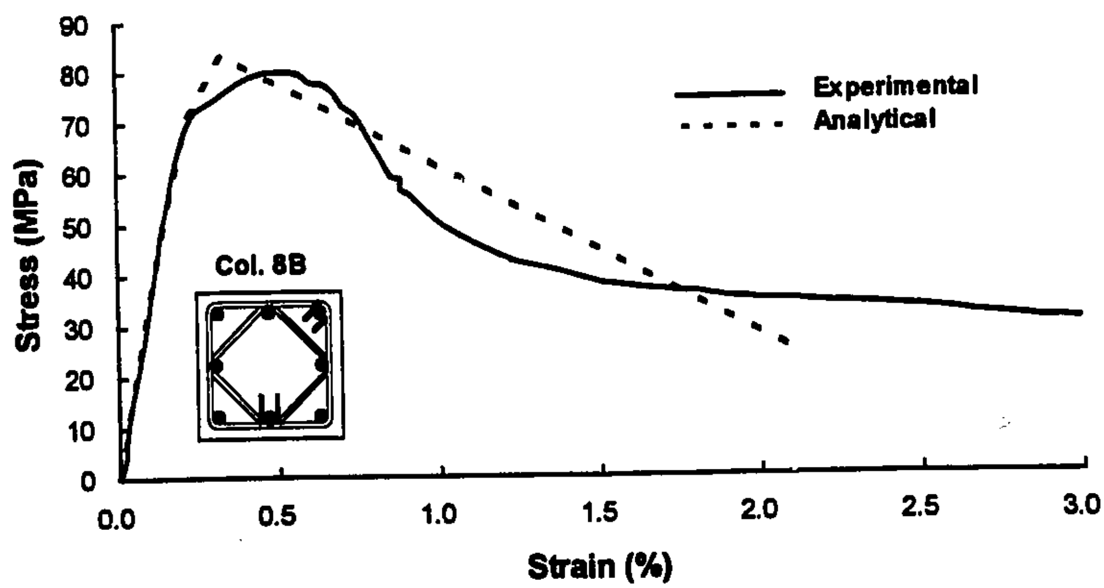

Figure 7.66: Square columns (5A and 8B) tested by Li (1994).

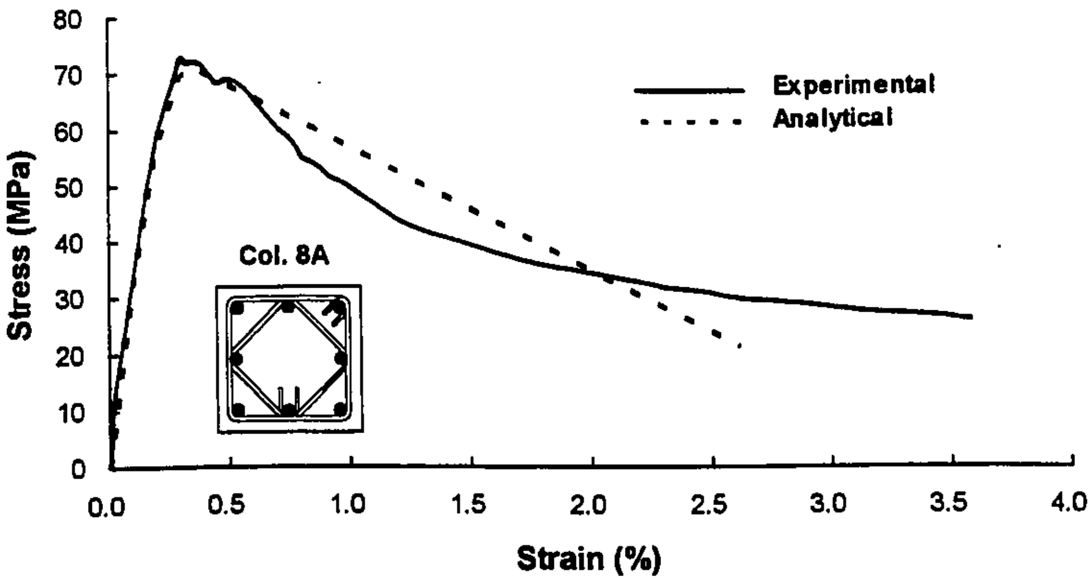

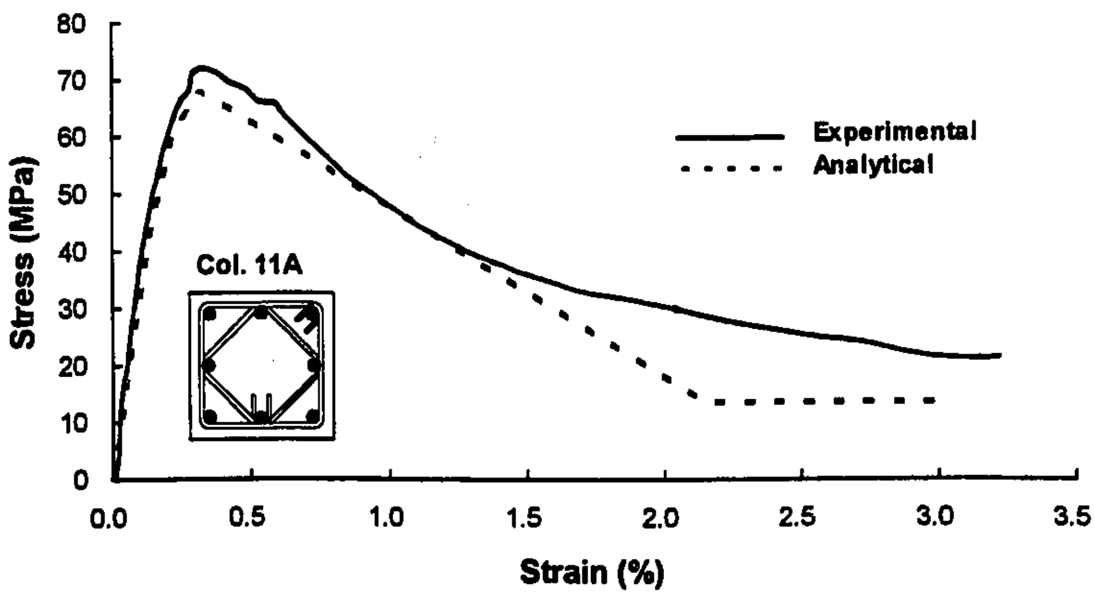

Figure 7.67: Square columns (8A and 11A) tested by Li (1994).

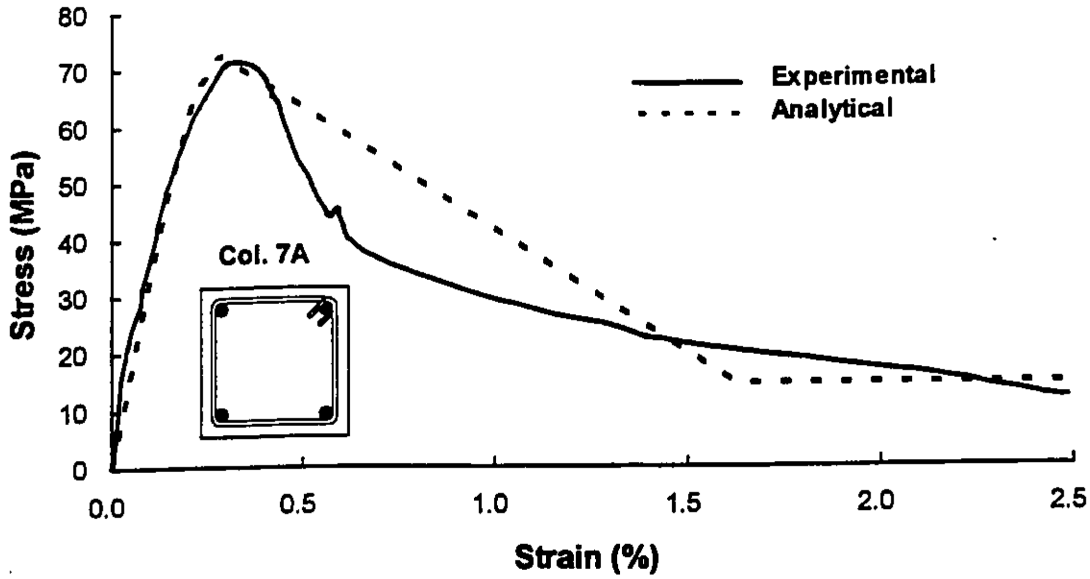

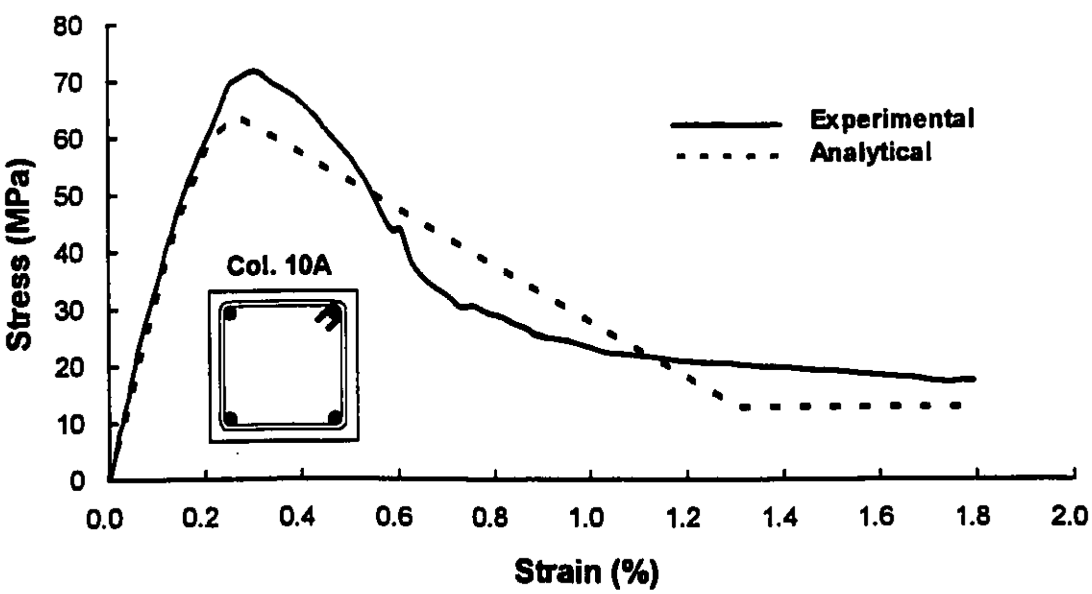

Figure 7.68: Square columns (7A and 10A) tested by Li (1994).

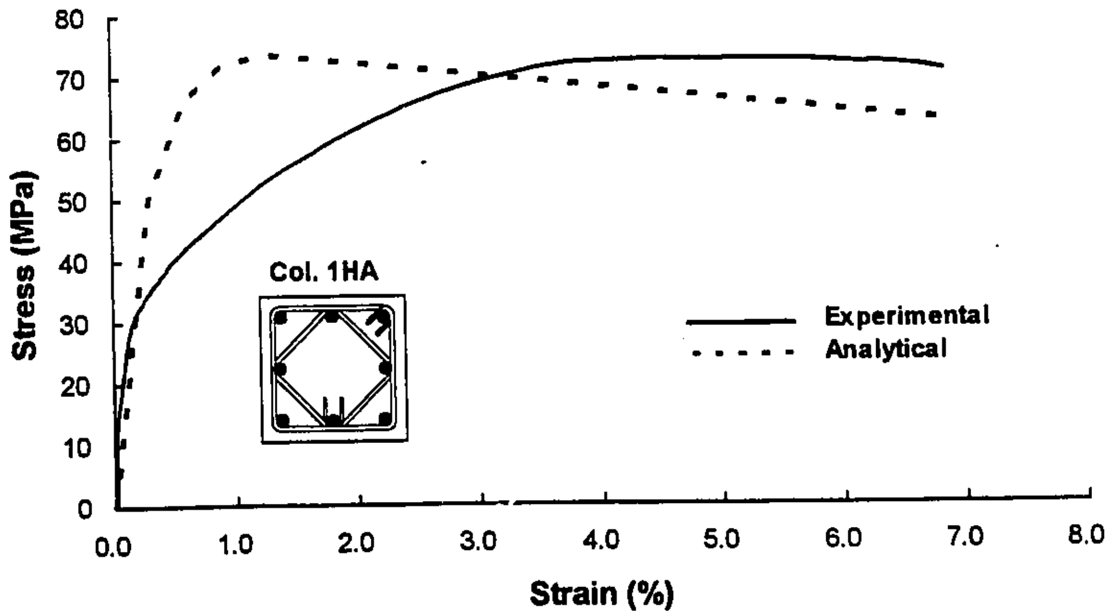

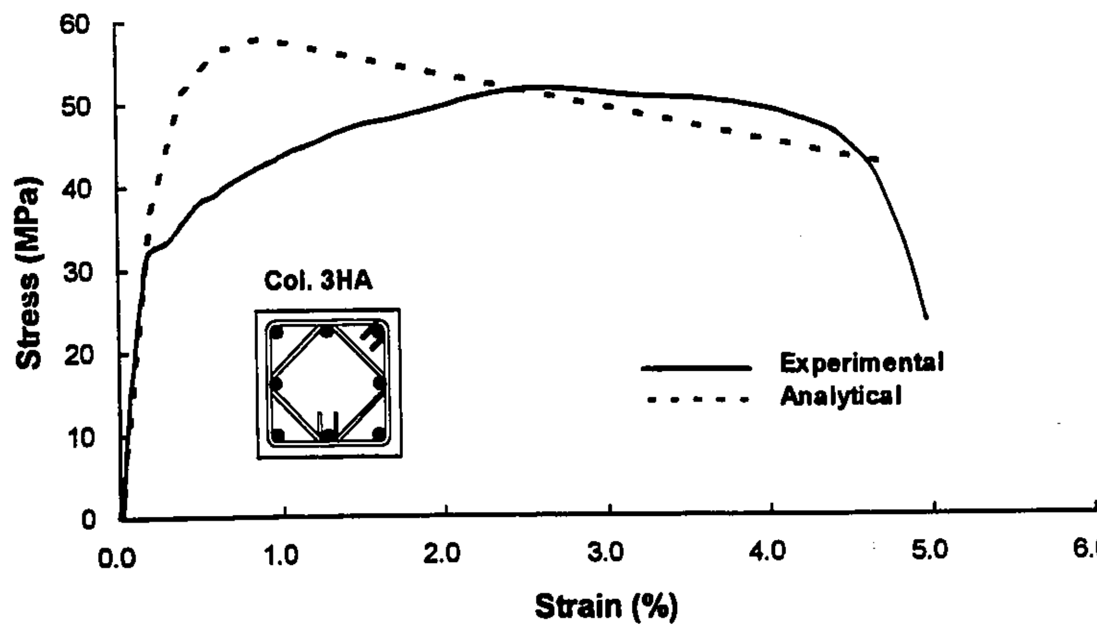

Figure 7.69: Square columns (1HA and 3HA) tested by Li (1994).

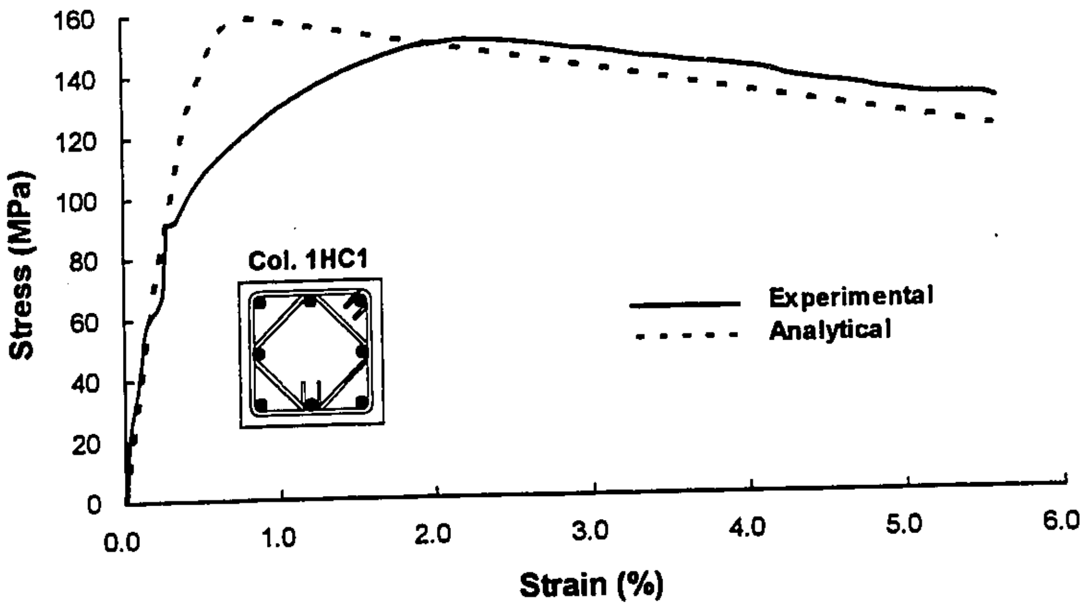

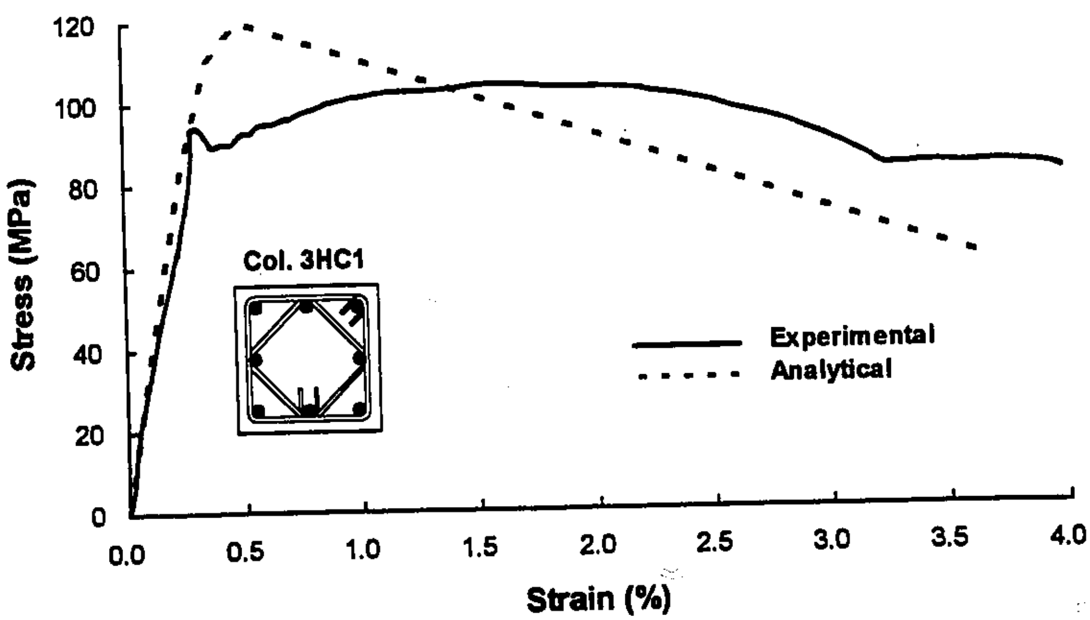

Figure 7.70: Square columns (1HC1 and 3HC1) tested by Li (1994).

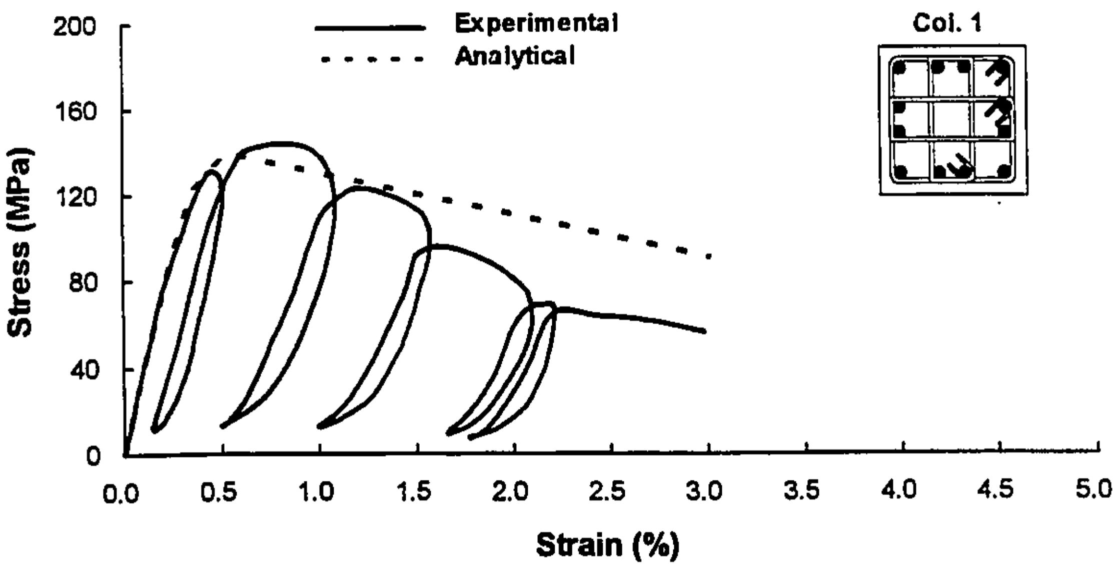

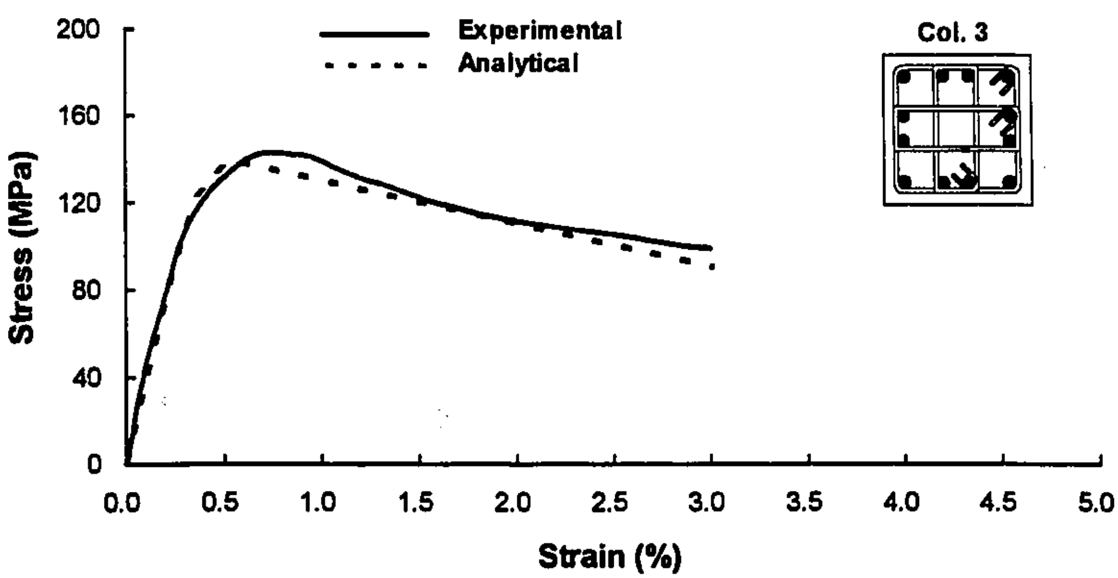

Figure 7.71: Square columns (1 and 3) tested by Nishiyama et al. (1993).

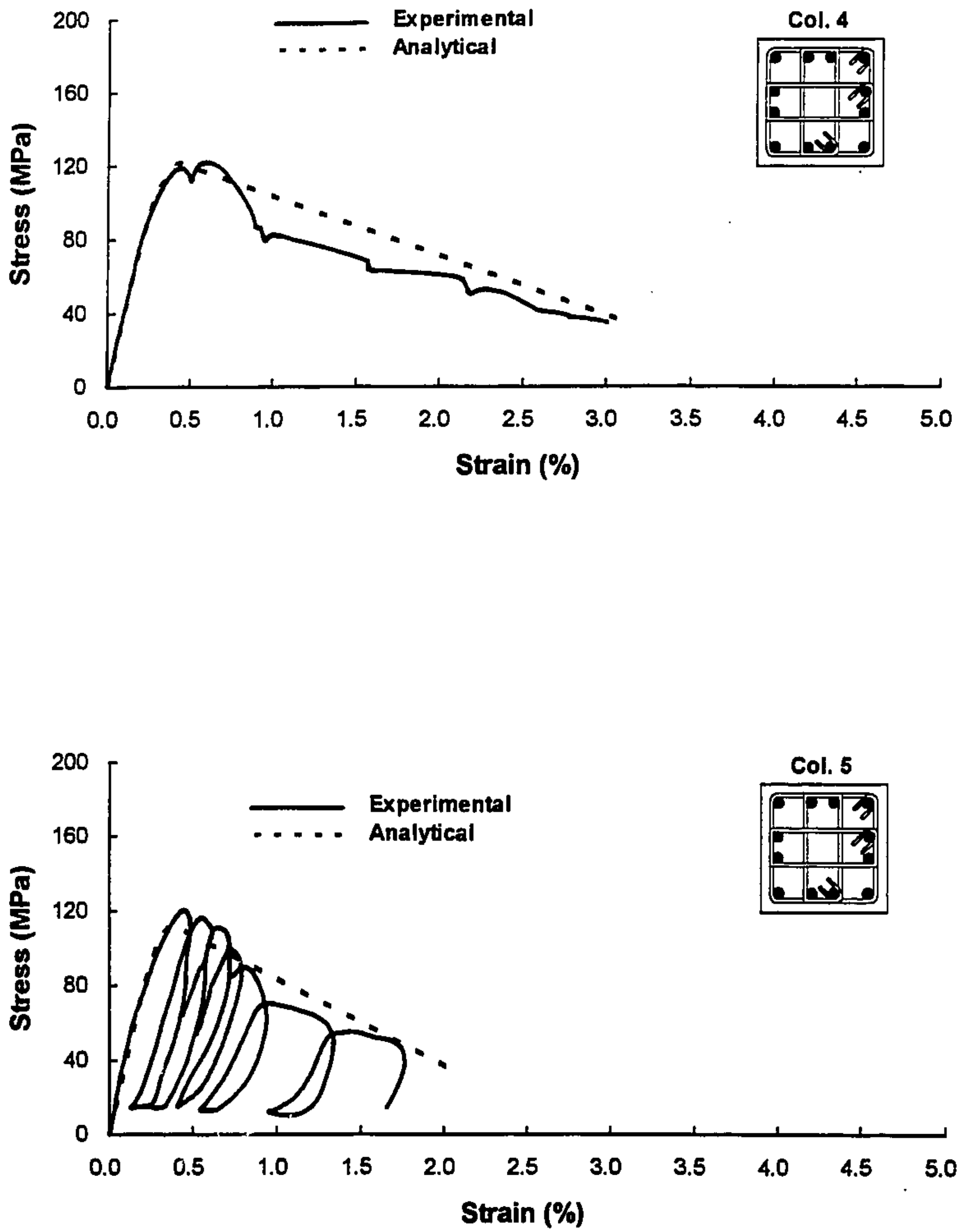

Figure 7.72: Square columns (4 and 5) tested by Nishiyama et al. (1993).

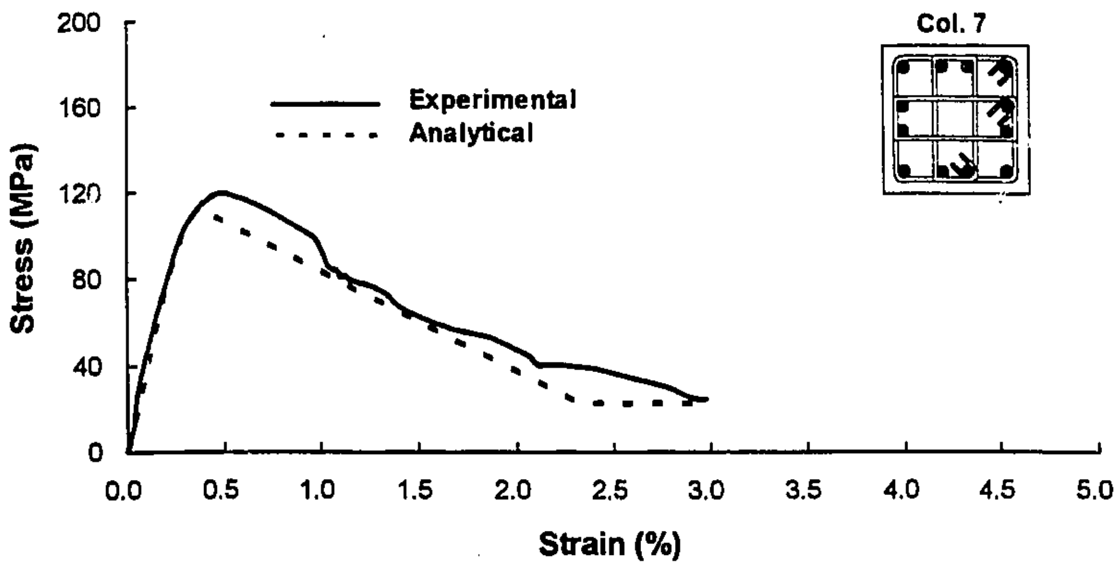

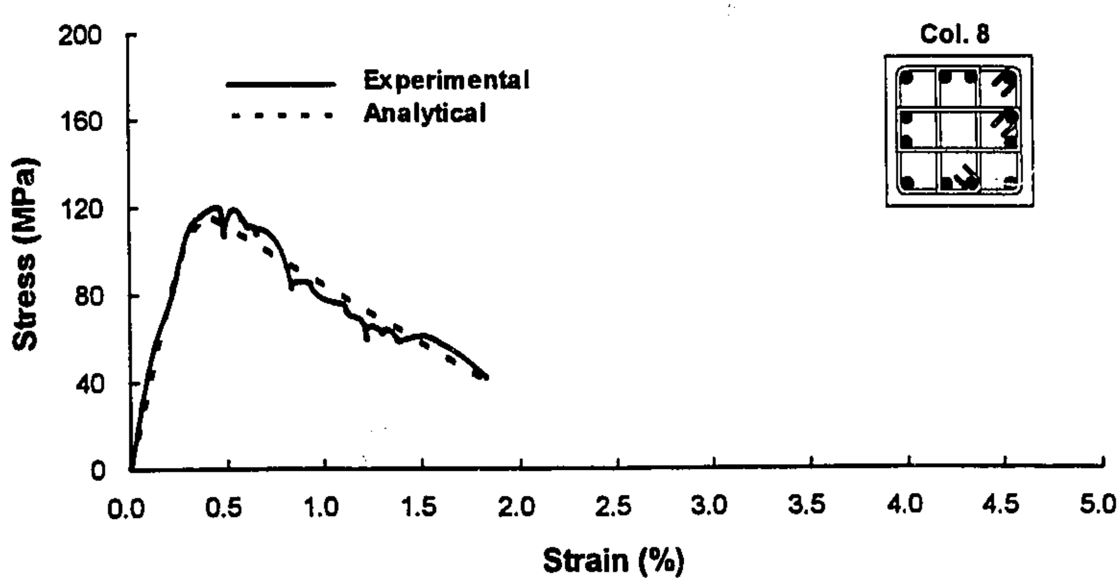

Figure 7.73: Square columns (7 and 8) tested by Nishiyama et al. (1993).

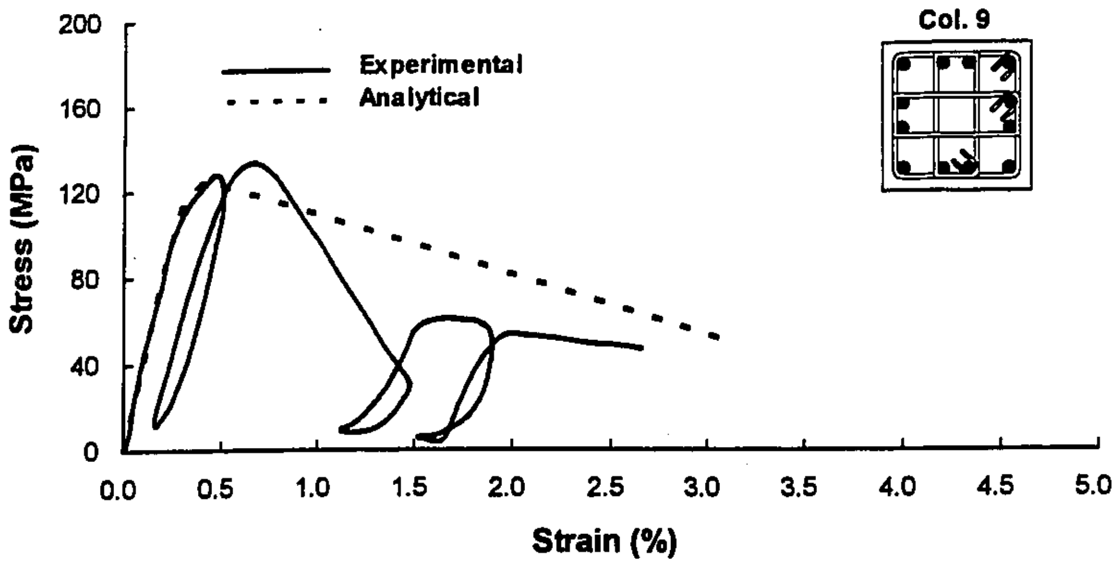

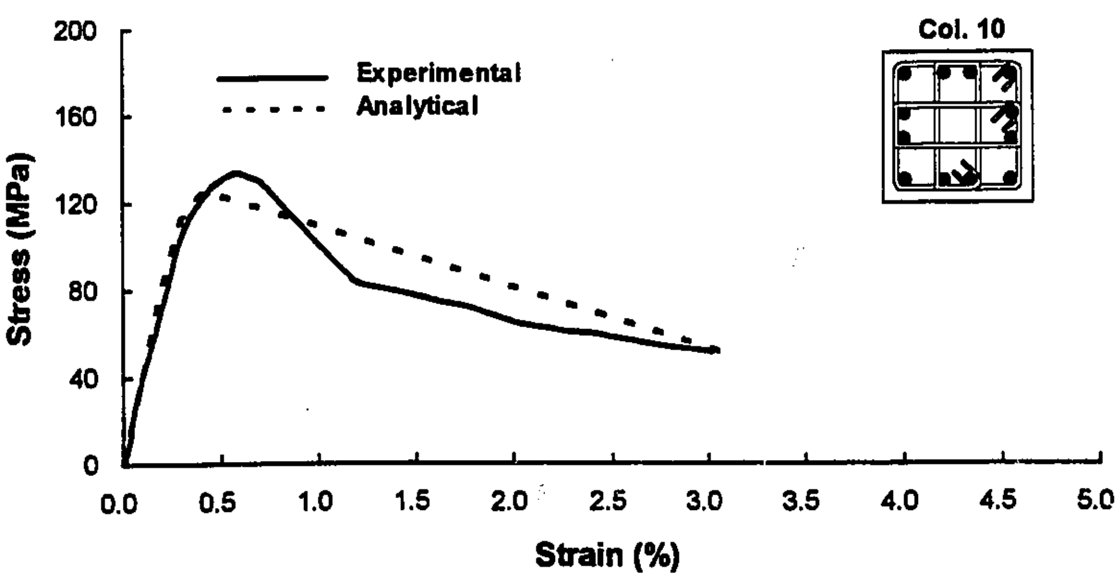

Figure 7.74: Square columns (9 and 10) tested by Nishiyama et al. (1993).

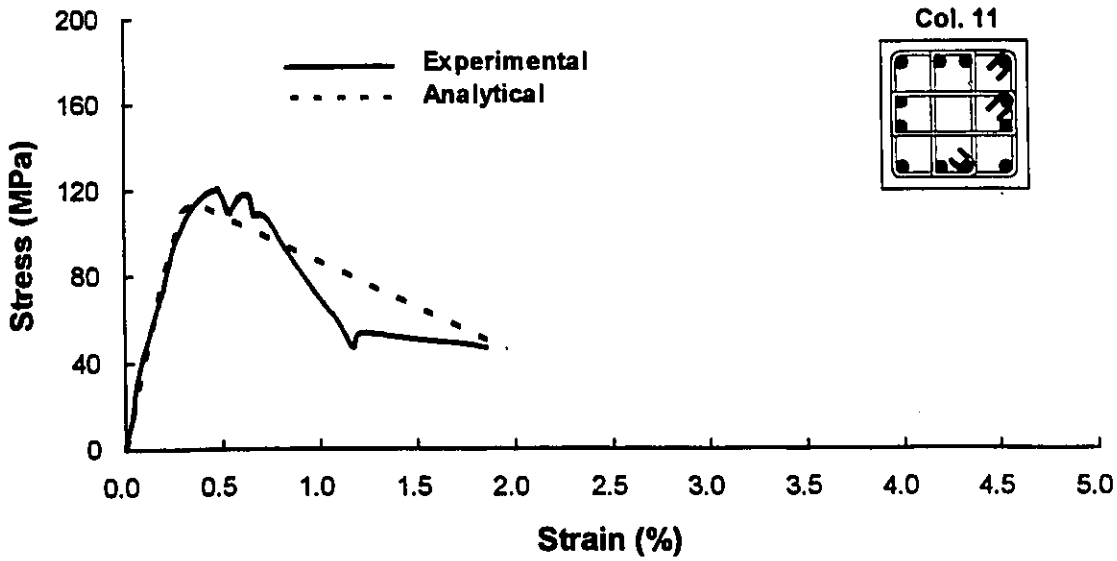

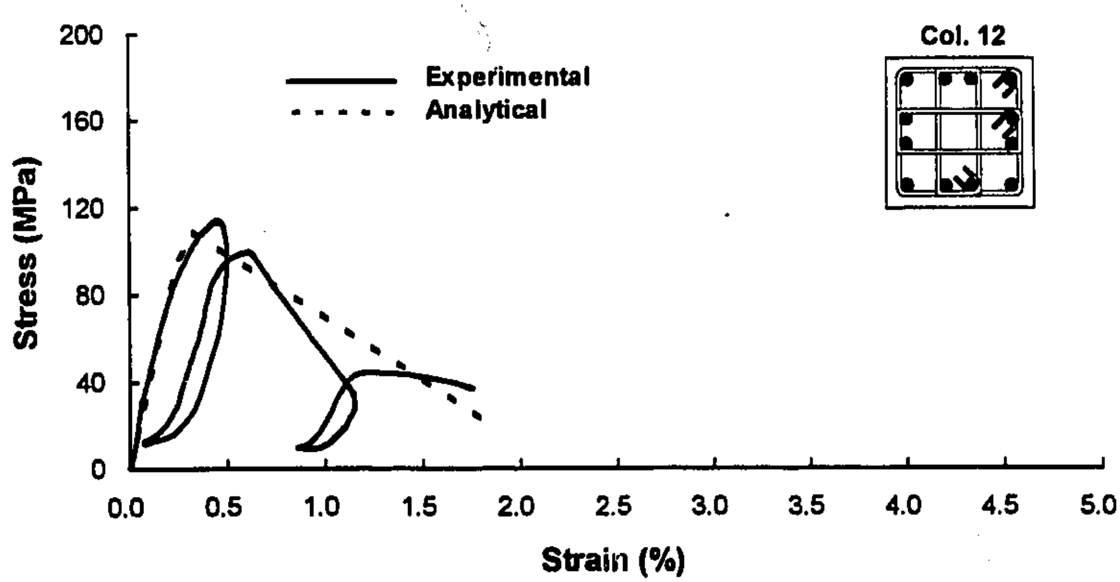

Figure 7.75: Square columns (11 and 12) tested by Nishiyama et al. (1993).

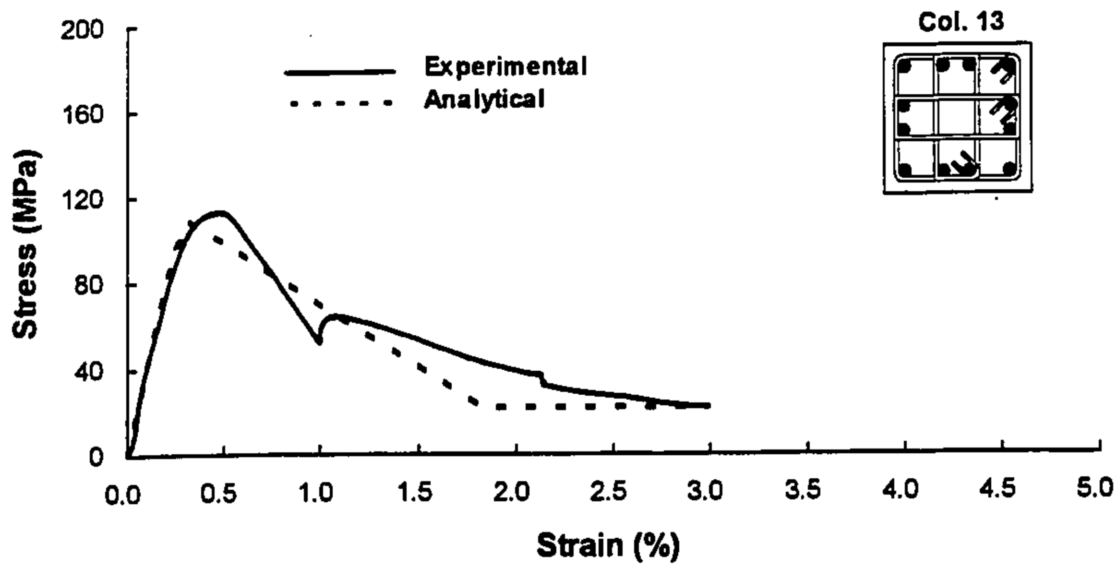

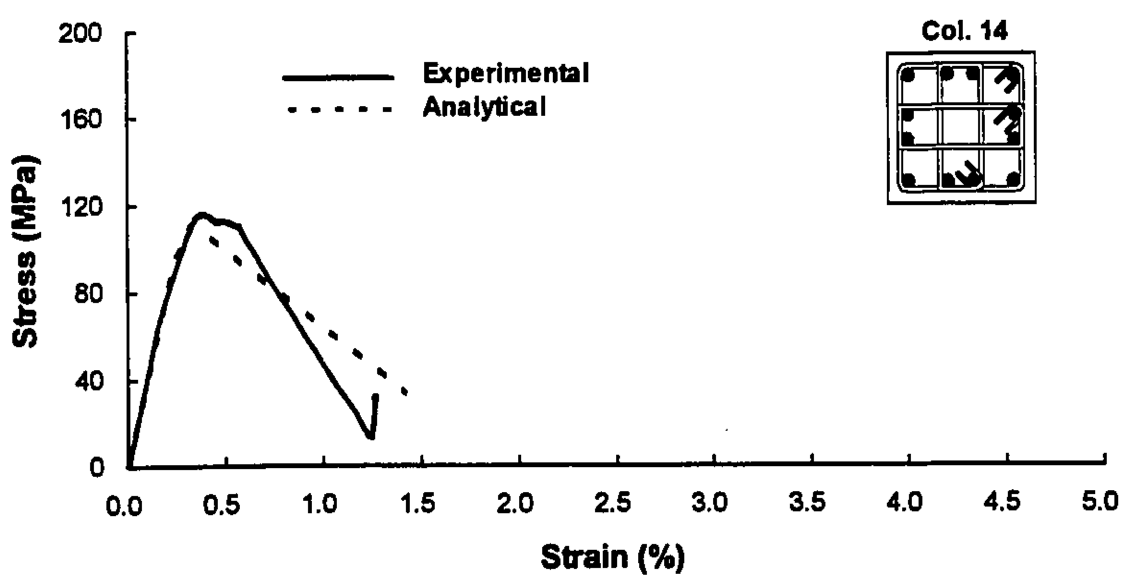

Figure 7.76: Square columns (13 and 14) tested by Nishiyama et al. (1993).

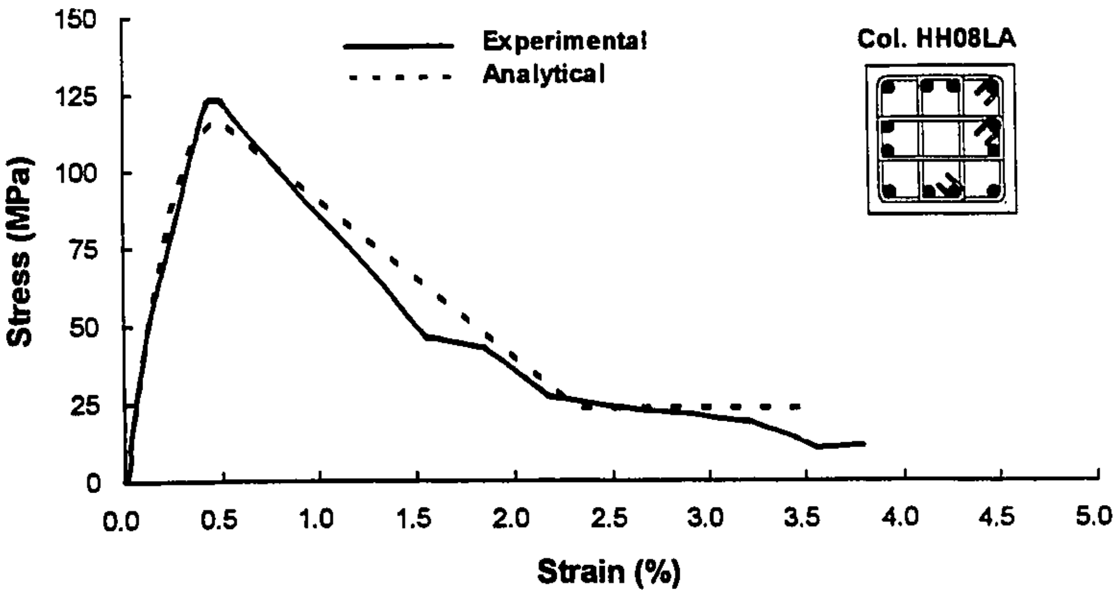

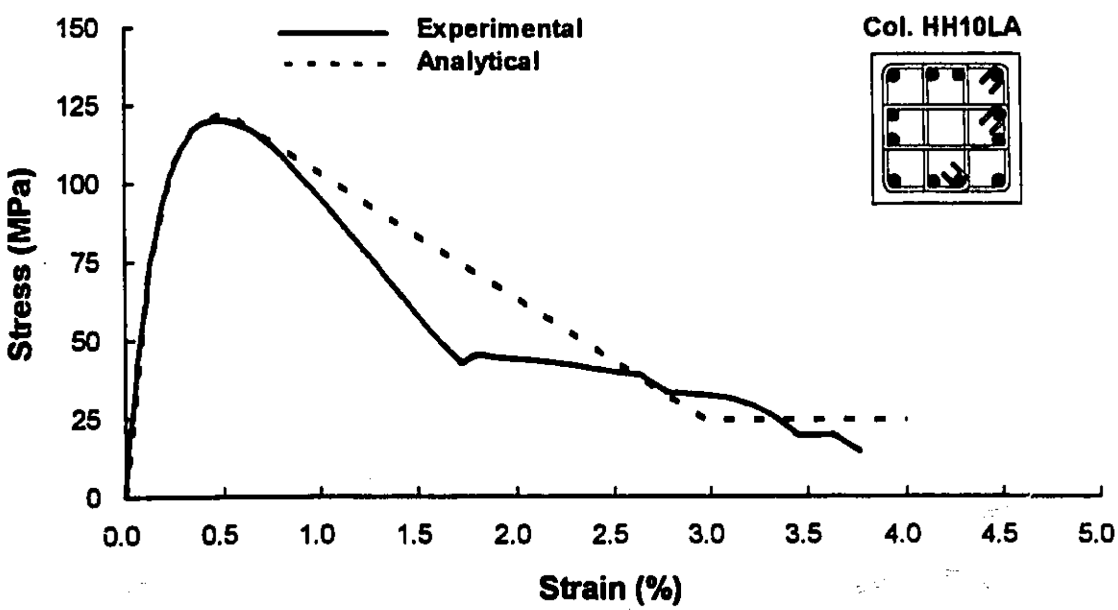

Figure 7.77: Square columns (HH08LA and HH10LA) tested by Nagashima et al. (1992).

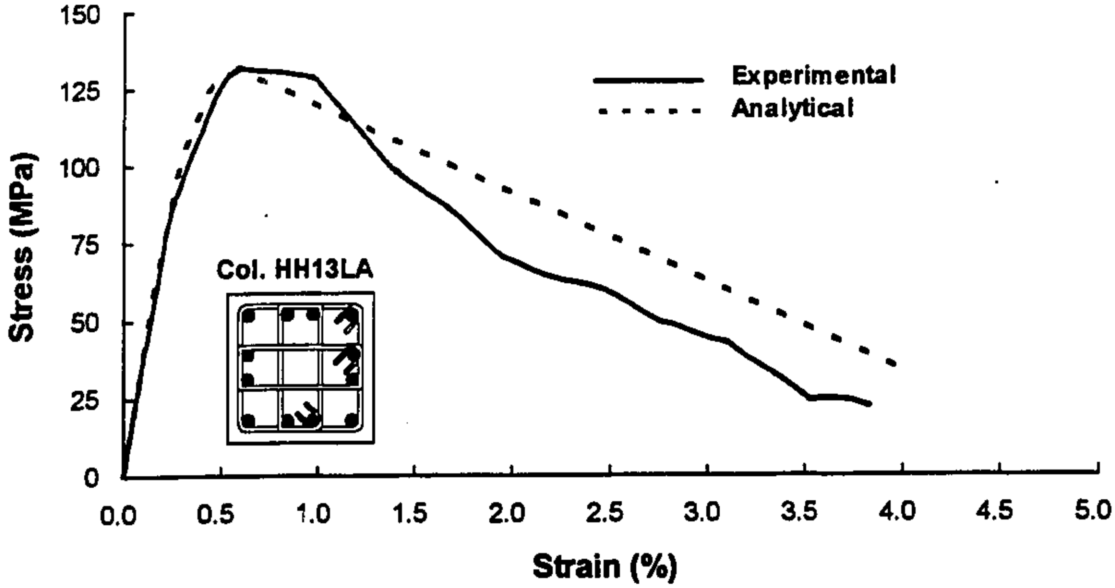

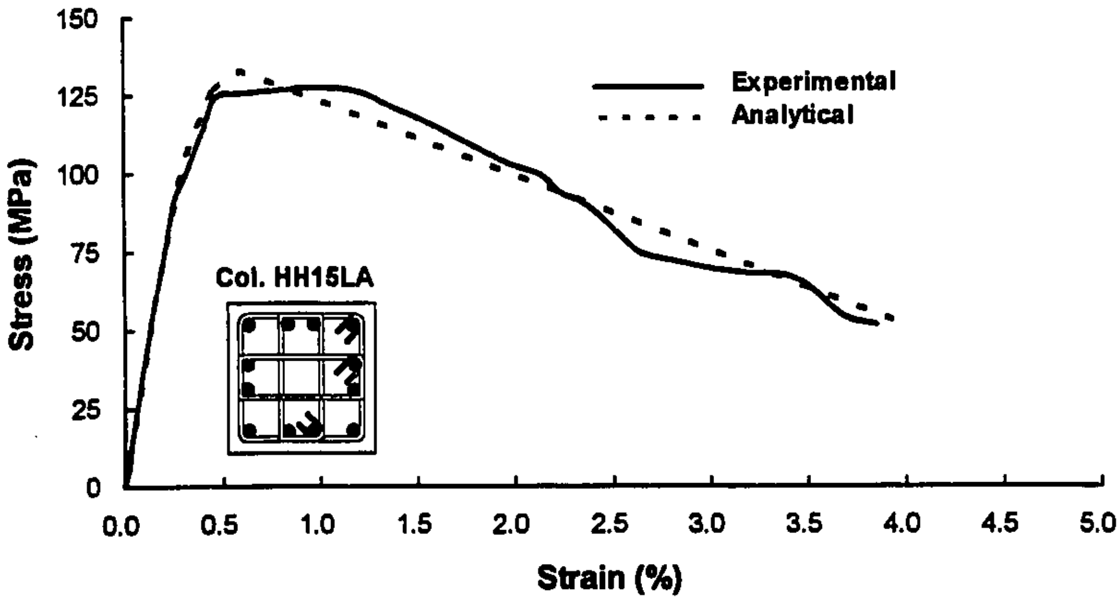

Figure 7.78: Square columns (HH13LA and HH15LA) tested by Nagashima et al. (1992).

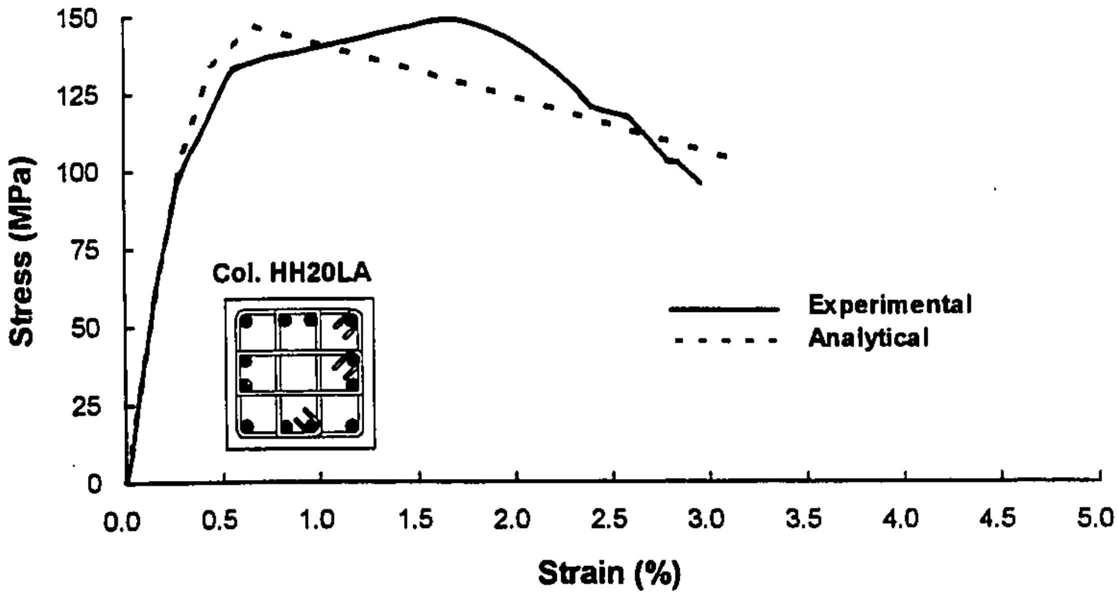

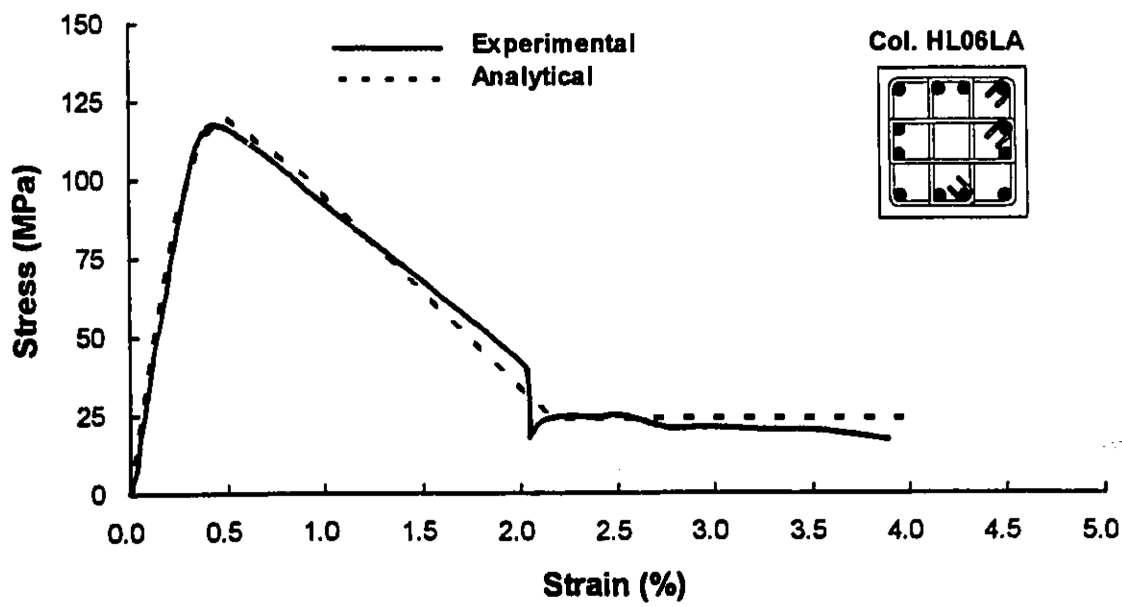

Figure 7.79: Square columns (HH20LA and HL06LA) tested by Nagashima et al. (1992).

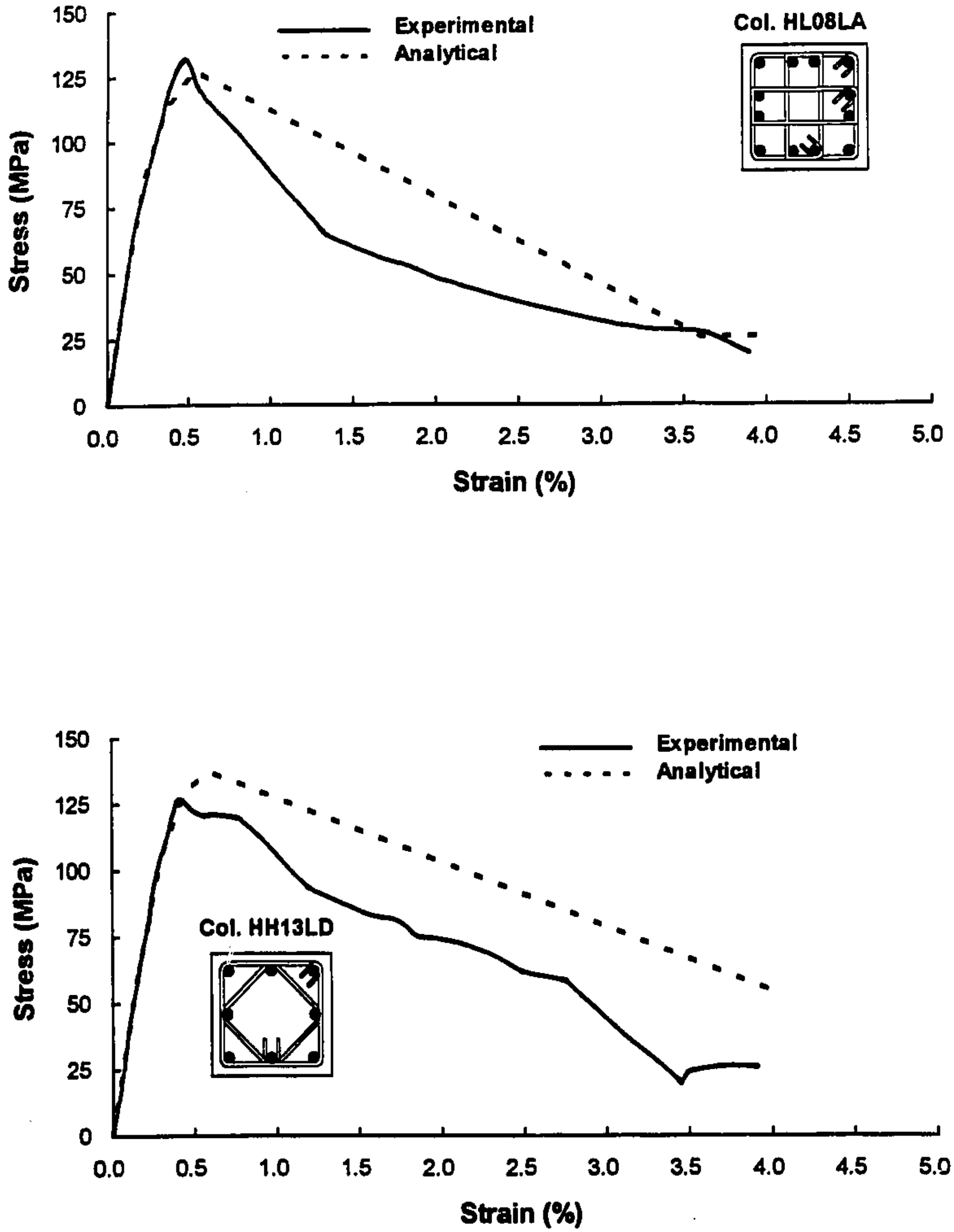

Figure 7.80: Square columns (HL08LA and HH13LD) tested by Nagashima et al. (1992).

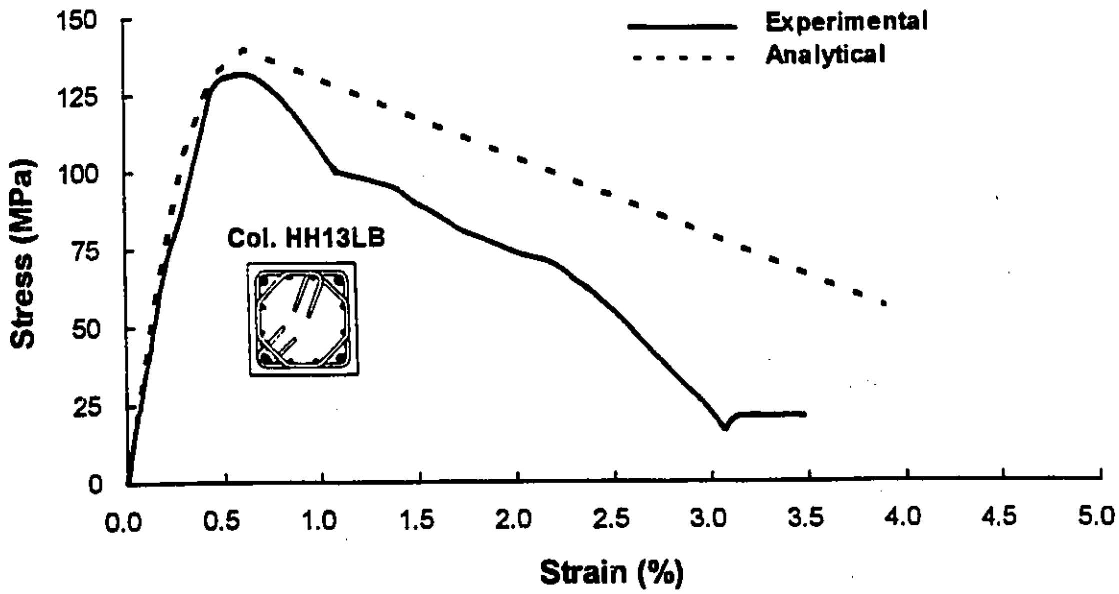

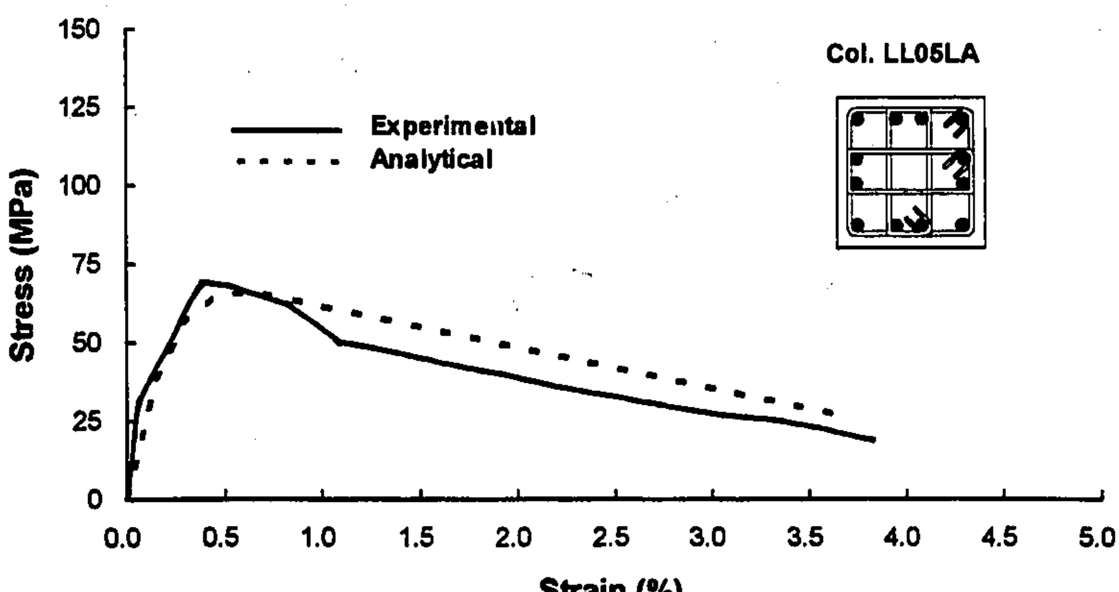

Figure 7.81: Square columns (HH13LB and LL05LA) tested by Nagashima et al. (1992).

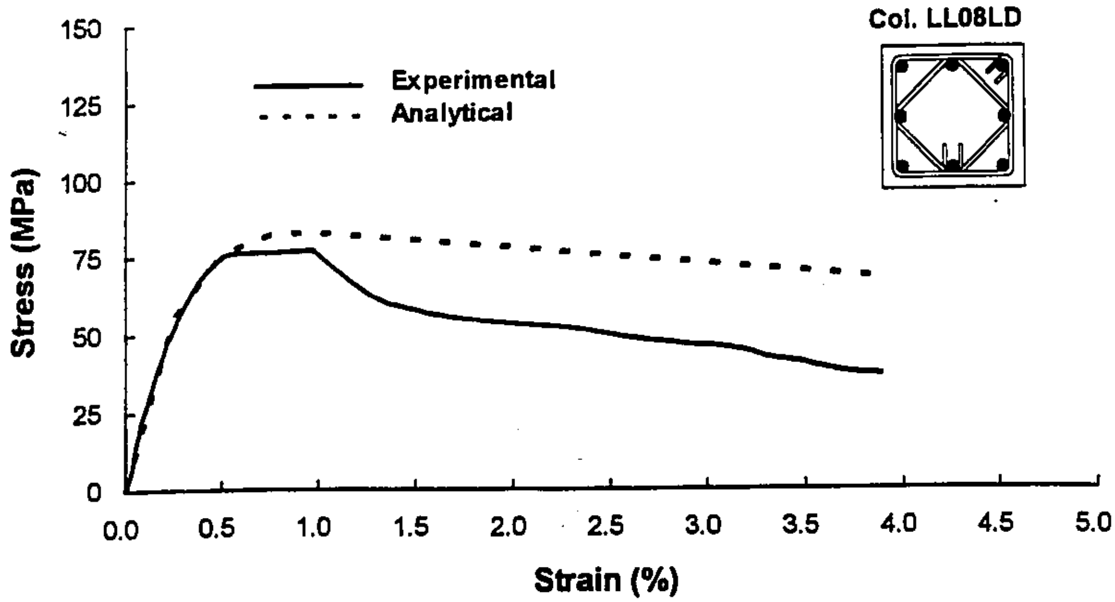

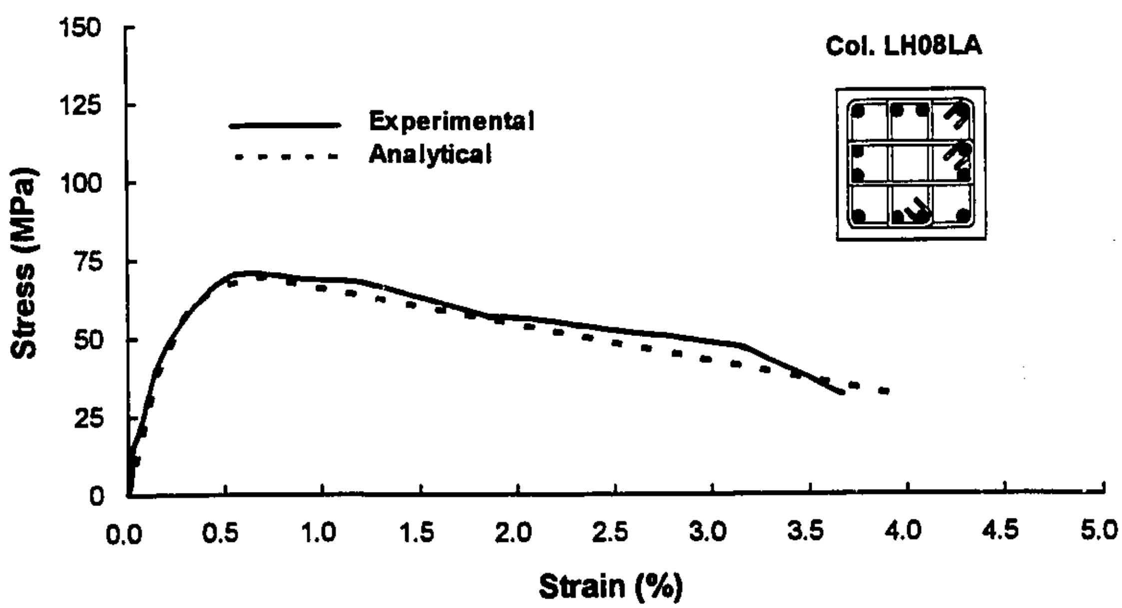

Figure 7.82: Square columns (LL08LD and LH08LA) tested by Nagashima et al. (1992).

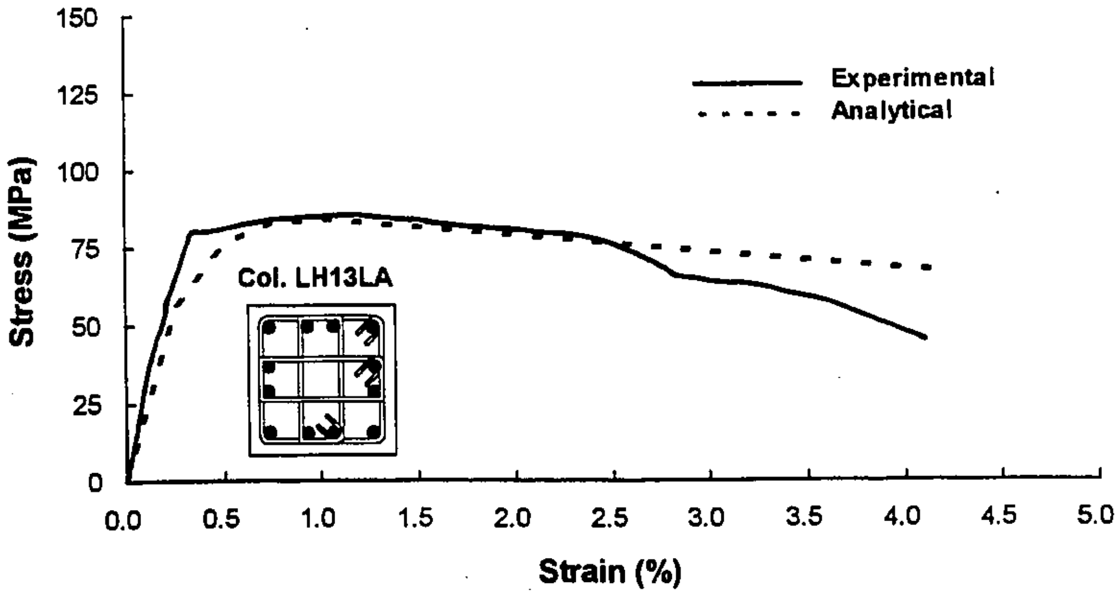

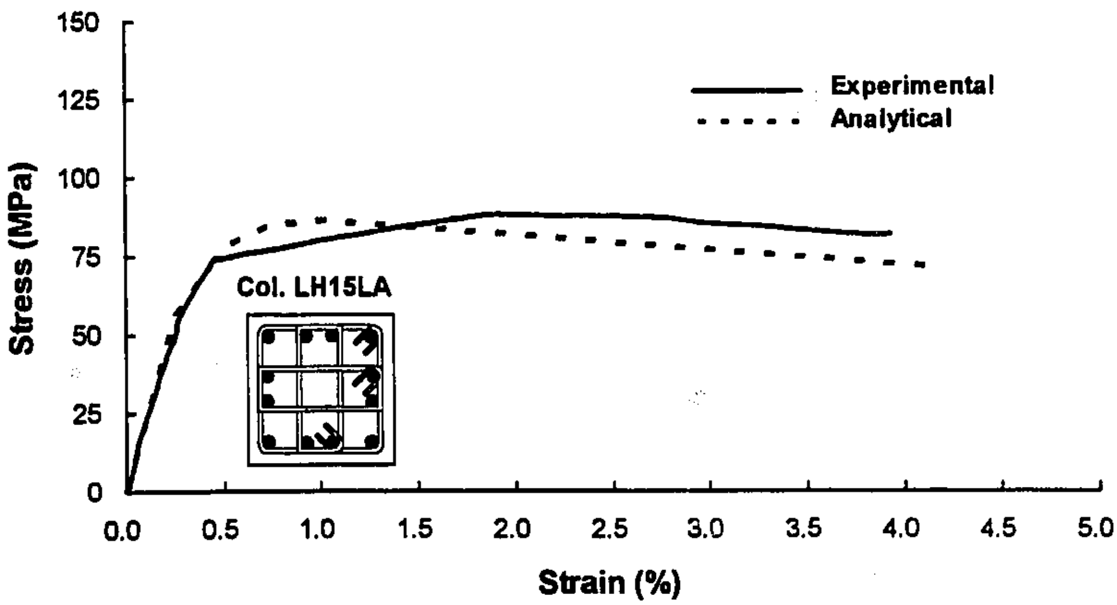

Figure 7.83: Square columns (LH13LA and LH15LA) tested by Nagashima et al. (1992).

Chapter 8

A Displacement Based Design Approach for Column Confinement

8.1 General

Reinforced concrete columns subjected to strong earthquakes may experience a large number of inelastic deformation cycles. Strength and stability of structures supported by such columns depend on deformability of these columns within the inelastic range. Column deformability can be improved significantly through confinement of the core concrete. Therefore, column confinement plays a major role on behavior of reinforced concrete structures during strong earthquakes.

Performance of structures during past earthquakes have demonstrated that the confinement requirements of ACI Building Code (1989), for normal strength concrete, provide satisfactory designs in many applications. However, the same requirements have been shown to produce unsafe column designs in certain cases, while also producing over conservative designs in other cases resulting in congestion of reinforcement, leading to constructibility problems (Saatcioglu 1989, Saatcioglu 1991). On the other hand, the state-of-knowledge on concrete confinement has improved substantially since the pioneering research of Richart et al. in 1928, which formed the basis for the current building code requirements. During the last two decades, a large volume of experimental data have been generated (Saatcioglu 1991), and a number of analytical models have been developed, describing stress-strain characteristics of confined normal strength concrete (Sheikh and Uzumeri 1982, Mander et al. 1988, Saatcioglu and Razvi 1992). The new information, which could eliminate most of the shortcomings of the current design provisions, has not yet found its way into the ACI Building Code. An improved design approach, for normal strength concrete, is presented in this chapter, reflecting recent developments in the area of column confinement.

8.2 Design Parameters

Performance of reinforced concrete columns during recent earthquakes and laboratory tests under simulated seismic loading have clearly demonstrated that a strong relationship exists between lateral drift and column confinement. The drift level imposed on a column during an earthquake varies substantially depending on the characteristics of ground excitation and the framing system. Columns of braced frames are expected to experience little interstory drift, remaining essentially elastic during seismic response. Inelastic deformability of these columns may not require substantial improvements through confinement. Columns of unbraced frames experience significant lateral drift when subjected strong ground excitations. The confinement requirements for these columns must be sufficiently stringent to ensure adequate inelastic deformability. Therefore, lateral drift is a design parameter that plays an important role on the required level of confinement.

The role of concrete becomes more dominant on column performance when the level of axial compression is high. Experiments have shown that the rate of strength decay under reversed cyclic loading increases rapidly with increasing axial compression (Saatcioglu and Ozcebe 1989, Saatcioglu 1991, Sheikh and Khoury 1993, Park et al. 1982, Muguruma et al. 1990). Furthermore, high axial compression combined with high lateral drift results in secondary stresses which produce additional deformations due to P-Δ effect. The P-Δ effect can be very significant, and may potentially lead to stability problems.

Lateral drift and axial compression may be classified as design parameters resulting from the actions imposed on structures during a seismic activity, and may be classified as offensive parameters. Parameters related to confinement reinforcement, on the other hand, may be viewed as defensive parameters, protecting columns against the actions arising from earthquakes. The primary defensive parameters include the amount, grade, spacing and arrangement of lateral confinement reinforcement. The proper combination of these parameters can improve column performance through increased confinement pressure and improved efficiency of this pressure. Confinement pressure can be increased by using high volumetric ratio and/or grade of confinement reinforcement. The efficiency of pressure can be improved by increasing its uniformity. This can be achieved by using an efficient reinforcement arrangement. Closely spaced circular hoops and spirals provide uniform lateral pressure resulting from uniform hoop tension, which can be considered as the most efficient confinement pressure. Rectilinear reinforcement can also provide near uniform pressure when used in the form of closely spaced longitudinal bars, where each bar is laterally supported by the corner of a closed hoop or the hook of a cross tie. Four bar arrangement, sometimes used in square and rectangular sections provide the least efficient reinforcement arrangement, resulting in high pressure peaks near the corners and low lateral pressure between the corners. In all cases, the lateral pressure is generated by tension in transverse reinforcement, which can not be developed unless the tie ends are well anchored into the confined core. Therefore, the tie ends, whether in the form of closed hoops or cross ties, should have bends well anchored into the confined core.

Strength and deformability of concrete are known to be inversely proportional. Therefore, higher strength concretes require higher lateral pressures (Razvi and Saatcioglu 1994). Hence, concrete strength should be considered in establishing the confinement steel requirements. Furthermore, column concrete consists of two different parts, with two distinctly different mechanical properties; unconfined concrete in the cover and confined concrete in the core. As the percentage of confined concrete in a section increases, the beneficial effect of confinement on overall column behavior also increases. A column with large cover area can not maintain most of its original strength beyond the spalling of cover, no matter how well the core concrete is confined. Therefore, in earthquake resistant columns it is advisable to use small cover. The ratio of gross-to-core area is another parameter that needs to be considered in design.

8.3 Current Design Approach

The design approach for column confinement used in CSA Standard A23.3-84 (1984) and ACI Code 318-89 (1989) is based on an arbitrary performance criterion. Accordingly, columns are expected to maintain their concentric capacities at high strain levels when the useful limit of transverse reinforcement is attained beyond the spalling of cover. This performance is achieved if strength and ductility of core concrete are improved sufficiently to account for the loss of strength associated with cover spalling. The amount of transverse reinforcement required to offset the effects of cover spalling can be derived as given in Eq. 8.1. This equation is derived based on the assumption that the increase in concrete strength due to confinement can be expressed as 4.1 times the uniform lateral pressure generated by confinement reinforcement. This is indicated in Eq. 8.2.

$$\rho_s = \left[0.415 \frac{f'_c}{f_{yt}} \left(\frac{A_g}{A_c} - 1 \right) + \frac{4 A_{sp} A_s}{d_s s A_c} \right] \tag{8.1}$$

$$f'_{cc} = 0.85f'_c + 4.1f_l \tag{8.2}$$

The ACI Code has adopted Eq. 8.1 after dropping the second term, and replacing coefficient 0.415 by 0.45. The Code expression is shown in Eq. 8.3.

$$\rho_s = 0.45\left(\frac{A_g}{A_c}-1\right)\frac{f'_c}{f_{yt}} \tag{8.3}$$

Eq. 8.3 gives the volumetric ratio of confinement reinforcement required in a circular column. It is a function of the ratio of the gross cross-sectional area to confined core area (A_g/A_c). Hence, it results in high volumetric ratios for columns with thick concrete covers. Columns with large cross-sectional areas may have A_g/A_c ratios approaching unity while the volumetric ratio requirement given in Eq. 8.3 approaching zero. This may result in unsafe levels of volumetric ratio. Therefore, the ACI Code (1989) provides a lower bound for the volumetric ratio by setting a limit on the A_g/A_c ratio not to be less than 1.25. This translates into Eq. 8.4.

$$\rho_s = 0.12\frac{f'_c}{f_{yt}} \tag{8.4}$$

The above requirements are based on test data obtained from concrete cylinders subjected to uniform hydrostatic pressure or passive confinement pressure provided by circular spirals. Hence, they are applicable to closely spaced spirally reinforced circular columns. Eqs. 8.3 and 8.4 form the volumetric steel requirements of ACI318 (1989) for circular spirals. The confinement steel requirements for square and rectangular columns, in the same building code, are based on an arbitrary extension of the above requirements, while recognizing that rectilinear reinforcement is not as effective as circular reinforcement. The code expression for the required area of rectilinear confinement reinforcement is obtained from Eq. 8.3, based on the premise that rectilinear reinforcement is 3/4 as effective as circular spirals. This implies that 1/3 more steel is needed in rectangular columns to attain deformabilities usually expected of spirally reinforced circular columns. The increased steel requirement, when expressed in terms of the area of lateral reinforcement, translates into Eq. 8.5. The lower limit of confinement reinforcement for rectangular sections is established to produce 50% more rectilinear reinforcement than that establish for spiral steel. This leads to Eq. 8.6.

$$A_{sh} = 0.3\left(sh_c\frac{f'_c}{f_{yt}}\right)\left[\left(\frac{A_g}{A_{ch}}\right)-1\right] \tag{8.5}$$

$$A_{sh} = 0.09sh_c\frac{f'_c}{f_{yt}} \tag{8.6}$$

Eqs. 8.5 and 8.6 give the area of confinement steel required in each cross-sectional direction by ACI318 (1989) for square and rectangular columns. The current ACI318 (1989) design approach does not explicitly address the relationship between lateral drift and corresponding confinement requirement. Instead, the code approach is based on axial deformability of columns under concentric loading, with implications that columns that have axial deformabilities are likely to have lateral deformabilities under seismic loading. Furthermore, axial load level is not a parameter in the current ACI318 (1989) approach. It becomes clear from the foregoing discussion that neither of the two major design parameters related to the actions arising from seismic effects, previously referred to as offensive parameters, is explicitly considered in the current code provisions.

The defensive parameters of confinement relevant to transverse reinforcement are addressed in the code for spirally reinforced circular columns, although they are not linked to the expected levels of lateral drift and axial compression. The design expressions have been derived with due considerations given to the magnitude and efficiency of confinement pressure. However, the code requirements for square and rectangular columns do not include the arrangement of reinforcement and resulting efficiency of confinement pressure as a parameter. Consequently, the difference in behavior between a column with four corner bars tied with perimeter hoops, and a column with well distributed longitudinal reinforcement laterally supported by overlapping hoops and/or cross ties, is not recognized in the code. Furthermore, hoop spacing is not included as a separate parameter other than the maximum spacing limit specified. The trade off between spacing, reinforcement arrangement and volumetric ratio is not considered, limiting flexibility in design, while promoting congestion of reinforcement. These shortcomings of the current ACI318 (1989) design approach are eliminated in the proposed approach, presented in the following section.

8.4 Proposed Design Procedure

The proposed design approach is based on the computation of lateral drift capacity of a column with specific confinement characteristics and imposed axial compression. The amount, grade, spacing, and arrangement of confinement reinforcement are determined for expected levels of lateral drift and axial compression.

The drift capacity is established from inelastic deformations of columns. Tests of reinforced concrete columns under simulated seismic loading indicate that lateral deflection of a column consists of components due to flexure, shear, and anchorage slip. Fig. 8.1 shows experimentally recorded displacement components in a typical test column (Saatcioglu and Ozcebe 1989). While the components due to flexure and anchorage slip may be equally significant, shear deformation in a typical column is negligibly small, forming approximately less than 10% of total displacement. Therefore, the effects of inelastic shear deformations on lateral drift capacity of flexure dominant columns can be ignored for simplicity. Treatment of shear dominant columns, as in the case of short columns, and design against shear forces, are beyond the scope of the procedure described in this chapter. This leaves components due to flexure and anchorage slip to be computed for establishing the lateral drift capacity.

8.4.1 Computation of Displacements due to Flexure

Inelastic displacement of a reinforced concrete column due to flexure can be established by following standard procedures outlined in text books (Park and Paulay 1975, Paulay and Priestley 1992). However, consideration of proper material properties, especially for confined concrete, and proper treatment of progression of plastic hinging are of utmost importance for reliability of results.

The first step in computing flexural displacements involves plane section analysis of the critical section. This requires the consideration of stress-strain characteristics for unconfined cover concrete, confined core concrete, and reinforcing steel with strain hardening. The confined concrete model proposed in Chapter 7 has been selected for the analysis. This model incorporates all the relevant parameters of confinement, and has been verified extensively against circular, square, and rectangular columns with different reinforcement arrangements, tested under concentric, eccentric, and reversed cyclic loadings. Confined concrete strength, f'_{cc}, is expressed in the model in terms of unconfined concrete strength, f'_{co}, and equivalent uniform confinement pressure, f_{le}.

$$f'_{cc} = f_{co} + k_1 f_{le} \tag{8.7}$$

$$k_1 = 6.7 (f_{le})^{-0.17} \tag{8.8}$$

$$f_{le} = k_2 \, f_l \tag{8.9}$$

The average lateral pressure, f_l, is computed by dividing the summation of yield forces in transverse reinforcement by the core area perpendicular to these forces. While the average pressure is representative of the actual uniform lateral pressure that develops in spirally reinforced circular columns, it is not representative of non-uniform pressure generated in square and rectangular columns. The confinement pressure resulting from closely spaced longitudinal and transverse reinforcement approaches uniform average pressure, while that resulting from four corner bars and perimeter hoops show significant variation in pressure between the corners. The average pressure needs to be reduced in the latter case before it can be used as equivalent uniform pressure. This is done through coefficient k_2. This coefficient reflects the reinforcement arrangement and the resulting efficiency in lateral pressure, and is equal to 1.0 for spirally reinforced circular columns and less than or equal to 1.0 for square and rectangular columns. Coefficient k_2 is used in the design procedure to introduce efficiency of reinforcement arrangement as a design parameter.

Moment-curvature relationships for square columns are computed and compared with those recorded experimentally. The comparisons shown in Figures 8.2 through 8.8 indicate good agreement between analytical and experimental sectional response.

Once the sectional moment-curvature relationship is determined for a given axial load level, the variation of curvature along column height can be established as illustrated in Fig. 8.9. The curvature diagram assumes different shapes depending on the stage of loading. As the moment capacity of the critical section is exceeded, the column resistance gradually drops, while the curvatures near the critical section continue increasing. This results in gradual formation of a plastic hinge which propagates towards the elastic region until it is fully developed. Fig. 8.9 illustrates the progression of plastic hinge in a column. The curvature diagram can then be used to compute inelastic rotation and resulting displacement as the area, and moment of the area under the curvature diagram, respectively. Fig. 8.10 illustrates comparisons of analytically obtained moment-flexural rotation relationships with envelopes of hysteretic relationships recorded during cyclic load tests. The comparisons shown in Figs. 8.2 through 8.8 and 8.10 indicate that flexural force-deformation relationships for columns can be established fairly accurately using the procedure described above, with the material models adopted.

8.4.2 Computation of Displacements due to Anchorage Slip

Deformations due to anchorage slip are caused by slippage and/or extension of longitudinal reinforcement within the adjoining member. Hence they are not included in the flexural analysis discussed earlier. These deformations can be as significant, and sometimes even more significant than those caused by flexure, increasing lateral drift and associated P-Δ effects. Omission of these deformations may lead to erroneous results, especially when significant yielding of longitudinal tension reinforcement is expected.

The extension of reinforcement in the adjoining member can not be prevented if the critical column section is located at the ends. It accounts for a major portion of total member end rotation due to anchorage slip. Hysteresis loops due to reinforcement extension is similar to those obtained for flexure, showing stable loops dissipating seismic induced energy. The other component of anchorage slip, caused by the slippage of reinforcement, however, results in significant pinching of the loops, and should be prevented to the extent possible through proper anchorage. The combination of extension and slippage of reinforcement is referred to as anchorage slip.

The anchorage slip deformation may form a significant portion of total lateral drift demand, especially in columns with relatively small axial compression. In this case, the remaining lateral drift due to flexure may not be high enough to justify stringent confinement requirements. On the other hand, if the drift component due to anchorage slip is excessive, it may lead to high P-Δ moments and a faster rate of strength degradation in the lateral load capacity. Furthermore, deformations due to anchorage slip are related to the strain condition at the critical column section, which is influenced by concrete confinement. Therefore, there is a close relationship between the confinement requirements, which are meant to improve behavior of column concrete in compression, and anchorage slip, that occurs outside the confined end regions. Consequently, anchorage slip must be an integral part of a displacement based design procedure for column confinement.

The analytical model recently proposed by Alsiwat and Saatcioglu (1992) has been adopted here to compute deformations resulting from anchorage slip. The model incorporates yield penetration and associated inelasticity in anchored reinforcement, as well as possibility of slip within this region. It can be used relatively easily, making it especially suitable for design. Inelastic deformations due to extension and slip are treated separately in this model. Extension of anchored reinforcement is computed by integrating the strains in reinforcement. Fig. 8.11 illustrates the assumed strain distribution along the straight lead length of a re-bar. The length of each region, shown in the figure, can be established from equilibrium of forces. This leads to Eq. 8.10.

$$L = \frac{\Delta f_s d_b}{4u} \tag{8.10}$$

Where, L represents the length of each region, L_e, L_{yp}, or L_{sh}, and Δf_s is the corresponding incremental steel stress between the beginning and end of each region. Diameter of reinforcement is denoted by d_b. The bar force is partially developed within each region depending on bond stress, u, between the concrete and steel. Frictional bond stress, u_f, and elastic bond stress, u_e, are used for inelastic and elastic regions, respectively. The inelastic region consists of strain hardening and yield plateau.

A local bond-slip model is used to establish the bar slip. Bar slip occurs only if the bar is strained to the cut-off point. In this case, the bond stress within the available elastic length is computed from Eq. 8.10, and the resulting value is used to obtain the corresponding bar slip from the bond-slip model. The details of the procedure, as well as hooked bars, and bars subjected to pull and push, are discussed elsewhere (Alsiwat and Saatcioglu 1992). Extensive verification of the model is also presented in the same reference. Figs. 8.12 and 8.13 includes some of the comparisons on pull out tests.

Bar slip and/or extension of reinforcement, δ_{as} results in member end rotations at column ends. This rotation, θ_{as}, and corresponding deflection, Δ_{as}, can be computed as shown below:

$$\theta_{as} = \frac{\delta_{as}}{d-c} \qquad \textbf{(8.11)}$$

$$\Delta_{as} = \theta_{as} H \qquad \textbf{(8.12)}$$

Where, d and c represent the effective section depth and neutral axis location, respectively. Column height at which deflection (Δ_{as}) is computed, is denoted by H.

Analytical rotations obtained by Eq. 8.11 are compared with those recorded experimentally in Fig. 8.14. The comparisons indicate that the procedure described above and the analytical model adopted can be used to obtain force-anchorage slip deformation relationships fairly accurately.

8.4.3 Maximum Usable Column Displacement and Drift Capacity

Superposition of displacement components due to flexure and anchorage slip gives total lateral displacement. Figs. 8.15 through 8.18 depict comparisons of analytically obtained total column displacements with those recorded experimentally. The comparisons, including ascending and descending branches of force-displacement relationships, show good correlations within a wide range of axial compression values.

Drift capacity is obtained when a column reaches its maximum usable lateral load capacity, beyond which it can be declared to have failed. During response to strong earthquakes confined columns of multistorey multi-bay frame systems do not fail immediately after the attainment of their peak loads. Instead, they continue carrying a significant portion of their peak load while deforming and dissipating seismic induced energy beyond the peak. It is generally believed that a well designed reinforced concrete element can tolerate some strength decay without jeopardizing strength and stability of the structure. In seismic design, where critical members are designed and detailed for inelasticity, it would be unduly conservative to take the displacement corresponding to peak load as the limiting displacement for design purposes. In this design approach, the displacement corresponding to 20% strength decay beyond the peak has been adopted as the maximum usable displacement beyond which the column can be considered to have failed. The maximum usable displacement and the corresponding lateral force capacity are obtained from force-displacement relationship under monotonic loading. It is assumed that the monotonic force-displacement curve is representative of the envelope of the force-displacement hysteretic relationship under reversed cyclic loading. Hence the definition of maximum displacement adopted here is consistent with that used earlier by Saatcioglu (1991) for columns under reversed cyclic loading. The maximum usable lateral displacement is divided by unsupported column height to obtain lateral drift capacity.

8.4.4 Design Aids

The drift capacity of a column with specific confinement characteristics and axial compression can be established by following the procedure described in previous sections. The drift capacity is then compared with the expected drift level (drift demand) for the ground motion expected in a given area of seismicity and soil conditions, and for the framing system used. Procedures used to calculate drift demand are not discussed in this chapter, and can be found elsewhere (Qi and Moehle 1991). If the drift capacity is different than the expected drift level, the iterative design process starts, and the procedure is repeated with a revised confinement reinforcement until a reasonable agreement is attained between the expected drift level and the provided drift capacity. Although the steps outlined above are straight forward to follow, the numerical procedure involved can be prohibitively excessive for design applications, unless a computer software is available. Therefore, a design table was generated for columns with different geometric and material properties, illustrating relationships between axial compression and drift capacity for columns with different confinement reinforcement. These relationships are also shown in Figure 8.19 for selected columns.

Table 8.1 provides a complete set of design data for four levels of confinement efficiency (arrangement and spacing of reinforcement as reflected by k_2) and three levels of A_g/A_c ratio. This table can be used to obtain reinforcement ratio ρ_c required for a given axial load, expected drift level, and reinforcement arrangement. The reinforcement ratio ρ_c is defined as the total area of transverse reinforcement in one direction (A_{st}) divided by the centre-to-centre spacing between the ties, s, and the core dimension, b_c perpendicular to the reinforcement. This is expressed in Eq. 8.13. The core dimension b_c is measured between the centre lines of perimeter hoops.

$$\rho_c = \frac{\sum A_{st}}{s\, b_c} \tag{8.13}$$

The test data used in developing the confinement model, for normal strength concrete, had $\rho_c < 2\%$ (or $\rho_s < 4\%$). Therefore, this value may be taken as the upper limit of reinforcement ratio for the proposed design procedure. Coefficient k_2, reflecting the efficiency of confinement reinforcement, is given below.

$$k_2 = 0.15\sqrt{\left(\frac{b_c}{s}\right)\left(\frac{b_c}{s_l}\right)} \leq 1.0 \tag{8.14}$$

For the most efficient reinforcement arrangement, i.e., closely spaced spirally reinforced circular columns $k_2 = 1.0$. For square and rectangular columns $k_2 < 1.0$, and may be approaching 1.0 only when closely spaced overlapping hoops and cross ties with closely spaced longitudinal reinforcement are used, producing near uniform confinement pressure. Eq. 8.14 implies that the same k_2 can be attained either by reducing the spacing of transverse reinforcement along column height, s, or by reducing the spacing of cross ties or hoop legs supporting longitudinal reinforcement in cross-sectional plane, s_l. The spacing quantities for rectilinear columns can be determined conveniently if Eq. 8.14 is re-written in the following form:

$$\left(\frac{b_c}{s}\right)\cdot\left(\frac{b_c}{s_l}\right) = 44\,(k_2)^2 \tag{8.15}$$

While Eq. 8.15 indicates that a trade off between s and s_l is possible to arrive at the same confinement efficiency (k_2), this trade off is limited by the maximum spacing limits specified in the next section.

The confinement model that forms the basis for the design procedure is applicable to square and rectangular sections with different confinement pressures in two orthogonal directions. While this generality is maintained in the design procedure, the following simplifying assumption is introduced in developing the design table. The assumption involves the use of equal confinement reinforcement ratio in each cross-sectional direction for square and rectangular columns, as in the case of current ACI318 requirements (ACI Code 1989). This assumption reflects the current practice and is not expected to hinder the design process.

It is to be noted that reinforcement arrangements used in rectangular sections may lead to different k_2 values in two cross-sectional directions. Therefore, when k_2 computed for one cross-sectional direction $(k_2)_1$, using $(b_c)_1$ and $(s_l)_1$ is not equal to k_2 computed in the other direction $(k_2)_2$, using $(b_c)_2$ and $(s_l)_2$, then k_2 can be calculated from the following equation;

$$k_2 = \frac{(k_2)_1\ (b_c)_1 + (k_2)_2\ (b_c)_2}{(b_c)_1 + (b_c)_2} \tag{8.16}$$

Table 8.1 was generated using a 600 mm square column section, with a total story height of 3.0 m. The columns were reinforced with 2% longitudinal reinforcement, equally distributed along the perimeter of the section. Straight bars were assumed in the anchorage region with 28 mm bar diameter. Concrete cylinder strength was 40 MPa and longitudinal and transverse steel grades were 400 MPa. The strain hardening in reinforcement was considered starting at 1% strain, and following a parabolic variation up to 10% strain at 560 MPa. The use of this design table for other columns requires assessment of the significance of these parameters on lateral drift. Therefore, an extensive parametric study was conducted. The parameters considered in this study include column height-to-width ratio, cross-sectional size and shape, aspect ratio of cross-section, distribution and percentage of longitudinal reinforcement, concrete strength, and bar size. The results are presented in Figures 8.20 through 8.25 and indicate that while these parameters have some effects on drift capacities, the effects are small, and in most cases negligible. Therefore, Table 8.1 can be used for all concrete columns that meet the spacing and reinforcement ratio limitations specified in this paper, and also conform to the requirements of ACI318 Building Code (1989), other than those for confinement.

Table 8.1 incorporates the effects of material strengths through $\rho_c f_{yt}/f'_c$ ratio. It was found in the parametric study that the reduction in drift capacity associated with an increase in concrete strength can be offset by an increase in confinement reinforcement ratio ρ_c, proportional to the increase in concrete strength. A review of experimental data on high-strength concrete columns has also shown that the lateral confinement pressure for high-strength concrete columns should be increased proportional to the increase in concrete strength to attain deformabilities expected in lower strength concrete columns (Razvi and Saatcioglu 1994). Therefore, the $\rho_c f_{yt}/f'_c$ ratio has been adopted in Table 8.1. However, it is recommended that the current ACI318 (1989) limit of 400 MPa be used for lateral confinement reinforcement (f_{yt}) for columns with normal-strength concrete.

8.4.5 Maximum Spacing Limitation

Most building codes provide maximum spacing limitations for transverse reinforcement as governed by confinement, shear, and stability of longitudinal reinforcement. Researchers have shown that transverse reinforcement with a spacing equal to 1.25 times the cross-sectional dimension, h, do not produce the beneficial effects of confinement (Ahmed and Shah 1982). Razvi and Saatcioglu (1989) indicated that transverse reinforcement with a spacing of $b_c/2$ show beneficial effects of confinement, degree of which depends on other parameters. On the other hand, the maximum spacing of transverse reinforcement, as governed by shear, is specified as h/2 in the building code (ACI318 1989).

An important aspect of design for confinement is the consideration of longitudinal bar stability under compression, especially within the inelastic range. Recent research on stability of longitudinal reinforcement indicates that a spacing of 6 times the longitudinal bar diameter or 150 mm (6 in) can be used as a limit for bar buckling (Paulay and Priestley 1992). This suggests that the current absolute limit of 100 mm (4 in) (ACI318 1989) can be relaxed, especially if a design procedure like the one proposed in this paper is employed, allowing the trade off between the spacings in the vertical and horizontal planes, s and s_l, respectively. The smaller of the following limits can then be used as the maximum spacing of transverse confinement reinforcement, s_{max}:

- One-half of the minimum core dimension ($b_c/2$).
- Six times the longitudinal bar diameter.
- 150 mm (6 in).

The effect of the spacing of laterally supported longitudinal reinforcement, s_l is included in the design procedure, and no further spacing limit is necessary for s_l, other than that indirectly imposed by the requirements set on the minimum number of longitudinal bars ACI318 (1989).

The design procedure is also applicable to columns reinforced with circular spirals confirming to the above spacing limitations and with a minimum of six longitudinal bars.

8.5 Application of Design Procedure to High-Strength Concrete Columns

The design procedure presented in this chapter was developed for confinement of normal-strength concrete columns. The procedure is based on the computation of lateral drift capacity of columns, which has two potentially significant components; flexure and anchorage slip. The procedure used for computation of the flexural component is equally applicable to high-strength concrete columns, since the confined concrete model used is applicable to both normal-strength and high-strength concrete columns. However, the applicability of the procedure used for anchorage slip deformations to high-strength concrete columns requires verification against test data. At this time, however, there is little experimental data available to verify and/or modify the elements of the anchorage slip model developed by Alsiwat and Saatcioglu (1992) for high-strength concrete columns. While the design procedure itself is independent of concrete strength, the design aid developed in this chapter can not be used for high-strength concrete columns, prior to verification against experimental data.

Table 8.1 Lateral Drift Capacities for Reinforced Concrete Columns

$\rho_c = A_{st} / (b_c\, s)$ $\qquad k_2 = 0.15 \sqrt{(b_c/s)(b_c/s_l)}$ $\qquad P_o = 0.85\, f'_c\, (A_g - A_s) + A_s\, f_y$

		Lateral Drift Capacity (%)											
	P/P_0	0.20			0.40			0.60			0.80		
$\rho_c\, f_{yt}/f'_c$ (%)	A_g/A_c k_2	1.2	1.4	1.6	1.2	1.4	1.6	1.2	1.4	1.6	1.2	1.4	1.6
Unconfined concrete		1.6	1.6	1.6	1.0	1.0	1.0	0.7	0.7	0.7	0.3	0.3	0.3
	0.25	3.0	2.6	2.2	1.3	1.2	1.2	1.0	1.0	1.0	0.5	0.4	0.4
4.0	0.50	3.3	2.9	2.4	1.4	1.3	1.2	1.1	1.1	1.1	0.6	0.5	0.4
	0.75	3.5	3.2	2.6	1.5	1.4	1.3	1.1	1.1	1.1	0.8	0.6	0.5
	1.00	3.6	3.4	2.9	1.7	1.4	1.3	1.2	1.1	1.1	1.0	0.7	0.6
	Circular		2.6	2.1	1.6	1.4	1.3	1.2	1.1	1.1	1.0	1.0	1.0
	0.25	4.6	4.1	3.0	1.8	1.4	1.3	1.1	1.1	1.1	0.8	0.6	0.5
8.0	0.50	5.4	4.9	3.9	2.3	1.8	1.4	1.3	1.2	1.1	1.2	0.8	0.6
	0.75	6.1	5.5	4.6	2.8	2.2	1.7	1.6	1.3	1.2	1.3	1.1	0.8
	1.00			5.2	3.2	2.6	2.0	1.8	1.5	1.3	1.5	1.3	1.0
	Circular		4.5	3.2	2.6	1.9	1.5	1.8	1.4	1.2	1.4	1.2	1.2
	0.25		5.5	4.0	2.5	1.8	1.3	1.4	1.2	1.1	1.1	0.7	0.6
12.0	0.50			5.4	3.3	2.5	1.8	1.8	1.4	1.2	1.4	1.1	0.8
	0.75				4.1	3.2	2.3	2.3	1.8	1.4	1.7	1.4	1.1
	1.00				4.9	3.9	2.9	2.7	2.2	1.6	2.0	1.6	1.3
	Circular			4.5	3.8	2.8	1.8	2.5	1.8	1.4	1.9	1.4	1.2
	0.25		6.4	4.9	3.1	2.2	1.5	1.7	1.2	1.1	1.2	0.9	0.6
	0.50				4.3	3.3	2.3	2.4	1.8	1.3	1.7	1.3	1.0
16.0	0.75				5.4	4.3	3.1	3.1	2.4	1.7	2.2	1.8	1.3
	1.00					5.0	3.7	3.8	3.0	2.3	2.6	2.3	1.6
	Circular			5.5	4.9	3.6	2.2	3.1	2.2	1.5	2.4	1.7	1.3

Notes:

1. **Reinforcement ratio ρ_c is to be provided in each cross-sectional direction.**
2. **The blanks in the table indicate rupturing of longitudinal tension reinforcement prior to 20% strength decay due to concrete crushing.**

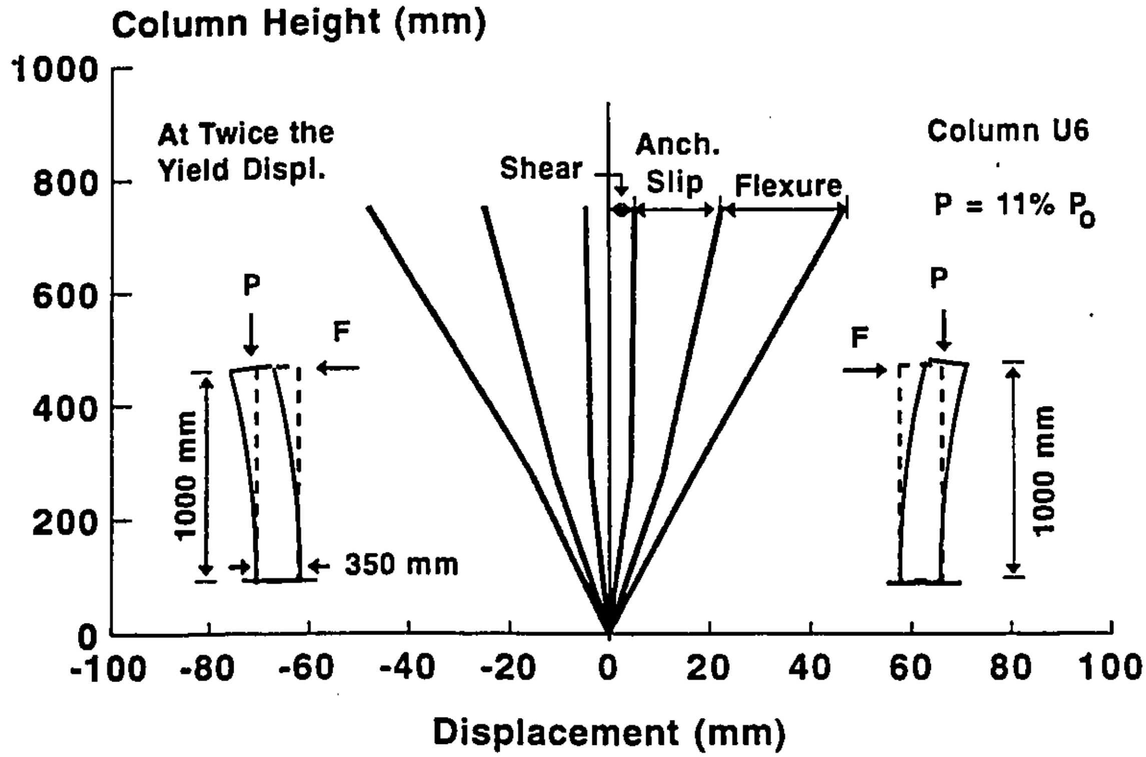

Figure 8.1: Components of displacement in a typical test column (Saatcioglu and Ozcebe 1989).

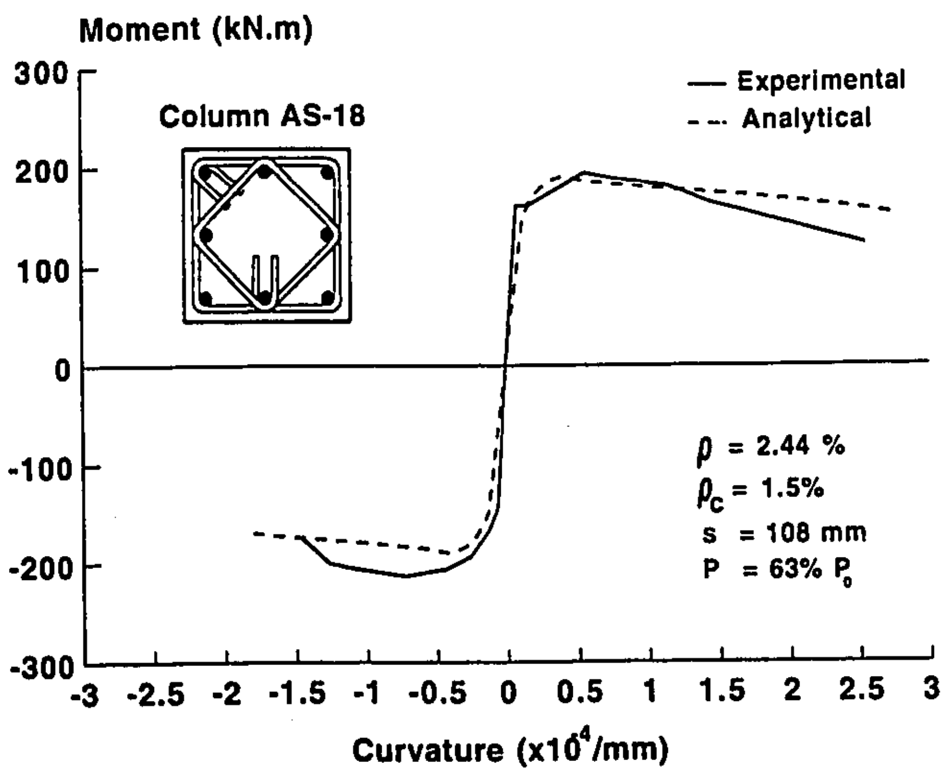

Figure 8.2: Comparison of analytical and experimental moment- curvature envelopes for column AS-18 tested under reversed cyclic loading (Sheikh and Khoury 1993).

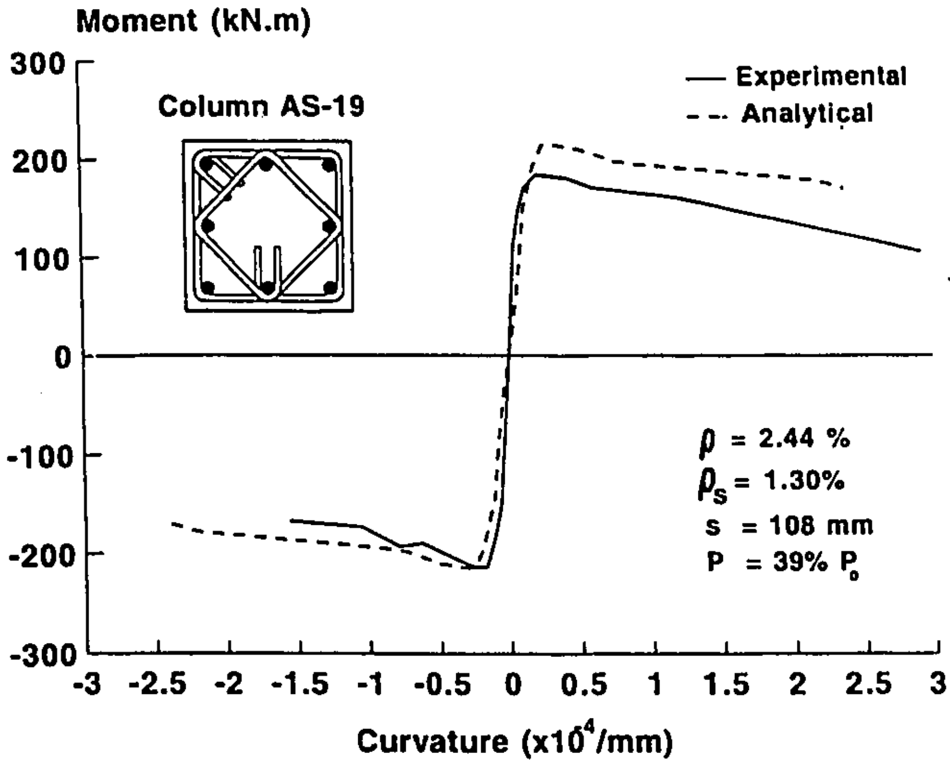

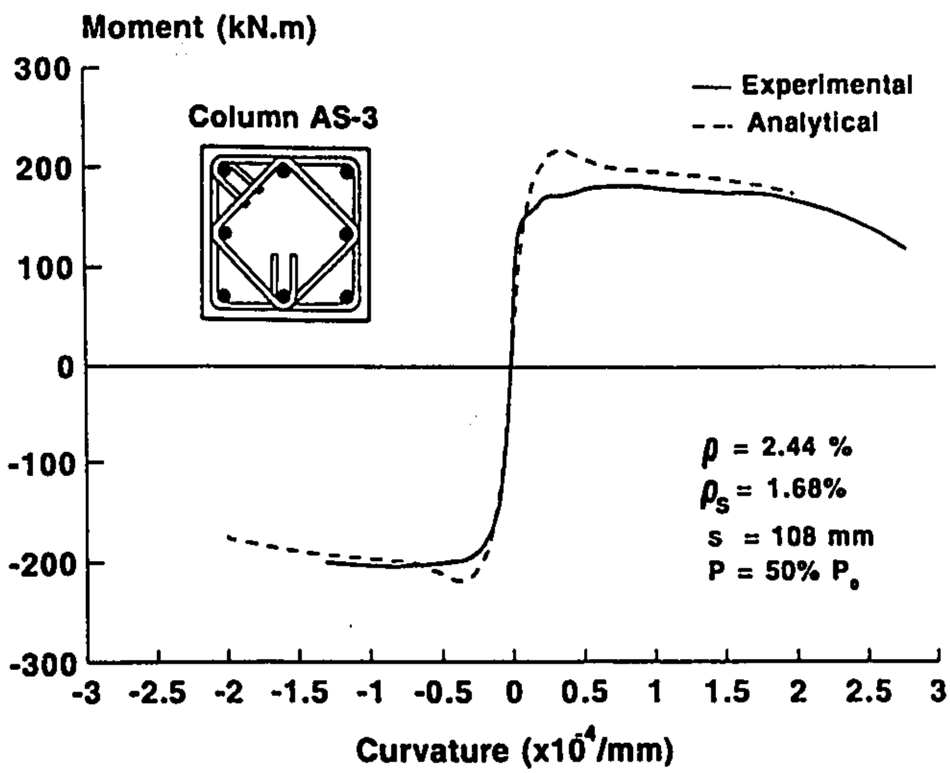

Figure 8.3: Comparison of analytical and experimental moment curvature envelopes for columns AS-19 and AS-3 tested under reversed cyclic loading (Sheikh and Khoury 1993).

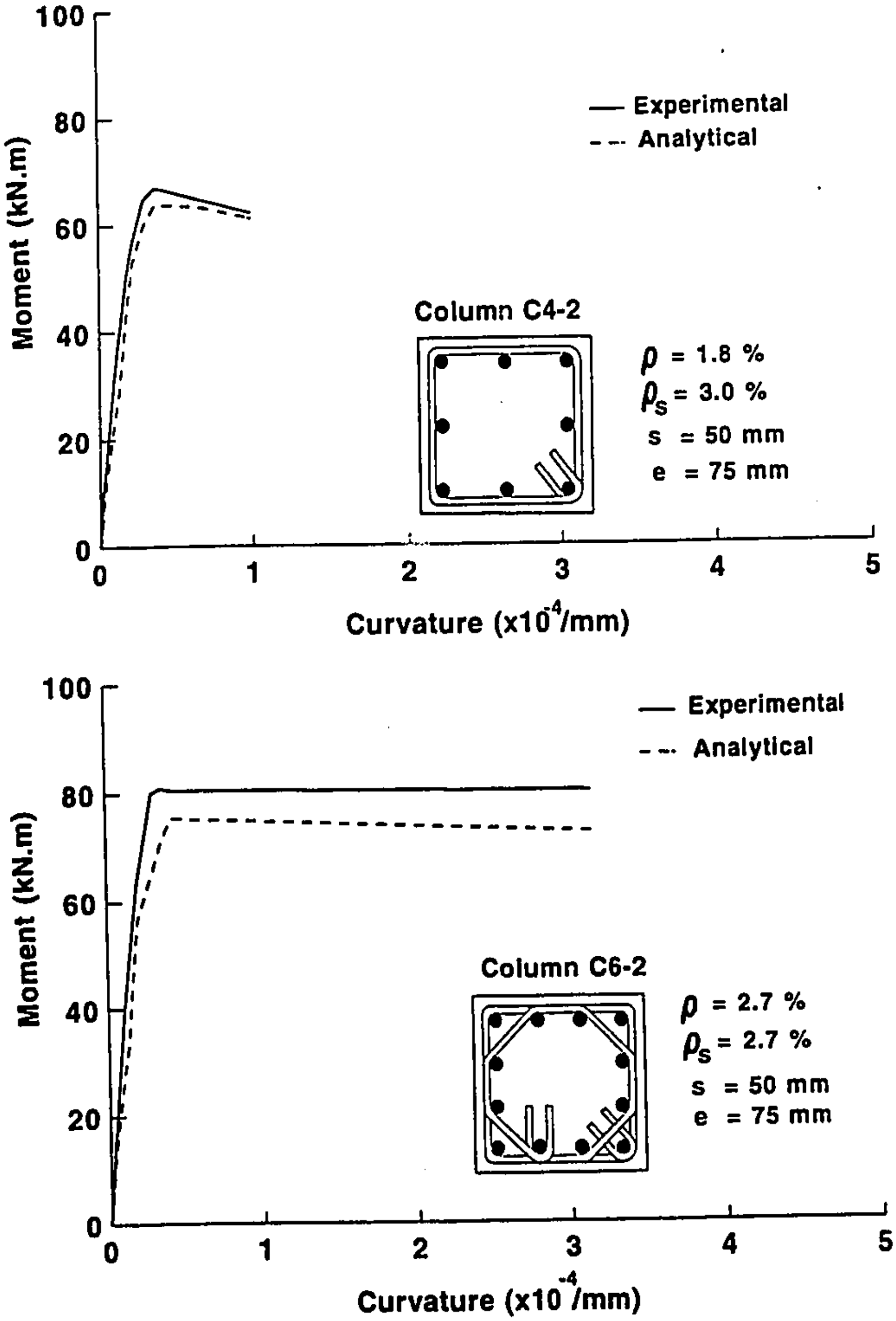

Figure 8.4: Comparison of analytical and experimental moment curvature relationships for columns C4-2 and C6-2 tested under monotonically increasing axial compression (Saatcioglu et al. 1995).

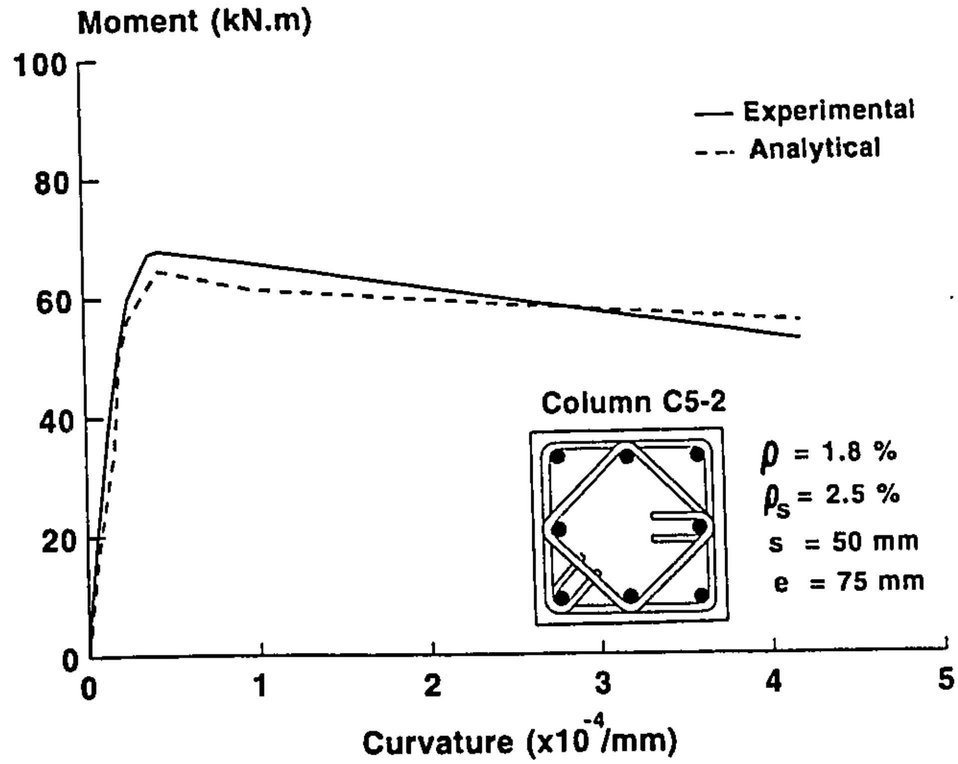

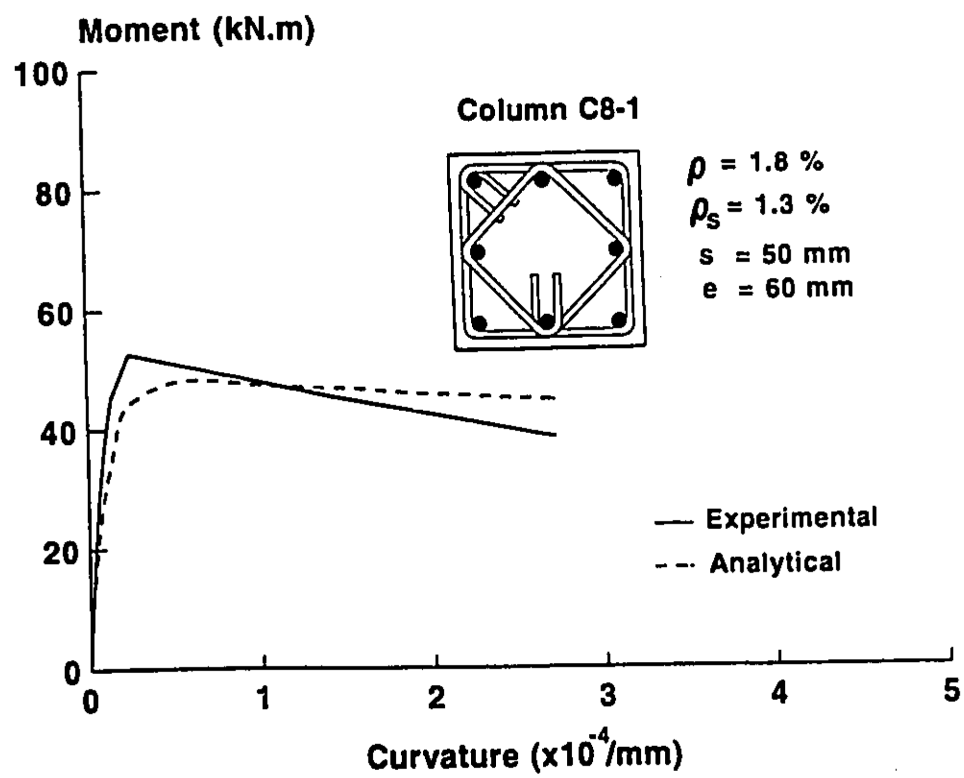

Figure 8.5: Comparison of analytical and experimental moment curvature relationships for columns C5-2 and C8-1 tested under monotonically increasing axial compression (Saatcioglu et al. 1995).

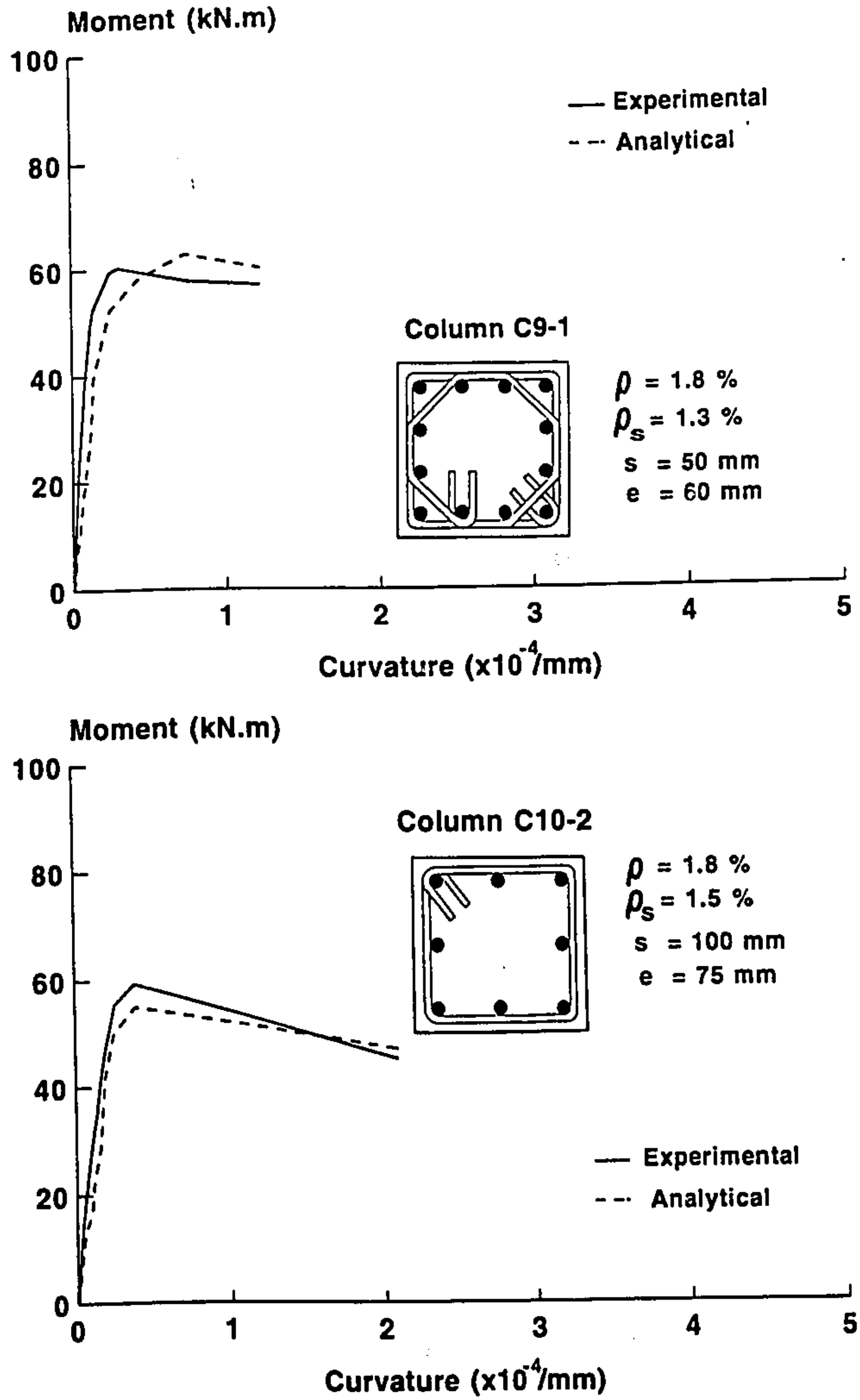

Figure 8.6: Comparison of analytical and experimental moment curvature relationships for columns C9-1 and C10-2 tested under monotonically increasing axial compression (Saatcioglu et al. 1995).

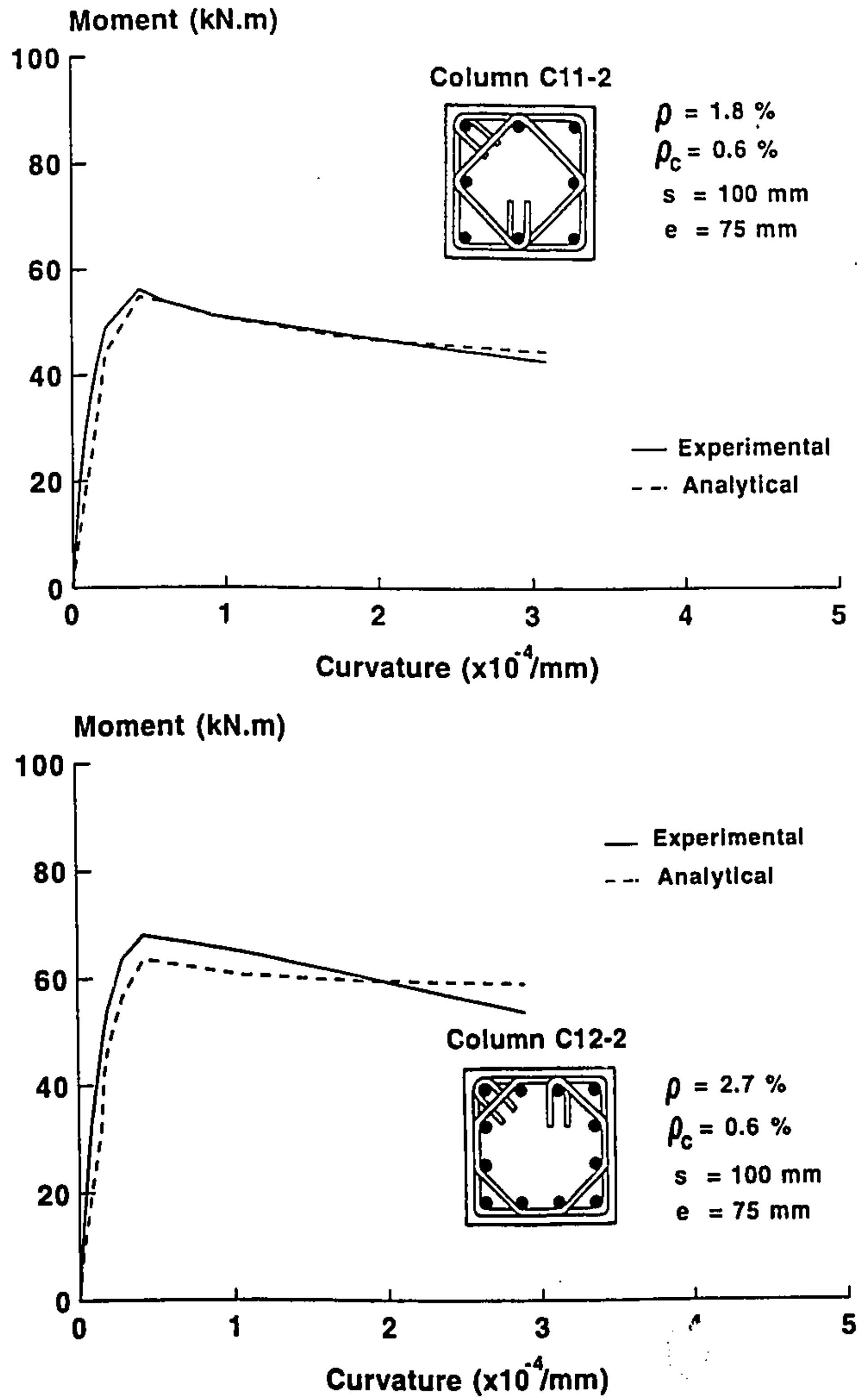

Figure 8.7: Comparison of analytical and experimental moment curvature relationships for columns C11-2 and C12-2 tested under monotonically increasing axial compression (Saatcioglu et al. 1995).

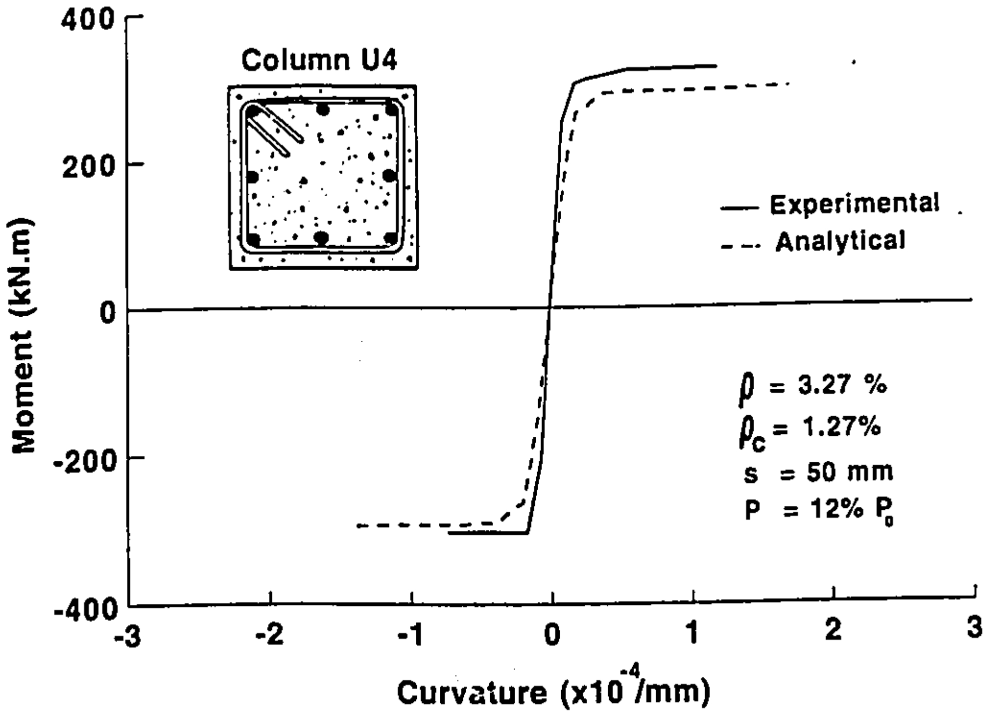

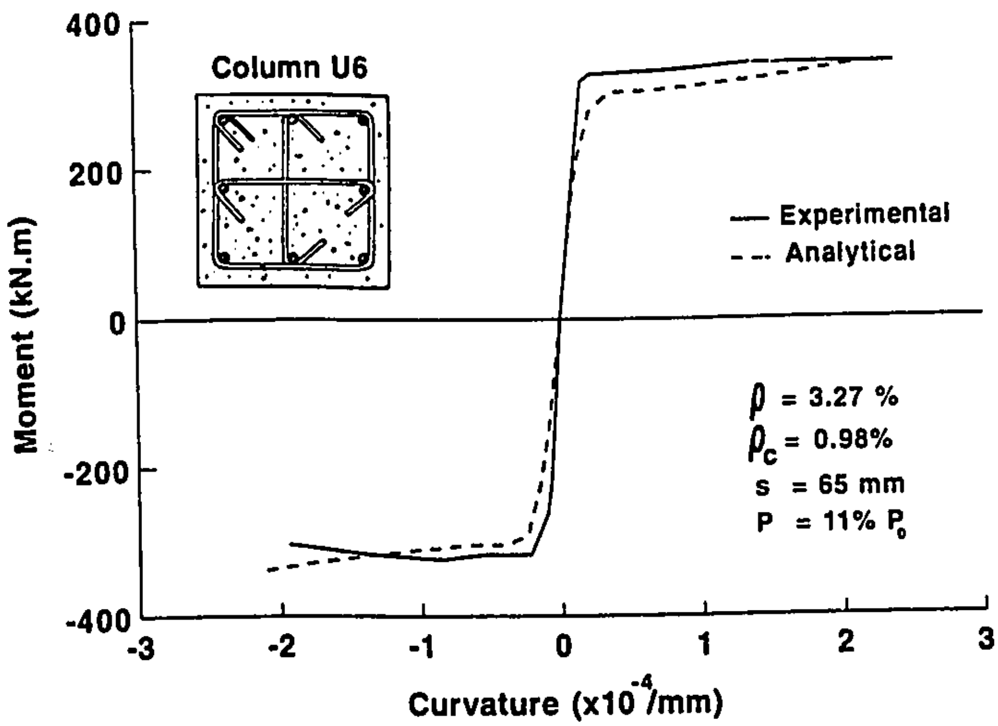

Figure 8.8: Comparison of analytical and experimental moment curvature envelopes for columns U4 and U6 tested under reversed cyclic loading (Saatcioglu and Ozcebe 1989).

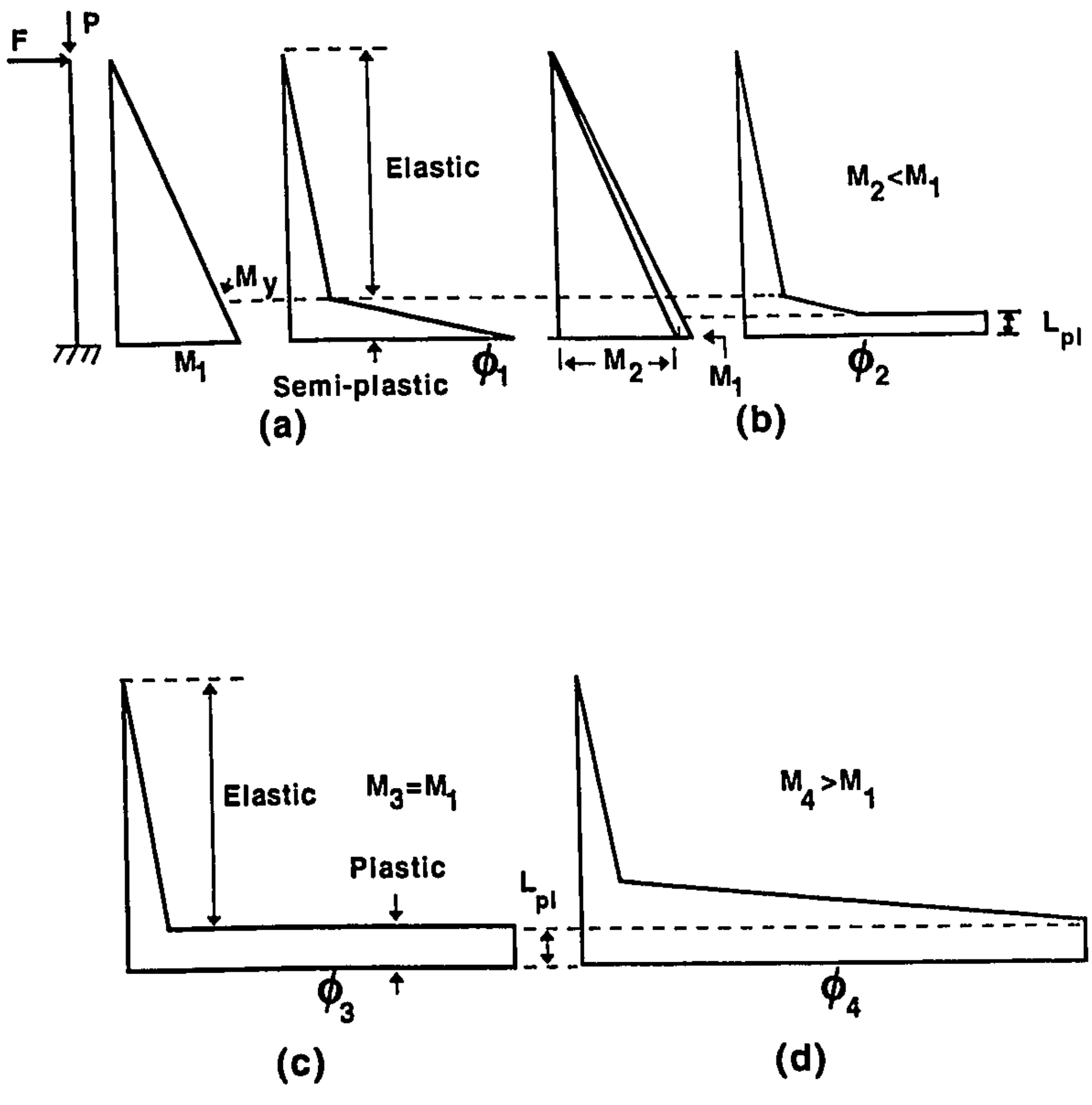

Figure 8.9: Progression of a plastic hinge.

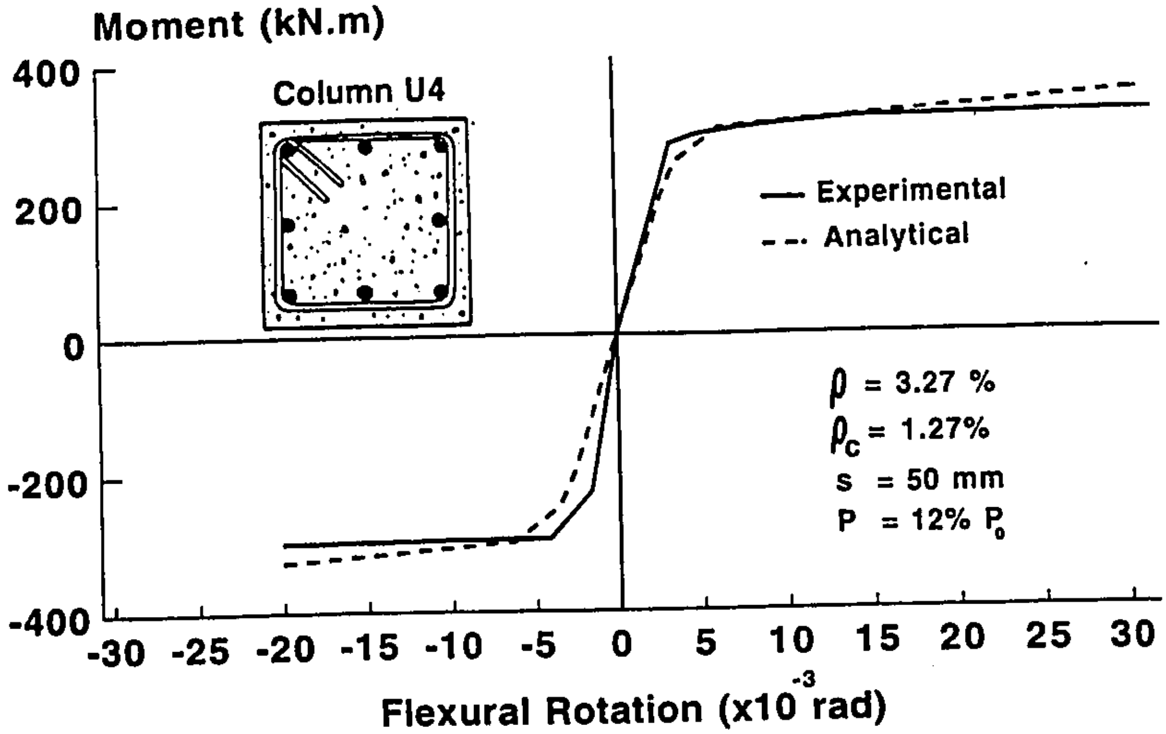

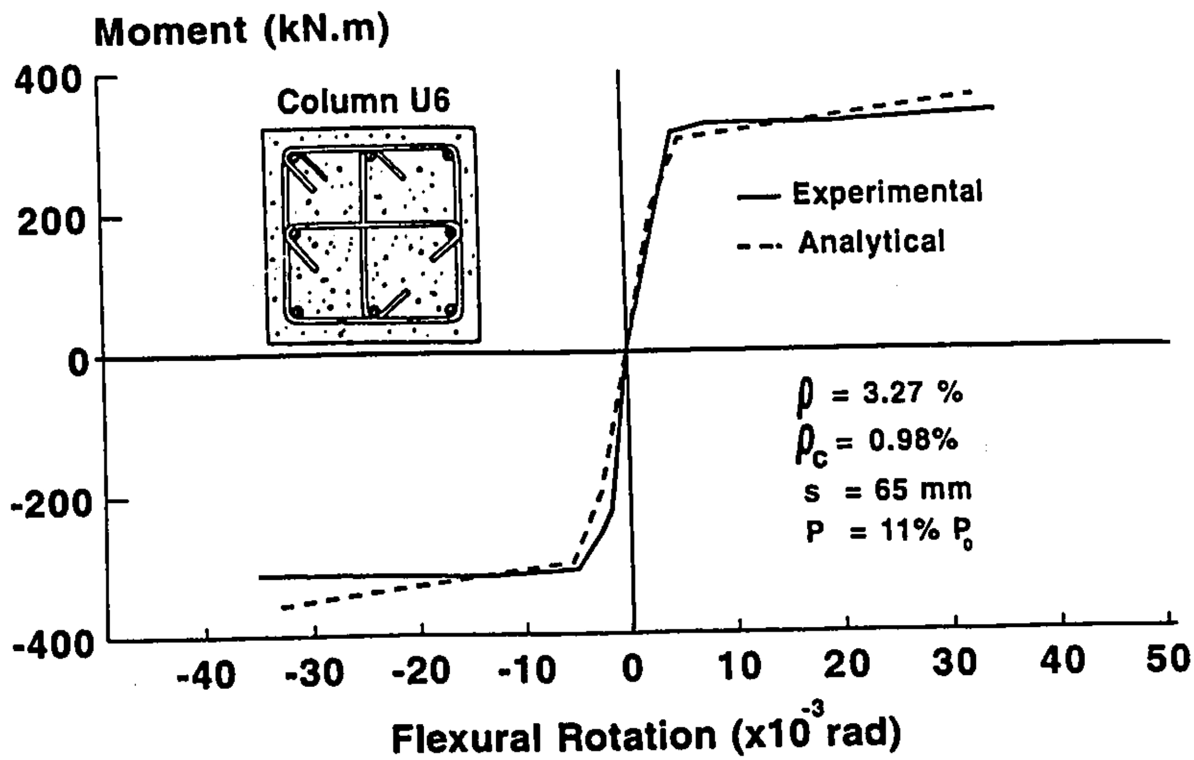

Figure 8.10: Comparisons of moment-flexural rotation relationships (Saatcioglu and Ozcebe 1989).

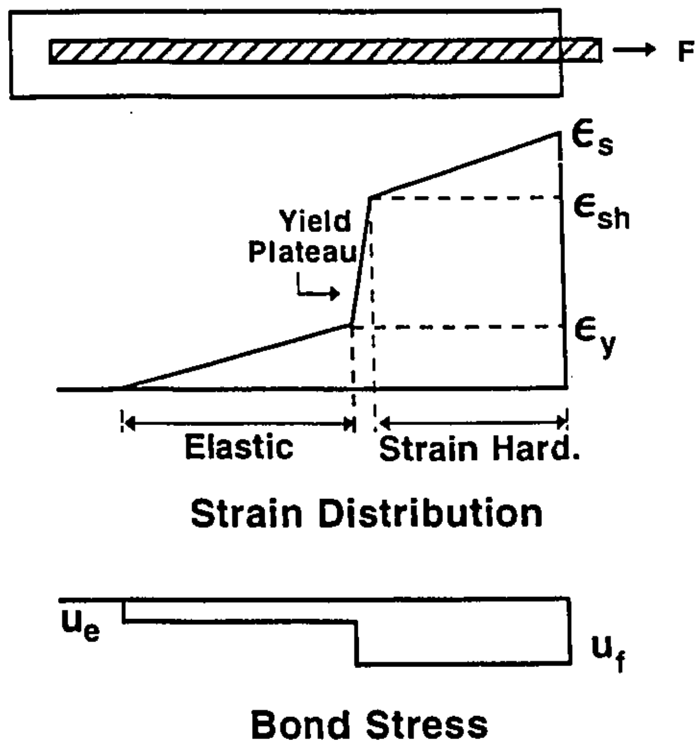

Figure 8.11: Strain and bond in anchored reinforcement (Alsiwat and Saatcioglu 1992).

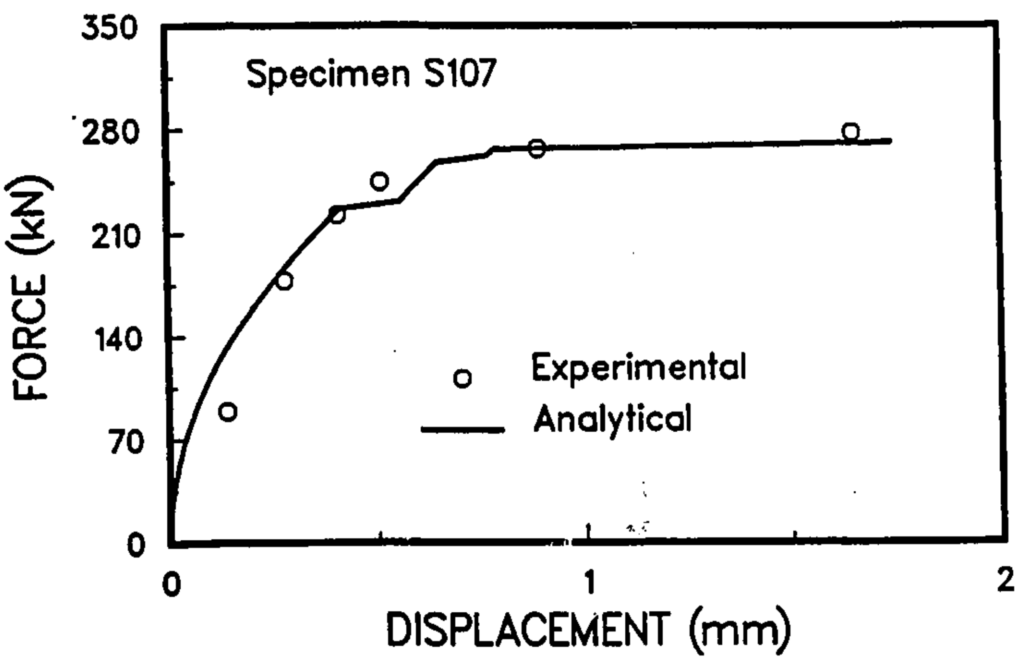

Figure 8.12: Comparison of pull-out test for specimen S107 (Alsiwat and Saatcioglu 1992).

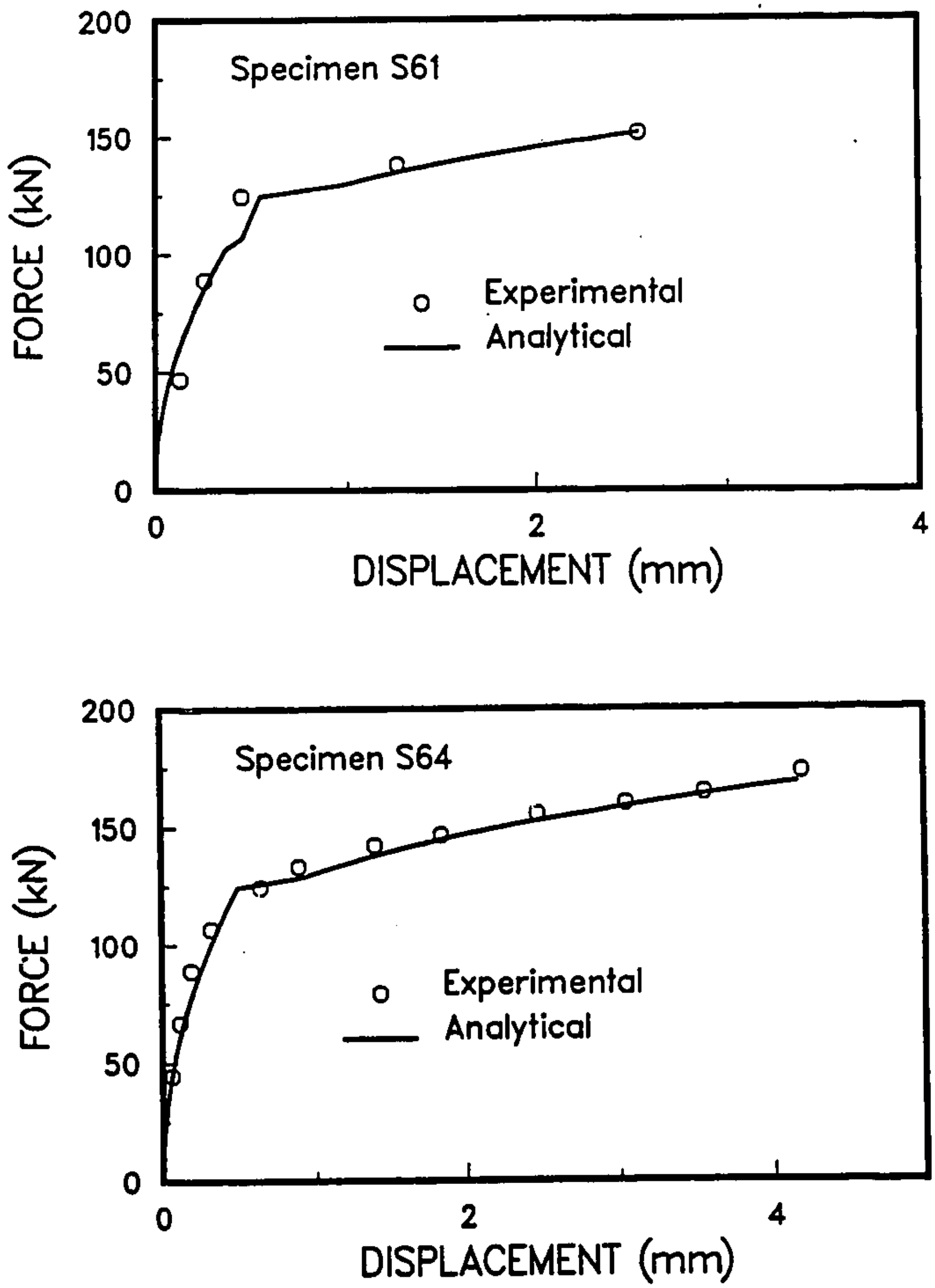

Figure 8.13: Comparison of pull-out tests for specimens S61 and S64 (Alsiwat and Saatcioglu 1992).

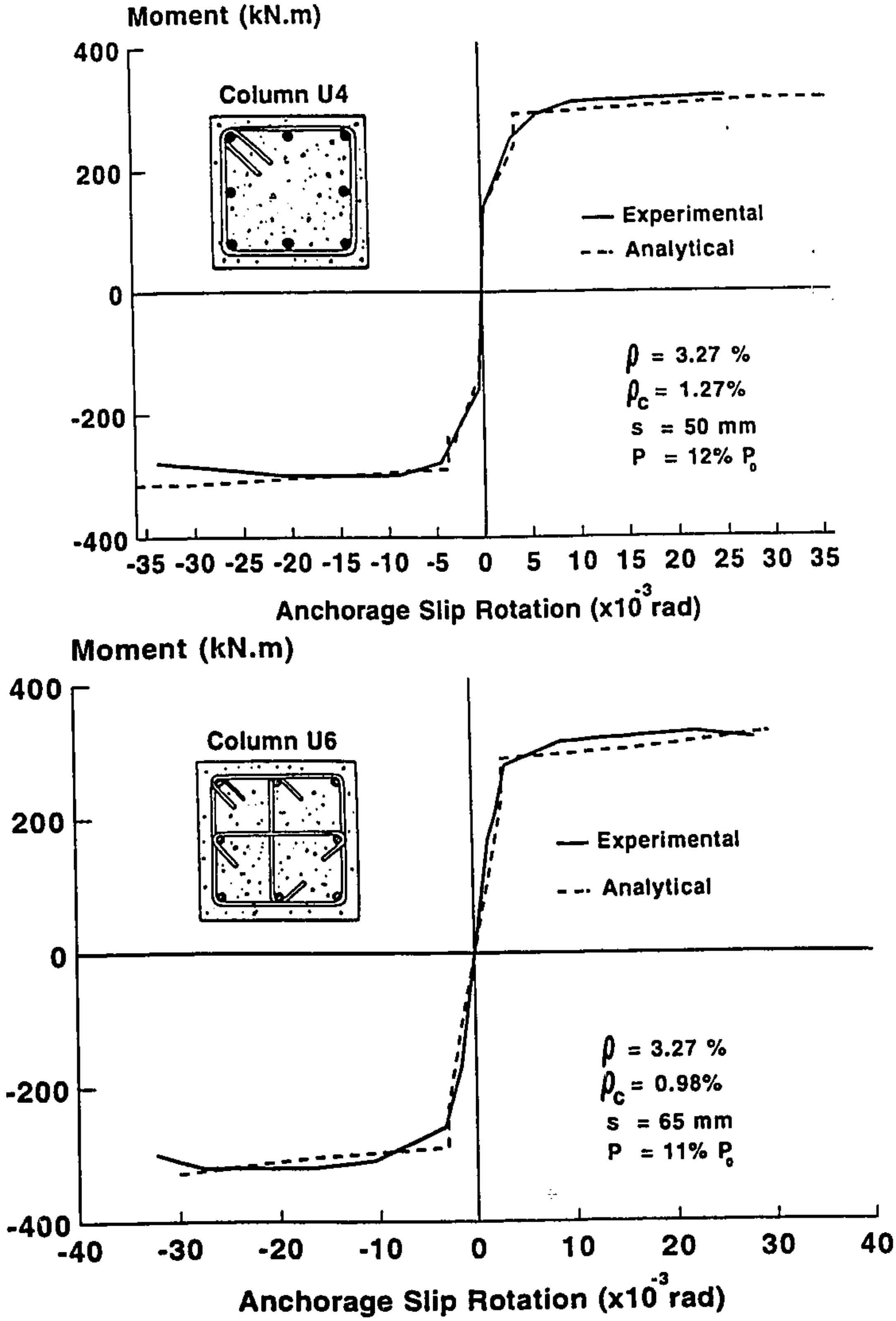

Figure 8.14: Comparisons of moment-anchorage slip rotation relationships (Saatcioglu and Ozcebe 1989).

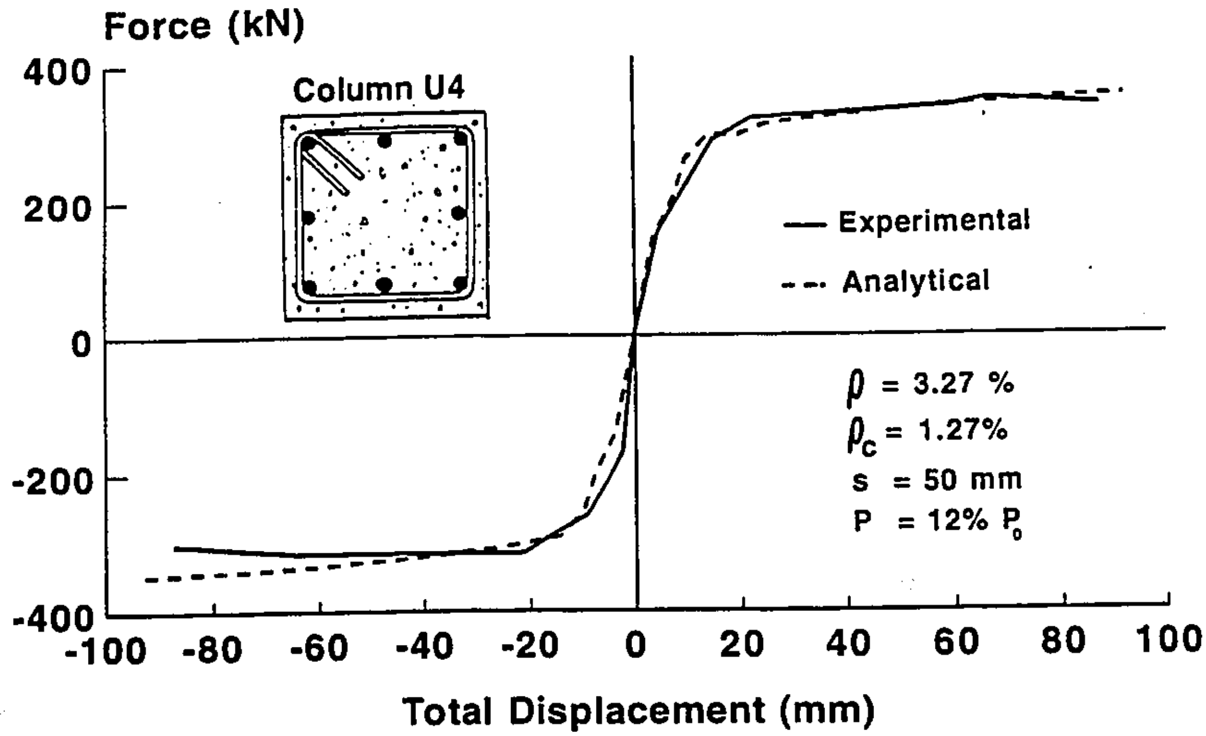

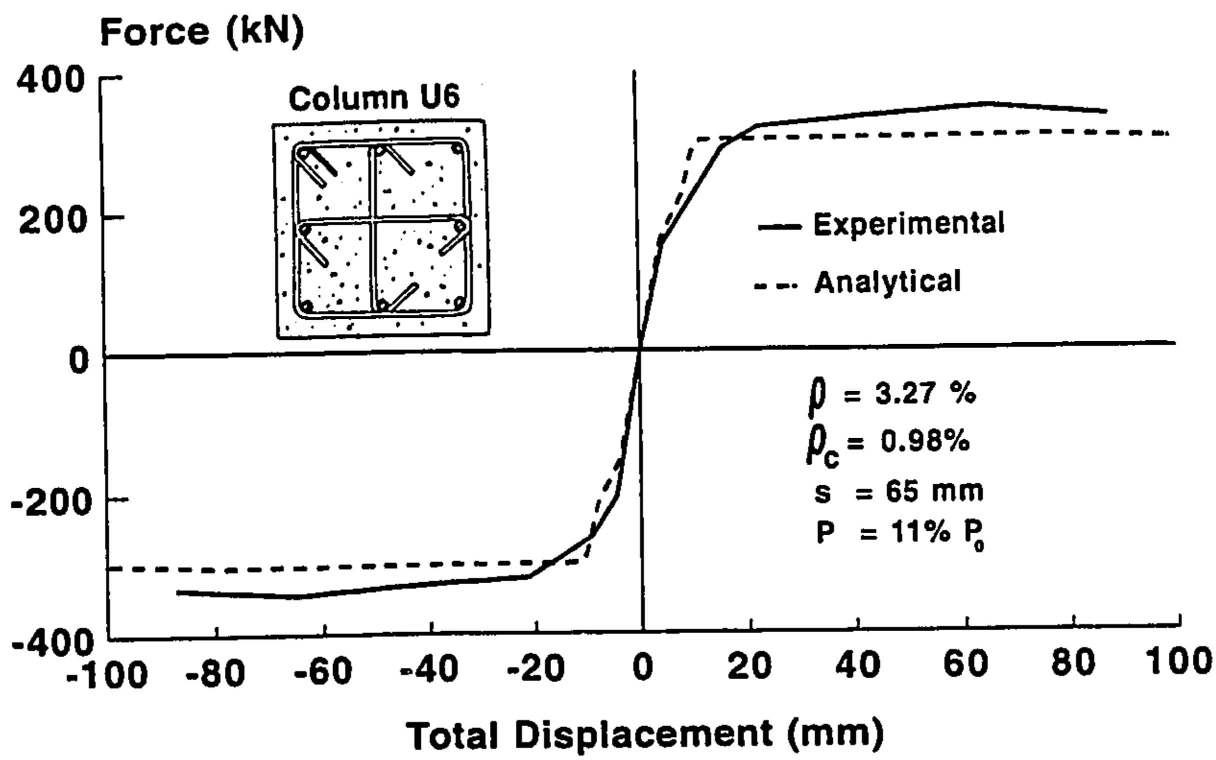

Figure 8.15: Comparison of lateral force-displacement relationships for columns U4 and U6 (Saatcioglu and Ozcebe 1989).

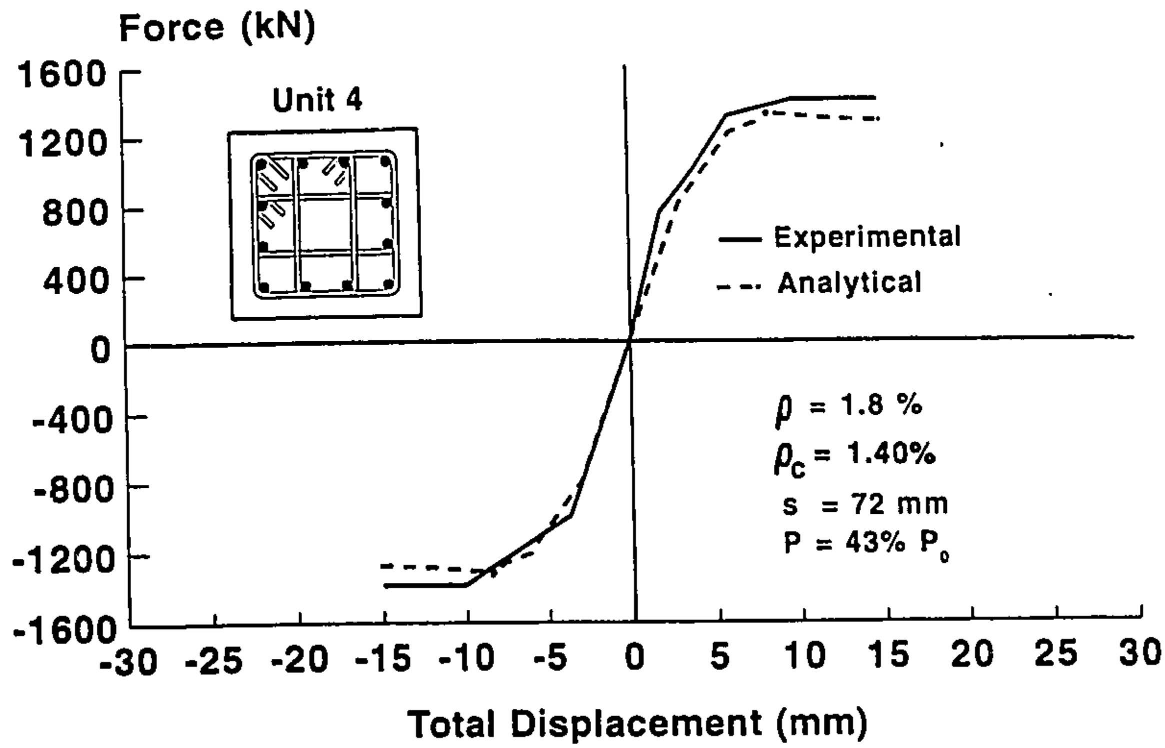

Figure 8.16: Comparison of lateral force-displacement relationships for column 4 (Park et al. 1982).

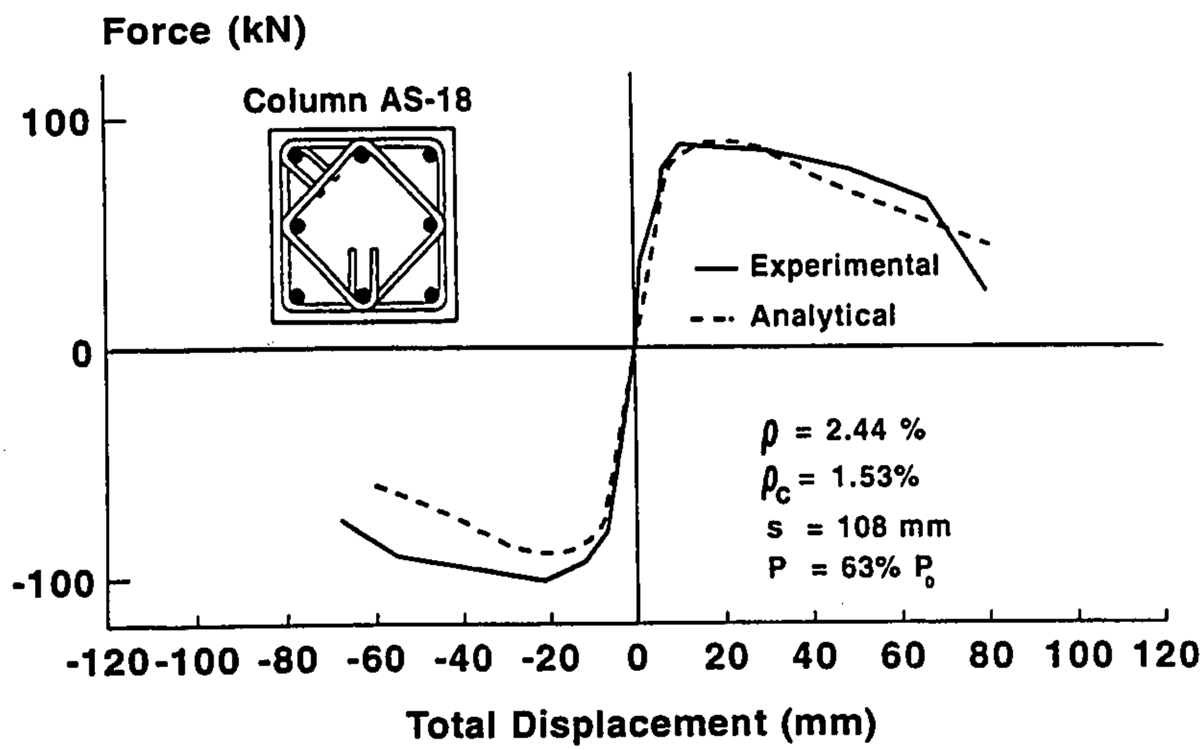

Figure 8.17: Comparison of lateral force-displacement relationships for column AS-18 (Sheikh and Khoury 1993).

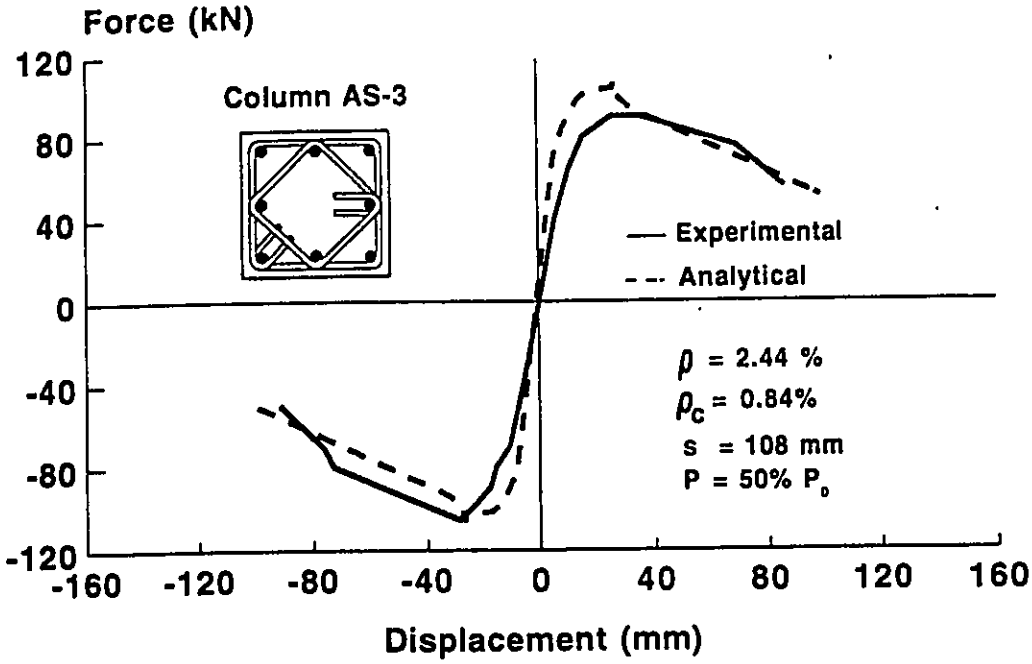

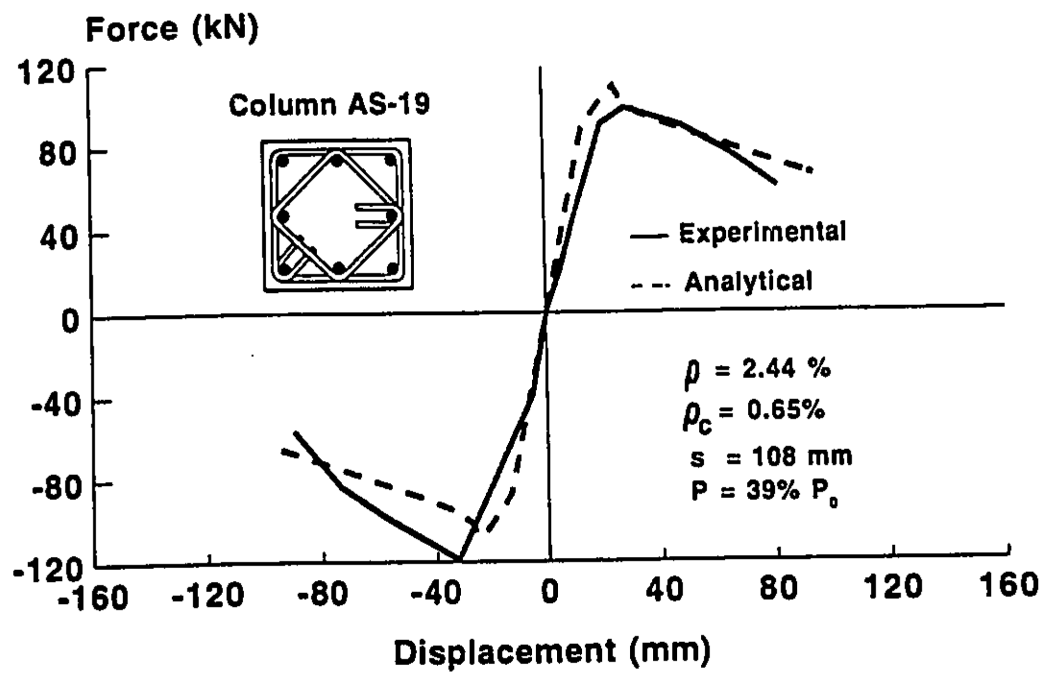

Figure 8.18: Comparison of lateral force-displacement relationships for columns AS-3 and AS-19 (Sheikh and Khoury 1993).

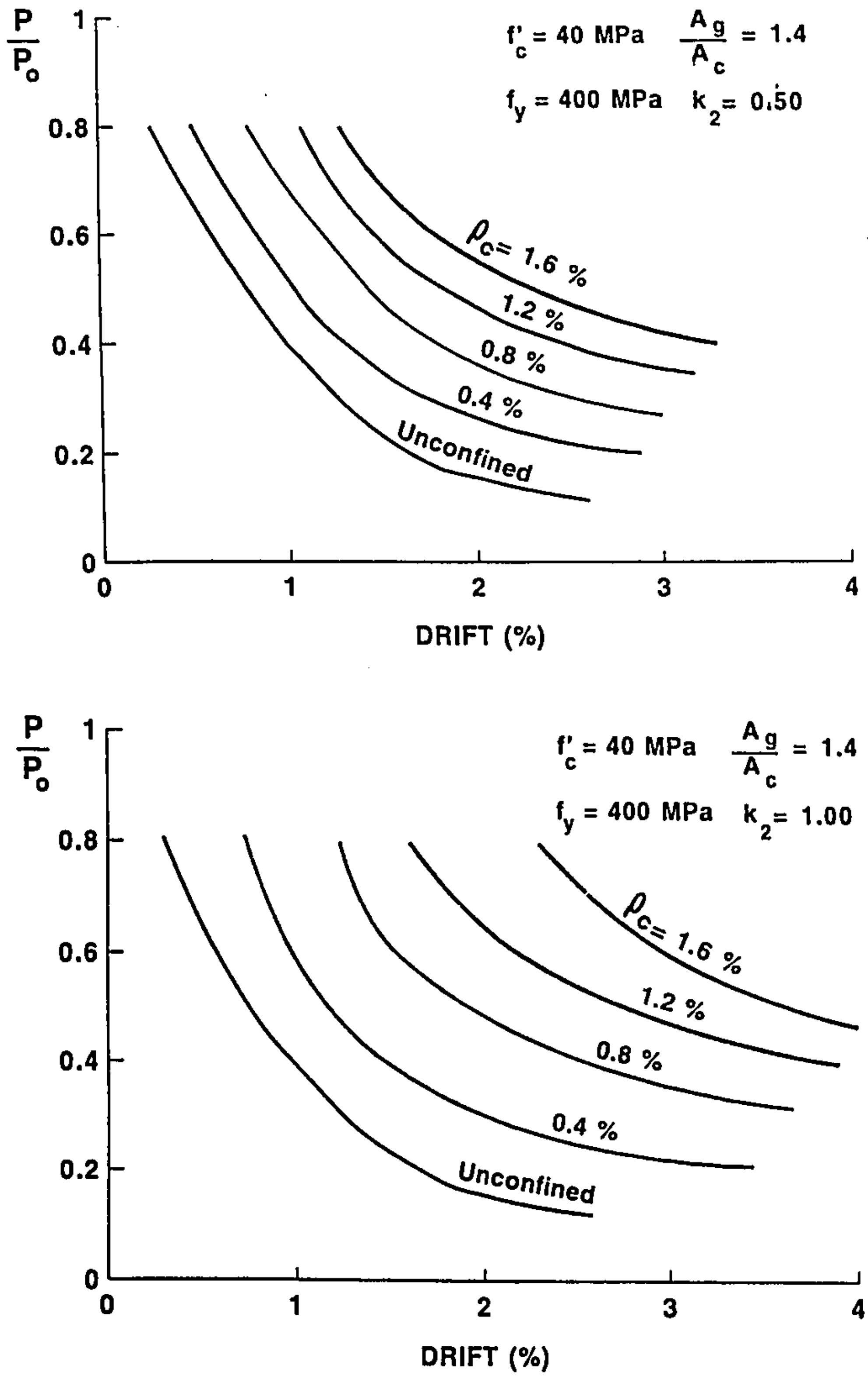

Figure 8.19: Axial compression-drift capacity relationships for columns with different confinement reinforcement.

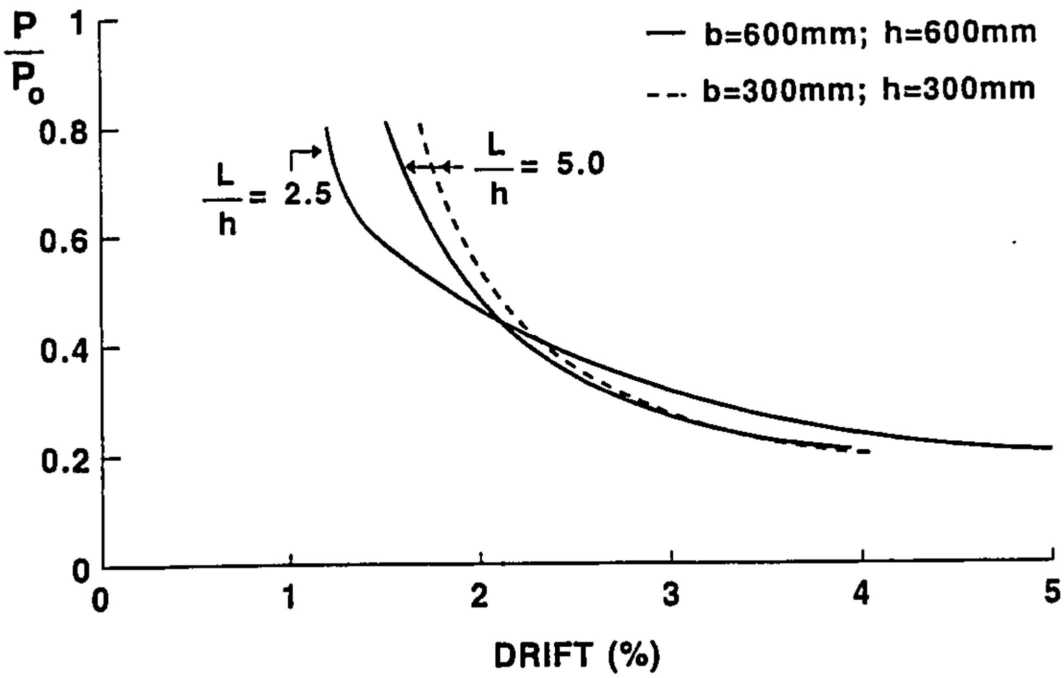

Figure 8.20: Effects of shear span-to-depth ratio and section size.

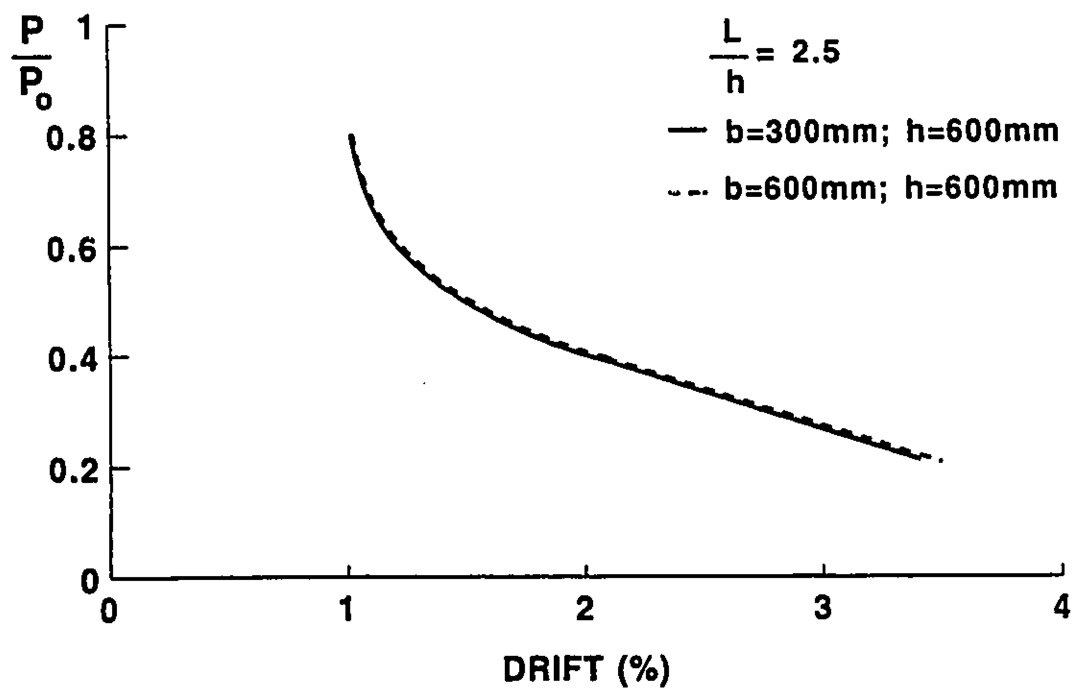

Figure 8.21: Effect of cross-sectional aspect ratio.

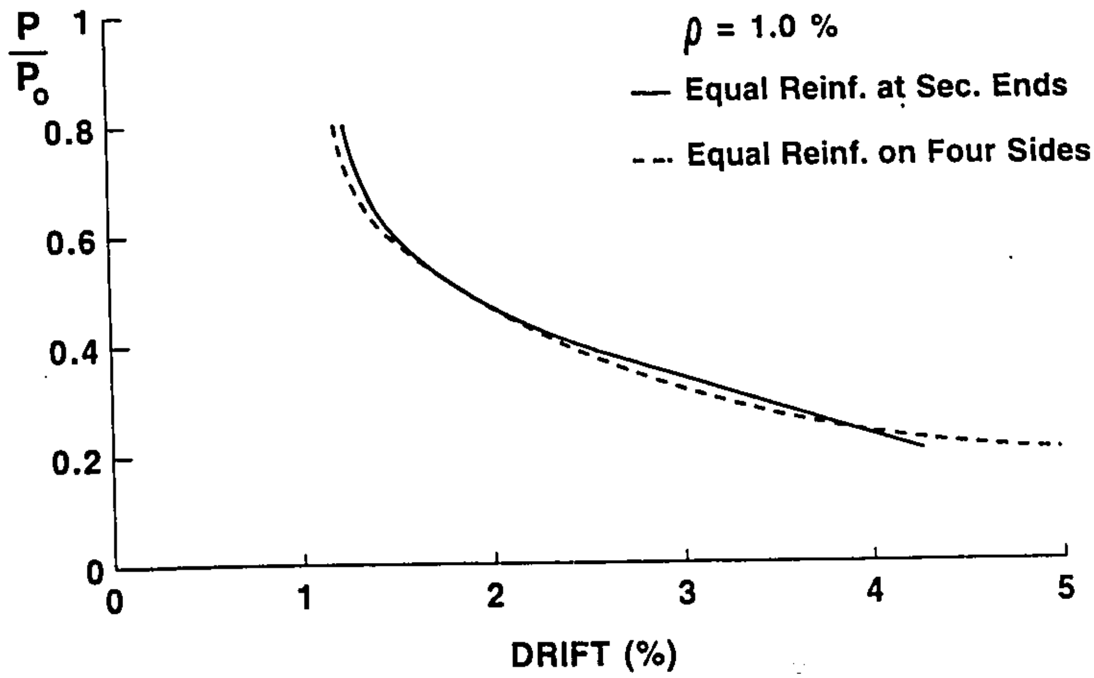

Figure 8.22: Effect of distribution of longitudinal steel.

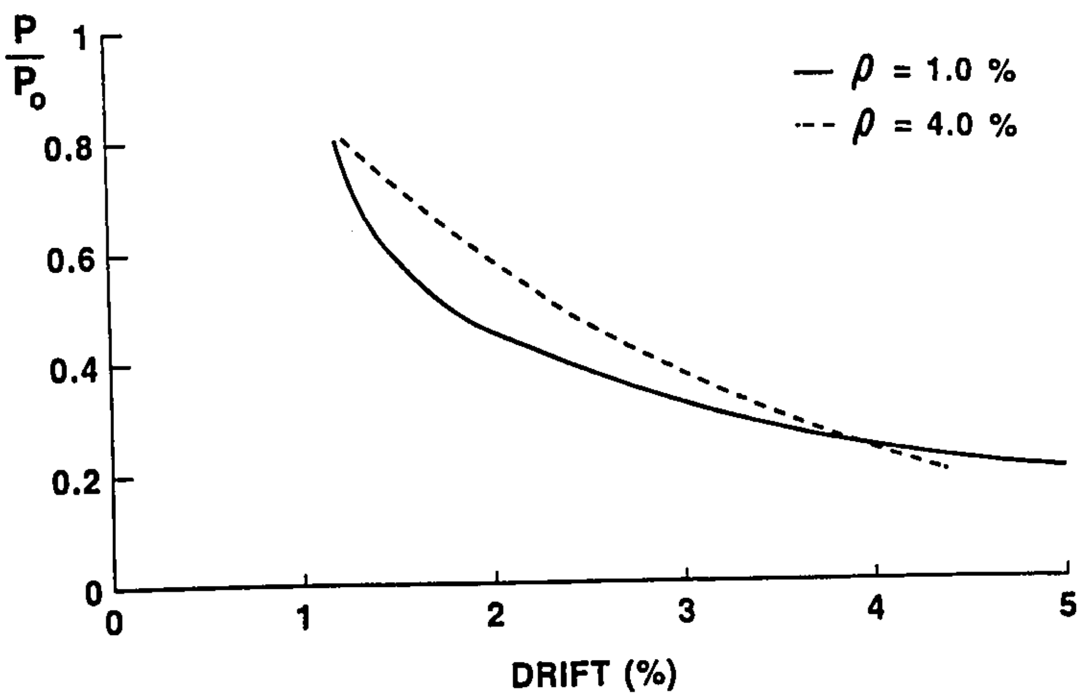

Figure 8.23: Effect of longitudinal steel ratio.

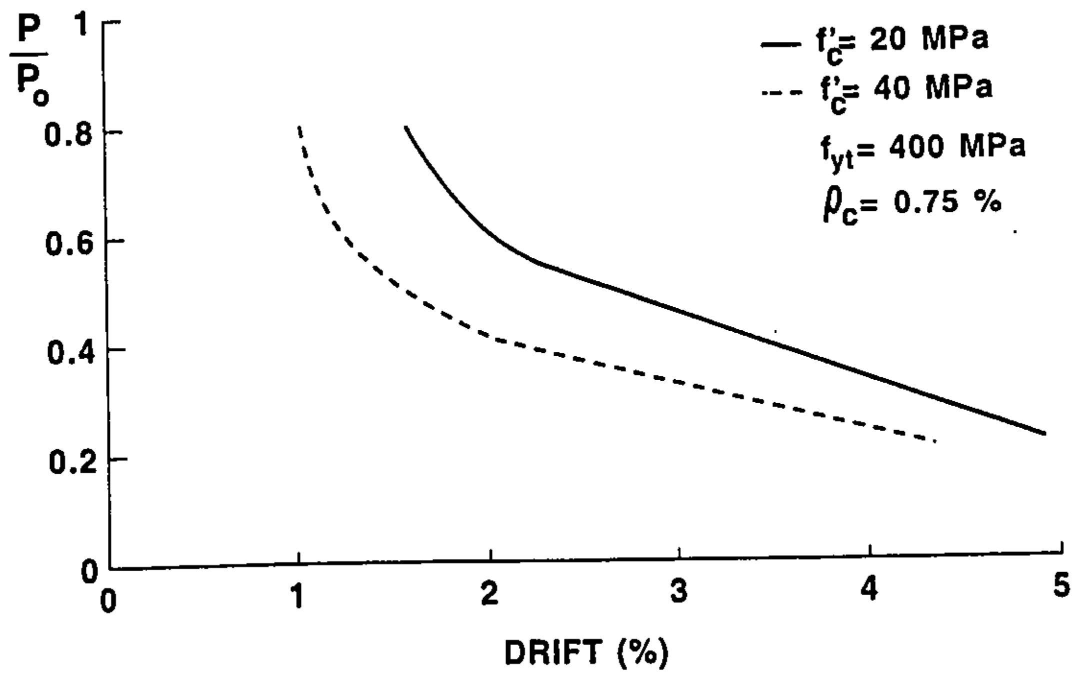

Figure 8.24: Effect of concrete strength.

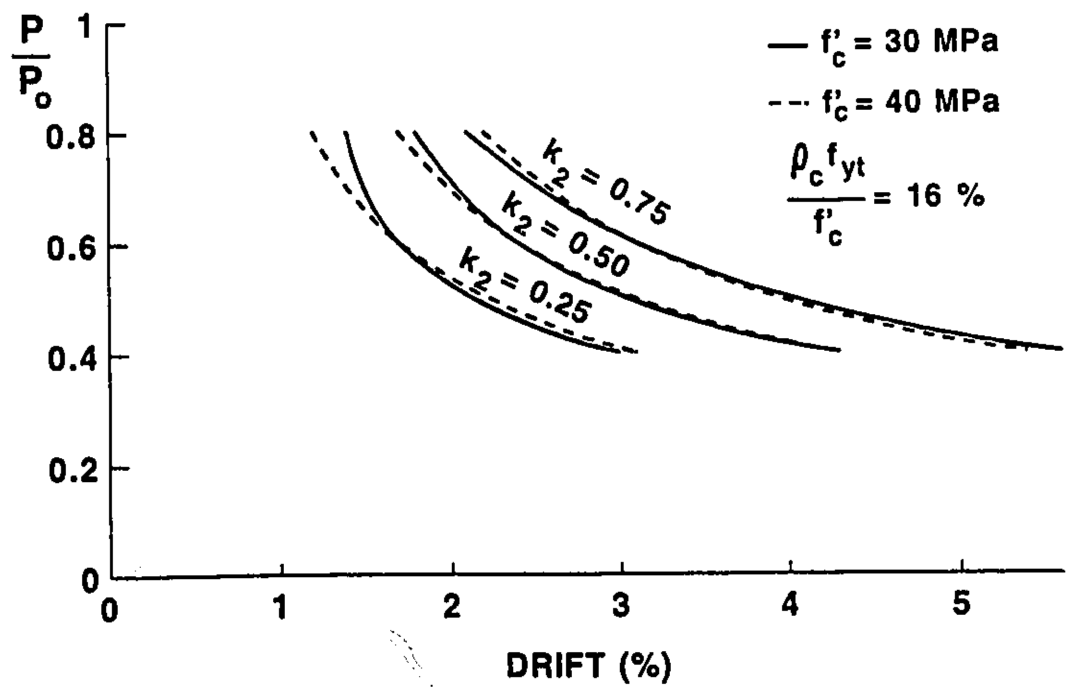

Figure 8.25: Effect of $\rho_s\ f_{yt}/f_c'$ ratio.

Chapter 9
Summary and Conclusions

9.1 Summary

A combined analytical and experimental investigation was conducted to study the confinement of concrete in columns. A comprehensive literature survey was first conducted to re-evaluate the existing data on column confinement. A similar comprehensive survey was conducted on available analytical models on column confinement.

The experimental investigation included tests of 46 full size high-strength concrete columns tested under monotonically increasing concentric compression. A preliminary test program was also conducted to investigate the characteristics of high-strength concrete mixes. The test data provided invaluable information on strength and deformability of high-strength concrete columns.

The experimental data was combined with available test data on confinement of normal-strength and high-strength concrete columns to develop an analytical model for stress-strain relationship of confined concrete. The model was verified against a large volume of experimental data, including normal-strength and high-strength concretes confined by normal-strength and high-strength reinforcement of different volumetric ratio, arrangement and spacing. The model was also verified against test data obtained under eccentric and reversed cyclic loadings, as well as under slow and fast strain rates.

The analytical model was used to develop a displacement based design procedure for column confinement. The procedure provides required confinement steel for columns with different deformation demands. A design aid was developed for use in practice.

9.2 Conclusions

The following conclusions can be drawn based on the experimental and analytical research reported in this thesis:

1. Parameters of column deformability can be viewed in three groups:
   a) Those related to applied loading; axial load level, shear stress, rate of loading, direction of lateral load, eccentricity of load, and loading history.
   b) Those related to confinement reinforcement; volumetric ratio, spacing, yield strength and arrangement of confinement reinforcement, and section geometry.
   c) Those related to concrete type; concrete strength and unit weight of aggregate.

2. Strength and deformability of concrete columns improve significantly if the core concrete is well confined, regardless of concrete strength. However, high-strength concrete columns require significantly higher volumetric ratio of confinement steel to attain deformabilities usually expected from normal-strength concrete columns.

3. High lateral pressure required to confine high-strength concrete, relative to normal-strength concrete, can be provided either by increasing the volumetric ratio of confinement steel and/or using high-strength lateral steel. High strength steel, with

1000 MPa yield strength, was found to be effective in confining high-strength concrete. Therefore, the required volumetric ratio can be reduced when high-strength steel is utilized with efficient arrangement of confinement reinforcement.

4. Although higher grade confinement reinforcement increases lateral pressure and hence improves behaviour, the volumetric ratio plays a more dominant role on concrete deformability. Hence, the increase in the grade of transverse reinforcement can not totally make up for a proportional reduction in volumetric ratio.

5. The descending slope of the stress-strain relationship of confined concrete is a function of amount, strength, arrangement of confinement reinforcement, and concrete strength.

6. Strain readings indicate that high-strength steel with f_{yt} = 1000 MPa yields at peak load or shortly thereafter. This indicates that high-strength steel can be fully utilized in confining the core concrete.

7. The results indicate a consistent decrease in deformability with increasing concrete strength. However, strength gain due to confinement is approximately constant for concretes with different unconfined strengths. Columns with different concrete strengths but similar confinement characteristics indicate approximately the same absolute gain in strength due to confinement. Therefore, if the same percentage of strength enhancement is desired, higher strength concrete columns are required to be confined more than those with lower strength concretes.

8. Unconfined concrete strength in column core varies approximately between 85% and 100% of concrete strength determined by a standard cylinder test. The average value of this variation appears to be higher for higher strength concretes.

9. Concentric capacity of plain or unconfined high-strength concrete columns can be predicted reasonably well with the use of current building code approach developed for normal-strength concrete, which assumes in-place strength of concrete to be 85% of cylinder strength.

10. High-strength concrete columns may be classified into three groups in terms of their capacities under concentric loading. The first group consists of plain or lightly reinforced unconfined columns, where early separation of cover concrete is not likely to occur. These columns may be able to develop capacities based on the current practice for normal-strength concrete. Columns confined with closely spaced longitudinal and transverse reinforcement experience loss of strength due to the early separation of cover. Depending on the thickness of the cover, concrete strength, and the degree of confinement of the core, the unconfined strength P_o, based on gross cross-sectional area may or may not be attained. When core confinement is not sufficient, the loss of strength associated with cover spalling can not be compensated by the concrete confinement. These columns form the second group. It may be more appropriate to compute concentric capacities of these columns on the basis of the core area. The third group consists of columns with sufficient confinement of the core to develop unconfined column capacities with core alone. The unconfined strength P_o, based on the current practice for normal-strength concrete may still be applicable to these columns, provided that the attainment of the ultimate load capacity beyond the spalling of the cover is an acceptable limit state for design purposes. More research is needed to establish the governing conditions for each category of columns, and the associated concentric load capacities.

11. Circular spirals are more effective in confining concrete than rectilinear ties. High-strength concrete columns confined with circular spirals showed improved strength and ductility when compared with columns confined with the same volumetric ratio

of rectilinear ties. However, it is possible to improve the behaviour of square columns up to the same level of performance as circular columns, or even higher level of performance, by improving the efficiency and/or the amount of confinement reinforcement.

12. The expressions given in ACI-318 (1989) and CSA A 23.3 (1984) overestimate the modulus of elasticity for high-strength concrete. The expression suggested by Carrasquillo et al. (1981) agrees well with the experimental data.

13. The review of available analytical models for normal and high-strength concrete indicates that existing analytical models for confined concrete have limitations. Models developed based on normal-strength concrete are not applicable to high-strength concrete. Available confinement models for high-strength concrete are mostly modified versions of models developed for normal-strength concrete, which are only applicable, in most cases, to test data based on which they were derived.

14. The analytical model proposed in this investigation for stress-strain relationship of confined concrete can be used for normal-strength and high-strength concretes confined by normal-strength and high-strength reinforcement of different volumetric ratios and arrangements, as evidenced by extensive verification against test data. The model can be used for concentric and eccentric loads.

15. Confinement steel requirements of ACI 318 (1989) Building Code for normal-strength concrete are based on an arbitrary design concept. Therefore, the code requirements tend to be conservative for columns subjected to low axial loads, and unsafe for columns under high axial loads. Furthermore, the arrangement of reinforcement in confining core concrete is not explicitly recognized There exist a need for a more rational design approach incorporating all the relevant parameters of confinement.

16. No specific confinement steel requirements for high-strength concrete are available in the ACI-318 (1989) building code. However, the extension of the current normal-strength concrete requirements to high-strength concrete may lead to conservative design under low axial load, and unsafe design under high axial load.

17. The displacement based design procedure developed in this investigation for column confinement incorporates all the relevant parameters of confinement and produces confinement steel requirements for different drift levels. Hence, it represents a significant improvement over the current building code procedure. While the procedure is applicable to both normal-strength and high-strength concrete columns, the design table developed is only applicable to normal-strength concrete, since the anchorage slip characteristics of high-strength concrete has not yet been established.

9.3 Recommendations for Future Research

The following recommendations are made for future research;

1. The effect of high-strength steel on confinement of high-strength concrete needs to be investigated using different grades of high-strength steel.

2. More research is needed to investigate behaviour of high strength concrete columns under high axial load and lateral load reversals.

3. The applicability of the procedure used for anchorage slip deformations to high-strength concrete columns needs to be verified against test data. There is a need for more experimental data to verify and/or modify the anchorage slip model developed by Alsiwat and Saatcioglu (1992).

References

1. Abdel-Fattah, H., and Ahmed, S.H., "Behavior of Hoop Confined High Strength Concrete under Axial and Shear Loads," ACI Structural Journal V.86, Nov.-Dec. 1989, pp.652-659.

2. Abdulkadir, R., "Strength and Ductility of Concrete Columns Reinforced with Welded Wire Fabric and/or Rebars," A Thesis Presented to the University of Ottawa, in 1991, in Partial Fulfilment of the Requirements for the Degree of Master of Applied Science.

3. ACI Committee 318, "Building Code Requirements for Reinforced Concrete (ACI 318-77)," American Concrete Institute, Detroit, 1977, 102 pp.

4. ACI Committee 318, "Building Code Requirements for Reinforced Concrete (ACI 318-89)," American Concrete Institute, Detroit, 1992, 348 pp.

5. ACI Committee 363, "State-of-the Art Report on High Strength Concrete," ACI Journal, Jul.-Aug. 1984, Vol.81, No.4, pp. 364-411.

6. Ahmed, S.H., and Shah, S.P., "Stress-Strain Curves of Concrete Confined by Spiral Reinforcement," ACI Journal, V.79, No.6, Nov.-Dec. 1982, pp.484-490.

7. Al-Hussaini, A., Regan, P.E., Xue, H.Y., Ramdane, K.E., "The Behavior of HSC Columns Under Axial Load," Proceedings of the Symposium on High-Strength Concrete, June 93, Norway, pp. 83-90.

8. Alsiwat, J., and Saatcioglu, M. "Reinforcement anchorage slip under monotonic loading," Journal of Structural Engineering, ASCE, V01.118, No.9, 1992, pp.

2421-2438.

9. Aitcin, P.C., Laplante, P., and Bedard, C., " Development and Experimental Use of 90 MPa (1300 psi) Field Concrete," ACI Special Publication, SP-87-5, American Concrete Institute, Detroit, 1985, pp.51-70.

10. Allseed, J., and Saatcioglu, M., "Reinforcement Anchorage Slip Under Monotonic Loading," Journal of Structural Engineering, ASCE, Vol. 118, No. 9, pp. 2421-2438.

11. Aoyama, H., "Recent Development in Design and Construction of High-Rise Reinforced Concrete Buildings in Japan," Sixth Canadian Conference on Earthquake Engineering, Toronto, 1991, pp.3-16.

12. AS 3600 "Standards Association of Australia," Australian Standard AS 3600 - 1994 Concrete Structures, Sydney, Australia, pp. 155.

13. Atalay, M. B. and Penzien, J., "The Seismic Behaviour of Critical Regions of Reinforced Concrete Components as Influenced by Moment, Shear, and Axial Force," Report No. EERC 75-19, College of Engineering, University of California, Berkeley, California, 1975, 226 pp.

14. Azizinamini, A., and Kuska, S.B., "Flexural Capacity and Ductility of High-Strength Concrete Columns," Proceedings of the Symposium on High-Strength Concrete, June 93, Norway, pp. 91-98.

15. Azizinamini, A., Kuska, S.S.B., Brungardt, P., and Hatfield, E., " Seismic Behavior of Square High-Strength Concrete Columns," ACI Structural Journal, Vol. 91, No.3, May-June 1994, pp. 336-345.

16. Baingo, D., and Saatcioglu, M., "Performance of Circular High Strength Concrete Columns Under Lateral Load Reversals," Research Report, Department of Civil Engineering, University of Ottawa, Ottawa, Canada, 1995.

17. Bakhsh, A. H., Wafa, F. F., and Akhtaruzzaman, A. A., " Torsional Behavior of Plain High-Strength Concrete Beams," ACI Structural Journal, Proceedings Vol. 87, No. 5, Sept.-Oct. 1990, pp. 583 - 588.

18. Balmer, G.G. "Shearing Strength of Concrete Under High Triaxial Stress-Computation of Mohr's Envelope as a Curve," Structural Research Lab. Report No. SP-23, U.S. Bureau of Reclamation, 1949, pp. 13.

19. Basset, R., "Behaviour of Reinforced High Strength Lightweight Concrete Columns with Rectangular Ties," M.A.Sc. Thesis, University of Toronto, Ontario, 1983, 108 pp.

20. Basset, R., and Uzumeri, S.M., "Effect of Confinement on the Behavior of High-Strength Lightweight Concrete Columns," Canadian Journal of Civil Engineering, Vol.13, No.6, Dec. 1986, pp. 741-751.

21. Bayrak, O., and Sheikh, S. A., "High Strength Concrete Columns Subjected to Earthquake Type Loading", Proceedings of the Seven Canadian Conference on Earthquake Engineering, Montreal, Quebec, 1995, pp. 477-484.

22. Bertero, V. V., "Earthquake Engineering," Structural Engineering Slide Library, Volumne 4; Set J. International Structural Slides, 1985.

23. Bertero, V.V., "Inelastic behavior of Structural Elements and Structures," Proceedings of the Workshop on High Strength Concrete, U.of Illinois at Chicago

Circle, Chicago, Illinois, Dec. 1979, pp. 96-167.

24. Bertero, V.V., and Felippa, C., Discussion of "Ductility of Concrete", by Roy, H.E., and Sozen, M.A., Proceedings of the International Symposium on the Flexural Mechanics of Reinforced Concrete, ASCE-ACI, Miami, November 1964, pp.227-234.

25. Bjerkeli, L., Tomaszewica, A., and Jensen, J.J., "Deformation Properties and Ductility of High Strength Concrete," High Strength Concrete, Second International Symposium, ACI SP-121-12, Detroit, 1990, pp.215-238.

26. Boulay, C., and de Larrard, F., " The Sand-Box: a New Capping Method for Testing High-Performance Concrete Cylinders, ACI, Concrete International, April 1993 (a).

27. Boulay, C., and de Larrard, F., " Capping High-Performance Concrete Cylinders with the 'Sand-Box'," Proceedings of the Symposium on High-Strength Concrete, June 1993 (b), Norway, pp. 1015-1023.

28. Bresler, B., and Gilbert, P.H., " Tie Requirement for Reinforced Concrete Columns," ACI Journal, Proceedings, Vol.58, No.5, November 1961, pp. 555-569.

29. British Standards Institution, " Structural Use of Concrete, Part1, Code of Practice for Design and Construction," 1985.

30. Burdette, Edwin G., and Hilsdorf, Hubert K., " Behaviour of Laterally Reinforced Concrete Columns," Journal of the Structural Division, Proceedings of the American Society of Civil Engineers, ST2, February 1971, pp. 587-602.

31. Carette, G.G, Malhotra, V.M., and Aitcin, P.C., " Preliminary Data on Long Term Strength Development of Condensed Silica Fume Concrete," Third International Conference on Fly Ash, Silica Fume, Slag / Natural Pozzolans in Concrete, Norway, 1989, Supplementary Papers, pp. 597-617.

32. Carrasquillo, R. L., Nilson, A. H., and Slate, F. O., " Properties of High-Strength Concrete Subjected to Short Term Loads," ACI Journal, Proceedings V. 78, No.3, May-June 1981, pp. 171-178.

33. CEB-FIP Model Code 1990. First Predraft 1988. Bulletin d'Information No 190 a et b, Juillet 1988.

34. Chan, W.L., " The Ultimate Strength and Deformations of Plastic Hinges in Reinforced Concrete Frameworks," Magazine of Concrete Research, Vol.7, No.21, November 1955, pp.121-132.

35. Chung, H., Hayashi, S. and Kokusho, S., "Reinforced High Strength Columns Subjected to Axial Forces, Bending Moments, and Shear Forces," Transactions of the Japan Concrete institute, Vol.2, 1980, pp. 335-342.

36. Cordon, W. A., and Gillespie, H. A., " Variables in Concrete Aggregates and Portland Cement Paste Which Influence the Strength of Concrete," ACI Journal, Proceedings, Vol. 60, No. 8, Aug. 1963, pp. 1029-1052.

37. CSA, "Design of Concrete Structures for Buildings (CAN3-A23.2-M84)," Canadian Standards Association, Ontario, 1984, 281 pp.

38. Cusson, D., and Paultre, P., " Experimental Study of High-Strength Concrete Columns Confined by Rectangular Ties," Proceedings of the Symposium on High-

Strength Concrete, June 1993, Norway, pp. 136-145.

39. Cusson, D., and Paultre, P., " High-Strength Concrete Columns Confined by Rectangular Ties," Journal of Structural Engineering, ASCE, Vol. 120, No.3, March 1994, pp.783-804.

40. Cusson, D., and Paultre, P., and Aitcin, P.C., "Le Confinement des Colonnes en Beton a Huate Performance Par des Entries Rectangulaires," Annual Conference of the Canadian Society for Civil Engineering, May 27-29, 1992, Quebec, pp.21-30.

41. Cusson, D., and Paultre, P., and Aitcin, P.C., "Le confinement des poteaux en beton a haute performance - Prediction du comportment, Bull. liaison Labo. P. et Ch., 192, juil-aout 1994, pp. 61-74.

42. Day, R.L., and Haque, M.N., "The Correlation Between Strength of Small-and Standard-Size Concrete Cylinders," A Paper Submitted to ACI Journal for Possible Publication, June 1992.

43. De Larrard, F., "A Survey of Recent Researches Performed in the French 'LPC' Network on High-Performance Concrete," Proceedings of the Symposium on High-Strength Concrete, June 1993, Norway, pp. 57-67.

44. Djellouli, J., Aitcin, P. C., and Chaallal, O., " Use of Ground Granulated Slag in High-Performance Concrete," High Strength Concrete, Second International Symposium, ACI SP-121-18, Detroit, 1990, pp. 351-368.

45. Fafitis, A. and Shah, S. P., "Lateral Reinforcement for High-Strength Concrete Columns," ACI Special Publication, SP-87-12, American Concrete Institute, Detroit, 1985(b), pp.213-232.

46. Fafitis, A. and Shah, S. P., "Prediction of Ultimate Behaviour of Confined Columns Subjected to Large Deformation," ACI Structural Journal, Vol. 82, July-August 1985 (a), pp.423-433.

47. Favre, R., Charif, H., and Jaccoud, J.-P., " Improved Serviceability of Reinforced Concrete Slabs with the Use of High-Strength Concrete," High Strength Concrete, Second International Symposium, ACI Sp-121-6, Detroit, 1990, pp. 89-108.

48. FIP/CEB, "High Strength Concrete, State of the Art Report," Bulletin d'Information No.197, Aug.1990, 61 pp.

49. Galeota, D., Giammatteo, M.M., and Marino, R., "Strength and Ductility of Confined High Strength Concrete," Proceedings of 10th World Conference on Earthquake Engineering, Madrid, 1992, pp. 2609-2613.

50. Gerd, R., " Influence of the Tensile Behavior on the Shear Strength of Longitudinally Reinforced Concrete Members," Proceedings of the First International Conference on Fracture Mechanics of Concrete Structures, Colorado, USA, 1-5 June 1992.

51. Goldman, A., and Bentur, A., " Bond Effect in High Strength Silica Fume Concrete," ACI Material Journal, Proceedings, Vol.86, No.4, 1989, pp. 440-447.

52. Hatanaka, S., and Tanigawa, Y., "Lateral Pressure Requirements for Compressive Concrete," Proc.of 10th World Conf.on Earthquake Engineering., Madrid, 1992, pp. 2603-2608.

53. Hibi, J., Mihara, Y., Otani, S., and Aoyama, H., "Behavior of Reinforced Concrete

Columns Using High Strength Concrete After Flexural Yielding," Transactions of The Japan Concrete Institute, Vol.13, 1991, pp. 395-402.

54. Hoff, G. C., " Utilization of High Strength Concrete in North America," Proceedings of the Symposium on High-Strength Concrete, June 93, Norway, pp. 28-36.

55. Hognestad, E., "A Study of Combined Bending and Axial Load in Reinforced Concrete Members, " University of Illinois, Engineering Experimental Station, Bulletin Series No. 399, November 1951, pp.128.

56. Hudson, Fred M., "Reinforced Concrete Columns: Effects of Lateral Tie Spacing on Ultimate Strength," Paper No.10, Symposium on Reinforced Concrete Columns, ACI, SP-13, 1966, pp. 235-244.

57. Ibrahim, H. H. H., and MacGregor, J. G., " Flexural Behavior of High Strength Concrete Columns," Structural Engineering Report No. 196, Department of Civil Engineering, University of Alberta, Alberta, March 1994, pp. 197.

58. Ichikawa, A., Sugano, S., Nagashima, T., Kimura, H., "An Experimental Study on Axial Compression Behavior of High-Strength Concrete Columns," (in Japanese), Proceedings of the Japan Concrete Institute, Vol. 13, No.2, 1991, pp. 403-408.

59. Imam, M., Vandewalle, L., and Mortelmans, F., " Indirect Tensile Strength of Very High Strength Concrete," Proceedings of the Symposium on High-Strength Concrete, June 93, Norway, pp. 1114 -1121.

60. Ishiwata, Y., Itakura, Y., Teshigawara, M., Takasaki, T., Hiraishi, H., Kawashima, S., Yagen, C., "Study on High-Strength RC Columns under Uniaxial Loading (Part 2 Behavior after Maximum Stress)," (in Japanese), Proceedings of the Annual

Conference of Japan Architectural Institute, Oct.1990, pp. 841-842.

61. Itakura, Y., Teshigawara, M., Takasaki, T., Ishiwatari, Y., Hiraishi, H., Kawashima, S., Yagen, C., "Study on High-Strength RC Columns under Uniaxial Loading (Part1 Outline of Test Results)," (in Japanese), Proceedings of the Annual Conference of Japan Architectural Institute, Oct.1990, pp. 839-840.

62. Itakura, Y., and Yagenji, A., "Compressive Test on High-Strength R/C Columns and Their Analysis Based on Energy Concept," Proceedings of 10th World Conference on Earthquake Engineering, Madrid, 1992, pp. 2599-2602.

63. Kaar, P.H., Fiorato, A.E., Carpenter, J.E., and Corely, W.G., " Limiting Strains of Concrete Confined by Rectangular Hoops," PCA, Research and Development Bulletin RD053.01D, 1978, pp.12.

64. Kabeyasawa, T., Li, K.N., and Huang, K., "Experimental Study on Strength and Deformability of Ultrahigh Strength Concrete Columns," Transactions of The Japan Concrete Institute, Vol.12, 1990, pp. 315-322.

65. Kabeyasawa, T., Shen, F.H., Kuramoto, H., and Rubiano, N.R., "Experimental Study on Behavior of Ultra-High-Strength Reinforced Concrete Columns under Tri-Axial Forces," Transactions of The Japan Concrete Institute, Vol.13, 1991, pp. 279-286.

66. Karasan, I.D., Jirsa, J.O., "Behaviour of Concrete under Varying Strain Gradient," Proceedings, ASCE, Vol.96, St8, August 1970, pp.1675-1696.

67. Kent, D.C., and Park, R., "Flexural Members with Confined Concrete," Journal of Structural Division, ASCE, Vol.97, 1971, pp. 1969-1990.

68. Khaloo, A. R., and Ahmed, S. H., " Behavior of High Strength Concrete Under Torsional Triaxial Compression," ACI Material Journal, Vol. 86, No.6, Nov.-Dec. 1989, pp. 550-558.

69. King, J.W.H., " The effect of Lateral Reinforcement in Reinforced Concrete Columns," The Structural Engineer, Vol. 24, No. 7, July 1946, pp. 355-388.

70. Kong, G., Bergner, H., Grimm, R., and Simsch, G., " Utilization of High-Strength Concrete in Europe," Proceedings of the Symposium on High-Strength Concrete, June 93, Norway, pp. 45-56.

71. Kumramoto, H., and Minami, K., "Experiments on the Shear Strength of ultra-High Strength Concrete Columns," Proceedings of 10th World Conference on Earthquake Engineering, 1992, Madrid, pp. 3001-3006.

72. Legeron, F., and Paultre, P. , "Seismic Behaviour of Columns Made of High-Strength Concrete", Proceedings of the Seven Canadian Conference on Earthquake Engineering, Montreal, Quebec, 1995, pp. 469-476.

73. Li, Bing, "Strength and Ductility of Reinforced Concrete Members and Frames Constructed Using High Strength Concrete," Research Report No. 94-5, University of Canterbury, Christchurch, New Zealand, May 1994, p. 389.

74. Limsuwan, E., "Strength of High-Strength Concrete Columns," Proceedings of the Symposium on High-Strength Concrete, June 93, Norway, pp. 277-284.

75. Lipien, W., and Saatcioglu, M., "Ductility of High-Strength Concrete Columns," Research Report, Department of Civil Engineering, University of Ottawa, Ottawa,

Canada, 1995.

76. Lloyd, N.A., and Rangan, B.V., "High Strength Concrete Columns under Eccentric Compression," Research Report No. 1/95, School of Civil Engineering, Curtin University of Technology, Australia, 1995, pp. 199.

77. Maage, M., Smeplass, S., and Johansen, R., " Long-Term Strength of High Strength Silica Fume Concrete," High Strength Concrete, Second International Symposium, ACI Sp-121-20, Detroit, 1990, pp. 399-408.

78. Malhotra, V.M., "Are 4 x 8 Inch Concrete Cylinders as Good as 6 x 12 Inch Cylinders for Quality Control of Concrete?," ACI Journal, Proceedings Vol.73, No.1, 1976, pp. 33-36.

79. Mander, J.B., Priestley, M.J.N., and Park R., "Observed Stress-Strain Behaviour of Confined Concrete," ASCE Structural Journal, Vol. 114, No.8, Aug. 1988(a), pp. 1827-1849.

80. Mander, J.B., Priestley, M.J.N., and Park R., "Theoretical Stress-Strain Model for Confined Concrete," ASCE Structural Journal, Vol. 114, No.8, Aug. 1988(b), pp. 1804-1826.

81. Martinez, S., Nilson, A.H., and Slate, F.O., "Spirally Reinforced High-Strength Concrete Columns," Research Report No. 82-10, Department of Structural Engineering, Cornell University, Ithaca, August 1982, 255 pp.

82. Martinez, S. Nilson A.H., and Slate, F.O., "Spirally Reinforced High-Strength Concrete Columns," ACI Journal, Sept.-Oct. 1984, pp. 431-442.

83. Mehta, P. K., and Aitcin, P. C., " Microstructural Basis of Selection of Materials and Mix Proportions for High-Strength Concrete," High Strength Concrete, Second International Symposium, ACI SP-121-14, Detroit, 1990, pp. 265-286.

84. Mizoguchi, M., Arakawa, T., and Arai, Y., "Strength Behavior of High Strength R/C Columns under Biaxial Bending-Shear and Varying Axial Load," Transactions of The Japan Concrete Institute, Vol.13, 1991, pp. 387-394.

85. Moreno, J. and Zils, J., "Optimization of High-Rise Concrete Buildings," Analysis and Design of High-Rise Buildings, ACI SP-97, 1985, Detroit.

86. Muguruma, H., Nishiyama, M., Watanabe, F., and Tanaka, H., "Ductile Behaviour of High Strength Concrete Columns Confined by High Strength Transverse Reinforcement," ACI International Conference on "Evaluation and Rehabilitation of Concrete Structures and Innovations in Design, " SP-128-54, Vol.2, Hong Kong, December 1991, pp. 877-891.

87. Muguruma, H., Watanabe, F., Iwashimizu, T., and Mitsueda, R., "Ductility Improvement of High Strength Concrete by Lateral Confinement," Transactions of the Japan Concrete Institute, Vol.5, 1983, pp. 403-410.

88. Muguruma, H., Watanabe, F., and Komuro, T, "Ductility Improvement of High Strength Concrete Columns with Lateral Confinement," High Strength Concrete, Second International Symposium, ACI Sp-121-4, Detroit, 1990, pp.47-60.

89. Nagashima, T., Sugano, S., Kimura, H., Ichikawa, A., "Monotonic Axial Compression Test on Ultra-High-Strength Concrete Tied Columns," Proc.of 10th World Conf.on Earthquake Engineering., Madrid, 1992, pp. 2983-2988.

90. Neville, A.M., "A General Relation for Strengths of Concrete Specimens of Different Shapes and Sizes," ACI Journal, Proceedings, Vol.63, No.10, 1966, pp.1095-1109.

91. Nilson, Arthur H., " Design Implications of Current Research on High-Strength Concrete," High Strength Concrete, ACI SP-87, 1985, pp.85-118, Detroit.

92. Nilson, Arthur H., " High-Strength Concrete - An Overview of Cornell Research," Utilization of High Strength Concrete Proceedings, Stavanger, Norway, Tapir Publisher, June 1987, pp. 27-38.

93. Nishiyama, M., Fukushima, I., Watanabe, F., Muguruma, H., "Axial Loading Tests on High-Strength Concrete Prisms Confined by Ordinary and High-Strength Steel," Proceedings of the Symposium on High-Strength Concrete, June 93, Norway, pp. 322-329.

94. Norwegian Standard NS 3473, Concrete Structures, Design rules, Norway, 1989.

95. Novokshchenov, V., "Factors Controlling the Compressive Strength of Silica Fume Concrete in the Range 100 to 150 MPa," Proceedings of the Symposium on High-Strength Concrete, June 93, Norway, pp. 863-873.

96. Otani, S., and Cheung, V.W., "Behaviour of Reinforced Concrete Columns Under Biaxial Lateral Load Reversals," Publication 81-02, Department of Civil Engineering, University of Toronto, Toronto, Canada, 1981, 127 pp.

97. Ozcebe, G., and Saatcioglu, M., "Confinement of Concrete Columns for Seismic Loading," ACI Structural Journal, Vol.84, No.4, 1987, pp.308-315.

98. Ozden, S., " Behaviour of High-Strength Concrete Under Strain Gradient," M.A.Sc. Thesis, Department of Civil Engineering, University of Toronto, Toronto, August 1992, pp. 165.

99. Park, R., Paulay, T., "Reinforced Concrete Structures," John Wiley and Sons, 1975, pp.769.

100. Park, R., Priestley, M.J.N., and Gill, W.D., "Ductility of Square Confined Concrete Columns," Journal of the Structural Division, ASCE, Vol.108, No. ST4, April 1982, pp. 929-951.

101. Paulay, T, and Priestley, M.J.N., "Seismic design of reinforced concrete and masonry buildings," John Wiley and Sons, 1992, pp. 744.

102. Pfister, J.F., " Influence of Ties on the Behaviour of Reinforced Concrete Columns," ACI Journal, Proceedings Vol.61, No.5, May 1964, pp. 521-536.

103. Polat, M.B., "Behaviour of Normal and High Strength Concrete under Axial Compression,"M.A.Sc thesis, Department of Civil Engineering., University of Toronto, Ontario, Canada, 1992, 175 pp.

104. Popovics, S., "Analytical Approach to Complete Stress-Strain Curves," Cement and Concrete Research, Vol.3, No.5, Sept. 1973, pp.583-599.

105. Potter, R.J., and Guirguis, S., " High Concrete in Australia," Proceedings of the Symposium on High-Strength Concrete, June 93, Norway, pp. 581-589.

106. Qi, X., and Moehle, J.P., "Displacement Design Approach for Reinforced Concrete

Structures Subjected to Earthquakes," Report No. UCB/EERC-91/2, Earthquake Engineering Research Center, University of California, Berkeley, January 1991.

107. Rabbat, B., Daniel, J.I., Weinmann, T.L., and Hanson, N.W. "Seismic Behaviour of Lightweight Concrete Columns," Report to NSF, Construction Technology Laboratories, Skokie, Illinois, 1982,263 pp.

108. Radain, A., Samman, T.A., and Wafa, F.F., "Mechanical Properties of High-Strength Concrete," Proceedings of the Symposium on High-Strength Concrete, June 93, Norway, pp. 1209-1216.

109. Rangan B. V., "Strength of Concrete Slender Columns," ACI Structural Journal, V87, No.1, January-February 1990, pp. 32-38.

110. Rangan, B.V., Saunders, P., and Seng, E.J., "Design of High-Strength Concrete Columns," Evaluation and Rehabilitation of Concrete Structures and Innovations in Design, ACI SP 128-52, 1991, pp. 851-862.

111. Razvi, S., " Behavior of Confined Concrete Columns Confined with Welded Wire Fabric," A Thesis Presented to the University of Ottawa, in 1988, in Partial Fulfilment of the Requirements for the Degree of Master of Applied Science, pp. 152.

112. Razvi, S., and Saatcioglu, M.," A Displacement Based Design Approach for Column Confinement," A Paper Submitted to ASCE for Possible Publication, 1994.

113. Razvi, S., and Saatcioglu, M., " Behaviour of Reinforced Concrete Columns Confined with Welded Wire Fabric and/or Rectilinear Ties," Research Report,

Department of Civil Engineering, University of Ottawa, Canada, 1989(a), pp.65.

114. Razvi, S., and Saatcioglu, M., " Confinement of Reinforced Concrete Columns with Welded Wire Fabric," ACI Structural Journal, Vol.86, No.5, September-October 1989(b), pp. 615-623.

115. Razvi, S., and Saatcioglu, M., "Discussion of Deformation Properties and Ductility of High-Strength Concrete," ACI Material Journal, Vol.88, No.6, 1991, pp. 674-675.

116. Razvi, S., and Saatcioglu, M., "Strength and Deformability of Confined High-Strength Concrete Columns," ACI Structural Journal, Nov.-Dec. 1994.

117. Read, P., Carette, G.G., and Malhotra, V.M., " Strength Development Characteristics of High-Strength Concrete Incorporating Supplementary Cementing Materials," A Paper Presented at the Second International Conference on High-Strength Concrete, Berkeley, California, April 1990.

118. Richart, F.E., Brandtzaeg, A., and Brown, R.L., " A Study of the Failure of Concrete Under Combined Compressive Stresses," University of Illinois, Engineering Experimental Station, Bulletin No. 185, 1928, pp. 104.

119. Richart, F.E., Brandtzaeg, A., and Brown, R.L., " The Failure of Plain and Spirally Reinforced Concrete in Compression," University of Illinois, Engineering Experimental Station, Bulletin No. 190, 1929, pp. 74.

120. Roy, H. E. M., and Sozen, M.A., " A Model to Simulate the Response of Concrete to Multi-Axial Loading," Structural Research Series No.268, Civil Engineering Studies, University of Illinois, 1963.

121. Russell, H., G., " Shortening of High-Strength Concrete Members," High Strength Concrete, Second International Symposium, ACI SP-121-1, Detroit, 1990, pp. 1-20.

122. Saatcioglu, M., "Performance of Reinforced Concrete Structures During the 1994 Northridge Earthquake," Preliminary Report on the Northridge, California, Earthquake of January 17, 1994, Canadian Association for Earthquake Engineering, Vancouver, Canada, 15 March 1994, pp. 226-250.

123. Saatcioglu, M., "Deformability of Reinforced Concrete Columns," Earthquake-Resistance Concrete Structures Inelastic Response and Design, ACI SP-127-10, 1991, pp. 421-452.

124. Saatcioglu, M., " Discussion of the proposed revisions to ACI 318-83," ACI Structural Journal, Vol. 86, No.3, 1989, pp. 345-347.

125. Saatcioglu, M., and Bruneau, M., "Performance of Structures during the 1992 Erzincan Earthquake," Canadian Journal of Civil Engineering, Volume 20, Number 2, 1993, pp. 305-325.

126. Saatcioglu, M. , and Ozcebe, G., "Response of Reinforced Concrete Columns to Simulated Seismic Loading," ACI Structural Journal, Vol.86, No.1, January-February 1989, pp.3-12.

127. Saatcioglu, M., and Razvi, S., "Analytical Model for Confined Concrete," Research Report No: 9101, Department of Civil Engineering, University of Ottawa, Ottawa, Ontario, 1991, pp. 59.

128. Saatcioglu, M., and Razvi, S., "Strength and Ductility of Confined Concrete,"

Journal of Structural Engineering, ASCE, Vol. 118, No. 6, 1992, pp. 1590-1607.

129. Saatcioglu, M., and Razvi, S., "Behaviour of Confined High-Strength Concrete Columns," Proceedings of CPCA/CSCE Structural Concrete Conference, May 19-21, 1993, Toronto, Canada, pp.37-50.

130. Saatcioglu, M., Salamat, A.H., and Razvi, S. R., "Confined Columns Under Eccentric Loading," Journal of Structural Engineering, ASCE, Nov. 1995.

131. Sakai, K., and Sheikh, S. A., " What Do We Know about Confinement in Reinforced Concrete Columns? (A Critical Review of Previous Work and Code Provisions)," ACI Structural Journal, Vol. 86, N0. 2, March-April 1989, pp. 192-207.

132. Sakai, Y., Hibi, J., Otani, S., and Aoyama, H., "Experimental Study of Flexural Behavior of Reinforced Concrete Columns using High Strength Concrete," Transaction of The Japan Concrete Inst., Vol.12, 1990, pp. 323-330.

133. Salamat, A., "Behaviour of Confined Concrete under Eccentric Loading," A Thesis Presented to the University of Ottawa, in 1991, in Partial Fulfilment of the Requirements for the Degree of Master of Applied Science.

134. Sargin, M., "Stress-Strain Relationship for Concrete and Analysis of Structural Concrete Sections," Study No.4, Solid Mechanics Division, University of Waterloo, 1971, pp.167.

135. Sato, T. and Ibushi, K. "Effect of Confinement on Ductile Behavior of Reinforced Concrete Short Columns," Transactions of the Japan Concrete Institute, 10(5), 1988, pp. 337-344.

136. Scott, B.D., Park, R., and Priestley, M.J.N., "Stress-Strain Behaviour of Concrete Confined by Overlapping Hoops at High and Low Strain Rates," ACI Journal, January-February 1982, pp. 13-27.

137. Schade, J.E., "Flexural Concrete Stress in High Strength Concrete Columns," M.A.Sc. Thesis, Department of Civil Engineering, University of Calgary, Alberta, 1992, pp.156.

138. Shah, S., and Rangan, B.V., "Effects of Reinforcement on Ductility of Concrete," Journal of Structural Division, ASCE, St6, June 1970, pp. 1167-1184.

139. Sheikh, S.A., "A Comparative Study of Confinement Models," ACI Structural Journal., Vol. 79, No. 4, 1982, pp.296-305.

140. Sheikh, S.A., and Khoury, S.S. "Confined Concrete Columns With Stub," ACI Structural Journal, Vol. 90, No. 4, 1993, pp. 414-431.

141. Sheikh, S.A., Shah, D. V., and Khoury, S.S. "Confinement of High-Strength Concrete Columns," ACI Structural Journal, Vol. 91, No. 1, Jan.-Feb. 1994, pp. 100-111.

142. Sheikh, S.A., and Toklucu, M. "Reinforced Concrete Columns Confined by Circular Spirals and Hoops," ACI Structural Journal, Vol. 90, No.5, Sept.-Oct. 1993, pp.542-553.

143. Sheikh, S.A., and Uzumeri, S.M., "Analytical Model for Concrete Confinement in Tied Columns," Journal of Structural Engineering, ASCE, Vol.108, No.5, December 1982, pp. 2703-2723.

144. Sheikh, S.A., and Uzumeri, S.M., "Strength and Ductility of Tied Concrete Columns," Journal of Structural Engineering, ASCE, Vol.106, No.5, 1980, pp. 1079-1102.

145. Sheikh, S.A., and Yeh, C.C., "Flexural Behavior of Confined Concrete Columns," ACI Structural Journal, May-June 1986, pp.389-404.

146. Sheikh, S.A., and Yeh, C.C., and Menzies, D., "Confined Concrete Columns," Pacific Conference on Earthquake Engineering, Wairakei, New Zeland, August 1987, pp. 177-188.

147. Shin, S.W., Kamara, M., and Ghosh, S.K., "Flexural Ductility, Strength Prediction, and Hysteretic Behavior of Ultra-High-Strength Concrete Members," High-Strength Concrete, 2nd Int.Symp.,ACI SP-121-13, pp.239-264.

148. Smith, Gregory J., and Rad, Franz N., "Economic Advantages of High Strength-Concretes in Columns," Concrete International, Design and Construction, Vol.11, No.4, April 1989, pp.37-43.

149. Soliman, M.T.M., and Yu, C.W., "Flexural Stress-Strain Relationship of Concrete Confined by Rectangular Transverse Reinforcement," Magazine of Concrete Research, Vol.19, No.61, December 1967, pp. 223-238.

150. Somes, Norman F., " Compression Tests on Hoop-Reinforced Concrete," Journal of the Structural Division, Proceedings of the American Society of Civil Engineers, ST7, July 1970, pp. 1495-1509.

151. Stockl, S., Discussion of "Ductility of Concrete", by Roy, H.E., and Sozen, M.A.,

Proceedings of the International Symposium on the Flexural Mechanics of Reinforced Concrete, ASCE-ACI, Miami, November 1964, pp.225-227.

152. Sturman, G. M., Shah, S.P., and Winter, G., "Effect of Flexural Strain Gradient on Microcracking and Stress-Strain Behaviour of Concrete," ACI Journal, Proceedings, July 1965, pp. 805-822.

153. Sudo, E., Masuda, Y., Abe, M., Yasuda, M., "Mechanical Properties of Confined High-Strength Concrete," Proceedings of the Symposium on High-Strength Concrete, June 93, Norway, pp. 369-376.

154. Sugano, S., Nagashima, T., Kimura, H., Tamura, A., and Ichikawa, A., "Experimental Studies on Seismic Behavior of Reinforced Concrete Members of High Strength Concrete," High Strength Concrete, Second International Symposium, ACI SP-121-5, Detroit, 1990, pp.61-87.

155. Sundararaj, P., "High Strength Concrete Columns Under Eccentric Load," M.A.Sc. Thesis, Department of Civil Engineering, University of Toronto, Toronto, 1991, pp. 261.

156. Szulcynski, T. , and Sozen, M.A., "Load-Deformation Characteristics of Reinforced Concrete Prisms with Rectilinear Transverse Reinforcement," Structural Research Series No.224, Civil Engineering Studies, University of Ilinois, Urbana, September 1961, 54 pp.

157. Tachibana, D., Imai, M., Yamazaki, N., Kawai, T., and Inada, Y., " High-Strength Concrete Incorporating Several Admixtures," High Strength Concrete, Second International Symposium, ACI SP-121-16, Detroit, 1990, pp.309-330.

158. Thomsen, J.H., and Wallace, J.W., "A Study of High-Strength Reinforced Concrete Columns Subjected to Lateral and Axial Loads," Research Report No. CU/CEE-92/6, Dept. of Civil Engineering, Clarkson University, 1992, 170 pp.

159. Thomsen, J.H., and Wallace, J.W., "Lateral Load Behavior of Reinforced Concrete Columns Constructed Using High-Strength Materials," ACI Structural Journal, Vol.91, No. 5, Sept.-Oct. 1994, pp. 605-615.

160. Tomosawa, F., Masuda, Y., Abe, M., Shimizu, A., and Nakane, S., " High-Strength Concretes for High-Rise Buildings in Japan," High Strength Concrete, Second International Symposium, ACI SP-121-3, Detroit, 1990, pp. 33-46.

161. Tomosawa, F., Noguchi, T., " Relationship Between Compressive Strength and Modulus of Elasticity of High-Strength Concrete," Proceedings of the Symposium on High-Strength Concrete, June 93, Norway, pp. 1247-1254.

162. Tomosawa, F., Noguchi, T., and Onoyama, K., "Test Method for Compressive Strength of High-Strength Concrete," Proceedings of the Symposium on High-Strength Concrete, June 93, Norway, pp. 1255-1262.

163. Vallenas, J., Bertero, V.V, Popov, E.P., "Concrete Confined by Rectangular Hoops and Subjected to Axial Load," Report No. UCB/EERC-77/13, Earthquake Engineering Research Center, College of Engineering, University of California, Berkeley, August 1977, pp.114.

164. Wafa, F.F., and Ashour, S. A., " Mechanical Properties of High-Strength Fiber Reinforced Concrete," Proceedings ACI Material Journal, Vol. 89, No.5, Sept.-Oct. 1992, pp. 449-455.

165. Watanabe, F., Muguruma, H., Matsutani, T., and Sanda, D., "Utilization of High Strength Concrete for Reinforced Concrete High-Rise Buildings in Seismic Area," Utilization of High Strength Concrete Proceedings, Stavanger, Norway, Tapir Publisher, June 1987, pp. 655-666.

166. Watanabe, F., Muguruma, H., Tanaka, H., and Katsuda, S., " Improving the Flexural Ductility of Prestressed Concrete Beam by Using the high Yield Strength Lateral Hoop Reinforcement," FIP, Symposia on Partial Prestressing and Practical Construction in Prestressed and Reinforced Concrete, Proceedings: Part 2, Sept. 1980, Bucuresti-Romania, pp.398-406.

167. Xie, J., Elwi, A. E., and MacGregor, J. G., "Numerical Investigation of Eccentrically loaded Tied High-Strength Concrete Columns," Structural Engineering Report No. 204, Department of Civil Engineering, University of Alberta, October 1994, pp. 190.

168. Yagenji, A., Hiraishi, H., Teshigawara, M., "Data Analysis of Uni-Axial Tests of RC Columns Based on Energy Principle," (in Japanese), Proceedings of the Annual Conference of Japan Architectural Institute, Sept. 1991, pp. 493-494.

169. Yong, Y.K., Nour, M.G., and Nawy, E.G., "Behavior of Laterally Confined High-Strength Concrete Under Axial Loads," ASCE Journal of Structural Engineering, Vol.114, No.2,1988, pp. 332-351.

170. Zagajeski, S.W., Bertero, V.V., and Bouwkamp, J.G., "Hysteretic Behaviour of Reinforced Concrete Columns Subjected to High Axial and Cyclic Shear Forces," Report No. UCB/EERC-78/05, College of Engineering, University of California, Berkeley, California, 1978, 208 pp.